BRS
BOARD REVIEW SERIES

Embryology

SIXTH EDITION

Ronald W. Dudek

- Outline format highlights the most tested topics for USMLE Step 1
- More than 280 board-style questions to help test your memorization and mastery
- Online access—offers greater study flexibility

Wolters Kluwer
Health

BRS
BOARD REVIEW SERIES

Embryology

SIXTH EDITION

BRS
BOARD REVIEW SERIES

Embryology

SIXTH EDITION

Ronald W. Dudek, Ph.D.
Professor
Department of Anatomy and Cell Biology
Brody School of Medicine
East Carolina University
Greenville, North Carolina

Wolters Kluwer
Health
Philadelphia • Baltimore • New York • London
Buenos Aires • Hong Kong • Sydney • Tokyo

Acquisitions Editor: Crystal Taylor
Product Manager: Catherine Noonan
Marketing Manager: Joy Fisher-Williams
Designer: Holly Reid McLaughlin
Compositor: S4Carlisle Publishing Servises

Sixth Edition

351 West Camden Street
Two Commerce Square
Baltimore, MD 21201

2001 Market Street
Philadelphia, PA 19103

Printed in China

Library of Congress Cataloging-in-Publication Data

ISBN 978-1-4511-9038-0

Cataloging-in-Publication data available on request from the Publisher.

To purchase additional copies of this book, call our customer service department at **(800) 638-3030** or fax orders to **(301) 223-2320**. International customers should call **(301) 223-2300**.

Visit Lippincott Williams & Wilkins on the Internet: http://www.lww.com. Lippincott Williams & Wilkins customer service representatives are available from 8:30 am to 6:00 pm, EST.

9 8 7 6 5 4 3 2 1

Preface

The sixth edition of BRS *Embryology* includes improvements based on suggestions and comments from the many medical students who have used this book in preparation for the USMLE Step 1 examination and those students who have reviewed the book. I pay close attention to these suggestions and comments in order to improve the quality of this book. The goal of BRS *Embryology* is to provide an accurate and quick review of important clinical aspects of embryology for the future physician. In addition, we have added color to the diagrams. In this regard, I have used the following color scheme. The ectoderm/neuroectoderm and derivatives are colored blue. The neural crest cells and derivatives are colored purple. The mesoderm and derivatives are colored red. When multiple mesodermal structures are involved (e.g., reproductive systems), I used light red and dark red. The endoderm and derivatives are colored yellow.

Many times in the history of science, certain biological concepts become entrenched and accepted as dogma even though recent evidence comes to light to challenge these concepts. One of these concepts is the process of twinning. Recent evidence calls into question the standard figures used in textbooks on how the process of twinning occurs. In particular, it is becoming increasingly difficult to ignore the fact that dizygotic twins are sometimes monochorionic. Although we by far do not know or attempt to explain exactly how twinning occurs, it seems that the interesting cell and molecular events involved in twinning occur in the first few cell divisions during first three or four days after fertilization. You are not a twin because the inner cell mass splits. The inner cell mass splits because you are a twin. This evidence warrants a new twinning figure (Figure 6.6) that does not comport with the standard figures but tries to embrace recent evidence, although many may call it controversial. Progress in our scientific understanding of twinning will never occur if our concept of the twinning process is overly simplistic and reinforced by standard figures repeated over and over in textbooks. Some published references that speak to this twinning issue include Boklage,[1,2] Yoon et al.,[3] Williams et al.,[4] and Hoekstra et al.[5]

I understand that BRS *Embryology* is a review book designed for a USMLE Step 1 review and that you will not be faced with a question regarding this twinning concept, but I know my readers are sophisticated enough to appreciate the scientific and clinical value of being challenged to question traditional concepts as "grist for the mill" in discussions with your colleagues.

I would appreciate receiving your comments and/or suggestions concerning BRS *Embryology* sixth edition, especially after you have taken the USMLE Step 1 examination. Your suggestions will find their way into the seventh edition. You may contact me at dudekr@ecu.edu.

Ronald W. Dudek, PhD

REFERENCES

1. Boklage CE. Traces of embryogenesis are the same in monozygotic and dizygotic twins: not compatible with double ovulation. *Hum Reprod*. 2009;24(6):1255–1266.
2. Boklage CE. *How New Humans Are Made: Cells and Embryos, Twins and Chimeras, Left and Right, Mind/Self/Soul, Sex, and Schizophrenia*. Hackensack, NJ: World Scientific Publishing; 2010.
3. Yoon G, Beischel LS, Johnson JP, et al. Dizygotic twin pregnancy conceived with assisted reproductive technology associated with chromosomal anomaly, imprinting disorder, and monochorionic placentation. *J Pediatr*. 2005;146:565–567.
4. Williams CA, Wallace MR, Drury KC, et al. Blood lymphocyte chimerism associated with IVF and monochorionic dizygous twinning: case report. *Hum Reprod*. 2004;19(12):2816–2821.
5. Hoekstra C, Zhao ZZ, Lambalk CB, et al. Dizygotic twinning. *Hum Reprod Update*. 2008;14(1):37–47.

Contents

chapter 1

Prefertilization Events

I. SEXUAL REPRODUCTION

Sexual reproduction occurs when female and male gametes (oocyte and spermatozoon, respectively) unite at fertilization. Gametes are direct descendants of **primordial germ cells**, which are first observed in **the wall of the yolk sac** at week 4 of embryonic development and subsequently migrate into the future gonad region. Gametes are produced by **gametogenesis** (called **oogenesis** in the female and **spermatogenesis** in the male). Gametogenesis employs a specialized process of cell division, **meiosis**, which uniquely distributes chromosomes among gametes.

II. CHROMOSOMES (FIGURE 1.1)

A single chromosome consists of two characteristic regions called **arms** (**p arm** = **short arm**; **q arm** = **long arm**), which are separated by a **centromere**. During meiosis I, **single chromosomes** undergo DNA replication, which duplicates the arms. This forms **duplicated chromosomes**, which consist of two sister **chromatids** attached at the centromere.

A. Ploidy and N number. Ploidy refers to the **number of chromosomes** in a cell. The N number refers to the **amount of DNA** in a cell.

1. **Normal somatic cells and primordial germ cells** contain **46 single chromosomes** and **2N amount of DNA**. The chromosomes occur in **23 homologous pairs**; one member (homologue) of each pair is of maternal origin, and the other is of paternal origin. The term "**diploid**" is classically used to refer to a cell containing 46 single chromosomes. Chromosome pairs 1–22 are **autosomal (nonsex) pairs**. Chromosome pair 23 consists of the **sex chromosomes** (XX for a female and XY for a male).
2. **Gametes** contain **23 single chromosomes** (22 autosomes and 1 sex chromosome) and **1N amount of DNA**. The term "**haploid**" is classically used to refer to a cell containing 23 single chromosomes. Female gametes contain only the X sex chromosome. Male gametes contain either the X or Y sex chromosome; therefore, the male gamete determines the genetic sex of the individual.

B. The X chromosome. A normal female somatic cell contains **two X chromosomes (XX)**. The female cell **permanently inactivates** one of the X chromosomes during week 1 of embryonic development. The choice of which X chromosome (maternal or paternal) is inactivated is random. The

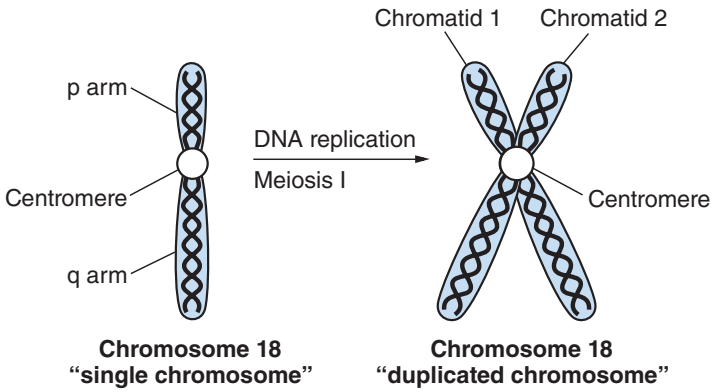

FIGURE 1.1. A schematic diagram of chromosome 18 showing it in its "single-chromosome" state and in the "duplicated-chromosome" state that is formed by DNA replication during meiosis I. It is important to understand that both the "single-chromosome" state and the "duplicated-chromosome" state will be counted as one chromosome 18. As long as the additional DNA in the "duplicated chromosome" is bound at the centromere, the structure will be counted as one chromosome 18 even though it has twice the amount of DNA.

inactivated X chromosome (called the **Barr body**) can be observed by light microscopy near the nuclear membrane.

C. **The Y chromosome.** A normal male somatic cell contains **one X chromosome** and **one Y chromosome (XY)**.

III. MEIOSIS

Meiosis is a specialized process of cell division that occurs only during the production of gametes within the female ovary or male testes. Meiosis consists of two divisions (meiosis I and II), which result in the formation of four gametes, each containing half the number of chromosomes (23 single chromosomes) and half the amount of DNA (1N) found in normal somatic cells (46 single chromosomes, 2N).

A. **Meiosis I.** Events that occur during meiosis I include the following:
1. **Synapsis:** pairing of 46 homologous duplicated chromosomes.
2. **Crossing over:** exchange of large segments of DNA.
3. **Alignment:** alignment of 46 homologous duplicated chromosomes at the metaphase plate.
4. **Disjunction:** separation of 46 homologous duplicated chromosomes from each other; **centromeres do not split**.
5. **Cell division:** formation of two secondary gametocytes (23 duplicated chromosomes, 2N).

B. **Meiosis II.** Events that occur during meiosis II include the following:
1. **Synapsis:** absent.
2. **Crossing over:** absent.
3. **Alignment:** alignment of 23 duplicated chromosomes at the metaphase plate.
4. **Disjunction:** separation of 23 duplicated chromosomes to form 23 single chromosomes; centromeres split.
5. **Cell division:** formation of four gametes (23 single chromosomes, 1N).

IV. OOGENESIS: FEMALE GAMETOGENESIS (FIGURE 1.2)

A. **Primordial germ cells (46, 2N)** from the wall of the yolk sac arrive in the ovary at **week 6** and differentiate into **oogonia (46, 2N)**, which populate the ovary through *mitotic* division.

B. Oogonia enter meiosis I and undergo DNA replication to form **primary oocytes (46, 4N)**. All primary oocytes are formed by **month 5 of fetal life**. No oogonia are present at birth.

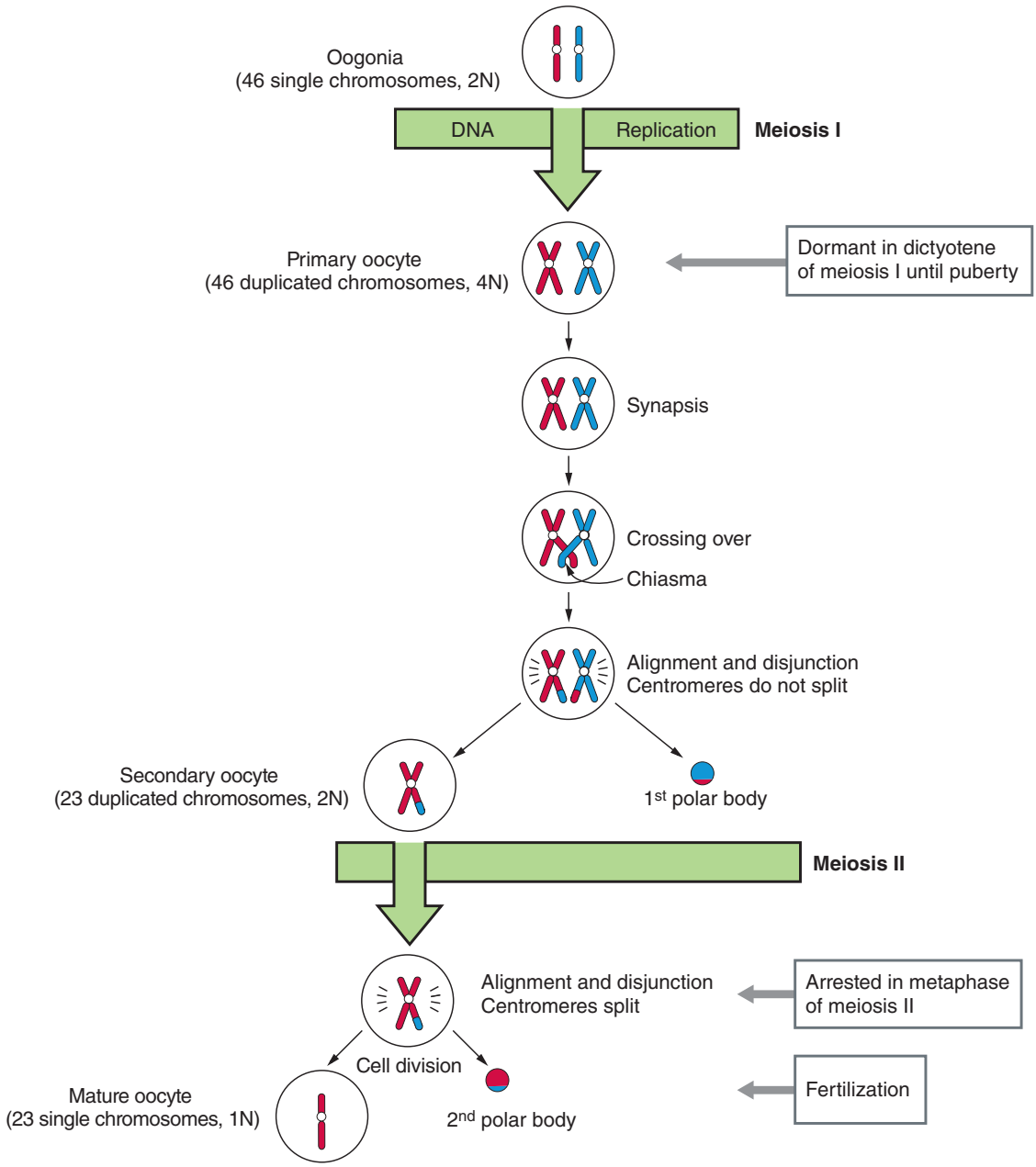

FIGURE 1.2. Oogenesis: female gametogenesis. Note that only one pair of homologous chromosomes is shown (*red,* maternal origin; *blue,* paternal origin). Synapsis is the process of pairing of homologous chromosomes. The point at which the DNA molecule crosses over is called the chiasma and is where exchange of small segments of maternal and paternal DNA occurs. Note that synapsis and crossing over occur only during meiosis I. The polar bodies are storage bodies for DNA unnecessary for the further function of the cell and probably degenerate. There is no evidence that polar bodies divide or undergo any other activity.

C. Primary oocytes remain **dormant in prophase (dictyotene) of meiosis I** from month 5 of fetal life until puberty. After puberty, 5 to 15 primary oocytes begin maturation with each ovarian cycle, with usually only 1 reaching full maturity in each cycle.

D. During the ovarian cycle and triggered by the **luteinizing hormone (LH) surge,** a primary oocyte completes meiosis I to form two daughter cells: the **secondary oocyte (23, 2N)** and the **first polar body**, which degenerates.

E. The secondary oocyte promptly begins meiosis II but is **arrested in metaphase of meiosis II** about 3 hours before ovulation. The secondary oocyte remains arrested in metaphase of meiosis II until fertilization occurs.

F. At fertilization, the secondary oocyte completes meiosis II to form a **mature oocyte (23, 1N)** and a **second polar body**.

G. Approximate number of oocytes

1. **Primary oocytes:** At month 5 of fetal life, 7 million primary oocytes are present. At birth, 2 million are present (5 million have degenerated). At puberty, 40,000 are present (1.96 million more have degenerated).
2. **Secondary oocytes:** Twelve secondary oocytes are ovulated per year, up to 480 over the entire reproductive life of the woman (40 years × 12 secondary oocytes per year = 480). This number (480) is obviously overly simplified since it is **reduced** in women who take birth control pills (which prevent ovulation), in women who become pregnant (ovulation stops during pregnancy), and in women who may have anovulatory cycles.

V. SPERMATOGENESIS: MALE GAMETOGENESIS (FIGURE 1.3)

Spermatogenesis is classically divided into three phases:

A. Spermatocytogenesis

1. **Primordial germ cells (46, 2N)** from the wall of the yolk sac arrive in the testes at **week 6** and remain **dormant until puberty**. At puberty, primordial germ cells differentiate into **type A spermatogonia (46, 2N)**.
2. Type A spermatogonia undergo mitosis to provide a continuous supply of stem cells throughout the reproductive life of the male. Some type A spermatogonia differentiate into **type B spermatogonia (46, 2N)**.

B. Meiosis

1. Type B spermatogonia enter meiosis I and undergo DNA replication to form **primary spermatocytes (46, 4N)**.
2. Primary spermatocytes complete meiosis I to form **secondary spermatocytes (23, 2N)**.
3. Secondary spermatocytes complete meiosis II to form four **spermatids (23, 1N)**.

C. Spermiogenesis

1. Spermatids undergo a **postmeiotic series of morphological changes** to form **sperm (23, 1N)**. These changes include the (a) formation of the acrosome, (b) condensation of the nucleus, and (c) formation of head, neck, and tail. The total time of sperm formation (from spermatogonia to spermatozoa) is about 64 days.
2. Newly ejaculated sperm are **incapable** of fertilization until they undergo **capacitation**, which occurs in the female reproductive tract and involves the unmasking of sperm glycosyltransferases and the removal of adherent plasma proteins coating the surface of the sperm.

VI. CLINICAL CONSIDERATIONS

A. Offspring of older women

1. Prolonged dormancy of primary oocytes may be the reason for the high incidence of chromosomal abnormalities in the offspring of older women. Since all primary oocytes are formed by month 5 of fetal life, a female infant is born with her entire supply of gametes. Primary oocytes remain dormant until ovulation; those ovulated late in the woman's reproductive life may have been dormant for as long as 40 years.
2. The incidence of **trisomy 21 (Down syndrome)** increases with advanced age of the mother. The primary cause of Down syndrome is maternal meiotic nondisjunction. Clinical findings

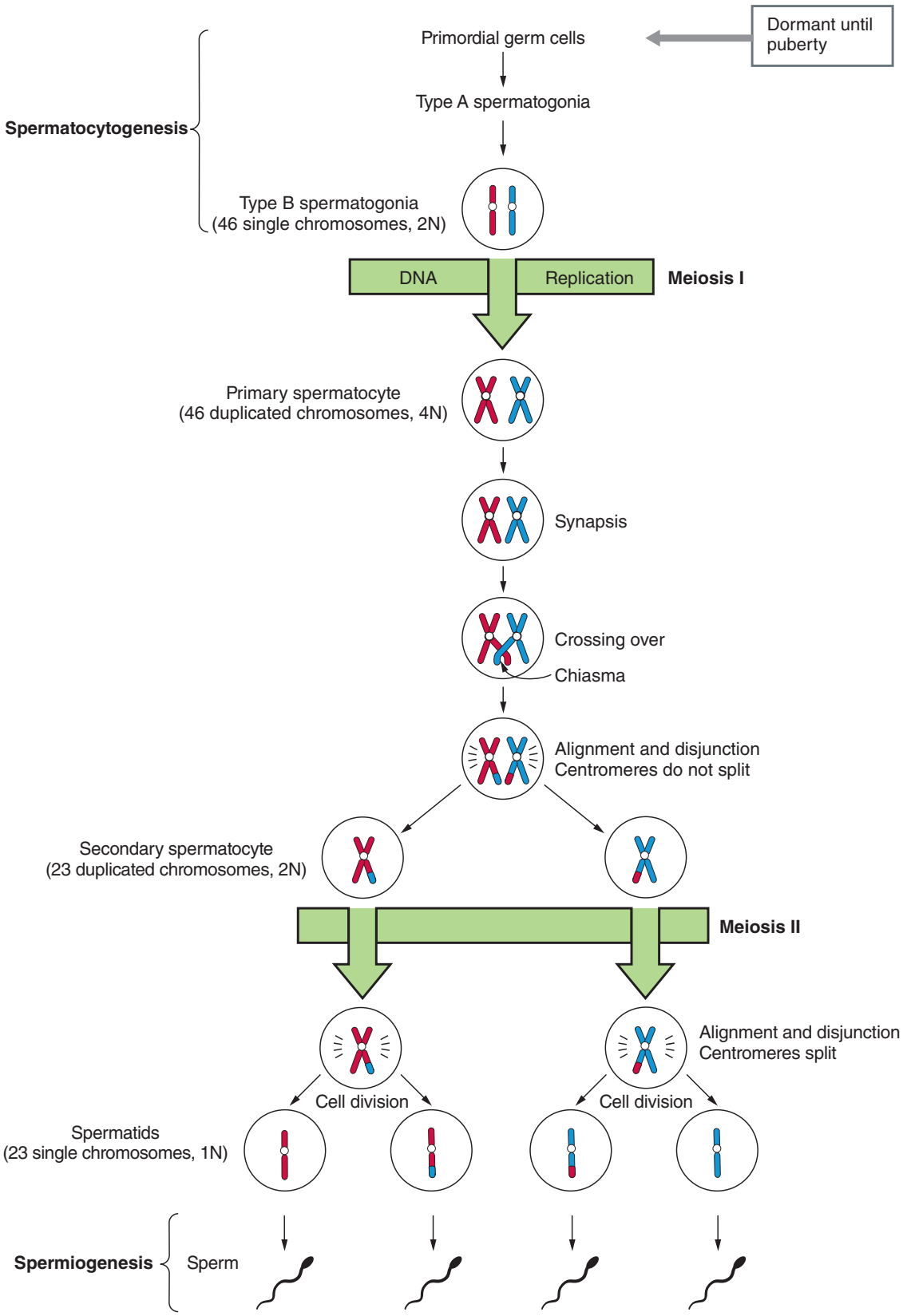

FIGURE 1.3. Spermatogenesis: male gametogenesis. Note that only one pair of homologous chromosomes is shown (*red*, maternal origin; *blue*, paternal origin). Synapsis is the process of pairing of homologous chromosomes. The point at which the DNA molecule crosses over is called the chiasma and is where exchange of small segments of maternal and paternal DNA occurs. Note that synapsis and crossing over occur only during meiosis I.

include moderate mental retardation, microcephaly, microphthalmia, colobomata, cataracts and glaucoma, flat nasal bridge, epicanthal folds, protruding tongue, Brushfield spots, simian crease in the hand, increased nuchal skin folds, congenital heart defects, and an association with a decrease in α-fetoprotein.

B. Offspring of older men

An increased incidence of achondroplasia (a congenital skeletal anomaly characterized by retarded bone growth) and Marfan syndrome are associated with advanced paternal age.

C. Male infertility

1. **Sperm number and motility:** Infertile males produce less than 10 million sperm/mL of semen. Fertile males produce from 20 to more than 100 million sperm/mL of semen. Normally, up to 10% of sperm in an ejaculate may be grossly deformed (two heads or two tails), but these sperm probably do not fertilize an oocyte because of their lack of motility.
2. **Hypogonadotropic hypogonadism** is a condition where the hypothalamus produces reduced levels of gonadotropin-releasing factor (GnRF), leading to reduced levels of follicle-stimulating hormone (FSH) and LH, and finally, reduced levels of testosterone. **Kallmann syndrome** is a genetic disorder characterized by hypogonadotropic hypogonadism and anosmia (loss of smell).
3. **Drugs:** cancer chemotherapy, anabolic steroids, cimetidine (histamine H_2-receptor antagonist that inhibits stomach HCl production), spironolactone (a K^+-sparing diuretic), phenytoin (an antiepileptic drug), sulfasalazine (a sulfa drug used to treat ulcerative colitis, Crohn disease, rheumatoid arthritis, and psoriatic arthritis), and nitrofurantoin (an antibiotic used to treat urinary tract infections).
4. **Other factors:** Klinefelter syndrome (XXY), seminoma, cryptochordism, varicocele, hydrocele, mumps, prostatitis, epididymitis, hypospadias, ductus deferens obstruction, and impotence.

D. Female infertility

1. **Anovulation** is the absence of ovulation in some women due to inadequate secretion of FSH and LH and is often treated with **clomiphene citrate** (a fertility drug). Clomiphene citrate competes with estrogen for binding sites in the adenohypophysis, thereby suppressing the normal negative feedback loop of estrogen on the adenohypophysis. This stimulates FSH and LH secretions and induces ovulation.
2. **Premature ovarian failure (primary ovarian insufficiency)** is the loss of function of the ovaries before age 40, resulting in infertility. The cause is generally idiopathic, but cases have been attributed to autoimmune disorders, Turner syndrome, Fragile X syndrome, chemotherapy, or radiation treatment. The onset can be seen in early teenage years, but varies widely. If a girl never begins menstruation, the condition is called **primary ovarian failure**. Clinical findings include amenorrhea, low estrogen levels, high FSH levels, and small ovaries without follicles (seen by ultrasound).
3. **Pelvic inflammatory disease (PID)** refers to the infection of the uterus, uterine tubes, and/or ovaries leading to inflammation and scar formation. The cause is generally a sexually transmitted infection (STI), usually by *Neisseria gonorrhea* or *Chlamydia trachomatis*; however, many other reasons are possible (lymphatic spread, hematogenous spread, postpartum infections, postabortal [miscarriage or abortion] infections, or intrauterine device infections). Clinical findings include fever, tenderness of the cervix, lower abdominal pain, discharge, painful intercourse, or irregular menstrual bleeding; some cases are asymptomatic.
4. **Polycystic ovarian syndrome** is a complex female endocrine disorder defined by oligo-ovulation (infrequent, irregular ovulations), androgen excess, multiple ovarian cysts (by ultrasound). The cause is uncertain, but a strong genetic component exists. Clinical findings include anovulation, irregular menstruation, amenorrhea, ovulation-related infertility, high androgen levels or activity resulting in acne and hirsutism, insulin resistance associated with obesity, and type 2 diabetes.
5. **Endometriosis** is the appearance of foci of endometrial tissue in abnormal locations outside the uterus (e.g., ovary, uterine ligaments, pelvic peritoneum). The ectopic endometrial

table 1.1 Chance of Pregnancy in Days Near Ovulation

Time	Chance of Pregnancy (%)
5 days before ovulation	10
4 days before ovulation	16
3 days before ovulation	14
2 days before ovulation	27
1 day before ovulation	31
Day of ovulation	33
Day after ovulation	0

tissue shows cyclic hormonal changes synchronous with the cyclic hormonal changes of the endometrium in the uterus. Clinical findings include infertility, dysmenorrhea, pelvic pain (most pronounced at the time of menstruation), dysuria, painful sex, and throbbing pain in the legs.

E. The estimated chance of pregnancy (fertility) in the days surrounding ovulation is shown in Table 1.1.

Study Questions for Chapter 1

1. Which of the following is a major characteristic of meiosis I?

(A) Splitting of the centromere
(B) Pairing of homologous chromosomes
(C) Reducing the amount of DNA to 1N
(D) Achieving the diploid number of chromosomes
(E) Producing primordial germ cells

2. A normal somatic cell contains a total of 46 chromosomes. What is the normal complement of chromosomes found in a sperm?

(A) 22 autosomes plus a sex chromosome
(B) 23 autosomes plus a sex chromosome
(C) 22 autosomes
(D) 23 autosomes
(E) 23 paired autosomes

3. Which of the following describes the number of chromosomes and amount of DNA in a gamete?

(A) 46 chromosomes, 1N
(B) 46 chromosomes, 2N
(C) 23 chromosomes, 1N
(D) 23 chromosomes, 2N
(E) 23 chromosomes, 4N

4. Which of the following chromosome compositions in a sperm normally results in the production of a genetic female if fertilization occurs?

(A) 23 homologous pairs of chromosomes
(B) 22 homologous pairs of chromosomes
(C) 23 autosomes plus an X chromosome
(D) 22 autosomes plus a Y chromosome
(E) 22 autosomes plus an X chromosome

5. In the process of meiosis, DNA replication of each chromosome occurs, forming a structure consisting of two sister chromatids attached to a single centromere. What is this structure?

(A) A duplicated chromosome
(B) Two chromosomes
(C) A synapsed chromosome
(D) A crossover chromosome
(E) A homologous pair

6. All primary oocytes are formed by

(A) week 4 of embryonic life
(B) month 5 of fetal life
(C) birth
(D) month 5 of infancy
(E) puberty

7. When does formation of primary spermatocytes begin?

(A) During week 4 of embryonic life
(B) During month 5 of fetal life
(C) At birth
(D) During month 5 of infancy
(E) At puberty

8. In the production of female gametes, which of the following cells can remain dormant for 12 to 40 years?

(A) Primordial germ cell
(B) Primary oocyte
(C) Secondary oocyte
(D) First polar body
(E) Second polar body

9. In the production of male gametes, which of the following cells remains dormant for 12 years?

(A) Primordial germ cell
(B) Primary spermatocyte
(C) Secondary spermatocyte
(D) Spermatid
(E) Sperm

10. Approximately how many sperm will be ejaculated by a normal fertile male during sexual intercourse?

(A) 10 million
(B) 20 million
(C) 35 million
(D) 100 million
(E) 350 million

11. A young woman enters puberty with approximately 40,000 primary oocytes in her ovary. About how many of these primary oocytes will be ovulated over the entire reproductive life of the woman?

(A) 40,000
(B) 35,000
(C) 480
(D) 48
(E) 12

12. Fetal sex can be diagnosed by noting the presence or absence of the Barr body in cells obtained from the amniotic fluid. What is the etiology of the Barr body?

(A) Inactivation of both X chromosomes
(B) Inactivation of homologous chromosomes
(C) Inactivation of one Y chromosome
(D) Inactivation of one X chromosome
(E) Inactivation of one chromatid

13. How much DNA does a primary spermatocyte contain?

(A) 1N
(B) 2N
(C) 4N
(D) 6N
(E) 8N

14. During meiosis, pairing of homologous chromosomes occurs, which permits large segments of DNA to be exchanged. What is this process called?

(A) Synapsis
(B) Nondisjunction
(C) Alignment
(D) Crossing over
(E) Disjunction

15. During ovulation, the secondary oocyte resides at what specific stage of meiosis?

(A) Prophase of meiosis I
(B) Prophase of meiosis II
(C) Metaphase of meiosis I
(D) Metaphase of meiosis II
(E) Meiosis is completed at the time of ovulation

16. Concerning maturation of the female gamete (oogenesis), when do the oogonia enter meiosis I and undergo DNA replication to form primary oocytes?

(A) During fetal life
(B) At birth
(C) At puberty
(D) With each ovarian cycle
(E) Following fertilization

17. Where do primordial germ cells initially develop?

(A) In the gonads at week 4 of embryonic development
(B) In the yolk sac at week 4 of embryonic development
(C) In the gonads at month 5 of embryonic development
(D) In the yolk sac at month 5 of embryonic development
(E) In the gonads at puberty

Answers and Explanations

1. **B.** Pairing of homologous chromosomes (synapsis) is a unique event that occurs only during meiosis I in the production of gametes. Synapsis is necessary so that crossing over can occur.
2. **A.** A normal gamete (sperm in this case) contains 23 single chromosomes. These 23 chromosomes consist of 22 autosomes plus 1 sex chromosome.
3. **C.** Gametes contain 23 chromosomes and 1N amount of DNA, so that when two gametes fuse at fertilization, a zygote containing 46 chromosomes and 2N amount of DNA is formed.
4. **E.** A sperm contains 22 autosomes and 1 sex chromosome. The sex chromosome in sperm may be either the X chromosome or the Y chromosome. The sex chromosome in a secondary oocyte is only the X chromosome. If an X-bearing sperm fertilizes a secondary oocyte, a genetic female (XX) is produced. Therefore, sperm is the arbiter of sex determination.
5. **A.** The structure formed is a duplicated chromosome. DNA replication occurs, so that the amount of DNA is doubled ($2 \times 2N = 4N$). However, the chromatids remain attached to the centromere, forming a duplicated chromosome.
6. **B.** During early fetal life, oogonia undergo mitotic divisions to populate the developing ovary. All the oogonia subsequently give rise to primary oocytes by month 5 of fetal life; at birth, no oogonia are present in the ovary. At birth, a female has her entire supply of primary oocytes to carry her through reproductive life.
7. **E.** At birth, a male has primordial germ cells in the testes that remain dormant until puberty, at which time they differentiate into type A spermatogonia. At puberty, some type A spermatogonia differentiate into type B spermatogonia and give rise to primary spermatocytes by undergoing DNA replication.
8. **B.** Primary oocytes are formed by month 5 of fetal life and remain dormant until puberty, when hormonal changes in the young woman stimulate the ovarian and menstrual cycles. From 5 to 15 oocytes will then begin maturation with each ovarian cycle throughout the woman's reproductive life.
9. **A.** Primordial germ cells migrate from the wall of the yolk sac during week 4 of embryonic life and enter the gonad of a genetic male, where they remain dormant until puberty (about age 12 years), when hormonal changes in the young man stimulate the production of sperm.
10. **E.** A normal fertile male will ejaculate about 3.5 mL of semen containing about 100 million sperm/mL ($3.5 \text{ mL} \times 100 \text{ million} = 350 \text{ million}$).
11. **C.** Over her reproductive life, a woman will ovulate approximately 480 oocytes. A woman will ovulate 12 primary oocytes per year, provided that she is not using oral contraceptives, does not become pregnant, or does not have any anovulatory cycles. Assuming a 40-year reproductive period gives $40 \times 12 = 480$.
12. **D.** The Barr body is formed from inactivation of one X chromosome in a female. All somatic cells of a normal female will contain two X chromosomes. The female has evolved a mechanism for permanent inactivation of one of the X chromosomes presumably because a double dose of X chromosome products would be lethal.
13. **C.** Type B spermatogonia give rise to primary spermatocytes by undergoing DNA replication, thereby doubling the amount of DNA ($2 \times 2N = 4N$) within the cell.

14. **D.** Synapsis (pairing of homologous chromosomes) is a unique event that occurs only during meiosis I in the production of gametes. Synapsis is necessary so that crossing over, whereby large segments of DNA are exchanged, can occur.

15. **D.** The secondary oocyte is arrested in metaphase of meiosis II about 3 hours before ovulation, and it remains in this meiotic stage until fertilization.

16. **A.** All primary oocytes are formed by month 5 of fetal life, so no oogonia are present at birth.

17. **B.** Primordial germ cells, the predecessors to gametes, are first seen in the wall of the yolk sac at week 4 of embryonic development, and they migrate into the gonads at week 6.

chapter 2

Week 1 of Human Development (Days 1–7)*

I. FERTILIZATION

Fertilization occurs in the **ampulla of the uterine tube** and includes three phases.

A. Phase 1: **Sperm penetration of corona radiata** involves the action of both sperm and uterine tube mucosal enzymes.

B. Phase 2: **Sperm binding and penetration of the zona pellucida**
   1. **Sperm binding** occurs through the interaction of sperm glycosyltransferases and ZP3 receptors located on the zona pellucida. Sperm binding triggers the **acrosome reaction**, which entails the fusion of the outer acrosomal membrane and sperm cell membrane, resulting in the release of acrosomal enzymes.
   2. **Penetration of the zona pellucida** requires acrosomal enzymes, specifically **acrosin**. Sperm contact with the cell membrane of a secondary oocyte triggers the **cortical reaction**, which entails the release of cortical granules (lysosomes) from the oocyte cytoplasm. This reaction changes the secondary oocyte cell membrane potential and inactivates sperm receptors on the zona pellucida. These changes are called the **polyspermy block**, which renders the secondary oocyte cell membrane impermeable to other sperm. However, efficiency of the polyspermy block remains questionable since **diandric triploidy** (an embryo with three sets of chromosomes, two of which come from the father) is quite common.

C. Phase 3: **Fusion of sperm and oocyte cell membranes** occurs with subsequent breakdown of both membranes at the fusion area.
   1. The entire sperm (except the cell membrane) enters the cytoplasm of the secondary oocyte arrested in metaphase of meiosis II. The sperm nuclear contents and the centriole pair persist, but the sperm mitochondria and tail degenerate. The sperm nucleus becomes the **male pronucleus**. Since all sperm mitochondria degenerate, all mitochondria within the zygote are of maternal origin (i.e., **all mitochondrial DNA is of maternal origin**). The oocyte loses its centriole pair during meiosis so that the establishment of a functional zygote depends upon the **sperm centriole pair** (a cardinal feature of human embryogenesis) to produce a microtubule-organizing center (MTOC).

*The age of a developing conceptus can be measured either from the estimated day of fertilization (fertilization age) or from the day of the last normal menstrual period (LNMP age). In this book, age is presented as the fertilization age.

2. The secondary oocyte completes meiosis II, forming a mature ovum and a second polar body. The nucleus of the mature ovum is now called the **female pronucleus**.
3. Male and female pronuclei fuse, forming a **zygote** (a new cell whose genotype is a combination of maternal and paternal chromosomes).
4. **Syngamy** is a term that describes the successful completion of fertilization, that is, the formation of a zygote. Syngamy occurs when the male and female pronuclei fuse and the cytoplasmic machinery for proper cell division exists.
5. The life span of a zygote is only a few hours because its existence terminates when the first cleavage division occurs.

II. CLEAVAGE AND BLASTOCYST FORMATION (FIGURE 2.1)

A. **Cleavage** is a series of **mitotic** divisions of the zygote where the plane of the first mitotic division passes through the area of the cell membrane where the polar bodies were previously extruded.

1. Cleavage in humans is **holoblastic**, which means the cells divide completely through their cytoplasm. Cleavage in humans is **asymmetrical**, which means the daughter cells are unequal in size (i.e., one cell gets more cytoplasm than the other) at least during the first few cell divisions. Cleavage in humans is **asynchronous**, which means only one cell will divide at a time; generally, the largest daughter cell will divide next at least during the first few cell divisions.
2. The process of cleavage eventually forms a **blastula** consisting of cells called **blastomeres.**

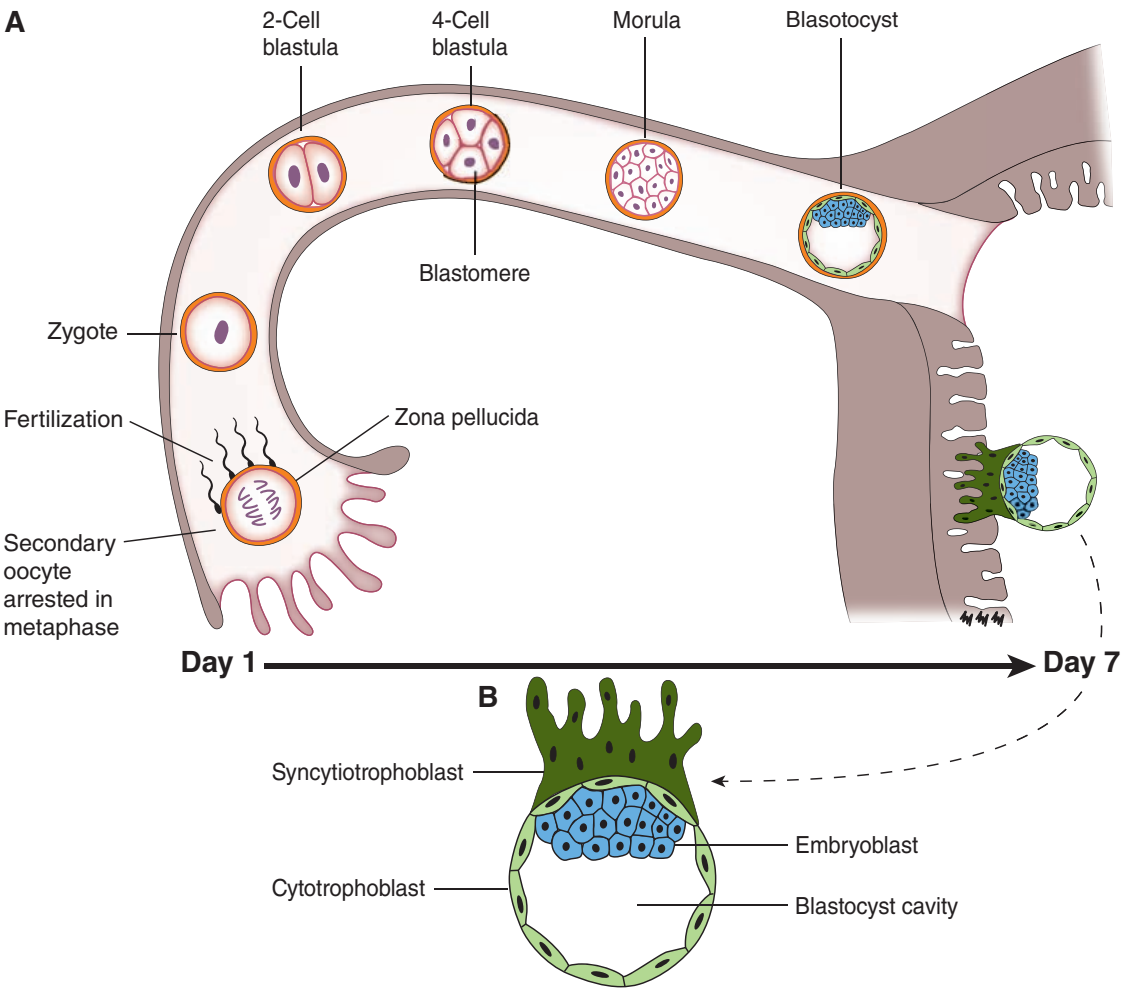

FIGURE 2.1. A. The stages of human development during week 1. **B.** A day 7 blastocyst.

3. A cluster of blastomeres (16–32 blastomeres) forms a **morula**.
4. Blastomeres are **totipotent** up to the eight-cell stage (i.e., each blastomere can form a complete embryo by itself). **Totipotency** refers to a stem cell that can differentiate into every cell within the organism, including extraembryonic tissues.

B. Blastocyst formation involves fluid secreted within the morula that forms the **blastocyst cavity**. The conceptus is now called a **blastocyst**.

1. The inner cell mass of the blastocyst is called the **embryoblast** (becomes the embryo). The embryoblast cells are **pluripotent**. **Pluripotency** refers to a stem cell that can differentiate into ectoderm, mesoderm, and endoderm.
2. The outer cell mass of the blastocyst is called the **trophoblast** (becomes the fetal portion of the placenta).

C. Zona pellucida degeneration occurs by day 4 after conception. The zona pellucida must degenerate for implantation to occur.

III. IMPLANTATION (FIGURE 2.1)

The blastocyst usually implants within the **posterior superior wall of the uterus** by day 7 after fertilization. Implantation occurs in the **functional layer of the endometrium** during the **progestational (secretory) phase** of the menstrual cycle. The trophoblast proliferates and differentiates into the **cytotrophoblast** and **syncytiotrophoblast**. Failure of implantation may involve immune rejection (graft-versus-host reaction) of the antigenic conceptus by the mother.

IV. CLINICAL CONSIDERATIONS

A. Ectopic tubal pregnancy (ETP)

1. ETP occurs when the blastocyst implants within the uterine tube due to **delayed transport**.
2. The **ampulla of the uterine tube** is the most common site of an ectopic pregnancy. The **rectouterine pouch (pouch of Douglas)** is a common site for an ectopic abdominal pregnancy.
3. ETP is most commonly seen in women with **endometriosis** or **pelvic inflammatory disease**.
4. ETP leads to uterine tube rupture and hemorrhage if surgical intervention (i.e., salpingectomy) is not performed.
5. ETP presents with **abnormal uterine bleeding, unilateral pelvic pain, increased levels of human chorionic gonadotropin (hCG)** (but lower than originally expected with uterine implantation pregnancy), and a **massive first-trimester bleed**.
6. ETP must be differentially diagnosed from **appendicitis**, an **aborting intrauterine pregnancy**, or a **bleeding corpus luteum** of a normal intrauterine pregnancy.

B. Testicular teratocarcinoma (TTC)

1. TTC is a germ cell neoplasm. In its early histologic stages, a TTC resembles a blastocyst with three primary germ layers and may be loosely referred to as "male pregnancy."
2. TTC contains well-differentiated cells and structures from each of the three primary germ layers: for example, colon glandular tissue (endoderm), cartilage (mesoderm), and squamous epithelium (ectoderm).
3. TTC also contains undifferentiated pluripotent stem cells called **embryonic carcinoma (EC) cells**.
4. TTC is associated with **elevated α-fetoprotein levels**.
5. TTC can be experimentally produced by implanting a blastocyst in an extrauterine site. The ability of blastocysts to form TTC suggests a relationship between the inner cell mass and EC cells. This relationship has been confirmed by isolation of cell lines from blastocysts called **embryonic stem (ES) cells**, which have biochemical characteristics remarkably similar to those of EC cells.

Study Questions for Chapter 2

1. A 20-year-old woman presents at the emergency department with severe abdominal pain on the right side with signs of internal bleeding. She indicated that she has been sexually active without contraception and missed her last menstrual period. Based on this information, which of the following disorders must be included as an option in the diagnosis?

(A) Ovarian cancer
(B) Appendicitis
(C) Normal pregnancy
(D) Ectopic tubal pregnancy
(E) Toxemia of pregnancy

2. When does a secondary oocyte complete its second meiotic division to become a mature ovum?

(A) At ovulation
(B) Before ovulation
(C) At fertilization
(D) At puberty
(E) Before birth

3. How soon after fertilization occurs within the uterine tube does the blastocyst begin implantation?

(A) Within minutes
(B) By 12 hours
(C) By day 1
(D) By day 2
(E) By day 7

4. Where does the blastocyst normally implant?

(A) Functional layer of the cervix
(B) Functional layer of the endometrium
(C) Basal layer of the endometrium
(D) Myometrium
(E) Perimetrium

5. Which of the following events is involved in the cleavage of the zygote during week 1 of development?

(A) A series of meiotic divisions forming blastomeres
(B) Production of highly differentiated blastomeres
(C) An increased cytoplasmic content of blastomeres
(D) An increase in size of blastomeres
(E) A decrease in size of blastomeres

6. Which of the following structures must degenerate for blastocyst implantation to occur?

(A) Endometrium in progestational phase
(B) Zona pellucida
(C) Syncytiotrophoblast
(D) Cytotrophoblast
(E) Functional layer of the endometrium

7. Which of the following is the origin of the mitochondrial DNA of all human adult cells?

(A) Paternal only
(B) Maternal only
(C) A combination of paternal and maternal
(D) Either paternal or maternal
(E) Unknown origin

8. Individual blastomeres were isolated from a blastula at the 4-cell stage. Each blastomere was cultured in vitro to the blastocyst stage and individually implanted into four pseudopregnant foster mothers. Which of the following would you expect to observe 9 months later?

(A) Birth of one baby
(B) Birth of four genetically different babies
(C) Birth of four genetically identical babies
(D) Birth of four grotesquely deformed babies
(E) No births

9. Embryonic carcinoma (EC) cells were isolated from a yellow-coated mouse with a teratocarcinoma. The EC cells were then microinjected into the inner cell mass of a blastocyst isolated from a black-coated mouse. The blastocyst was subsequently implanted into the uterus of a white-coated foster mouse. Which of the following would be observed after full-term pregnancy?

(A) A yellow-coated offspring
(B) A black-coated offspring
(C) A white-coated offspring
(D) A yellow- and black-coated offspring
(E) A yellow- and white-coated offspring

10. In oogenesis, which of the following events occurs immediately following the completions of meiosis II?

(A) Degeneration of the zona pellucida
(B) Sperm penetration of the corona radiata
(C) Formation of a female pronucleus
(D) Appearance of the blastocyst
(E) Completion of cleavage

Answers and Explanations

1. **D.** Ectopic tubal pregnancy must always be an option in the diagnosis when a woman in her reproductive years presents with such symptoms. Ninety percent of ectopic implantations occur in the uterine tube. Ectopic tubal pregnancies result in rupture of the uterine tube and internal hemorrhage, which presents a major threat to the woman's life. The uterine tube and embryo must be surgically removed. The symptoms may sometimes be confused with appendicitis.
2. **C.** At ovulation, a secondary oocyte begins meiosis II, but this division is arrested at metaphase. The secondary oocyte will remain arrested in metaphase until a sperm penetrates it at fertilization. Therefore, the term "mature ovum'" is somewhat of a misnomer because it is a secondary oocyte that is fertilized, and, once fertilized, the new diploid cell is known as a zygote. If fertilization does not occur, the secondary oocyte degenerates.
3. **E.** The blastocyst begins implantation by day 7 after fertilization.
4. **B.** The blastocyst implants in the functional layer of the uterine endometrium. The uterus is composed of the perimetrium, myometrium, and endometrium. Two layers are identified within the endometrium: (1) the functional layer, which is sloughed off at menstruation, and (2) the basal layer, which is retained at menstruation and serves as the source of regeneration of the functional layer. During the progestational phase of the menstrual cycle, the functional layer undergoes dramatic changes; uterine glands enlarge and vascularity increases in preparation for blastocyst implantation.
5. **E.** Cleavage is a series of mitotic divisions by which the large amount of zygote cytoplasm is successively partitioned among the newly formed blastomeres. Although the number of blastomeres increases during cleavage, the size of individual blastomeres decreases until they resemble adult cells in size.
6. **B.** The zona pellucida must degenerate for implantation to occur. Early cleavage states of the blastula are surrounded by a zona pellucida, which prevents implantation in the uterine tube.
7. **B.** The mitochondrial DNA of all human adult cells is of maternal origin only. In human fertilization, the entire sperm enters the secondary oocyte cytoplasm. However, sperm mitochondria degenerate along with the sperm's tail. Therefore, only mitochondria present within the secondary oocyte (maternal) remain in the fertilized zygote.
8. **C.** This scenario would result in four genetically identical children. Blastomeres at the 4- to 8-cell stage are totipotent, that is, capable of forming an entire embryo. Since blastomeres arise by mitosis of the same cell (zygote), they are genetically identical. This phenomenon is important in explaining monozygotic (identical) twins. About 30% of monozygotic twins arise by early separation of blastomeres. The remaining 70% originate at the end of week 1 of development by a splitting of the inner cell mass.
9. **D.** This scenario would result in a yellow- and black-coated offspring. Because EC cells and inner cell mass cells have very similar biochemical characteristics, they readily mix with each other, and development proceeds unencumbered. Because the mixture contains cells with yellow-coat genotype and black-coat genotype, offspring with coats of two colors (yellow and black) will be produced. The offspring are known as mosaic mice.
10. **C.** The secondary oocyte is arrested in metaphase of meiosis II, and it will remain in this meiotic stage until fertilization occurs. Following fertilization, the secondary oocyte completes meiosis II, forming a mature ovum and a polar body. The nucleus of the mature ovum is called the female pronucleus, which fuses with the male pronucleus to form a zygote.

chapter 3

Week 2 of Human Development (Days 8–14)

I. FURTHER DEVELOPMENT OF THE EMBRYOBLAST (FIGURE 3.1)

During this period, the embryoblast differentiates into two distinct cellular layers: the dorsal **epiblast** layer (columnar cells) and the ventral **hypoblast** layer (cuboidal cells). The epiblast and hypoblast together form a flat, ovoid-shaped disk known as the **bilaminar embryonic disk**. Within the epiblast, clefts develop and eventually coalesce to form the **amniotic cavity**. Hypoblast cells migrate and line the inner surface of the cytotrophoblast to form the **exocoelomic membrane**, which delimits a space called the **exocoelomic cavity** (or **primitive yolk sac**). The primitive yolk sac is later called the **definitive yolk sac** when a portion of the exocoelomic cavity pinches off as an **exocoelomic cyst**. At the future site of the mouth, hypoblast cells become columnar shaped and fuse with epiblast cells to form a circular, midline thickening called the **prochordal plate**.

II. FURTHER DEVELOPMENT OF THE TROPHOBLAST (FIGURE 3.1)

A. Syncytiotrophoblast. The syncytiotrophoblast is the outer multinucleated zone of the trophoblast where no mitosis occurs (i.e., it arises from the cytotrophoblast). During this period, the syncytiotrophoblast continues its invasion of the endometrium, thereby eroding endometrial blood vessels and endometrial glands. Lacunae form within the syncytiotrophoblast and become filled with maternal blood and glandular secretions. In addition, endometrial stromal cells (**decidual cells**) at the site of implantation become filled with glycogen and lipids and also supply nutrients to the embryoblast. The isolated lacunae fuse to form a **lacunar network** through which maternal blood flows, thus establishing early **uteroplacental circulation**. Although a primitive circulation is established between the uterus and future placenta, the embryoblast receives its nutrition via **diffusion** only at this time.

B. Cytotrophoblast. The cytotrophoblast is mitotically active as new cytotrophoblastic cells migrate into the syncytiotrophoblast, thereby fueling the growth of the syncytiotrophoblast. In addition, cytotrophoblastic cells also produce local mounds called **primary chorionic villi** that bulge into the surrounding syncytiotrophoblast.

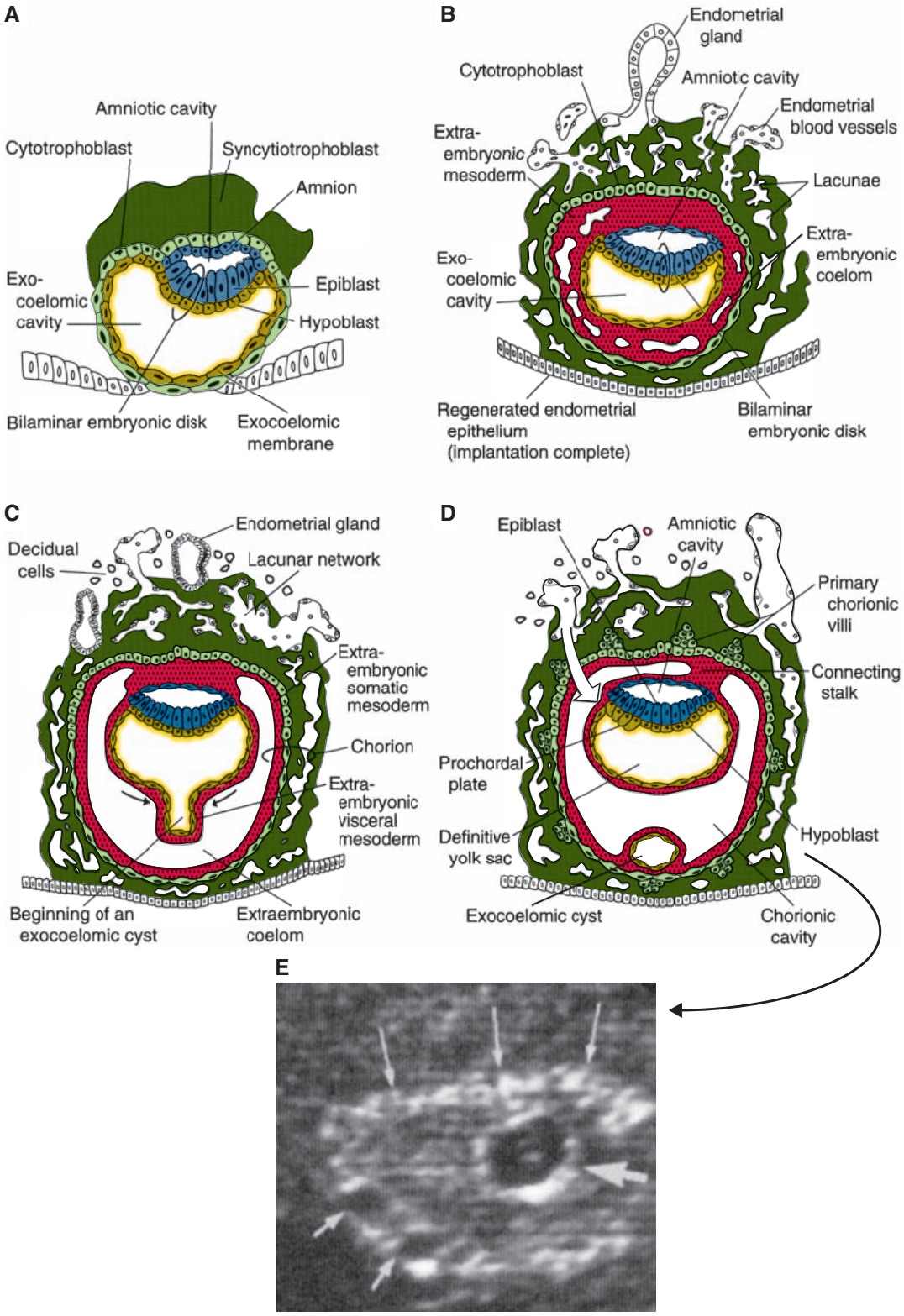

FIGURE 3.1. **A.** A **day 8 blastocyst** is shown partially implanted into the endometrium. Extraembryonic mesoderm (EEM) has not formed yet. **B.** A **day 12 blastocyst** is shown completely implanted within the endometrium, and epithelium has regenerated. This type of implantation is known as interstitial implantation. EEM begins to form. **C.** A **day 13 blastocyst.** A lacunar network forms, establishing an early uteroplacental circulation. An exocoelomic cyst begins to pinch off (*small arrows*). **D.** A **day 14 blastocyst.** The embryoblast can be described as two balloons (amniotic cavity and yolk sac) pressed together at the bilaminar embryonic disk. The *curved open arrow* indicates that the embryoblast receives maternal nutrients via diffusion. **E.** A sonogram at about week 3 shows a hyperechoic rim representing the chorion (*thick arrow*) surrounding the chorionic cavity (or gestational sac). Within the chorionic cavity, two tiny cystic areas (i.e., the amnion and yolk sac) separated by a thin echogenic line (i.e., embryonic disk) can be observed. Note the hyperechoic base of the endometrium (*long arrows*) and two endometrial cysts (*short arrows*).

III. DEVELOPMENT OF EXTRAEMBRYONIC MESODERM (FIGURE 3.1)

The extraembryonic mesoderm develops from the epiblast and consists of loosely arranged cells that fill the space between the exocoelomic membrane and the cytotrophoblast. Large spaces develop in the extraembryonic mesoderm and coalesce to form the **extraembryonic coelom**. The extraembryonic coelom divides the extraembryonic mesoderm into the **extraembryonic somatic mesoderm** and **extraembryonic visceral mesoderm**.

The extraembryonic somatic mesoderm lines the trophoblast, forms the connecting stalk, and covers the amnion. The extraembryonic visceral mesoderm covers the yolk sac. As soon as the extraembryonic somatic mesoderm and extraembryonic visceral mesoderm form, one can delineate the **chorion,** which consists of the extraembryonic somatic mesoderm, cytotrophoblast, and syncytiotrophoblast. As the chorion is delineated, the extraembryonic coelom is now called the **chorionic cavity**. The conceptus is suspended by the **connecting stalk** within the chorionic cavity.

IV. CLINICAL CONSIDERATIONS

A. Human chorionic gonadotropin (hCG) is a glycoprotein **produced by the syncytiotrophoblast,** which stimulates the production of progesterone by the corpus luteum (i.e., maintains corpus luteum function). This is clinically significant because progesterone produced by the corpus luteum is essential for the maintenance of pregnancy until week 8. The placenta then takes over progesterone production. hCG can be assayed in **maternal blood at day 8** or **maternal urine at day 10** and is the basis of pregnancy testing. hCG is detectable throughout a pregnancy. **Low hCG values** may predict a spontaneous abortion or indicate an ectopic pregnancy. **Elevated hCG values** may indicate a multiple pregnancy, hydatidiform mole, or gestational trophoblastic neoplasia.

B. RU-486 (mifepristone; Mifeprex) initiates menstruation when taken within 8–10 weeks of the start of the last menstrual period. If implantation of a conceptus has occurred, the conceptus will be sloughed along with the endometrium. RU-486 is a **progesterone-receptor antagonist (blocker)** used in conjunction with **misoprostol (Cytotec; a prostaglandin E_1 [PGE_1] analogue)** and is 96% effective at terminating pregnancy.

C. Hydatidiform mole (complete or partial; Figure 3.2) represents an abnormal placenta characterized by marked enlargement of chorionic villi. A complete mole is distinguished from a partial mole by the amount of chorionic villous involvement. The hallmarks of a complete mole include gross, generalized edema of chorionic villi forming grape-like, transparent vesicles, hyperplastic proliferation of surrounding trophoblastic cells, and absence of an embryo/fetus. Clinical signs diagnostic of a mole include preeclampsia during

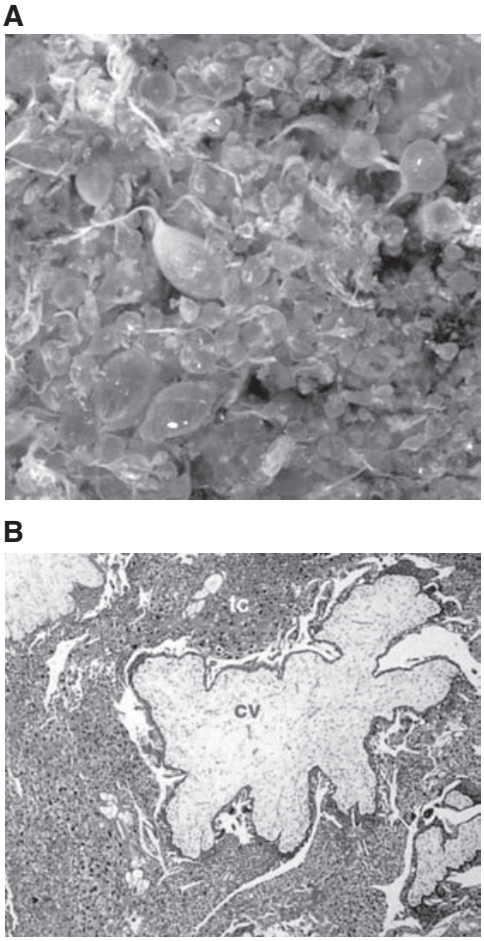

FIGURE 3.2. Hydatidiform mole.

the first trimester, elevated hCG levels (>100,000 mIU/mL), and an enlarged uterus with bleeding. About 3% to 5% of moles develop into gestational trophoblastic neoplasia, so follow-up visits after a mole is detected are essential. The photograph (Figure 3.2A) shows gross edema of the chorionic villi forming grape-like vesicles. The light micrograph (Figure 3.2B) shows edema of the chorionic villi (cv) surrounded by hyperplastic trophoblastic cells (tc).

D. Gestational trophoblastic neoplasia (GTN; choriocarcinoma; Figure 3.3) is a malignant tumor of the trophoblast that may occur following a normal or ectopic pregnancy, abortion, or hydatidiform mole. With a high degree of suspicion, elevated hCG levels are diagnostic. Nonmetastatic GTN (i.e., confined to the uterus) is the most common form of the neoplasia, and treatment is highly successful. However, the prognosis of metastatic GTN is poor if it spreads to the liver or brain. The photograph (Figure 3.3A) shows hemorrhagic nodules metastatic to the liver. This is due to the rapid proliferation of trophoblastic cells combined with marked propensity to invade blood vessels. The central portion of the lesion is hemorrhagic and necrotic, with only a thin rim of trophoblastic cells at the periphery. The light micrograph (Figure 3.3B) shows the distinctive alternating arrangement of mononuclear cytotrophoblastic cells (cy) and multinucleated syncytiotrophoblastic cells (sy).

E. Oncofetal antigens (Table 3.1) are cell surface antigens that normally appear only on embryonic cells but for unknown reasons are re-expressed in human malignant cells. Monoclonal antibodies directed against specific oncofetal antigens provide an avenue for cancer therapy.

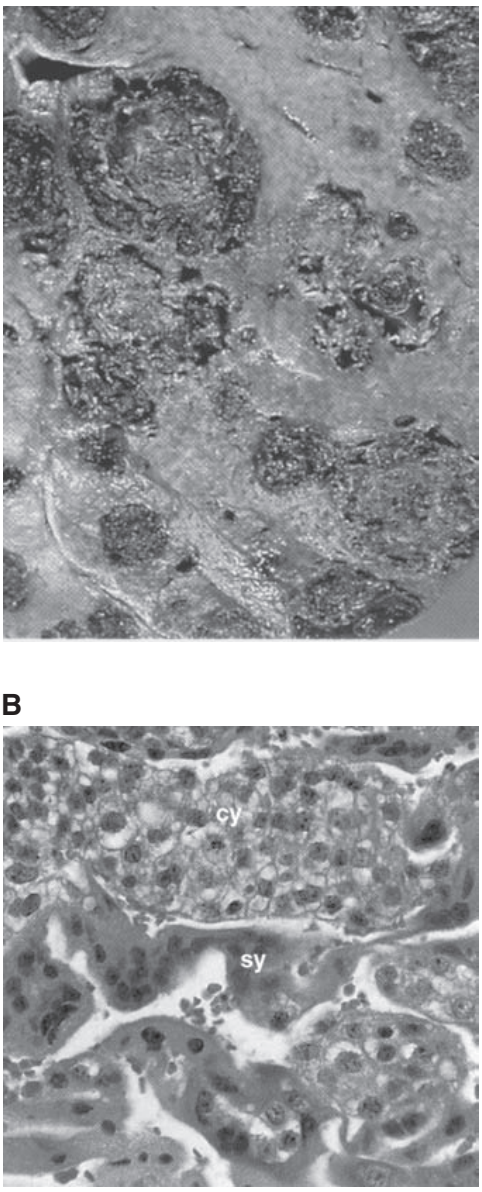

FIGURE 3.3. Gestational trophoblastic neoplasia.

table 3.1 Oncofetal Antigens and Tumor Markers

Antigen	Associated Tumor
α-Fetoprotein (AFP)	Hepatocellular carcinoma, germ cell neoplasms, yolk sac or endodermal sinus tumors of the testicle or ovary
α-1-Antitrypsin (AAT)	Hepatocellular carcinoma, yolk sac or endodermal sinus tumors of the testicle or ovary
Carcinoembryonic antigen (CEA)	Colorectal cancer, pancreatic cancer, breast cancer, and small cell cancer of the lung; bad prognostic sign if elevated preoperatively
β_2-Microglobulin	Multiple myeloma (excellent prognostic factor), light chains in urine (Bence Jones protein)
CA 125	Surface-derived ovarian cancer
CA 15-3	Breast cancer
CA 19-9	Pancreatic cancer (excellent marker)
Neuron-specific enolase (NSE)	Small cell carcinoma of the lung, seminoma, neuroblastoma
Prostate-specific antigen (PSA)	Prostate cancer
Human chorionic gonadotropin (hCG)	Trophoblastic tumors, hydatidiform mole (benign), choriocarcinoma (malignant)
Bombesin	Small cell carcinoma of the lung, neuroblastoma
Lactate dehydrogenase (LDH)	Hodgkin disease

CA, cancer antigen.

Study Questions for Chapter 3

1. Which of the following components plays the most active role in invading the endometrium during blastocyst implantation?

(A) Epiblast
(B) Syncytiotrophoblast
(C) Hypoblast
(D) Extraembryonic somatic mesoderm
(E) Extraembryonic visceral mesoderm

2. Between which two layers is the extraembryonic mesoderm located?

(A) Epiblast and hypoblast
(B) Syncytiotrophoblast and cytotrophoblast
(C) Syncytiotrophoblast and endometrium
(D) Exocoelomic membrane and syncytiotrophoblast
(E) Exocoelomic membrane and cytotrophoblast

3. During week 2 of development, the embryoblast receives its nutrients via

(A) diffusion
(B) osmosis
(C) reverse osmosis
(D) fetal capillaries
(E) yolk sac nourishment

4. The prochordal plate marks the site of the future

(A) umbilical cord
(B) heart
(C) mouth
(D) anus
(E) nose

5. Which of the following are components of the definitive chorion?

(A) Extraembryonic somatic mesoderm and epiblast
(B) Extraembryonic somatic mesoderm and cytotrophoblast
(C) Extraembryonic somatic mesoderm and syncytiotrophoblast
(D) Extraembryonic somatic mesoderm, cytotrophoblast, and syncytiotrophoblast
(E) Extraembryonic visceral mesoderm, cytotrophoblast, and syncytiotrophoblast

6. A 16-year-old girl presents on May 10 in obvious emotional distress. On questioning, she relates that on May 1 she experienced sexual intercourse for the first time, without using any means of birth control. Most of her anxiety stems from her fear of pregnancy. What should the physician do to alleviate her fear?

(A) Prescribe diazepam and wait to see if she misses her next menstrual period
(B) Use ultrasonography to document pregnancy
(C) Order a laboratory assay for serum hCG
(D) Order a laboratory assay for serum progesterone
(E) Prescribe diethylstilbestrol ("morning-after pill")

7. Carcinoembryonic antigen (CEA) is an oncofetal antigen that is generally associated with which one of the following tumors?

(A) Hepatoma
(B) Germ cell tumor
(C) Squamous cell carcinoma
(D) Colorectal carcinoma
(E) Teratocarcinoma

For each of Questions 8–13 concerning a 14-day-old blastocyst, select the most appropriate structure in the accompanying diagram.

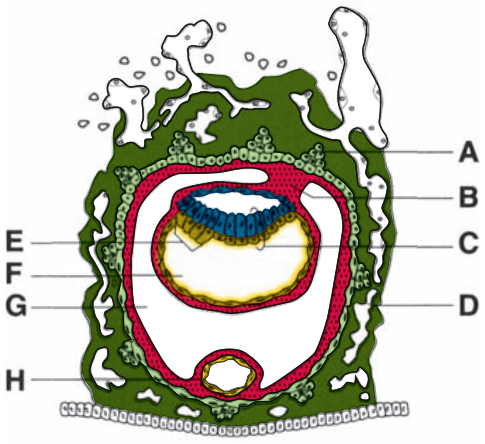

8. Future site of the mouth

9. Forms definitive structures found in the adult

10. Chorion

11. Chorionic cavity

12. Primary chorionic villi

13. Connecting stalk

14. A 42-year-old woman presents with complaints of severe headaches, blurred vision, slurred speech, and loss of muscle coordination. Her last pregnancy 5 years ago resulted in a hydatidiform mole. Laboratory results show a high hCG level. Which of the following conditions is a probable diagnosis?

(A) Vasa previa
(B) Placenta previa
(C) Succenturiate placenta
(D) Choriocarcinoma
(E) Membranous placenta

15. At what location does the amniotic cavity develop?

(A) Between the cytotrophoblast and syncytiotrophoblast
(B) Within the extraembryonic mesoderm
(C) Between the endoderm and mesoderm
(D) Within the hypoblast
(E) Within the epiblast

16. At the end of week 2 of development (day 14), what is the composition of the embryonic disk?

(A) Epiblast only
(B) Epiblast and hypoblast
(C) Ectoderm and endoderm
(D) Ectoderm, mesoderm, and endoderm
(E) Epiblast, mesoderm, and hypoblast

Answers and Explanations

1. **B.** The syncytiotrophoblast plays the most active role in invading the endometrium of the mother's uterus. During the invasion, endometrial blood vessels and endometrial glands are eroded and a lacunar network is formed.

2. **E.** The extraembryonic mesoderm is derived from the epiblast and is located between the exocoelomic membrane and the cytotrophoblast. The overall effect is to completely separate the embryoblast from the trophoblast, with the extraembryonic mesoderm serving as a conduit (connection) between them.

3. **A.** During week 2 of development, the embryoblast receives its nutrients from endometrial blood vessels, endometrial glands, and decidual cells via diffusion. Diffusion of nutrients does not pose a problem, given the small size of the blastocyst during week 2. Although the beginnings of a uteroplacental circulation are established during week 2, no blood vessels have yet formed in the extraembryonic mesoderm to carry nutrients directly to the embryoblast (this occurs in week 3).

4. **C.** The prochordal plate is a circular, midline thickening of hypoblast cells that are firmly attached to the overlying epiblast cells. The plate will eventually develop into a membrane called the oropharyngeal membrane at the site of the future mouth. It is interesting to note that at this early stage of development the cranial versus caudal region of the embryo is established by the prochordal plate, and since the prochordal plate is located in the midline, bilateral symmetry is also established.

5. **D.** The definitive chorion consists of three components: extraembryonic somatic mesoderm, cytotrophoblast, and syncytiotrophoblast. The chorion defines the chorionic cavity in which the embryoblast is suspended and is vital in the formation of the placenta.

6. **C.** Human chorionic gonadotropin (hCG) can be assayed in maternal serum at day 8 of development and in urine at day 10. If this teenager is pregnant, the blastocyst would be in week 2 of development (day 10). Laboratory assay of hCG in either the serum or urine can be completed; however, serum hCG might be more reliable. It is important to note that if she is pregnant, she will not miss a menstrual period until May 15, at which time the embryo will be entering week 3 of development.

7. **D.** Oncofetal antigens are normally expressed during embryonic development, remain unexpressed in normal adult cells, but are re-expressed on transformation to malignant neoplastic tissue. CEA is associated with colorectal carcinoma.

8. **E.** The prochordal plate indicates the site of the future mouth. At this early stage of development, the orientation of the embryo in the cranial versus caudal direction is established. The prochordal plate is a thickening of hypoblast cells that are firmly attached to the epiblast cells.

9. **C.** The bilaminar embryonic disk develops definitive adult structures after gastrulation occurs, as contrasted with the trophoblast, which is involved in placental formation.

10. **D.** The chorion consists of three layers—extraembryonic somatic mesoderm, cytotrophoblast, and syncytiotrophoblast. The chorion is vital in the formation of placenta.

11. **G.** The chorion forms the walls of the chorionic cavity in which the conceptus is suspended by the connecting stalk. Note that the inner lining of the chorionic cavity is extraembryonic mesoderm.

12. **A.** The cytotrophoblast is mitotically active, so that local mounds of cells (primary chorionic villi) form that bulge into the surrounding syncytiotrophoblast. As development continues,

primary chorionic villi form secondary chorionic villi and finally tertiary chorionic villi as part of placental formation.

13. B. The extraembryonic mesoderm can be thought of as initially forming in a continuous layer and then splitting as isolated cavities begin to appear everywhere except dorsally near the amniotic cavity and epiblast. When the isolated cavities coalesce, the extraembryonic coelom (or chorion cavity) and connecting stalk are formed.

14. D. After a hydatidiform mole, it is very important to assure that all the invasive trophoblastic tissue is removed. High levels of hCG are a good indicator of retained trophoblastic tissue because such tissue produces this hormone. In this case, the trophoblastic tissue has developed into a malignant choriocarcinoma and metastasized to the brain, causing her symptoms of headache, blurred vision, and so on.

15. E. The amniotic cavity develops within the epiblast, and it is a cavity that contains the embryo and amniotic fluid.

16. B. The embryoblast consists of the two distinct cell layers (epiblast and hypoblast) at the end of development week 2 (day 14) and forms the bilaminar embryonic disk.

chapter 4

Embryonic Period (Weeks 3–8)

I. GENERAL CONSIDERATIONS

A. By the end of the embryonic period, all major organ systems begin development, although functionality may be minimal.

B. During the embryonic period, the uteroplacental circulation cannot satisfy the increasing nutritional needs of the rapidly developing embryo, so development of the cardiovascular system is essential.

C. During the embryonic period, folding of the embryo occurs in two distinct planes. **Craniocaudal folding** progresses due to the growth of the central nervous system (CNS) and the amnion. **Lateral folding** progresses due to the growth of the somites, amnion, and other components of the lateral body wall.

D. Both the craniocaudal folding and lateral folding change the shape of the embryo from a two-dimensional disk to a three-dimensional cylinder.

E. By the end of week 8, the embryo has a distinct human appearance.

F. During the embryonic period, the basic segmentation of the human embryo in the craniocaudal direction is controlled by the **Hox (homeobox) complex** of genes.

G. The development of each individual organ system will be reviewed in forthcoming chapters. However, it is important to realize that all organ systems develop simultaneously during the embryonic period. In addition, embryogenesis proceeds at a slower pace in the female embryo compared with the male embryo due to the presence of the paternally imprinted X chromosome.

II. FURTHER DEVELOPMENT OF THE EMBRYOBLAST

A. Gastrulation (Figure 4.1)

1. Gastrulation is the process that establishes the three definitive germ layers of the embryo (**ectoderm, intraembryonic mesoderm,** and **endoderm**), forming a **trilaminar embryonic disk** by day 21 of development. These three germ layers give rise to all the tissues and organs of the adult.

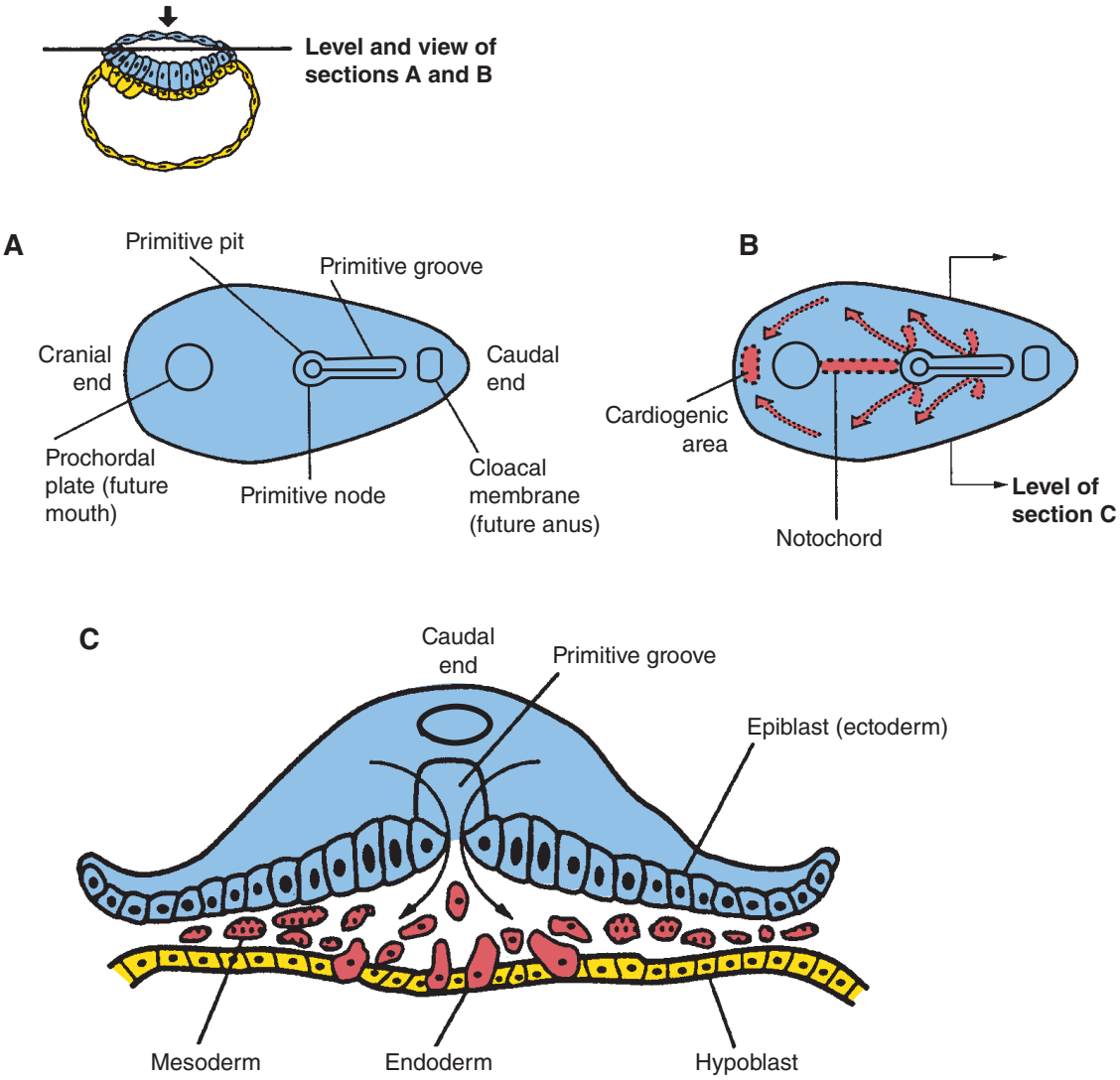

FIGURE 4.1. Schematic representation of gastrulation. Embryoblast at the upper left is for orientation. **A.** Dorsal view of the epiblast (blue). **B.** *Dotted arrows (red)* show the migration of cells through the primitive streak during gastrulation. **C.** Cross section showing the migration of cells that will form the intraembryonic mesoderm *(red)* and displace the hypoblast *(yellow)* to form the endoderm. Epiblast cells migrate to the primitive streak and invaginate into a space between the epiblast and hypoblast. Some of these migrating epiblast cells displace the hypoblast to form the definitive endoderm. The remainder of the epiblast cells migrates laterally, cranially, and along the midline to form the definitive intraembryonic mesoderm (e.g., cardiogenic area, notochord). After the formation of the endoderm and intraembryonic mesoderm, the epiblast is called the definitive ectoderm.

2. Gastrulation is heralded by the formation of the **primitive streak** and is caused by a proliferation of epiblast cells. The primitive streak consists of the **primitive groove, primitive node**, and **primitive pit**.
3. As early as the bilaminar and trilaminar stages of embryogenesis, the **left side/right side (L/R) axis determination** begins with the asymmetric activity of **sonic hedgehog protein (Shh)** only on the future left side since Shh activity is suppressed on the future right side by **activin**. In addition, the neurotransmitter **serotonin (5HT)** plays an important role in L/R axis determination.
4. The **cloacal membrane** is the future site of the anus where the epiblast and hypoblase cells fuse. The cloacal membrane is located caudal to the primitive streak.
5. The ectoderm, intraembryonic mesoderm, and endoderm of the trilaminar embryonic disk are all derived from the epiblast. The term *intraembryonic mesoderm* describes the germ layer that forms during week 3 (gastrulation), in contrast to the *extraembryonic mesoderm*, which forms during week 2.

6. Intraembryonic mesoderm forms various tissues and organs found in the adult, whereas extraembryonic mesoderm is involved in placenta formation. In this regard, later chapters do not use the term "intraembryonic mesoderm" when discussing tissue and organ development of the adult, but instead shorten the term to "mesoderm."

B. Changes involving intraembryonic mesoderm (Figure 4.2)

1. **Paraxial mesoderm** is a thick plate of mesoderm located on each side of the midline. Paraxial mesoderm becomes organized into segments known as **somitomeres**, which form in a craniocaudal sequence. **Somitomeres 1–7** do not form somites but contribute mesoderm to the pharyngeal arches. The remaining somitomeres further condense in a craniocaudal sequence to form **42–44 pairs of somites**. The first pair of somites forms on day 20, and new somites appear at a rate of 3 per day. The caudal-most somites eventually disappear to give a final count of approximately **35 pairs of somites**. The number of somites is one of the criteria for determining the age of the embryo. Somites further differentiate into the following components:
   a. **Sclerotome** forms the cartilage and bone components of the vertebral column.
   b. **Myotome** forms epimeric and hypomeric muscles.
   c. **Dermatome** forms dermis and subcutaneous area of skin.
2. **Intermediate mesoderm** is a longitudinal dorsal ridge of mesoderm located between the paraxial mesoderm and lateral mesoderm. This ridge develops into the **urogenital ridge**, which forms the future kidneys and gonads.
3. **Lateral mesoderm** is a thin plate of mesoderm located along the lateral sides of the embryo. Large spaces develop in the lateral mesoderm and coalesce to form the **intraembryonic coelom**. The intraembryonic coelom divides the lateral mesoderm into two layers:
   a. **Intraembryonic somatic mesoderm** (also called **somatopleure**)
   b. **Intraembryonic visceral mesoderm** (also called **visceropleure** or **splanchnopleure**)
4. **Notochord** is a solid cylinder of mesoderm extending in the midline of the trilaminar embryonic disk from the primitive node to the prochordal plate. It has a number of important functions, which include the following:
   a. The notochord induces the overlying ectoderm to differentiate into neuroectoderm to form the neural plate.
   b. The notochord induces the formation of the vertebral body of each of the vertebrae.
   c. The notochord forms the nucleus pulposus of each intervertebral disk.
5. **Cardiogenic region** is a horseshoe-shaped region of mesoderm located at the cranial end of the trilaminar embryonic disk rostral to the prochordal plate. This region forms the future heart.
6. Specific derivatives of mesoderm are indicated in Table 4.1.

C. Changes involving ectoderm.

The major change involving a specific portion of ectoderm is its induction by the underlying notochord to differentiate into neuroectoderm and neural crest cells, thereby forming the future nervous system. Specific derivatives of ectoderm are indicated in Table 4.1.

D. Changes involving endoderm.

Specific derivatives of endoderm are indicated in Table 4.1.

III. VASCULOGENESIS (DE NOVO BLOOD VESSEL FORMATION)

Vasculogenesis occurs in two general locations as follows.

A. In extraembryonic mesoderm:

1. Angiogenesis occurs first within extraembryonic visceral mesoderm around the yolk sac on day 17.
2. By day 21, angiogenesis extends into extraembryonic somatic mesoderm located around the connecting stalk to form the **umbilical vessels** and in secondary villi to form **tertiary chorionic villi.**

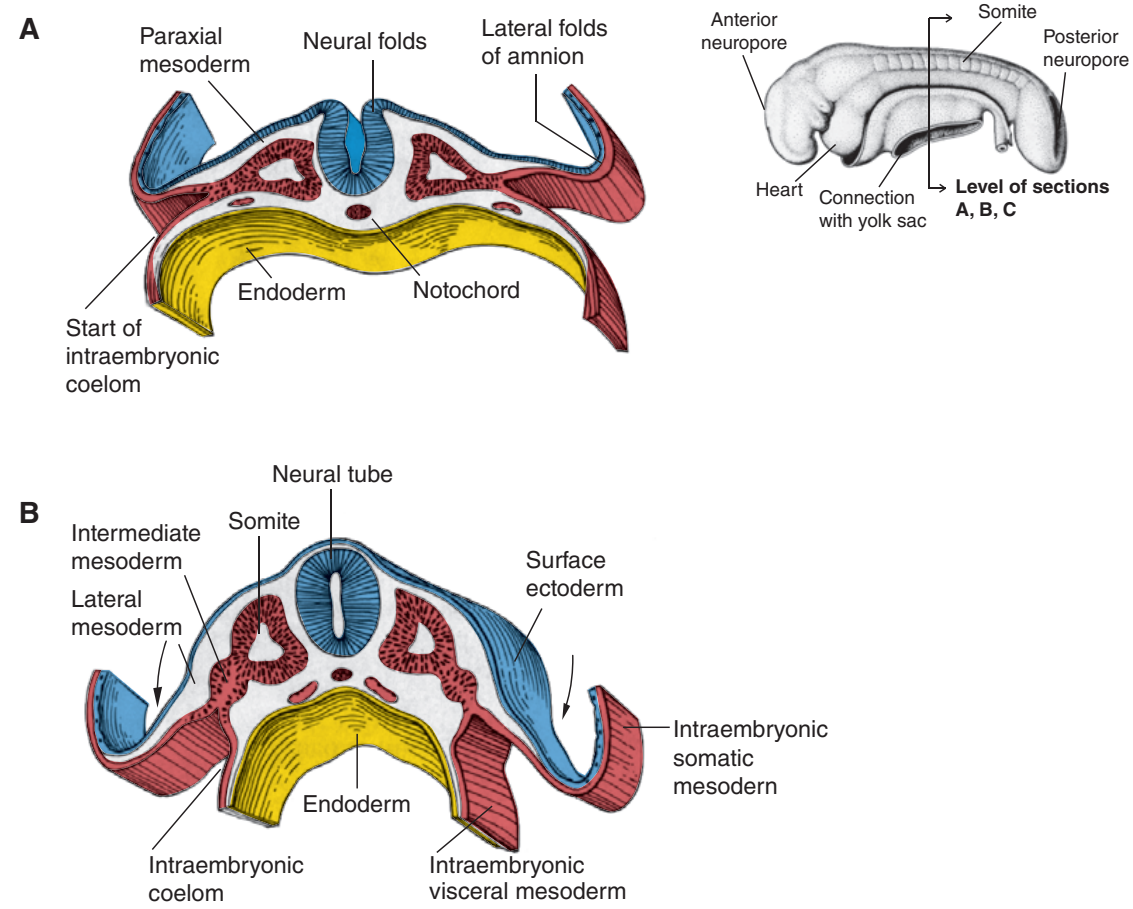

FIGURE 4.2. Schematic representation showing changes involving intraembryonic mesoderm. Picture in the upper right is for orientation. **A.** Cross section at day 19. **B.** Cross section at day 21, with *arrows* indicating lateral folding of the embryo. **C.** Cross section showing differentiation of the somite. Ectoderm and neuroectoderm, blue; mesoderm, red; endoderm, yellow.

table 4.1 Germ Layer Derivatives

Ectoderm	Mesoderm	Endoderm
Epidermis, hair, nails, sweat and sebaceous glands Utricle, semicircular ducts, vestibular ganglion of CN VIII Saccule, cochlear duct (organ of Corti), spiral ganglion of CN VIII Olfactory placode, CN I Ameloblasts (enamel of teeth) Adenohypophysis Lens of eye Anterior epithelium of cornea Acinar cells of parotid gland Acinar cells of mammary gland Epithelial lining of: Lower anal canal Distal part of male urethra External auditory meatus	Muscle (smooth, cardiac, skeletal) Extraocular muscles, ciliary muscle of eye, iris stroma, ciliary body stroma Substantia propria of cornea, corneal endothelium, sclera, choroid Muscles of tongue (occipital somites) Pharyngeal arch muscles Laryngeal cartilages Connective tissue Dermis and subcutaneous layer of skin Bone and cartilage Dura mater Endothelium of blood and lymph vessels Red blood cells, white blood cells, microglia, and Kupffer cells Spleen Kidney Adrenal cortex Testes, epididymis, ductus deferens, seminal vesicle, ejaculatory duct Ovary, uterus, uterine tubes, superior 1/3 of vagina	Hepatocytes Principal and oxyphil cells of parathyroid Thyroid follicular cells thymus Epithelial reticular cells of thymus Acinar and islet cells of pancreas Acinar cells of submandibular and sublingual glands Epithelial lining of: Gastrointestinal tract Trachea, bronchii, lungs Biliary apparatus Urinary bladder, female urethra, most of male urethra Inferior 2/3 of vagina Auditory tube, middle ear cavity Crypts of palatine tonsils

Derivatives

Neuroectoderm

All neurons within brain and spinal cord
Retina, iris epithelium, ciliary body epithelium, optic nerve (CN II), optic chiasm, optic tract, dilator and sphincter pupillae muscles
Astrocytes, oligodendrocytes, ependymocytes, tanycytes, choroid plexus cells
Neurohypophysis
Pineal gland

Neural Crest

Cranial neural crest cells:
- Pharyngeal arch skeletal and connective tissue components
- Bones of neurocranium
- Pia and arachnoid
- Parafollicular (C) cells of thyroid
- Aorticopulmonary septum
- Odontoblasts (dentin of teeth)
- Sensory ganglia of CN V, CN VII, CN IX, CN X
- Ciliary (CN III), pterygopalatine (CN VII), submandibular (CN VII), and otic (CN IX) parasympathetic ganglia

Trunk neural crest cells:
- Melanocytes
- Schwann cells
- Chromaffin cells of adrenal medulla
- Dorsal root ganglia
- Sympathetic chain ganglia
- Prevertebral sympathetic ganglia
- Enteric parasympathetic ganglia of the gut (Meissner and Auerbach; CN X)
- Abdominal/pelvic cavity parasympathetic ganglia

CN, cranial nerve.

3. Angiogenesis occurs by a process by which extraembryonic mesoderm differentiates into **angioblasts**, which form clusters known as **angiogenic cell clusters**.
4. The angioblasts located at the periphery of angiogenic cell clusters give rise to **endothelial cells**, which fuse with each other to form small blood vessels.

B. In intraembryonic mesoderm:

1. Blood vessels form within the embryo by the same mechanism as in extraembryonic mesoderm.
2. Eventually, blood vessels formed in the extraembryonic mesoderm become continuous with blood vessels within the embryo, thereby establishing a blood vascular system between the embryo and placenta.

IV. HEMATOPOIESIS (BLOOD CELL FORMATION; FIGURE 4.3)

Hematopoiesis first occurs within the **extraembryonic visceral mesoderm around the yolk sac** during week 3 of development. During this process, angioblasts within the center of angiogenic cell clusters give rise to primitive blood cells. Beginning at week 5, hematopoiesis is taken over by a sequence of embryonic organs: **liver, thymus, spleen**, and **bone marrow**.

V. CLINICAL CONSIDERATIONS

A. Chordoma (CD) is a benign or malignant tumor that arises from remnants of the notochord. CD may be found either intracranially or in the sacral region and occurs more commonly in men late in adult life (age 50 years).

B. First missed menstrual period is usually the first indication of pregnancy. Week 3 of embryonic development coincides with the first missed menstrual period. Note that at this time the embryo has already undergone 2 weeks of development. It is crucial that the woman become aware of a pregnancy as soon as possible because the embryonic period is a period of high susceptibility to teratogens.

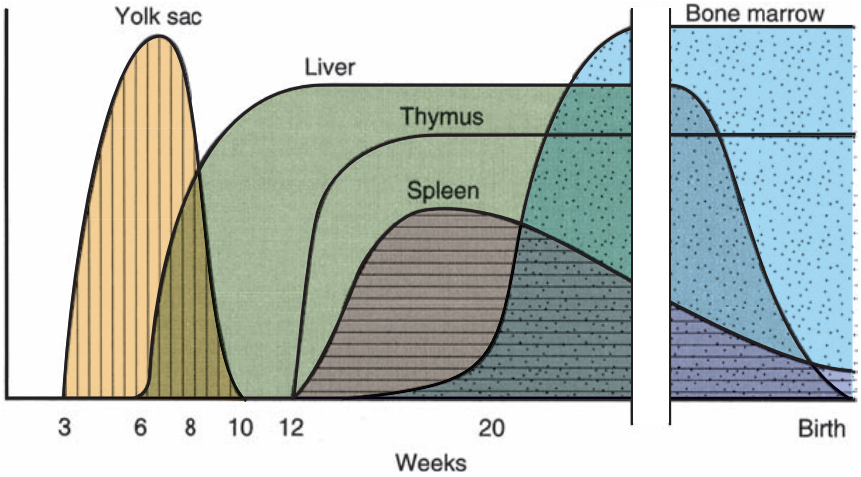

FIGURE 4.3. A schematic diagram showing the contribution of various organs to hematopoiesis during development. During the period of yolk sac hematopoiesis, the earliest **embryonic form** of hemoglobin is synthesized, called **hemoglobin** $\xi_2\varepsilon_2$**.** During the period of liver hematopoiesis, the **fetal form** of hemoglobin (**HbF**) is synthesized, called **hemoglobin** $\alpha_2\gamma_2$**.** During the period of bone marrow hematopoiesis (about week 30), the **adult form** of hemoglobin (**HbA**) is synthesized, called **hemoglobin** $\alpha_2\beta_2$**,** and gradually replaces hemoglobin $\alpha_2\gamma_2$**. Hemoglobin** $\alpha_2\gamma_2$ is the predominant form of hemoglobin during pregnancy because it has a higher affinity for oxygen than the adult form of hemoglobin and thereby "pulls" oxygen from the maternal blood into fetal blood.

C. Thalassemia syndromes are a heterogeneous group of genetic defects characterized by the lack or decreased synthesis of either the α-globin chain **(α-thalassemia)** or β-globin chain **(β-thalassemia)** of hemoglobin $\alpha_2\beta_2$. α-Thalassemia is an autosomal recessive genetic disorder most commonly caused by a deletion of the **HBA1 gene** and/or the **HBA2 gene** on **chromosome 16p13.3** for the **α_1-globin subunit of hemoglobin and α_2-globin subunit of hemoglobin**, respectively. β-Thalassemia is an autosomal recessive genetic disorder caused by >200 missense or frameshift mutations in the **HBB gene** on **chromosome 11p15.5** for the **β-globin subunit of hemoglobin**.

1. **Hydrops fetalis** is the most severe form of α-thalassemia and causes severe pallor, generalized edema, and massive hepatosplenomegaly and invariably leads to intrauterine fetal death.
2. **β-Thalassemia major (Cooley anemia)** is the most severe form of β-thalassemia and causes a severe, transfusion-dependent anemia. It is most common in Mediterranean countries and parts of Africa and Southeast Asia.

D. Hydroxyurea (a cytotoxic drug) promotes fetal hemoglobin (HbF) production by the reactivation of γ-chain synthesis. Hydroxyurea has been especially useful in the treatment of **sickle cell disease**, in which the presence of HbF counteracts the low oxygen affinity of HbS and inhibits the sickling process.

E. Sacrococcygeal teratoma (ST; Figure 4.4) is a tumor that arises from remnants of the primitive streak, which normally degenerates and disappears. ST is the most common germ cell tumor of childhood. ST is derived from pluripotent cells of the primitive streak and often contains various types of tissue (e.g., bone, nerve, hair). ST occurs more commonly in female infants and usually becomes malignant during infancy (must be surgically removed by age 6 months). The photograph (Figure 4.4) shows an infant with an ST.

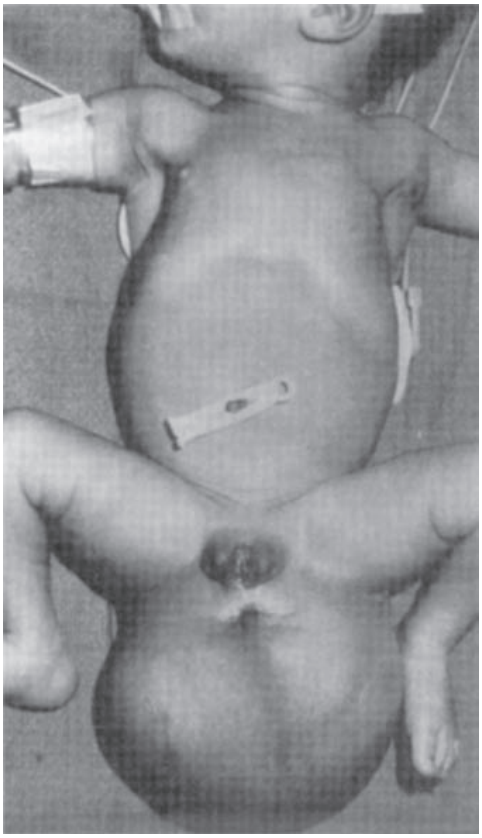

FIGURE 4.4. Sacrococcygeal teratoma.

F. Caudal dysplasia (sirenomelia; Figure 4.5) refers to a constellation of syndromes ranging from minor lesions of lower vertebrae to complete fusion of the lower limbs. Caudal dysplasia is caused by abnormal gastrulation, in which the migration of mesoderm is disturbed. It can be associated with various cranial anomalies:

1. **VATER,** which includes **v**ertebral defects, **a**nal atresia, **t**racheo**e**sophageal fistula, and **r**enal defects.
2. **VACTERL,** which is similar to VATER but also includes **cardiovascular** defects and upper **l**imb defects.

The photograph (Figure 4.5) shows an infant with caudal dysplasia (sirenomelia).

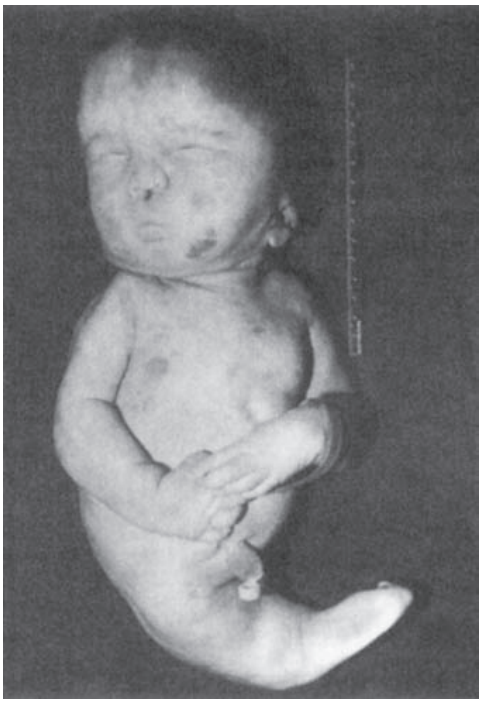

FIGURE 4.5. Caudal dysplasia (sirenomelia).

Study Questions for Chapter 4

1. Which germ layers are present at the end of week 3 of development (day 21)?

(A) Epiblast only
(B) Epiblast and hypoblast
(C) Ectoderm and endoderm
(D) Ectoderm, mesoderm, and endoderm
(E) Epiblast, mesoderm, and hypoblast

2. Which process establishes the three definitive germ layers?

(A) Neurulation
(B) Gastrulation
(C) Craniocaudal folding
(D) Lateral folding
(E) Angiogenesis

3. The first indication of gastrulation in the embryo is

(A) formation of the primitive streak
(B) formation of the notochord
(C) formation of the neural tube
(D) formation of extraembryonic mesoderm
(E) formation of tertiary chorionic villi

4. Somites may differentiate into which of the following?

(A) Urogenital ridge
(B) Kidneys
(C) Notochord
(D) Epimeric and hypomeric muscles
(E) Epithelial lining of the gastrointestinal tract

5. Intermediate mesoderm will give rise to the

(A) neural tube
(B) heart
(C) kidneys and gonads
(D) somites
(E) notochord

6. The developing embryo has a distinct human appearance by the end of

(A) week 4
(B) week 5
(C) week 6
(D) week 7
(E) week 8

7. The lateral mesoderm is divided into two distinct layers by the formation of the

(A) extraembryonic coelom
(B) intraembryonic coelom
(C) cardiogenic region
(D) notochord
(E) yolk sac

8. Very often the first indication a woman has that she is pregnant is a missed menstrual period. In which week of embryonic development will a woman experience her first missed menstrual period?

(A) Start of week 3
(B) Start of week 4
(C) Start of week 5
(D) Start of week 8
(E) End of week 8

9. A female newborn was found to have a large midline tumor in the lower sacral area, which was diagnosed as a sacrococcygeal tumor. Which of the following courses of treatment is recommended for this child?

(A) Immediate chemotherapy and radiation treatment
(B) Surgical removal by age 6 months
(C) Surgical removal at age 4–5 years
(D) Surgical removal at age 13–15 years
(E) No treatment because this tumor normally regresses with age

10. A woman has her pregnancy suddenly terminated due to intrauterine fetal death. At autopsy, the fetus shows severe pallor, generalized edema, and hepatosplenomegaly. Which of the following would you suspect?

(A) VATER
(B) β-Thalassemia minor
(C) β-Thalassemia major
(D) Hydrops fetalis
(E) VACTERL

11. The specialized group of mesenchymal cells that aggregate to form blood islands centrally and primitive blood vessels peripherally are called

(A) fibroblasts
(B) cardiac progenitor cells
(C) angioblasts
(D) myoblasts
(E) osteoblasts

12. The epiblast is capable of forming which of the following germ layers?

(A) Ectoderm only
(B) Ectoderm and mesoderm only
(C) Ectoderm and endoderm only
(D) Ectoderm, mesoderm, endoderm
(E) Mesoderm and endoderm only

13. A male newborn has a hemangioma on the left frontotemporal region of his face and scalp. The cells forming the hemangioma are derived from which of the following cell layers?

(A) Ectoderm only
(B) Mesoderm only
(C) Endoderm only
(D) Ectoderm and mesoderm
(E) Endoderm and mesoderm

14. Which structure is derived from the same embryonic primordium as the dorsal root ganglia?

(A) Gonads
(B) Kidney
(C) Pineal gland
(D) Liver
(E) Adrenal medulla

15. Which structure is derived from the same embryonic primordium as the kidney?

(A) Gonads
(B) Epidermis
(C) Pineal gland
(D) Liver
(E) Adrenal medulla

Answers and Explanations

1. **D.** During week 3 of development, the process of gastrulation, which establishes the three primary germ layers (ectoderm, intraembryonic mesoderm, and endoderm), occurs. The origin of all tissues and organs of the adult can be traced to one of these germ layers because these are whence they "germinate."

2. **B.** Gastrulation establishes the three primary germ layers during week 3 of development. Neurulation is the process by which neuroectoderm forms the neural plate, which eventually folds to form the neural tube.

3. **A.** The formation of the primitive streak on the dorsal surface of the bilaminar embryonic disk is the first indication of gastrulation.

4. **D.** Approximately 35 pairs of somites form. They are derived from a specific subdivision of intraembryonic mesoderm called paraxial mesoderm. Somites differentiate into the components called sclerotome (cartilage and bone of the vertebral column), myotome (epimeric and hypomeric muscle), and dermatome (dermis and subcutaneous area of skin).

5. **C.** Intermediate mesoderm is a subdivision of intraembryonic mesoderm that forms a longitudinal dorsal ridge called the urogenital ridge from which the kidneys and gonads develop.

6. **E.** The embryo starts the embryonic period as a two-dimensional disk and ends as a three-dimensional cylinder. This dramatic change in geometry is caused by formation of all the major organ systems. As the organ systems gradually develop during the embryonic period, the embryo appears more and more human-like; it has a distinct human appearance at the end of week 8.

7. **B.** The lateral mesoderm is a subdivision of intraembryonic mesoderm and initially is a solid plate of mesoderm. The intraembryonic coelom forms in the middle of the lateral mesoderm, thereby dividing it into the intraembryonic somatic mesoderm and intraembryonic visceral mesoderm.

8. **A.** Given a regular 28-day menstrual cycle, a woman who starts menses on, say, February 1 will ovulate on February 14, and the secondary oocyte will be fertilized, if she becomes pregnant, within 24 hours. So, the zygote undergoes week 1 of development from February 15 to 21. Week 2 of development is from February 22 to 28. On the next day, March 1, the woman would enter her next menstrual cycle if she were not pregnant, but because she is pregnant, she does not menstruate. Therefore, this first missed menstrual period corresponds with the start of week 3 of embryonic development. The embryonic period (week 3–week 8) is a time of high susceptibility to teratogens.

9. **B.** The preponderance of sacrococcygeal tumors is found in female newborns. Because these tumors develop from pluripotent cells of primitive streak origin, malignancy is of great concern, and the tumor should be surgically removed by age 6 months. Occasionally, these tumors may recur after surgery, demonstrating malignant properties.

10. **D.** Hydrops fetalis is the most severe form of α-thalassemia, and is a direct result of the lack or decreased synthesis of the α-globin chain of hemoglobin $\alpha_2\beta_2$.

11. **B.** The angioblasts are the mesenchymal cells that form blood vessels in embryonic development, as well as embryonic blood cells.

12. **D.** The epiblast is capable of forming all three germ layers (ectoderm, mesoderm, and endoderm) during gastrulation. Epiblast cells migrate to the primitive streak and invaginate into a space between the epiblast and hypoblast. Some of these epiblast cells displace the hypoblast to

form the definitive endoderm. Migrating epiblast cells also form the intraembryonic mesoderm. The remaining epiblast cells form the ectoderm.

13. B. A hemangioma is a vascular tumor that can be present at birth in which the abnormal proliferation of blood vessels leads to a mass resembling a neoplasm. Hemangiomas are mesodermal in origin, in that they are formed by embryonic blood cells and the vascular endothelium formed by angioblasts.

14. E. Both the chromaffin cells of the adrenal medulla and the dorsal root ganglia are derived from neural crest cells.

15. A. Both the kidneys and the gonads are derived from intermediate mesoderm. This longitudinal dorsal ridge of mesoderm forms the gonadal ridge, which is involved with the formation of the future kidneys and gonads.

chapter 5

Cardiovascular System

I. FORMATION OF HEART TUBE (FIGURE 5.1)

A. Lateral plate mesoderm located at the cephalic area of the embryo splits into a somatic layer and splanchnic layer, thus forming the **pericardial cavity**.

B. **Precardiac mesoderm** preferentially migrates into the splanchnic layer and forms the **heart-forming regions (HFRs)**.

C. As lateral folding of the embryo occurs, the HFRs fuse in the midline and form a continuous sheet of mesoderm.

D. Hypertrophied foregut endoderm secretes **vascular endothelial growth factor (VEGF)**, which induces the sheet of mesoderm to form discontinuous vascular channels that remodel into a single **endocardial tube (endocardium)**.

E. Mesoderm around the endocardium forms the **myocardium**, which secretes a layer of extracellular matrix proteins called **cardiac jelly**.

F. Mesoderm that migrates from the coelomic wall near the liver into the cardiac region forms the **epicardium**.

II. PRIMITIVE HEART TUBE DILATIONS (FIGURE 5.2)

A. Five dilations appear along the length of the tube, namely, the **truncus arteriosus, bulbus cordis, primitive ventricle, primitive atrium**, and **sinus venosus.**

B. These five dilations undergo **dextral looping** and develop into the adult structures of the heart.

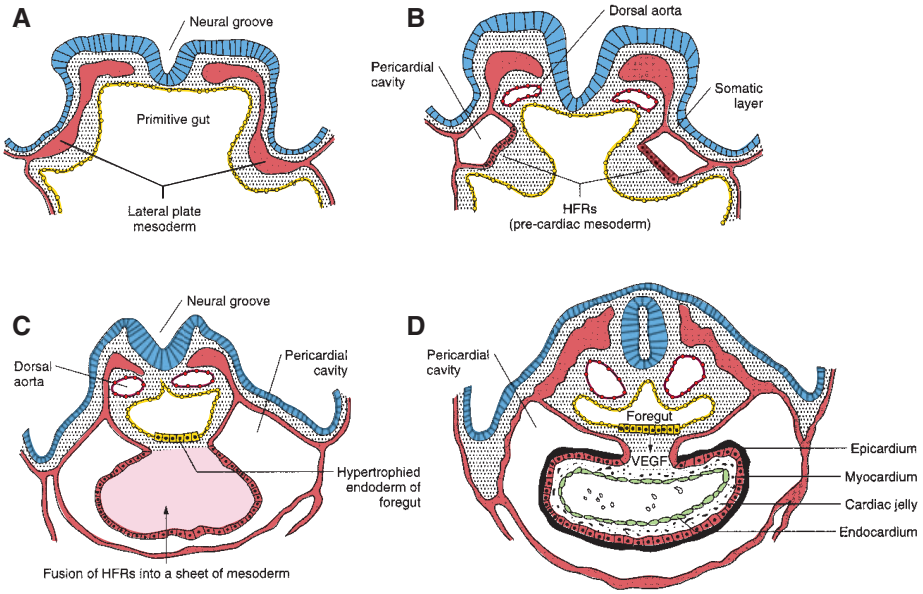

FIGURE 5.1. Schematic diagrams depict cross sections of an embryo at the level of the developing heart. **A.** Formation of lateral plate mesoderm. **B.** Splitting of lateral plate mesoderm. **C.** Fusion of heart-forming regions (HFRs) in the midline into a sheet of mesoderm. **D.** Vascular endothelial growth factor (VEGF) induction of single endocardial tube. Neuroectoderm and ectoderm, blue; mesoderm, red; endoderm, yellow; epicardium, black; and endocardium, green.

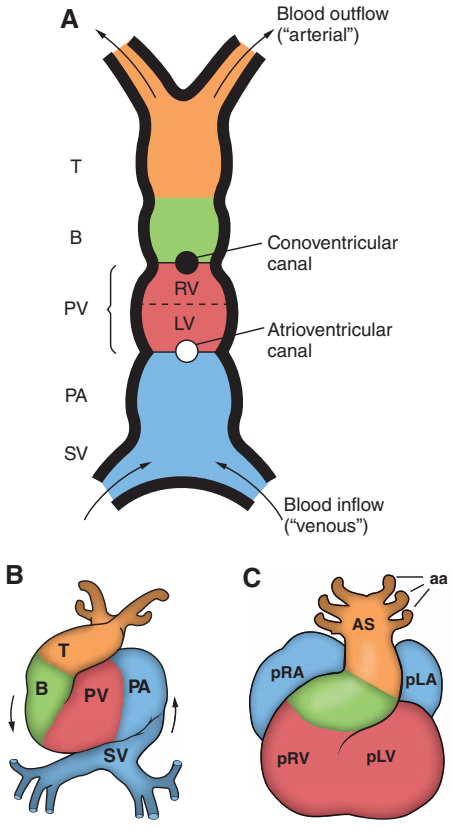

Embryonic Dilation	Adult Structure
Truncus asteriosus (T)	Aorta Pulmonary trunk
Bulbus cordis (B)	Smooth part of right ventricle **(conus arteriosus)** Smooth part of left ventricle **(aortic vestibule)**
Primitive ventricle (PV)	Trabeculated part of right ventricle (RV) Trabeculated part of left ventricle (LV)
Primitive atrium (PA)	Trabeculated part of right atrium Trabeculated part of left atrium
Sinus venosus (SV)	Smooth part of right atrium **(sinus venarum)**[a] Coronary sinus Oblique vein of left atrium

[a] The smooth part of the left atrium is formed by incorporation of parts of the **pulmonary veins** into the atrial wall. The junction of the trabeculated and smooth part of the right atrium is called the **crista terminalis**.

FIGURE 5.2. Schematic diagrams depict the primitive heart tube and its five dilations. **A.** At 22 days. Note the location of the atrioventricular canal and conoventricular canal. *Arrows* show the direction of blood flow from the "venous" blood inflow at the sinus venosus to the "arterial" blood outflow at the truncus arteriosus. Note that "venous" blood inflow enters the left ventricle (LV) before it enters the right ventricle (RV). **B.** At 26 days. Note that the straight heart tube begins dextral looping (*curved arrows*). T = truncus arteriosus; B = bulbus cordis; PV = primitive ventricle; PA = primitive atrium; SV = sinus venosus. **C.** At 30–35 days. Dextral looping is complete, and the four primitive heart chambers are apparent. aa = aortic arches; AS = aortic sac; pRA = primitive right atrium; pRV = primitive right ventricle; pLA = primitive left atrium; pLV = primitive left ventricle.

III. THE AORTICOPULMONARY SEPTUM (FIGURE 5.3)

A. Formation. Neural crest cells migrate from the hindbrain region through pharyngeal arches 3, 4, and 6 and invade both the **truncal ridges** and **bulbar ridges**. The truncal and bulbar ridges grow and twist around each other in a spiral fashion and fuse to form the aorticopulmonary (AP) septum. The AP septum divides the truncus arteriosus and bulbus cordis into the aorta and pulmonary trunk.

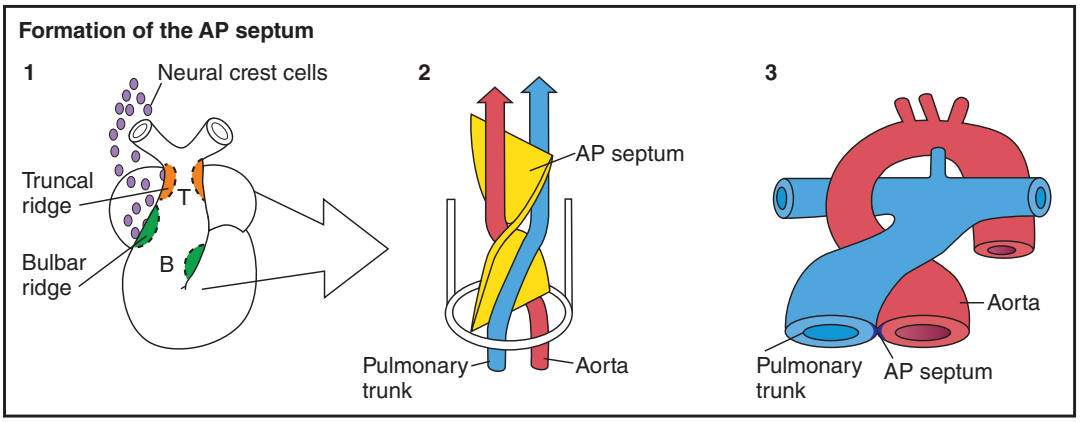

FIGURE 5.3. Formation of the aorticopulmonary (AP) septum. T = truncal ridges (*orange*), B = bulbar ridges (*green*).

B. Clinical considerations

1. **Persistent truncus arteriosus (PTA; Figure 5.4)** is caused by abnormal neural crest cell migration such that only *partial* development of the AP septum occurs. PTA results in a condition in which one large vessel leaves the heart and receives blood from both the right and left ventricles. PTA is usually accompanied by a membranous ventricular septal defect (VSD) and is associated clinically with **marked cyanosis (right–left shunting of blood)**. Figure 5.4 shows PTA. *Arrows* indicate the direction of blood flow.

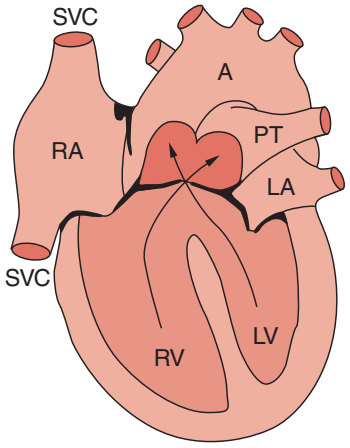

FIGURE 5.4. Persistent truncus arteriosus. SVC = superior vena cava; RA = right atrium; IVC = inferior vena cava; RV = right ventricle; LV = left ventricle; A = aorta; PT = pulmonary trunk; LA = left atrium.

2. **D-Transposition of the great arteries (complete; Figure 5.5)** is caused by abnormal neural crest cell migration such that *nonspiral* development of the AP septum occurs. D-Transposition results in a condition in which the aorta arises abnormally from the right ventricle and the pulmonary trunk arises abnormally from the left ventricle; hence the systemic and pulmonary circulations are *completely* separated from each other. It is incompatible with life unless an accompanying shunt exists, like a VSD, patent foramen ovale, or patent ductus arteriosus. It is associated clinically with **marked cyanosis (right–left shunting of blood)**. Figure 5.5A shows D-transposition of the great arteries (complete). *Arrows* indicate the direction of blood flow.

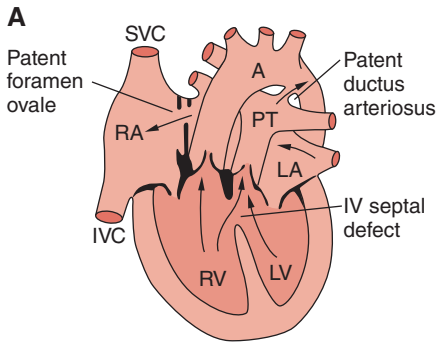

FIGURE 5.5. A. D-Transposition of the great arteries (complete). SVC = superior vena cava; RA = right atrium; IVC = inferior vena cava; RV = right ventricle; LV = left ventricle; A = aorta; PT = pulmonary trunk; LA = left atrium; IV = interventricular; P = pulmonary artery.

The MRI (Figure 5.5B) shows the ascending aorta (A) abnormally positioned anterior to the pulmonary artery (P). The ascending aorta is normally positioned posterior and to the right of the pulmonary artery at the level of the semilunar valves.

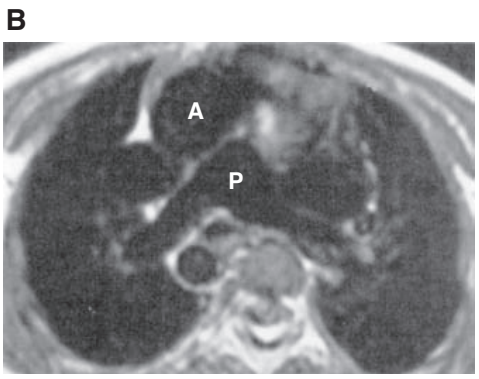

FIGURE 5.5. **B.** MRI.

3. **L-Transposition of the great vessels (corrected; Figure 5.6)** is characterized by the transposition of the aorta and pulmonary trunk along with "inverted" ventricles such that the anatomical right ventricle lies on the left side and the anatomical left ventricle lies on the right side. These two major deviations offset one another such that the blood flow pattern is normal. Figure 5.6 shows L-transposition of the great arteries (corrected).

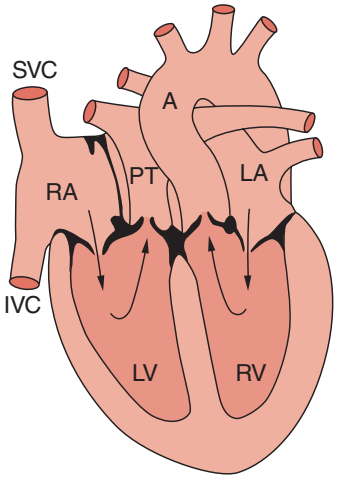

FIGURE 5.6. L-Transposition of the great arteries (*corrected*). *Arrows* indicate the direction of blood flow. SVC = superior vena cava; RA = right atrium; IVC = inferior vena cava; RV = right ventricle; LV = left ventricle; A = aorta; PT = pulmonary trunk; LA = left atrium.

4. **Tetralogy of Fallot (TF; Figure 5.7)** is caused by an abnormal neural crest cell migration such that a *skewed* development of the AP septum occurs. TF results in a condition in which the pulmonary trunk exhibits a small diameter and the aorta exhibits a large diameter. TF is characterized by four classic malformations: **pulmonary stenosis, right ventricular hypertrophy, overriding aorta,** and **ventricular septal defect,** giving the mnemonic **PROVE**. TF is associated clinically with **marked cyanosis (right–left shunting of blood)**, whereby the clinical consequences depend primarily on the severity of the pulmonary stenosis. Figure 5.7A shows

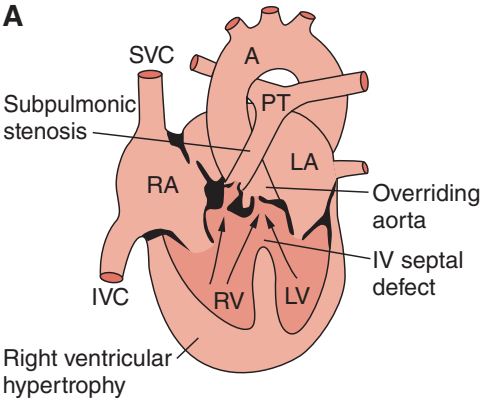

FIGURE 5.7. Tetralogy of Fallot. **A.** *Arrows* indicate the direction of blood flow. SVC = superior vena cava; RA = right atrium; IVC = inferior vena cava; RV = right ventricle; LV = left ventricle; A = aorta; PT = pulmonary trunk; LA = left atrium; IV = interventricular.

TF. The MRI (Figure 5.7B) shows the small right pulmonary artery (R) and the larger but still diminutive left pulmonary artery (L). Note also the very large diameter of the aortic arch (A).

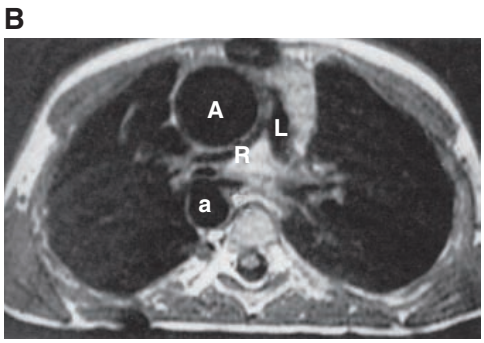

FIGURE 5.7. B. MRI. R = right pulmonary artery; L = left pulmonary artery; A = aortic arch; a = descending aorta.

IV. THE ATRIAL SEPTUM (FIGURE 5.8)

A. Formation

1. The crescent-shaped **septum primum** forms in the roof of the primitive atrium and grows toward the atrioventricular (AV) cushions in the AV canal.
2. The **foramen primum** forms between the free edge of the septum primum and the AV cushions. The foramen primum closes when the septum primum fuses with the AV cushions.
3. The **foramen secundum** forms in the center of the septum primum.
4. The crescent-shaped **septum secundum** forms to the right of the septum primum.
5. The **foramen ovale** is the opening between the upper and lower limbs of the septum secundum.
6. During embryonic life, blood is shunted from the right atrium to the left atrium via the foramen ovale.
7. Immediately after birth, functional closure of the foramen ovale is facilitated both by a **decrease in right atrial pressure** from occlusion of placental circulation and by an **increase in left atrial pressure** due to increased pulmonary venous return.
8. Later in life, the septum primum and septum secundum anatomically fuse to complete the formation of the atrial septum.

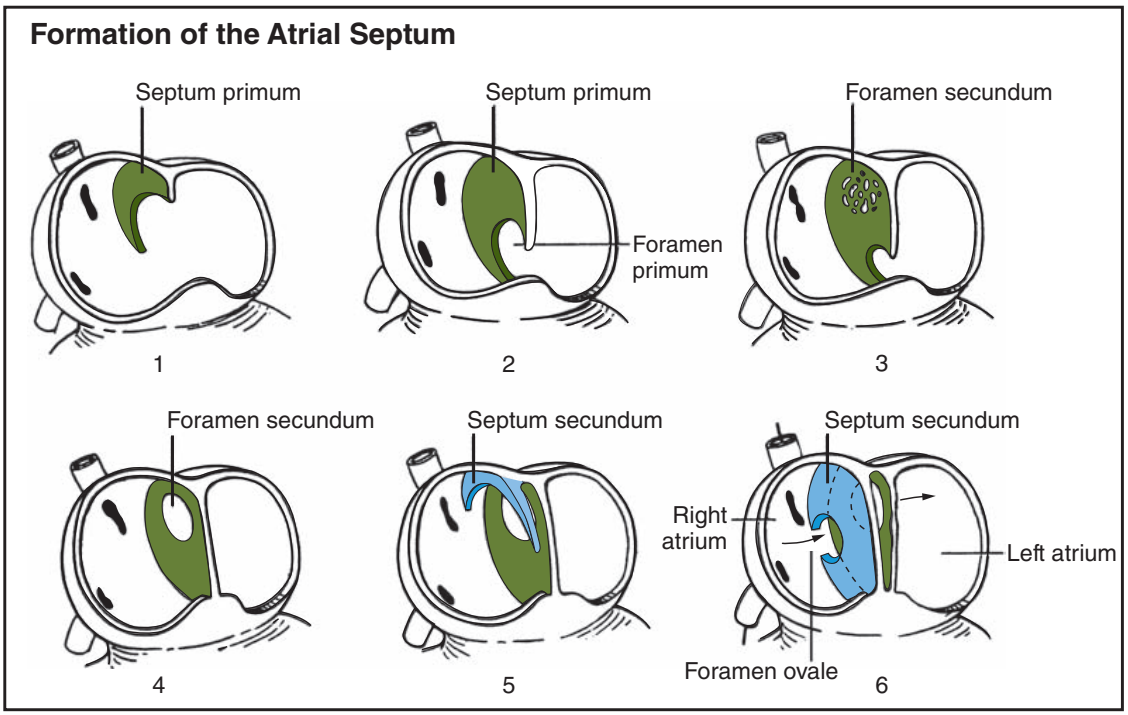

FIGURE 5.8. Formation of the atrial septum. The *arrows* in 6 indicate the direction of blood flow from the right atrium to the left atrium across the fully developed atrial septum. Septum primum = green, septum secundum = blue.

B. Clinical considerations: Atrial septal defects

1. **Probe patency of the foramen ovale** is caused by incomplete anatomic fusion of septum primum and septum secundum. It is present in approximately 25% of the population and is usually of no clinical importance.
2. **Premature closure of the foramen ovale** is closure of the foramen ovale during prenatal life. It results in hypertrophy of the right side of the heart and underdevelopment of the left side of the heart.
3. **Foramen secundum defect (Figure 5.9)** is caused by excessive resorption of septum primum, septum secundum, or both. This results in a condition in which there is an opening between the right and left atria. Some defects can be tolerated for a long time, with clinical symptoms manifesting as late as age 30 years. It is the most common clinically significant atrial septal defect (ASD). Figure 5.9A shows a foramen secundum defect. The AP radiograph (Figure 5.9B) shows cardiomegaly due to enlargement of the right atrium and right ventricle (left atrium and ventricle are generally normal sized), enlargement of the pulmonary artery (*arrow*), and increased pulmonary vascularity. The enlarged pulmonary arteries prevent the aorta from forming the normal left border of the heart (i.e., the aortic knob is small).

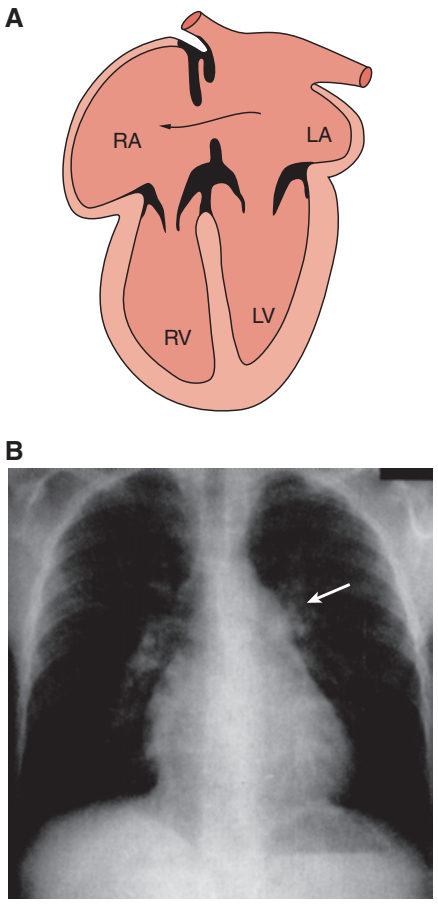

FIGURE 5.9. Foramen secundum defect. **A.** RA = right atrium; RV = right ventricle; LA = left atrium; LV = left ventricle. *Arrow* shows the direction of blood flow. **B.** AP radiograph.

4. **Common atrium (cor triloculare biventriculare; Figure 5.10)** is caused by the complete failure of septum primum and septum secundum to develop. This results in a condition in which there is formation of only one atrium. Figure 5.10 shows a common atrium defect.

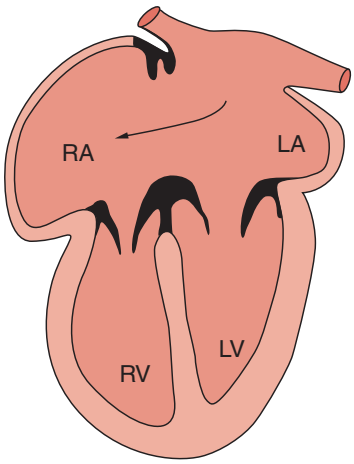

FIGURE 5.10. Common atrium. RA = right atrium; RV = right ventricle; LA = left atrium; LV = left ventricle. *Arrow* shows the direction of blood flow.

V. THE ATRIOVENTRICULAR SEPTUM (FIGURE 5.11)

A. Formation. The **dorsal atrioventricular (AV) cushion** and **ventral AV cushion** approach each other and fuse to form the AV septum. The AV septum partitions the AV canal into the right AV canal and left AV canal.

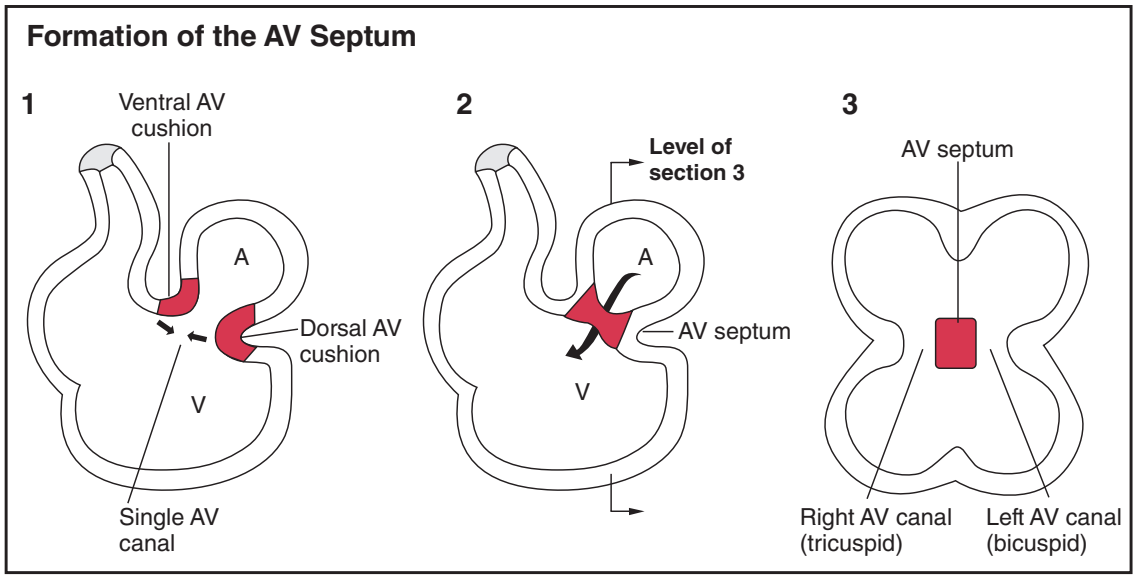

FIGURE 5.11. Formation of the atrioventricular (AV) septum. The AV septum partitions the atrioventricular canal. AV septum = red.

B. Clinical considerations

1. **Persistent common AV canal (Figure 5.12)** is caused by failure of fusion of the dorsal and ventral AV cushions. It results in a condition in which the common AV canal fails to partition into the right and left AV canals, so that a large opening exists in the center of the heart. Consequently, the tricuspid and bicuspid valves are represented by one valve (common AV valve) common to both sides of the heart. Two common hemodynamic abnormalities are found:
   a. **Left–right shunting** of blood from the left atrium to the right atrium causes an enlarged right atrium and right ventricle.
   b. **Mitral valve regurgitation** causes an enlarged left atrium and left ventricle.

   Figure 5.12 shows a persistent common AV canal defect. *Arrows* indicate the direction of blood flow.

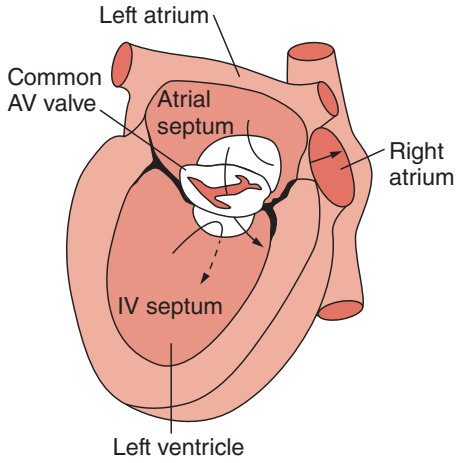

FIGURE 5.12. Persistent common atrioventricular (AV) canal. *Top arrow:* blood flows from left atrium to right atrium. *Middle arrow:* blood flows from the right and left atria to the left ventricle. *Bottom arrow:* blood flows from left ventricle to the right ventricle.

2. **Ebstein anomaly (Figure 5.13)** is caused by the failure of the posterior and septal leaflets of the tricuspid valve to attach normally to the annulus fibrosus; instead they are displaced inferiorly into the right ventricle. It results in a division of the right ventricle into a large, upper, "atrialized" portion and a small, lower, functional portion. There is a reduced amount of blood available to the pulmonary trunk due to the small, functional portion of the right ventricle. It is usually associated with an ASD and maternal lithium exposure. Figure 5.13A shows Ebstein anomaly. The AP radiograph (Figure 5.13B) shows massive cardiomegaly due to enlargement of the right atrium. The left cardiac contour is also abnormal because of displacement of the right ventricular outflow tract.

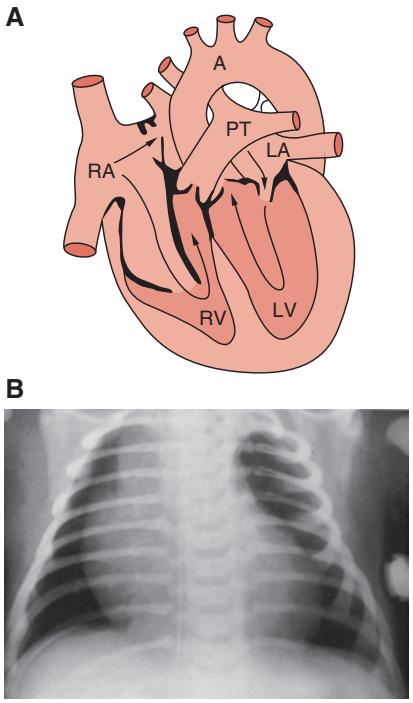

FIGURE 5.13. Ebstein anomaly. **A.** A = aorta; RA = right atrium; RV = right ventricle; LV = left ventricle; LA = left atrium; PT = pulmonary trunk. *Arrows* indicate the direction of blood flow. **B.** AP radiograph.

3. **Foramen primum defect (Figure 5.14)** is caused by a failure of the AV septum to fuse with the septum primum. It results in a failure of the foramen primum to close (patent foramen primum) and is generally accompanied by an abnormal mitral valve. Figure 5.14 shows a foramen primum defect.

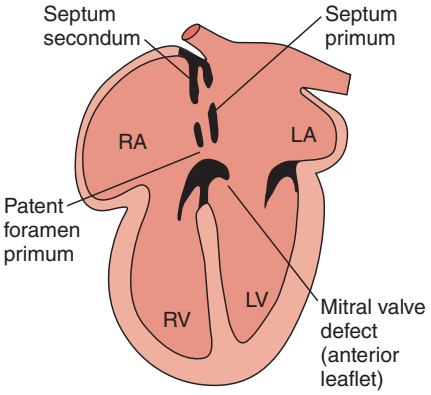

FIGURE 5.14. Foramen primum defect. RA = right atrium; RV = right ventricle; LA = left atrium; LV = left ventricle.

4. **Tricuspid atresia (hypoplastic right heart; Figure 5.15)** is caused by an insufficient amount of AV cushion tissue available for the formation of the tricuspid valve. It results in a complete agenesis of the tricuspid valve so that no communication between the right atrium and right ventricle exists. It is associated clinically with **marked cyanosis** and is always accompanied by the following: **patent foramen ovale, interventricular septum defect, overdeveloped left ventricle,** and **underdeveloped right ventricle**. Figure 5.15A

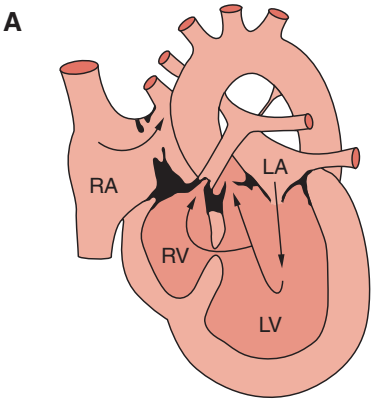

FIGURE 5.15. Tricuspid atresia. **A.** RA = right atrium; RV = right ventricle; LA = left atrium; LV = left ventricle. *Arrows* indicate the direction of blood flow.

shows a tricuspid atresia defect. The AP radiograph (Figure 5.15B) shows a normal-sized heart with a convex left cardiac contour.

B

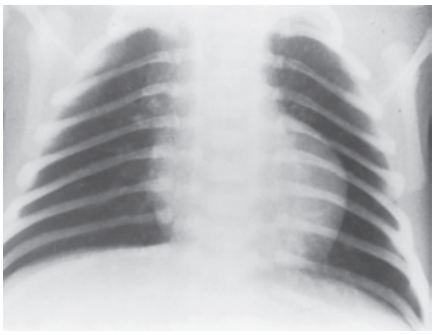

FIGURE 5.15. B. AP radiograph.

VI. THE INTERVENTRICULAR SEPTUM (FIGURE 5.16)

A. Formation

1. The **muscular interventricular (IV) septum** develops in the midline on the floor of the primitive ventricle and grows toward the fused AV cushions.
2. The **IV foramen** is located between the free edge of the muscular IV septum and the fused AV cushions.
3. The IV foramen is closed by the **membranous IV septum**.
4. The membranous IV septum forms by the proliferation and fusion of tissue from three sources: the **right bulbar ridge, left bulbar ridge**, and **AV cushions**.

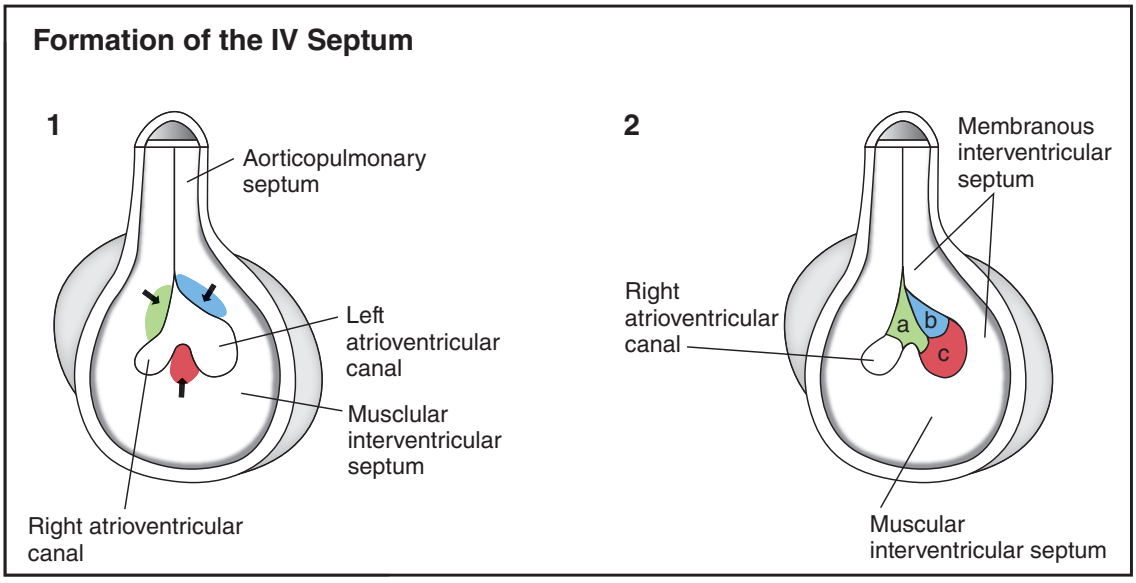

FIGURE 5.16. Formation of the interventricular (IV) septum. The IV septum partitions the primitive ventricle. The three sources of the membranous interventricular septum are indicated: a = right bulbar ridge (*green*); b = left bulbar ridge (*blue*); c = atrioventricular (AV) cushions (*red*).

B. Clinical considerations: IV septal defects (VSDs)

1. **Muscular VSD** is caused by single or multiple perforations in the muscular IV septum.
2. **Common ventricle (cor triloculare biatriatum)** is caused by failure of the membranous and muscular IV septa to form.

3. **Membranous VSD (Figure 5.17)** is caused by faulty fusion of the **right bulbar ridge, left bulbar ridge**, and **AV cushions**. It results in an opening between the right and left ventricles, which allows free flow of blood. A large VSD is initially associated with a **left–right shunting of blood,** increased pulmonary blood flow, and pulmonary hypertension. One of the secondary effects of a large VSD and its associated pulmonary hypertension is proliferation of the tunica intima and tunica media of pulmonary muscular arteries and arterioles, resulting in a narrowing of their lumen. Ultimately, pulmonary resistance becomes higher than systemic resistance and causes **right–left shunting of blood** and cyanosis. At this stage, the characteristic of the patient is called the "**Eisenmenger complex.**" This is an important concept that distinguishes a "**blue baby**" (cyanotic at birth) and a "**blue kid**" (late-onset cyanosis). A membranous VSD is the most common type of VSD. Figure 5.17A shows a membranous VSD. The left anterior oblique (LAO) ventriculograph (Figure 5.17B) demonstrates the flow of contrast material from the left ventricle (LV) through the membranous VSD defect into the right ventricle (RV).

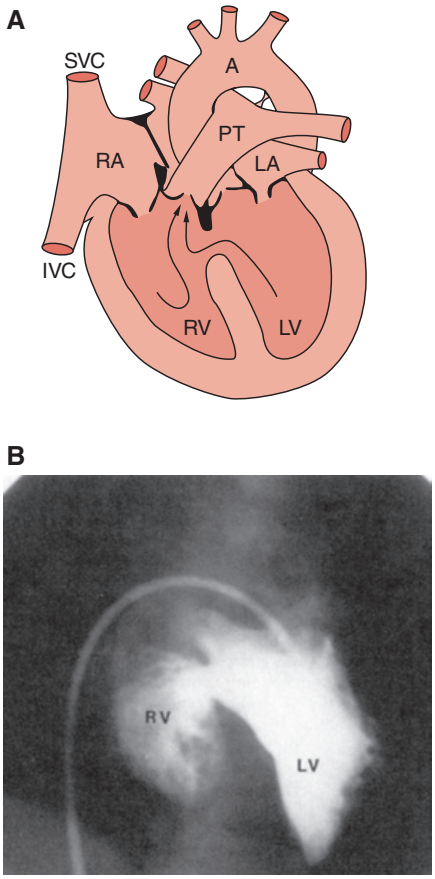

FIGURE 5.17. Membranous ventricular septal defect (VSD). SVC = superior vena cava; IVC = inferior vena cava; RA = right atrium; RV = right ventricle; LA = left atrium; LV = left ventricle; PT = pulmonary trunk; A = aorta. *Arrows* indicate the direction of blood flow. **B.** LAO ventriculograph.

VII. THE CONDUCTION SYSTEM OF THE HEART

A. At week 5, cardiac myocytes in the sinus venosus region of the primitive heart tube begin to undergo spontaneous electrical depolarizations at a *faster rate* than cardiac myocytes in other regions.

B. The sinus venous incorporates into the right atrium due to dextral looping. The fast-rate depolarizing cardiac myocytes in this area become the **sinoatrial (SA) node** and the **atrioventricular (AV) node**.

C. In the adult, the cardiac myocytes of the SA and AV nodes remain committed to a fast rate of electrical depolarizations instead of developing contractile properties.

D. As the atria and ventricles become electrically isolated by the formation of the **fibrous skeleton** of the heart, the **AV node** provides the *only* pathway for depolarizations to flow from the atria to ventricles.

E. The **AV bundle** or **bundle of His** develops from a ringlike cluster of cells found at the AV junction that specifically expresses the homeobox gene, ***msx-2***.

F. The **intramural network of Purkinje myocytes** have a distinct embryological origin (versus the bundle of His), in that Purkinje myocytes develop from already contractile cardiac myocytes within the myocardium and can therefore be considered as **modified cardiac myocytes**.

VIII. CORONARY ARTERIES

A. Progenitor stem cells from the liver migrate into the primitive heart tube and take residence beneath the epicardium.

B. These progenitor stem cells form vascular channels that grow toward the truncus arteriosus (future aorta) and form a **peritruncal capillary ring**. Only two of these capillaries survive, and these become the proximal portions of the right and left coronary arteries.

IX. DEVELOPMENT OF THE ARTERIAL SYSTEM (FIGURE 5.18)

A. General pattern

1. In the head and neck region, the arterial pattern develops mainly from six pairs of arteries (called **aortic arches**) that course through the pharyngeal arches.
2. The aortic arch arteries undergo a complex remodeling process that results in the adult arterial pattern.
3. In the rest of the body, the arterial patterns develop mainly from the **right and left dorsal aortae**.
4. The right and left dorsal aortae fuse to form the **dorsal aorta**, which then sprouts **posterolateral arteries, lateral arteries**, and **ventral arteries (vitelline and umbilical)**.

B. Clinical considerations. Most anomalies of the great arteries occur as a result of the persistence of parts of the aortic arch system that normally regress and the regression of parts that should normally persist.

1. **Abnormal origin of the right subclavian artery** occurs when right aortic arch 4 and the right dorsal aorta cranial to the seventh intersegmental artery abnormally regress. As development continues, the right subclavian artery lies on the left side just inferior to the left subclavian artery. The right subclavian artery must therefore cross the midline posterior to the trachea and esophagus to supply the right arm. This anomaly may constrict the trachea or esophagus. However, it is generally not clinically significant.
2. **Double aortic arch** occurs when an abnormal right aortic arch develops in addition to a left aortic arch due to persistence of the distal portion of the right dorsal aorta. This forms a vascular ring around the trachea and esophagus, which causes difficulties in breathing and swallowing.
3. **Right aortic arch** occurs when the entire right dorsal aorta abnormally persists and part of the left dorsal aorta regresses. The right aortic arch may pass anterior or posterior (retroesophageal right arch) to the esophagus and trachea. A retroesophageal right arch may cause difficulties in swallowing or breathing.
4. **Patent ductus arteriosus (PDA)** occurs when the ductus arteriosus (a connection between the left pulmonary artery and aorta) fails to close. The ductus arteriosus normally undergoes functional closure within a few hours after birth via smooth muscle contraction to ultimately form the **ligamentum arteriosum**. A patent ductus arteriosus causes a left → right shunting of oxygen-rich blood from the aorta back into the pulmonary circulation. This can be treated with prostaglandin synthesis inhibitors (e.g., indomethacin), which promote closure. PDA is very common in premature infants and maternal rubella infection. Clinical signs include a **harsh, machine-like, continuous murmur** in the upper left parasternal area.
5. **Postductal coarctation of the aorta** occurs when the aorta is abnormally constricted. A postductal coarctation is found distal to the origin of the left subclavian artery and inferior to the ductus arteriosus. It is clinically associated with increased blood pressure in the upper extremities, lack of pulse in femoral artery, high risk of both cerebral hemorrhage and bacterial endocarditis, and Turner syndrome. A **preductal coarctation of the aorta** in which the constriction is located superior to the ductus arteriosus occurs less commonly.

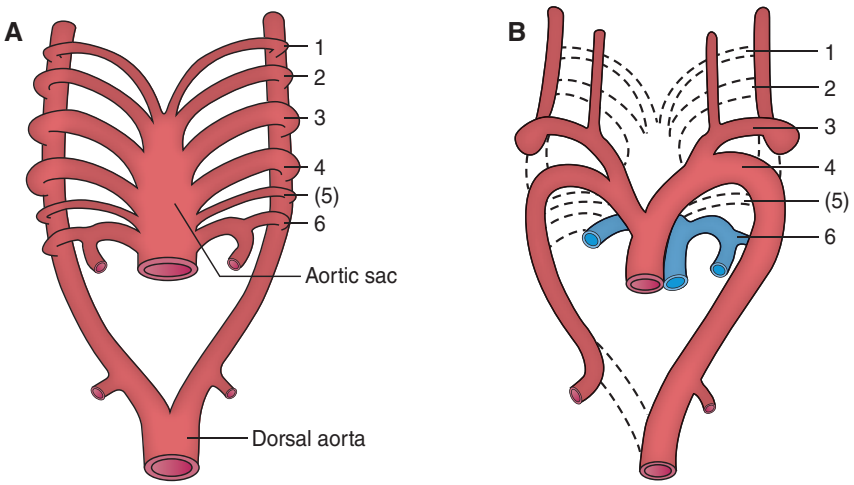

C

Embryonic	Adult
Aortic arch arteries	
1	Maxillary artery (portion of)
2	Stapedial artery (portion of)
3	Right and left common carotid arteries (portion of) Right and left internal carotid arteries
4	Right subclavian artery (portion of) Arch of the aorta (portion of)
5	Regresses in humans
6[a]	Right and left pulmonary arteries (portion of) Ductus arteriosus
Dorsal Aorta	
Posterolateral arteries	Arteries to the upper and lower extremities, intercostal, lumbar, and lateral sacral arteries
Lateral arteries	Renal, suprarenal, and gonadal arteries
Ventral arteries	
Vitelline	Celiac, superior mesenteric, and inferior mesenteric arteries
Umbilical	Medial umbilical ligaments

[a]Early in development, the recurrent laryngeal nerves hook around aortic arch 6. On the right side, the distal part of aortic arch 6 regresses, and the right recurrent laryngeal nerve moves up to hook around the right subclavian artery. On the left side, aortic arch 6 persists as the ductus arteriosus (or ligamentum arteriosus in the adult); the left recurrent laryngeal nerve remains hooked around the ductus arteriosus.

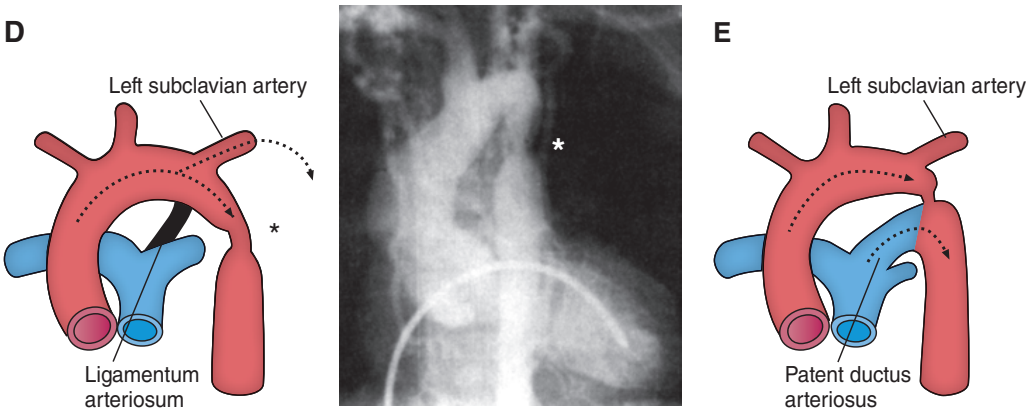

FIGURE 5.18. Development of the arterial system. **A, B.** Development and fate of the aortic arches during the remodeling process. Note the portions of the aortic arches that degenerate during the remodeling process (*dashed lines*). **C.** Table showing the correspondence of embryonic arteries to their derivative adult counterparts. **D.** Postductal coarctation of the aorta. In a postductal coarctation, blood reaches the lower part of the body via collateral circulation through the left subclavian, intercostal, and internal thoracic arteries. An angiogram of a postductal coarctation (at the *) with well-developed collateral blood vessels is shown. **E.** Preductal coarctation of the aorta. In a preductal coartation, blood reaches the lower part of the body via a patent ductus arteriosus. Prostaglandin treatment is required to maintain the patent ductus arteriosus until surgery. * stands for point of constriction. *Dotted arrows* = direction of blood flow.

X. DEVELOPMENT OF THE VENOUS SYSTEM (FIGURE 5.19)

A. General pattern. The general pattern develops mainly from three pairs of veins: the **vitelline veins, umbilical veins**, and **cardinal veins** that empty blood into the sinus venosus. These veins undergo remodeling due to a left → right shunting of venous blood to the right atrium.

B. Clinical considerations. Most anomalies of the venous system occur as a result of persistence of the veins on the left side of the body that normally regress during the left → right shunting of blood.

1. **Double inferior vena cava** occurs when the left supracardinal vein persists, forming an additional inferior vena cava below the level of the kidneys.
2. **Left superior vena cava** occurs when the left anterior cardinal vein persists, forming a superior vena cava on the left side. The right anterior cardinal vein abnormally regresses.
3. **Double superior vena cava** occurs when the left anterior cardinal vein persists, forming a superior vena cava on the left side. The right anterior cardinal vein also forms a superior vena cava on the right side.
4. **Absence of the hepatic portion of the inferior vena cava** occurs when the right vitelline vein fails to form a segment of the inferior vena cava. Consequently, blood from the lower part of the body reaches the right atrium via the azygos vein, hemiazygos vein, and superior vena cava.

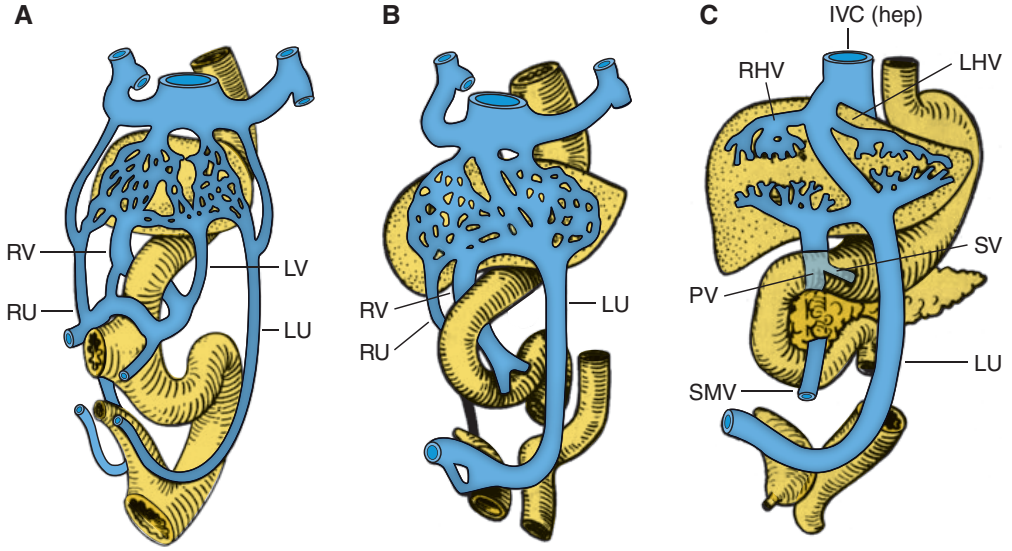

D

Embryonic	Adult
Vitelline veins	
Right and left	Portion of the IVC,[a] hepatic veins and sinusoids, ductus venosus, portal vein, inferior mesenteric vein, superior mesenteric vein, splenic vein
Umbilical veins	
Right	Degenerates early in fetal life
Left	Ligamentum teres
Cardinal veins	
Anterior	SVC, internal jugular veins
Posterior	Portion of IVC, common iliac veins
Subcardinal	Portion of IVC, renal veins, gonadal veins
Supracardinal	Portion of IVC, intercostal veins, hemiazygos vein, azygos vein

IVC = inferior vena cava, SVC = superior vena cava.
[a]Note that the IVC is derived embryologically from four different sources.

FIGURE 5.19. Development of the venous system. **A.** Week 5. **B.** Month 2. **C.** Month 3. Due to the left–right shunting of venous blood, the right vitelline vein enlarges, whereas the proximal part of the left vitelline vein disappears. Note that the right umbilical vein degenerates early in fetal life, whereas the left umbilical vein enlarges to carry oxygenated blood from the placenta to the fetus. **D.** Table showing the correspondence of the embryonic veins to their adult counterparts. IVC (hep) = inferior vena cava, LHV = left hepatic vein, LU = left umbilical vein, LV = left vitelline vein, PV = portal vein, RHV = right hepatic vein, RU = right umbilical vein, RV = right vitelline vein, SMV = superior mesenteric vein, SV = splenic vein.

Study Questions for Chapter 5

1. The most common interventricular septal defect (VSD) seen clinically is

(A) persistent truncus arteriosus
(B) membranous VSD
(C) common ventricle
(D) foramen secundum defect
(E) premature closure of foramen ovale

2. Which of the following clinical signs would be most obvious on examination of a patient with either tetralogy of Fallot or transposition of the great vessels?

(A) Sweaty palms
(B) Lack of femoral artery pulse
(C) Pulmonary hypertension
(D) Cyanosis
(E) Diffuse red rash

3. Which of the following congenital cardiovascular malformations is most commonly associated with maternal rubella infection?

(A) Isolated dextrocardia
(B) Patent ductus arteriosus
(C) Persistent truncus arteriosus
(D) Coarctation of the aorta
(E) Double aortic arch

4. The most common atrial septal defect (ASD) seen clinically is

(A) common atrium
(B) foramen secundum defect
(C) premature closure of the foramen ovale
(D) persistent truncus arteriosus
(E) probe patency of the foramen ovale

5. The ventral surface of the adult heart as seen on gross examination or radiography is comprised primarily of the

(A) left atrium
(B) left ventricle
(C) inferior vena cava
(D) bulbus cordis
(E) right ventricle

6. The left recurrent laryngeal nerve recurs around the

(A) left primary bronchus
(B) left subclavian artery
(C) left subclavian vein
(D) ductus arteriosus
(E) left common carotid artery

7. Which of the three primary germ layers forms the histologically definitive endocardium of the adult heart?

(A) Ectoderm
(B) Endoderm
(C) Mesoderm
(D) Epiblast
(E) Hypoblast

8. Which of the following is responsible for the proper alignment of the atrioventricular canal and the conoventricular canal?

(A) Lateral folding of the embryo
(B) Craniocaudal folding of the embryo
(C) Programmed cell migration
(D) Formation of the aorticopulmonary septum
(E) Dextral looping

9. The hepatic sinusoids that can be observed histologically in an adult liver are derived from the

(A) supracardinal veins
(B) anterior cardinal veins
(C) posterior cardinal veins
(D) vitelline veins
(E) subcardinal veins

10. Which of the following arterial malformations is very common in premature infants?

(A) Patent ductus arteriosus
(B) Coarctation of the aorta
(C) Right aortic arch
(D) Double aortic arch
(E) Abnormal origin of the right subclavian artery

11. A physician monitoring a newborn infant's heart sounds using a stethoscope hears the characteristic murmur of a patent ductus arteriosus. How soon after birth should this murmur normally disappear?

(A) 1–2 months
(B) 1–2 weeks

(C) 1–2 days
(D) 1–2 hours
(E) Immediately

12. How soon after birth does the foramen ovale close?

(A) 1–2 months
(B) 1–2 weeks
(C) 1–2 days
(D) 1–2 hours
(E) Immediately

13. A 9-year-old boy presents with complaints of numbness and tingling in both feet. Examination reveals no pulse in the femoral artery, increased blood pressure in the arteries of the upper extremity, and enlarged intercostal veins. Which of the following abnormalities would be suspected?

(A) Double aortic arch
(B) Tetralogy of Fallot
(C) Postductal coarctation of the aorta
(D) Right aortic arch
(E) Abnormal origin of the right subclavian artery

14. The coronary sinus is derived from which of the following?

(A) Truncus arteriosus
(B) Bulbus cordis
(C) Primitive ventricle
(D) Primitive atrium
(E) Sinus venosus

15. The conus arteriosus is derived from which of the following?

(A) Truncus arteriosus
(B) Bulbus cordis
(C) Primitive ventricle
(D) Primitive atrium
(E) Sinus venosus

16. The proximal part of the aorta is derived from which of the following?

(A) Truncus arteriosus
(B) Bulbus cordis
(C) Primitive ventricle
(D) Primitive atrium
(E) Sinus venosus

17. The trabeculated part of the right ventricle is derived from which of the following?

(A) Truncus arteriosus
(B) Bulbus cordis
(C) Primitive ventricle
(D) Primitive atrium
(E) Sinus venosus

18. Tricuspid atresia is a cardiac malformation that involves which of the following septa?

(A) Aorticopulmonary septum
(B) Atrial septum
(C) Atrioventricular septum
(D) Interventricular septum

19. A muscular VSD is a cardiac malformation that involves which of the following septa?

(A) Aorticopulmonary septum
(B) Atrial septum
(C) Atrioventricular septum
(D) Interventricular septum

20. Tetralogy of Fallot is a cardiac malformation that involves which of the following septa?

(A) Aorticopulmonary septum
(B) Atrial septum
(C) Atrioventricular septum
(D) Interventricular septum

21. D-Transposition of the great arteries is a cardiac malformation that involves which of the following septa?

(A) Aorticopulmonary septum
(B) Atrial septum
(C) Atrioventricular septum
(D) Interventricular septum

22. An insufficient amount of AV cushion material will result in which of the following?

(A) Persistent truncus arteriosus (PTA)
(B) Ebstein anomaly
(C) Transposition of the great arteries
(D) Common ventricle
(E) Tricuspid atresia

23. A partial development of the aorticopulmonary septum will result in which of the following?

(A) Persistent truncus arteriosus (PTA)
(B) Ebstein anomaly
(C) Transposition of the great arteries
(D) Common ventricle
(E) Tricuspid atresia

24. A failure of the tricuspid leaflets to attach to the annulus fibrosus will result in which of the following?

(A) Persistent truncus arteriosus (PTA)
(B) Ebstein anomaly

(C) Transposition of the great arteries
(D) Common ventricle
(E) Tricuspid atresia

25. A faulty fusion of the right and left bulbar ridges and AV cushion will result in which of the following?

(A) Persistent truncus arteriosus (PTA)
(B) Ebstein anomaly
(C) Transposition of the great arteries
(D) Common ventricle
(E) Membranous VSD

26. The superior mesenteric artery is derived from which of the following?

(A) Posterolateral arteries
(B) Lateral arteries
(C) Ventral arteries

27. The arteries to the upper extremity are derived from which of the following?

(A) Posterolateral arteries
(B) Lateral arteries
(C) Ventral arteries

28. The gonadal arteries are derived from which of the following?

(A) Posterolateral arteries
(B) Lateral arteries
(C) Ventral arteries

29. The proximal part of the internal carotid artery is derived from which of the following?

(A) Aortic arch 1
(B) Aortic arch 2
(C) Aortic arch 3
(D) Aortic arch 4
(E) Aortic arch 6

30. A portion of the arch of the aorta is derived from which of the following?

(A) Aortic arch 1
(B) Aortic arch 2
(C) Aortic arch 3
(D) Aortic arch 4
(E) Aortic arch 6

31. The proximal part of the right subclavian artery is derived from which of the following?

(A) Aortic arch 1
(B) Aortic arch 2
(C) Aortic arch 3
(D) Aortic arch 4
(E) Aortic arch 6

32. The portal vein is derived from which of the following?

(A) Vitelline veins
(B) Umbilical veins
(C) Anterior cardinal veins
(D) Posterior cardinal veins
(E) Subcardinal veins

33. The renal veins are derived from which of the following?

(A) Vitelline veins
(B) Umbilical veins
(C) Anterior cardinal veins
(D) Posterior cardinal veins
(E) Subcardinal veins

34. The superior mesenteric vein is derived from which of the following?

(A) Vitelline veins
(B) Umbilical veins
(C) Anterior cardinal veins
(D) Posterior cardinal veins
(E) Subcardinal veins

35. Closure of the foramen primum results from fusion of which of the following structures?

(A) Septum secundum and the fused atrioventricular cushions
(B) Septum secundum and the septum primum
(C) Septum primum and the fused atrioventricular cushions
(D) Septum primum and the septum spurium
(E) Septum primum and the sinoatrial valves

36. A 3-day-old boy delivered at 32 weeks of gestation is experiencing respiratory distress syndrome. The physician detects a heart murmur characteristic of a patent ductus arteriosus, a diagnosis that is confirmed with an echocardiogram. Which embryonic structure is involved in this diagnosis?

(A) Left third aortic arch
(B) Right third aortic arch
(C) Left sixth aortic arch
(D) Umbilical arteries
(E) Vitelline arteries

Answers and Explanations

1. **B.** The most common of all cardiac congenital malformations seen clinically are membranous VSDs. The membranous interventricular septum forms by the proliferation and fusion of tissue from three different sources: the right and left bulbar ridges and the atrioventricular (AV) cushions. Because of this complex formation, the probability of defects is very high.

2. **D.** Marked cyanosis is a distinct clinical sign in both tetralogy of Fallot and transposition of the great vessels. Any congenital cardiac malformation that allows right-to-left shunting of blood is sometimes called cyanotic heart disease. Right-to-left shunting allows poorly oxygenated blood from the right side of the heart to mix with highly oxygenated blood on the left side of the heart. This causes decreased oxygen tension to peripheral tissues, leading to a characteristic blue tinge (cyanosis) and bulbous thickening of the fingers and toes (clubbing).

3. **B.** Patent ductus arteriosus (PDA) is the most common congenital cardiac malformation associated with rubella infection of the mother. It is unclear how the rubella virus acts to cause PDA.

4. **B.** The most common ASD is foramen secundum defect, which is caused by excessive resorption of the septum primum or the septum secundum. This results in an opening between the atria (patent foramen ovale). Some of these defects may remain undiagnosed and may be tolerated for a long time (up to age 30 years before the person presents clinically).

5. **E.** During embryological formation of the heart, the arterial and venous ends of the heart tube are fixed in place. As further growth continues, the heart tube folds to the right. This greatly contributes to the ventral surface of the adult heart being comprised primarily of the right ventricle. The definitive anatomical orientation of the adult heart within the thorax is not at all similar to the strong image we have in our minds of the classic Valentine's Day heart.

6. **D.** The left recurrent laryngeal nerve recurs around the ductus arteriosus (ligamentum arteriosus in the adult). Early in embryological development, both the right and left recurrent laryngeal nerves hook (recur) around aortic arch 6. The left aortic arch 6 persists as the ductus arteriosus.

7. **C.** The entire cardiovascular system is of mesodermal origin.

8. **E.** Dextral looping aligns these two canals through early looping, convergence, wedging, and repositioning. This is especially important in correcting the unusual blood flow pattern in the primitive heart tube where venous blood flows into the left ventricle prior to the right ventricle.

9. **D.** Because of the location of the vitelline veins and the tremendous growth of the developing liver (hepatic diverticulum), the vitelline veins are surrounded by the liver and give rise to the hepatic sinusoids. The umbilical veins also contribute to the hepatic sinusoidal network.

10. **A.** Patent ductus arteriosus (PDA) is very common in premature infants. Infants with birth weight less than 1750 grams typically have a PDA during the first 24 hours postnatally. PDA is more common in female infants than in male infants.

11. **D.** The ductus arteriosus functionally closes within 1–2 hours after birth via smooth muscle contraction of the tunica media. Before birth, the patency of the ductus arteriosus is controlled by the low oxygen content of the blood flowing through it, which in turn stimulates production of prostaglandins, which cause smooth muscle to relax. After birth, the high oxygen content of the blood due to lung ventilation inhibits production of prostaglandins, causing smooth muscle contraction. Premature infants can be treated with prostaglandin synthesis inhibitors (such as indomethacin) to promote closure of the ductus arteriosus.

12. **E.** The foramen ovale functionally closes almost immediately after birth as pressure in the right atrium decreases and pressure in the left atrium increases, thereby pushing the septum primum

against the septum secundum. Anatomical fusion occurs much later in life; more than 25% of the population has probe patency of the foramen ovale, in which anatomical fusion does not occur.

13. C. No pulse in the femoral artery, increased blood pressure in the arteries of the upper extremity, enlarged intercostal veins, and numbness and tingling in both feet are clinical symptoms indicative of postductal coarctation of the aorta. Because of the constriction of the aorta, the blood supply to the lower extremity is compromised.

14. E. The coronary sinus is derived from the sinus venosus.

15. B. The smooth part of the right ventricle, known as the conus arteriosus, is derived from the bulbus cordis.

16. A. The proximal part of the aorta is derived from the truncus arteriosus.

17. C. The trabeculated part of the right ventricle is derived from the primitive ventricle.

18. C. Tricuspid atresia involves the atrioventricular septum.

19. D. Muscular VSD is caused by perforations in the muscular interventricular septum.

20. A. Tetralogy of Fallot involves the aorticopulmonary septum.

21. A. D-Transposition involves the aorticopulmonary septum.

22. E. Insufficient amount of AV cushion material will cause tricuspid atresia.

23. A. Partial development of the aorticopulmonary septum will cause persistent truncus arteriosus.

24. B. Failure of fusion of the tricuspid leaflets with the annulus fibrosus results in Ebstein anomaly.

25. E. Faulty fusion of the right and left bulbar ridges and AV cushions will cause membranous VSD.

26. C. The superior mesenteric artery is derived from ventral branches of the dorsal aorta, specifically the vitelline arteries.

27. A. Arteries to the upper extremity are derived from posterolateral branches of the dorsal aorta.

28. B. The gonadal arteries are derived from lateral branches of the dorsal aorta.

29. C. The proximal part of the internal carotid artery is derived from aortic arch 3.

30. D. Part of the arch of the aorta is derived from aortic arch 4.

31. D. The proximal part of the right subclavian artery is derived from aortic arch 4.

32. A. The portal vein is derived from the right vitelline vein.

33. E. The renal veins are derived from the subcardinal veins.

34. A. The superior mesenteric vein is derived from the vitelline veins.

35. C. The foramen primum forms between the free edge of the septum primum and the atrioventricular (AV) cushions. It is closed when the septum primum fuses with the AV cushions.

36. C. Patent ductus arteriosus (PDA) is a condition in which the ductus arteriosus, a blood vessel that allows blood to bypass the baby's lungs before birth, fails to normally close after birth. The ductus arteriosus is derived from the distal portion of the left sixth aortic arch.

chapter 6

Placenta and Amniotic Fluid

I. FORMATION OF THE PLACENTA (FIGURE 6.1)

The placenta develops as the embryo invades the endometrium of the uterus and as the trophoblast forms the villous chorion. The formation of the villous chorion proceeds through three stages: **primary chorionic villi**, **secondary chorionic villi**, and **tertiary chorionic villi**.

II. PLACENTAL COMPONENTS: DECIDUA BASALIS AND VILLOUS CHORION (FIGURE 6.2)

The human placenta is **hemochorial** (i.e., maternal blood comes in direct contact with the chorion) and **discoid-shaped**.

A. The maternal component

1. The maternal component of the placenta consists of the **decidua basalis**. The decidua basalis includes the portion of the endometrium located between the blastocyst and the myometrium (i.e., the site of implantation). The **decidua parietalis** includes all portions of the endometrium other than the site of implantation.
2. The decidua basalis and decidua parietalis shed as part of the afterbirth.
3. The **decidua capsularis** includes the portion of endometrium that covers the blastocyst and separates the blastocyst from the uterine cavity. The decidua capsularis attenuates and degenerates at week 22 of development because of a reduced blood supply.
4. The term *decidua* means "falling off," "shed," or "sloughed off."
5. The **maternal surface** of the placenta is characterized by 8–10 compartments called **cotyledons**, which impart a **cobblestone appearance** to the maternal surface. The cotyledons are separated from each other by decidual (placental) septa.
6. The maternal surface is **dark red and oozes blood** due to torn maternal blood vessels.

B. The fetal component

1. The fetal component of the placenta consists of **tertiary chorionic villi** derived from both the trophoblast and extraembryonic mesoderm, which collectively are called the **villous (bushy) chorion**.
2. The villous chorion develops prolifically at the decidua basalis.
3. The villous chorion contrasts to an area of no villous development known as the **smooth chorion**. The smooth chorion contacts the decidua capsularis.

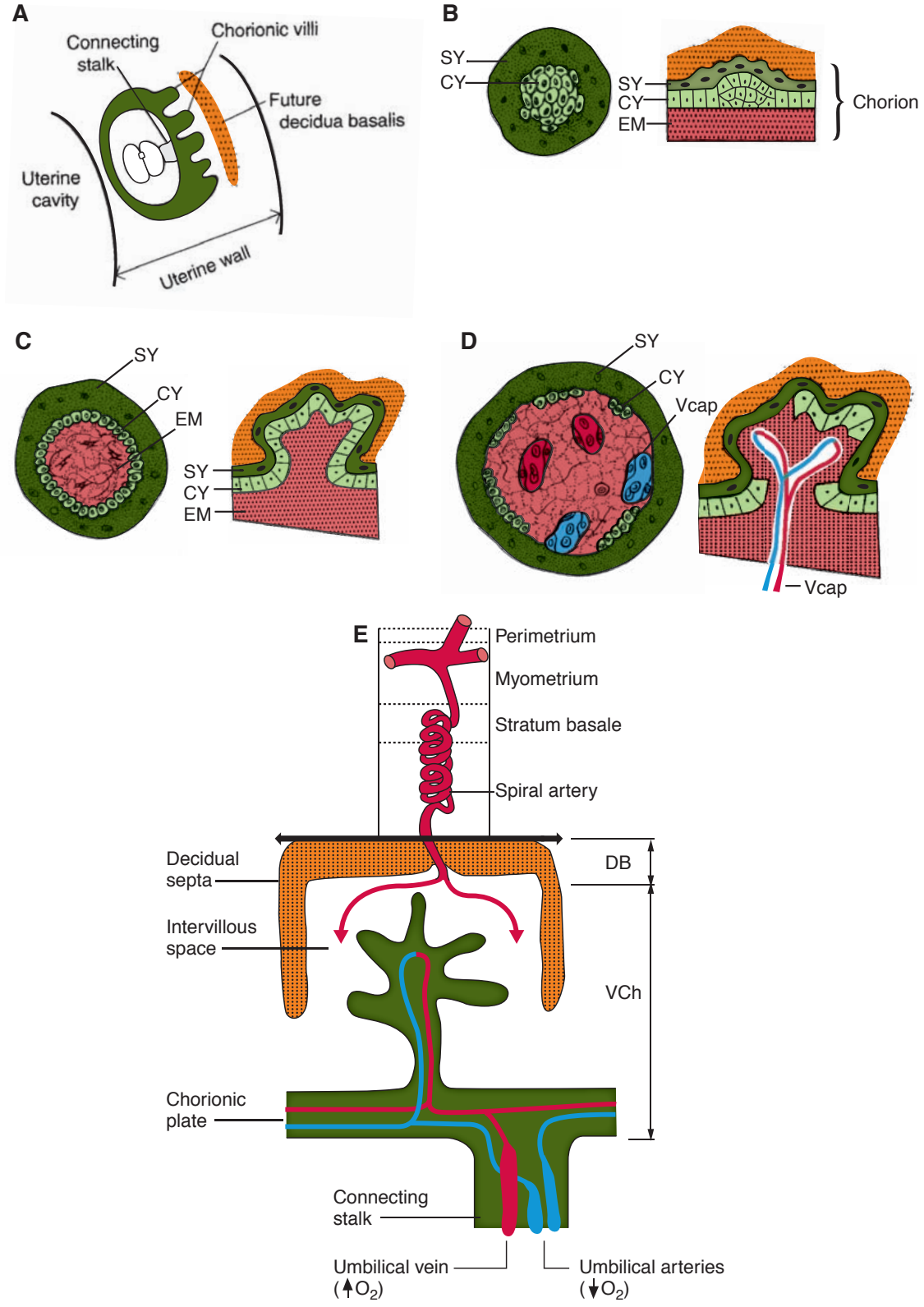

FIGURE 6.1. Diagram of the various stages of villous chorion formation. **A.** A week 2 embryo completely embedded in the wall of the uterus. **B.** Primary chorionic villus during week 2. A primary villus consists of a core of cytotrophoblastic cells (CY, *light green*) surrounded by syncytiotrophoblast (SY, *dark green*). **C.** Secondary chorionic villus during the start of week 3. A secondary villus consists of a core of extraembryonic mesoderm (EM, *light red*) surrounded by cytotrophoblastic cells (CY, *light green*) and syncytiotrophoblast (SY, *dark green*). **D.** Tertiary chorionic villus at the end of week 3. A tertiary villus consists of a core of villous (fetal) capillaries (Vcap, *red* and *blue*) surrounded by scattered cytotrophoblastic cells (CY, *light green*) and syncytiotrophoblast (SY, *dark green*). **E.** The villous chorion (VCh), which consists of tertiary chorionic villi, and the decidua basalis (DB) constitute the definitive placenta. The thick, *double-headed arrow* indicates the plane of separation when the placenta is shed during the afterbirth. The cytotrophoblast penetrates the syncytiotrophoblast to make contact with the decidua basalis and form the outer cytotrophoblast shell (not shown), which secures the tertiary chorionic villus in an upright position. (Note: The stratum basale is not part of the placenta.)

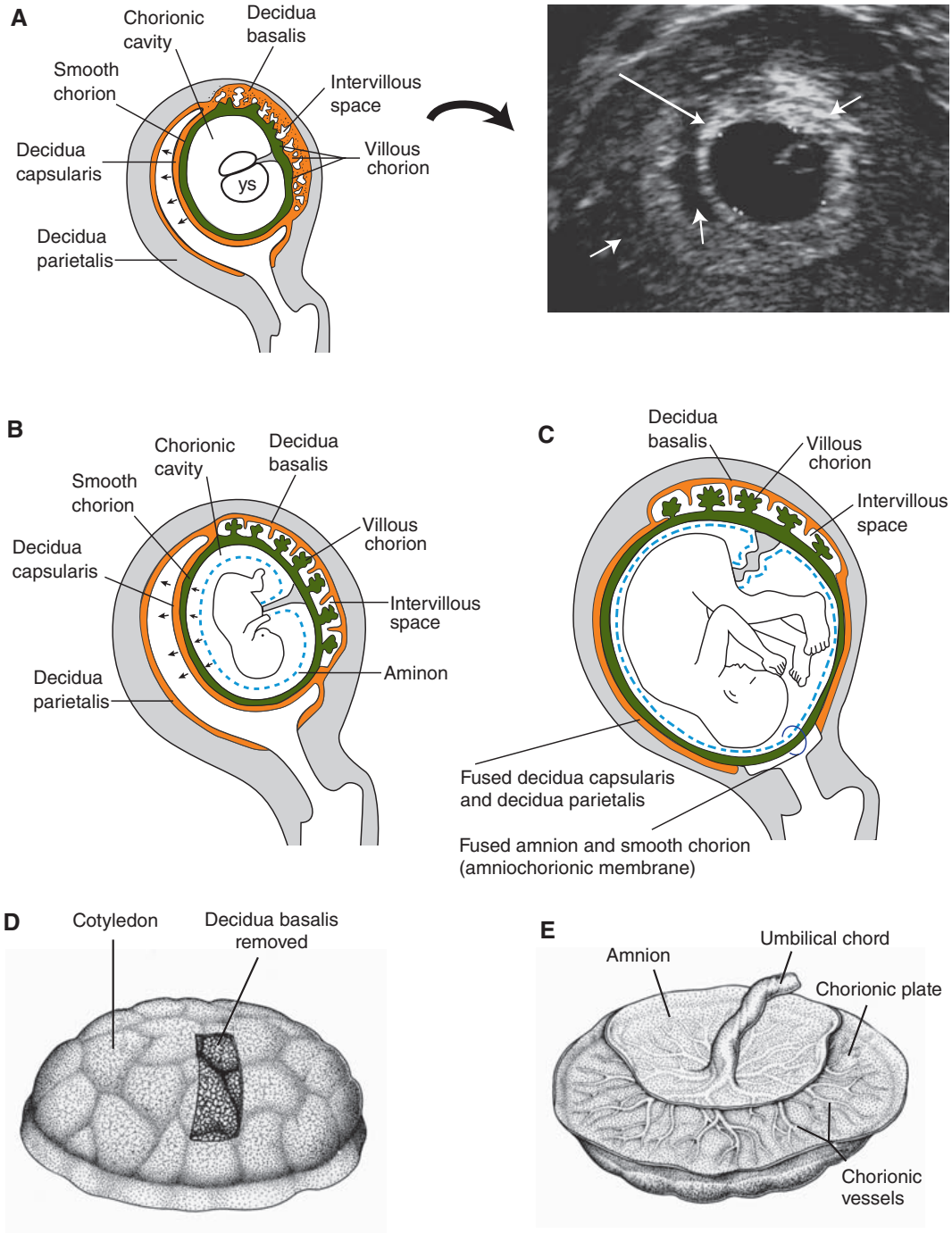

FIGURE 6.2. Diagram showing the relationship of the fetus, uterus, and placenta. **A.** Week 4. The diagram shows the early stages of placenta formation. The sonogram shows the decidua basalis (db), decidua parietalis (dp), and decidua capsularis and smooth chorion (dc+sc). Note the location of the uterine cavity (uc) and chorionic cavity (cc). Within the chorionic cavity, the yolk sac can be observed. **B.** Early fetal period. The *arrows* (outer set) indicate that as the fetus grows within the uterine wall, the decidua capsularis expands toward and fuses with the decidua parietalis, thereby obliterating the uterine cavity. The *arrows* (inner set) indicate that as the fetus grows, the amnion expands toward and fuses with the smooth chorion, thereby forming the amniochorionic membrane and obliterating the chorionic cavity. **C.** Late fetal period. The uterine cavity and chorionic cavity are obliterated. The fused amnion and smooth chorion form the amniochorionic membrane ("bag of waters"), which passes over the cervical opening. **D.** Maternal surface of the placenta. **E.** Fetal surface of the placenta.

4. The **fetal surface** of the placenta is characterized by the well-vascularized chorionic plate containing the chorionic (fetal) blood vessels.
5. The fetal surface has a **smooth, shiny, light-blue or blue-pink appearance** (because the amnion covers the fetal surface), and 5–8 large chorionic (fetal) blood vessels.

III. PLACENTAL MEMBRANE (FIGURE 6.3)

The placental membrane separates maternal blood from fetal blood. A common misperception is that the placental membrane acts as a strict "barrier." However, a wide variety of substances freely cross the placental membrane. Some substances that cross can be either beneficial or harmful. Some substances do not cross the placental membrane. The composition of the placental membrane changes during pregnancy.

A. **In early pregnancy,** the placental membrane has four layers: **syncytiotrophoblast, cytotrophoblast, connective tissue,** and the **endothelium of fetal capillaries**. Several cell types have been identified within the connective tissue, which includes mesenchymal cells, reticular cells, myofibroblasts,

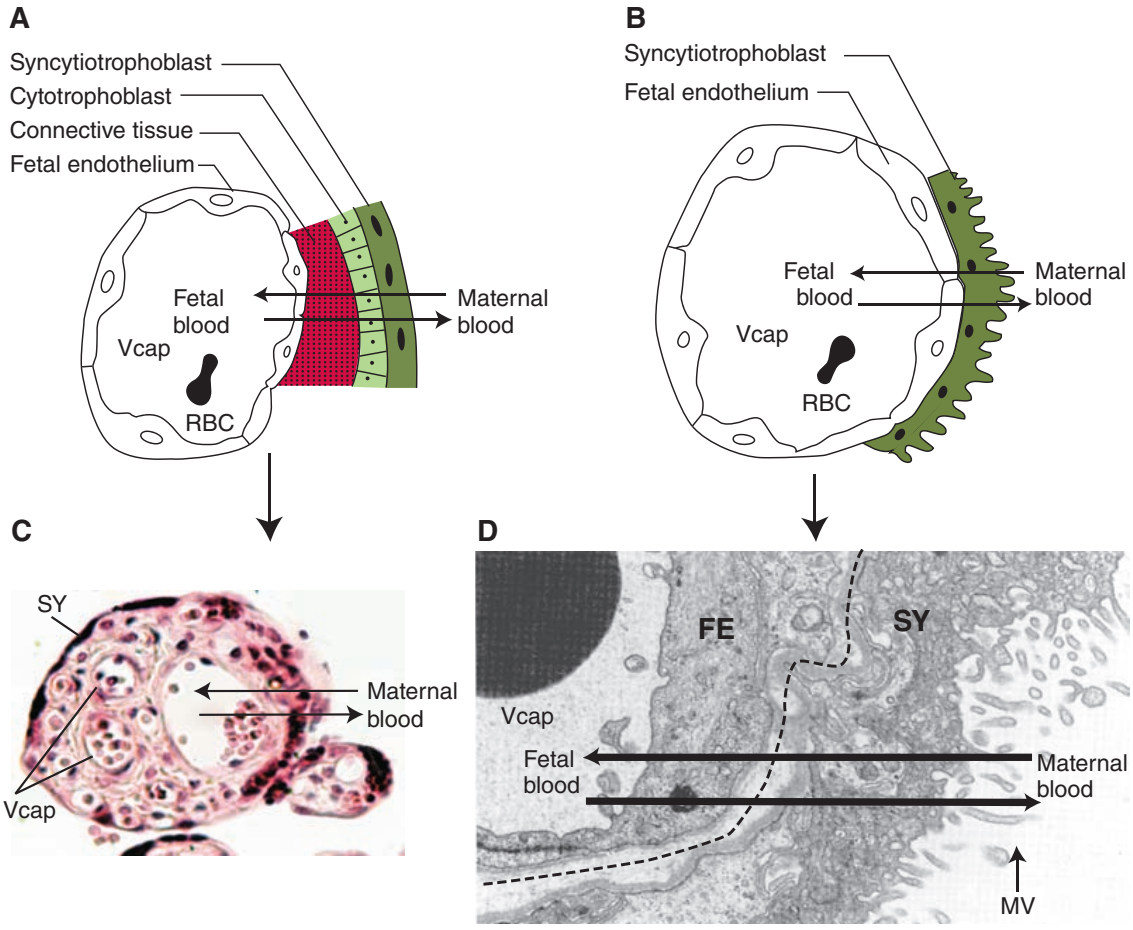

FIGURE 6.3. The placental membrane. **A.** In early pregnancy. **B.** In late pregnancy. **C.** Light micrograph of a tertiary chorionic villus shows the placental membrane in an early pregnancy. Note the location of maternal and fetal blood. **D.** Electron microscopy of a tertiary chorionic villus showing the placental membrane in a late pregnancy. Note the location of maternal and fetal blood and the microvillous border (MV) of the syncytiotrophoblast cells. FE = fetal endothelium; SY = syncytiotrophoblast; RBC = red blood cell; Vcap = villous (fetal) capillaries. **E.** Table of substances that cross and that do not cross the placental membrane. Substances cross the placenta by simple diffusion, facilitated diffusion (e.g., glucose), active transport (e.g., many amino acids), receptor-mediated endocytosis (e.g., immunoglobulin G [IgG] and IgA), and pinocytosis (e.g., large proteins).

E

SUBSTANCES THAT CROSS OR DO NOT CROSS THE PLACENTAL MEMBRANE

BENEFICIAL SUBSTANCES THAT CROSS THE PLACENTAL MEMBRANE

- O_2, CO_2
- Glucose, L-form amino acids, free fatty acids, vitamins
- H_2O, Na^+, Cl^-, K^+, I^-, CA^{2+}, PO_4^{2+}
- Urea, uric acid, bilirubin
- Fetal and maternal RBCs
- Maternal serum proteins, α-fetoprotein, transferrin–Fe^{2+}complex, LDL, prolactin
- Steroid hormones (unconjugated)
- IgG, IgA

HARMFUL SUBSTANCES THAT CROSS THE PLACENTAL MEMBRANE

- Viruses—e.g., rubella, cytomegalovirus, herpes simplex type 2, varicella zoster, Coxsackie, variola, measles, poliomyelitis
- Category X drugs (absolute contraindication in pregnancy)—e.g., thalidomide, aminopterin, methotrexate, busulfan (Myleran), chlorambucil (Leukeran), cyclophosphamide (Cytoxan), phenytoin (Dilantin), triazolam (Halcion), estazolam (ProSom), warfarin (Coumadin), isotretinoin (Accutane), clomiphene (Clomid), diethylstilbestrol (DES), ethisterone, norethisterone, megestrol (Megace), oral contraceptives (Ovcon, Levlen, Norinyl), nicotine, alcohol, ACE inhibitors (Captopril, enalapril)
- Category D drugs (definite evidence of risk to fetus)—e.g., tetracycline (Achromycin), doxycycline (Vibramycin), streptomycin, amikacin, tobramycin (Nebcin), phenobarbital (Donnatal), pentobarbital (Nembutal), valproic acid (Depakene), diazepam (Valium), chlordiazepoxide (Librium), alprazolam (Xanax), lorazepam (Ativan), lithium, hydrochlorothiazide (Diuril)
- Carbon monoxide
- Organic mercury, lead, polychlorinated biphenyls (PCBs), potassium iodide
- Cocaine, heroin
- *Toxoplasma gondii*, *Treponema pallidum*, *Listeria monocytogenes*
- Rubella virus vaccine
- Anti-Rh antibodies

SUBSTANCES THAT DO NOT CROSS THE PLACENTAL MEMBRANE

- Maternally derived cholesterol, triglycerides, and phospholipids
- Protein hormones (e.g., insulin)
- Drugs (e.g., succinylcholine, curare, heparin, methyldopa, drugs similar to amino acids)
- IgD, IgE, IgM
- Bacteria in general

FIGURE 6.3. *(Continued)*

smooth muscle cells, macrophages, and fetal placental antigen-presenting cells (or **Hofbauer cells**).

B. In late pregnancy, the placental membrane has two layers: the **syncytiotrophoblast** and the **endothelium of fetal capillaries**.

IV. THE PLACENTA AS AN ENDOCRINE ORGAN

The placenta produces both protein and steroid hormones as follows:

A. Human chorionic gonadotropin (hCG) is a glycoprotein hormone that stimulates the production of progesterone by the corpus luteum.

B. Human placental lactogen (hPL) is a protein hormone that induces lipolysis (thus elevating free fatty acid levels in the mother) and inhibits insulin secretion (thereby playing a role in gestational diabetes). hPL is considered the "growth hormone of the fetus."

C. Estrone, estradiol (most potent), and estriol are steroid hormones produced by the placenta, but little is known about their specific functions in either the mother or the fetus.

D. Progesterone is a steroid hormone that maintains the endometrium during pregnancy, serves as a precursor for glucocorticoid/mineralocorticoid synthesis in the fetal adrenal cortex, and serves as a precursor for testosterone synthesis in the fetal testes.

V. THE UMBILICAL CORD (FIGURE 6.4)

A. A patent opening called the **primitive umbilical ring** exists on the ventral surface of the developing embryo through which three structures pass: the **yolk sac** (**vitelline duct**), **connecting stalk**, and **allantois**.

B. The nonfunctional allantois degenerates to form the **median umbilical ligament** in the adult.

C. As the amnion expands, the aminion squeezes the vitelline duct, connecting stalk, and allantois together to form the **primitive umbilical cord**.

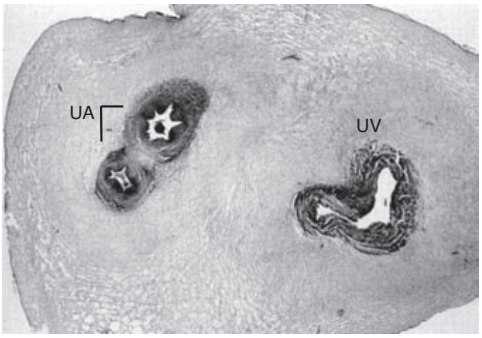

FIGURE 6.4. Light micrograph of a normal umbilical cord showing the two umbilical arteries (UA) and one umbilical vein (UV).

D. At week 6, the gut tube connected to the yolk sac herniates (called the **physiological umbilical herniation**) into the extraembryonic coelom. The herniation reduces by week 11 as the gut tube returns to the abdominal cavity. The yolk sac (vitelline duct) and allantois degenerate.

E. The definitive umbilical cord at term is pearl-white, 1–2 cm in diameter, 50–60 cm long, eccentrically positioned, and contains the **right and left umbilical arteries, left umbilical vein**, and **mucus connective tissue (Wharton jelly)**.

F. Physical inspection of the umbilicus in a newborn may reveal a light gray, shiny sac, indicating an **omphalocele**; fecal (meconium) discharge, indicating an **ileal (Meckel) diverticulum**; or a urine discharge, indicating a **urachal fistula**.

VI. CIRCULATORY SYSTEM OF THE FETUS (FIGURE 6.5)

Fetal circulation involves three shunts: the **ductus venosus**, the **ductus arteriosus**, and the **foramen ovale**.

A. Highly oxygenated and nutrient-enriched blood returns to the fetus from the placenta via the **left umbilical vein**. (Note: Highly oxygenated blood is carried by the left umbilical vein, not by an artery.)

B. From the left umbilical vein, blood enters the liver, where most of the blood bypasses the hepatic sinusoids by coursing through the **ductus venosus** to enter the inferior vena cava (IVC).

C. From the IVC, blood enters the right atrium where most of the blood bypasses the right ventricle by coursing through the **foramen ovale** to enter the left atrium.

D. From the left atrium, blood enters the left ventricle and is delivered to fetal tissues via the aorta.

E. Poorly oxygenated and nutrient-poor fetal blood returns to the placenta via **right and left umbilical arteries**.

F. Some blood in the right atrium enters the right ventricle. The blood in the right ventricle enters the pulmonary trunk, but most of the blood bypasses the lungs by coursing through the **ductus arteriosus**.

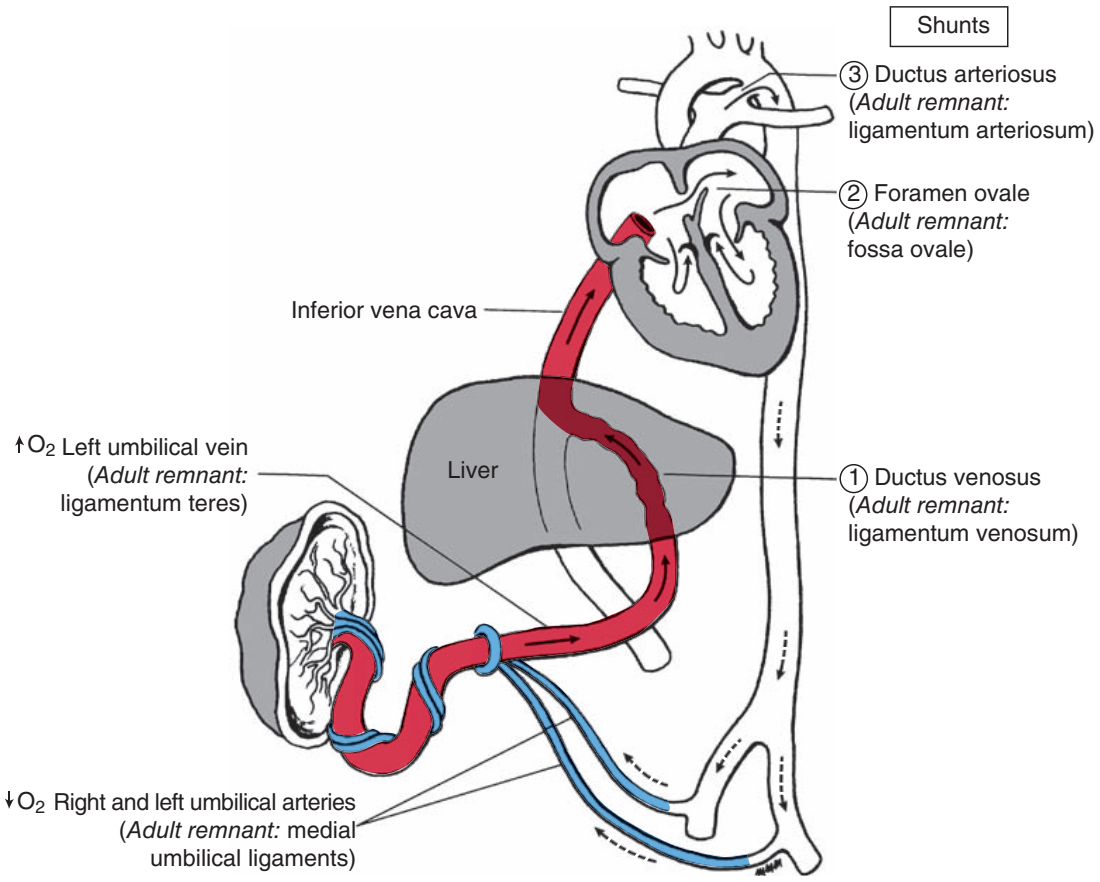

Remnants Created by Closure of Fetal Circulatory Structures	
Fetal Structure	**Adult Remnant**
Right and left umbilical arteries	Medial umbilical ligaments
Left umbilical vein	Ligamentum teres
Ductus venosus	Ligamentum venosum
Foramen ovale	Fossa ovale
Ductus arteriosus	Ligamentum arteriosum

FIGURE 6.5. Schematic diagram of fetal circulation and remnants of fetal circulatory structures.

G. Fetal lungs receive only a minimal amount of blood for growth and development. The blood is returned to the left ventricle via pulmonary veins.

H. Fetal lungs are not capable of respiratory function because they are functionally immature and the fetus is underwater (amniotic fluid). The placenta provides respiratory function for the fetus.

I. Circulatory system changes at birth are facilitated by a **decrease in right atrial pressure** due to occlusion of placental circulation and by an **increase in left atrial pressure** due to increased pulmonary venous return.

J. Changes include closure of all of the following: right and left umbilical arteries, left umbilical vein, ductus venosus, ductus arteriosus, and foramen ovale.

VII. AMNIOTIC FLUID

Amniotic fluid is maternally derived water that contains the following: electrolytes, carbohydrates, amino acids, lipids, proteins (hormones, enzymes, *a*-fetoprotein), urea, creatinine, lactate, pyruvate, desquamated fetal cells, fetal urine, fetal feces (meconium), and fetal lung liquid (useful for lecithin/sphingomyelin [L/S] ratio measurement for lung maturity).

A. Production of amniotic fluid

1. Amniotic fluid is constantly produced during pregnancy by the following: **direct transfer** from maternal circulation in response to osmotic and hydrostatic forces and **excretion of fetal urine by the kidneys** into the amniotic sac.
2. Kidney defects (e.g., bilateral kidney agenesis or Potter syndrome) result in **oligohydramnios**.

B. Resorption of amniotic fluid

1. Amniotic fluid is constantly resorbed during pregnancy by the following sequence of events: the fetus swallows amniotic fluid, amniotic fluid is absorbed into fetal blood through the gastrointestinal tract, and excess amniotic fluid is removed via the placenta and passed into maternal blood.
2. Swallowing defects (e.g., esophageal atresia) or absorption defects (e.g., duodenal atresia) result in **polyhydramnios**.

C. The amount of amniotic fluid

1. The amount of amniotic fluid is gradually increased during pregnancy from **50 mL at week 12** to **1000 mL at term**.
2. The rate of water exchange within the amniotic sac at term is 400–500 mL/hr, with a net flow of 125–200 mL/hr moving from the amniotic fluid into the maternal blood.
3. The near-term fetus excretes about 500 mL of urine daily, which is mostly water because the placenta exchanges metabolic wastes.
4. The fetus swallows about 400 mL of amniotic fluid daily.

D. Estimation of amniotic fluid volume (AFV). AFV is clinically measured by ultrasonography by calculating the **amniotic fluid index (AFI)**. The AFI is calculated by dividing the uterus into four quadrants, using the linea nigra (pigmented linea alba) for the right and left divisions and the umbilicus for the upper and lower quadrants. The maximum vertical amniotic fluid pocket diameter in each quadrant not containing the umbilical cord or fetal extremities is measured in centimeters. The sum of these measurements is the AFI.

1. **AFI 0 to <5 cm indicates oligohydramnios**
2. **AFI 5–25 cm indicates normal**
3. **AFI >25 cm indicates polyhydramnios**

VIII. TWINNING (FIGURE 6.6)

A. Steps in Monozygotic (Identical) Twinning

1. A secondary oocyte arrested in metaphase of meiosis II is fertilized by one sperm. The nuclear contents and centriole pair of the sperm enter the oocyte cytoplasm.
2. The secondary oocyte completes meiosis II forming the second polar body. The female and male pronuclei form.
3. The female and male pronuclei fuse and the centriole pair provide the cytoplasmic machinery for cleavage cell divisions to occur. A zygote is formed.
4. Cleavage divisions produce a cluster of blastomeres called a morula surrounded by a zona pellucida. The molecular mechanisms that establish twin embryogenesis are active in the morula and are responsible for the latter "splitting" of the inner cell mass. In other words,

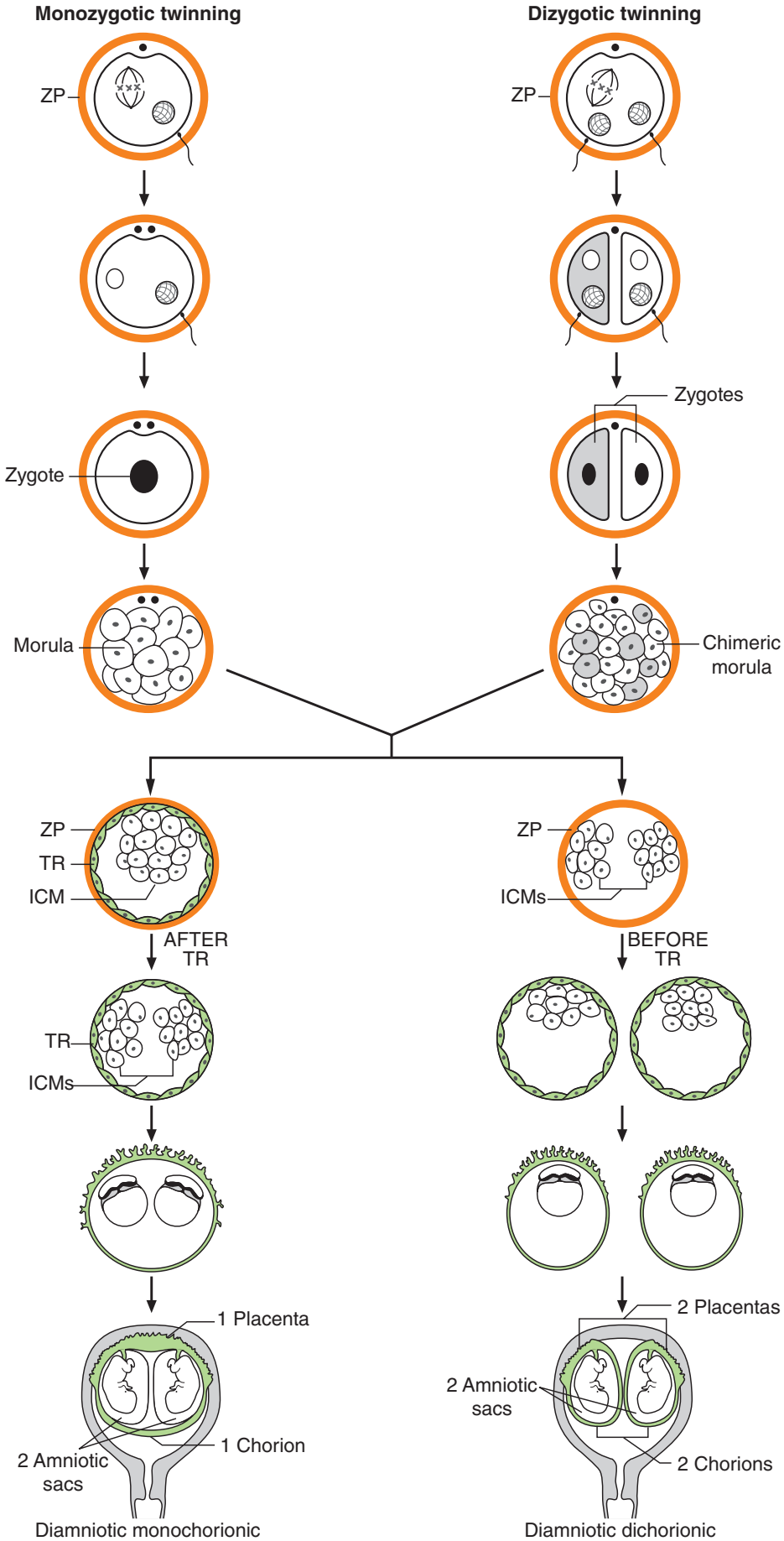

FIGURE 6.6. Diagram of monozygotic and dizygotic twinning. ZP=zona pellucida, TR=trophoblast, ICM=inner cell mass.

twinning causes the "splitting," not vice versa. The twinning morula can travel two different routes, leading to either monochorionic or dichorionic twins.

5. If "splitting" occurs AFTER the differentiation of the trophoblast, then monochorionic twins will form.
6. If "splitting" occurs BEFORE the differentiation of the trophoblast, then dichorionic twins will form.

B. Steps in Dizygotic (Fraternal) Twinning

1. A secondary oocyte arrested in metaphase of meiosis II is fertilized by two sperm. The nuclear contents and centriole pair of both sperm enter the oocyte cytoplasm.
2. The secondary oocyte completes meiosis II but does not form a secondary polar body. Instead, the DNA that would have been sequestered in second polar body forms another female pronucleus. There are now two separate cellular entities within the zona pellucida, each containing a female and male pronucleus.
3. The female and male pronuclei fuse and the centriole pair provides the cytoplasmic machinery for cleavage cell divisions to occur. Two zygotes are formed with two different genotypes.
4. Cleavage divisions produce a cluster of blastomeres called a morula surrounded by a zona pellucida. The morula is a **chimera** consisting of an assortment of cells with two different genotypes. The molecular mechanisms that establish twin embryogenesis are active in the chimeric morula and are responsible for the latter "splitting" of the inner cell mass. In other words, twinning causes the "splitting," not vice versa. The twinning chimeric morula can travel two different routes, leading to either monochorionic or dichorionic twins.
5. If "splitting" occurs AFTER the differentiation of the trophoblast, then monochorionic twins will form.
6. If "splitting" occurs BEFORE the differentiation of the trophoblast, then dichorionic twins will form.

C. Conjoined (Siamese) Twining (Figure 6.7)

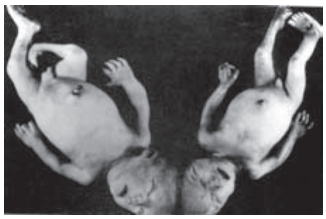

FIGURE 6.7. Craniophagus.

1. Occurs exactly like monozygotic twins except that there is incomplete "splitting" of the inner cell mass. The exact molecular mechanisms involved are not clear.
2. All conjoined twins (except parasitic twins) are symmetrical (i.e., like parts are fused to like parts).
3. The most common types of conjoined twins are: 1) thoracomphalopagus (fusion from upper chest to lower chest, 2) thoracopagus (fusion from upper chest to lower abdomen), 3) omphalopagus (fusion at lower chest), craniopagus (fusion of skulls), and parasitic twins (asymmetrically conjoined; one twin is small and dependent on the larger twin).
4. Conjoined twins are monoamniotic (i.e., one amnion) and monochorionic (i.e., one chorion). This photograph (Figure 6.7) shows twins that are conjoined at the head (called craniophagus).

IX. CLINICAL CONSIDERATIONS

A. **Velamentous placenta (Figure 6.8)** occurs when the umbilical (fetal) blood vessels abnormally travel through the amniochorionic membrane before reaching the placenta proper. If the umbilical blood vessels cross the internal os, a serious condition called **vasa previa** exists. In vasa previa, if one of the umbilical (fetal) blood vessels ruptures during pregnancy, labor, or delivery, the fetus will bleed to death. This photograph (Figure 6.8) shows a velamentous placenta with umbilical (fetal) blood vessels traveling through the amniochorionic membrane (*arrow*).

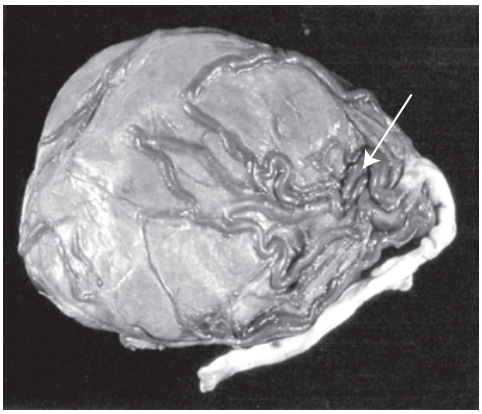

FIGURE 6.8. Velamentous placenta.

B. **Circumvallate placenta (Figure 6.9)** is a placenta peripheral, cuplike attachment of the amnion on the fetal surface of the placenta. This photograph (Figure 6.9) shows a circumvallate placenta with a peripheral, cuplike attachment of the amnion (*arrow*).

C. **Bipartite or tripartite placenta** is a placenta made up of two or three connected lobes.

D. **Duplex or triplex placenta** is a placenta made up of two or three separate lobes.

E. **Succenturiate placenta** is a placenta consisting of small accessory lobes completely separate from the main placenta. Care must be taken to ensure that the accessory lobes are eliminated in the afterbirth.

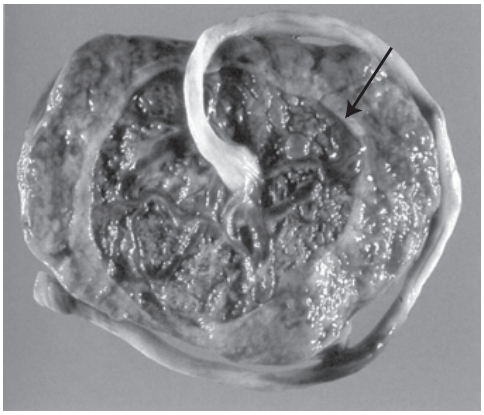

FIGURE 6.9. Circumvallate placenta.

F. **Membranous placenta** is a thin placenta that forms over the greater part of the uterine cavity. Care must be taken to ensure that the entire placenta is eliminated during the afterbirth; the condition may require curettage.

G. **Placenta previa** occurs when the placenta attaches in the lower part of the uterus, **covering the internal os**. The placenta normally implants in the posterior superior wall of the uterus. Uterine (maternal) blood vessels rupture during the later part of pregnancy as the uterus begins to gradually dilate. The mother may bleed to death, and the fetus will also be placed in jeopardy because of the compromised blood supply. Because the placenta blocks the cervical opening, delivery is usually accomplished by cesarean section. This condition is clinically associated with **repeated episodes of bright, red vaginal bleeding**.

H. **Placental abruption** occurs when a normally implanted placenta prematurely separates from the uterus before delivery of the fetus. It is associated with maternal hypertension.

I. **Placental accreta** occurs when there is abnormal adherence of the chorionic villi to the uterine wall with partial or complete absence of the decidua basalis.

J. **Placental percreta** occurs when the chorionic villi penetrate the myometrium to reach the perimetrium.

K. Premature rupture of the amniochorionic membrane is the most common cause of premature labor and oligohydramnios. It is commonly referred to as "breaking of the waters."

L. Amniotic band syndrome (Figure 6.10) occurs when bands of amniotic membrane encircle and constrict various parts of the fetus, causing limb amputations and craniofacial anomalies. This photograph (Figure 6.10) shows amniotic band syndrome with a constriction of the right leg (*arrow*) and amputation of the left leg (*arrow*).

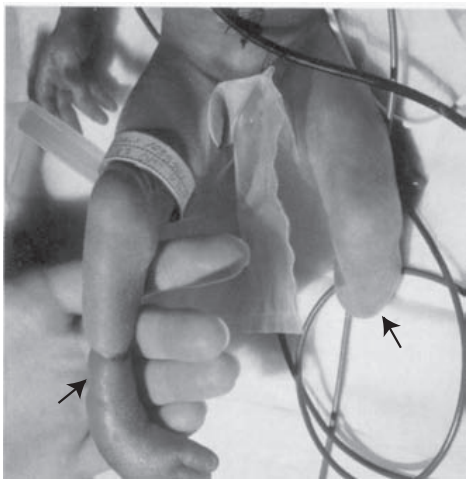

FIGURE 6.10. Amniotic band syndrome.

M. Presence of a single umbilical artery (SUA) within the cord is an abnormal condition that is associated with poor intrauterine fetal growth, prematurity, and cardiovascular anomalies. (Normally two umbilical arteries are present.)

N. Umbilical cord knots (Figure 6.11). The umbilical cord frequently forms loops producing a **false knot**, which is of no clinical significance. However, in some cases, **true knots** form, which may cause fetal death due to fetal anoxia. This photograph (Figure 6.11) shows a **true knot** (*arrow*) of the umbilical cord that caused fetal death.

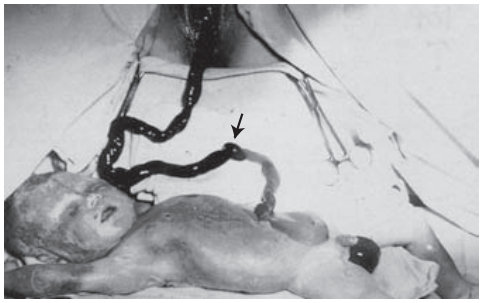

FIGURE 6.11. A true knot.

O. Erythroblastosis fetalis

1. The **Rh factor** is clinically important in pregnancy. If the mother is Rh^-, she will produce Rh antibodies if the fetus is Rh+. This situation will not affect the first pregnancy, but it will affect the second pregnancy with an Rh+ fetus.
2. In the second pregnancy with an Rh^+ fetus, a hemolytic condition of red blood cells (RBCs) occurs, known as **Rh-hemolytic disease of newborn (erythroblastosis fetalis)**.
3. This causes destruction of fetal RBCs, which leads to the release of large amounts of **bilirubin** (a breakdown product of hemoglobin). This causes fetal brain damage due to a condition called kernicterus, which is a pathological deposition of bilirubin in the basal ganglia.
4. **Severe hemolytic disease**, whereby the fetus is severely anemic and demonstrates total body edema (i.e., **hydrops fetalis**), may lead to death. In these cases, an intrauterine transfusion is indicated.
5. **Rh_0(D) immune globulin (RhoGAM, MICRhoGAM)** is a human immunoglobulin (IgG) preparation that contains antibodies against Rh factor and prevents a maternal antibody response to Rh+ cells that may enter the maternal bloodstream of an Rh– mother. This drug is administered to Rh– mothers within 72 hours after the birth of an Rh+ baby to prevent erythroblastosis fetalis during subsequent pregnancies.
6. There are two main treatments for erythroblastosis fetalis:
   a. **Intravascular transfusion (IVT)** of RBCs is indicated for the treatment of severe fetal anemia in preterm fetuses in the following conditions: **RBC alloimmunization** (the most prevalent antibodies are anti-D, anti-K1, and anti-c); **parvovirus infection**, which is due to the arrest of bone marrow precursors; **chronic fetomaternal hemorrhage**, which presents as a perception by the mother of decreased fetal movements; and **inherited RBC disorders** (e.g., α-thalassemia, congenital dyserythropoietic anemia). The access site for IVT is the **umbilical vein at the umbilical cord insertion** into the placenta (using the umbilical arteries is associated with fetal bradycardia) or the **intrahepatic part of the umbilical vein**. IVTs

are performed between **18 and 35 weeks of gestation**. IVTs prior to 18 weeks of gestation are rarely successful because of the small size of anatomical structures and limited visualization. IVTs after 35 weeks of gestation are not done because IVT-related morbidity is greater than morbidity associated with delivery.

b. **Rh_0(D) immune globulin (RhoGAM, MICRhoGAM)** is a human IgG preparation that contains antibodies against Rh factor and prevents a maternal antibody response to Rh+ cells that may enter the maternal bloodstream of an Rh– mother. This drug is administered to Rh– mothers within 72 hours after the birth of an Rh+ baby to prevent erythroblastosis fetalis during subsequent pregnancies.

P. **Oligohydramnios** occurs when there is a low amount of amniotic fluid **(<400 mL in late pregnancy)**. Oligohydramnios may be associated with the inability of the fetus to excrete urine into the amniotic sac due to **renal agenesis**. This results in many fetal deformities (**Potter syndrome**) and **hypoplastic lungs** due to increased pressure on the fetal thorax.

Q. **Polyhydramnios** occurs when there is a high amount of amniotic fluid **(>2,000 mL in late pregnancy)**. Polyhydramnios may be associated with the inability of the fetus to swallow due to **tracheoesophageal fistula**, esophageal **atresia**, or **anencephaly**. Polyhydramnios is commonly associated with **maternal diabetes**.

R. **α-Fetoprotein (AFP)** is "fetal albumin" produced by fetal hepatocytes. AFP is routinely assayed in amniotic fluid and maternal serum between **weeks 14 and 18** of gestation. AFP levels change with gestational age, so proper interpretation of AFP levels depends upon an accurate gestational age.

1. **Elevated AFP levels** are associated with **neural tube defects** (e.g., **spina bifida or anencephaly**), **omphalocele** (which allows fetal serum to leak into the amniotic fluid), and **esophageal** and **duodenal atresia** (which interfere with fetal swallowing).
2. **Reduced AFP levels** are associated with **Down syndrome**.

S. **Preeclampsia and eclampsia**

1. Preeclampsia is a complication of pregnancy characterized by hypertension, edema, and/or proteinuria.
2. Severe preeclampsia refers to the sudden development of **maternal hypertension (>160/110 mm Hg), edema (hands and/or face), and proteinuria (>5 g/24 hours)**, usually after week 32 of gestation (third trimester).
3. Eclampsia includes the additional symptom of convulsions.
4. The pathophysiology of preeclampsia involves a **generalized arteriolar constriction** that affects the brain (seizures and stroke), kidneys (oliguria and renal failure), liver (edema), and small blood vessels (thrombocytopenia and disseminated intravascular coagulation).
5. Treatment of severe preeclampsia involves **magnesium sulfate** (for seizure prophylaxis) and **hydralazine** (blood pressure control); once the patient is stabilized, delivery of the fetus should ensue immediately.
6. Risk factors include the following: nulliparity, diabetes, hypertension, renal disease, twin gestation, or hydatidiform mole (produces **first trimester preeclampsia**).

Study Questions for Chapter 6

1. During the later stages of pregnancy, maternal blood is separated from fetal blood by the

(A) syncytiotrophoblast only
(B) cytotrophoblast only
(C) syncytiotrophoblast and cytotrophoblast
(D) syncytiotrophoblast and fetal endothelium
(E) cytotrophoblast and fetal endothelium

2. The maternal and fetal components of the placenta are

(A) decidua basalis and secondary chorionic villi
(B) decidua capsularis and secondary chorionic villi
(C) decidua parietalis and tertiary chorionic villi
(D) decidua capsularis and villous chorion
(E) decidua basalis and villous chorion

3. The intervillous space of the placenta contains

(A) maternal blood
(B) fetal blood
(C) maternal and fetal blood
(D) amniotic fluid
(E) maternal blood and amniotic fluid

4. A young insulin-dependent diabetic woman in her first pregnancy is concerned that her daily injection of insulin will cause a congenital malformation in her baby. What should the physician tell her?

(A) Insulin is highly teratogenic; discontinue treatment
(B) Insulin does not cross the placental membrane
(C) Insulin crosses the placental membrane but is degraded rapidly
(D) Insulin will benefit her baby by increasing glucose metabolism
(E) Insulin crosses the placental membrane but is not teratogenic

5. What is a normal amount of amniotic fluid at term?

(A) 50 mL
(B) 500 mL
(C) 1000 mL
(D) 1500 mL
(E) 2000 mL

6. Which of the following does not pass through the primitive umbilical ring?

(A) Allantois
(B) Amnion
(C) Yolk sac
(D) Connecting stalk
(E) Space connecting the intraembryonic and extraembryonic coeloms

7. Which of the following best describes the placental components of dizygotic twins?

(A) One placenta, two amniotic sacs, one chorion
(B) One placenta, two amniotic sacs, two chorions
(C) Two placentas, two amniotic sacs, one chorion
(D) Two placentas, two amniotic sacs, two chorions
(E) One placenta, two amniotic sacs, two chorions

8. A 26-year-old pregnant woman experiences repeated episodes of bright red vaginal bleeding at week 28, week 32, and week 34 of pregnancy. The bleeding spontaneously subsided each time. Use of ultrasound shows that the placenta is located in the lower right portion of the uterus over the internal os. What is the diagnosis?

(A) Hydatidiform mole
(B) Vasa previa
(C) Placenta previa
(D) Placental abruption
(E) Premature rupture of the amniochorionic membrane

9. A 19-year-old woman in week 32 of a complication-free pregnancy is rushed to the emergency department because of profuse vaginal bleeding. The bleeding subsides, but afterward no fetal heart sounds can be heard, indicating intrauterine fetal death. The woman goes into labor and delivers a stillborn infant. On examination of the afterbirth, a velamentous placenta

is detected. Although not much can be done at this point, what is the diagnosis?

(A) Placenta previa
(B) Vasa previa
(C) Hydatidiform mole
(D) Premature rupture of the amniochorionic membrane
(E) Amniotic band syndrome

10. A 32-year-old pregnant woman at 30 weeks of gestation comes to her physician because of excess weight gain in a 2-week period. Ultrasonography reveals polyhydramnios. Which fetal abnormality is most likely responsible for the polyhydramnios?

(A) Bilateral kidney agenesis
(B) Umbilical cord knots
(C) Velamentous placenta
(D) Hypoplastic lungs
(E) Esophageal atresia

11. A 25-year-old pregnant woman at 17 weeks of gestation comes to her OB/GYN for a normal examination. During routine blood tests, her serum α-fetoprotein (AFP) concentration is found to be markedly decreased for her gestational age. Which abnormality will the physician need to rule out based on these low AFP levels?

(A) Spina bifida
(B) Anencephaly
(C) Omphalocele
(D) Down syndrome
(E) Esophageal atresia

Answers and Explanations

1. **D.** During the later stages of pregnancy, the placental membrane becomes very thin and consists of two layers—the syncytiotrophoblast and the fetal endothelium.
2. **E.** The placenta is a unique organ, in that it is a composite of tissue from two different sources—the mother and fetus. The maternal component is the decidua basalis, and the fetal component is the villous chorion.
3. **A.** The intervillous space contains only maternal blood as the spiral arteries of the endometrium penetrate the outer cytotrophoblast shell.
4. **B.** Insulin, like all protein hormones, does not cross the placental membrane in significant amounts.
5. **C.** The normal amount of amniotic fluid at term is 1000 mL. However, the amount of amniotic fluid at various stages of pregnancy can be indicative of congenital malformations. Oligohydramnios (400 mL in late pregnancy) may be indicative of renal agenesis. Polyhydramnios (2000 mL in late pregnancy) may be indicative of either anencephaly or esophageal atresia.
6. **B.** The amnion does not pass through the primitive umbilical ring. As craniocaudal folding occurs, the amnion becomes the outer covering of the umbilical cord.
7. **D.** Dizygotic twins and 35% of monozygotic twins have two placentas, two amniotic sacs, and two chorions ("222").
8. **C.** A placenta implanted in the lower part of the uterus near the internal os is called placenta previa. The repeated episodes of bright-red vaginal bleeding are caused by the gradual dilation of the uterus in the later stages of pregnancy. As the uterus dilates, spiral arteries and veins supplying the placenta are ruptured. The mother may bleed to death, and the fetus is placed in jeopardy because of the compromised maternal blood flow.
9. **B.** A velamentous placenta occurs when umbilical blood vessels abnormally travel through the amniochorionic membrane before reaching the placenta proper. If the vessels cross the internal os, a serious condition called vasa previa exists. As the fetus grows during pregnancy and the amniochorionic membrane stretches, the umbilical vessels may rupture. When that happens, the fetus will bleed to death. The mother is in no danger of bleeding to death in vasa previa because only the umbilical vessels rupture.
10. **E.** Polyhydramnios is associated with the inability of the fetus to swallow because of esophageal atresia or anencephaly. Polyhydramnios can also result from absorption defects such as duodenal atresia. The inability of the embryo to swallow the amniotic fluid means that the fluid cannot be absorbed into the fetal blood and removed by the placenta and passed into the maternal blood.
11. **D.** Reduced AFP levels are associated with Down syndrome. All of the other defects (neural tube defects such as spina bifida and anencephaly, omphalocele, and esophageal atresias) are associated with elevated AFP levels.

chapter 7

Nervous System

I. OVERVIEW

A. **Central nervous system (CNS)** is formed in week 3 of development, during which time the **neural plate** develops. The neural plate consists of **neuroectoderm** and becomes the **neural tube**, which gives rise to the brain and spinal cord.

B. **Peripheral nervous system (PNS)** is derived from three sources:
1. Neural crest cells (see Section III)
2. Neural tube, which gives rise to all preganglionic autonomic nerves (sympathetic and parasympathetic) and all nerves (α-motoneurons and γ-motoneurons) that innervate skeletal muscles
3. Mesoderm, which gives rise to the dura mater and to connective tissue investments of peripheral nerve fibers (endoneurium, perineurium, and epineurium)

II. DEVELOPMENT OF THE NEURAL TUBE (FIGURE 7.1)

Neurulation refers to the formation and closure of the neural tube. **BMP-4** (bone morphogenetic protein), **noggin** (an inductor protein), **chordin** (an inductor protein), **FGF-8** (fibroblast growth factor), and **N-CAM** (neural cell adhesion molecule) play a role in neurulation. The events of neurulation occur as follows:

A. The **notochord** induces the overlying ectoderm to differentiate into **neuroectoderm** and form the **neural plate**. The notochord forms the **nucleus pulposus** of the intervertebral disk in the adult.

B. The neural plate folds to give rise to the **neural tube**, which is open at both ends at the **anterior** and **posterior neuropores**. The anterior and posterior neuropores connect the lumen of the neural tube with the amniotic cavity.
1. The **anterior neuropore** closes during week 4 (day 25) and becomes the **lamina terminalis**. Failure of the anterior neuropore to close results in upper neural tube defects (NTDs; e.g., **anencephaly**).
2. The **posterior neuropore** closes during week 4 (day 27). Failure of the posterior neuropore to close results in lower NTDs (e.g., **spina bifida with myeloschisis**).

C. As the neural plate folds, some cells differentiate into **neural crest cells**.

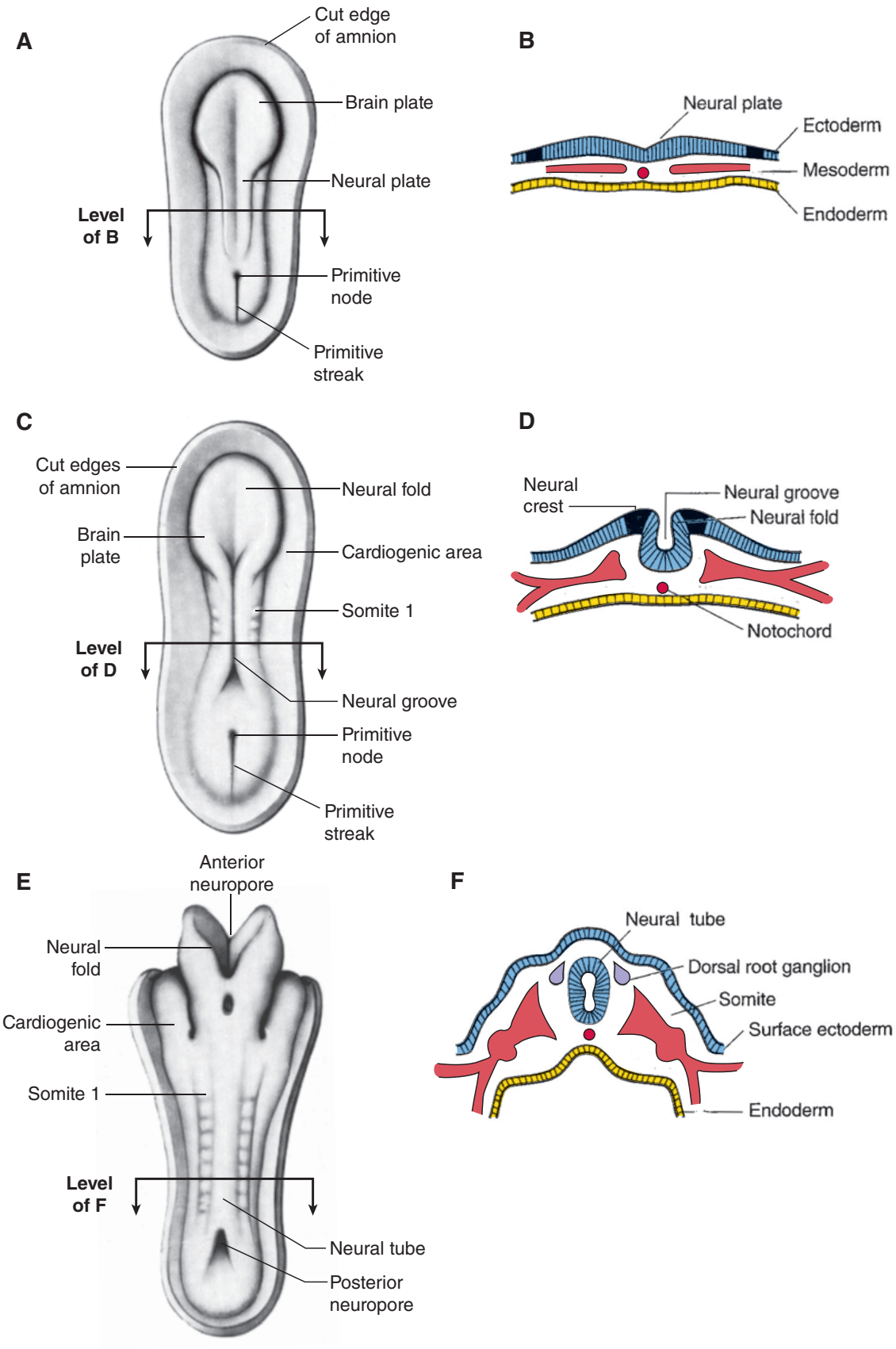

FIGURE 7.1. Development of the neural tube. **(A, B)** Neural plate stage. **(A)** Dorsal view of a human embryo. **(B)** Transverse section of a human embryo at the level shown in panel A. **(C, D)** Neural groove stage. **(C)** Dorsal view of a human embryo. **(D)** Transverse section of a human embryo at the level shown in panel C. **(E, F)** Early neural tube stage. **(E)** Dorsal view of a human embryo. **(F)** Transverse section of a human embryo at the level shown in panel E.

D. The rostral part of the neural tube becomes the adult **brain**.

E. The caudal part of the neural tube becomes the adult **spinal cord**.

F. The lumen of the neural tube gives rise to the **ventricular system** of the brain and **central canal** of the spinal cord.

III. NEURAL CREST CELLS (FIGURE 7.1)

The neural crest cells differentiate from cells located along the lateral border of the neural plate, which is mediated by **BMP-4** and **BMP-7**. Neural crest cells undergo a prolific migration throughout the embryo (both the cranial region and trunk region) and ultimately differentiate into a wide array of adult cells and structures (see Chapter 4, Table 4.1).

A. Cranial neural crest cells

1. There is a remarkable relationship between the origin of cranial neural crest cells from the rhombencephalon (hindbrain) and their final migration into pharyngeal arches (see Chapter 12, Table 12.1).
2. The rhombencephalon is divided into eight segments called **rhombomeres (R1–R8)**.
3. Cranial neural crest cells from R1 and R2 migrate into pharyngeal arch 1 (which also receives neural crest cells from the midbrain area).
4. Cranial neural crest cells from R4 migrate into pharyngeal arch 2.
5. Cranial neural crest cells from R6 and R7 migrate into pharyngeal arch 3.
6. Cranial neural crest cells differentiate into the following adult cells and structures:
   a. **Pharyngeal arch skeletal and connective tissue components**
   b. **Bones of neurocranium**
   c. **Pia and arachnoid**
   d. **Parafollicular (C) cells of thyroid**
   e. **Aorticopulmonary septum**
   f. **Odontoblasts (dentin of teeth)**
   g. **Sensory ganglia of cranial nerve (CN) V, CN VII, CN IX, and CN X**
   h. **Ciliary (CN III), pterygopalatine (CN VII), submandibular (CN VII), and otic (CN IX) parasympathetic ganglia**.

B. Trunk neural crest cells

1. Trunk neural crest cells extend from somite 6 to the most caudal somites and migrate in a dorsolateral, ventral, and ventrolateral direction throughout the embryo.
2. Trunk neural crest cells differentiate into the following adult cells and structures:
   a. **Melanocytes**
   b. **Schwann cells**
   c. **Chromaffin cells of adrenal medulla**
   d. **Dorsal root ganglia**
   e. **Sympathetic chain ganglia**
   f. **Prevertebral sympathetic ganglia**
   g. **Enteric parasympathetic ganglia of the gut (Meissner and Auerbach; CN X)**
   h. **Abdominal/pelvic cavity parasympathetic ganglia**.

C. Clinical considerations.

Neurocristopathy is a term used to describe any disease related to maldevelopment of neural crest cells.

1. **Medullary carcinoma of thyroid (MC).** MC is an endocrine neoplasm of the parafollicular (C) cells of neural crest origin that secrete calcitonin. The carcinoma cells are usually arranged in cell nests surrounded by bands of stroma containing amyloid. MC can be either sporadic (80% of cases) or familial (20% of cases). The familial type of MC is associated with the **MEN (multiple endocrine neoplasia) 2A and 2B syndromes**. The familial MEN type 2A syndrome consists of

medullary carcinoma of the thyroid, parathyroid adenoma, and a pheochromocytoma. The familial MEN type 2B syndrome consists of medullary carcinoma of the thyroid, mucosal neuromas of the lips and tongue, pheochromocytoma, and a marfanoid habitus. The MEN syndrome is an autosomal dominant genetic disorder caused by a mutation in the ***RET* protooncogene** on **chromosome 10q11.2** for the **ret receptor tyrosine kinase**. Mutations in the *RET* protooncogene result in a **gain-of-function mutation**, whereby the ret receptor tyrosine kinase becomes constitutively activated.

2. **Schwannoma.** A schwannoma is a benign tumor of Schwann cells of neural crest origin. These tumors are well-circumscribed, encapsulated masses that may or not be attached to the nerve. The most common location within the cranial vault is at the cerebellopontine angle near the vestibular branch of CN VIII (often referred to as an **acoustic neuroma**). **Clinical features include** tinnitus and hearing loss. CN V (trigeminal nerve) is also commonly affected.
3. **Neurofibromatosis type 1 (NF1; von Recklinghausen disease; Figure 7.2).** NF1 is a relatively common autosomal dominant genetic disorder caused by a mutation in the ***NF1* gene** on **chromosome 17q11.2** for the **neurofibromin** protein. More than 500 different mutations of the *NF1* gene have been identified, which include **missense, nonsense**, and **frameshift mutations, whole-gene deletions, intragenic deletions**, and **RNA-splicing mutations**, all of which result in a **loss-of-function mutation**. Neurofibromin downregulates **p21 ras oncoprotein**, so the *NF1* gene belongs to the family of **tumor-suppressor genes** and regulates cAMP levels. **Clinical features include** multiple neural tumors (called **neurofibromas**) that are widely dispersed over the body and reveal proliferation of all elements of a peripheral nerve, including neurites, fibroblasts, and Schwann cells of neural crest origin, numerous pigmented skin lesions (called **café au lait spots**) probably associated with melanocytes of neural crest origin, axillary and inguinal freckling, scoliosis, vertebral dysplasia, and pigmented iris hamartomas (called **Lisch nodules**). The photograph (Figure 7.2) shows a woman with generalized neurofibromas on the face and arms.

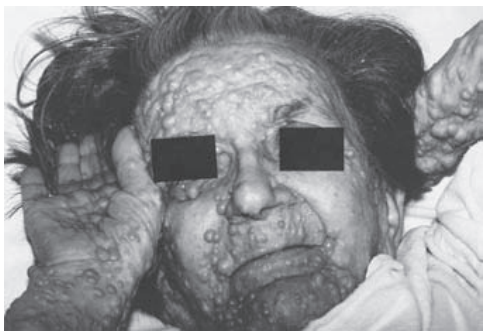

FIGURE 7.2. Neurofibromatosis type 1; von Recklinghausen disease.

4. **Waardenburg syndrome (WS; Figure 7.3)** is an autosomal dominant genetic disorder caused by a mutation in either the ***PAX3* gene** on **chromosome 2q35** (for type I WS) encoding for the **paired box protein PAX3** or the ***MITF* gene** on **chromosome 3p14.3-p14.1** (for type II WS) encoding for the **microphthalmia-associated transcription factor**. Paired box protein gene *PAX3* is one of a family of nine human PAX genes coding for **DNA-binding transcription factors** that are expressed in the early embryo. The mutations of the *PAX3* gene include **missense, nonsense, and frameshift mutations, whole-gene deletions, intragenic deletions**, and **RNA-splicing mutations**, all of which result in a **loss-of-function mutation. Clinical features include** dystopia canthorum (malposition of the eyelid), growing together of eyebrows, lateral displacement of lacrimal puncta, a broad nasal root, heterochromia of the iris, congenital deafness or hearing impairment, and piebaldism, including a white forelock and a triangular area of hypopigmentation. The photograph (Figure 7.3) shows a woman with a white forelock and bilateral profound hearing loss.

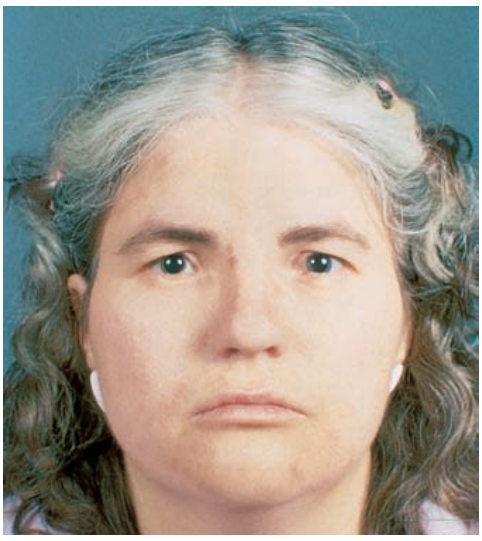

FIGURE 7.3. Waardenburg syndrome.

5. **CHARGE association.** The CHARGE association is understandable only if the wide distribution of neural crest cell derivatives is appreciated. The cause of CHARGE is unknown, but it seems to involve an insult during the second month of gestation, probably involving the neural crest cells. **Clinical features include c**oloboma of the retina, lens, or choroid; **h**eart defects (e.g., tetralogy of Fallot, ventricular septal defect [VSD], patent ductus arteriosus [PDA]); **a**tresia choanae; **r**etardation of growth; **g**enital abnormalities in male infants (e.g., cryptorchidism, microphallus); and **e**ar abnormalities or deafness.
6. **Hirschsprung disease.** See Chapter 10, Section IV.B.
7. **Cleft palate and lip.** See Chapter 12, Sections VIII.G and VIII.H.
8. **DiGeorge syndrome.** See Chapter 12, Section VIII.I.
9. **Pheochromocytoma.** See Chapter 13, Section IX.C.
10. **Neuroblastoma.** See Chapter 13, Section IX.C.

IV. PLACODES

Placodes are localized thickenings of surface **ectoderm**. They give rise to cells that migrate into underlying mesoderm and develop into sensory receptive organs of cranial nerves (CN I and CN VIII) and the lens of the eye. There are three placodes:

A. **Nasal (olfactory) placode.** The nasal (olfactory) placodes differentiate into neurosensory cells that give rise to the **olfactory nerve (CN I)** and induce formation of olfactory bulbs.

B. **Otic placode.** The otic placodes give rise to the **otic vesicle**, which forms the following:
1. Utricle, semicircular ducts, and vestibular ganglion of CN VIII
2. Saccule, cochlear duct (organ of Corti), spiral ganglion of CN VIII
3. Vestibulocochlear nerve (CN VIII)

C. **Lens placode.** The lens placode gives rise to the **lens** and is induced by the optic vesicles.

V. VESICLE DEVELOPMENT OF THE NEURAL TUBE (FIGURE 7.4)

A. The three **primary brain vesicles** and two associated **flexures** develop during week 4.
1. Primary brain vesicles
   a. **Prosencephalon (forebrain)** is associated with the appearance of the **optic vesicles** and gives rise to the **telencephalon** and **diencephalon**.
   b. **Mesencephalon (midbrain)** remains as the **mesencephalon**.
   c. **Rhombencephalon (hindbrain)** gives rise to the **metencephalon** and **myelencephalon**.
2. **Flexures**
   a. **Cephalic flexure (midbrain flexure)** is located between the prosencephalon and the rhombencephalon.
   b. **Cervical flexure** is located between the rhombencephalon and the future spinal cord.

B. The five **secondary brain vesicles** become visible in week 6 of development and form various adult derivatives of the brain.
1. **Telencephalon** gives rise to the cerebral hemispheres, caudate, and putamen.
2. **Diencephalon** gives rise to the epithalamus, subthalamus, thalamus, hypothalamus, mammillary bodies, neurohypophysis, pineal gland, globus pallidus, retina, iris, ciliary body, optic nerve (CN II), optic chiasm, and optic tract.
3. **Mesencephalon** gives rise to the midbrain.
4. **Metencephalon** gives rise to the pons and cerebellum.
5. **Myelencephalon** gives rise to the medulla.

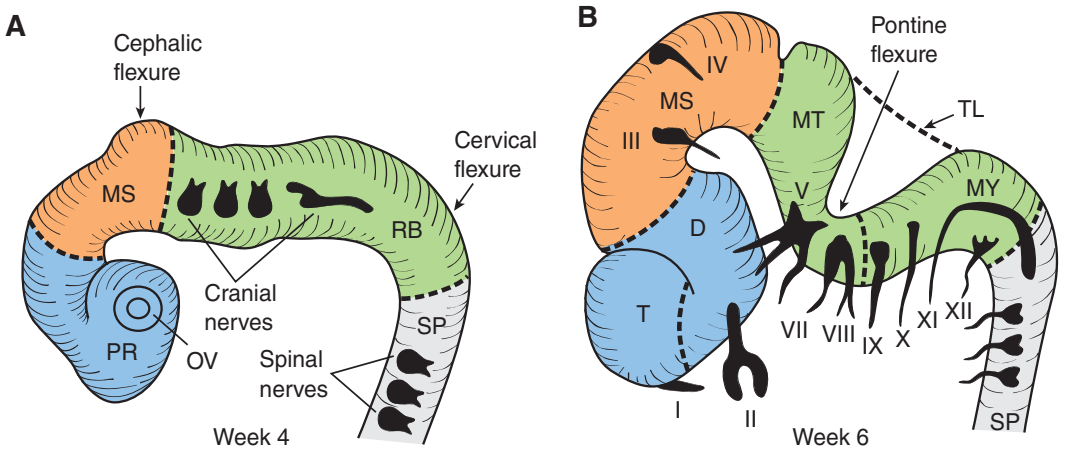

C

BRAIN VESICLES AND THEIR ADULT DERIVATIVES

Primary Vesicles	Secondary Vesicles	Adult Derivatives
Prosencephalon	**Telencephalon**	Cerebral hemispheres, caudate, putamen, amygdaloid claustrum, lamina terminalis, olfactory bulbs, hippocampus
	Diencephalon	Epithalamus, subthalamus, thalamus, hypothalamus, mammillary bodies, neurohypophysis, pineal gland, globus pallidus, retina, iris, ciliary body, optic nerve (CN II), optic chiasm, optic tract
Mesencephalon	**Mesencephalon**	Midbrain
Rhombencephalon	**Metencephalon**	Pons, cerebellum
	Myelencephalon	Medulla

FIGURE 7.4. Schematic illustrations of the developing brain vesicles. **A.** Three-vesicle stage of the brain in a 4-week-old embryo. Divisions are indicated by dashed lines. PR = prosencephalon (*blue*); MS = mesencephalon (*orange*); RB = rhombencephalon (*green*); SP = spinal cord; OV = optic vesicle. **B.** Five-vesicle stage of the brain in a 6-week-old embryo. Divisions are indicated by dashed lines. Cranial nerves (CN) are indicated by Roman numerals. CN VI is not shown because it exits the brain stem from the ventral surface. T = telencephalon; D = diencephalon; MS = mesencephalon; MT = metencephalon; MY = myelencephalon; TL = tela choroidea; SP = spinal cord. **C.** Table indicating the brain vesicles and their adult derivatives.

VI. HISTOGENESIS OF THE NEURAL TUBE

The cells of the neural tube are neuroectodermal (or neuroepithelial) cells that give rise to the following cell types:

A. Neuroblasts form all neurons found in the CNS.

B. Glioblasts (spongioblasts) are, for the most part, formed after cessation of neuroblast formation. Radial glial cells are an exception and develop before neurogenesis is complete. Glioblasts form the supporting cells of the CNS and include the following:

1. **Astrocytes (Figure 7.5)** have the following characteristics and functions: project foot processes to capillaries that contribute to the blood–brain barrier, play a role in the metabolism of neurotransmitters (e.g., glutamate, γ-aminobutyrate [GABA], serotonin), buffer the $[K^+]$ of the CNS extracellular space, form the external and internal glial-limiting membrane in the CNS, form glial scars

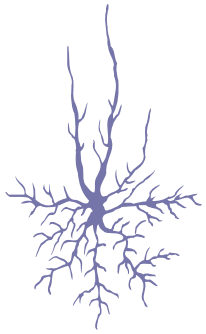

FIGURE 7.5. Protoplasmic astrocyte.

in a damaged area of the CNS (i.e., astrogliosis), undergo hypertrophy and hyperplasia in reaction to CNS injury, and contain the **glial fibrillary acidic protein (GFAP)** and **glutamine synthetase**, which are good markers for astrocytes. The drawing (Figure 7.5) shows a protoplasmic astrocyte.

2. **Oligodendrocytes (Figure 7.6)** produce the **myelin** in the CNS. A single oligodendrocyte can myelinate several (up to 30) axons. The drawing (Figure 7.6) shows an oligodendrocyte.
3. **Ependymocytes (Figure 7.7)** line the central canal and ventricles of the brain. These cells are not joined by tight junctions, so that exchange between the cerebrospinal fluid (CSF) and CNS extracellular fluid occurs freely. The drawing (Figure 7.7) shows ependymocytes lining the ventricle of the brain.
4. **Tanycytes (Figure 7.8)** are modified ependymal cells that mediate transport between CSF in the ventricles and the neuropil. These cells usually project to hypothalamic nuclei that regulate the release of gonadotropic hormones from the adenohypophysis. The drawing (Figure 7.8) shows a tanycyte within the ependymal lining of the ventricle.
5. **Choroid plexus cells (Figure 7.9)** are a continuation of the ependymal lining that is reflected over the choroid plexus villi. Choroid plexus cells are modified ependymocytes and **secrete CSF** by selective transport of molecules from blood coming from the highly vascularized pia mater (called the tela choroidea). These cells are joined by **tight junctions (zonula occludens)**, which are the basis of the **blood–CSF barrier**. CSF is normally **clear**. A **yellow color (xanthochromia)** indicates previous bleeding (subarachnoid hemorrhage) or increased protein. A **pinkish color** is usually due to a bloody tap. **Turbidity** is due to the presence of leukocytes. The drawing (Figure 7.9) shows choroid plexus cells.

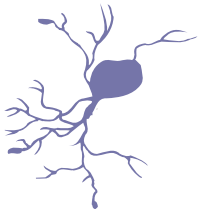

FIGURE 7.6. Oligodendrocyte.

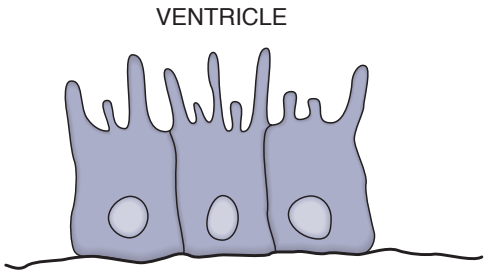

FIGURE 7.7. Ependymal cells.

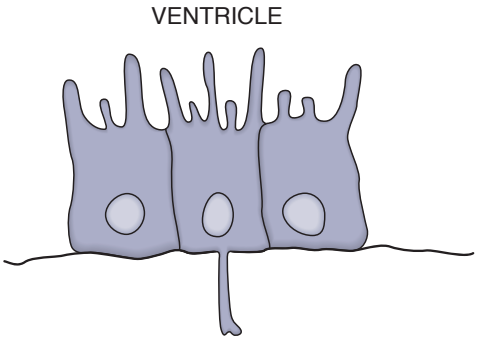

FIGURE 7.8. Tanycyte.

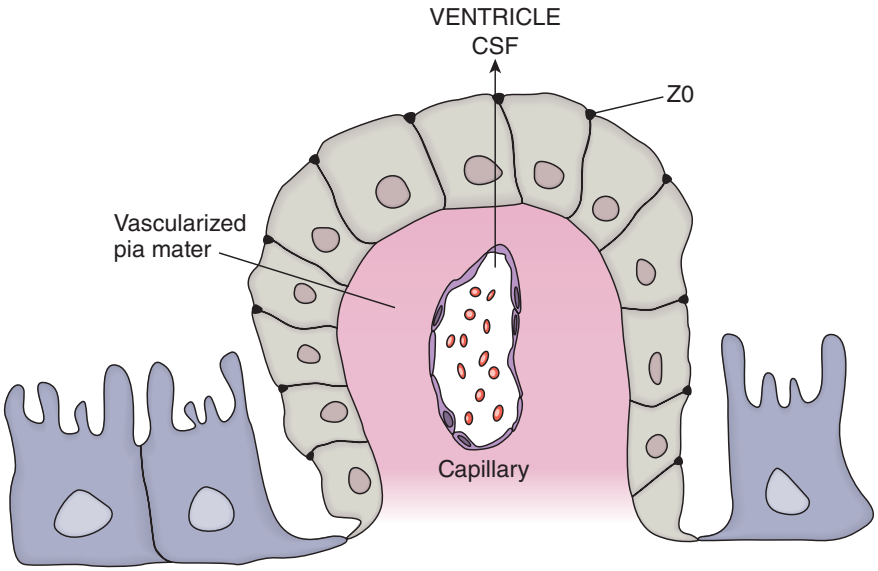

FIGURE 7.9. Choroid plexus cells. CSF = cerebrospinal fluid; Z0 = zonula occludens.

6. **Microglia (Hortega cells; Figure 7.10)** are the macrophages of the CNS, which arise from monocytes and invade the developing nervous system in week 3 along with the developing blood vessels. The drawing (Figure 7.10) shows a microglial cell.

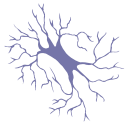

FIGURE 7.10. Microglial cell.

VII. LAYERS OF THE EARLY NEURAL TUBE (FIGURE 7.11)

A. Ventricular zone

1. The early neural tube consists of neuroectoderm arranged in a pseudostratified columnar arrangement.
2. A first wave of proliferation and differentiation of the neuroectoderm gives rise to **neuroblasts**, which migrate into the intermediate zone.
3. A second wave of proliferation and differentiation of the neuroectoderm gives rise to **glioblasts**, which migrate into the intermediate zone and marginal zone.
4. The neuroectoderm that remains in the ventricular zone gives rise to **ependymocytes, tanycytes**, and **choroid plexus cells**.

B. Intermediate zone

1. The intermediate zone contains **neuroblasts**, which differentiate into **neurons** with dendrites and axons.
2. The intermediate zone also contains **glioblasts**, which differentiate into **astrocytes** and **oligodendrocytes**.
3. The intermediate zone forms the **gray matter** of the CNS.
4. The intermediate zone is divided into the **alar plate**, associated with sensory (afferent) functions, and the **basal plate**, associated with motor (efferent) functions.

C. Marginal zone

1. The marginal zone contains **axons** from neurons within the intermediate zone.
2. The marginal zone also contains **glioblasts**, which differentiate into **astrocytes** and **oligodendrocytes**.
3. The marginal zone forms the **white matter** of the CNS.

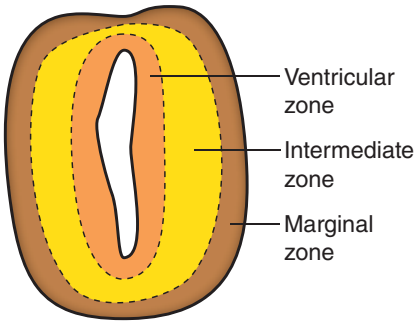

FIGURE 7.11. Layers of the early neural tube.

VIII. DEVELOPMENT OF THE SPINAL CORD (FIGURE 7.12)

The spinal cord develops from the neural tube caudal to the fourth pair of somites.

A. Alar (sensory) plate

1. The alar plate is a **dorsolateral** thickening of the intermediate zone of the neural tube.
2. The alar plate gives rise to **sensory neuroblasts of the dorsal horn** (general somatic afferent [GSA] and general visceral afferent [GVA] cell regions).
3. The alar plate receives axons from the dorsal root ganglia that become the **dorsal (sensory) roots**.
4. The alar plate becomes the **dorsal horn of the spinal cord**.

B. Basal (motor) plate

1. The basal plate is a **ventrolateral** thickening of the intermediate zone of the neural tube.
2. The basal plate gives rise to **motor neuroblasts of the ventral and lateral horns** (general somatic efferent [GSE] and general visceral efferent [GVE] cell regions).
3. The basal plate projects axons from motor neuroblasts, which exit the spinal cord and become the **ventral (motor) roots**.
4. The basal plate becomes the **ventral horn of the spinal cord**.

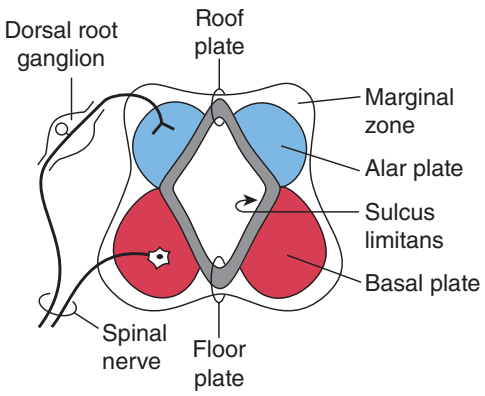

FIGURE 7.12. Development of the spinal cord.

C. Sulcus limitans (SL)

1. The SL is a **longitudinal groove** in the lateral wall of the neural tube that appears during week 4 of development and separates the alar and basal plates.
2. The SL disappears in the adult spinal cord but is retained in the rhomboid fossa of the brain stem.
3. The SL extends from the spinal cord to the rostral midbrain.

D.

The **roof plate** is the nonneural roof of the central canal, which connects the two alar plates.

E.

The **floor plate** is the nonneural floor of the central canal, which connects the two basal plates. The floor plate contains the ventral white commissure.

F. Myelination

1. Myelination of the spinal cord begins during month 4 in the ventral (motor) roots.
2. **Oligodendrocytes** accomplish myelination in the **CNS**.
3. **Schwann cells** accomplish myelination in the **PNS**.
4. Myelination of the corticospinal tracts is not completed until the end of 2 years of age (i.e., when the corticospinal tracts become myelinated and functional).
5. Myelination of the **association neocortex** extends to 30 years of age.

G. Positional changes of the spinal cord

1. **At week 8** of development, the spinal cord extends the length of the vertebral canal.
2. **At birth**, the **conus medullaris** extends to the level of the third lumbar vertebra (**L3**).
3. **In adults**, the conus medullaris terminates at **L1–L2 interspace**.
4. Disparate growth between the vertebral column and the spinal cord results in the formation of the **cauda equina**, consisting of dorsal and ventral roots (L3–Co), which descends below the level of the conus medullaris.
5. Disparate growth results in the nonneural **filum terminale**, which anchors the spinal cord to the coccyx.

IX. DEVELOPMENT OF THE MYELENCEPHALON (FIGURE 7.13)

The myelencephalon develops from the caudal **rhombencephalon** and gives rise to the **medulla oblongata**.

A. Alar plate sensory neuroblasts give rise to the following:

1. **Cochlear and vestibular nuclei**, which form the special somatic afferent (SSA) column and in the medullopontine junction

2. **Spinal trigeminal nucleus**, which forms the GSA column
3. **Solitary nucleus**, which forms the special visceral afferent (SVA; taste) and GVA columns
4. **Dorsal column nuclei**, which consist of the gracile and cuneate nuclei
5. **Inferior olivary nuclei**, which are cerebellar relay nuclei and are derived from the alar plate by migrating to a ventral position (see *arrow* in Figure 7.13)

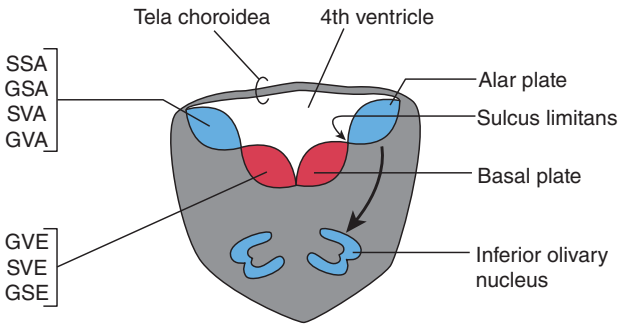

FIGURE 7.13. Development of myelencephalon. SSA = special somatic afferent; GSA = general somatic afferent; SVA = special visceral afferent; GVA = general visceral afferent; GVE = general visceral efferent; SVE = special visceral efferent; GSE = general somatic efferent.

B. Basal plate motor neuroblasts give rise to the following:

1. Dorsal motor nucleus of the vagus nerve (CN X) and the inferior salivatory nucleus of the glossopharyngeal nerve (CN IX), which form the GVE column
2. Nucleus ambiguus, which forms the special visceral efferent (SVE) column (CN IX, CN X, and CN XI)
3. Hypoglossal nucleus, which forms the GSE column

C. The **roof plate** forms the roof of the fourth ventricle. The roof plate is called the **tela choroidea**, which is a monolayer of ependymal cells covered with pia mater. The tela choroidea is invaginated by pial blood vessels to form the **choroid plexus** of the fourth ventricle.

D. The **open (rostral) medulla** extends from the obex to the stria medullares of the rhomboid fossa. The lateral walls of the rostral medulla open like a book and form the rhomboid fossa (i.e., the floor of the fourth ventricle) due to the formation of the pontine flexure.

X. DEVELOPMENT OF THE METENCEPHALON

The metencephalon develops from the rostral **rhombencephalon** and gives rise to the **pons** and **cerebellum**.

A. Pons (Figure 7.14)

1. **Alar plate sensory neuroblasts** give rise to the following:
   a. **Cochlear and vestibular nuclei**, which form the SSA column of CN VIII
   b. **Spinal and principal trigeminal nuclei**, which form the GSA column of CN V
   c. **Solitary nucleus**, which forms the SVA (taste) and GVA columns of CN VII
   d. **Pontine nuclei**, which consist of cerebellar relay nuclei (pontine gray) and are derived from the alar plate by migrating to a ventral position (*arrow* in Figure 7.14)

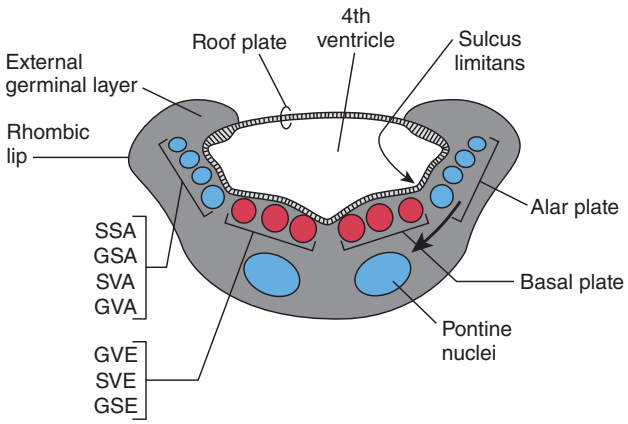

FIGURE 7.14. Development of the metencephalon: pons. SSA = special somatic afferent; GSA = general somatic afferent; SVA = special visceral afferent; GVA = general visceral afferent; GVE = general visceral efferent; SVE = special visceral efferent; GSE = general somatic efferent.

2. **Basal plate motor neuroblasts** give rise to the following:
   a. **Superior salivatory nucleus**, which forms the GVE column of CN VII
   b. **Facial (CN VII) and motor trigeminal (CN V) nuclei**, which form the SVE column
   c. **Abducent (CN VI) nucleus**, which forms the GSE column
3. **Base of the pons**. The base of the pons contains the following:
   a. Pontine nuclei from the alar plate
   b. Corticobulbar, corticospinal, and corticopontine fibers, whose cell bodies are located in the cerebral cortex
   c. Pontocerebellar fibers

B. Cerebellum

1. The cerebellum is formed from the **rhombic lips**, which are the two dorsolateral thickened alar plates.
2. The rhombic lips thicken at week 6 to form the **cerebellar plate**, which has a dumbbell appearance.
3. The cerebellar plate is separated into cranial and caudal portions by a **transverse groove**.
4. The caudal portion forms the **flocculonodular lobe**, which is the most primitive part of the cerebellum.
5. The cranial portion forms the **vermis** and the **cerebellar hemispheres**, both of which undergo extensive formation of **fissures** and **folia**.
6. Like the rest of the neural tube, the rhombic lips consist of neuroectoderm arranged in the ventricular zone, intermediate zone, and marginal zone.
7. In month 3, the neuroectoderm in the ventricular zone undergoes another wave of proliferation to form the **internal germinal layer**. The internal germinal layer gives rise to the following:
   a. **Deep cerebellar nuclei** (i.e., dentate, emboliform, globose, and fastigial nuclei)
   b. **Purkinje cells**
   c. **Golgi cells**
8. Some neuroectodermal cells from the internal germinal layer migrate through the marginal zone to form the **external germinal layer**. The external germinal layer gives rise to the following:
   a. **Basket cells**
   b. **Granule cells**
   c. **Stellate cells**
9. Both the external and internal germinal layers give rise to **astrocytes, Bergmann cells**, and **oligodendrocytes** within the cerebellum.

XI. DEVELOPMENT OF THE MESENCEPHALON (FIGURE 7.15)

The mesencephalon remains unchanged during primary to secondary vesicle formation and gives rise to the **midbrain**.

A. Alar plate sensory neuroblasts gives rise to the **superior colliculi** and the **inferior colliculi** (*arrows* in Figure 7.15 indicate the direction of migration)

B. Basal plate motor neuroblasts give rise to the following:

1. **Edinger-Westphal nucleus of CN III**, which forms the GVE column
2. **Oculomotor (CN III) nucleus**, which forms the GSE column
3. **Substantia nigra** (*arrows* indicate direction of migration)
4. **Red nucleus** (*arrows* indicate direction of migration)

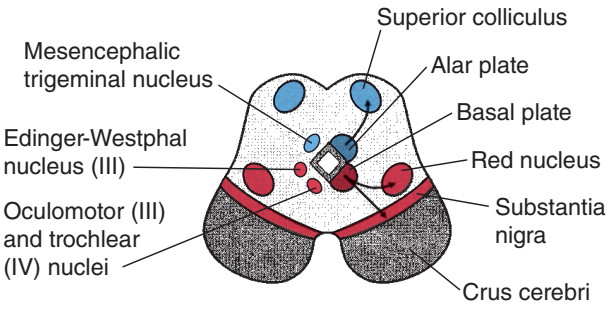

FIGURE 7.15. Transverse section of the development of the midbrain.

C. Crus cerebri contain corticobulbar, corticospinal, and corticopontine fibers, derived from the cerebral cortex of the telencephalon.

D. The **trochlear (CN IV) nucleus** and a portion of the sensory **mesencephalic trigeminal (CN V) nucleus** originate in the metencephalon and secondarily migrate into the mesencephalon.

XII. DEVELOPMENT OF THE DIENCEPHALON, OPTIC STRUCTURES, AND HYPOPHYSIS

A. Diencephalon (Figure 7.16) develops from the prosencephalon within the walls of the primitive third ventricle. The alar plates remain prominent in the prosencephalon, but the basal plates regress. The diencephalon gives rise to the **epithalamus, thalamus, subthalamus**, and **hypothalamus**.

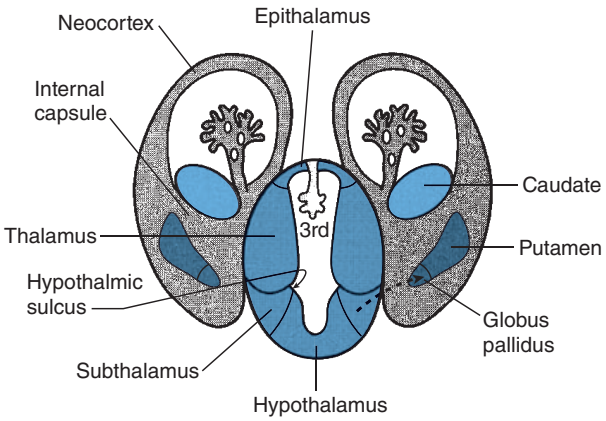

FIGURE 7.16. Transverse section of the development of the forebrain.

1. **Epithalamus** develops from the alar plate and the embryonic roof plate. The epithalamus gives rise to the following: **pineal body (epiphysis), habenular nuclei, habenular commissure, posterior commissure, tela choroidea**, and the **choroid plexus** of the third ventricle.
2. **Thalamus** develops from the alar plate. The thalamus gives rise to the following: **thalamic nuclei, lateral geniculate body**, and the **medial geniculate body**.
3. **Subthalamus** develops from the alar plate. The subthalamus gives rise to the following: **subthalamic nucleus, zona incerta**, and **lenticular and thalamic fasciculi (fields of Fortel)**. Neuroblasts within the subthalamus migrate (*arrow* in Figure 7.16) into the telencephalic white matter to become the globus pallidus.
4. **Hypothalamus** develops from the alar plate and floor plate ventral to the hypothalamic sulcus. The hypothalamus gives rise to the following: **hypothalamic nuclei, mammillary bodies**, and **neurohypophysis**.

B. Optic vesicles, cups, and stalks are derivatives of diencephalon. They give rise to the **retina, iris, ciliary body, optic nerve (CNII), optic chiasm**, and **optic tract** (see Chapter 9).

C. Hypophysis (pituitary gland) (Figure 7.17) is attached to the hypothalamus by the pituitary stalk and consists of the **anterior lobe (adenohypophysis)** and the **posterior lobe (neurohypophysis)**.

1. **Anterior lobe (adenohypophysis)** develops from **Rathke pouch**, which is an ectodermal diverticulum of the primitive oral cavity (**stomodeum**). The diagram (Figure 17.17A) shows a midsagittal view of an embryo at week 6 indicating Rathke pouch and the infundibulum. Remnants of Rathke pouch may give rise to a **craniopharyngioma**. A craniopharyngioma is the most common supratentorial tumor occurring in childhood and is the most common cause of hypopituitarism in children. The MRI (Figure 7.17B) shows a craniopharyngioma (*arrows*), which lies suprasellar in the midline, compressing the optic chiasm and hypothalamus.
2. **Posterior lobe (neurohypophysis)** develops from the **infundibulum**, which is a neuroectodermal ventral evagination of the hypothalamus.

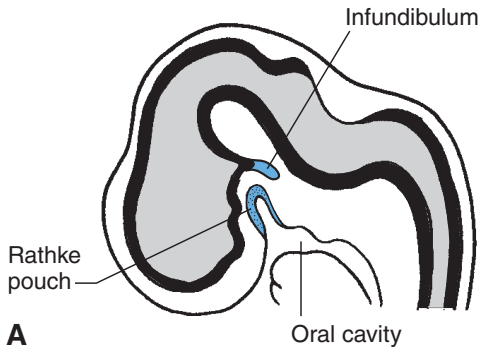

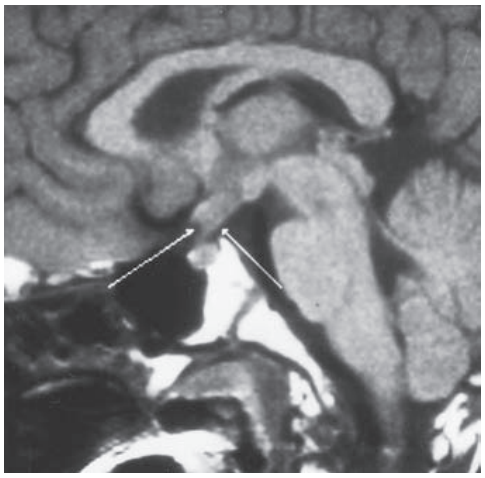

FIGURE 7.17. Hypophysis (pituitary gland).

XIII. DEVELOPMENT OF THE TELENCEPHALON

The telencephalon develops from the prosencephalon. The telencephalon gives rise to the following: **cerebral hemispheres, caudate, putamen, amygdaloid, claustrum, lamina terminalis, olfactory bulbs,** and **hippocampus**.

A. Cerebral hemispheres (Figure 7.18) develop as bilateral evaginations of the lateral walls of the **prosencephalic vesicle** and contain the **cerebral cortex, cerebral white matter, basal ganglia**, and **lateral ventricles**. The cerebral hemispheres are interconnected by three commissures: the **corpus callosum, anterior commissure**, and **hippocampal (fornical) commissure**. Continuous hemispheric growth gives rise to frontal, parietal, occipital, and temporal lobes, which overlie the insula and dorsal brain stem. The diagram (Figure 7.18) shows the development of the cerebral cortex at month 6, month 8, and at term. Note the change in the cerebral cortex from a smooth surface or lissencephalic structure to a convoluted surface or gyrencephalic structure. As growth proceeds, a complex pattern of **sulci (grooves)** and **gyri (elevations)** develops.

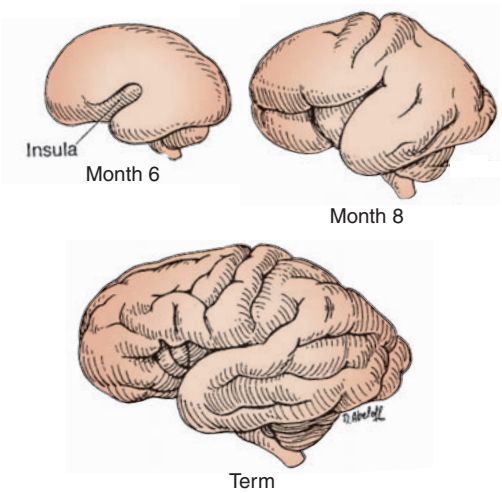

FIGURE 7.18. Development of the cerebral cortex.

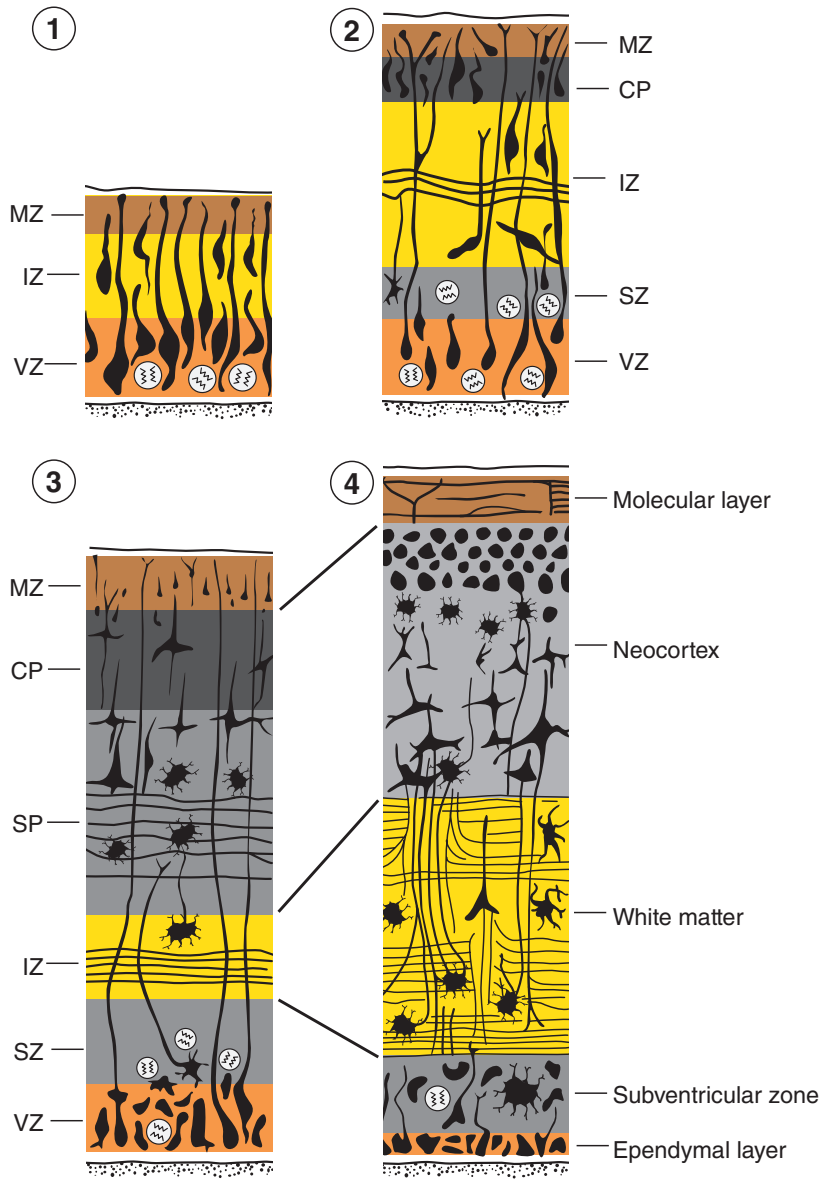

FIGURE 7.19. Cerebral cortex (pallium). MZ = marginal zone; IZ = intermediate zone; VZ = ventricular zone; CP = cortical plate; SP = subplate zone; SZ = subventricular zone.

B. Cerebral cortex (pallium; Figure 7.19)

1. Like the rest of the neural tube, the wall of the telencephalon consists of neuroectoderm arranged in the ventricular zone, intermediate zone, and marginal zone.
2. Neuroblasts from the ventricular zone and the intermediate zone migrate peripherally to form a transient layer called the **cortical plate**.
3. Neuroblasts in the ventricular zone undergo a wave of proliferation to form the **subventricular zone**.
4. Neuroblasts from the subventricular zone migrate peripherally to form the **subplate zone**.
5. The cortical plate and subplate zone together form the **cerebral neocortex**.
6. The intermediate zone becomes devoid of neuroblasts and develops into the **white matter** of the cerebral hemispheres.
7. The marginal zone develops into the **molecular layer** of the cerebral cortex.
8. The cerebral cortex is classified as the **neocortex** and **allocortex**.
   a. **Neocortex (isocortex)** is a six-layered cortex that represents 90% of the cortical mantle.
   b. **Allocortex** is a three-layered cortex that represents 10% of the cortical mantle. The allocortex is subdivided into the **archicortex** (which includes the hippocampal formation) and the **paleocortex** (which includes the olfactory cortex).

9. The diagram (Figure 7.19) shows the temporal sequence (early to late: 1–4, respectively) of cytodifferentiation of the cerebral cortex.

C. Corpus striatum (striatal eminence)

1. The corpus striatum appears in week 5 of development in the floor of the telencephalic vesicle.
2. The corpus striatum gives rise to the basal ganglia: the **caudate nucleus, putamen, amygdaloid nucleus**, and **claustrum**.
3. The corpus striatum is divided into the caudate nucleus and the lentiform nucleus by corticofugal and corticopetal fibers (which make up the internal capsule).
4. The neurons of the globus pallidus (also a basal ganglion) originate in the subthalamus. These neurons then migrate into the telencephalic white matter and become the medial segments of the lentiform nucleus.

D. Commissures are fiber bundles that interconnect the two cerebral hemispheres and cross the midline via the embryonic lamina terminalis (commissural plate).

1. **Anterior commissure** is the first commissure to appear and interconnects the olfactory structures and the middle and inferior temporal gyri.
2. **Hippocampal (fornical) commissure** is the second commissure to appear and interconnects the two hippocampi.
3. **Corpus callosum** is the third commissure to appear (between weeks 12 and 22). The corpus callosum is the largest commissure of the brain and interconnects homologous neocortical areas of the two cerebral hemispheres.

XIV. DEVELOPMENT OF THE SYMPATHETIC NERVOUS SYSTEM

The **sympathetic nervous system** originates from the basal plate of the neural tube and neural crest cells.

A. The **basal plate** of the neural tube gives rise to **preganglionic sympathetic neurons** within the **intermediolateral cell column** of the spinal cord, which form white communicating rami found between T1 and L3.

B. The **neural crest cells** give rise to **postganglionic sympathetic neurons** within the **sympathetic chain ganglia, prevertebral sympathetic ganglia** (e.g., celiac ganglia), and **chromaffin cells of adrenal medulla**.

XV. DEVELOPMENT OF THE PARASYMPATHETIC NERVOUS SYSTEM

The **parasympathetic nervous system** originates from the basal plate of the neural tube and neural crest cells.

A. The **basal plate** of the neural tube gives rise **to preganglionic parasympathetic neurons** within the nuclei of the **midbrain (CN III), pons (CNVII), medulla (CN IX, X)**, and **spinal cord at S2–S4**.

B. The **neural crest cells** give rise to **postganglionic parasympathetic neurons** within the **ciliary ganglion (CN III), pterygopalatine ganglion (CN VII), submandibular ganglion (CN VII), otic ganglion (CN IX), enteric ganglia of the gut (Meissner and Auerbach; CN X)**, and **abdominal/pelvic cavity parasympathetic ganglia**.

XVI. DEVELOPMENT OF THE CRANIAL NERVES

A. **Olfactory nerve (CN I)** is derived from the **nasal (olfactory) placode** and mediates smell (olfaction). CN I is capable of regeneration.

B. **Optic nerve (CN II)** is derived from the **ganglion cells of the retina** (which is a diverticulum of the diencephalon) and mediates vision. CN II is not capable of regeneration after transection. CN II is not a true cranial nerve, but a tract of the diencephalon.

C. **Oculomotor nerve (CN III)** is derived from the **basal plate of the rostral midbrain** and mediates eye movements by innervation of the medial rectus muscle, superior rectus muscle, inferior rectus muscle, and inferior oblique muscle, upper eyelid movement by innervation of the levator palpebrae muscle, pupillary constriction by innervation of sphincter pupillae muscle of the iris, and accommodation by innervation of the ciliary muscle.

D. **Trochlear nerve (CN IV)** is derived from the **basal plate of the caudal midbrain** and mediates eye movements by innervation of the superior oblique muscle.

E. **Trigeminal nerve (CN V).** The motor division of CN V is derived from the **basal plate of the rostral pons**. The sensory division of CN V is derived from the cranial **neural crest cells**. CN V mediates the sensory and motor innervation of pharyngeal arch 1 derivatives.

F. **Abducent nerve (CN VI)** is derived from the **basal plate of the caudal pons** and mediates eye movements by innervation of the lateral rectus muscle.

G. **Facial nerve (CN VII).** The motor division of CN VII is derived from the **basal plate of the pons**. The sensory division of CN VII is derived from the cranial **neural crest cells**. CN VII mediates the sensory and motor innervation of pharyngeal arch 2 derivatives.

H. **Vestibulocochlear nerve (CN VIII)** is derived from the **otic placode**. The vestibular division of CN VIII mediates balance and equilibrium. The cochlear division of CN VIII mediates hearing.

I. **Glossopharyngeal nerve (CN IX).** The motor division of CN IX is derived from the **basal plate of the medulla**. The sensory division of CN IX is derived from the cranial **neural crest cells**. CN IX mediates the sensory and motor innervation of pharyngeal arch 3 derivatives.

J. **Vagal nerve (CN X).** The motor division of CN X is derived from the **basal plate of the medulla**. The sensory division of CN X is derived from the cranial **neural crest cells**. CN X mediates the sensory and motor innervation of pharyngeal arches 4 and 6 derivatives.

K. **Accessory nerve (CN XI)** is derived from the **basal plate of the spinal segments C1–C6**. CN XI innervates the sternocleidomastoid and trapezius muscles.

L. **Hypoglossal nerve (CN XII)** is derived from the **basal plate of the medulla**. CN XIII innervates the intrinsic and extrinsic muscles of the tongue.

XVII. DEVELOPMENT OF THE CHOROID PLEXUS

The choroid plexus develops from the **roof plates of the rhombencephalon and diencephalon** and within the **choroid fissure of the telencephalon**. The choroid plexus consists of **choroid plexus cells** (i.e., modified ependymocytes) and a vascular pia mater (tela choroidea). The choroid plexus produces 500 mL of CSF per day. The CSF is returned to the venous system via the **arachnoid (granulations) villi** of the venous dural sinuses (e.g., superior sagittal sinus).

XVIII. CONGENITAL MALFORMATIONS OF THE CENTRAL NERVOUS SYSTEM

A. Variations of spina bifida (Figure 7.20). Spina bifida occurs when the **bony vertebral arches** fail to form properly, thereby creating a vertebral defect, usually in the **lumbosacral region**.

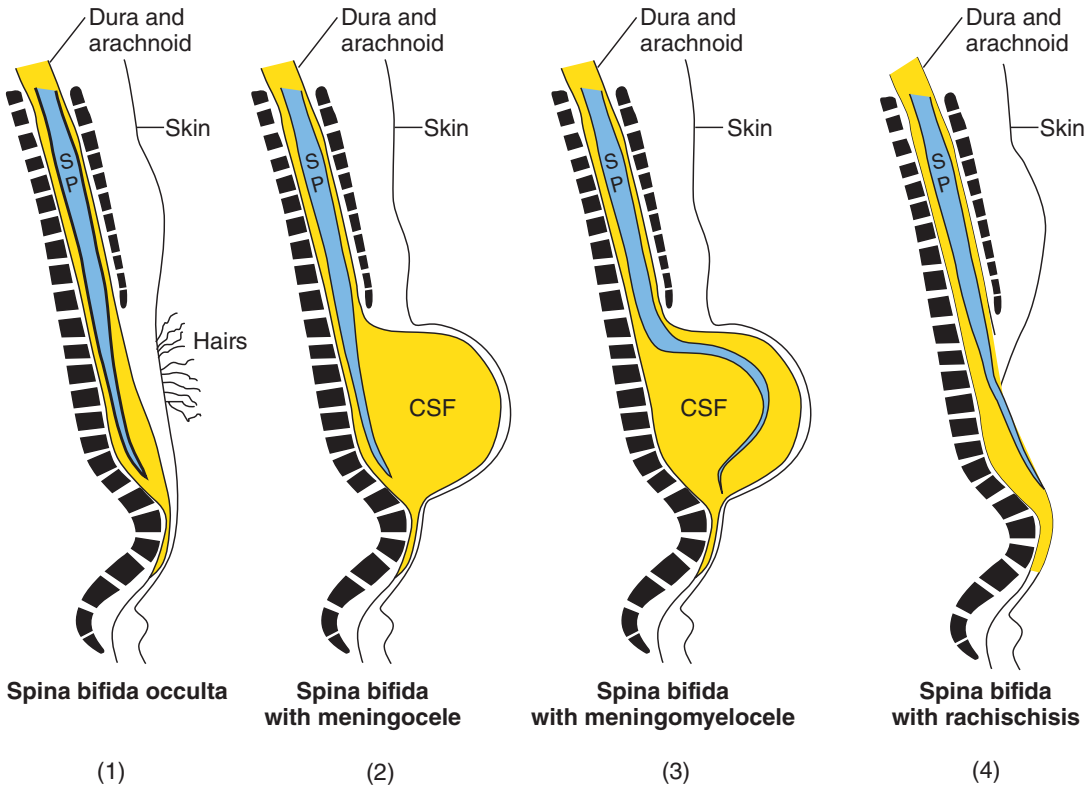

FIGURE 7.20. Schematic drawings illustrating the various types of spina bifida. SP = spinal cord; CSF = cerebrospinal fluid.

1. **Spina bifida occulta (Figure 7.21)** is evidenced by a tuft of hair in the lumbosacral region. It is the least severe variation and occurs in 10% of the population. The MRI (Figure 7.21) of spina bifida occulta shows the presence of the bony vertebral bodies (VB) along the entire length of the vertebral column. However, the bony spinous processes terminate much higher (*asterisk*) because the vertebral arches fail to form properly. This creates a bony vertebral defect. The spinal cord is intact.

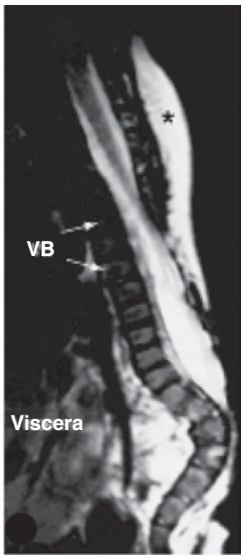

FIGURE 7.21. Spina bifida occulta.

2. **Spina bifida with meningocele (Figure 7.22)** occurs when the meninges protrude through a vertebral defect and form a sac filled with CSF. The spinal cord remains in its normal position. The sonogram (Figure 7.22) of spina bifida with meningomyelocele shows the spinal cord (*arrows*), CSF-filled sac, a small subcutaneous lipoma (L), and the filum terminale (*arrowhead*).
3. **Spina bifida with meningomyelocele** occurs when the meninges and spinal cord protrude through a vertebral defect and form a sac filled with CSF.

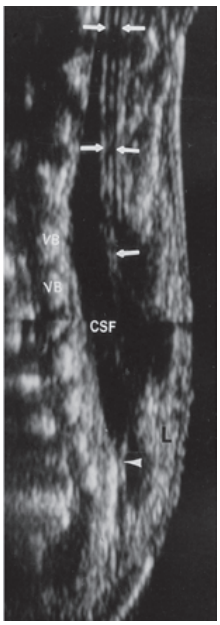

FIGURE 7.22. Spina bifida with meningomyelocele.

4. **Spina bifida with rachischisis (Figure 7.23)** occurs when the posterior neuropore of the neural tube fails to close during week 4 of development. This condition is the most severe type of spina bifida, causing paralysis from the level of the defect caudally. This variation presents clinically as an **open neural tube** that lies on the surface of the back. This condition also falls into a classification called **NTDs. Lower NTDs** (i.e., spina bifida with rachischisis) result from a failure of the **posterior neuropore** to close during week 4 of development and usually occur in the lumbosacral region. **Upper NTDs** (e.g., anencephaly) result from a failure of the **anterior neuropore** to close during week 4 of development. NTDs can be diagnosed prenatally by detecting elevated levels of α-**fetoprotein** in the amniotic fluid. About 75% of all NTDs can be prevented if all women capable of becoming pregnant consume **folic acid** (dose: 0.4 mg of folic acid per day). The photograph (Figure 7.23) of spina bifida with rachischisis shows a newborn infant with an open neural tube on the back.

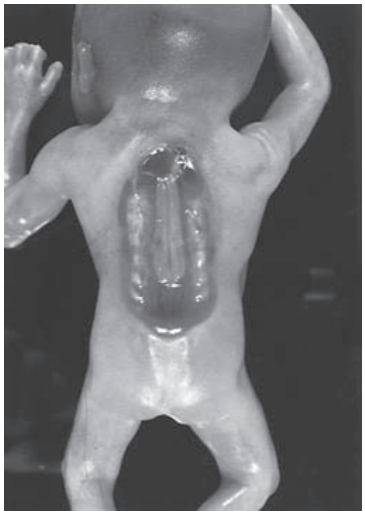

FIGURE 7.23. Spina bifida with rachischisis.

B. Variations of cranium bifida (Figure 7.24). Cranium bifida occurs when the **bony skull** fails to form properly, thereby creating a skull defect, usually in the **occipital region**.

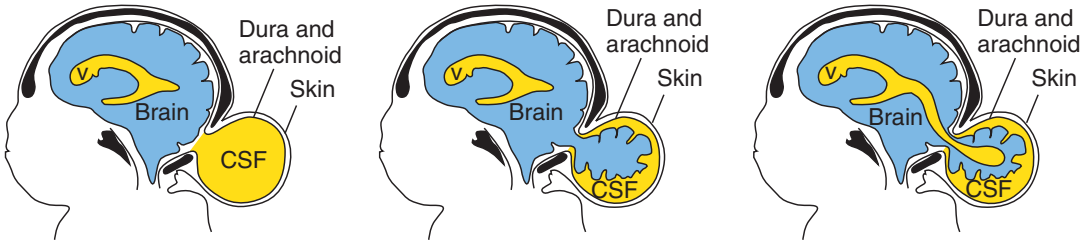

FIGURE 7.24. Schematic drawings illustrating the various types of cranium bifidum.

1. **Cranium bifida with meningocele (Figure 7.25)** occurs when the meninges protrude through the skull defect and form a sac filled with CSF. The photograph (Figure 7.25) shows a fetus with an occipital meningocele (*asterisk*).

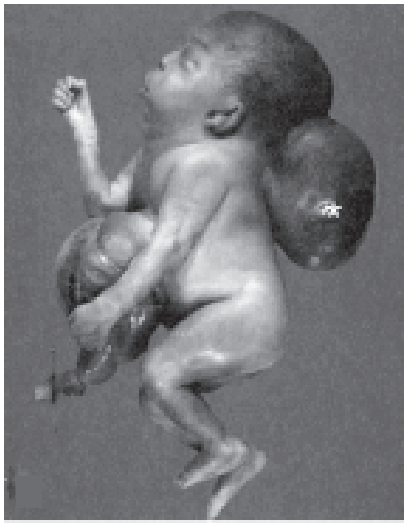

FIGURE 7.25. Fetus with an occipital meningocele

2. **Cranium bifida with meningoencephalocele (Figure 7.26)** occurs when the meninges and brain protrude through the skull defect and form a sac filled with CSF. This defect usually comes to medical attention within the infant's first few days or weeks of life. The outcome is poor (75% of the infants die or have severe retardation). The MRI (Figure 7.26) of a meningoencephalocele shows a large protrusion (*arrows*) extending through an occipital bone defect, which contains brain tissue (B).
3. **Cranium bifida with meningohydroencephalocele** occurs when the meninges, brain, and a portion of the ventricle protrude through the skull defect.

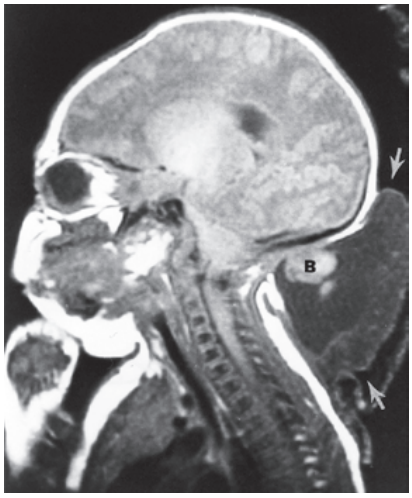

FIGURE 7.26. Magnetic resonance imaging of a meningoencephalocele.

C. Anencephaly (meroanencephaly; Figure 7.27) is a type of **upper NTD** that occurs when the **anterior neuropore** fails to close during week 4 of development. This results in the following: failure of the brain to develop (however, a rudimentary brain is present), failure of the lamina terminalis to form, and failure of the bony cranial vault to form. Anencephaly is incompatible with extrauterine life. If not stillborn, infants with anencephaly survive from only a few hours to a few weeks. Anencephaly is the common serious birth defect seen in stillborn fetuses. Anencephaly is easily diagnosed by ultrasound, and a therapeutic abortion is usually performed at the mother's request. The photograph (Figure 7.27) shows a newborn infant with anencephaly.

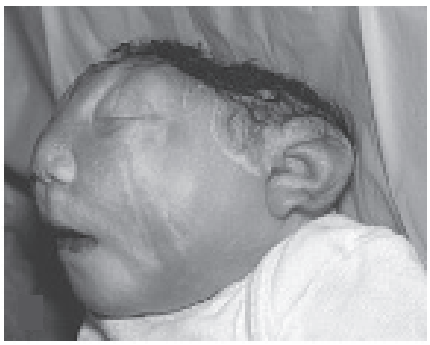

FIGURE 7.27. Newborn infant with anencephaly.

D. Arnold-Chiari malformation (Figure 7.28) occurs when the caudal vermis and tonsils of the cerebellum and the medulla oblongata herniate through the foramen magnum. This results in a compression of the medulla oblongata and stretching of CN IX, CN X, and CN XII. **Clinical features include** spastic dysphonia, difficulty in swallowing, laryngeal stridor (vibrating sound heard during respiration as a result of obstructed airways), diminished gag reflex, apnea, and vocal cord paralysis.

This malformation is commonly associated with a **lumbar meningomyelocele, platybasia** (bone malformation of base of skull) along with malformation of the occipitovertebral joint, and obstructive **hydrocephalus** (due to obliteration of the foramen of Magendie and foramina of Luschka of the fourth ventricle; however, about 50% of cases demonstrate **aqueductal stenosis**). The MRI (Figure 7.28) shows the Arnold-Chiari malformation. Note the herniation of the brain stem and cerebellum (*arrows*) through foramen magnum. Note the presence of a syrinx (S) in the cervical spinal cord.

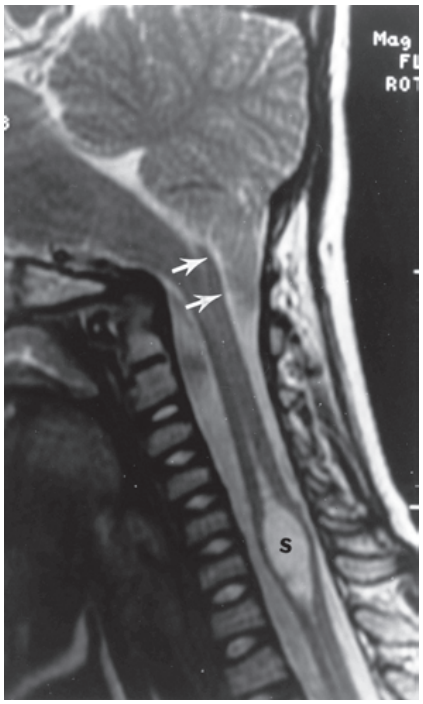

FIGURE 7.28. Magnetic resonance imaging of the Arnold-Chiari malformation.

E. Hydrocephalus is a dilation of the ventricles due to an excess of CSF that may result from either a blockage of CSF circulation or, rarely, an overproduction of CSF (e.g., due to a choroid plexus papilloma). There are two general categories of hydrocephalus:

1. **Communicating (or nonobstructive) hydrocephalus (Figure 7.29)**. In this type of hydrocephalus, there is free communication between the ventricles and the subarachnoid space. The blockage of CSF in this type of hydrocephalus is usually in the subarachnoid space or arachnoid granulations and results in the enlargement of all the ventricular cavities as well as the subarachnoid space. The sonogram (Figure 7.29) shows the dilated lateral ventricle (L) communicating through a dilated foramen of Monro with a dilated third ventricle (3) and dilated fourth ventricle (4). The cisterna magna (C) is also shown.

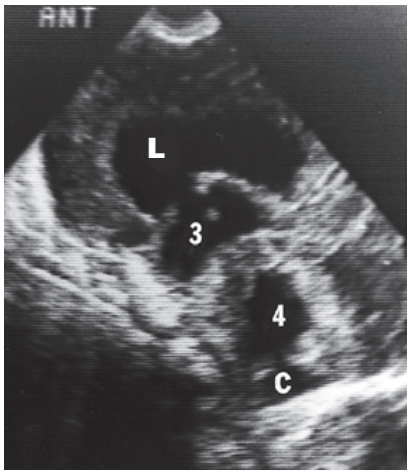

FIGURE 7.29. Communicating (or nonobstructive) hydrocephalus.

2. **Noncommunicating (or obstructive) hydrocephalus.** In this type of hydrocephalus, there is a lack of communication between the ventricles and the subarachnoid space. The blockage of CSF in this type of hydrocephalus is in the foramen of Monro, the cerebral aqueduct, or the foramen of Magendie/foramina of Luschka and results in the enlargement of only those ventricular cavities proximal to the blockage. There are two types of **congenital hydrocephalus**, both of which produce a noncommunicating (obstructive) hydrocephalus:
   a. **Congenital aqueductal stenosis (Figure 7.30)** is the most common cause of congenital hydrocephalus. This type may be transmitted by an X-linked trait, or it may be caused by cytomegalovirus or toxoplasmosis. The sonogram (Figure 7.30) shows dilated lateral ventricles (L), dilated third ventricle (3), but normal-size fourth ventricle (4). Therefore, obstruction at the cerebral aqueduct is presumed.
   b. **Dandy-Walker syndrome (Figure 7.31)** is associated with **atresia of the foramen of Magendie and foramina of Luschka** (although it remains controversial). This syndrome is usually associated with dilation of the fourth ventricle, posterior fossa cyst, agenesis of the cerebellar vermis, small cerebellar hemispheres, occipital meningocele, and, frequently, agenesis of the splenium of the corpus callosum. The MRI (Figure 7.31) shows a dilated fourth ventricle (4) communicating with a posterior fossa cyst (CY) along with small cerebellar hemispheres.

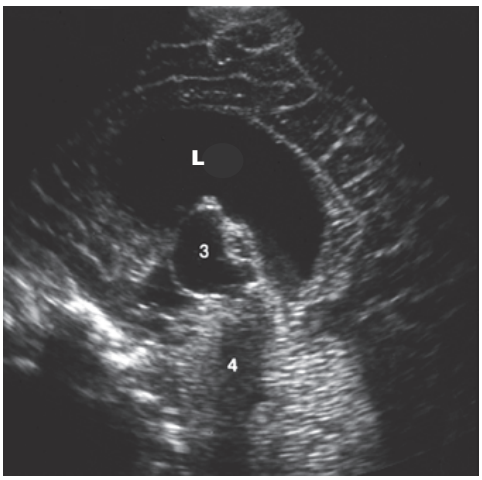

FIGURE 7.30. Congenital aqueductal stenosis.

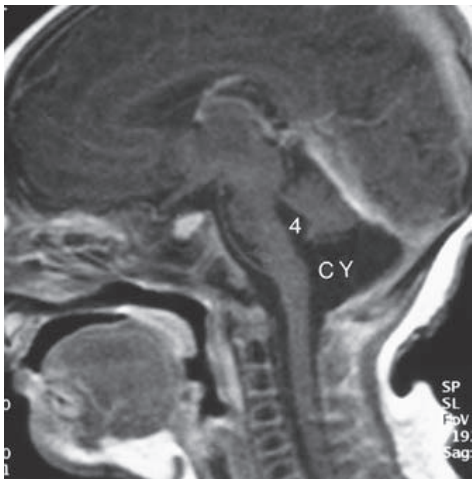

FIGURE 7.31. Dandy-Walker syndrome.

F. **Porencephaly (encephaloclastic porencephaly; Figure 7.32)** is the presence of one or more fluid-filled cystic cavities within the brain that may communicate with the ventricles but do not extend to the cerebral cortical surface. The cysts are lined by ependyma and have smooth or irregular walls. These cysts form as a result of brain destruction early in gestation before the brain is capable of a glial response to form a scar. The sonogram (Figure 7.32) shows a fluid-filled cystic cavity (*asterisk*) communicating with the right lateral ventricle (Ch denotes the choroid plexus).

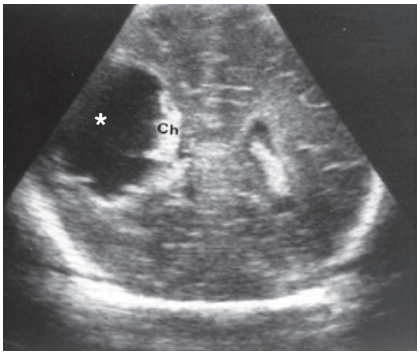

FIGURE 7.32. Porencephaly.

G. Hydranencephaly (Figure 7.33) is the presence of a huge, fluid-filled cystic cavity that completely replaces the cerebral hemispheres. The cyst is lined by glial and meningeal elements. This cystic cavity forms as a result of occlusion of the **internal carotid arteries** in utero, causing widespread destruction of the cerebral cortex (the brain stem and cerebellum are usually spared because vertebrobasilar circulation is not affected). Other causes include toxoplasmosis, rubella, cytomegalovirus, and herpes virus. The MRI (Figure 7.33) shows a huge, fluid-filled cystic cavity within the supratentorial compartment (*asterisk*) that replaces the cerebral hemispheres. Note that the brain stem and cerebellum remain intact.

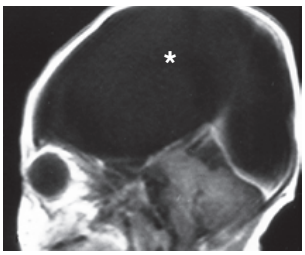

FIGURE 7.33. Hydranencephaly.

H. Schizencephaly (Figure 7.34) is the presence of a cerebral cortical cleft of brain tissue that extends from the ventricles to the cerebral cortical surface. The cleft is lined by cortical brain tissue and is fluid filled (i.e., a fluid-filled cleft). The cleft forms as a result of abnormal neuronal migration during embryological formation of the brain. The MRI (Figure 7.34) shows a cleft of brain tissue in the left cerebral hemisphere (*arrows*). This cleft is fluid filled and communicates with the lateral ventricles.

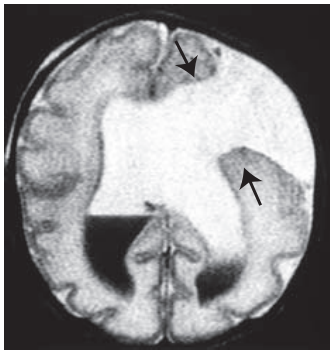

FIGURE 7.34. Schizencephaly.

I. Holoprosencephaly (arhinencephaly; Figure 7.35) occurs when the prosencephalon fails to cleave down the midline such that the telencephalon contains a single ventricle. It is characterized by the absence of olfactory bulbs and tracts (arhinencephaly) and is often seen in trisomy 13 (Patau syndrome), trisomy 18 (Edward syndrome), short-arm deletion of chromosome 18, and Meckel syndrome. Because the fetal face develops at the same time as the brain, facial anomalies (e.g., cyclopia, cleft lip, cleft palate) are commonly seen with holoprosencephaly. Holoprosencephaly is the most severe manifestation of **fetal alcohol syndrome** resulting from alcohol abuse during pregnancy (especially in the first 4 weeks of pregnancy). The sonogram (Figure 7.35) shows a single, horseshoe-shaped ventricle (V) and fused thalami (T) typical of holoprosencephaly. There are three types of holoprosencephaly:

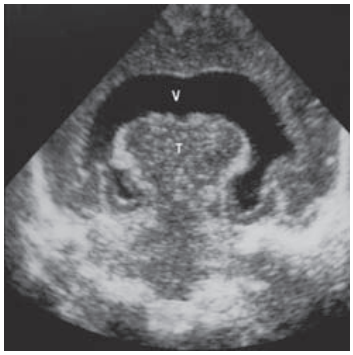

FIGURE 7.35. Holoprosencephaly (arhinencephaly).

J. Tethered spinal cord (filum terminale syndrome; Figure 7.36) occurs when a thick, short filum terminale forms. The result is weakness and sensory deficits in the lower extremity and a neurogenic bladder. Tethered spinal cord is frequently associated with lipomatous tumors or meningomyeloceles. Deficits usually improve after transection. The MRI (Figure 7.36) shows a low-positioned spinal cord (*arrows*) attached to an intraspinal lipoma (L) typical of a tethered spinal cord.

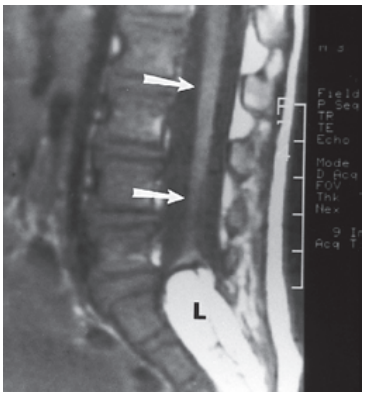

FIGURE 7.36. Tethered spinal cord.

K. Chordoma is a tumor that arises from remnants of the notochord.

Study Questions for Chapter 7

1. Which one of following basal ganglia is derived from the diencephalon?

(A) Amygdaloid nucleus
(B) Head of the caudate nucleus
(C) Tail of the caudate nucleus
(D) Globus pallidus
(E) Putamen

2. When are the axons of the corticospinal tracts fully myelinated?

(A) In the late embryonic period
(B) In the midfetal period
(C) At birth
(D) By the end of the first postnatal year
(E) By the end of the second postnatal year

3. Which of the following represents the general somatic efferent (GSE) column of the pons?

(A) Abducent nucleus
(B) Nucleus ambiguus
(C) Hypoglossal nucleus
(D) Inferior olivary nucleus
(E) Inferior salivatory nucleus

4. Which of the following represents the general visceral efferent (GVE) column of the pons?

(A) The cerebellum
(B) The spinal trigeminal nucleus
(C) The principal trigeminal nucleus
(D) The superior salivatory nucleus
(E) The pontine nuclei

5. The external germinal layer of the cerebellum gives rise to which of the following?

(A) Outer stellate cells
(B) Purkinje cells
(C) Granule cells
(D) Basket cells
(E) Giant cells of Betz

6. Which of the following statements best describes the pathogenesis of hydranencephaly?

(A) Results from failure of midline cleavage of the embryonic forebrain
(B) Results from atresia of the outlet foramina of the fourth ventricle
(C) Results from blockage of the cerebral aqueduct
(D) Results from internal carotid artery occlusion
(E) Results from failure of the anterior neuropore to close

7. The anterior and posterior neuropores close during which week of embryonic development?

(A) Week 2
(B) Week 3
(C) Week 4
(D) Week 5
(E) Week 6

8. At birth the conus medullaris is found at which vertebral level?

(A) T12
(B) L1
(C) L3
(D) S1
(E) S4

9. Which of the following structures is derived from the telencephalon?

(A) Pineal gland
(B) Hypothalamus
(C) Hippocampus
(D) Optic nerve (CN II)
(E) Globus pallidus

10. Which of the following conditions results from failure of the anterior neuropore to close?

(A) Hydrocephalus
(B) Anencephaly
(C) Mongolism
(D) Craniosynostosis
(E) Meningoencephalocele

11. Which of the following structures is derived from the diencephalon?

(A) Caudate nucleus
(B) Cerebellum
(C) Olfactory bulbs
(D) Neurohypophysis
(E) Adenohypophysis

12. Caudal herniation of the cerebellar tonsils and medulla through the foramen magnum is called

(A) Dandy-Walker syndrome
(B) Down syndrome
(C) Arnold-Chiari syndrome
(D) cranium bifidum
(E) myeloschisis

13. The flexure that develops between the metencephalon and the myelencephalon is called the

(A) cephalic flexure
(B) mesencephalic flexure
(C) pontine flexure
(D) cerebellar flexure
(E) cervical flexure

14. Which of the following statements best describes the sulcus limitans?

(A) It is found in the interpeduncular fossa
(B) It is located between the alar and basal plates
(C) It separates the medulla from the pons
(D) It separates the hypothalamus from the thalamus
(E) It separates the neocortex from the allocortex

15. Myelinated preganglionic sympathetic neurons have their cell bodies in

(A) Clarke column
(B) substantia gelatinosa
(C) intermediolateral cell column
(D) intermediomedial cell column

16. The choroid plexus of the fourth ventricle is derived from the

(A) alar plate
(B) basal plate
(C) floor plate
(D) rhombic lip
(E) roof plate

17. Tanycytes are found principally in the

(A) area postrema
(B) cerebral aqueduct
(C) lateral ventricles
(D) third ventricle
(E) fourth ventricle

18. Which of the following most accurately describes the herniation of meninges and brain tissue through a defect in occipital bone?

(A) Cranium bifidum with meningoencephalocele
(B) Cranium bifidum with meningohydroencephalocele
(C) Cranium bifidum with meningocele
(D) Arnold-Chiari syndrome
(E) Dandy-Walker syndrome

19. Which of the following is the most common cause of congenital hydrocephalus?

(A) Cranium bifidum with meningoencephalocele
(B) Cranium bifidum with meningohydroencephalocele
(C) Aqueductal stenosis
(D) Arnold-Chiari syndrome
(E) Dandy-Walker syndrome

20. Which of the following is associated with atresia of the foramen of Magendie and foramina of Luschka?

(A) Cranium bifidum with meningoencephalocele
(B) Cranium bifidum with meningohydroencephalocele
(C) Aqueductal stenosis
(D) Arnold-Chiari syndrome
(E) Dandy-Walker syndrome

21. Which of the following is associated with platybasia and malformation of the occipitovertebral joint?

(A) Cranium bifidum with meningoencephalocele
(B) Cranium bifidum with meningohydroencephalocele
(C) Aqueductal stenosis
(D) Arnold-Chiari syndrome
(E) Dandy-Walker syndrome

22. A 22-year-old pregnant woman at 20 weeks of gestation comes to her ON/GYN for a normal examination. During routine blood tests, her serum α-fetoprotein (AFP) concentration is markedly increased for her gestational age. Ultrasonography reveals spina bifida in the fetus. At what week of gestation did this defect most likely occur?

(A) 1–2
(B) 4–6
(C) 9–11
(D) 12–15
(E) 16–19

23. Which structure is derived from the cranial neural crest cells?

(A) Lens of the eye
(B) Pia mater
(C) Dura mater
(D) Pineal gland
(E) Olfactory placode, CN I

Answers and Explanations

1. **D.** The globus pallidus has its origin from the diencephalon. Neuroblasts from the subthalamus migrate into the telencephalic white matter to form the globus pallidus.

2. **E.** Axons of the corticospinal tracts are fully myelinated by the end of the second postnatal year; Babinski sign (extensor plantar reflex) is usually not elicitable before myelination of the corticospinal tracts.

3. **A.** The abducent nucleus represents the general somatic efferent (GSE) column of the pons.

4. **D.** The superior salivatory nucleus represents the general visceral efferent (GVE) column of the pons. All somatic and visceral motor nuclei are derived from the basal plate. The cerebellum and pontine nuclei and the sensory nuclei of cranial nerves are derivatives of the alar plate.

5. **C.** New evidence documents that the external granular layer gives rise only to the granule cells of the internal granular layer and not to the basket (inner stellate) or stellate (outer stellate) neurons, as was long thought. The giant cells of Betz are found in the cerebral cortex.

6. **D.** Hydranencephaly consists of huge intracerebral cavitation resulting from infarction in the territory of the internal carotid artery.

7. **C.** The anterior and posterior neuropores close during week 4 of development—the anterior on day 25, the posterior on day 27. Failure of the anterior neuropore to close results in anencephaly; failure of the posterior neuropore to close results in myeloschisis.

8. **C.** At birth, the conus medullaris extends to L3, and in the adult it extends to the L1–L2 interspace. At 8 weeks, the spinal cord extends the entire length of the vertebral canal.

9. **C.** The hippocampus develops from the telencephalon. The pineal gland, hypothalamus, CN II, and the globus pallidus are derived from the diencephalon.

10. **B.** Failure of the anterior neuropore to close results in anencephaly. The brain fails to develop; no cranial vault is formed.

11. **D.** The neurohypophysis develops from the diencephalon. The adenohypophysis (pars distalis, pars tuberalis, and pars intermedia) develops from Rathke pouch, an ectodermal diverticulum of the stomodeum. The caudate nucleus and olfactory bulbs develop from the telencephalon. The cerebellum develops from the metencephalon.

12. **C.** Arnold-Chiari syndrome is a cerebellomedullary malformation in which the caudal vermis and medulla herniate through the foramen magnum, resulting in communicating hydrocephalus. Arnold-Chiari syndrome is frequently associated with spina bifida.

13. **C.** The pontine flexure develops between the metencephalon (pons) and the myelencephalon (medulla). The pontine flexure results in lateral expansion of the walls of the metencephalon and myelencephalon, stretching of the roof of the fourth ventricle, and widening of the floor of the fourth ventricle (rhomboid fossa).

14. **B.** The sulcus limitans separates the sensory alar from the motor basal plates. It is found in the developing spinal cord and on the surface of the adult rhomboid fossa of the fourth ventricle. The bulbopontine sulcus (inferior pontine sulcus) separates the medulla from the pons. The hypothalamic sulcus separates the thalamus from the hypothalamus. The rhinal sulcus separates the neocortex from the allocortex.

15. **C.** Myelinated preganglionic sympathetic neurons have their cell bodies in the intermediolateral cell column of the lateral horn; this cell column extends from C8 to L1. Myelinated

preganglionic parasympathetic neurons have their cell bodies in the sacral autonomic nucleus, from S2 to S4.

16. **E.** The roof plate and its pial covering give rise to the choroid plexus, which invaginates into the fourth ventricle. The alar plate gives rise to sensory neurons; the basal plate gives rise to motor neurons; the floor plate contains decussating fibers; the rhombic lips give rise to the cerebellum.

17. **D.** Tanycytes are modified ependymal cells, found principally in the third ventricle. Tanycytes transport substances from the CSF to the hypophyseal portal system.

18. **A.** Cranium bifidum with meningoencephalocele consists of the herniation of meninges and brain tissue through a defect in occipital bone.

19. **C.** The most common cause of congenital hydrocephalus is aqueductal stenosis.

20. **E.** Dandy-Walker syndrome is congenital hydrocephalus associated with atresia of the outlet foramina of Magendie and Luschka. It is associated with agenesis of the cerebellar vermis and agenesis of the splenium of the corpus callosum.

21. **D.** Arnold-Chiari syndrome, a common congenital malformation, is frequently associated with platybasia and malformation of the occipitovertebral joint; other anomalies frequently seen are beaking of the tectum, aqueductal stenosis, kinking and herniation of the medulla, and herniation of the cerebellar vermis through the foramen magnum. Meningomyelocele (spina bifida) is a common component of the syndrome.

22. **B.** The posterior neuropore closes during week 4 (day 27). Failure of the posterior neuropore to close results in lower neural tube defects, such as spina bifida.

23. **B.** The pia mater is the only listed structure that is derived from cranial neural crest cells. For a summary of germ cell derivatives refer to Table 4.1.

chapter 8

Ear

I. OVERVIEW

The ear is the organ of **balance** and **hearing**. The ear consists of an **internal**, a **middle**, and an **external ear**.

II. THE INTERNAL EAR (FIGURE 8.1; TABLE 8.1)

The internal ear develops in week 4 from a thickening of the surface **ectoderm** called the **otic placode**. The otic placode invaginates into the underlying mesoderm (or mesenchyme) adjacent to the rhombencephalon and becomes the **otic vesicle**. The otic vesicle divides into **utricular** and **saccular portions**.

A. **Utricular portion** of the otic vesicle gives rise to the following:

1. **Utricle** contains the sensory hair cells and otoliths of the macula utriculi. The utricle responds to **linear acceleration** and the **force of gravity**.
2. **Semicircular ducts** contain the sensory hair cells of the cristae ampullares. The semicircular ducts respond to **angular acceleration**.
3. **Vestibular ganglion of cranial nerve (CN) VIII** lies at the base of the internal auditory meatus.
4. **Endolymphatic duct and sac** is a membranous duct that connects the saccule to the utricle and terminates in a blind sac beneath the dura. The endolymphatic sac absorbs endolymph.

B. **Saccular portion** of the otic vesicle gives rise to the following:

1. **Saccule** contains the sensory hair cells and otoliths of the macula sacculi. The saccule responds to **linear acceleration** and the **force of gravity**.
2. **Cochlear duct (organ of Corti)** is involved in hearing. This duct has pitch (tonopic) localization whereby high-frequency sound waves (20,000 Hz) are detected at the base and low-frequency sound waves (20 Hz) are detected at the apex.
3. **Spiral ganglion of CN VIII** lies in the modiolus of the bony labyrinth.

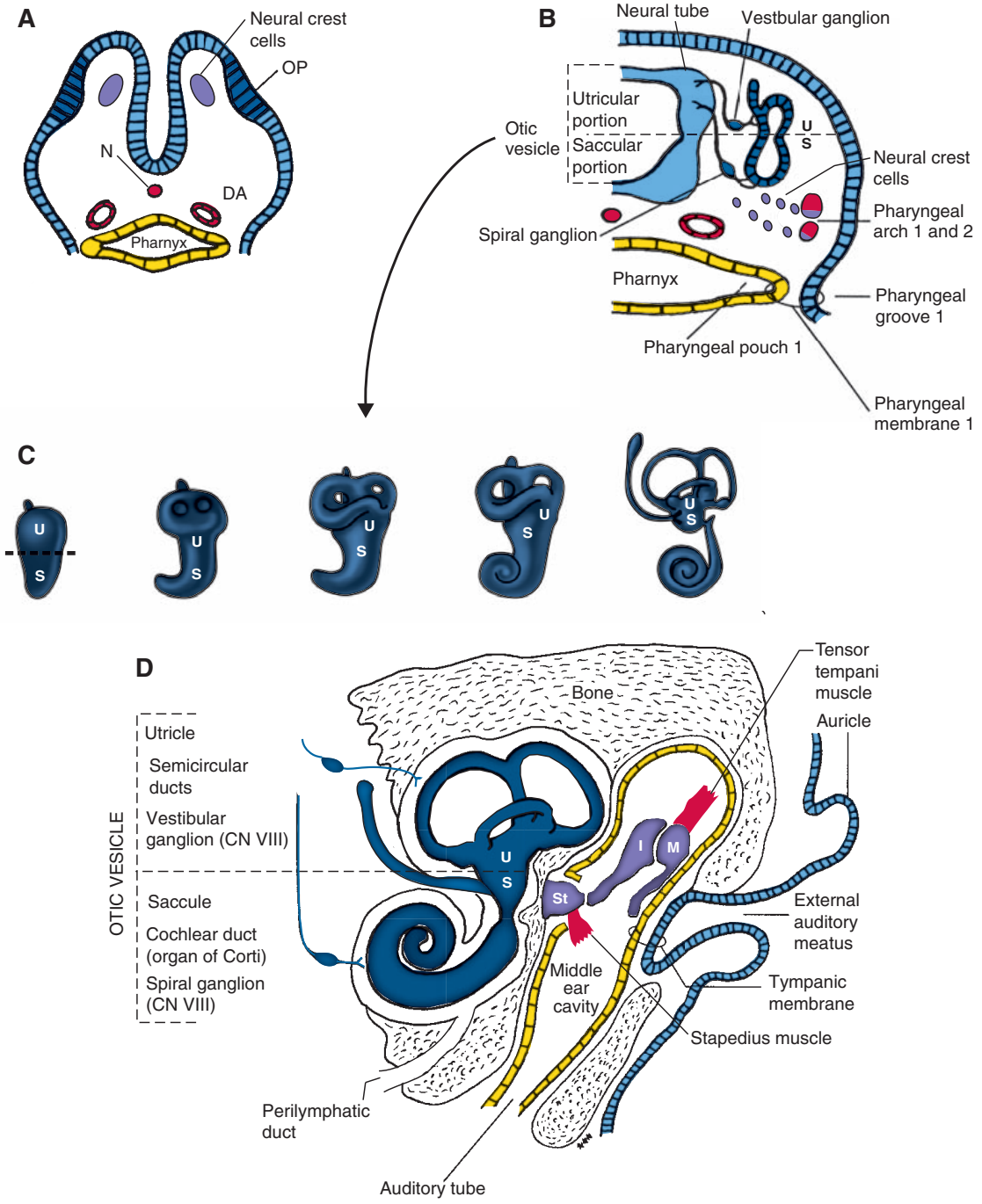

FIGURE 8.1. Schematic transverse sections show the formation of the otic placode and otic vesicle from the surface ectoderm. **(A)** The otic placode (*dark blue*) is distinguished by a thickening of the surface ectoderm (*light blue*). DA = dorsal aorta (*red*); N = notochord (*red*); OP = otic placode (*dark blue*); neural crest cells (*purple*). **(B)** The otic placode invaginates into the underlying mesenchyme and becomes the otic vesicle (*dark blue*). **(C)** The otic vesicle undergoes extensive changes to form the adult membranous labyrinth (*dark blue*). U = utricle (*dark blue*); S = saccule (*dark blue*). **(D)** The adult ear. U=utricle (*dark blue*); S=saccule (*dark blue*); M = malleus (*purple*); I = incus (*purple*); St = stapes (*purple*); tensor tympani muscle (*red*); stapedius muscle (*red*); epithelial lining of auditory tube and middle ear cavity (*yellow*); epithelial lining of external auditory meatus and skin of the auricle (*light blue*).

table 8.1 Embryonic Ear Structures and Their Adult Derivatives

Embryonic Structure	Adult Derivative
	Internal ear
Otic Vesicle	
Utricular portion (Ectoderm)	Utricle, semicircular ducts, vestibular ganglion of CN VIII, endolymphatic duct and sac
Saccular portion (Ectoderm)	Saccule, cochlear duct (organ of Corti), spiral ganglion of CN VIII
	Middle ear
Pharyngeal arch 1	Malleus (Meckel cartilage; neural crest cells) Incus (Meckel cartilage; neural crest cells) Tensor tympani muscle (mesoderm)
Pharyngeal arch 2	Stapes (Reichert cartilage; neural crest cells) Stapedius muscle (mesoderm)
Pharyngeal pouch 1	Epithelial lining of the auditory tube (endoderm) Epithelial lining of the middle ear cavity (endoderm)
Pharyngeal membrane 1	Tympanic membrane (ectoderm, mesoderm and neural crest cells, and endoderm)
	External ear
Pharyngeal groove 1	Epithelial lining of the external auditory meatus (ectoderm)
Auricular hillocks	Auricle

III. THE MEMBRANOUS AND BONY LABYRINTHS

A. The membranous labyrinth consists of all the structures derived from the otic vesicle (see Table 8.1).

B. The membranous labyrinth is initially surrounded by neural crest cells that form a connective tissue covering. This connective tissue becomes cartilaginous and then ossifies to become the **bony labyrinth** of the temporal bone.

C. The connective tissue closest to the membranous labyrinth degenerates, thus forming the **perilymphatic space** containing **perilymph**.

D. This establishes an interesting anatomical relationship in which the membranous labyrinth floats in perilymph within the bony labyrinth.

E. Perilymph, which is similar in composition to **cerebrospinal fluid**, communicates with the subarachnoid space via the **perilymphatic duct**.

IV. MIDDLE EAR (FIGURE 8.1; TABLE 8.1)

A. Ossicles of the middle ear

1. The **malleus** develops from Meckel cartilage derived from neural crest cells within **pharyngeal arch 1**. The malleus is attached to the tympanic membrane and is moved by the **tensor tympani muscle** derived from mesoderm within **pharyngeal arch 1**. The tensor tympani muscle is innervated by CN V_3.
2. The **incus** develops from Meckel cartilage derived from neural crest cells within **pharyngeal arch 1**. The incus articulates with the malleus and stapes.
3. The **stapes** develops from Reichert cartilage derived from neural crest cells within **pharyngeal arch 2**. The stapes is attached to the oval window of the vestibule and is moved by the **stapedius muscle** derived from mesoderm within **pharyngeal arch 2**. The stapedius muscle is innervated by CN VII.

B. The **epithelial lining of the auditory tube** and **epithelial lining of the middle ear cavity** develop from endoderm of **pharyngeal pouch 1**.

C. The **tympanic membrane** develops from ectoderm, intervening mesoderm and neural crest cells, and endoderm of **pharyngeal membrane 1**. The tympanic membrane separates the middle ear from the external auditory meatus of the external ear. The tympanic membrane is innervated by CN V_3 and CN IX.

V. EXTERNAL EAR (FIGURE 8.2; TABLE 8.1)

A. The **epithelial lining of the external auditory meatus** develops from ectoderm of **pharyngeal groove 1**. The external auditory meatus becomes filled with ectodermal cells that form a temporary **meatal plug**, which disappears before birth. The external auditory meatus is innervated by CN V_3 and CN IX.

B. **Auricle (or pinna)** develops from **six auricular hillocks** that surround pharyngeal groove 1. The auricle is innervated by CN V_3, CN VII, CN IX, and CN X and cervical nerves C_2 and C_3. Figure 8.2 shows all the structures of the adult external ear.

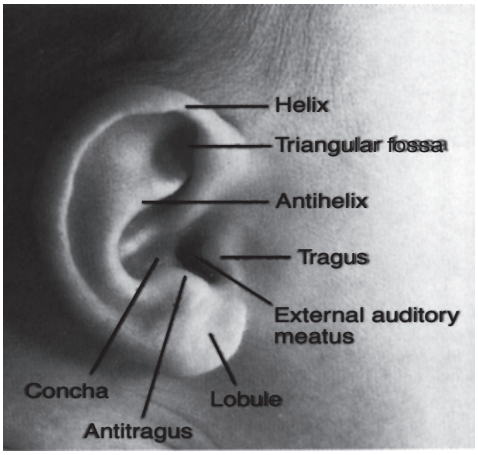

FIGURE 8.2. Nomenclature of the adult auricle.

VI. CONGENITAL MALFORMATIONS OF THE EAR

A. **Minor auricular malformations (Figure 8.3)** are commonly found and raise only cosmetic issues. However, auricular malformations are seen in **Down syndrome (trisomy 21), Patau syndrome (trisomy 13)**, and **Edwards syndrome (trisomy 18)**. The photograph (Figure 8.3) shows a minor auricular variation with a partially folded helix and a prominent antihelix (*arrow*).

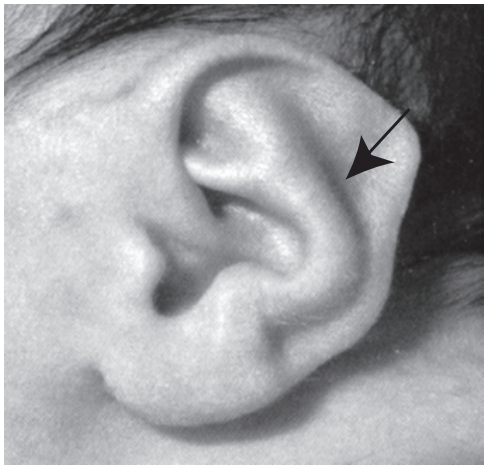

FIGURE 8.3. Minor auricular variation: partially folded helix.

B. Low-set slanted auricles (Figure 8.4) are auricles that are located below a line extended from the corner of the eye to the occiput. This condition may indicate chromosomal abnormalities. The photograph (Figure 8.4) shows a severely low-set and posteriorly rotated auricle in a Stickler syndrome infant. Stickler syndrome is a type of skeletal dysplasia caused by a mutation either in the *COL2A1* **gene** on **chromosome 12q12-13.2** for **collagen α-1(II) chain protein** or in the *COL11A1* **gene** on chromosome 1p21 for **collagen α-1(XI) chain protein**.

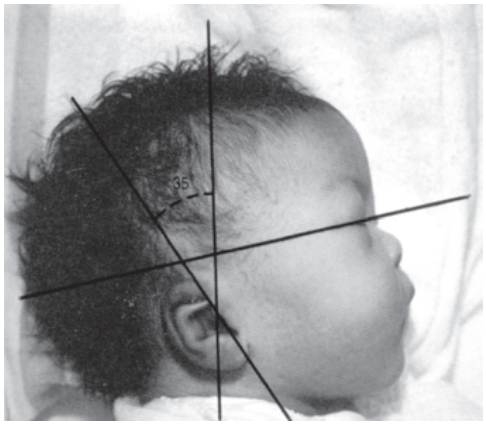

FIGURE 8.4. Stickler syndrome.

C. Preauricular sinus (Figure 8.5) is a narrow tube or shallow pit that has a pinpoint external opening that is most often asymptomatic and of minor cosmetic importance, although infections may occur. The embryological basis is uncertain but probably involves pharyngeal groove 1. The photograph (Figure 8.5) shows a preauricular sinus in the pre-tragal area.

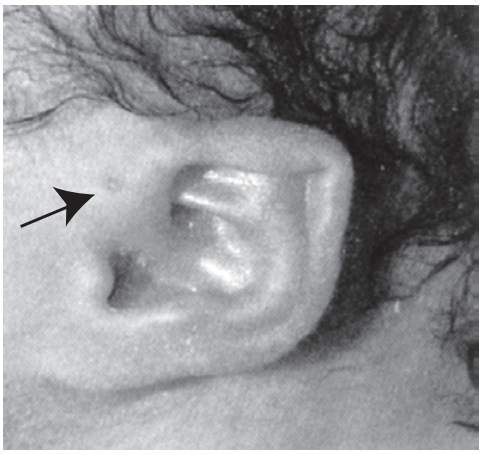

FIGURE 8.5. Preauricular sinus.

D. Auricular appendages (Figure 8.6) are skin tags that are commonly found anterior to the auricle (i.e., pre-tragal area) and raise only cosmetic issues. The embryological basis is the formation of accessory auricle hillocks. The photograph (Figure 8.6) shows auricular appendages (i.e., skin tags) in the pre-tragal area (*arrows*).

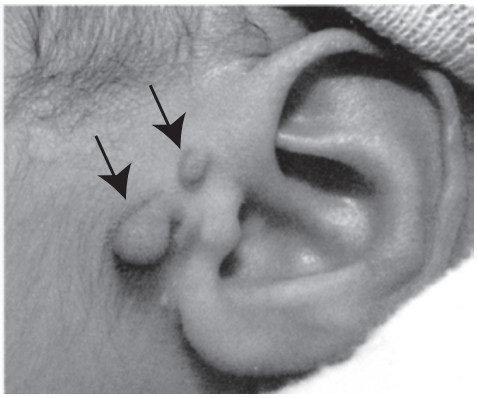

FIGURE 8.6. Auricular appendages.

E. Atresia of the external auditory meatus (Figure 8.7). A **complete atresia** consists of a bony plate in the location of the tympanic membrane. A **partial atresia** consists of a soft tissue plug in the location of the tympanic membrane. This results in conduction deafness and is usually associated with a first arch syndrome. The embryological basis is the failure of the meatal plug to canalize. The photograph (Figure 8.7) shows the absence of the external auditory meatus in this infant.

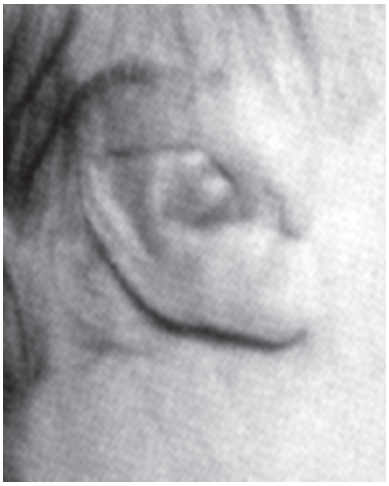

FIGURE 8.7. Atresia of the external auditory meatus.

F. Congenital cholesteatoma (epidermoid cyst; Figure 8.8) is a benign tumor found in the middle ear cavity that results in conduction deafness. The embryological basis is the proliferation of endodermal cells lining the middle ear cavity. The light micrograph (Figure 8.8) shows a large epidermoid formation (*arrow*).

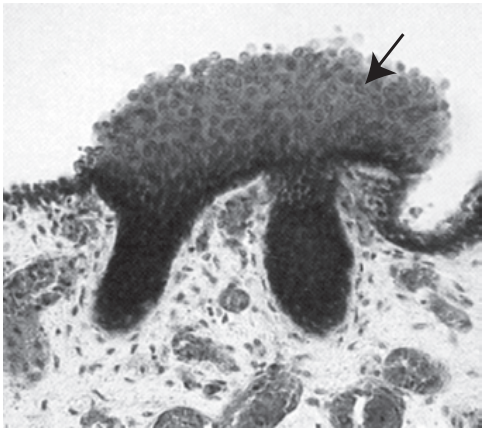

FIGURE 8.8. Epidermoid cyst.

G. Microtia (Figure 8.9) is a severely disorganized auricle that is associated with other malformations resulting in deafness. The embryological basis is impaired proliferation or fusion of the auricular hillocks. The photograph (Figure 8.9) shows a severely disorganized auricle (*arrow*).

H. Congenital deafness. The organ of Corti may be damaged by exposure to **rubella virus**, especially during weeks 7 and 8 of development.

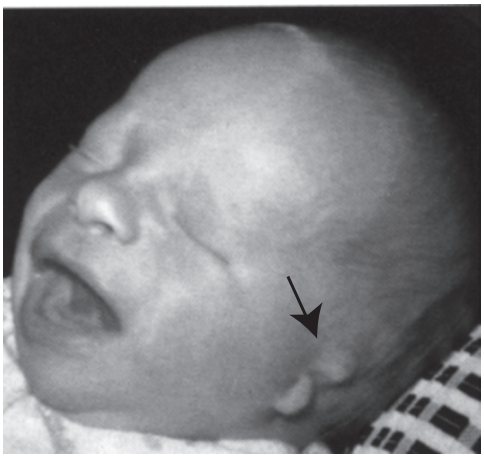

FIGURE 8.9. Microtia.

Study Questions for Chapter 8

1. The cochlear duct contains the spiral organ of Corti and is derived from which of the following?

(A) From both ectoderm and mesoderm
(B) Neural crest
(C) Endoderm
(D) Mesoderm
(E) Ectoderm

2. The middle ear cavity

(A) is of mesodermal origin
(B) develops from pharyngeal pouch 1
(C) develops from pharyngeal arch 1
(D) develops from pharyngeal arch 2
(E) develops from the otic vesicle

3. The otic vesicle

(A) gives rise to the bony labyrinth
(B) is found adjacent to the rhombencephalon
(C) is derived from neuroectoderm
(D) gives rise to the auricle (pinna)
(E) gives rise to the tympanic membrane

4. The auricle (pinna) of the external ear is innervated by which of the following nerves?

(A) CN V_3
(B) CN V_2
(C) CN XII
(D) CN III
(E) CN VIII

5. The stapedius muscle, which moves the stapes ossicle, is innervated by

(A) CN V_3
(B) CN XII
(C) CN III
(D) CN VII
(E) cervical nerves C_2 and C_3

6. The utricular portion of the otic vesicle gives rise to the

(A) ductus reuniens
(B) cochlear duct
(C) endolymphatic sac
(D) scala vestibuli
(E) scala tympani

7. The saccular portion of the otic vesicle gives rise to the

(A) organ of Corti
(B) endolymphatic duct
(C) superior semicircular canal
(D) crus commune nonampullare
(E) lateral semicircular canal

8. The tubotympanic recess gives rise to

(A) a conduit that interconnects the middle ear and the nasopharynx
(B) the external auditory meatus
(C) the internal auditory meatus
(D) the facial canal
(E) a conduit that interconnects the perilymphatic space with the subarachnoid space

9. Perilymph enters the subarachnoid space via the

(A) cochlear duct
(B) ductus reuniens
(C) perilymphatic duct
(D) vestibular aqueduct
(E) utriculosaccular duct

10. Pharyngeal groove 1 gives rise to the

(A) internal auditory meatus
(B) external auditory meatus
(C) eustachian tube
(D) cervical sinus
(E) primary tympanic cavity

Answers and Explanations

1. **E.** The cochlear duct is derived from a thickening of the surface ectoderm called the otic placode.
2. **B.** The middle ear cavity develops from pharyngeal pouch 1 as it evaginates to form the tubotympanic recess.
3. **B.** The otic vesicle arises from an invagination of the surface ectoderm called the otic placode. The otic vesicle is found adjacent to the rhombencephalon.
4. **A.** The auricle (pinna) of the external ear is innervated by cranial nerves V_3 (mandibular division), VII, IX, and X; cervical nerves C_2 and C_3 also innervate the auricle.
5. **D.** The stapes is innervated by CN VII.
6. **C.** The utricular region of the otic vesicle gives rise to the endolymphatic sac and duct and semicircular ducts.
7. **A.** The saccular region of the otic vesicle gives rise to the cochlear duct, which houses the spiral organ of Corti.
8. **A.** The tubotympanic recess is derived from pharyngeal pouch 1. It gives rise to the tympanic cavity and the auditory (eustachian) tube; the auditory tube interconnects the tympanic cavity with the nasopharynx.
9. **C.** The perilymph enters the subarachnoid space of the posterior cranial fossa via the cochlear aqueduct, which contains the perilymphatic duct.
10. **B.** Pharyngeal groove 1 gives rise to the external auditory meatus.

chapter 9

Eye

I. DEVELOPMENT OF THE OPTIC VESICLE (FIGURE 9.1; TABLE 9.1)

A. The development of the optic vesicle begins at day 22 with the formation of **optic sulcus**, which evaginates from the wall of the diencephalon as the **optic vesicle**, consisting of **neuroectoderm**.

B. The optic vesicle invaginates and forms a double-layered **optic cup** and **optic stalk**.

C. ***PAX6*** is the master homeotic gene in eye development. *PAX6* is expressed predominately in the optic cup and lens placode. *PAX2* is expressed predominately in the optic stalk.

D. The optic cup and its derivatives. The double-layered optic cup consists of an **outer pigment layer** and an **inner neural layer**.

1. **Retina**
   - **a.** The outer pigment layer of the optic cup gives rise to the **pigment layer of the retina**.
   - **b.** The **intraretinal space** separates the outer pigment layer from the inner neural layer. Although the intraretinal space is obliterated in the adult, it remains a weakened area prone to **retinal detachment**.
   - **c.** The inner neural layer of the optic cup gives rise to the **neural layer of the retina** (i.e., the rods and cones, bipolar cells, ganglion cells, etc.).
2. **Iris (Figure 9.2)**
   - **a.** The epithelium of the iris develops from the anterior portions of both the outer pigment layer and inner neural layer of the optic cup, which explains its histological appearance of two layers of columnar epithelium.
   - **b.** The stroma develops from mesoderm continuous with the choroid.
   - **c.** The iris contains the **dilator pupillae muscle** and **sphincter pupillae muscle**, which are formed from the epithelium of the outer pigment layer by a transformation of these epithelial cells into contractile cells.
3. **Ciliary body (Figure 9.2)**
   - **a.** The epithelium of the ciliary body develops from the anterior portions of both the outer pigment layer and inner neural layer of the optic cup, which explains its histological appearance of two layers of columnar epithelium.
   - **b.** The stroma develops from mesoderm continuous with the choroid.
   - **c.** The ciliary body contains the **ciliary muscle**, which is formed from mesoderm within the choroid.

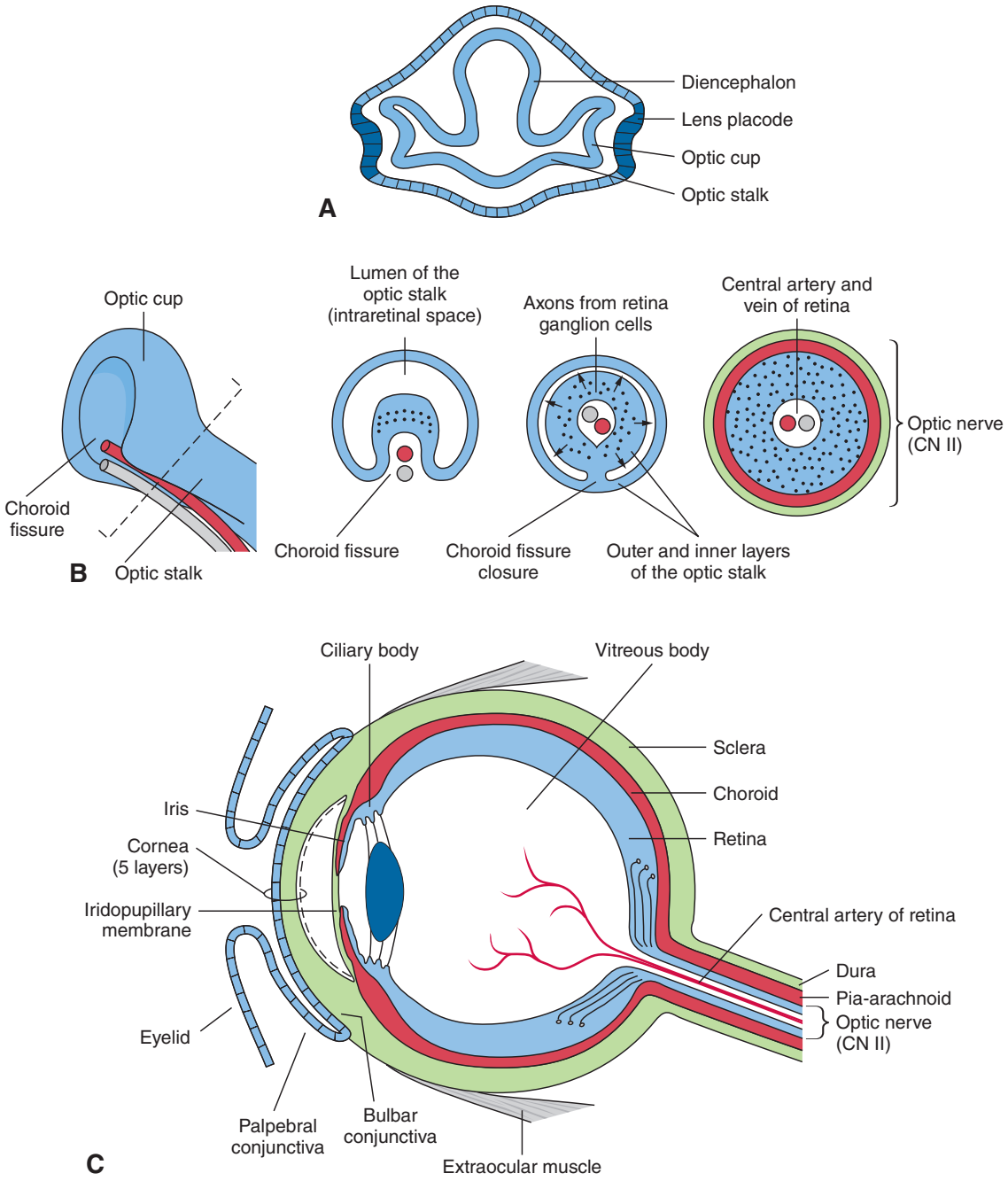

FIGURE 9.1. A. The optic cup (*light blue*) and optic stalk (*light blue*) are evaginations of the diencephalon (*light blue*). The optic cup induces surface ectoderm to differentiate into the lens placode (*dark blue*). **B**. Formation of the optic nerve (CN II) from the optic stalk. The choroid fissure, which is located on the undersurface of the optic stalk, permits access of the hyaloid artery (*red*) and vein to the inner aspect of the eye. The choroid fissure eventually closes. As ganglion cells form in the retina, axons accumulate in the optic stalk and cause the inner and outer layers of the optic stalk to fuse, obliterating the lumen (or intraretinal space) and forming the optic nerve. **C**. The adult eye. Note that the sclera (*green*) is continuous with the dura mater (*green*) and the choroid (*red*) is continuous with the pia-arachnoid (*red*). The iridopupillary membrane is normally obliterated.

table 9.1 Embryonic Eye Structures and Their Adult Derivatives

Embryonic Structure	Adult Derivative
Diencephalon	
Optic cup (neuroectoderm)	Retina, iris epithelium, dilator and sphincter pupillae muscles of iris, ciliary body epithelium
Optic stalk (neuroectoderm)	Optic nerve (CN II), optic chiasm, optic tract
Surface ectoderm	Lens, anterior epithelium of cornea, bulbar and palpebral conjunctiva
Mesoderm	Sclera, choroid, stroma of iris, stroma of ciliary body, ciliary muscle, substantia propria of cornea, corneal endothelium, vitreous body, central artery and vein of retina, extraocular muscles

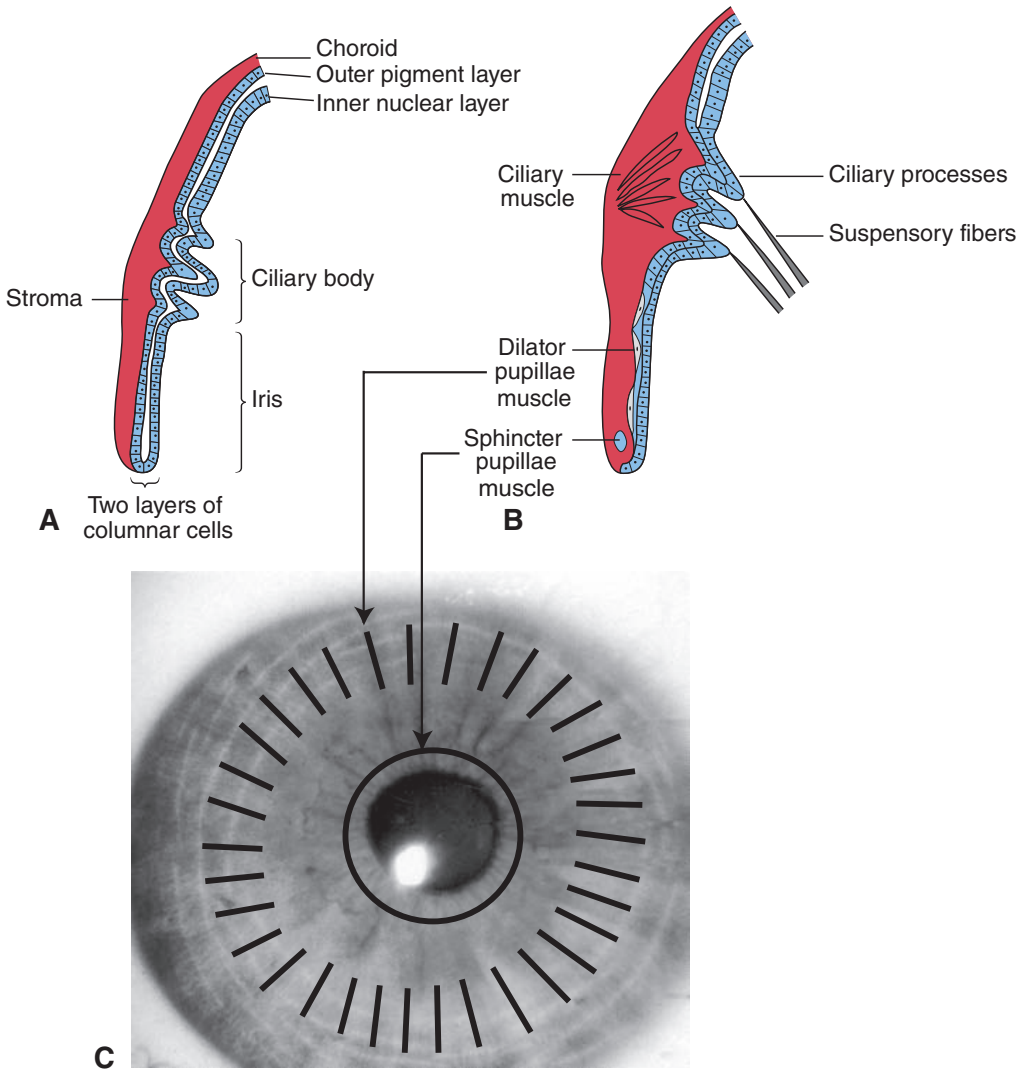

FIGURE 9.2. A, B. Sagittal sections through the developing iris and ciliary body. The iris and ciliary body form from the outer pigment layer (*light blue*) and inner neural layer (*light blue*) of the optic cup. In the adult, this embryological origin is reflected histologically by two layers of simple columnar epithelium that line both the iris and ciliary body. Note the dilator and sphincter pupillae muscles (*light blue*) associated with the iris and the ciliary muscle (*red*) associated with the ciliary body. **C**. Photograph of the human eye. Note the radial arrangement (spokelike pattern) of the dilator pupillae muscle around the entire iris. Note the circular arrangement of the sphincter pupillae muscle around the edge of the entire iris.

d. The **ciliary processes** are components of the ciliary body and produce **aqueous humor**. The aqueous humor circulates through the posterior chamber, then the anterior chamber, and finally drains into the venous circulation via the **trabecular meshwork** and the **canal of Schlemm**.

e. The ciliary processes give rise to the **suspensory fibers** of the lens (ciliary zonule), which are attached to and suspend the lens.

E. The optic stalk and its derivatives

1. The optic stalk contains the **choroid fissure**, in which the **hyaloid artery and vein** are found.
2. The hyaloid artery and vein later become the **central artery and vein of the retina**.
3. The optic stalk contains axons from the ganglion cell layer of the retina.
4. The choroid fissure closes during week 7, so that the optic stalk, together with the axons of the ganglion cells, forms the **optic nerve (CN II), optic chiasm, and optic tract**.
5. The optic nerve (CN II) is a tract of the diencephalon and has the following characteristics:
   a. The optic nerve is not completely myelinated until 3 months after birth; it is myelinated by oligodendrocytes.

b. The optic nerve is not capable of regeneration after transection.
c. The optic nerve is invested by the meninges and therefore is surrounded by a subarachnoid space, which plays a role in papilledema.

II. DEVELOPMENT OF OTHER EYE STRUCTURES

A. Sclera. The sclera develops from mesoderm surrounding the optic cup. The sclera forms an outer **fibrous** layer that is continuous with the dura mater posteriorly and the cornea anteriorly.

B. Choroid. The choroid develops from mesoderm surrounding the optic cup. The choroid forms a **vascular** layer that is continuous with the pia/arachnoid posteriorly and iris/ciliary body anteriorly.

C. Anterior chamber

1. The anterior chamber develops from mesoderm over the anterior aspect of the eye that is continuous with the sclera and undergoes vacuolization to form a chamber.
2. The anterior chamber essentially splits the mesoderm into two layers:
   a. The mesoderm posterior to the anterior chamber is called the **iridopupillary membrane**, which is normally resorbed prior to birth.
   b. The mesoderm anterior to the anterior chamber develops into the **substantia propria of the cornea** and **corneal endothelium**.

D. Cornea

1. The cornea develops from both surface ectoderm and mesoderm lying anterior to the anterior chamber.
2. The surface ectoderm forms the **anterior epithelium of the cornea** which has a high regenerative capacity.
3. The mesoderm forms the **substantia propria of the cornea (i.e., Bowman layer, stroma**, and **Descemet membrane)** and **corneal endothelium**.

E. Lens

1. The lens develops from surface ectoderm, which forms the **lens placode**.
2. The lens placode invaginates to form the **lens vesicle**.
3. The adult lens is completely surrounded by a **lens capsule**.
4. The **lens epithelium** is a simple cuboidal epithelium located beneath the capsule only on the anterior surface. The lens epithelium is mitotically active and migrates to the equatorial region of the lens.
5. The **lens fibers** are prismatic remnants of the lens epithelium that lose their nuclei and organelles.
6. The lens fibers are filled with cytoskeletal proteins called **filensin and a,b,g-crystallin**, which maintain the conformation and transparency of the lens.

F. Vitreous body. The vitreous body develops from mesoderm that migrates through the choroid fissure and forms a transparent gelatinous substance between the lens and retina. The vitreous body contains the **hyaloid artery**, which is later obliterated to form the **hyaloid canal** of the adult eye.

G. Canal of Schlemm. The canal of Schlemm is found at the sclerocorneal junction called the **limbus** and drains the aqueous humor into the venous circulation. An obstruction of the canal of Schlemm results in increased intraocular pressure **(glaucoma)**.

H. Extraocular muscles. The extraocular muscles develop from mesoderm that surrounds the optic cup.

III. CONGENITAL MALFORMATIONS OF THE EYE

A. Coloboma iridis (Figure 9.3) is a cleft in the iris caused by failure of the choroid fissure to close in week 7 of development and may extend into the ciliary body, retina, choroid, or optic nerve. A **palpebral coloboma**, a notch in the eyelid, results from a defect in the developing eyelid. The photograph (Figure 9.3) shows the cleft in the iris.

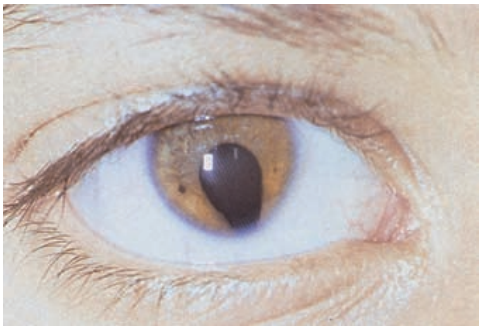

FIGURE 9.3. Coloboma iridis.

B. Congenital cataracts (Figure 9.4) are opacities of the lens and are usually bilateral. They are fairly common and may result from the following: rubella virus infection, toxoplasmosis, congenital syphilis, Down syndrome (trisomy 21), or galactosemia (an inborn error of metabolism). The photograph (Figure 9.4) shows lens opacities in both eyes.

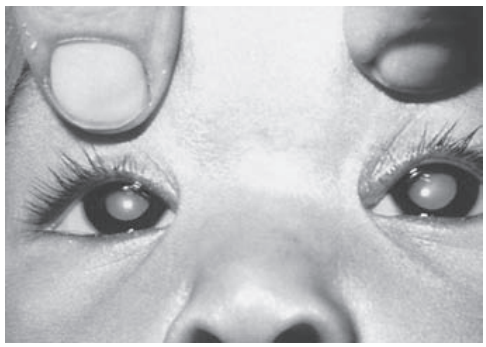

FIGURE 9.4. Congenital cataracts.

C. Congenital glaucoma (buphthalmos; Figure 9.5) is increased intraocular pressure due to abnormal development of the canal of Schlemm or the iridocorneal filtration angle. It is usually genetically determined but may result from maternal rubella infection.

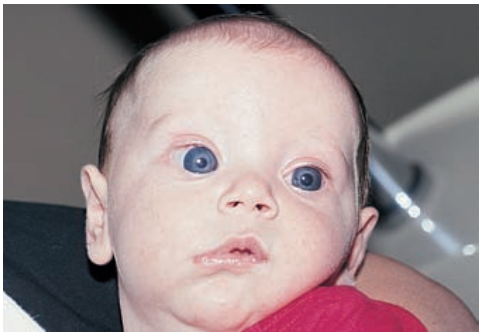

FIGURE 9.5. Congenital glaucoma (buphthalmos).

D. Detached retina (Figure 9.6) may result from head trauma or may be congenital. The site of detachment is between the outer and inner layers of the optic cup (i.e., between the retinal pigment epithelial layer and outer segment layer of rods and cones of the neural retina). The photograph (Figure 9.6) shows a detached retina. Note the retina (*arrow*) detached from the choroid and sclera (L denotes the lens).

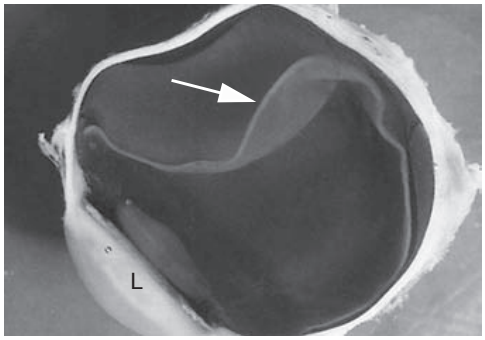

FIGURE 9.6. Detached retina.

E. Persistent iridopupillary membrane (Figure 9.7) consists of strands of connective tissue that partially cover the pupil; however, it seldom affects vision. The photograph (Figure 9.7) shows a persistent iridopupillary membrane. Note the strands of connective tissue that partially cover the pupil.

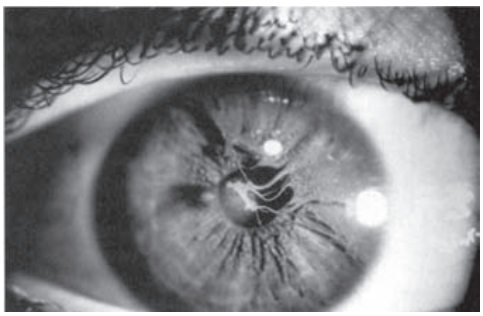

FIGURE 9.7. Persistent iridopupillary membrane.

F. Microphthalmia (Figure 9.8) is a small eye, usually associated with intrauterine infections from the TORCH group of microorganisms (*To*xoplasma, *r*ubella virus, *c*ytomegalovirus, and *h*erpes simplex virus). The CT scan (Figure 9.8) shows exophthalmos, small right globe, and a retroocular mass (*arrows*).

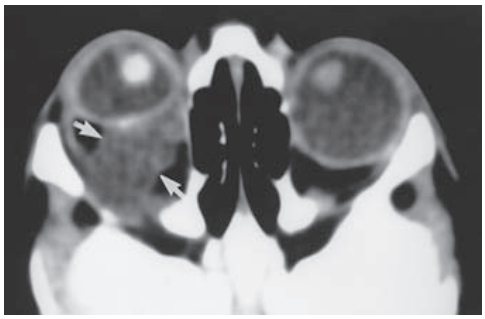

FIGURE 9.8. Microphthalmia.

G. Hereditary retinoblastoma (RB; Figure 9.9) Hereditary RB is an autosomal dominant genetic disorder caused by a mutation in the *RB1* **gene** on **chromosome 13q14.1** for the **retinoblastoma (RB) protein**. More than 1,000 different mutations of the *RB1* gene have been identified, which include missense, frameshift, and RNA splicing mutations that result in a premature STOP codon and a **loss-of-function mutation**. RB protein binds to E2F (a gene-regulatory protein) such that there is no expression of target genes whose products stimulate the cell cycle at the G1 checkpoint. RB protein belongs to the family of **tumor-suppressor genes**. **Clinical features include** a malignant tumor of the retina that develops in children younger than 5 years of age, a whitish mass in the pupillary area behind the lens (leukokoria; the "cat's eye"), and strabismus. The CT scan (Figure 9.9) of RB shows multiple tumor calcifications (*arrows*) within the left intraorbital mass.

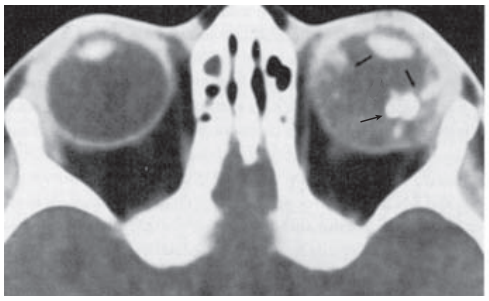

FIGURE 9.9. Retinoblastoma.

H. Anophthalmia is absence of the eye. It is due to failure of the optic vesicle to form.

I. Cyclopia is a single orbit and one eye. It is due to failure of median cerebral structures to develop.

J. Retinocele results from herniation of the retina into the sclera or from failure of the choroid fissure to close.

K. Retrolental fibroplasia (retinopathy of prematurity) is an oxygen-induced retinopathy seen in premature infants.

L. **Papilledema** is edema of the optic disk (papilla) due to increased intracranial pressure. This pressure is reflected into the subarachnoid space, which surrounds the optic nerve (CN II).

M. **Retinitis pigmentosa (RP)** is a hereditary degeneration and atrophy of the retina. RP may be transmitted as an autosomal recessive, autosomal dominant, or X-linked trait. RP is characterized by a degeneration of the rods, night blindness (nyctalopia), and "gun barrel vision." RP may also be due to abetalipoproteinemia (Bassen-Kornzweig syndrome), which may be arrested with massive doses of vitamin A.

Study Questions for Chapter 9

1. The surface ectoderm gives rise to which of the following structures?

(A) Dilator pupillae muscle
(B) Retina
(C) Lens
(D) Sclera
(E) Choroid

2. Failure of the choroid fissure to close results in

(A) congenital detached retina
(B) congenital aniridia
(C) congenital aphakia
(D) coloboma iridis
(E) microphthalmos

3. The optic cup is an evagination of which of the following?

(A) Telencephalon
(B) Diencephalon
(C) Mesencephalon
(D) Metencephalon
(E) Myelencephalon

4. The epithelium of the ciliary body is derived from

(A) ectoderm
(B) mesoderm
(C) endoderm
(D) neuroectoderm
(E) neural crest cells

5. Hyperoxygenation of premature infants may result in

(A) congenital glaucoma
(B) microphthalmia
(C) coloboma
(D) retrolental fibroplasia
(E) persistent pupillary membrane

6. The optic nerve is a tract of the diencephalons that is not completely myelinated until

(A) 5 years after birth
(B) 2 years after birth
(C) 1 year after birth
(D) 3 weeks after birth
(E) 3 months after birth

7. The hyaloid canal is found in the

(A) vitreous body
(B) choroid
(C) optic stalk
(D) ciliary body
(E) intraretinal space

8. Aqueous humor is produced by the

(A) choroid plexus
(B) trabecular meshwork
(C) ciliary processes
(D) vitreous body
(E) lens vesicle

9. Aqueous humor enters the venous circulation via

(A) arachnoid villi
(B) scleral canal
(C) hyaloid canal
(D) canal of Schlemm
(E) Cloquet's canal

10. In a detached retina, the site of detachment is found

(A) within the outer plexiform layer
(B) within the inner plexiform layer
(C) between the inner nuclear layer and the outer nuclear layer
(D) between the choriocapillaris and the pigment epithelial layer
(E) between the pigment epithelial layer and the layer of outer segments of rods and cones

Answers and Explanations

1. **C.** The lens forms from the lens placode that is induced by the optic cup.
2. **D.** Failure of the choroid (optic) fissure to close results in a cleft of the iris—a coloboma iridis. This defect may extend into the ciliary body, choroid, optic nerve, or retina. Congenital aphakia—absence of the lens—may result from defective development of the lens placode.
3. **B.** The optic cup and its derivatives—the retina and optic nerve—develop from the diencephalon.
4. **D.** The ciliary body is derived from the anterior two layers of the optic cup (neuroectoderm), which form the epithelium, and from an anterior extension of the choroid (mesoderm).
5. **D.** Retrolental fibroplasia results from hyperoxygenation of premature infants. In premature infants, high oxygen concentration results in vaso-obliteration of the terminal arterioles, leading to hemorrhage and infarction of the retina. This phenomenon is peculiar to the incompletely vascularized peripheral retina.
6. **E.** The axons of the optic nerve are not completely myelinated until 3 months after birth. Myelinated axons are normally not found in the retina. The optic nerve is not a true peripheral nerve but a tract of the diencephalon; when severed, the optic nerve does not regenerate. Myelination in the central nervous system (CNS) is accomplished by oligodendrocytes; oligodendrocytes are not found in the retina.
7. **A.** The hyaloid canal (Cloquet's canal) is found in the vitreous body. In early development, a hyaloid artery passes through the vitreous body to perfuse the developing lens; in the late fetal period, this artery is obliterated to form the hyaloid canal.
8. **C.** Aqueous humor is produced by the ciliary processes of the ciliary body. It flows from the posterior chamber, through the pupil, into the anterior chamber, and finally to the canal of Schlemm, which empties into the extraocular veins.
9. **D.** Aqueous humor enters the venous circulation via the canal of Schlemm. Blockage of this canal results in increased intraocular pressure (glaucoma).
10. **E.** The site of retinal detachment is between the pigment epithelial layer and the layer of outer segments of rods and cones; this corresponds to the intraretinal space between the inner and outer layers of the optic cup. Retinal detachment occurs when fluid from the vitreous compartment passes through a retinal hole and separates the pigment epithelial layer from the layer of outer segments of rods and cones.

chapter 10

Digestive System

I. OVERVIEW (FIGURE 10.1)

A. The **primitive gut tube** is formed from the incorporation of the dorsal part of the yolk sac into the embryo due to the craniocaudal folding and lateral folding of the embryo.

B. The primitive gut tube extends from the **oropharyngeal membrane** to the **cloacal membrane** and is divided into the **foregut, midgut**, and **hindgut**.

C. Histologically, the general plan of the adult gastrointestinal tract consists of a **mucosa** (epithelial lining and glands, lamina propria, and muscularis mucosae), **submucosa, muscularis externa**, and **adventitia** or **serosa**.

D. Embryologically, the epithelial lining and glands of the mucosa are derived from **endoderm**, whereas the other components are derived from **visceral mesoderm**.

E. Early in development, the epithelial lining the gut tube proliferates rapidly and obliterates the lumen. Later, **recanalization** occurs.

II. DERIVATIVES OF THE FOREGUT

Derivatives of the foregut are supplied by the **celiac trunk**. The exception to this is the esophagus, for which the intraabdominal portion is supplied by the celiac trunk, whereas the intrathoracic portion is supplied by other branches of the aorta.

A. Esophagus

1. **Development.** The foregut is divided into the esophagus dorsally and the trachea ventrally by the **tracheoesophageal folds**, which fuse to form the **tracheoesophageal septum**. The esophagus is initially short but lengthens with descent of the heart and lungs. During development, the endodermal lining of the esophagus proliferates rapidly and obliterates the lumen; later, recanalization occurs.
2. **Sources.** The stratified squamous epithelium, mucosal glands, and submucosal glands of the definitive esophagus are derived from **endoderm**. The lamina propria, muscularis mucosae, submucosa, skeletal muscle and smooth muscle of muscularis externa, and adventitia of the definitive esophagus are derived from **visceral mesoderm**.

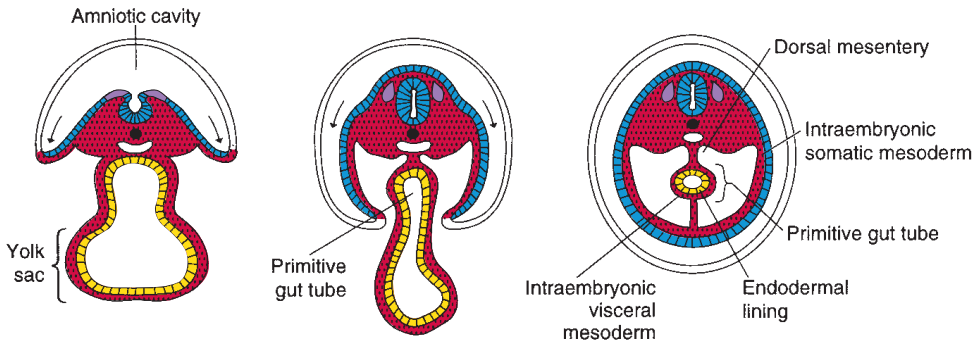

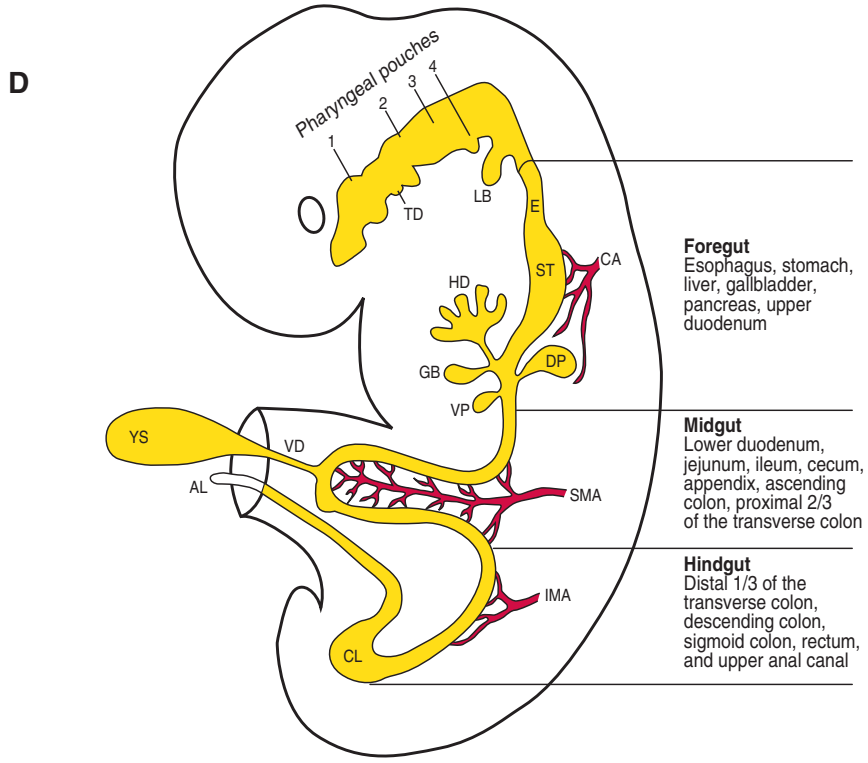

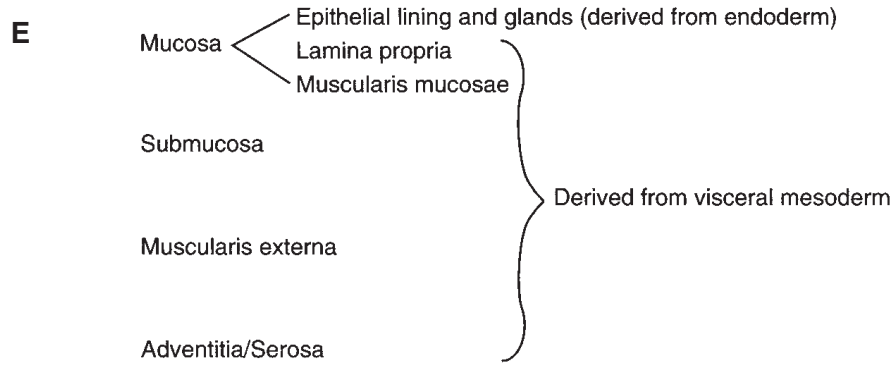

FIGURE 10.1. **A–C**. Cross sections of an embryo showing the formation of the primitive gut tube. **D**. Development of gastrointestinal tract showing the foregut, midgut, and hindgut along with the adult derivatives. The entire length of the endodermal gut tube is shown from the mouth to the anus. The fates of the lung bud (LB), pharyngeal pouches (1–4), and thyroid diverticulum (TD) are covered in later chapters. E = esophagus; ST = stomach; HD = hepatic diverticulum; GB = gall bladder; VP = ventral pancreatic bud; DP = dorsal pancreatic bud; CA = celiac artery; YS = yolk sac; VD = vitelline duct; AL = allantois; SMA = superior mesenteric artery; CL = cloaca; IMA = inferior mesenteric artery. **E**. Diagram showing the general plan of histological and embryological organization of the adult gastrointestinal tract.

3. **Clinical considerations**

   a. **Esophageal atresia (Figure 10.2)** occurs when the tracheoesophageal septum deviates too far dorsally, causing the esophagus to end as a closed tube. About 33% of patients with esophageal atresia also have other congenital defects associated with the VATER (**v**ertebral defects, **a**nal atresia, **t**racheo**e**sophageal fistula, and **r**enal defects) or VACTERL (similar to VATER plus **c**ardiovascular defects and upper **l**imb defects) syndromes. It is associated clinically with polyhydramnios (the fetus is unable to swallow amniotic fluid) and a tracheoesophageal fistula. The photograph (Figure 10.2; posterior view) shows that the esophagus terminates blindly in a blunted esophageal pouch (*arrow*). There is a distal esophageal connection with the trachea at the carina (*arrowhead*).

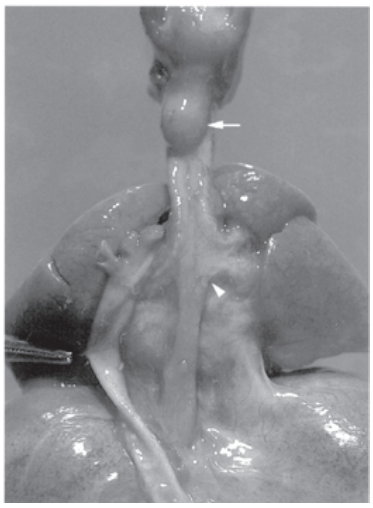

FIGURE 10.2. Esophageal atresia.

   b. **Esophageal stenosis (Figure 10.3)** occurs when the lumen of the esophagus is narrowed and usually involves the midesophagus. The stenosis may be caused by submucosal/muscularis externa hypertrophy, remnants of the tracheal cartilaginous ring within the wall of the esophagus, a membranous diaphragm obstructing the lumen, probably due to incomplete recanalization. The light micrograph (Figure 10.3) shows the stratified squamous epithelial lining of the esophagus and submucosal glands. Note that a portion of the muscular wall contains remnants of cartilage (*arrow*), which contributes to a stenosis.

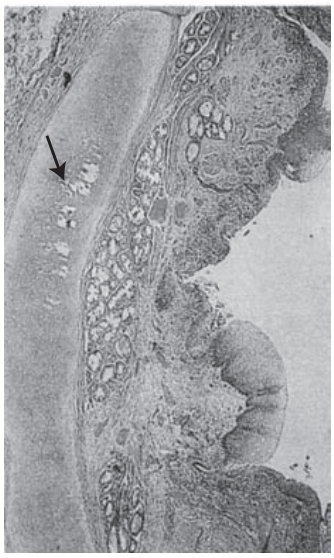

FIGURE 10.3. Esophageal stenosis.

   c. **Esophageal duplication (Figure 10.4)** occurs most commonly due to a congenital esophageal cyst, which is usually found (60% of the cases) in the lower esophagus. Duplication cysts may lie on the posterior aspect of the esophagus, where they protrude into the posterior mediastinum or within the wall of the esophagus (i.e., intramural). The barium esophagram (Figure 10.4) demonstrates a large intramural duplication cyst in the proximal esophagus (dashed lines). The cyst shows acute angles with the esophageal lumen, indicating its intramural location.

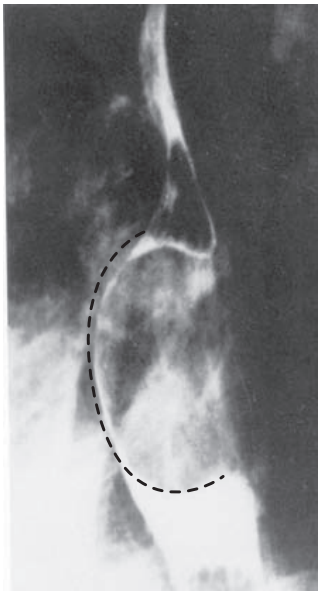

FIGURE 10.4. Esophageal duplication.

d. Vascular compression of the esophagus (Figure 10.5) occurs due to the abnormal origin of the **right subclavian artery** due to developmental anomalies of the aortic arches. The anomalous right subclavian artery passes from the aortic arch behind the esophagus and may cause dysphagia ("dysphagia lusoria"). The barium esophagram (Figure 10.5) reveals an oblique compression of the esophagus (*arrow*) due to the anomalous right subclavian artery.

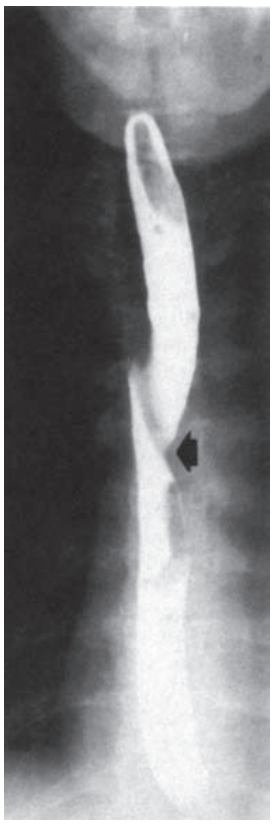

FIGURE 10.5. Vascular compression of the esophagus.

e. Achalasia (Figure 10.6) occurs due to the loss of ganglion cells in the myenteric plexus (Auerbach) and is characterized by the failure to relax the lower esophageal sphincter, which causes progressive dysphagia and difficulty in swallowing. The barium esophagram of the distal esophagus (Figure 10.6) shows a long, narrowed segment **("bird beak")** of the esophagus secondary to muscular hypertrophy in long-standing achalasia.

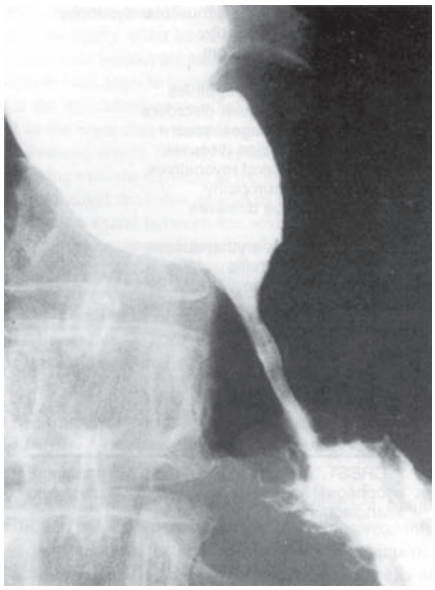

FIGURE 10.6. Achalasia.

B. Stomach (Figure 10.7)

1. **Development.** A fusiform dilation forms in the foregut in week 4 that gives rise to the **primitive stomach**. The dorsal part of the primitive stomach grows faster than the ventral part, thereby resulting in the greater and lesser curvatures, respectively. The primitive stomach rotates 90° clockwise around its longitudinal axis. The 90° rotation affects all foregut structures and is responsible for the adult anatomical relationship of foregut viscera. As a result of this clockwise

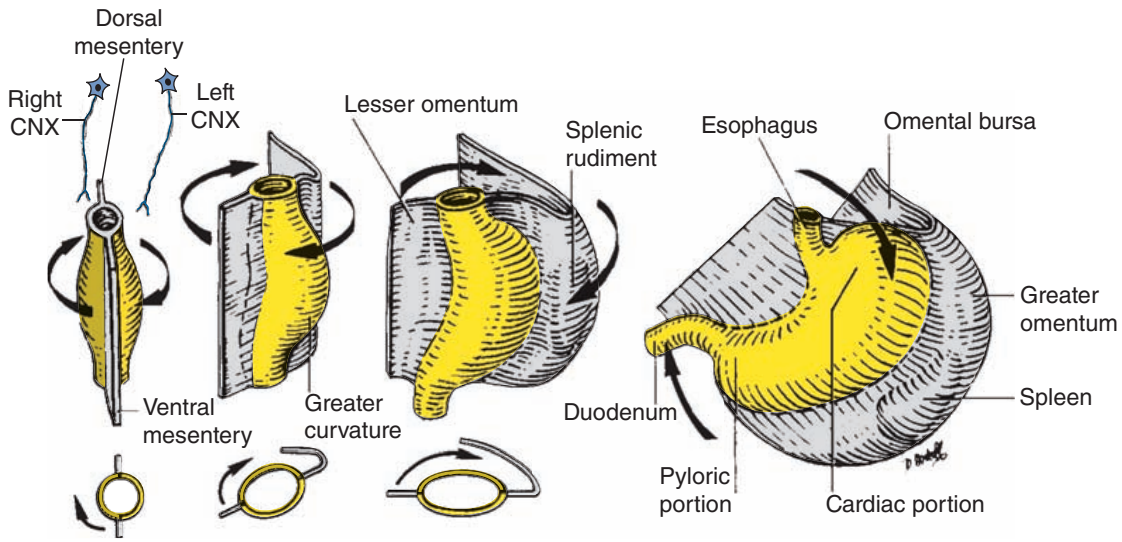

FIGURE 10.7. Diagram depicting the development and 90° rotation of the stomach from week 4 through week 6. CNX = cranial nerve X.

rotation, the dorsal mesentery is carried to the left and eventually forms the **greater omentum;** the **left vagus nerve (CNX)** innervates the ventral surface of the stomach; and the **right vagus nerve (CN X)** innervates the dorsal surface of the stomach.

2. **Sources.** The surface mucous cells lining the stomach, mucous neck cells, parietal cells, chief cells, and enteroendocrine cells comprising the gastric glands of the definitive stomach are derived from **endoderm**. The lamina propria, muscularis mucosae, submucosa, smooth muscle layers of the muscularis externa, and serosa of the definitive stomach are derived from **visceral mesoderm**.
3. **Hypertrophic pyloric stenosis (Figure 10.8)** occurs when the muscularis externa in the pyloric region hypertrophies and forms a small palpable mass (**"olive"**), causing a narrow pyloric lumen that obstructs food passage. It is associated clinically with projectile, nonbilious vomiting after feeding and a small, palpable mass at the right costal margin. Increased incidence has been found in infants treated with the antibiotic erythromycin. The pathogenesis of pyloric stenosis is the inability of the pyloric sphincter to relax due to a faulty migration of neural crest cells so that the ganglion cells of the enteric nervous system are not properly populated. The barium contrast radiograph (Figure 10.8) shows the long, narrow, double channel of the pylorus (*arrows*) in a patient with hypertrophic pyloric stenosis.

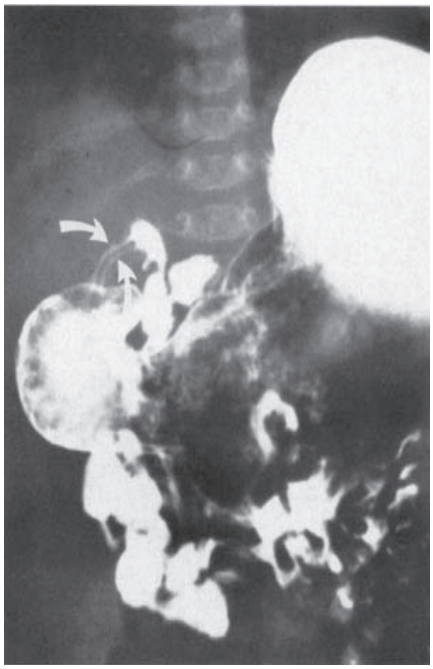

FIGURE 10.8. Hypertrophic pyloric stenosis.

C. Liver (Figure 10.9)

1. **Development.** The endodermal lining of the foregut forms an outgrowth (**hepatic diverticulum**) into the surrounding mesoderm of the **septum transversum** through induction by **fibroblast growth factors (FGFs) FGF-1, FGF-2, and FGF-8** released by **cardiac mesoderm** (which is in close vicinity). The mesoderm of the septum transversum is involved in the formation of the **diaphragm**, which explains the intimate gross anatomical relationship between the liver and

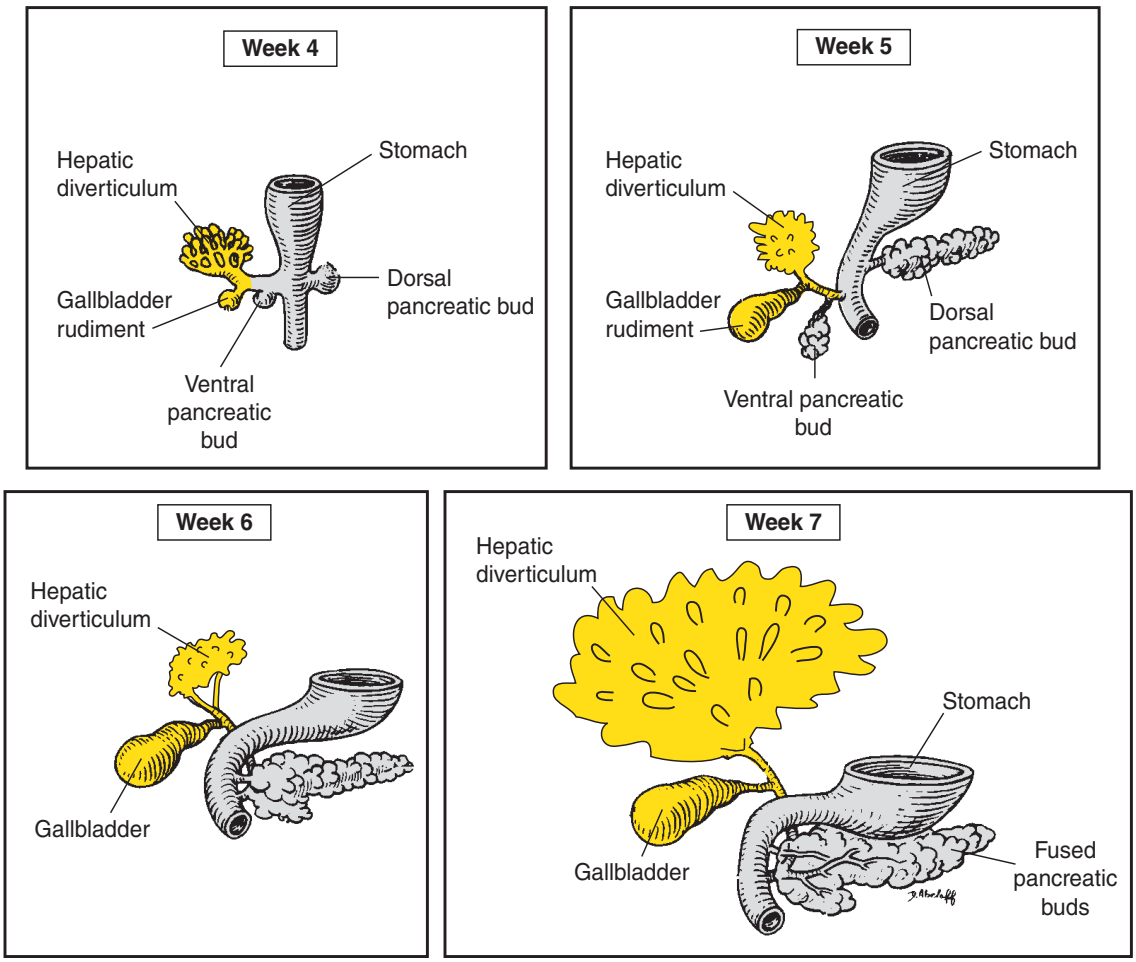

FIGURE 10.9. Sequence of events in the development of the hepatic diverticulum and gall bladder rudiment from week 4 through week 7.

diaphragm. Cords of hepatoblasts (called **hepatic cords**) from the hepatic diverticulum grow into the mesoderm of the septum transversum, where critical hepatoblast/mesoderm interactions occur. The hepatic cords arrange themselves around the **vitelline veins** and **umbilical veins**, which course through the septum transversum and form the **hepatic sinusoids**. Due to the tremendous growth of the liver, the liver bulges into the abdominal cavity which stretches the septum transversum to form the **ventral mesentery**. The ventral mesentery consists of the **falciform ligament** and the **lesser omentum**. The falciform ligament contains the **left umbilical vein**, which regresses after birth to form the **ligamentum teres**. The lesser omentum can be divided into the **hepatogastric ligament** and **hepatoduodenal ligament**. The hepatoduodenal ligament contains the **bile duct, portal vein**, and **hepatic artery** (i.e., **portal triad**).

2. **Sources.** The hepatocytes and simple columnar or cuboidal epithelium lining the biliary tree of the definitive liver are derived from **endoderm**. Kupffer cells, hematopoietic cells, endothelium of the sinusoids, and fibroblasts (connective tissue) of the definitive liver are derived from **mesoderm**.
3. **Clinical considerations.** Congenital malformations of the liver are rare except for minor gross anatomical variations.

D. Gallbladder and extrahepatic bile ducts (Figure 10.9)

1. **Development.** The connection between the hepatic diverticulum and the foregut narrows to form the **primitive bile duct**. An outgrowth from the primitive bile duct gives rise to the **gallbladder rudiment** and **cystic duct**. The cystic duct divides the primitive bile duct into the **common hepatic duct** and the definitive **bile duct**. During development, the endodermal lining of the gallbladder and extrahepatic bile ducts proliferates rapidly and obliterates the lumen; later, recanalization occurs.

2. **Sources.** The simple columnar epithelium lining the definitive gallbladder and simple columnar or cuboidal epithelium lining the definitive extrahepatic bile ducts are derived from **endoderm**. The lamina propria, muscularis externa, and adventitia of the definitive gallbladder are derived from **visceral mesoderm**.
3. **Clinical considerations**
   a. **Developmental anomalies of the gall bladder (Figure 10.10)** anatomy are fairly common in which two, bilobed, diverticula, and septated gall bladders are found. The drawings (Figure 10.10) show the developmental anomalies of the gall bladder. Septated gall bladder is most likely due to incomplete recanalization of the lumen.

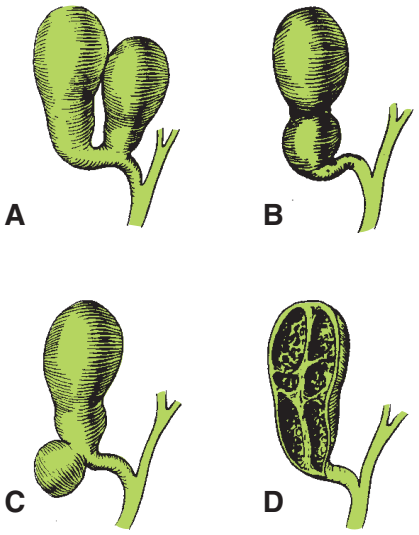

FIGURE 10.10. Developmental anomalies of the gallbladder. **A**. Two gall bladders. **B**. Bilobed gall bladder. **C**. Diverticulum of the gall bladder. **D**. Septated gall bladder.

   b. **Developmental anomalies of the cystic duct (Figure 10.11)** anatomy are fairly common. The drawings (Figure 10.11) show various developmental anomalies of the cystic duct.

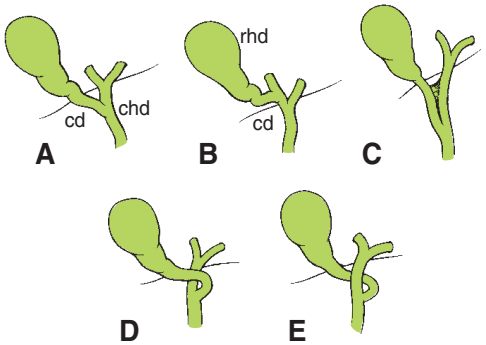

FIGURE 10.11. Developmental anomalies of the cystic duct. **A**. The cystic duct (cd) joins the common hepatic duct (chd) directly (most common anatomical arrangement). **B**. The cystic duct joins the right hepatic duct (rhd). **C**. Low junction of the cystic duct with the common hepatic duct. **D**. Anterior spiral of the cystic duct. **E**. Posterior spiral of the cystic duct.

   c. **Biliary atresia (Figure 10.12)** is defined as the obliteration of extrahepatic and/or intrahepatic ducts. The ducts are replaced by fibrotic tissue due to acute and chronic inflammation. **Clinical features include** progressive neonatal jaundice with onset soon after birth; white clay-colored stool; dark-colored urine; 12–19-month average survival time with a 100% mortality rate; can be treated by liver transplantation. The drawings (Figure 10.12) show different forms of extrahepatic biliary atresia.
   d. **Intrahepatic gall bladder** occurs when the gallbladder rudiment advances beyond the hepatic diverticulum and becomes buried within the substance of the liver.

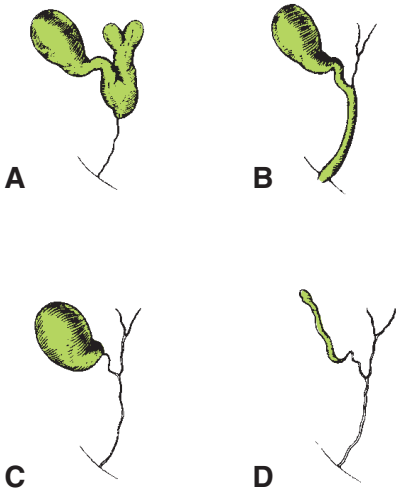

FIGURE 10.12. Different forms of extrahepatic biliary atresia. **A–C**. Partial. **D**. Complete.

e. **Floating gall bladder** occurs when the gallbladder rudiment lags behind the hepatic diverticulum and thereby becomes suspended from the liver by a mesentery. A floating gall bladder is at risk for **torsion** (i.e., a twisting or rotation around the axis of the mesentery).

E. Pancreas (Figure 10.9)

1. **Development.** The **dorsal pancreatic bud** is a direct outgrowth of foregut endoderm, whose formation is induced by the notochord. The **ventral pancreatic bud** is a direct outgrowth of foregut endoderm, whose formation is induced by hepatic mesoderm. Within both pancreatic buds, endodermal tubules surrounded by mesoderm branch repeatedly to form acinar cells and ducts (i.e., exocrine pancreas). Isolated clumps of endodermal cells bud from the tubules and accumulate within the mesoderm to form **islet cells** (i.e., endocrine pancreas). The islet cells form in the following sequence (first → last): **alpha cells** (glucagon) **beta cells** (insulin) **delta cells** (somatostatin) and **PP cells** (pancreatic polypeptide). Because of the 90° clockwise rotation of the duodenum, the ventral bud rotates dorsally and fuses with the dorsal bud to form the definitive adult pancreas. The ventral bud forms the **uncinate process** and a **portion of the head of the pancreas**. The dorsal bud forms the **remaining portion of the head, body**, and **tail of the pancreas**. The main pancreatic duct is formed by the anatomosis of the **distal two-thirds of the dorsal pancreatic duct** (the proximal one-third regresses) and the **entire ventral pancreatic duct** (48% incidence). The main pancreatic duct and common bile duct form a single opening (**hepatopancreatic ampulla of Vater**) into the duodenum at the tip of a major papillae **(hepatopancreatic papillae)**.
2. **Sources.** The acinar cells, islet cells, and simple columnar or cuboidal epithelium lining the pancreatic ducts of the definitive pancreas are derived from **endoderm**. The surrounding connective tissue and vascular components of the definitive pancreas are derived from **visceral mesoderm**.
3. **Clinical considerations**
   a. **Accessory pancreatic duct (Figure 10.13)** develops when the proximal one-third of the dorsal pancreatic duct persists and opens into the duodenum through minor papillae at a site proximal to the ampulla of Vater (33% incidence). The drawing (Figure 10.13) shows an accessory pancreatic duct.

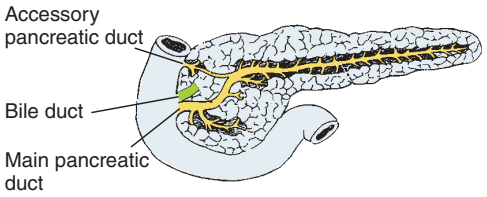

FIGURE 10.13. Accessory pancreatic duct.

   b. **Pancreas divisum (Figure 10.14)** occurs when the **distal two-thirds of the dorsal pancreatic duct** and the **entire ventral pancreatic duct** fail to anastomose and the proximal one-third of the dorsal pancreatic duct persists, thereby forming two separate duct systems (4% incidence). The dorsal pancreatic duct drains a **portion of the head, body**, and **tail of the pancreas** by opening into the duodenum through minor papillae. The ventral pancreatic duct drains the **uncinate process** and a **portion of the head of the pancreas** by opening into the duodenum through the major papillae. Patients with pancreas divisum are prone to pancreatitis, especially if the opening of the dorsal pancreatic duct at the minor papillae is small. The drawing (Figure 10.14A) shows pancreas divisum. Note that the distal two-thirds of the dorsal pancreatic duct and the ventral pancreatic bud fail to anastomose,

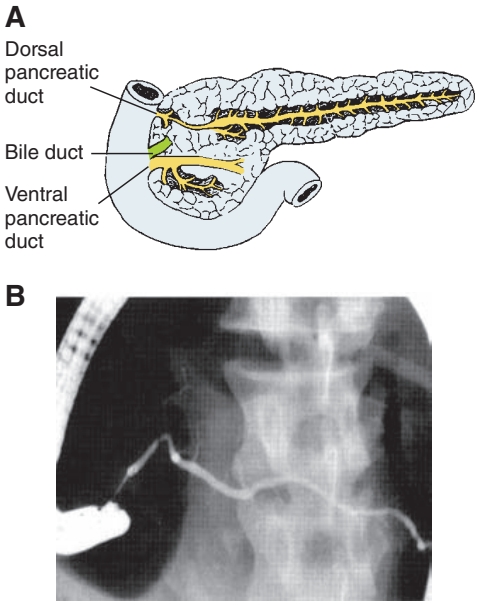

FIGURE 10.14. Pancreas divisum.

thereby forming two separate duct systems. An endoscopic retrograde pancreatogram (Figure 10.14B) performed through the accessory minor papillae shows the dorsal pancreatic duct in pancreatic divisum.

c. **Annular pancreas (Figure 10.15)** occurs when the ventral pancreatic bud fuses with the dorsal bud both dorsally and ventrally, thereby forming a **ring of pancreatic tissue** around the duodenum and causing severe **duodenal obstruction**. Newborns and infants are intolerant of oral feeding and often have bilious vomiting. Radiographic evidence of an annular pancreas is indicated by a duodenal obstruction, where a **"double bubble" sign** is often seen due to dilation of the stomach and distal duodenum (also associated with Down syndrome). The barium contrast radiograph (Figure 10.15) shows a partial duodenal obstruction consistent with an annular pancreas.

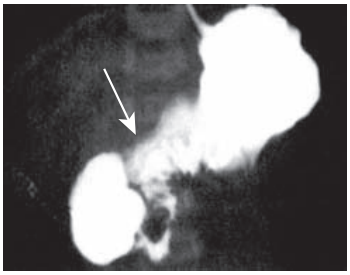

FIGURE 10.15. Annular pancreas.

d. **Hyperplasia of pancreatic islets** occurs when fetal islets are exposed to high blood glucose levels, as frequently happens in **infants of diabetic mothers**. Glucose freely crosses the placenta and stimulates fetal islet hyperplasia and insulin secretion, which causes increased fat and glycogen deposition in fetal tissues. This results in increased birth weight of infants at term (i.e., **macrosomia**) and serious episodes of **hypoglycemia** in the postnatal period.

F. **Upper duodenum** develops from the caudal-most part of the foregut.

III. DERIVATIVES OF THE MIDGUT (FIGURE 10.16)

Derivatives of the midgut are supplied by the **superior mesenteric artery**.

A. **Lower duodenum** develops from the cranial-most part of the midgut. The junction of the upper and lower duodenum is just distal to the opening of the bile duct.

B. **Jejunum, ileum, cecum, appendix, ascending colon, and the proximal two-thirds of the transverse colon (Figure 10.16)**

1. **Development.** The midgut forms a U-shaped loop (**midgut loop**) that herniates through the primitive umbilical ring into the extraembryonic coelom (i.e., **physiological umbilical herniation**) beginning at week 6. The midgut loop consists of a **cranial limb** and a **caudal limb**. The cranial limb forms the **jejunum** and **upper part of the ileum**. The caudal limb forms the **cecal diverticulum**, from which the **cecum** and **appendix** develop. The rest of the caudal limb forms the **lower part of the ileum, ascending colon**, and **proximal two-thirds of the transverse colon**. The midgut loop rotates a total of **270° counterclockwise** around the **superior mesenteric artery** as it returns to the abdominal cavity, thus reducing the physiological herniation, around week 11.
2. **Sources.** The simple columnar absorptive cells lining midgut derivatives, goblet cells, Paneth cells, and enteroendocrine cells comprising the intestinal glands are derived from **endoderm**. The lamina propria, muscularis mucosae, submucosa, and inner circular and outer longitudinal smooth muscle of the muscularis externa, and serosa are derived from **visceral mesoderm**.

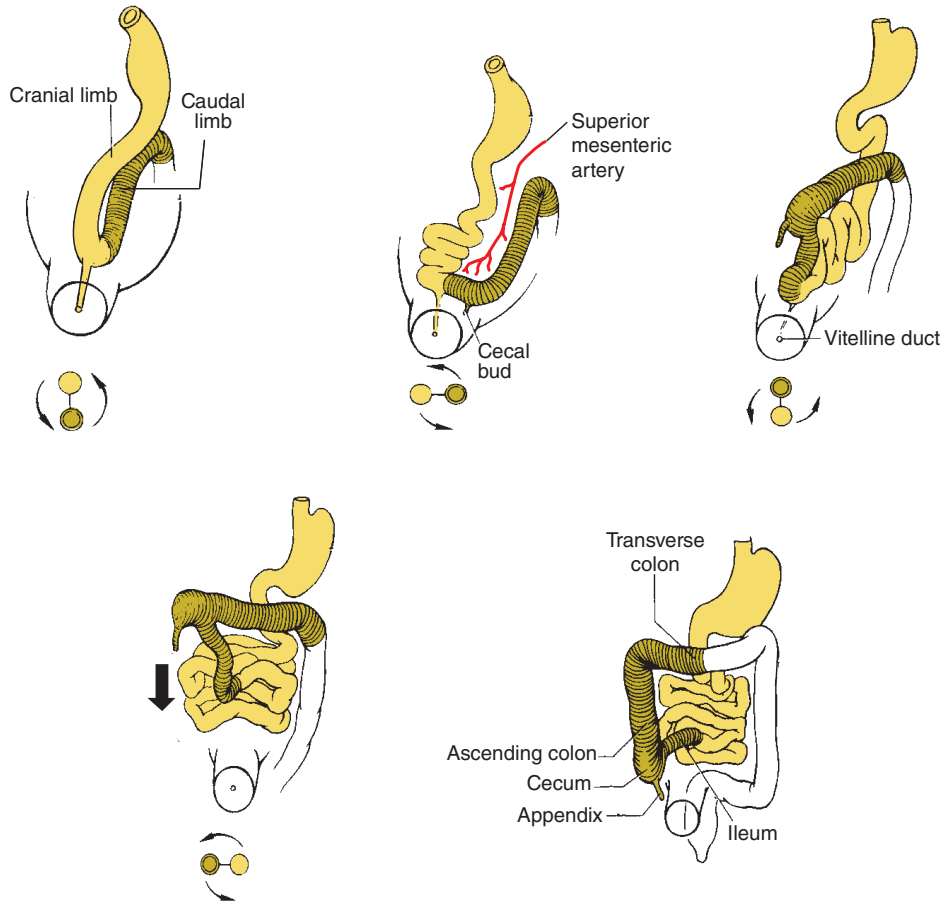

FIGURE 10.16. Diagram depicting the 270° counterclockwise rotation of the midgut loop. Note that after the 270° rotation (see *curved arrows*), the cecum and appendix are located in the upper abdominal cavity. Later in development, growth in the direction indicated by the *bold arrow* occurs so that the cecum and appendix position in the lower right quadrant.

3. Clinical considerations

a. Omphalocele (Figure 10.17) occurs when abdominal contents herniate through the umbilical ring and persist outside the body, covered variably by a translucent peritoneal membrane sac (a light gray, shiny sac) protruding from the base of the umbilical cord. Large omphaloceles may contain stomach, liver, and intestines. Small omphaloceles contain only intestines. Omphaloceles are usually associated with other congenital anomalies (e.g., trisomy 13, trisomy 18, or Beckwith-Wiedemann syndrome) and with increased levels of α-**fetoprotein**. The photograph (Figure 10.17) shows an infant with an omphalocele.

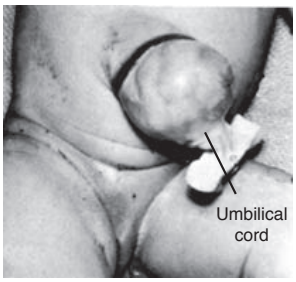

FIGURE 10.17. Omphalocele.

b. Gastroschisis (Figure 10.18) occurs when there is a defect in the ventral abdominal wall, usually to the right of the umbilical ring, through which there is a massive evisceration of intestines (other organs may also be involved). The intestines are not covered by

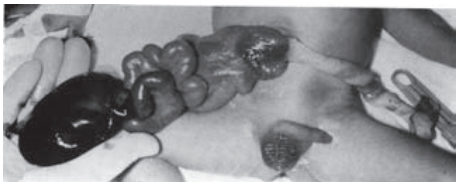

FIGURE 10.18. Gastroschisis.

a peritoneal membrane, are directly exposed to amniotic fluid, are thickened, and are covered with adhesions. The photograph (Figure 10.18) shows an infant with gastroschisis.

c. **Ileal diverticulum (Meckel's diverticulum; Figure 10.19)** occurs when a remnant of the vitelline duct persists, thereby forming an outpouching located on the **antimesenteric border** of the ileum. The outpouching may connect to the umbilicus via a fibrous cord or fistula. A Meckel diverticulum is usually located about 30 cm proximal to the ileocecal valve in infants and varies in length from 2 to 15 cm. **Heterotopic gastric mucosa** may be present, which leads to ulceration, perforation, or gastrointestinal bleeding, especially if a large number of parietal cells are present. It is associated clinically with symptoms resembling appendicitis and bright-red or dark-red stools (i.e., bloody). The photograph (Figure 10.19) shows a Meckel's diverticulum (*arrow*; IL denotes the ileum).

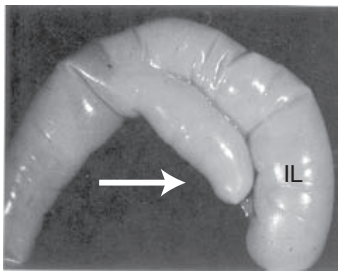

FIGURE 10.19. Meckel diverticulum.

d. **Nonrotation of the midgut loop (Figure 10.20)** occurs when the midgut loop rotates only 90° counterclockwise, thereby positioning the small intestine entirely on the right side and the large intestine entirely on the left side, with the cecum located either in the left upper quadrant or the left iliac fossa. The photograph (Figure 10.20) shows nonrotation of the midgut loop. Note the small intestines (SI) on the right side and the large intestines (LI) on the left side.

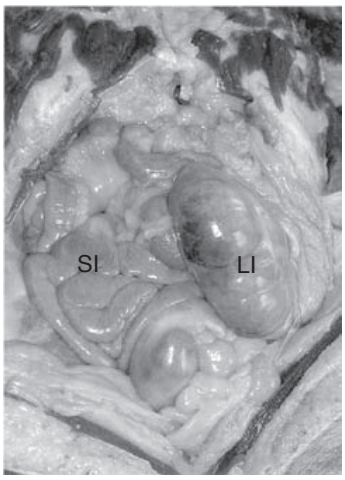

FIGURE 10.20. Nonrotation of the midgut loop.

e. **Malrotation of the midgut loop (Figure 10.21)** occurs when the midgut loop undergoes only partial counterclockwise rotation. This results in the cecum and appendix lying in a subpyloric or subhepatic location and the small intestine suspended by only a vascular pedicle (i.e., not a broad mesentery). A major clinical complication of malrotation is **volvulus** (twisting of the small intestines around the vascular pedicle), which may cause necrosis due to compromised blood supply. (Note: The abnormal position of the appendix due to malrotation of the midgut should be considered when diagnosing appendicitis.) When malrotation is surgically corrected, the appendix is removed to prevent delayed or missed diagnosis of appendicitis given the atypical abdominal pain location at presentation. The photograph (Figure 10.21) shows the condition of volvulus. Note the twisting (*arrow*) of the small intestines around the axis of the mesentery.

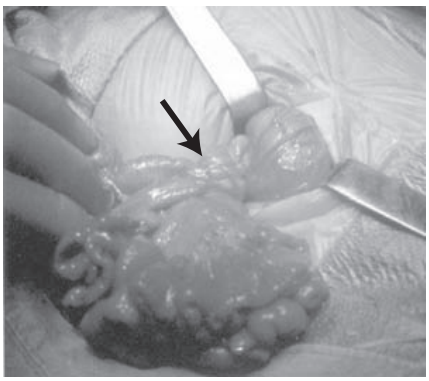
FIGURE 10.21. Volvulus.

f. **Reversed rotation of the midgut loop** occurs when the midgut loop rotates clockwise instead of counterclockwise, causing the large intestine

to enter the abdominal cavity first. This results in the large intestine anatomically being located posterior to the duodenum and superior mesenteric artery.

g. **Intestinal atresia and stenosis**. Atresia occurs when the lumen of the intestines is completely occluded, whereas stenosis occurs when the lumen of the intestines is narrowed. The causes of these conditions seem to be both failed recanalization and/or an ischemic intrauterine event ("vascular accident").

1. **Type I atresia** is characterized by a membranous septum or diaphragm of mucosa and submucosa that obstructs the lumen.
2. **Type II atresia (Figure 10.22)** is characterized by two blind bowel ends connected by a fibrous cord with an intact mesentery. The photograph (Figure 10.22) shows type II atresia. Note the fibrous cord (*arrow*).

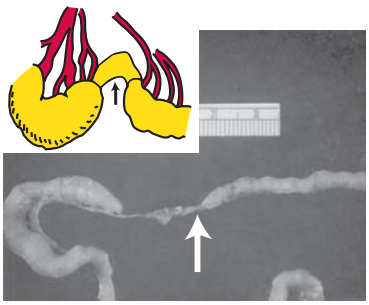

FIGURE 10.22. Type II atresia.

3. **Type IIIa atresia (Figure 10.23)** is characterized by two blind bowel ends separated by a gap in the mesentery. The photograph (Figure 10.23) shows type IIIa atresia. Note the gap in the mesentery (*asterisk*).

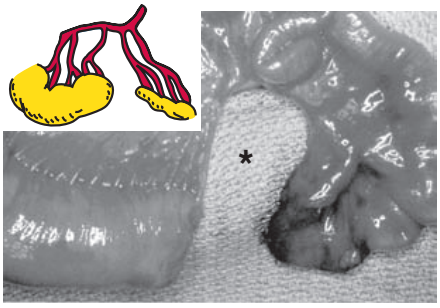

FIGURE 10.23. Type IIIa atresia.

4. **Type IIIb atresia ("apple peel" atresia; Figure 10.24)** is characterized by a bowel segment (distal to the atresia) that is shortened, coiled around a mesentery remnant, and lacking a blood supply from the superior mesentery artery (blood supply to this bowel segment is via collateral circulation). The photograph (Figure 10.24) shows "apple peel" atresia. Note the coiled bowel segment (*arrow*).
5. **Type IV atresia** is characterized by multiple atresia throughout the bowel having the appearance of a "string of sausages." Proximal atresias are associated clinically with polyhydramnios and bilious vomiting early after birth. Distal atresias are associated clinically with normal amniotic fluid, abdominal distention, later vomiting, and failure to pass meconium.

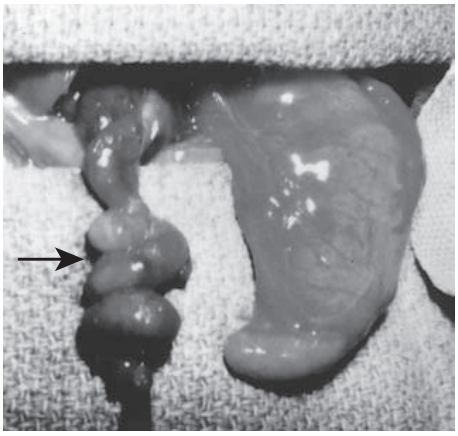

FIGURE 10.24. Type IIIb atresia.

h. **Duplication of the intestines (Figure 10.25)** occurs when a segment of the intestines is duplicated as a result of abnormal recanalization (most commonly near the ileocecal valve). The duplication is found on the mesenteric border. Its lumen generally communicates with the normal bowel, shares the same blood supply as the normal bowel, and is lined by normal intestinal epithelium, but heterotopic gastric and pancreatic tissue has been identified. It is associated clinically with an abdominal mass, bouts of abdominal pain, vomiting, chronic rectal bleeding, intussusception, and perforation. The photographs (Figure 10.25) show a duplication of the intestines. Note the larger diameter of the normal bowel segment (N) and the smaller diameter of the duplicated segment (D). Atretic areas (*arrows*) are indicated in the duplicated segment.

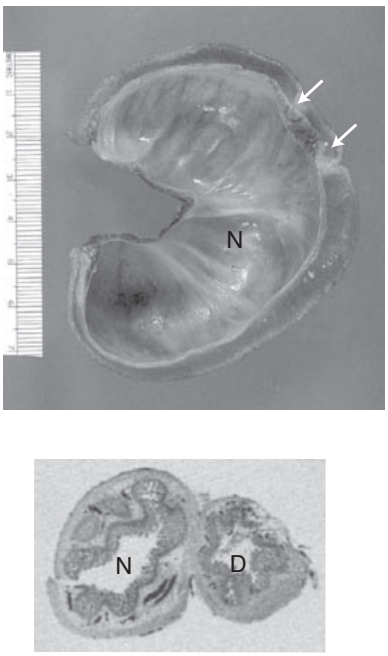

FIGURE 10.25. Duplication of the intestines.

i. **Intussusception** occurs when a segment of bowel invaginates or telescopes into an adjacent bowel segment, leading to obstruction or ischemia. This is one of the most common causes of obstruction in children younger than 2 years of age, is most often idiopathic, and is most commonly involves the ileum and colon (i.e., ileocolic). It is associated clinically with acute onset of intermittent abdominal pain, vomiting, bloody stools, diarrhea, and somnolence.

j. **Retrocecal and retrocolic appendix** occurs when the appendix is located on the posterior side of the cecum or colon, respectively. These anomalies are very common and important to remember during appendectomies. Note: The appendix is normally found on the medial side of the cecum.

k. **Superior mesenteric artery (SMA) syndrome** occurs when the third portion of the duodenum is compressed due to a decreased angle (as low as 6°) between the SMA and the aorta. This syndrome is caused by a loss of the intervening mesenteric fat pad due to a significant weight loss (e.g., bariatric surgery, anorexia nervosa), severe debilitating illnesses (e.g., malignant cancer), spinal cord injury, or corrective surgery for scoliosis.

IV. DERIVATIVES OF THE HINDGUT (FIGURE 10.26)

Derivatives of the hindgut are supplied by the **inferior mesenteric artery**.

A. Distal one-third of the transverse colon, descending colon, sigmoid colon.

1. **Development.** The cranial end of the hindgut develops into the distal one-third of the transverse colon, descending colon, and sigmoid colon. The terminal end of the hindgut is an endoderm-lined pouch called the **cloaca**, which contacts the surface ectoderm of the **proctodeum** to form the **cloacal membrane**.
2. **Sources.** The simple columnar absorptive cells lining hindgut derivatives, goblet cells, and enteroendocrine cells comprising the intestinal glands are derived from **endoderm**. The lamina propria, muscularis mucosae, submucosa, inner circular and outer longitudinal (taeniae coli) smooth muscle of the muscularis externa, and serosa are derived from **visceral mesoderm**.

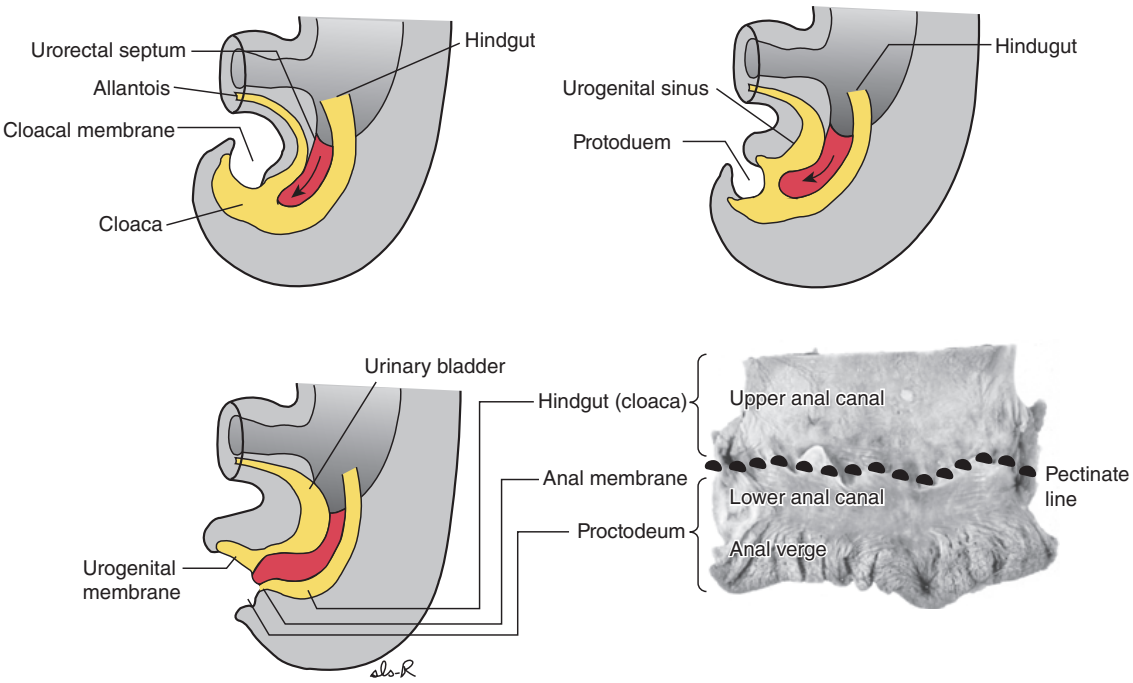

FIGURE 10.26. Diagram depicting the partitioning of the cloaca by urorectal septum. The *bold arrow* shows the direction of growth of the urorectal septum.

B. Rectum and upper anal canal

1. **Development.** The cloaca is partitioned by the **urorectal septum** into the **rectum/upper anal canal** and the **urogenital sinus**. The cloacal membrane is partitioned by the urorectal septum into the **anal membrane** and **urogenital membrane**. Note: The urorectal septum fuses with the cloacal membrane at the future site of the gross anatomical **perineal body**.
2. **Sources.** As mentioned in Section IVA2.
3. **Clinical considerations**
   a. **Colonic aganglionosis (Hirschsprung disease; Figure 10.27)** is caused by the arrest of the caudal migration of neural crest cells. The hallmark is the absence of ganglionic cells in the myenteric and submucosal plexuses, most commonly in the sigmoid colon and rectum, resulting in a narrow segment of colon (i.e., the colon fails to relax). Although the ganglionic cells are absent, there is a proliferation of hypertrophied nerve fiber bundles. The most characteristic functional finding is the failure of internal anal sphincter to relax following rectal distention (i.e., abnormal rectoanal reflex). Mutations of the ***RET* protooncogene** (chromosome 10q.11.2) have been associated with Hirschsprung disease. It is associated clinically with a distended abdomen, inability to pass meconium, gushing of fecal material on a rectal digital exam, and a loss of peristalsis in the colon segment distal to the

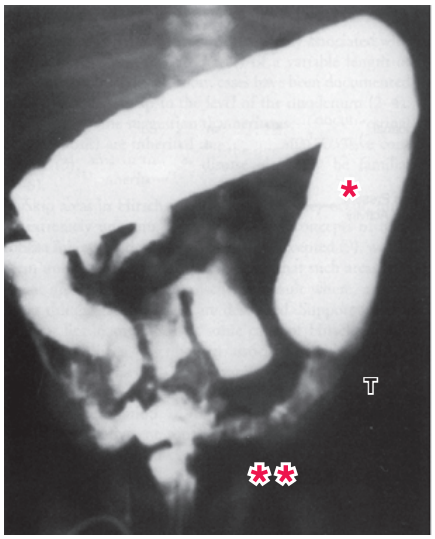

FIGURE 10.27. Colonic aganglionosis (Hirschsprung disease).

normal innervated colon. The radiograph (Figure 10.27) was taken after a barium enema of a patient with Hirschsprung disease. The upper segment of the normal colon (*single asterisk*) is distended with fecal material. The lower segment of the colon (*double asterisk*) is narrow. The lower segment is the portion of the colon where the ganglionic cells in the myenteric and submucosal plexuses are absent. The case shows a low transition zone (T) between the normal colon and the aganglionic colon.

b. Rectovesical fistula (Figure 10.28) is an abnormal communication between the rectum and the urinary bladder due to abnormal formation of the urorectal septum. This fistula is clinically associated with the presence of meconium in the urine. The diagram (Figure 10.28) shows a rectovesical fistula.

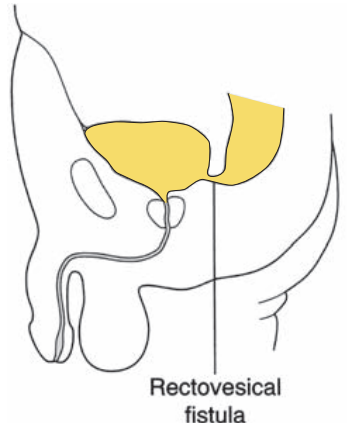

FIGURE 10.28. Rectovesical fistula.

c. Rectourethral fistula (Figure 10.29) is an abnormal communication between the rectum and the urethra due to abnormal formation of the urorectal septum. This fistula is clinically associated with the presence of meconium in the urine. A rectourethral fistula that generally occurs in males is associated with the prostatic urethra and is therefore sometimes called a **rectoprostatic fistula**. The diagram (Figure 10.29) shows a rectourethral fistula.

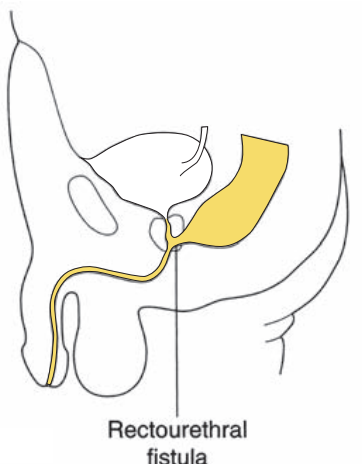

FIGURE 10.29. Rectourethral fistula.

d. Rectovaginal fistula (Figure 10.30) is an abnormal communication between the rectum and vagina due to abnormal formation of the urorectal septum. This fistula is associated clinically with the presence of meconium in the vagina. The diagram (Figure 10.30) shows a rectovaginal fistula.

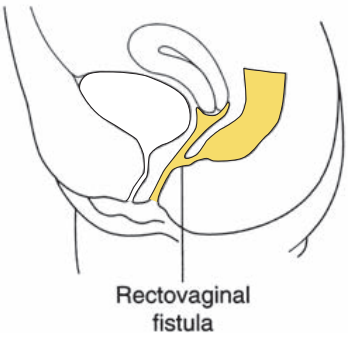

FIGURE 10.30. Rectovaginal fistula.

V. ANAL CANAL (FIGURE 10.26)

A. Development. The **upper anal canal** develops from the **hindgut**. The **lower anal canal** develops from the **proctodeum**, which is an invagination of surface ectoderm caused by a proliferation of mesoderm surrounding the anal membrane. The dual components (hindgut and proctodeum) involved in the embryological formation of the entire anal canal determine the gross anatomy of this area, which becomes important when considering the characteristics and metastasis of anorectal tumors. The junction between the upper and lower anal canals is indicated by the **pectinate line**, which also marks the site of the former **anal membrane**. In the adults, the pectinate line is located at the lower border of the anal columns.

B. Sources. The simple columnar epithelium lining the upper anal canal is derived from **endoderm**. The simple columnar and stratified columnar epithelia lining the lower anal canal are derived from **ectoderm**. The lamina propria, muscularis mucosae, submucosa, muscularis externa consisting of the internal and external anal sphincters, and adventitia are derived from **mesoderm**.

C. Clinical considerations

1. **Imperforate anus** occurs when the anal membrane fails to perforate; a layer of tissue separates the anal canal from the exterior.
2. **Anal agenesis** occurs when the anal canal ends as a blind sac **below the puborectalis muscle** due to abnormal formation of the urorectal septum. It is usually associated with rectovesical, rectourethral, or rectovaginal fistula.
3. **Anorectal agenesis** occurs when the rectum ends as a blind sac **above the puborectalis muscle** due to abnormal formation of the urorectal septum. It is the most common type of anorectal malformation and is usually associated with a rectovesical, rectourethral, or rectovaginal fistula.
4. **Rectal atresia** occurs when both the rectum and anal canal are present but remain unconnected due to either abnormal recanalization or a compromised blood supply causing focal atresia.

VI. MESENTERIES

The primitive is suspended within the peritoneal cavity of the embryo by the **ventral mesentery** and **dorsal mesentery**, from which all adult mesenteries are derived (Table 10.1).

table 10.1 Derivation of Adult Mesenteries

Embryonic Mesentery	Adult Mesentery
Ventral	Lesser omentum (hepatoduodenal and hepatogastric ligaments), falciform ligament of liver, coronary ligament of liver, triangular ligament of liver
Dorsal	Greater omentum (gastrorenal, gastrosplenic, gastrocolic, and splenorenal ligaments), mesentery of small intestine, mesoappendix, transverse mesocolon, sigmoid mesocolon

Study Questions for Chapter 10

1. Pancreatic islets consist of alpha, beta, and delta cells, which secrete glucagon, insulin, and somatostatin, respectively. These cells are derived from

(A) mesoderm
(B) endoderm
(C) ectoderm
(D) neuroectoderm
(E) neural crest cells

2. A 2-month-old baby with severe jaundice also has dark-colored urine (deep yellow) and white clay-colored stool. Which of the following disorders might be suspected?

(A) Esophageal stenosis
(B) Annular pancreas
(C) Hypertrophic pyloric stenosis
(D) Extrahepatic biliary atresia
(E) Duodenal atresia

3. A 28-day-old baby is brought to the physician because of projectile vomiting after feeding. Until this time, the baby has had no problems in feeding. On examination, a small knot is palpated at the right costal margin. Which of the following disorders might be suspected?

(A) Esophageal stenosis
(B) Annular pancreas
(C) Hypertrophic pyloric stenosis
(D) Extrahepatic biliary atresia
(E) Duodenal atresia

4. Which of the following arteries supplies foregut derivatives of the digestive system?

(A) Celiac trunk
(B) Superior mesenteric artery
(C) Inferior mesenteric artery
(D) Right umbilical artery
(E) Intercostal artery

5. The most common type of anorectal malformation is

(A) imperforate anus
(B) anal agenesis
(C) anorectal agenesis
(D) rectal atresia
(E) colonic aganglionosis

6. The simple columnar or cuboidal epithelium lining the extrahepatic biliary ducts is derived from

(A) mesoderm
(B) endoderm
(C) ectoderm
(D) neuroectoderm
(E) neural crest cells

7. A 4-day-old baby boy has not defecated since coming home from the hospital even though feeding has been normal without any excessive vomiting. Rectal examination reveals a normal anus, anal canal, and rectum. However, a large fecal mass is found in the colon, and a large release of flatus and feces follows the rectal examination. Which of the following conditions would be suspected?

(A) Imperforate anus
(B) Anal agenesis
(C) Anorectal agenesis
(D) Rectal atresia
(E) Colonic aganglionosis

8. Which one of the following structures is derived from the midgut?

(A) Appendix
(B) Stomach
(C) Liver
(D) Pancreas
(E) Sigmoid colon

9. A 3-month-old baby girl presents with a swollen umbilicus that has failed to heal normally. The umbilicus drains secretions, and there is passage of fecal material through the umbilicus at times. What is the most likely diagnosis?

(A) Omphalocele
(B) Gastroschisis
(C) Anal agenesis
(D) Ileal diverticulum
(E) Intestinal stenosis

10. The midgut loop normally herniates through the primitive umbilical ring into the extraembryonic coelom during week 6 of development. Failure of the intestinal loops to return

to the abdominal cavity by week 11 results in the formation of

(A) omphalocele
(B) gastroschisis
(C) anal agenesis
(D) ileal diverticulum
(E) intestinal stenosis

11. Kupffer cells present in the adult liver are derived from

(A) mesoderm
(B) endoderm
(C) ectoderm
(D) neuroectoderm
(E) neural crest cells

12. The simple columnar and stratified columnar epithelia lining the lower part of the anal canal is derived from

(A) mesoderm
(B) endoderm
(C) ectoderm
(D) neuroectoderm
(E) neural crest cells

13. A baby born to a young woman whose pregnancy was complicated by polyhydramnios was placed in the intensive care unit because of repeated vomiting containing bile. The stomach was markedly distended, and only small amounts of meconium had passed through the anus. What is the most likely diagnosis?

(A) Esophageal stenosis
(B) Annular pancreas
(C) Hypertrophic pyloric stenosis
(D) Extrahepatic biliary atresia
(E) Duodenal atresia

Answers and Explanations

1. **B.** Pancreatic islets form as isolated clumps of cells that bud from endodermal tubules.
2. **D.** The baby is suffering from extrahepatic biliary atresia, which results from failure of the bile ducts to recanalize during development. This prevents bile from entering the duodenum.
3. **C.** The baby is suffering from hypertrophic pyloric stenosis. This occurs when the smooth muscle in the pyloric region of the stomach hypertrophies and obstructs passage of food. The hypertrophied muscle can be palpated at the right costal margin. The exact cause of this condition is not known.
4. **A.** The artery that supplies foregut derivatives of the digestive system is the celiac trunk. The celiac trunk consists of the left gastric artery, splenic artery, and common hepatic artery. The superior mesenteric artery supplies the midgut, and the inferior mesenteric artery supplies the hindgut.
5. **C.** The most common type of malformation involving the anal canal and rectum is anorectal agenesis, in which the rectum ends as a blind sac above the puborectalis muscle. The anal canal may form normally but does not connect with the rectum. This malformation is accompanied by various fistulas.
6. **B.** The epithelium lining the extrahepatic biliary ducts is derived from endoderm. The intrahepatic biliary ducts are also derived from endoderm.
7. **E.** This baby boy suffers from colonic aganglionosis, or Hirschsprung disease, which results in the retention of fecal material, causing the normal colon to enlarge. The retention of fecal material results from a lack of peristalsis in the narrow segment of colon distal to the enlarged colon. A biopsy of the narrow segment of colon would reveal the absence of parasympathetic ganglion cells in the myenteric plexus caused by failure of neural crest migration.
8. **A.** The appendix is derived from the midgut. The midgut normally undergoes a 270° counterclockwise rotation during development; malrotation of the midgut may result in the appendix lying in the upper part of the abdominal cavity, which may affect a diagnosis of appendicitis.
9. **D.** This baby girl has an ileal diverticulum (Meckel diverticulum), which occurs when a remnant of the vitelline duct persists. In this case, a fistula is present by which contents of the ileum can be discharged onto the surface of the skin.
10. **A.** An omphalocele results when intestinal loops fail to return to the abdominal cavity. Instead, the intestinal loops remain in the umbilical cord covered by amnion.
11. **A.** Kupffer cells are actually macrophages and are derived from mesoderm. Hepatocytes and the epithelial lining of the intrahepatic biliary tree are derived from endoderm.
12. **C.** The anal canal is formed from two components—the hindgut and proctodeum. The epithelium lining the lower anal canal is derived from ectoderm lining the proctodeum.
13. **E.** This baby is suffering from duodenal atresia at a level distal to the opening of the common bile duct. This causes a reflux of bile and its presence in the vomitus. The pregnancy was complicated by polyhydramnios because the duodenal atresia prevented passage of amniotic fluid into the intestines for absorption.

chapter 11

Respiratory System

I. UPPER RESPIRATORY SYSTEM

The upper respiratory system consists of the **nose, nasopharynx**, and **oropharynx**.

II. LOWER RESPIRATORY SYSTEM (FIGURE 11.1)

The lower respiratory system consists of the **larynx, trachea, bronchi**, and **lungs**. The first sign of development is the formation of the **respiratory (or laryngotracheal) diverticulum** in the ventral wall of the primitive foregut during week 4. The distal end of the respiratory diverticulum enlarges to form the **lung bud**. The lung bud divides into two **bronchial buds** that branch into the **main (primary), lobar (secondary), segmental (tertiary)**, and **subsegmental bronchi**. The respiratory diverticulum initially is in open communication with the foregut, but eventually they become separated by indentations of mesoderm, the **tracheoesophageal folds**. When the tracheoesophageal folds fuse in the midline to form the **tracheoesophageal septum**, the foregut is divided into the trachea ventrally and esophagus dorsally.

A. Development of the larynx. The opening of the respiratory diverticulum into the foregut becomes the **laryngeal orifice**. The laryngeal epithelium and glands are derived from **endoderm**. The laryngeal muscles are derived from **somitomeric mesoderm of pharyngeal arches 4 and 6** and therefore are innervated by branches of the vagus nerve CN X; i.e., the superior laryngeal nerve and recurrent laryngeal nerve, respectively. The laryngeal cartilages (thyroid, cricoid, arytenoid, corniculate, and cuneiform) are derived from **somitomeric mesoderm of pharyngeal arches 4 and 6**.

B. Development of the trachea

1. **Sources.** The tracheal epithelium and glands are derived from **endoderm**. The tracheal smooth muscle, connective tissue, and C-shaped cartilage rings are derived from **visceral mesoderm**.
2. **Clinical consideration. Tracheoesophageal fistula** is an abnormal communication between the trachea and esophagus that results from improper division of foregut by the tracheoesophageal septum. It is generally associated with **esophageal atresia**, which will then result in **polyhydramnios. Clinical features include** excessive accumulation of saliva or mucus in the nose and mouth; episodes of gagging and cyanosis after swallowing milk; abdominal distention after crying; and reflux of gastric contents into lungs, causing pneumonitis. **Diagnostic features include** inability to pass a catheter into the stomach and radiographs demonstrating air in the infant's stomach. There are five different anatomical types of esophagus and trachea malformations as follows:

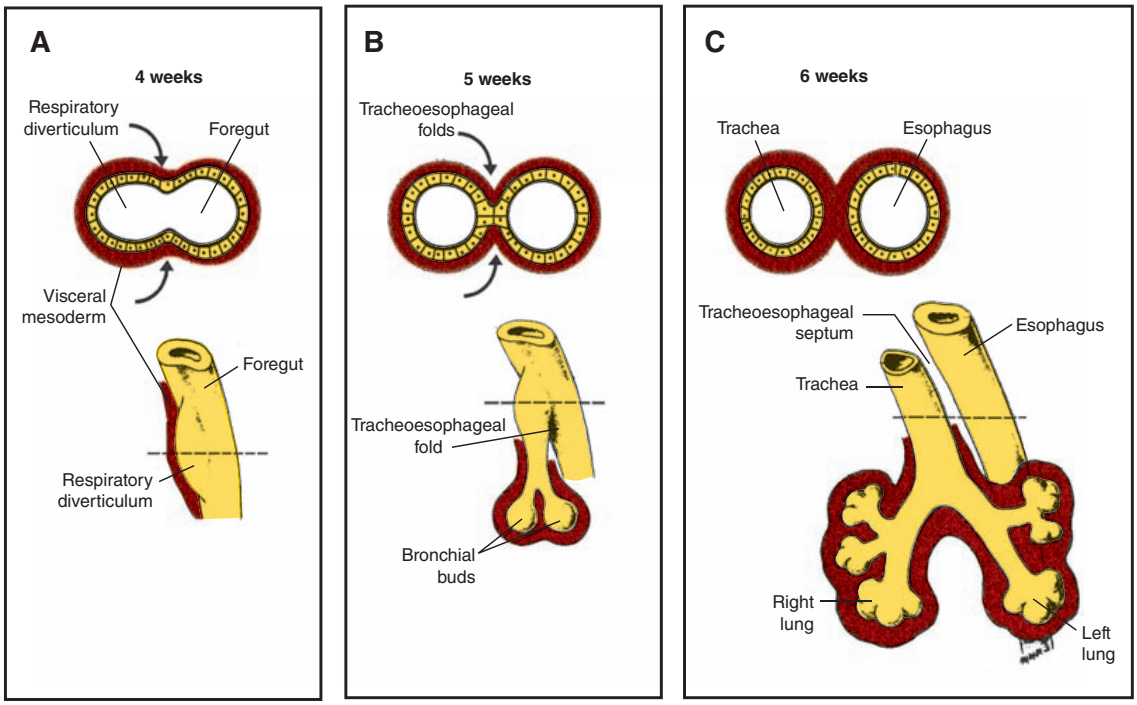

FIGURE 11.1. Development of respiratory system at **(A)** 4 weeks, **(B)** 5 weeks, and **(C)** 6 weeks. Both lateral views and cross-sectional views are shown. Note the relationship of the respiratory diverticulum and foregut. *Curved arrows* indicate the movement of the tracheoesophageal folds as the tracheoesophageal septum forms between the trachea and esophagus.

a. Esophageal atresia with a tracheoesophageal fistula at the distal one-third end of the trachea (Figure 11.2). This is the most common type, occurring in 82% of cases. The AP radiograph (Figure 11.2) of this malformation shows an enteric tube (*arrow*) coiled in the upper esophageal pouch. The air in the bowel indicates a distal tracheoesophageal fistula.

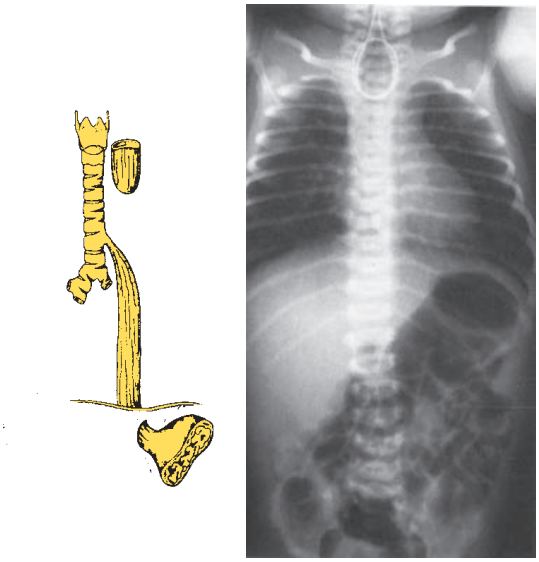

FIGURE 11.2. Esophageal atresia with a tracheoesophageal fistula at the distal one-third end of the trachea.

b. Esophageal atresia only (Figure 11.3). This malformation occurs in 9% of cases.

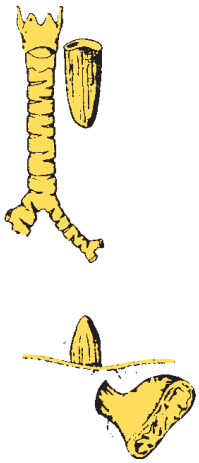

FIGURE 11.3. Esophageal atresia.

c. H-type tracheoesophageal fistula only (Figure 11.4). This malformation occurs in 6% of cases. The barium swallow radiograph (Figure 11.4) shows a normal esophagus (E), but dye has spilled into the trachea (T) through the fistula and outlines the upper trachea and larynx.

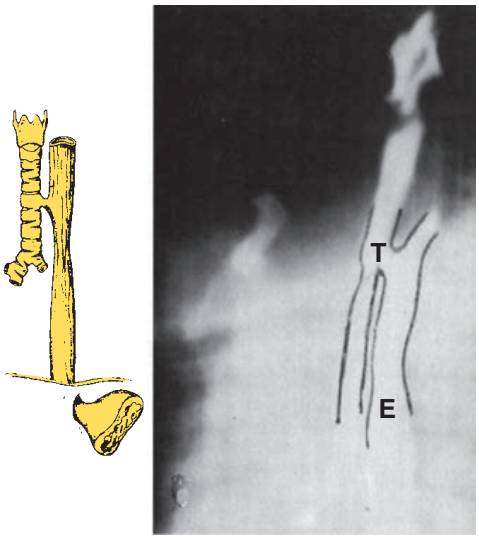

FIGURE 11.4. H-type tracheoesophageal fistula.

d. Esophageal atresia with a tracheoesophageal fistula at both proximal and distal ends (Figure 11.5). This malformation occurs in 2% of cases.

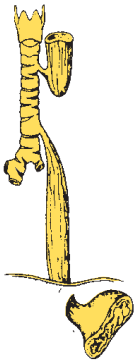

FIGURE 11.5. Esophageal atresia with a tracheoesophageal fistula at both proximal and distal ends.

e. Esophageal atresia with a tracheoesophageal fistula at the proximal end (Figure 11.6). This malformation occurs in 1% of cases.

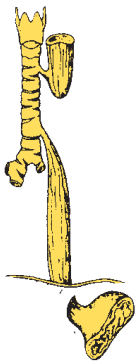

FIGURE 11.6. Esophageal atresia with a tracheoesophageal fistula at the proximal end.

C. Development of the bronchi (Figure 11.7)

1. Stages of development

a. The lung bud divides into two **bronchial buds**.

b. In week 5 of development, bronchial buds enlarge to form **main (primary) bronchi**.

c. The right main bronchus is larger and more vertical than the left main bronchus. This relationship persists throughout adult life and accounts for the greater likelihood of foreign bodies lodging on the right side than on the left.

d. The main bronchi further subdivide into **lobar (secondary) bronchi** (three on the right side and two on the left side, corresponding to the lobes of the adult lung).

e. The lobar bronchi further subdivide into **segmental (tertiary) bronchi** (10 on the right side and 9 on the left side), which further subdivide into **subsegmental bronchi**.

f. The segmental bronchi are the primordia of the **bronchopulmonary segments**, which are morphologically and functionally separate respiratory units of the lung.

g. As the bronchi develop, they expand laterally and caudally into a space known as the primitive pleural cavity.

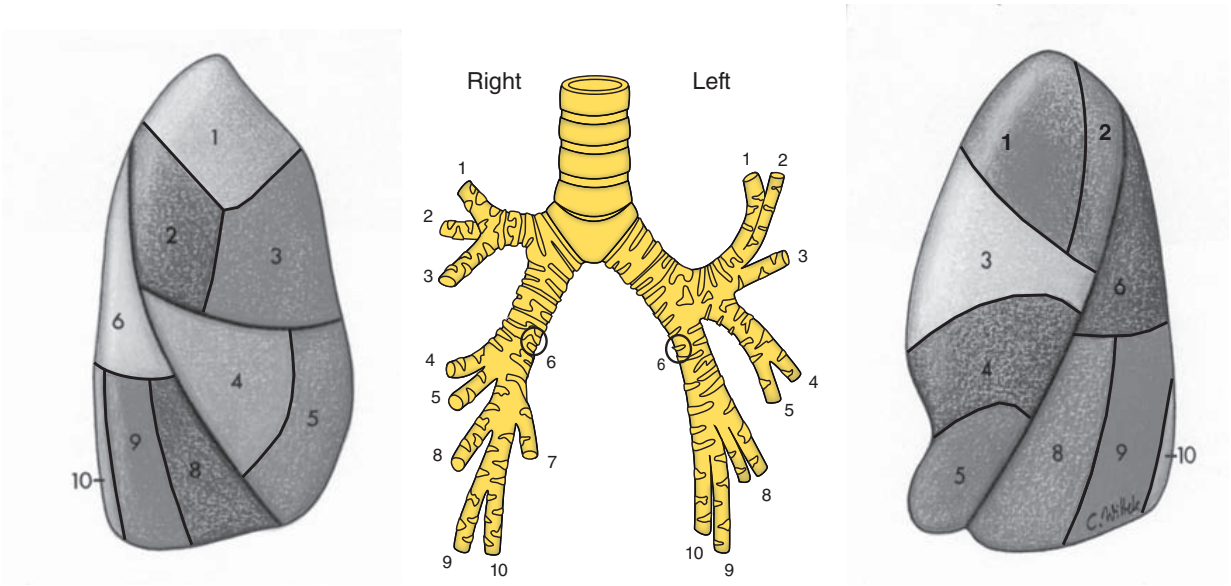

FIGURE 11.7. Distribution of bronchopulmonary segments and their relationship to the tracheobronchial tree. Segmental bronchi of the right and left lungs are numbered. Right lung: 1, 2, 3 = segmental bronchi that branch from the upper lobar bronchus; 4, 5 = segmental bronchi that branch from the middle lobar bronchus; 6, 7, 8, 9, 10: segmental bronchi that branch from the lower lobar bronchus. Note that bronchopulmonary segment 7 is not represented on the outer costal surface of the right lung (7 is located on the inner mediastinal surface). Left lung: 1+2, 3, 4, 5: segmental bronchi that branch from the upper lobar bronchus; 6, 8, 9, 10: segmental bronchi that branch from the lower lobar bronchus. Note that there is no number 7 segmental bronchus associated with the left lung.

h. The visceral mesoderm covering the outside of the bronchi develops into **visceral pleura**, and somatic mesoderm covering the inside of the body wall develops into **parietal pleura**.
i. The space between the visceral and parietal pleura is called the **pleural cavity**.

2. **Sources.** The bronchial epithelium and glands are derived from **endoderm**. The bronchial smooth muscle, connective tissue, and cartilage are derived from **visceral mesoderm**.
3. **Clinical considerations**
   a. **Bronchopulmonary segment** is a segment of lung tissue supplied by a segmental (tertiary) bronchus. Surgeons can resect diseased lung tissue along bronchopulmonary segments rather than remove the entire lobe.
   b. **Congenital lobar emphysema (CLE; Figure 11.8)** is characterized by progressive overdistention of one of the upper lobes or the right middle lobe with **air**. The term "emphysema" is a misnomer because there is no destruction of the alveolar walls. Although the exact etiology remains unknown, many cases involve **collapsed bronchi due to failure of bronchial cartilage formation**. In this situation, air can be inspired through collapsed bronchi but cannot be expired. During the first few days of life, fluid may be trapped in the involved lobe, producing an opaque, enlarged hemithorax. Later, the fluid is resorbed, and the classic radiological appearance of an emphysematous lobe with generalized radiolucency (hyperlucent) is apparent. The expiratory AP radiograph (Figure 11.8) shows a hyperlucent area in the emphysematous right upper lobe due to air trapping.

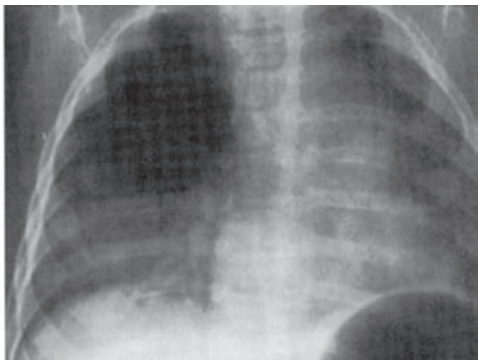

FIGURE 11.8. Congenital lobar emphysema.

   c. **Congenital bronchogenic cysts (Figure 11.9)** represent an abnormality in bronchial branching and may be found within the mediastinum (most commonly) or intrapulmonary. Intrapulmonary cysts are **round, solitary, sharply marginated, fluid filled** and do not initially communicate with the tracheobronchial tree. Because intrapulmonary bronchogenic cysts contain fluid, they appear as water-density masses on chest radiographs. These cysts may become air filled as a result of infection or instrumentation. The AP radiograph (Figure 11.9) shows a large opaque area in the right upper lobe due to a fluid-filled cyst.

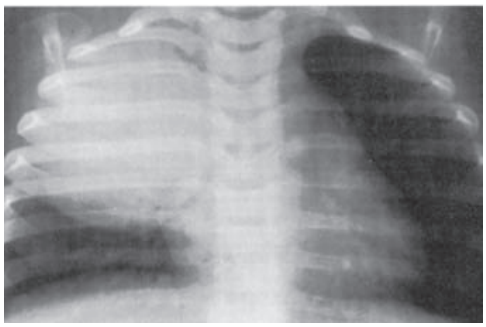

FIGURE 11.9. Congenital bronchogenic cyst.

   d. **Bronchiectasis** is the abnormal, permanent dilatation of bronchi due to chronic necrotizing infection (e.g., *Staphylococcus*, *Streptococcus*, *Haemophilus influenzae*), bronchial obstruction (e.g., foreign body, mucous plugs, or tumors), or congenital conditions (e.g., Kartagener syndrome, cystic fibrosis, immunodeficiency disorders). The lower lobes of the lung are predominately affected, and the affected bronchi have a saccular appearance. **Clinical features include** cough, fever, and expectoration of large amounts of foul-smelling purulent sputum. Bronchiectasis may also be classified to a group of disorders known as chronic obstructive pulmonary disease (COPD), which are characterized by increased resistance to airflow during both inspiration and expiration due to airway obstruction. Other members of COPD include emphysema, chronic bronchitis, and asthma.

D. Development of the lungs

1. **Periods of development.** The lung matures in a proximal–distal direction, beginning with the largest bronchi and proceeding outward. As a result, lung development is heterogeneous; proximal pulmonary tissue will be in a more advanced period of development than distal pulmonary tissue.

   a. **Pseudoglandular period (weeks 7–16; Figure 11.10).** During this period, the developing lung resembles an exocrine gland. The numerous **endodermal tubules (ETs)** are lined by **simple columnar epithelium** and are surrounded by mesoderm containing a **modest capillary network**. Each endodermal tubule branches into 15–25 **terminal bronchioles (TBs)**. During this period, respiration is not possible, and premature infants cannot survive. Figure 11.10 shows the lung in the pseudoglandular period.

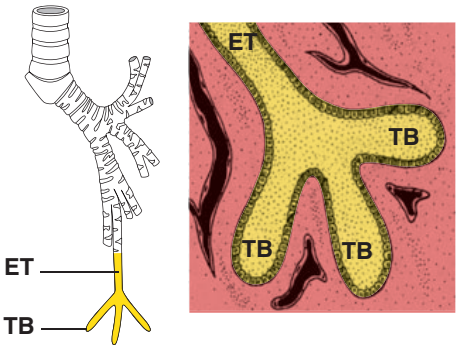

FIGURE 11.10. Pseudoglandular period.

   b. **Canalicular period (weeks 16–24; Figure 11.11).** During this period, the TBs branch into three or more **respiratory bronchioles (RBs)**. The RBs subsequently branch into three to six **alveolar ducts (ADs)**. The TBs, RBs, and ADs are now lined by a **simple cuboidal epithelium** and are surrounded by mesoderm containing a **prominent capillary network**. Premature infants born before week 20 rarely survive. Figure 11.11 shows the lung in the canalicular period.

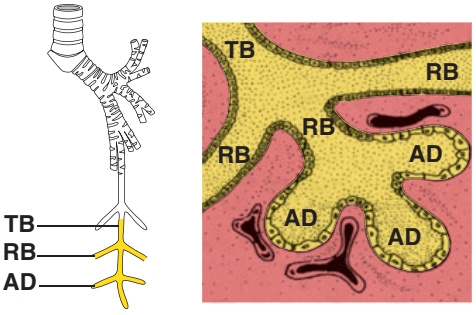

FIGURE 11.11. Canalicular period.

   c. **Terminal sac period (week 24 to birth; Figure 11.12).** During this period, **terminal sacs (TSs)** bud off the ADs and then dilate and expand into the surrounding mesoderm. The TSc are separated from each other by **primary septae**. The simple cuboidal epithelium within the TSc differentiates into **type I pneumocytes** (thin, flat cells that make up part of the blood–air barrier) and **type II pneumocytes** (which produce surfactant). The TSc are surrounded by mesoderm containing a **rapidly proliferating capillary network**. The capillaries make intimate contact with the TSs and thereby establish a **blood–air barrier** with the type I pneumocytes. **Premature infants born between week 25 and week 28 can survive with intensive care**. Adequate vascularization and surfactant levels are the most important factors for the survival of premature infants. Figure 11.12 shows the lung in the terminal sac period.

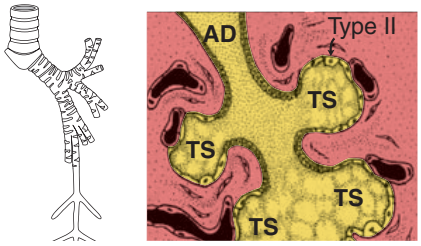

FIGURE 11.12. Terminal sac period.

d. Alveolar period (week 32–age 8 years; Figure 11.13). During this period, TSc are partitioned by **secondary septae** to form adult **alveoli**. About 20–70 million alveoli are present at birth. About 300–400 million alveoli are present by 8 years of age. The major mechanism for the increase in the number of alveoli is the formation of secondary septae that partition existing alveoli. After birth, the increase in the size of the lung is due to an **increase in the number of RBs**. On chest radiographs, lungs of a newborn infant are denser than an adult lung because of the fewer number of mature alveoli.

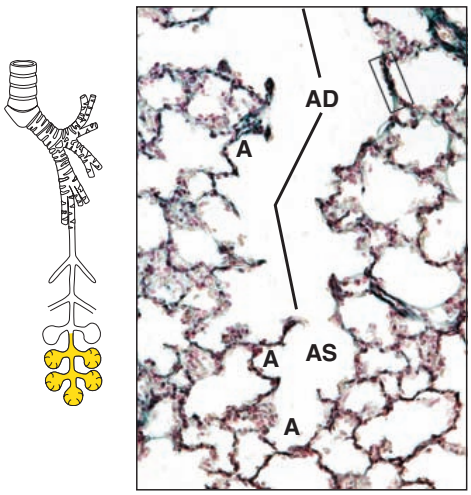

FIGURE 11.13. Alveolar period. A = adult alveoli; AD = alveolar duct; AS = alveolar sac.

2. Clinical considerations

a. Aeration at birth is the replacement of lung liquid with air in the newborn's lungs. In the fetal state, the functional residual capacity (FRC) of the lung is filled with liquid secreted by fetal lung epithelium via Cl^- transport using CFTR (cystic fibrosis transmembrane protein). At birth, lung liquid is eliminated by a reduction in lung liquid secretion via Na^+ transport by type II pneumocytes and resorption into pulmonary capillaries (major route) and lymphatics (minor route). Lungs of a stillborn baby will sink when placed in water because they contain fluid rather than air.

b. Hyaline Membrane Disease (HMD; Figure 11.14).

1. HMD is caused by a deficiency or absence of **surfactant** that is produced by **type II pneumocytes**.
2. Surfactant is composed of **dipalmitoylphosphatidylcholine** (the strongest surfactant molecule), **other lipids** (phosphatidylcholine, phosphatidylglycerol, neutral lipids, cholesterol), and **surfactant proteins A, B, C, and D**. Surfactant is a surface active agent that coats the inside of alveoli to maintain alveolar patency.
3. HMD is prevalent in premature infants (accounts for 50%–70% of deaths in premature infants), infants of diabetic mothers, infants who experienced fetal asphyxia or maternofetal hemorrhage (damages type II pneumocytes), and multiple-birth infants.
4. **Clinical features include** dyspnea, tachypnea, inspiratory retractions of chest wall, expiratory grunting, cyanosis, and nasal flaring.
5. **Treatments include** administration of betamethasone (a corticosteroid)

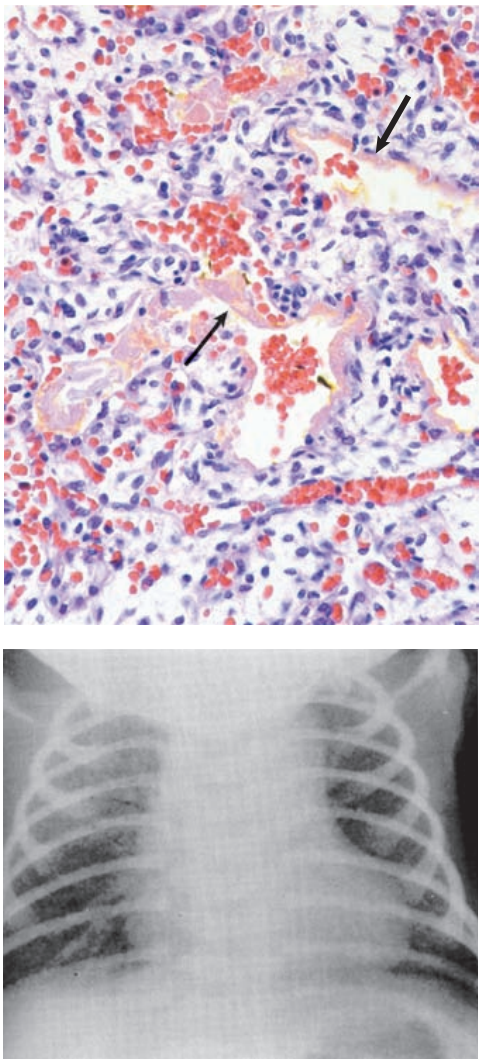

FIGURE 11.14. Hyaline membrane disease (HMD).

to the mother for several days before delivery (i.e., antenatal) to increase surfactant production, postnatal administration of an artificial surfactant solution, and postnatal high-frequency ventilation.

6. HMD in premature infants cannot be discussed without mentioning **germinal matrix hemorrhage (GMS)**. The germinal matrix is the site of proliferation of neuronal and glial precursors in the developing brain that is located above the caudate nucleus, in the floor of the lateral ventricles, and the caudo–thalamic groove. The germinal matrix also contains a rich network of fragile, thin-walled blood vessels.
7. The brain of the premature infant lacks the ability to autoregulate the cerebral blood pressure.
8. Consequently, increased arterial blood pressure in these blood vessels leads to rupture and hemorrhage into the germinal matrix. This leads to significant neurological sequelae, including cerebral palsy, mental retardation, and seizures.
9. Antenatal corticosteroid administration has a clear role in reducing the incidence of GMH is premature infants.
10. The light micrograph (Figure 11.14) shows the pathological hallmarks of HMD, which are acinar atelectasis (i.e., collapse of the respiratory acinus, which includes the RBs, ADs, and alveoli), dilation of TBs (shown by the asterisk), and deposition of an eosinophilic hyaline membrane material (*arrows*) that consists of fibrin and necrotic cells.
11. The AP radiograph (Figure 11.14) shows the radiological hallmarks of HMD, which are a bell-shaped thorax due to under-aeration and reticulogranularity of the lungs caused by acinar atelectasis.

c. **Pulmonary agenesis** is the complete absence of a lung or a lobe and its bronchi. This is a rare condition caused by failure of bronchial buds to develop. Unilateral pulmonary agenesis is compatible with life.
d. **Pulmonary aplasia** is the absence of lung tissue but the presence of a rudimentary bronchus.
e. **Pulmonary hypoplasia (PH)** is a poorly developed bronchial tree with abnormal histology. PH classically involves the right lung in association with right-sided obstructive congenital heart defects. PH can also be found in association with **congenital diaphragmatic hernia** (i.e., herniation of abdominal contents into the thorax), which compresses the developing lung. PH can also be found in association with **bilateral renal agenesis or Potter syndrome**, which causes an insufficient amount of amniotic fluid (oligohydramnios) to be produced, which in turn increases pressure on the fetal thorax.
f. **Cystic fibrosis (CF)** is an autosomal recessive genetic disorder caused by >1,000 mutations in the ***CFTR* gene** on **chromosome 7q31.2** for the **cystic fibrosis transmembrane conductance regulator**, which functions as a chloride ion (Cl^-) channel. CF is most commonly (approximately 70% of cases in the North American population) caused by a **three base pair deletion** at the site that codes for the amino acid **phenylalanine** at **position 508** (hence the mutation is called delta F508) of *CFTR*, such that phenylalanine is missing from the *CFTR*. However, there are a large number of deletions that can cause CF, and parents of an affected child can carry different deletions of *CFTR*. These mutations result in absent/near-absent *CFTR* synthesis, a block in *CFTR* regulation, or a destruction of Cl^- transport. **Clinical features include** production of abnormally thick mucus by epithelial cells lining the respiratory tract, resulting in obstruction of pulmonary airways, recurrent respiratory bacterial infections, and end-stage lung disease; pancreatic insufficiency with malabsorption; acute salt depletion; and chronic metabolic alkalosis. Males are almost always sterile due to the obstruction or absence of the vas deferens. Whites are the most commonly affected ethnic group, with CF occurring in 1 of 2,500 live births.

Study Questions for Chapter 11

1. A young mother brings her recently born infant into your office and complains that the infant gags and chokes after swallowing milk. A physical examination indicates excessive saliva and mucus around the mouth and nose, abdominal distention, pneumonitis, and radiographs indicate air in the infant's stomach. What is the most likely cause?

(A) Hypertrophic pyloric stenosis
(B) Tracheoesophageal fistula
(C) Congenital lobar emphysema
(D) Respiratory distress syndrome
(E) Pulmonary hypoplasia

2. Within hours after birth, a baby whose mother is diabetic had a rising respiratory rate and labored breathing. The baby became cyanotic and died. Postmortem histological examination revealed collapsed alveoli lined with eosinophilic material. What is the diagnosis?

(A) Congenital emphysema
(B) Respiratory distress syndrome
(C) Cystic fibrosis
(D) Tracheoesophageal fistula
(E) Pulmonary carcinoma

3. The trachea is lined with pseudostratified ciliated columnar epithelium with goblet cells. This epithelium is derived from

(A) neuroectoderm
(B) endoderm
(C) ectoderm
(D) visceral mesoderm
(E) mesoderm of fourth and sixth pharyngeal arches

4. Smooth muscle, connective tissue, and cartilage of primary bronchi are derived from which of the following sources?

(A) Neuroectoderm
(B) Endoderm
(C) Ectoderm
(D) Visceral mesoderm
(E) Mesoderm of pharyngeal arches 4 and 6

5. Components of the blood–air barrier in the lung are derived from which of the following sources?

(A) Ectoderm only
(B) Visceral mesoderm only
(C) Visceral mesoderm and ectoderm
(D) Endoderm and ectoderm
(E) Visceral mesoderm and endoderm

6. The respiratory diverticulum initially is in open communication with the primitive foregut. Which of the following embryonic structures is responsible for separating these two structures?

(A) Laryngotracheal groove
(B) Posterior esophageal folds
(C) Laryngotracheal diverticulum
(D) Tracheoesophageal septum
(E) Bronchopulmonary segment

7. Collapse of bronchi caused by failure of bronchial cartilage development is indicative of which one of the following congenital malformations?

(A) Congenital bronchial cysts
(B) Congenital neonatal emphysema
(C) Tracheoesophageal fistula
(D) Hyaline membrane disease
(E) Pulmonary hypoplasia

8. Pulmonary hypoplasia is commonly associated with which condition?

(A) Hyaline membrane disease
(B) Diaphragmatic hernia
(C) Tracheoesophageal fistula
(D) Congenital bronchial cysts
(E) Congenital neonatal emphysema

9. Development of which of the following is the first sign of respiratory system development?

(A) Tracheoesophageal septum
(B) Hypobranchial eminence
(C) Primitive foregut
(D) Tracheoesophageal fistula
(E) Respiratory diverticulum

10. In which stage of lung maturation is the blood–air barrier established?

(A) Embryonic period
(B) Pseudoglandular period
(C) Canalicular period
(D) Terminal sac period
(E) Alveolar period

Answers and Explanations

1. **B.** Tracheoesophageal fistula is an abnormal communication between the trachea and esophagus that results from an improper division of the foregut by the tracheoesophageal septum. It is generally associated with esophageal atresia and polyhydramnios.
2. **B.** Respiratory distress syndrome is common in premature infants and infants of diabetic mothers. It is caused by a deficiency or absence of surfactant. Collapsed alveoli and eosinophilic material consisting of fibrin (hyaline membrane) can be observed histologically, indicating associated hyaline membrane disease.
3. **B.** The epithelial lining of the entire respiratory system (from tracheal epithelium to type I pneumocytes lining alveoli) is derived from endoderm.
4. **D.** The epithelium of primary bronchi is derived from endoderm; the other components are derived from visceral mesoderm.
5. **E.** The blood–air barrier comprises the structures through which gaseous exchange occurs between air in alveoli and blood in pulmonary capillaries. The attenuated pulmonary epithelium (type I pneumocytes) is derived from endoderm. The simple, squamous epithelium (endothelium) lining pulmonary capillaries is derived from visceral mesoderm.
6. **D.** When the tracheoesophageal folds fuse in the midline, they form the tracheoesophageal septum. This septum is responsible for separating the adult trachea ventrally from the esophagus dorsally.
7. **B.** Congenital neonatal emphysema is a malformation involving the bronchi. One or more lobes of the lungs are overdistended with air because air can be inspired through collapsed bronchi but cannot be expired.
8. **B.** During normal development, a space is provided for the prolific growth of the bronchial buds in a lateral and caudal direction. This space, which is part of the intraembryonic coelom, is called the primitive pleural cavity. If this space is reduced by herniation of abdominal viscera, lung development will be severely compromised.
9. **E.** Development of the respiratory system begins in week 4; the first sign of development is formation of the respiratory diverticulum in the ventral wall of the primitive foregut.
10. **D.** The simple cuboidal epithelium within the terminal sacs differentiates into pneumocytes within the terminal sac period. The rapidly proliferating capillary network makes intimate contact with the terminal sacs, and the blood–air barrier is established with type I pneumocytes. These events take place in the terminal sac period, which runs from embryonic week 24 until birth.

chapter 12

Head and Neck

I. PHARYNGEAL APPARATUS (FIGURE 12.1; TABLE 12.1)

The pharyngeal apparatus consists of the **pharyngeal arches, pharyngeal pouches, pharyngeal grooves**, and **pharyngeal membranes**, all of which contribute greatly to the formation of the head and neck. The pharyngeal apparatus is first observed in week 4 of development and gives the embryo its distinctive appearance. There are five pharyngeal arches (1, 2, 3, 4, and 6), four pharyngeal pouches (1, 2, 3, and 4), four pharyngeal grooves (1, 2, 3, and 4), and four pharyngeal membranes (1, 2, 3, and 4). Pharyngeal arch 5 and pharyngeal pouch 5 completely regress in the human. Aortic arch 5 also completely regresses (see Chapter 5). The **Hox complex** and **retinoic acid** appear to be important factors in early head and neck formation. A lack or excess of retinoic acid causes striking facial anomalies.

A. **Pharyngeal arches (1, 2, 3, 4, 6)** contain **somitomeric mesoderm** and **neural crest cells**. The somitomeric mesoderm differentiates into **muscles** and **arteries** (i.e., aortic arches 1–6), whereas the neural crest cells differentiate into **bone** and **connective tissue**. In addition, each pharyngeal arch has a **cranial nerve** associated with it.

B. **Pharyngeal pouches (1, 2, 3, 4)** are evaginations of **endoderm** that lines the foregut.

C. **Pharyngeal grooves (1, 2, 3, 4)** are invaginations of **ectoderm** located between each pharyngeal arch.

D. **Pharyngeal membranes (1, 2, 3, 4)** are structures consisting of **ectoderm, intervening mesoderm and neural crest**, and **endoderm**. The pharyngeal membranes are located between each pharyngeal arch.

II. DEVELOPMENT OF THE THYROID GLAND

In the midline of the pharynx floor, the endodermal lining of the foregut forms the **thyroid diverticulum**. The thyroid diverticulum migrates caudally, passing ventral to the hyoid bone and laryngeal cartilages. During this migration, the thyroid remains connected to the tongue by the **thyroglossal duct**, which later is obliterated. The site of the thyroglossal duct is indicated in the adult by the **foramen cecum**.

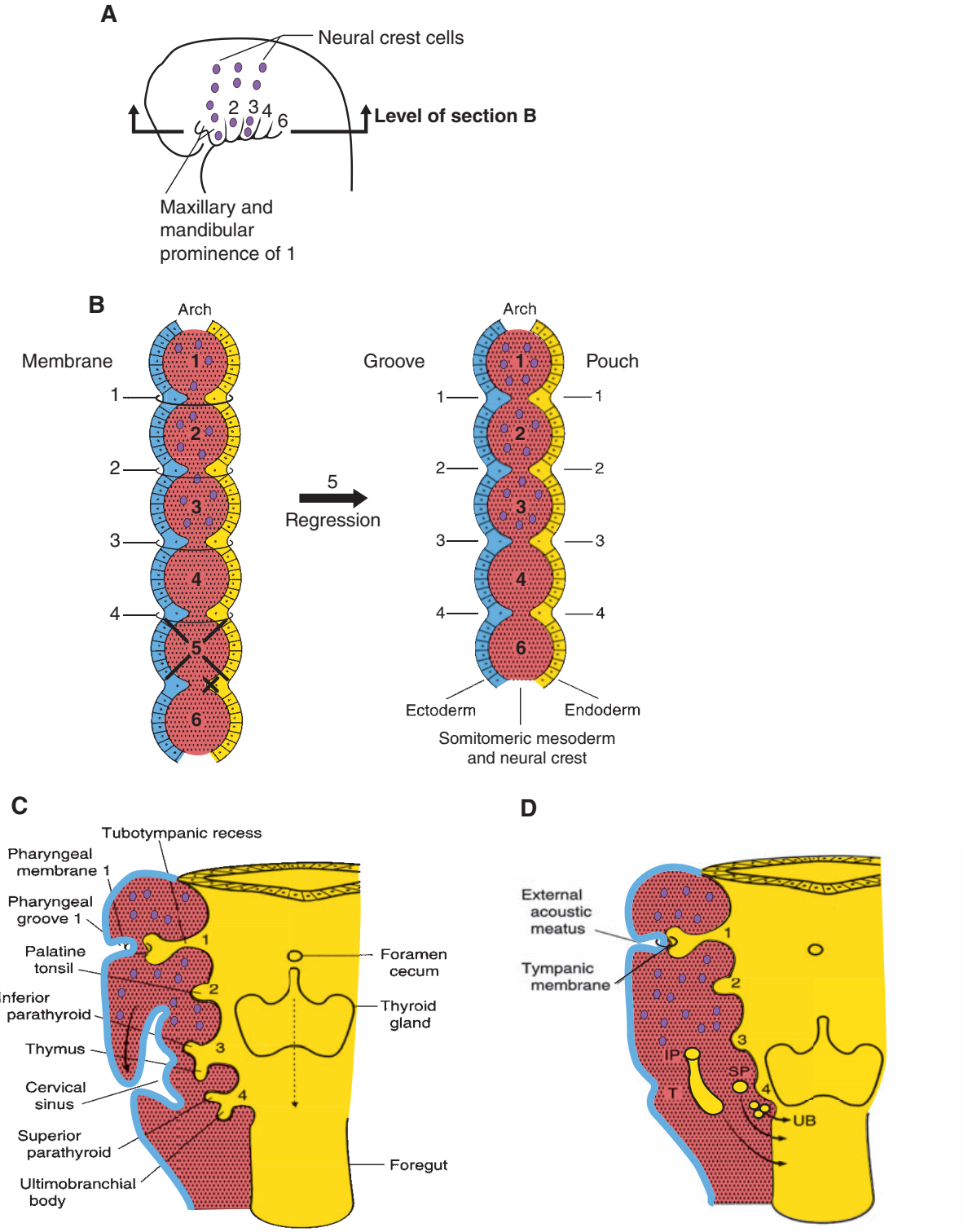

FIGURE 12.1. A. Lateral view of an embryo in week 4 of development, showing the pharyngeal arches and neural crest cells migrating into pharyngeal arches 1, 2, and 3. Note that pharyngeal arch 1 consists of a maxillary prominence and a mandibular prominence, which can cause some confusion in numbering of the arches. **B**. A schematic diagram indicating a convenient way to understand the numbering of the arches, pouches, grooves, and membranes. The X's indicate regression of pharyngeal arch 5 and pouch 5. The pharyngeal arches 1, 2, and 3 consist of somitomeric mesoderm (*red*) and neural crest cells (*purple*). The pharyngeal arches 4 and 6 consist of somitomeric mesoderm (*red*) only. The pharyngeal pouches 1, 2, 3, and 4 are lined by endoderm (*yellow*). The pharyngeal grooves 1, 2, 3, and 4 are lined by ectoderm (*blue*).The pharyngeal membranes 1, 2, 3, and 4 consist of ectoderm (*blue*), mesoderm (*red*), and endoderm (*yellow*). **C, D**. Schematic diagrams of the fate of the pharyngeal arches, pouches, grooves, and membranes. **C**. The *solid arrow* indicates the downward growth and fusion of pharyngeal arch 2, thereby forming a smooth contour at the neck region. The *dotted arrow* indicates downward migration of the thyroid gland. Note the fate of pharyngeal groove 1, pharyngeal membrane 1, and pharyngeal pouch 1 in the formation of the ear (See Chapter 8; Table 8-1). **D.** The *curved arrows* indicate the migratory direction of the inferior parathyroid (IP; yellow), thymus (T; *yellow*), superior parathyroid (SP; *yellow*), and ultimobranchial bodies (UB; yellow). Note that the parathyroid tissue derived from pharyngeal pouch 3 is carried farther caudally by the descent of the thymus than parathyroid tissue from pharyngeal pouch 4.

table 12.1 Adult Derivatives of Pharyngeal Arches, Pouches, Grooves, and Membranes

Arch	Nerve	Adult Derivatives
1	CN V	Mesoderm: Muscles of mastication, mylohyoid, anterior belly of digastric, tensor veli palatini, tensor tympani Neural crest from R1 and R2: Maxilla, mandible, malleus, incus, zygomatic bone, squamous temporal bone, palatine bone, vomer, sphenomandibular ligament, and Meckel cartilage
2	CN VII	Mesoderm: Muscles of facial expression, posterior belly of digastric, stylohyoid, stapedius Neural crest from R4: Stapes, styloid process, stylohyoid ligament, lesser horn and upper body of hyoid bone, and Reichert cartilage
3	CN IX	Mesoderm: Stylopharyngeus, common carotid arteries, internal carotid arteries Neural crest from R6 and R7: Greater horn and lower body of hyoid bone
4	CN X(superior laryngeal nerve)	Mesoderm: Muscles of soft palate (except tensor veli palatini), muscles of the pharynx (except stylopharyngeus) cricothyroid, cricopharyngeus, laryngeal cartilages, right subclavian artery, arch of aorta Neural crest: none
6	CN X(recurrent laryngeal nerve)	Mesoderm: Intrinsic muscles of larynx (except cricothyroid), upper muscles of the esophagus, laryngeal cartilages, pulmonary arteries, ductus arteriosus Neural crest: none
Pouch		
1		Epithelial lining of auditory tube and middle ear cavity, and mastoid air cells
2		Epithelial lining of palatine tonsil crypts
3		Inferior parathyroid gland
		Thymus
4		Superior parathyroid gland
		Ultimobranchial body[a]
Groove		
1		Epithelial lining of the external auditory meatus
2,3,4		Obliterated
Membrane		
1		Tympanic membrane
2,3,4		Obliterated

[a]Neural crest cells migrate into the ultimobranchial body to form parafollicular cells (C cells) of the thyroid, which secrete calcitonin

III. DEVELOPMENT OF THE TONGUE (FIGURE 12.2)

A. Oral part (anterior two-thirds) of the tongue

1. The oral part of the tongue forms from the **median tongue bud** and **two distal tongue buds** that develop in the pharynx floor due to a proliferation of mesoderm associated with **pharyngeal arch 1**.
2. The distal tongue buds overgrow the median tongue bud and fuse in the midline, forming the **median sulcus**.
3. The oral part is characterized by **filiform papillae** (no taste buds), **fungiform papillae** (taste buds present), **foliate papillae** (taste buds present), and **circumvallate papillae** (taste buds present).
4. General sensation from the mucosa is carried by the **lingual branch of the trigeminal nerve (cranial nerve [CN] V)**.
5. Taste sensation from the mucosa is carried by the **chorda tympani branch of the facial nerve (CN VII)**. Special visceral afferent (SVA) neurons convey taste sensation from the anterior two-thirds of the tongue to the central nervous system. The cell bodies for these neurons lie in the **geniculate ganglion**. The peripheral processes "hitch a ride" with the **lingual nerve** and **chorda tympani nerve**. The central processes enter the brain stem via the **intermediate nerve** and terminate in the rostral portion of the **solitary nucleus**.

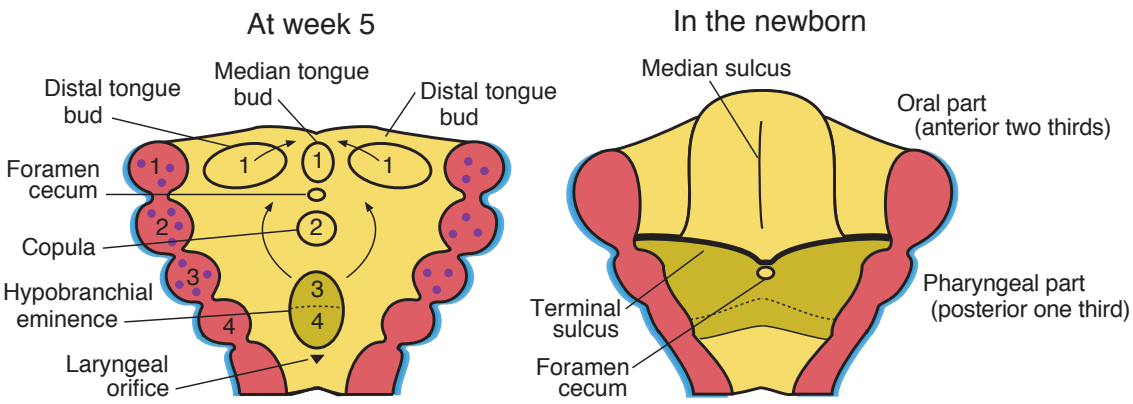

FIGURE 12.2. Development of the tongue at week 5 and in the newborn. The pharynx floor is lined by endoderm (*yellow*). The pharyngeal arches 1, 2, and 3 at week 5 contain somitomeric mesoderm (*red*) and neural crest cells (*purple*). The pharyngeal grooves are lined by ectoderm (*blue*). The upper curved arrows at week 5 indicate that the distal tongue buds overgrow the median tongue bud. The lower curved arrows at week 5 indicate that the hypobranchial eminence overgrows the copula.

B. Pharyngeal part (posterior one-third) of the tongue

1. The pharyngeal part of the tongue forms from the **copula (pharyngeal arch 2)** and **hypobranchial eminence (pharyngeal arches 3 and 4)** that develops in the pharynx floor due to a proliferation of mesoderm associated with **pharyngeal arches 2, 3, and 4**.
2. The copula (pharyngeal arch 2) is overgrown by the hypobranchial eminence (pharyngeal arches 3 and 4), thereby eliminating any contribution of the copula (pharyngeal arch 2) in the formation of the definitive adult tongue.
3. The line of fusion between the oral and pharyngeal parts of the tongue is indicated by the **terminal sulcus**.
4. The pharyngeal part is characterized by the **lingual tonsil**, which forms along with the palatine tonsil and pharyngeal tonsil (adenoids) **Waldeyer ring**.
5. General sensation from the mucosa is carried primarily by the **glossopharyngeal nerve (CN IX)**.
6. Taste sensation from the mucosa is carried predominantly by the **glossopharyngeal nerve (CN IX)**.

C. Muscles of the tongue

1. The intrinsic muscles and extrinsic muscles (styloglossus, hyoglossus, genioglossus, and palatoglossus) are derived from myoblasts that migrate into the tongue region from **occipital somites**.
2. Motor innervation is supplied by the **hypoglossal nerve (CN XII)**, except for palatoglossus muscle, which is innervated by CN X.

IV. DEVELOPMENT OF THE FACE (FIGURE 12.3)

A. The face is formed by three swellings: the **frontonasal prominence, maxillary prominence (pharyngeal arch 1)**, and **mandibular prominence (pharyngeal arch 1)**.

B. Bilateral ectodermal thickenings called **nasal placodes** develop on the ventrolateral aspects of the frontonasal prominence.

C. The nasal placodes invaginate into the underlying mesoderm to form the nasal pits, thereby producing a ridge of tissue that forms the **medial nasal prominence** and **lateral nasal prominence**.

D. A deep groove called the nasolacrimal groove forms between the maxillary prominence and the lateral nasal prominence and eventually forms the **nasolacrimal duct** and **lacrimal sac**.

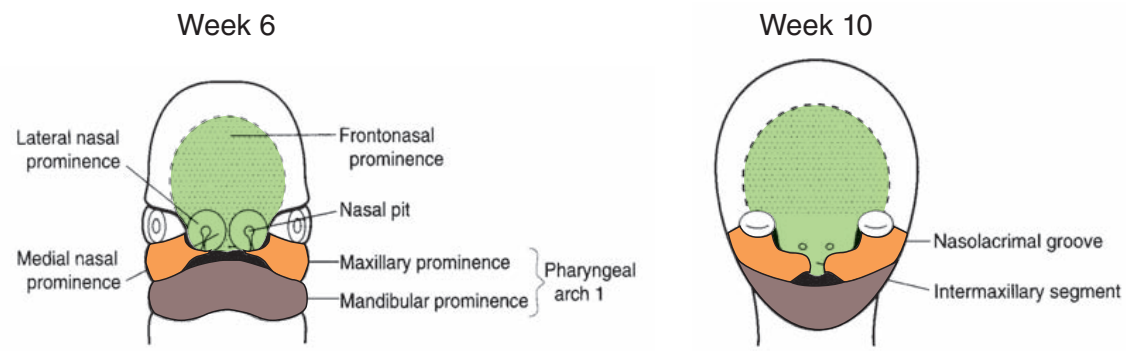

FIGURE 12.3. Development of the face at weeks 6 and 10. Frontonasal prominence = green, lateral nasal prominences = green, medial nasal prominences = green, maxillary prominences of pharyngeal arch 1 = orange, mandibular prominences of pharyngeal arch 1 = brown

V. DEVELOPMENT OF THE PALATE (FIGURE 12.4)

A. Intermaxillary segment

1. The intermaxillary segment forms when the two medial nasal prominences fuse together at the midline due to the growth of the maxillary prominences of pharyngeal arch 1 toward the midline.
2. The intermaxillary segment forms the **philtrum of the lip, four incisor teeth**, and **primary palate**.

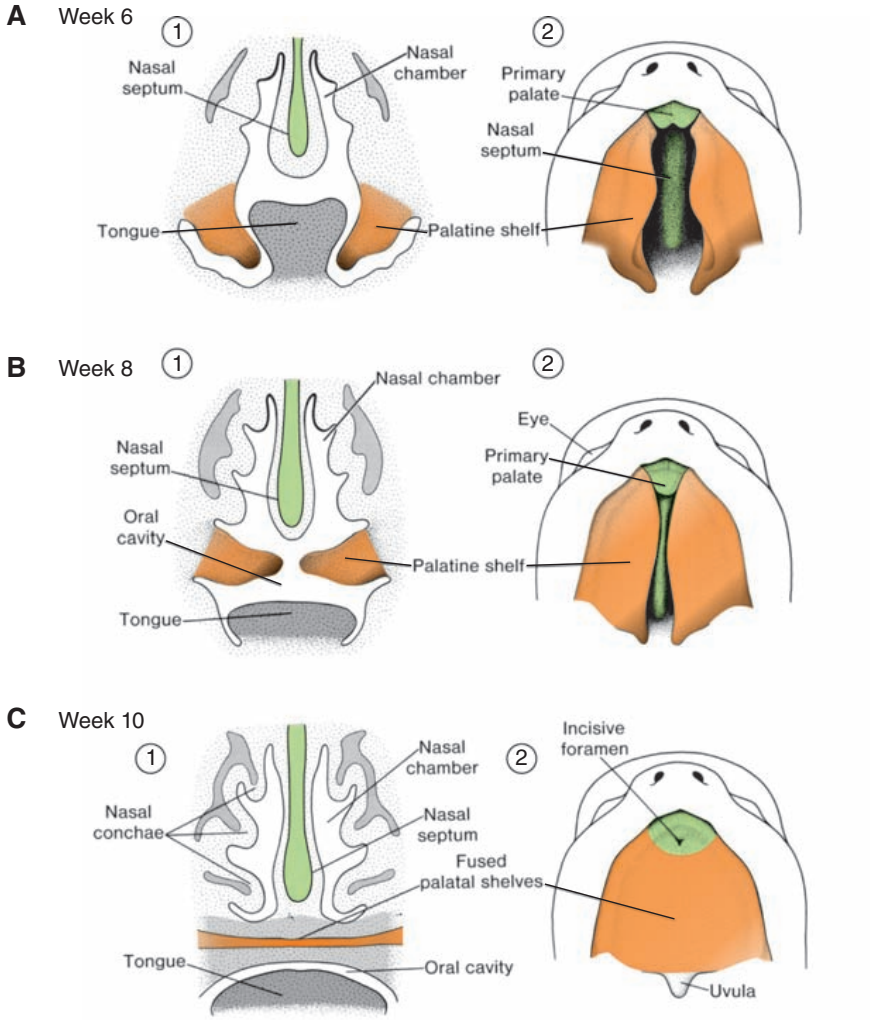

FIGURE 12.4. Development of the palate at weeks 6, 8, and 10. **(1)** Horizontal sections. **(2)** Roof of the mouth. Palatine shelves from maxillary prominence of pharyngeal arch 1 = orange, nasal septum from the medial nasal prominences = green, primary palate from the medial nasal prominences = green

B. Secondary palate

1. The secondary palate forms from outgrowths of the maxillary prominences of pharyngeal arch 1 called the **palatine shelves**.
2. Initially the palatine shelves project downward on either side of the tongue but later attain a horizontal position and fuse along the **palatine raphe** to form the **secondary palate**.
3. The primary and secondary palate fuse at the **incisive foramen** to form the **definitive palate**.
4. Bone develops in both the primary palate and anterior part of the secondary palate. Bone does not develop in the posterior part of the secondary palate, which eventually forms the **soft palate** and **uvula**.
5. The **nasal septum** develops from the medial nasal prominences and fuses with the definitive palate.

VI. DEVELOPMENT OF THE MOUTH

A. The mouth is formed from a surface depression called the **stomodeum**, which is lined by ectoderm, and the **cephalic end of the foregut**, which is lined by endoderm.

B. The stomodeum and foregut meet at the **oropharyngeal membrane**.

C. The epithelium of the **oral part of the tongue, hard palate, sides of the mouth, lips, parotid gland and ducts, Rathke pouch**, and **enamel of the teeth** are derived from ectoderm.

D. The epithelium of the **pharyngeal part of the tongue, floor of the mouth, palatoglossal fold, palatopharyngeal fold, soft palate, sublingual gland and ducts**, and **submandibular gland and ducts** are derived from endoderm.

VII. DEVELOPMENT OF THE NASAL CAVITIES

A. The nasal placodes deepen considerably to form the nasal pits and finally the **nasal sacs**.

B. The nasal sacs remain separated from the oral cavity by the **oronasal membrane**, but it soon ruptures; the nasal cavities and oral cavity are then continuous via the **primitive choanae**.

C. Swellings in the lateral wall of each nasal cavity form the **superior, middle, and inferior conchae**.

D. In the roof of each nasal cavity, the ectoderm of the nasal placode forms a thickened patch—the **olfactory epithelium**.

E. Olfactory epithelium contains **sustentacular cells, basal cells**, and **ciliated cells**. These ciliated cells are bipolar neurons that give rise to the **olfactory nerve (CN I)**, have a lifespan of 1–2 months, and are continuously regenerated.

VIII. CLINICAL CONSIDERATIONS

A. **First arch syndrome (Figure 12.5)** results from abnormal development of **pharyngeal arch 1** and produces various facial anomalies. It is caused by a lack of migration of neural crest cells into pharyngeal arch 1. Two well-described first arch syndromes are **Treacher Collins syndrome (mandibulofacial dysostosis)** and **Pierre Robin syndrome**. Treacher Collins syndrome is an autosomal dominant genetic disorder caused by a mutation in the *TCOF1* **gene** on **chromosome 5q32-q33.1** for the **treacle protein**. The treacle protein is a nucleolar protein that seems to be involved in microtubule dynamics. **Clinical features include** hypoplasia of the zygomatic bones and mandible, resulting in midface hypoplasia, micrognathia, and retrognathia; external ear abnormalities, including small, absent, malformed, or rotated ears; and lower eyelid abnormalities, including coloboma. The photograph (Figure 12.5) shows a young boy with Treacher Collins syndrome. Note the hearing aid cord.

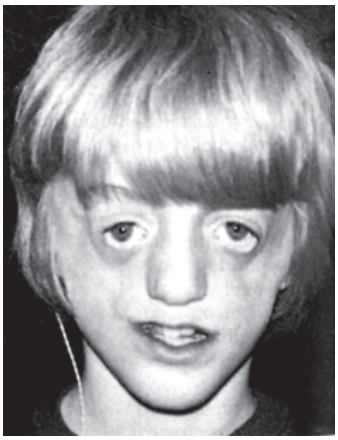

FIGURE 12.5. Treacher Collins syndrome (mandibulofacial dysostosis).

B. **Pharyngeal fistula (Figure 12.6)** occurs when **pharyngeal pouch 2** and **pharyngeal groove 2** persist, thereby forming a patent opening from the internal tonsillar area to the external neck. It is generally found along the **anterior border of the sternocleidomastoid muscle**. The radiograph (Figure 12.6) after injection of a contrast medium shows the course of the fistula through the neck (*arrow*). The fistula may begin inside the throat near the tonsils, travel through the neck, and open to the outside near the anterior border of the sternocleidomastoid muscle.

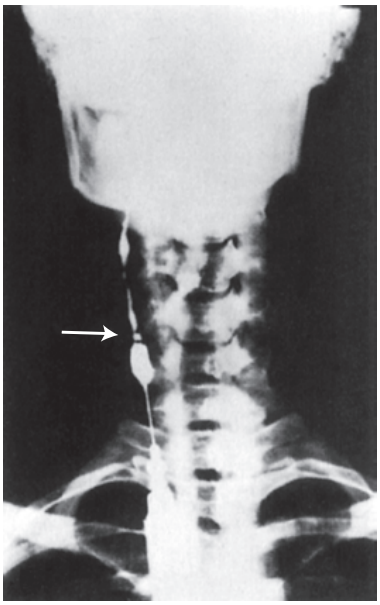

FIGURE 12.6. Pharyngeal fistula.

C. **Pharyngeal cyst (Figure 12.7)** occurs when parts of the **pharyngeal grooves 2, 3, and 4** that are normally obliterated persist, thereby forming a cyst. It is generally found near the **angle of the mandible**. The photograph (Figure 12.7) shows a fluid-filled cyst (*dotted circle*) near the angle of the mandible (*arrow*).

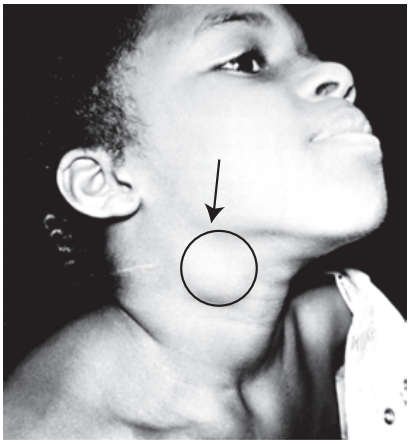

FIGURE 12.7. Pharyngeal cyst.

D. Ectopic thymus, parathyroid, or thyroid tissue (Figure 12.8) result from the abnormal migration of these glands from their embryonic position to their definitive adult location. Glandular tissue may be found anywhere along their migratory path. The photograph (Figure 12.8) shows a sublingual thyroid mass (*dotted circle*) in a 5-year-old euthyroid girl. The [^{99M}Tc] pertechnetate scan (Figure 12.8) localizes the position and the extent of the sublingual thyroid gland. There is no evidence of functioning thyroid tissue in the lower neck (i.e., in the normal anatomical position).

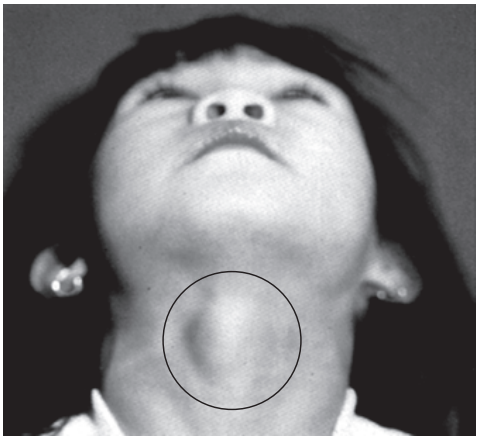

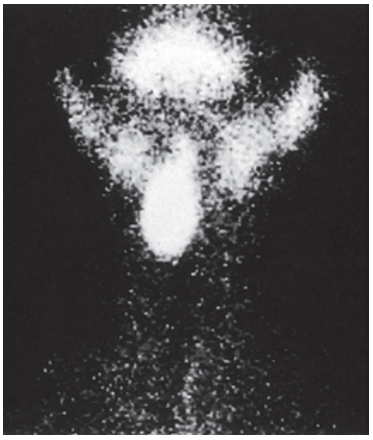

FIGURE 12.8. Ectopic thyroid tissue.

E. Thyroglossal duct cyst (Figure 12.9) occurs when parts of the thyroglossal duct persist and thereby form a cyst. It is most commonly located in the midline near the hyoid bone, but it may also be located at the base of the tongue, when it is then called a **lingual cyst**. The photograph (Figure 12.9A) shows a **thyroglossal duct cyst** (*arrow*), which is one of the most frequent congenital anomalies in the neck and is found along the midline most frequently below the hyoid bone. The MRI (Figure 12.9B) shows a **lingual cyst** consisting of a mass of thyroid tissue (*arrow*) at the base of the tongue.

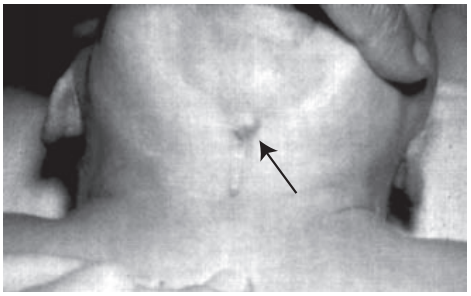

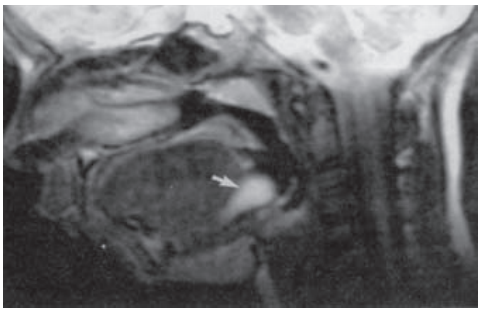

FIGURE 12.9. A. Thyroglossal duct cyst. **B.** Lingual cyst.

F. Congenital hypothyroidism (cretinism; Figure 12.10) occurs when a thyroid deficiency exists during the early fetal period due to a severe lack of dietary iodine, thyroid agenesis, or mutations involving the biosynthesis of thyroid hormone. This condition causes impaired skeletal growth and mental retardation. This condition is characterized by dry, rough skin, wide-set eyes, periorbital puffiness, a flat, broad nose, and large, protuberant tongue. The photograph (Figure 12.10) shows a child with impaired skeletal growth and mental retardation. Note the dry, rough skin (myxedema) and protuberant tongue.

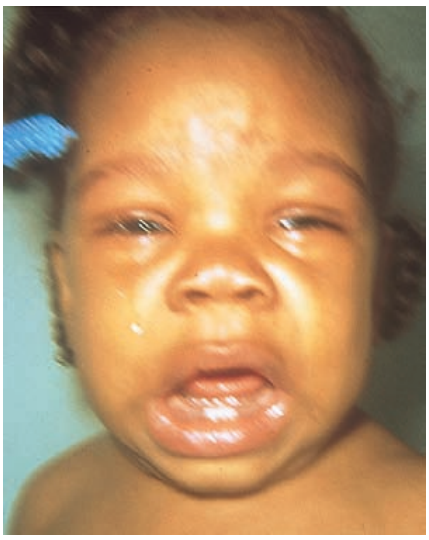

FIGURE 12.10. Congenital hypothyroidism (cretinism).

G. Cleft palate has multifactorial causes, including neural crest cell participation. It is classified as anterior or posterior. The anatomical landmark that separates anterior from posterior cleft palate defects is the incisive foramen.

1. **Anterior cleft palate** occurs when the palatine shelves fail to fuse with the primary palate.
2. **Posterior cleft palate** occurs when the palatine shelves fail to fuse with each other and with the nasal septum.
3. **Anteroposterior cleft palate** occurs when there is a combination of both defects.

H. Cleft lip (Figure 12.11) has multifactorial causes, including neural crest cells participation. Cleft lip and cleft palate are distinct malformations based on their embryological formation, even though they often occur together. They may occur unilaterally or bilaterally. Unilateral cleft lip is the most common congenital malformation of the head and neck. It results from the following:

1. The maxillary prominence fails to fuse with the medial nasal prominence.
2. The underlying somitomeric mesoderm and neural crest fail to expand, resulting in a **persistent labial groove**. The photograph (Figure 12.11) shows a child with a cleft palate and a unilateral cleft lip.

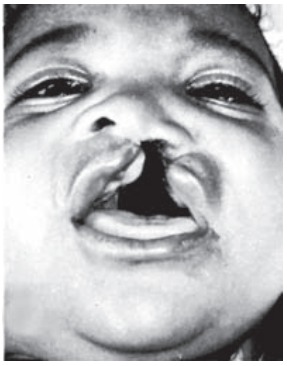

FIGURE 12.11. Unilateral cleft lip and cleft palate.

I. DiGeorge syndrome (DS; "catch 22"; 22q11 syndrome) is caused by a microdeletion of a region in chromosome 22q11.2 that is also called the *DiGeorge chromosomal region*. This results in the failure of **pharyngeal pouches 3 and 4** to differentiate into the thymus and parathyroid glands. DS is usually accompanied by facial anomalies resembling first arch syndrome (micrognathia, low-set ears) due to abnormal neural crest cell migration, cardiovascular anomalies due to abnormal neural crest cell migration during formation of the aorticopulmonary septum, immunodeficiency due to the absence of the thymus gland, and hypocalcemia due to the absence of parathyroid glands.

J. Ankyloglossia ("tongue-tie") occurs when the frenulum of the tongue extends to the tip of the tongue, thereby preventing protrusion.

Study Questions for Chapter 12

1. The most common site of a thyroglossal cyst is

(A) dorsal aspect of the neck
(B) anterior border of the sternocleidomastoid muscle
(C) superior mediastinum
(D) midline close to the hyoid bone
(E) base of the tongue

2. Taste sensation from the oral part (anterior two-thirds) of the tongue is predominantly carried by

(A) trigeminal nerve (CN V)
(B) chorda tympani branch of the facial nerve (CN VII)
(C) glossopharyngeal nerve (CN IX)
(D) superior laryngeal branch of the vagus nerve (CN X)
(E) recurrent laryngeal branch of the vagus nerve (CN X)

3. The intermaxillary segment forms via the fusion of the

(A) maxillary prominences
(B) mandibular prominences
(C) palatine shelves
(D) lateral nasal prominences
(E) medial nasal prominences

4. The most common site of a pharyngeal fistula is the

(A) dorsal aspect of neck
(B) anterior border of sternocleidomastoid muscle
(C) superior mediastinum
(D) midline close to the hyoid bone
(E) base of the tongue

5. What is the most common congenital malformation of the head and neck region?

(A) Anterior cleft palate
(B) Posterior cleft palate
(C) Thyroglossal duct cyst
(D) Unilateral cleft lip
(E) Ankyloglossia

6. Which pharyngeal arch is associated with Treacher Collins syndrome?

(A) Pharyngeal arch 1
(B) Pharyngeal arch 2
(C) Pharyngeal arch 3
(D) Pharyngeal arch 4
(E) Pharyngeal arch 6

7. During surgery for the removal of a thyroid tumor, a number of small masses of glandular tissue are noted just lateral to the thyroid gland. Metastasis from the thyroid tumor is suspected, but histological analysis of a biopsy reveals parathyroid tissue and remnants of thymus. How can this finding be explained?

(A) Tumor tissue has differentiated into normal tissue
(B) A parathyroid gland tumor is also present
(C) Ectopic glandular tissue is commonly found in this region
(D) The patient has DiGeorge syndrome
(E) The glandular tissue is a result of a thyroglossal duct cyst

8. A newborn presents with midfacial and mandibular hypoplasia, defects of the first pharyngeal arch consistent with the diagnosis of Treacher Collins syndrome. What structure would most likely be involved with the syndrome?

(A) Hyoid bone
(B) Stapes
(C) Malleus
(D) Thyroid gland
(E) Inferior parathyroid gland

Answers and Explanations

1. **D.** The thyroid gland forms from a diverticulum in the midline of the floor of the pharynx. The thyroid migrates caudally and passes ventral to the hyoid bone. During this migration, the thyroid remains connected to the tongue by the thyroglossal duct. If a part of the thyroglossal duct persists, a cyst will develop, usually near the hyoid bone.
2. **B.** Taste sensation from the mucosa for the oral part of the tongue is carried by the chorda tympani branch of the facial nerve (CN VII). This part of the tongue forms from pharyngeal arch 1, so the trigeminal nerve (CN V) will carry sensory innervation from the mucosa.
3. **E.** The intermaxillary segment, which plays a critical role in the formation of the definitive adult palate, forms when the two medial nasal prominences fuse in the midline.
4. **B.** A pharyngeal fistula forms when pharyngeal pouch 2 and pharyngeal groove 2 persist. Therefore, these fistulas are found on the lateral aspect of the neck, usually along the anterior border of the sternocleidomastoid muscle.
5. **D.** Unilateral cleft lip is the most common congenital malformation of the head and neck. Cleft lip occurs when the maxillary prominences fail to fuse with the medial nasal prominences and when the underlying somitomeric mesoderm and neural crest fail to proliferate, resulting in a persistent labial groove. Cleft lip occurs in 1 of 900 births and may be unilateral or bilateral.
6. **A.** First arch syndrome results from abnormal development of pharyngeal arch 1 due to a lack of migration of neural crest cells. Treacher Collins syndrome is associated with underdevelopment of the zygomatic bone, down-slanting palpebral fissures, and deformed lower eyelids and external ears.
7. **C.** The parathyroid and thymus migrate in a caudal and medial direction during development; therefore, ectopic glandular tissue may be found anywhere along the migratory path.
8. **C.** The malleus is the only structure on this list derived from the neural crest of the first pharyngeal arch.

chapter 13

Urinary System

I. OVERVIEW (FIGURE 13.1)

The **intermediate mesoderm** forms a longitudinal elevation along the dorsal body wall called the **urogenital ridge**. A portion of the urogenital ridge forms the **nephrogenic cord**, which gives rise to the urinary system. The nephrogenic cord develops into three sets of nephric structures: the **pronephros**, the **mesonephros**, and the **metanephros**.

A. **The pronephros** develops by the differentiation of **mesoderm** within the nephrogenic cord to form **pronephric tubules** and the **pronephric duct**. The pronephros is the cranial-most nephric structure and is a transitory structure that regresses completely by week 5. The pronephros is not functional in humans.

B. **The mesonephros** develops by the differentiation of **mesoderm** within the nephrogenic cord to form **mesonephric tubules** and the **mesonephric duct (Wolffian duct)**. The mesonephros is the middle nephric structure and is a partially transitory structure. Most of the mesonephric tubules regress, but the mesonephric duct persists and opens into the urogenital sinus. The mesonephros is functional for a short period.

C. **The metanephros** develops from an outgrowth of the mesonephric duct (called the **ureteric bud**) and from a condensation of mesoderm within the nephrogenic cord called the **metanephric mesoderm**. The metanephros is the caudal-most nephric structure. The metanephros begins to form at week 5 and is functional in the fetus at about week 10. The metanephros develops into the **definitive adult kidney**. The fetal kidney is divided into lobes, in contrast to the definitive adult kidney, which has a smooth contour.

II. DEVELOPMENT OF THE METANEPHROS (FIGURE 13.2)

A. **Development of the collecting system.** The ureteric bud is an outgrowth of the mesonephric duct. This outgrowth is regulated by ***WT-1*** (an anti-oncogene), **GDNF** (glial cell line-derived neurotrophic factor), and **c-Ret** (a tyrosine kinase receptor). The ureteric bud initially penetrates the metanephric mesoderm and then undergoes repeated branching to form the **ureters, renal pelvis, major calyces, minor calyces**, and **collecting ducts**.

B. **Development of the nephron.** The inductive influence of the collecting ducts causes the metanephric mesoderm to differentiate into **metanephric vesicles**, which later give rise to primitive **S-shaped**

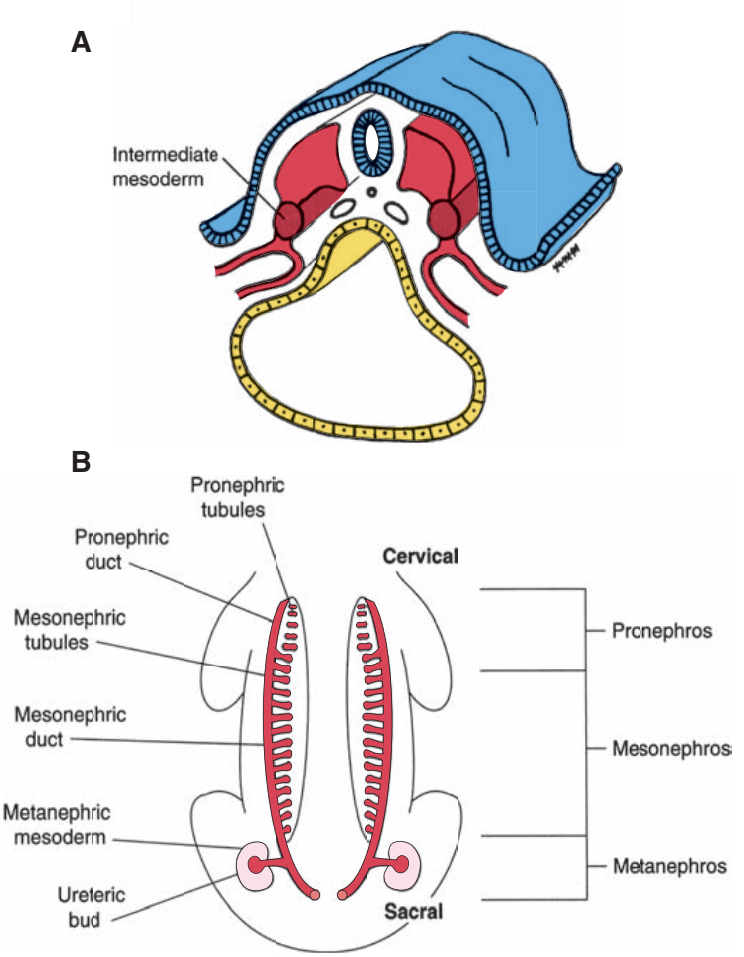

FIGURE 13.1. A.Cross-sectional view of an embryo at week 4. This diagram illustrates the intermediate mesoderm (*dark red*) as a cord of mesoderm that extends from the cervical to sacral levels. The intermediate mesoderm forms the urogenital ridge and nephrogenic cord. **B**. Frontal view of an embryo. This diagram depicts the pronephros, mesonephros, and metanephros. Note that nephric structures develop from cervical through sacral levels. Pronephric tubules and duct = dark red, mesonephric tubules and duct = dark red, ureteric bud= dark red, metanephric mesoderm= light red

renal tubules, which are critical to nephron formation. The S-shaped renal tubules differentiate into the **connecting tubule, distal convoluted tubule, loop of Henle, proximal convoluted tubule**, and **Bowman capsule**. Tufts of capillaries called **glomeruli** protrude into Bowman capsule. Nephron formation is complete at birth, but functional maturation of nephrons continues throughout infancy.

C. Tissue sources

1. The transitional epithelium lining the ureter, pelvis, major calyx, and minor calyx and the simple cuboidal epithelium lining the collecting tubules are derived from **mesoderm of the ureteric bud**.
2. The simple cuboidal epithelium lining the connecting tubule and distal convoluted tubule, the simple squamous epithelium lining the loop of Henle, the simple columnar epithelium lining the proximal convoluted tubule, and the podocytes and simple squamous epithelium lining Bowman's capsule are derived from **metanephric mesoderm**.

III. RELATIVE ASCENT OF THE KIDNEYS (FIGURE 13.3)

A. The fetal metanephros is located at vertebral level **S1–S2**, whereas the definitive adult kidney is located at vertebral level **T12–L3**.

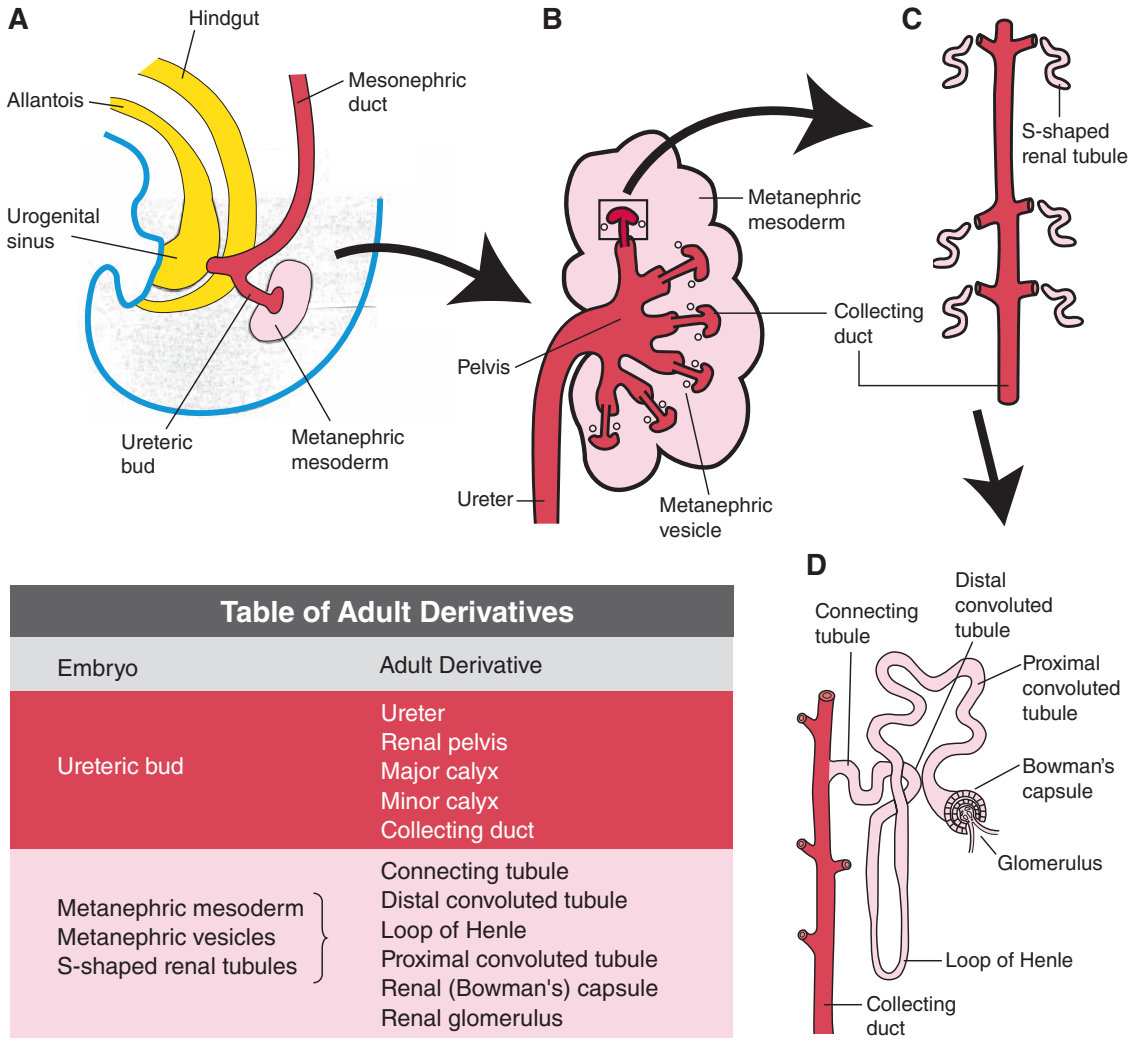

Table of Adult Derivatives

Embryo	Adult Derivative
Ureteric bud	Ureter Renal pelvis Major calyx Minor calyx Collecting duct
Metanephric mesoderm Metanephric vesicles S-shaped renal tubules	Connecting tubule Distal convoluted tubule Loop of Henle Proximal convoluted tubule Renal (Bowman's) capsule Renal glomerulus

FIGURE 13.2. A.Lateral view of the embryo. This diagram shows the relationship between the mesonephric duct (*dark red*), ureteric bud (*dark red*), and metanephric mesoderm (*light red*). In addition, note the urogenital sinus (*yellow*), hindgut (*yellow*), and allantois (*yellow*). **B**. Lateral view of a fetal kidney. This diagram indicates the structures formed from the ureteric bud (*dark red*). Note the repeated branching of the ureteric bud into the metanephric mesoderm (*light red*). At the tip of the each collecting duct, the formation of metanephric vesicles (*light red*) is induced. Note the outer lobulated appearance of a fetal kidney. **C**. Enlarged view of the rectangle shown in panel B. This diagram illustrates the further branching of a collecting duct (*dark red*) and the formation of primitive S-shaped renal tubules (*light red*). **D**. A summary table of derivatives and a diagram of an adult nephron. This table and diagram show the adult structures that derive from the ureteric bud (*dark red*) and the metanephric mesoderm, metanephric vesicles, or the S-shaped renal tubules (*light red*).

B. The change in location results from a disproportionate growth of the embryo caudal to the metanephros.

C. During the relative ascent, the kidneys **rotate 90°**, causing the hilum, which initially faces ventrally, to finally face medially.

IV. BLOOD SUPPLY OF THE KIDNEYS

A. During the relative ascent of the kidneys, they will receive their blood supply from arteries at progressively higher levels until the definitive renal arteries develop at **L2**.

B. Arteries formed during the ascent may persist and are called **supernumerary arteries**.

C. Supernumerary arteries are **end arteries**. Therefore, any damage to them will result in necrosis of kidney parenchyma.

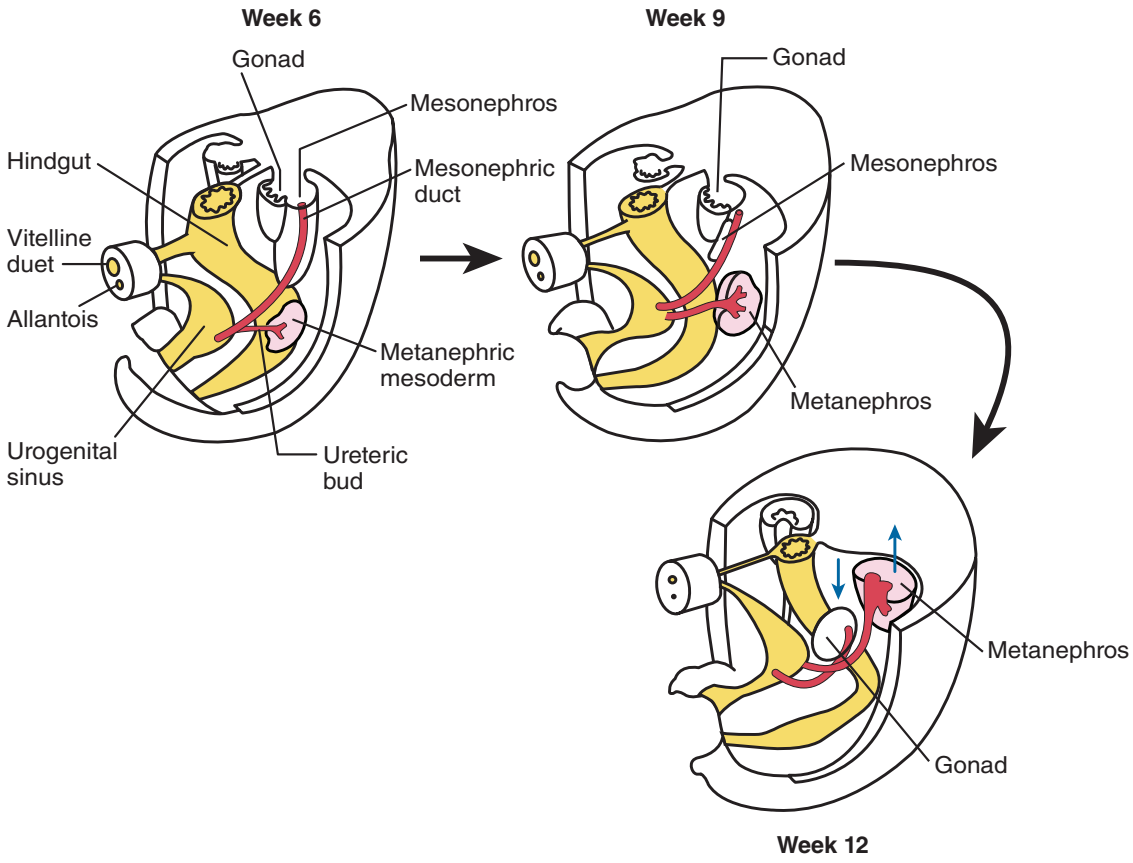

FIGURE 13.3. Relative ascent of the kidneys. This diagram demonstrates the relationship between the gonad and the metanephric (adult) kidney during development at weeks 6, 9, and 12. Note that the gonad descends (*blue arrow*) while the metanephric (adult) kidney ascends (*blue arrow*). Note the change in the relationship between the mesonephric duct and the ureteric bud as they enter the urogenital sinus. Mesonephric duct = dark red, ureteric bud = dark red, metanephric mesoderm (*light red*), urogenital sinus = yellow, hindgut = yellow.

V. DEVELOPMENT OF THE URINARY BLADDER (FIGURE 13.4)

A. The urinary bladder is formed from the upper portion of the **urogenital sinus**, which is continuous with the **allantois**.

B. The allantois becomes a fibrous cord called the **urachus** (or **median umbilical ligament** in the adult).

C. The lower ends of the mesonephric ducts become incorporated into the posterior wall of the bladder to form the **trigone of the bladder**.

D. The mesonephric ducts eventually open into the urogenital sinus below the bladder.

E. The **transitional epithelium** lining the urinary bladder is derived from **endoderm** because of its etiology from the urogenital sinus and gut tube.

VI. DEVELOPMENT OF THE FEMALE URETHRA (FIGURE 13.4)

A. The female urethra is formed from the lower portion of the urogenital sinus.

B. The female urethra develops **endodermal outgrowths** into the surrounding mesoderm to form the **urethral glands** and **paraurethral glands of Skene** (which are homologous to the prostate gland in the male).

C. The paraurethral glands of Skene open on each side of the external urethral orifice.

D. The female urethra ends at **navicular fossa**, which empties into the **vestibule of the vagina**, which also forms from the urogenital sinus.

E. The vestibule of the vagina develops **endodermal outgrowths** into the surrounding mesoderm to form the **lesser vestibular glands** and **greater vestibular glands of Bartholin** (which are homologous to the bulbourethral glands of Cowper in the male).

F. The greater vestibular glands of Bartholin open on each side of the vaginal orifice.

G. The transitional epithelium and stratified squamous epithelium lining the female urethra are derived from **endoderm**.

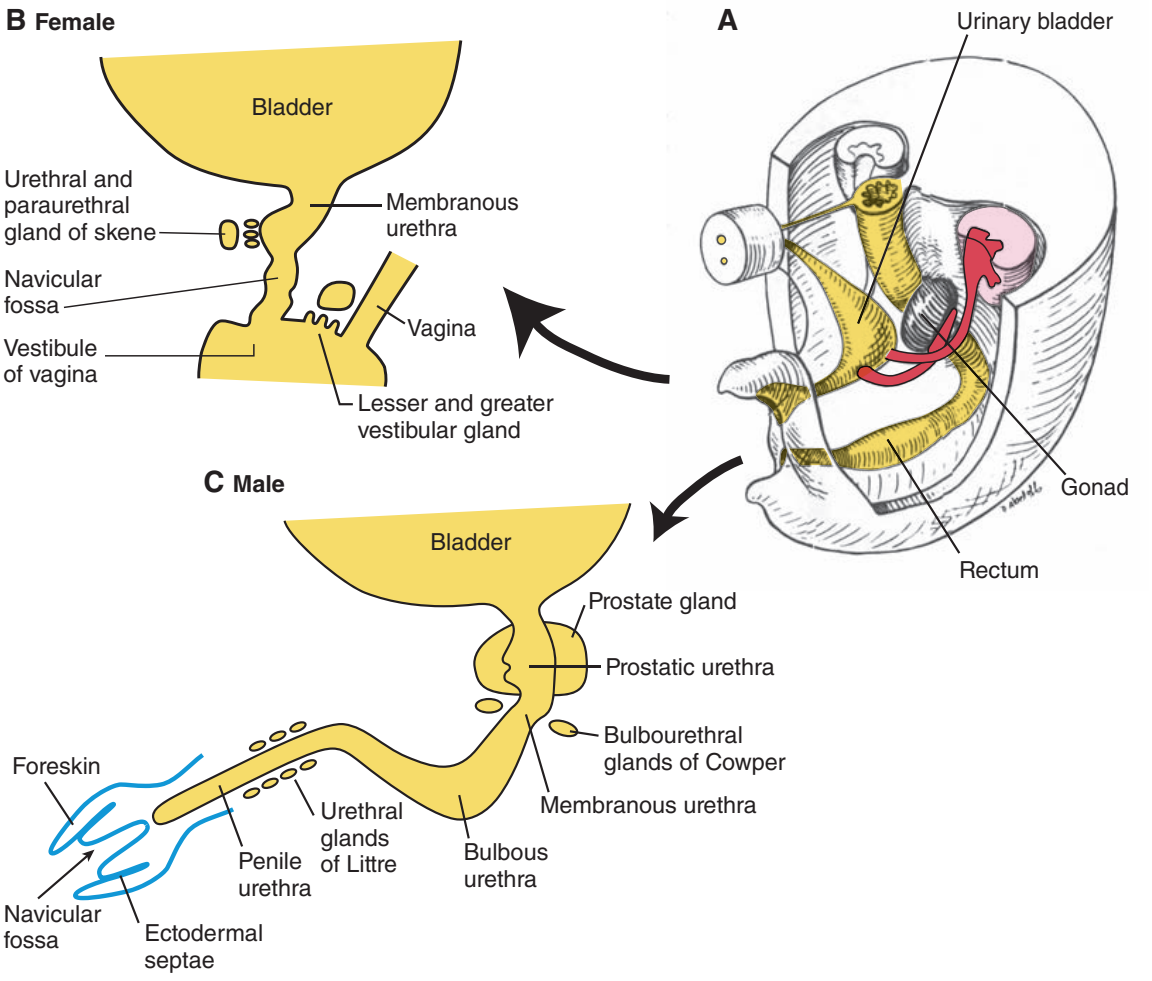

FIGURE 13.4. **A**. Diagram of an embryo showing the development of the upper portion of urogenital sinus into urinary bladder (*yellow*) and the lower portion into the female and male urethra. **B**. Female urethra. The urinary bladder (*yellow*), membranous portion of the female urethra (*yellow*), and navicular fossa (*yellow*) all empty into the vestibule of the vagina (*yellow*). **C**. Male urethra. The urinary bladder (*yellow*), prostatic urethra (*yellow*), membranous urethra (*yellow*), bulbous urethra (*yellow*), proximal part of the penile urethra (*yellow*), and navicular fossa (blue) are shown.

VII. DEVELOPMENT OF THE MALE URETHRA (FIGURE 13.4)

A. **Prostatic urethra, membranous urethra, bulbous urethra**, and **proximal part of penile urethra**. These parts of the urethra are formed from the lower portion of the urogenital sinus. The transitional epithelium and stratified columnar epithelium lining these parts of the urethra are derived from **endoderm**.

1. **The prostatic urethra** develops **endodermal outgrowths** into the surrounding mesoderm to form the **prostate gland**. The posterior wall of the prostatic urethra has an elevation called the **urethral crest**. The **prostatic sinus** is a groove on either side of the urethral crest that receives most of the prostatic ducts from the prostate gland. At a specific site along the urethral crest, there is an ovoid enlargement called the **seminal colliculus** (also called the **verumontanum**), which contains the **openings of the ejaculatory ducts** and the **prostatic utricle** (a vestigial remnant of the paramesonephric ducts in the male that is involved in the development of the vagina and uterus).
2. **The membranous urethra** develops **endodermal outgrowths** into the surrounding mesoderm to form the **bulbourethral glands of Cowper**.
3. **The bulbous urethra** contains the openings of the bulbourethral glands of Cowper.
4. **The proximal part of the penile urethra** develops **endodermal outgrowths** into the surrounding mesoderm to form **urethral glands of Littre**.

B. **Distal part of the penile urethra** is formed from an ingrowth of **surface ectoderm** called the **glandular plate**. The glandular plate joins the proximal penile urethra and becomes canalized to form the **navicular fossa. Ectodermal septa** appear lateral to the navicular fossa and become canalized to form the **foreskin**. The stratified squamous epithelium lining of the distal penile urethra is derived from **ectoderm**.

VIII. CLINICAL CONSIDERATIONS

A. **Renal agenesis** occurs when the ureteric bud fails to develop, thereby eliminating the induction of metanephric vesicles and nephron formation.

1. **Unilateral renal agenesis** is relatively common (more common in males). Therefore, a physician should never assume a patient has two kidneys. It is asymptomatic and compatible with life because the remaining kidney hypertrophies.
2. **Bilateral renal agenesis** is relatively uncommon. It causes oligohydramnios, which causes compression of the fetus, resulting in **Potter syndrome** (deformed limbs, wrinkly skin, and abnormal facial appearance). These infants are usually stillborn or die shortly after birth.

B. **Renal hypoplasia** occurs when there is a congenitally small kidney with no pathological evidence of dysplasia.

C. **Renal dysplasia** occurs when there is a disorganization of renal parenchyma with abnormally developed and immature nephrons.

D. **Renal ectopia** occurs when one or both kidneys fail to ascend and therefore remain in the pelvis or lower lumbar area (i.e., **pelvic kidney**). In some cases, two pelvic kidneys fuse to form a solid mass, commonly called a **pancake kidney**.

E. Renal fusion (Figure 13.5). The most common type of renal fusion is the **horseshoe kidney**. A horseshoe kidney occurs when the inferior poles of the kidneys fuse across the midline. Normal ascent of the kidneys is arrested because the fused portion gets trapped behind the **inferior mesenteric artery**. Kidney rotation is also arrested, so that the hilum faces ventrally. The photograph (Figure 13.5) shows a horseshoe kidney. The computed tomography (CT) scan shows a band of renal tissue (*arrow*) that extends across the midline.

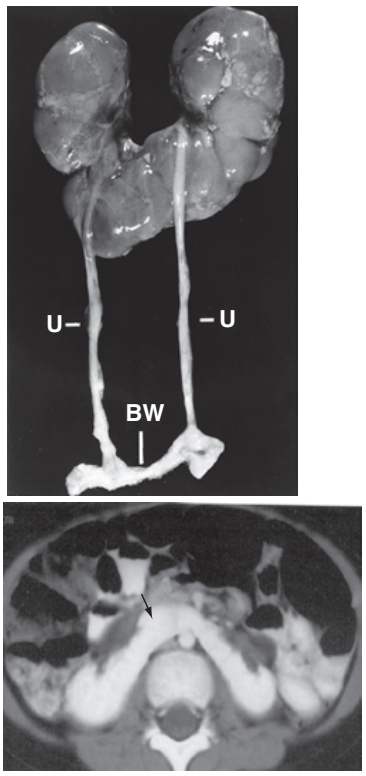

FIGURE 13.5. Horseshoe kidney. U = ureter; BW = bladder wall.

F. Renal artery stenosis (Figure 13.6) is the most common cause of renovascular hypertension in children. The stenosis may occur in the main renal artery of segmental renal arteries. The angiogram (Figure 13.6) shows bilateral renal artery stenosis (*arrows*).

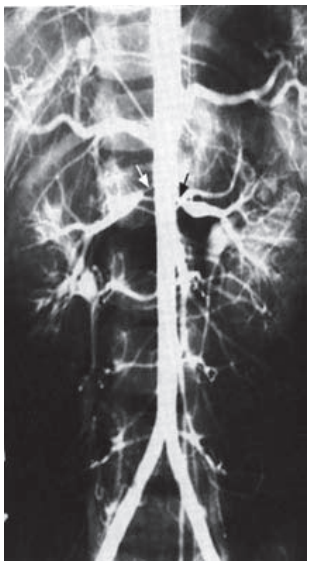

FIGURE 13.6. Renal artery stenosis.

G. Ureteropelvic junction obstruction (UPJ; Figure 13.7) occurs when there is an obstruction to the urine flow from the renal pelvis to the proximal ureter. UPJ is the most common congenital obstruction of the urinary tract. If there is severe uteropelvic atresia, a **multicystic dysplastic kidney** is found in which the cysts are actually dilated calyces. In this case, the kidney consists of grapelike, smooth-walled cysts of variable size. Dysplastic glomeruli and atrophic tubules are found between the cysts. The photograph (Figure 13.7) shows numerous cysts within the kidney. The sonogram shows many anechoic cysts (C) separated by renal septae.

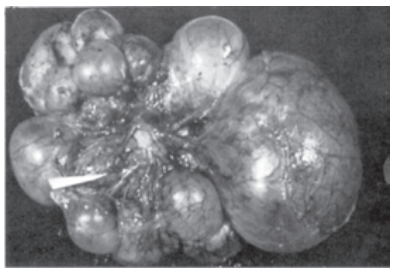

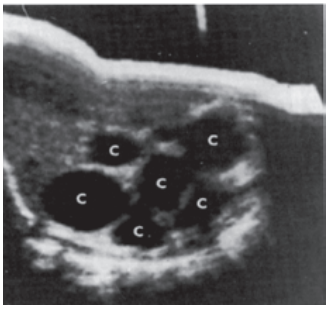

FIGURE 13.7. Multidysplastic kidney.

H. Childhood polycystic kidney disease (PCKD; Figure 13.8) is an autosomal recessive disease that has been mapped to the short arm of chromosome 6 (p6). In childhood PCKD, the kidneys are huge and spongy and contain numerous cysts due to the dilation of collecting ducts and tubules, which severely compromises kidney function. Childhood PCKD is associated clinically with cysts of the liver, pancreas, and lungs. Treatment includes dialysis and kidney transplant. The photograph (Figure 13.8) shows an infant with polycystic kidney (*arrow*). The light micrograph (Figure 13.8) shows large, fluid-filled cysts (CY) throughout the substance of the kidney. Between the cysts, some functioning nephrons can be observed.

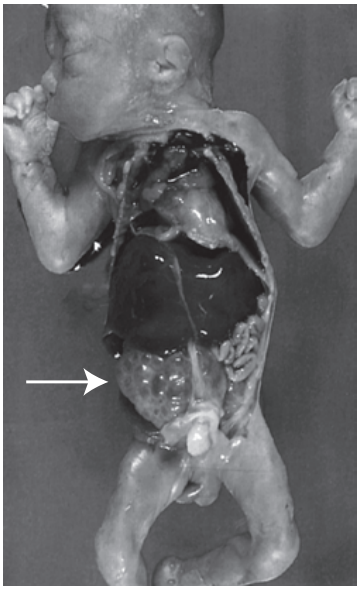

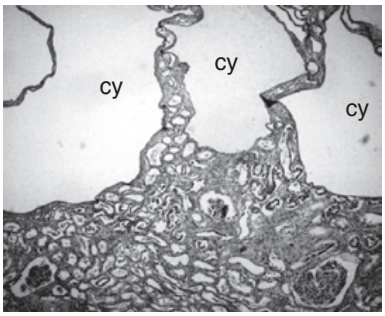

FIGURE 13.8. Childhood polycystic kidney disease.

I. **Wilms tumor (WT; Figure 13.9)** is the **most common renal malignancy of childhood**. WT presents as a large, solitary, well-circumscribed mass that on cut section is soft, homogeneous, and tan-gray in color. WT is interesting histologically, in that it tends to recapitulate different stages of embryological formation of the kidney, so that three classic histological areas are described: a stromal area; a blastemal area of tightly packed embryonic cells; and a tubular area. The photograph (Figure 13.9) shows a WT extending from normal kidney tissue (*arrow*). The light micrograph (Figure 13.9) shows the tumor that is characterized histologically by recognizable attempts to recapitulate embryonic development of the kidney. In this regard, the following three components are seen: (1) metanephric blastema elements (blas) consisting of clumps of small, tightly packed embryonic cells, (2) stromal elements (str), and (3) epithelial elements generally in the form of abortive attempts at forming tubules (t) or glomeruli.

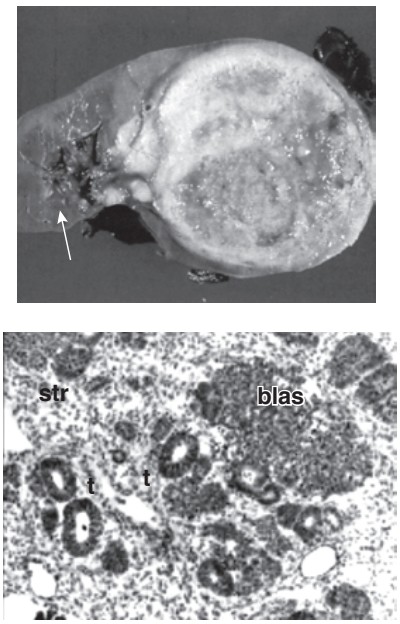

FIGURE 13.9. Wilms tumor.

J. **Ureteropelvic duplications (Figure 13.10)** occur when the ureteric bud prematurely divides before penetrating the metanephric blastema. This results in either a double kidney or a duplicated ureter and renal pelvis. The term duplex kidney refers to a configuration in which two ureters drain one kidney. The intravenous urogram (IVU) on the left (Figure 13.10) shows a bilateral duplication of the collecting system (*arrows*). The cystogram on the right (Figure 13.10) shows reflux into both of the lower collecting systems (*arrows*) only.

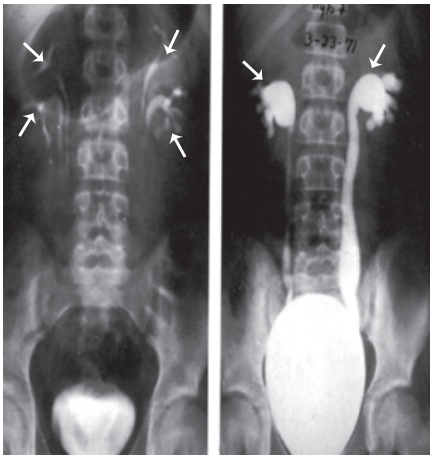

FIGURE 13.10. Ureteropelvic duplication.

K. **Exstrophy of the bladder** occurs when the posterior wall of the urinary bladder is exposed to the exterior. It is caused by a failure of the anterior abdominal wall and anterior wall of the bladder to develop properly. It is associated clinically with urine drainage to the exterior and epispadias. Surgical reconstruction is difficult and prolonged.

L. **Urachal fistula or cyst** occurs when a remnant of the allantois persists, thereby forming fistula or cyst. It is found along the midline on a path from the umbilicus to the apex of the urinary bladder. A urachal fistula forms a direct connection between the urinary bladder and the outside of the body at the umbilicus, causing **urine drainage** from the umbilicus.

M. **Ectopic opening of the ureter occurs** when the ureteric bud fails to separate from the mesonephric duct, which results in the opening of the ureter to be carried to a point distal to its normal position. The most common ectopic opening is a **lateral ureteral ectopia**, in which the opening is lateral to its normal position.

1. **In males**, the ectopic openings are most commonly located in the prostatic urethra, ejaculatory ducts, ductus deferens, or rectum. Because the ectopic openings are all located above the external urethral sphincter, boys with an ectopic opening of the ureter do not present with urine incontinence.
2. **In females**, the ectopic openings are most commonly located in the urethra, vestibule, or vagina. Because the ectopic openings are all located below the external urethral sphincter, girls with an ectopic opening of the ureter generally present with urine incontinence.

N. Ureterocele (Figure 13.11)

1. **Simple ureterocele** occurs when the distal end of the ureter has a cystlike protrusion into the submucosal layer of the urinary bladder.
2. **Ectopic ureterocele** occurs when the distal end of the ureter has a cystlike protrusion into the submucosal layer of the urinary bladder that is almost invariably associated with an ectopic ureter and duplication. In this situation, the ureterocele is at the end of the ureter from the upper renal segment and is located inferior to the other ureter opening. Figure 13.11 shows an ectopic ureterocele located at the end of an enlarged ureter from the upper renal segment. The opening of the enlarged ureter is located inferior to the normal-sized ureter from the lower renal segment.

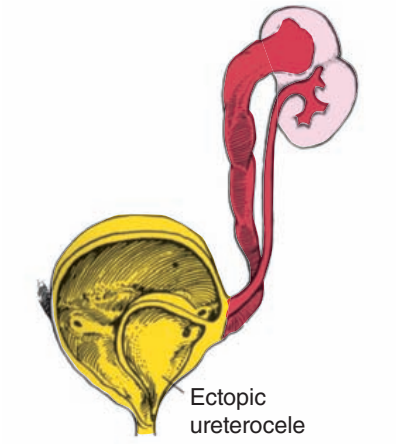

FIGURE 13.11. Ectopic ureterocele.

IX. DEVELOPMENT OF THE SUPRARENAL GLAND (FIGURE 13.12)

A. Cortex

1. The cortex forms from two episodes of mesoderm proliferation that occur between the root of the dorsal mesentery and the gonad.
2. The first episode forms the inner fetal **cortex**.
3. The second episode forms the outer **adult cortex**, by which mesoderm proliferation occurs at the periphery of the fetal cortex.
4. During the fetal period and at birth, the suprarenal glands are very large due to the size of the fetal cortex.
5. The suprarenal glands become smaller as the fetal cortex involutes rapidly during the first 2 weeks after birth and continues to involute during the first year of life.
6. The zona glomerulosa and zona fasciculata of the adult cortex are present at birth, but the zona reticularis is not formed until age 3 years.

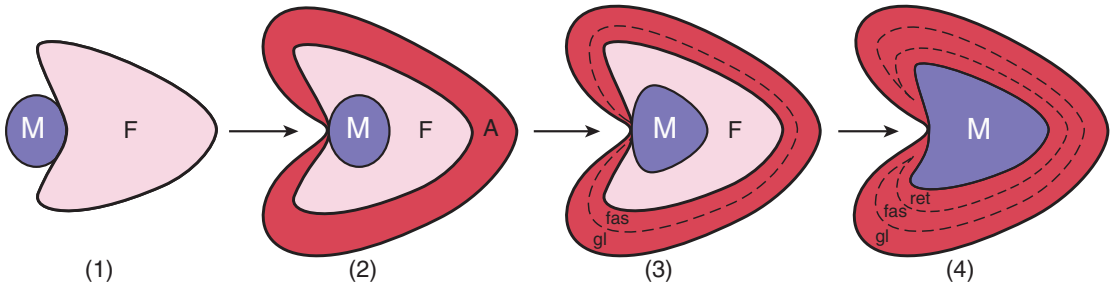

FIGURE 13.12. Development of the suprarenal gland. **(1)** At week 6, the fetal cortex (F; *light red*) and medulla (M; *purple*) at the medial aspect of the adrenal gland are both apparent. **(2)** At week 9, the adult cortex (A; *dark red*) has formed at the periphery of the fetal cortex. Note that the medulla is completely surrounded by the adult and fetal cortex. **(3)** At birth, the fetal cortex (*light red*) is still present and the adult cortex (*dark red*) has differentiated into the zona glomerulosa (gl) and zona fasciculate (fas). **(4)** At 3 years of age, the fetal cortex has completely involuted, thus reducing the size of the suprarenal gland. The adult cortex has further differentiated to form the zona reticularis (ret).

B. Medulla

1. The medulla forms when neural crest cells aggregate at the medial aspect of the fetal cortex and eventually become surrounded by the fetal and adult cortex.
2. The neural crest cells differentiate into **chromaffin cells**, which stain yellow-brown with chromium salts.
3. Chromaffin cells can be found in extrasuprarenal sites at birth, but these sites normally regress completely by puberty.
4. In a normal adult, chromaffin cells are found only in the suprarenal medulla.

C. Clinical considerations

1. **Neuroblastoma (NB; Figure 13.13)** is a common extracranial neoplasm containing **primitive neuroblasts** (small cells arranged in **Homer-Wright pseudorosettes**) of **neural crest origin**. NB occurs mainly in children and is found in extraadrenal sites usually along the sympathetic chain ganglia (60%) or within the adrenal medulla (40%). NB metastasizes widely to the bone marrow, bone, and lymph nodes. A common laboratory finding is increased urine vanillylmandelic acid (VMA) and metanephrine levels. Neuroblastomas vary in size from 1 cm to filling the entire abdomen. They are generally soft and white to gray-pink in color. As the size increases, the tumors become hemorrhagic and undergo calcification and cyst formation. The photograph (Figure 13.13) shows a NB. Note the nodular appearance of this tumor, with the kidney apparent on its left border (*arrow*). The light micrograph (Figure 13.13) shows that the neoplastic cells are small, primitive-looking cells with dark nuclei and scant cytoplasm. The cells are generally arranged as solid sheets, and some cells arrange around a central fibrillar area, forming Homer-Wright pseudorosettes (*asterisk*).

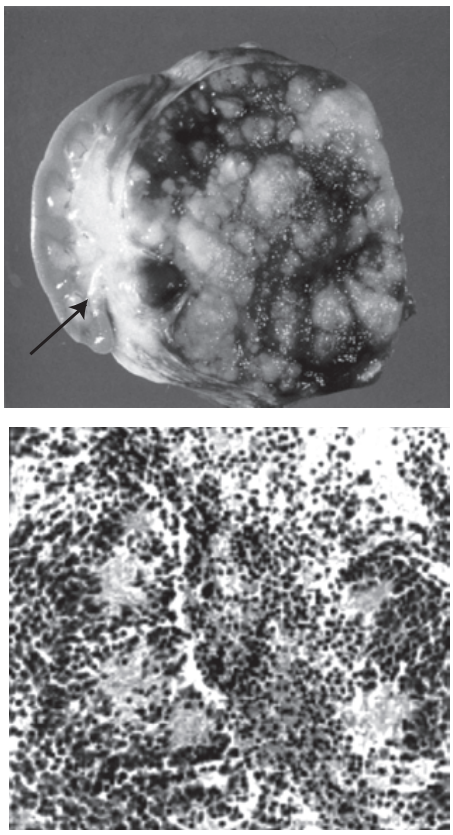

FIGURE 13.13. Neuroblastoma.

2. **Pheochromocytoma (PH; Figure 13.14)** is a relatively rare neoplasm that contains both epinephrine and norepinephrine. PH occurs mainly in adults 40–60 years old and is generally found in the region of the adrenal gland, but it may be found in extrasuprarenal sites. PH is associated with persistent or paroxysmal hypertension, anxiety, tremor, profuse sweating, pallor, chest pain, and abdominal pain. Laboratory findings include increased urine VMA and metanephrine levels, inability to suppress catecholamines with clonidine, and hyperglycemia. PH is treated by surgery or phenoxybenzamine (an α-adrenergic antagonist). Pheochromocytomas vary in size from 3 to 5 cm in diameter. They are gray-white to pink-tan in color. Exposure of the cut surface often results in darkening of the surface due to formation of yellow-brown adrenochrome pigment. The photograph (Figure 13.14) shows a pheochromocytoma. The light micrograph (Figure 13.14) shows neoplastic cells that have abundant cytoplasm with small, centrally located nuclei. The cells are generally found in clusters separated by a slender stroma and numerous capillaries. Numerous cytoplasmic hyaline eosinophilic globules are sometimes present that are derived from membranes of secretory granules.

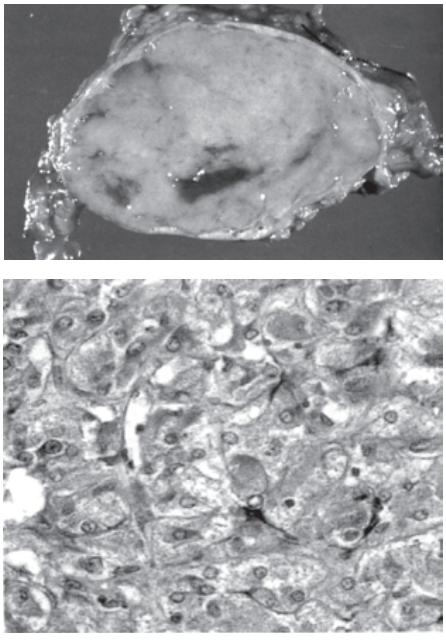

FIGURE 13.14. Pheochromocytoma.

3. **Congenital adrenal hyperplasia (CAH; Figure 13.15)**
   - **a.** CAH is caused most commonly by mutations in genes for enzymes involved in adrenocortical steroid biosynthesis (e.g., **21-hydroxylase deficiency, 11b-hydroxylase deficiency**).
   - **b.** 21-hydroxylase deficiency (current terminology is **CYP21A2 deficiency**) accounts for 90% of all cases of CAH.
   - **c.** CYP21A2 deficiency is an autosomal recessive genetic disorder caused by a mutation in the ***CYP21A2* gene** located on **chromosome 6p21.3**, which encodes for the **21-hydroxylase enzyme**.
   - **d.** In CYP21A2 deficiency, there is defective conversion of 17-hydroxyprogesterone to 11-deoxycortisol. There is virtually no synthesis of the cortisol or aldosterone, so that intermediates are funneled into androgen biosynthesis, thereby elevating androgen levels.
   - **e.** In CYP21A2 deficiency, the characteristic biochemical finding is **elevated serum concentration of 17-hydroxyprogesterone** (i.e., >3500 ng/dL, or 105 nmol/L)
   - **f.** The elevated levels of androgens lead to **masculinization of a female fetus** (i.e., **female pseudo-intersexuality**).
   - **g.** Female pseudo-intersexuality produces the following clinical findings: mild clitoral enlargement, complete labioscrotal fusion with a phalloid organ, or macrogenitosomia (in the male fetus). In clinical practice, most CYP21A2 deficiency cases are subcomplete, so that other symptoms may be the presenting condition, such as precocious puberty, virilization, and infertility.
   - **h.** Because cortisol cannot be synthesized, negative feedback to the adenohypophysis does not occur, so adrenocorticotropic hormone (ACTH) continues to stimulate the adrenal cortex, resulting in adrenal hyperplasia.
   - **i.** Because aldosterone cannot be synthesized, the patient presents with **hyponatremia ("salt-wasting")** with accompanying **dehydration** and **hyperkalemia**.
   - **j.** Treatment includes immediate infusion of intravenous saline and long-term steroid hormone replacement—both cortisol and mineralocorticoids (9α-fludrocortisone).
   - **k.** The photographs (Figure 13.15) show a patient (XX genotype) with CYP21A2 deficiency. This 10-year-old girl is clearly masculinized (left panel). After 9 months of cortisone therapy, there is marked improvement (right panel).

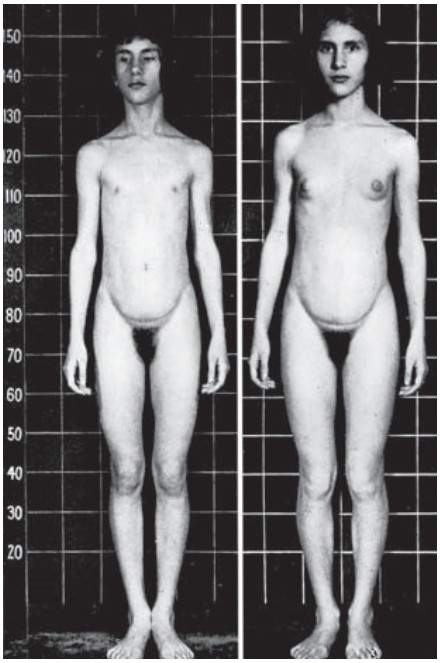

FIGURE 13.15. CYP21A2 deficiency (congenital adrenal hyperplasia)

Study Questions for Chapter 13

1. When does the metanephros become functional?

(A) At week 3 of development
(B) At week 4 of development
(C) At week 10 of development
(D) Just before birth
(E) Just after birth

2. A urachal cyst is a remnant of the

(A) urogenital sinus
(B) urogenital ridge
(C) cloaca
(D) allantois
(E) mesonephric duct

3. During surgery for a benign cyst on the kidney, the surgeon notes that the patient's right kidney has two ureters and two renal pelves. This malformation is

(A) an abnormal division of the pronephros
(B) an abnormal division of the mesonephros
(C) formation of an extra mass of intermediate mesoderm
(D) a premature division of the metanephric blastema
(E) a premature division of the ureteric bud

4. The transitional epithelium lining the urinary bladder is derived from

(A) ectoderm
(B) endoderm
(C) mesoderm
(D) endoderm and mesoderm
(E) neural crest cells

5. The transitional epithelium lining the ureter is derived from

(A) ectoderm
(B) endoderm
(C) mesoderm
(D) endoderm and mesoderm
(E) neural crest cells

6. The podocytes of Bowman capsule are derived from

(A) ectoderm
(B) endoderm
(C) mesoderm
(D) endoderm and mesoderm
(E) neural crest cells

7. The proximal convoluted tubules of the definitive adult kidney are derived from the

(A) ureteric bud
(B) metanephric vesicle
(C) mesonephric duct
(D) mesonephric tubules
(E) pronephric tubules

8. The trigone on the posterior wall of the urinary bladder is formed by the

(A) incorporation of the lower end of the mesonephric ducts
(B) incorporation of the lower end of the pronephric ducts
(C) incorporation of the metanephric blastema
(D) incorporation of the mesonephric tubules
(E) incorporation of the pronephric tubules

9. A 6-year-old girl presents with a large abdominal mass just superior to the pubic symphysis. The mass is tender when palpated and fixed in location. During surgery, a fluid-filled mass is noted connected to the umbilicus superiorly and to the urinary bladder inferiorly. What is the diagnosis?

(A) Pelvic kidney
(B) Horseshoe kidney
(C) Polycystic disease of the kidney
(D) Urachal cyst
(E) Exstrophy of the bladder

10. Immediately after birth of a boy, a moist, red protrusion of tissue is noted just superior to his pubic symphysis. After observation, urine drainage is noted from the upper lateral corners of this tissue mass. What is the diagnosis?

(A) Pelvic kidney
(B) Horseshoe kidney
(C) Polycystic disease of the kidney
(D) Urachal cyst
(E) Exstrophy of the bladder

Answers and Explanations

1. **C.** The metanephros begins to form at week 5 and starts to function in the fetus at about week 10. The pronephros is not functional in humans. The mesonephros is the interim kidney, which functions until the metanephros is ready.
2. **D.** The upper end of the urogenital sinus is in patent communication with the allantois, which lies in the umbilical cord. The allantois normally regresses and forms a fibrous cord. If a remnant persists, it forms a urachal cyst or sinus.
3. **E.** The ureteric bud seems to be preprogrammed to undergo repeated divisions. These divisions normally begin on contact with the metanephric blastema. If the ureteric bud undergoes division prematurely, duplication of the ureter and renal pelvis occurs. In some circumstances, two separate kidneys may form.
4. **B.** The transitional epithelium lining the urinary bladder is derived from endoderm because the urinary bladder develops from the upper end of the urogenital sinus. The origin of the urogenital sinus can be traced back to the gut tube, which is lined by endoderm.
5. **C.** The transitional epithelium lining the ureter is derived from mesoderm because the ureter develops from the ureteric bud. The ureteric bud is a diverticulum from the mesonephric duct whose origin can be traced back to the intermediate mesoderm.
6. **C.** The podocytes of Bowman capsule develop from the metanephric vesicles, which are of mesodermal origin.
7. **B.** The distal convoluted tubule, loop of Henle, proximal convoluted tubule, and Bowman capsule are all derived from the metanephric vesicle.
8. **A.** The lower ends of the mesonephric ducts are incorporated into the posterior wall of the urinary bladder. The mesonephric ducts contribute to the connective tissue component of the posterior wall at the trigone. It is generally believed that the transitional epithelium lining the entire bladder (even the trigone) is of endodermal origin.
9. **D.** A urachal cyst or sinus forms from a remnant of the allantois and is found along the midline on a path from the umbilicus to the apex of the urinary bladder. The epithelium lining the cyst produces secretions that gradually fill the remnant with fluid. Very rarely, the entire allantois persists, forming a fistula that is patent from the urinary bladder to the exterior at the umbilicus.
10. **E.** The moist, red tissue mass that is exposed to the exterior is actually the posterior wall of the urinary bladder. This is called exstrophy of the bladder and is caused when the anterior abdominal wall and anterior wall of the bladder fail to form. The ureters open onto the posterior wall; therefore, urine drainage is apparent.

chapter 14

Female Reproductive System

I. THE INDIFFERENT EMBRYO

A. The genotype of the embryo (46, XX or 46, XY) is established at fertilization.

B. **During weeks 1–6,** the embryo remains in a sexually indifferent or undifferentiated stage. This means that genetically female embryos and genetically male embryos are phenotypically indistinguishable.

C. **During week 7,** the indifferent embryo begins phenotypic sexual differentiation.

D. **By week 12,** female or male characteristics of the external genitalia can be recognized.

E. **By week 20,** phenotypic differentiation is complete.

1. **Phenotypic sexual differentiation**
   - **a.** Phenotypic sexual differentiation is determined by the *SRY* **gene** and may result in individuals with a **female phenotype**, an **intersex phenotype**, or a **male phenotype**.
   - **b.** The *SRY* gene on chromosome Yp11.3 encodes for a **sex-determining region Y protein** (also called **testes-determining factor [TDF]**).
   - **c.** TDF is a 220–amino acid nonhistone protein that contains a highly conserved DNA-binding region called a **high mobility group box**.
   - **d.** As the indifferent gonad develops into the testes, **Leydig cells** differentiate to produce **testosterone** and **Sertoli cells** differentiate to produce **Müllerian-inhibiting factor (MIF)**.
   - **e.** **In the presence of TDF, testosterone, and MIF**, the indifferent embryo will be directed to the male phenotype.
   - **f.** **In the absence of TDF, testosterone, and MIF**, the indifferent embryo will be directed to the female phenotype.
2. **Components of the indifferent embryo**
   - **a.** The components of the indifferent embryo that are remodeled to form the adult female reproductive system include the **gonads, genital ducts**, and **primordia of external genitalia**.
   - **b.** Phenotypic sexual differentiation occurs in a sequence beginning with the gonads, then the genital ducts, and finally the primordia of external genitalia.

II. DEVELOPMENT OF THE GONADS (FIGURE 14.1)

A. **The ovary**

1. The **intermediate mesoderm** forms a longitudinal elevation along the dorsal body wall, the **urogenital ridge**.

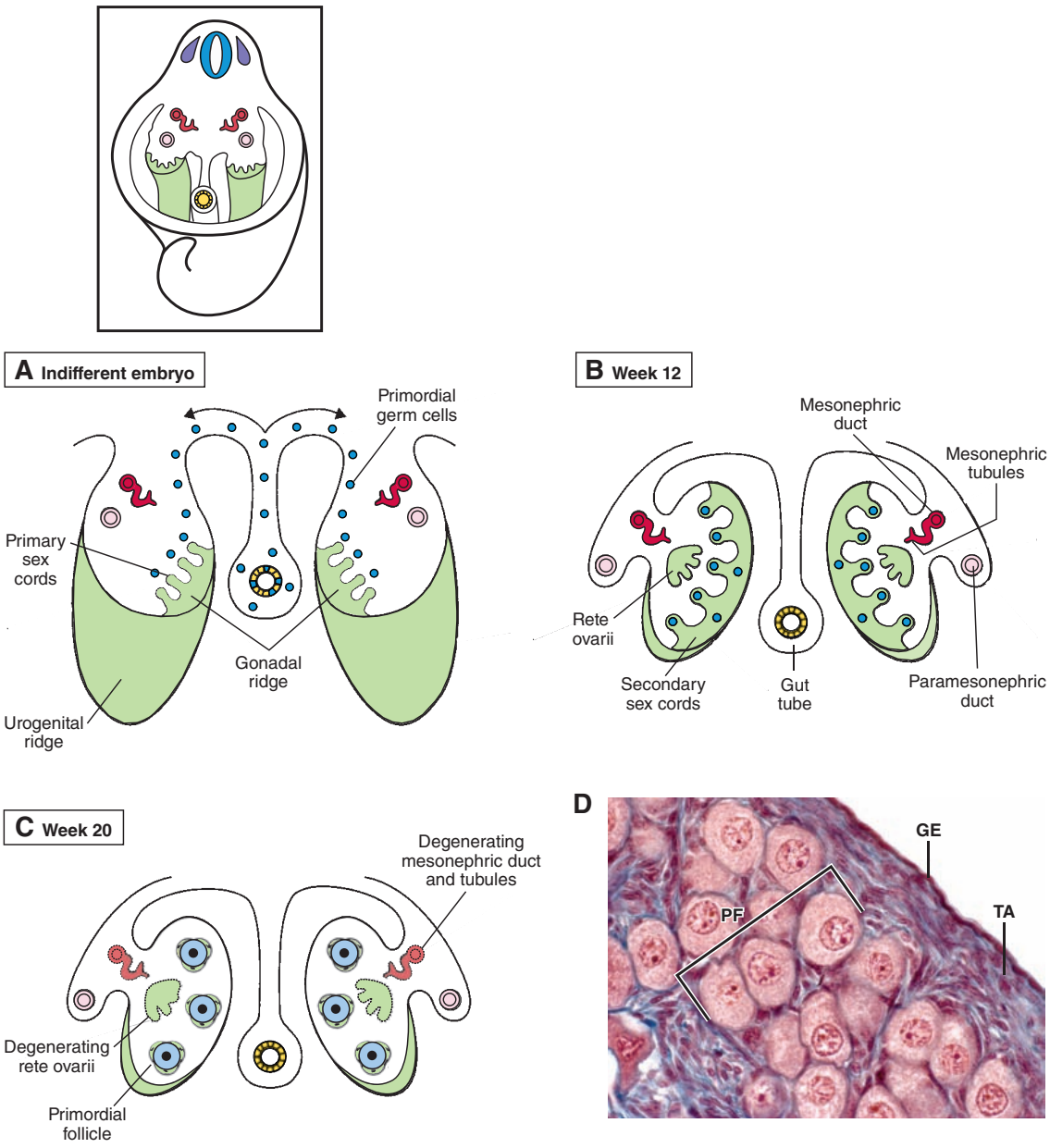

FIGURE 14.1. Development of the gonads. This diagram demonstrates the differentiation of the gonad in the female. The small figure in the box is a cross section of the embryo at the level of the urogenital ridge for orientation. **A**. Gonad in the indifferent embryo. This diagram shows primordial germ cells (*blue*) migrating from the yolk sac into the gonad. Urogenital ridge = green, primary sex cords = green, paramesonephric duct = light red, mesonephric duct = dark red, endodermal lining of yolk sac = yellow. **B**. Ovary at week 12. This diagram shows the secondary sex cords (*green*) that have incorporated primordial germ cells (*blue*). **C**. Ovary at week 20. This diagram shows the degenerating mesonephric duct and tubules (*dark red*) and degenerating rete ovarii (*green*). Primordial follicles that contain primary oocytes (*blue*) and are surrounded by a single layer of squamous cells (*green*) are shown. **D**. This light micrograph of the definitive adult ovary shows several primordial follicles (PFs). Each PF consists of a primary oocyte surrounded by a single layer of squamous cells. The nucleus of a primary oocyte is typically large, but many times the nucleus is not in the plane of section, so that only the cytoplasm of the primary oocyte is observed. GE = germinal epithelium; TA = tunica albuginea.

2. The coelomic epithelium and underlying mesoderm of the urogenital ridge proliferate to form the **gonadal ridge**.
3. **Primary sex cords** develop from the gonadal ridge and incorporate primordial germ cells (XX genotype), which migrate into the gonad from the wall of the yolk sac. The primordial germ cells originate from the **epiblast** in week 2 of development and then migrate into the endoderm and mesoderm layers of the yolk sac.
4. Primary sex cords extend into the medulla and develop into the **rete ovarii**, which eventually degenerates. Later, **secondary sex cords** develop and incorporate primordial germ cells as a thin **tunica albuginea** forms.
5. The secondary sex cords break apart and form isolated cell clusters called **primordial follicles**, which contain **primary oocytes** surrounded by a layer of **simple squamous cells**.
6. The primary oocytes are derived from primordial germ cells. Whereas, the simple squamous cells of the primordial follicle and the ovarian connective tissue stroma are derived from **mesoderm.**

B. Relative descent of the ovaries

1. The ovaries originally develop within the abdomen but later undergo a relative descent into the pelvis as a result of disproportionate growth of the upper abdominal region away from the pelvic region.
2. Other factors in this movement are uncertain but probably include the **gubernaculum**.
3. The gubernaculum is a band of fibrous tissue along the posterior wall that extends from the medial pole of the ovary to the uterus at the junction of the uterine tubes, forming the **ovarian ligament**.
4. The gubernaculum then continues into the labia majora, forming the **round ligament of the uterus**.
5. The peritoneum evaginates alongside the gubernaculum to form the **processus vaginalis**, which is obliterated in the female later in development.

III. DEVELOPMENT OF THE GENITAL DUCTS (FIGURE 14.2)

A. Paramesonephric (Müllerian) ducts

1. The paramesonephric ducts develop as **mesodermal** invaginations of the lateral surface of the urogenital ridge.
2. The cranial portions of the paramesonephric ducts develop into the **uterine tubes**.
3. The caudal portions of the paramesonephric ducts fuse in the midline to form the **uterovaginal primordium**, and thereby bring together two peritoneal folds called the **broad ligament**.
4. The uterovaginal primordium develops into the **uterus, cervix**, and **superior one third of the vagina**.
5. The paramesonephric ducts project into the dorsal wall of the cloaca and induce the formation of the **sinovaginal bulbs**.
6. The sinovaginal bulbs fuse to form the solid **vaginal plate**, which canalizes and develops into the **inferior two thirds of the vagina**.
7. Although the vagina has a dual origin, most authorities agree that the epithelial lining of the entire vagina is of **endodermal** origin.

B. Mesonephric (Wolffian) ducts and tubules

1. The mesonephric ducts and tubules develop in the female as part of the urinary system because these ducts are critical in the formation of the definitive metanephric kidney. However, they degenerate in the female after formation of the metanephric kidney.

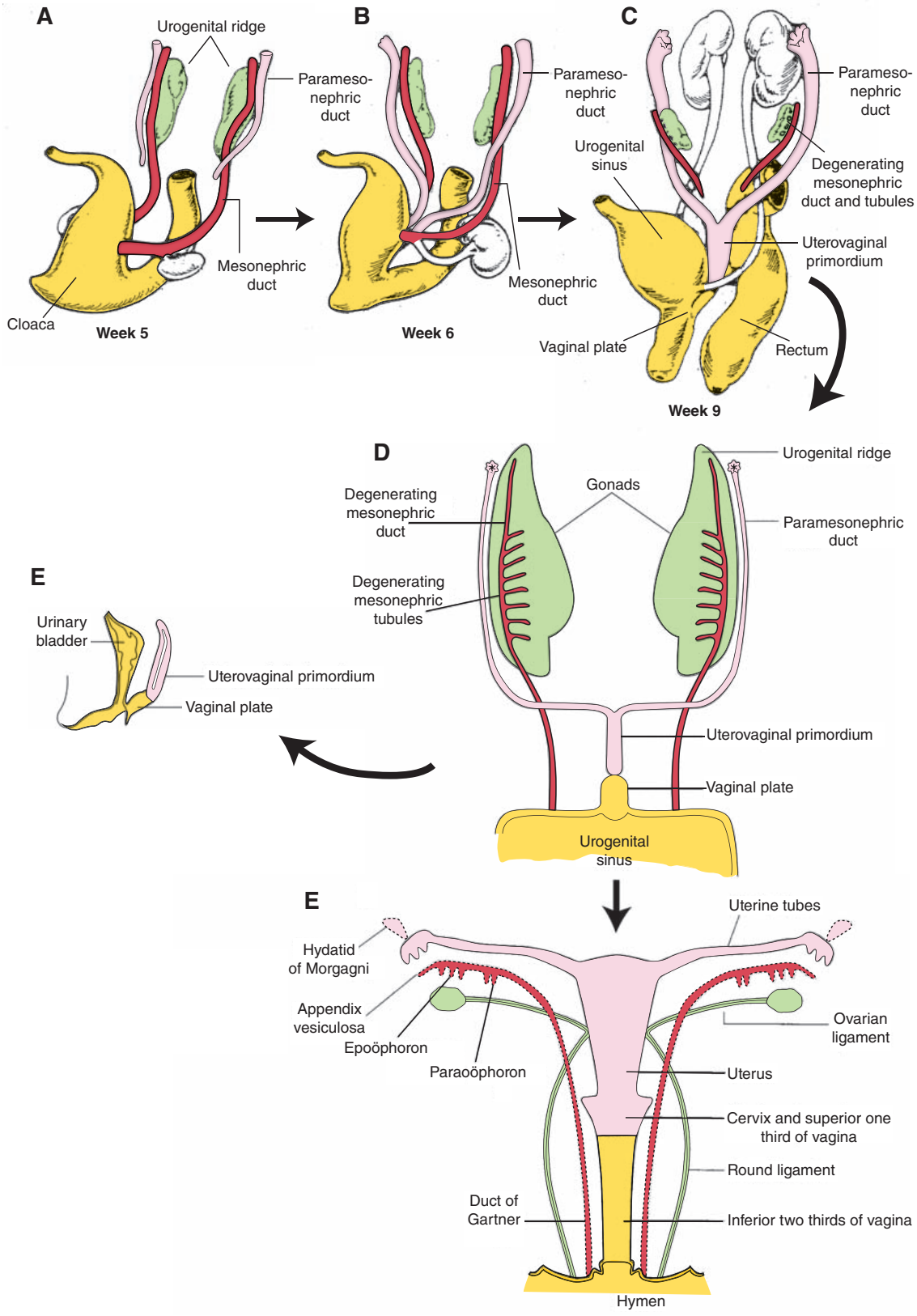

FIGURE 14.2. Development of the genital ducts. **A–C**. Lateral views of the embryo. **A**. At week 5. The paired paramesonephric ducts (*light red*) begin to form along the lateral surface of the urogenital ridge (*green*) and grow in close association to the mesonephric duct (*dark red*). **B**. At week 6. The paramesonephric ducts (*light red*) grow caudally and project into the dorsal wall of the cloaca (*yellow*) and induce the formation of the sinovaginal bulbs (not shown). The mesonephric ducts (*dark red*) continue to prosper. **C**. At week 9. The caudal portions of the paramesonephric ducts (*light red*) fuse in the midline to form the uterovaginal primordium (*light red*), and the sinovaginal bulbs fuse to form the vaginal plate (*yellow*) at the urogenital sinus (*yellow*). During this time period, the mesonephric duct (*dark red*) and mesonephric tubules (*dark red*) both degenerate in the female. **D**. Genital ducts in the indifferent embryo. **E**. Lateral view showing the dual origin of the vagina. **F**. Female components and vestigial remnants (*dotted lines*) at birth.

C. Vestigial remnants (Figure 14.3). The formation of cysts is related to vestigial remnants of the genital ducts. The diagram (Figure 14.3) shows the location of various cysts in the female reproductive tract:

1. A hydatid cyst of Morgagni (1) arises from hydatid of Morgagni, which is a remnant of the paramesonephric duct.
2. A Kobelt cyst (2) arises from the appendix vesiculosa, which is a remnant of the mesonephric duct.
3. A cyst of the epoophoron (3) arises from the epoophoron, which is a remnant of the mesonephric tubules.
4. A cyst of the paroophoron (4) arises from the paroophoron, which is a remnant of the mesonephric tubules.
5. A Gartner duct cyst (5) arises from the duct of Gartner, which is a remnant of the mesonephric duct.

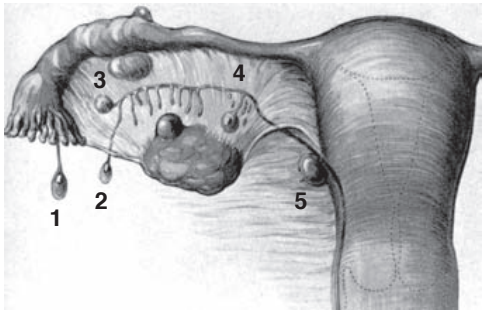

FIGURE 14.3. Location of various cysts in the female reproductive tract. See text for key.

IV. DEVELOPMENT OF THE PRIMORDIA OF EXTERNAL GENITALIA (FIGURE 14.4)

A. A proliferation of **mesoderm** around the cloacal membrane causes the overlying **ectoderm** to rise up so that three structures are visible externally: the **phallus, urogenital folds,** and **labioscrotal swellings.**

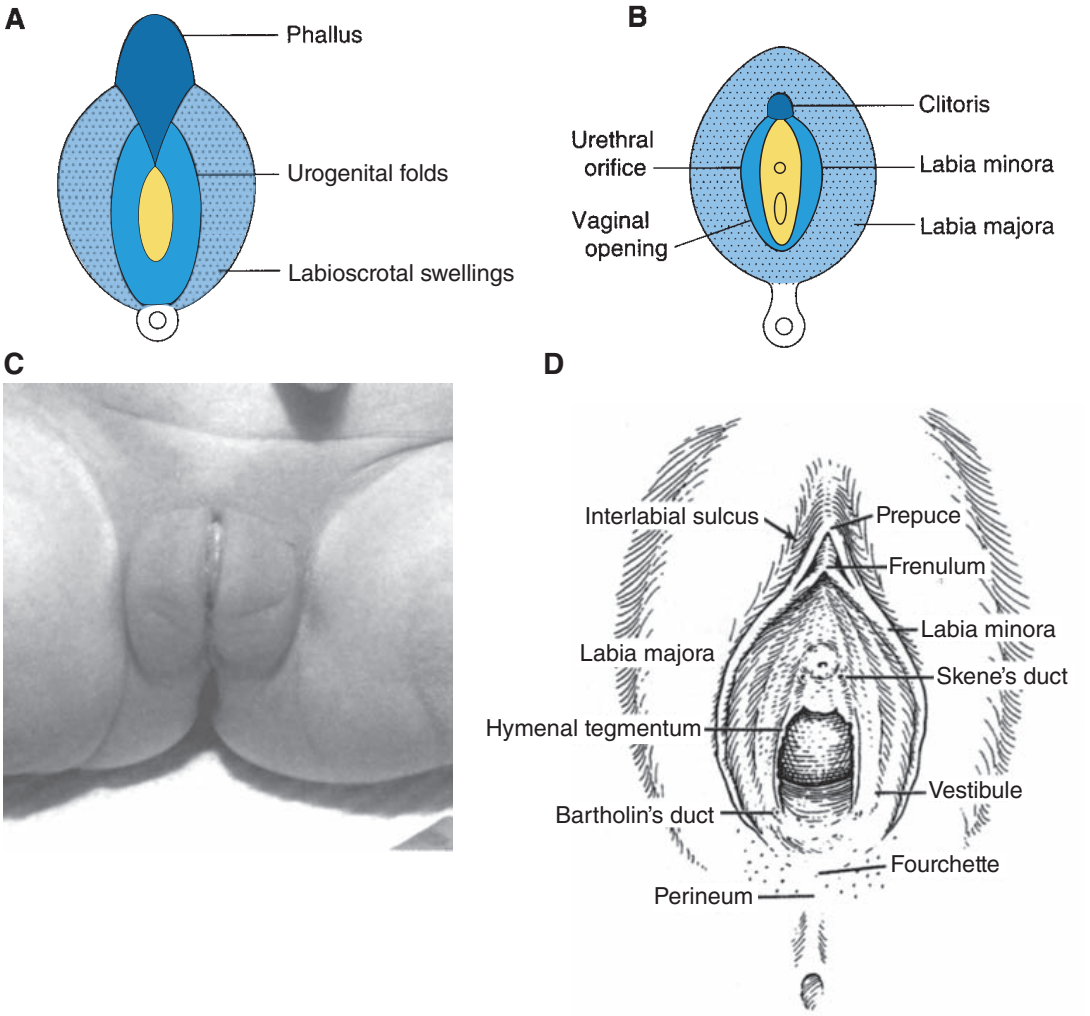

FIGURE 14.4. Development of the external genitalia. **A** and **B** indicate the differentiation of the phallus (*dark blue*), urogenital folds (*light blue*), and labioscrotal swellings (*blue shading*) in the female. **A**. At week 5. **B**. At birth. **C**. Appearance of normal female genitalia at birth. **D**. Diagram of the gross anatomy of the vulvar region in the adult female.

B. The phallus forms the **clitoris (glans clitoris, corpora cavernosa clitoris**, and **vestibular bulbs)**.

C. The urogenital folds form the **labia minora**.

D. The labioscrotal swellings form the **labia majora** and **mons pubis**.

V. TANNER STAGES OF FEMALE SEXUAL DEVELOPMENT (TABLE 14.1)

The Tanner scale includes stages of physical development in children, adolescents, and adults. The stages define physical measurements of development based on external primary and secondary sex characteristics. Due to natural variation, individuals may pass through the Tanner stages at different rates, depending on the timing of puberty.

table 14.1 Tanner Stages for the Female

Tanner Stage	Age (years)	Characteristics
I	<10	Height increases at 5–6 cm/yr Breasts have papillae elevations only Pubic hair is villus hair only (no coarse, pigmented hair)
II	9–13	Height increases at 7–8 cm/yr Breasts have palpable buds, and areolae enlarge Pubic hair is minimally coarse, pigmented hair mainly on the labia
III	12–14	Height increases at 8 cm/yr (peak rate) Breasts show elevation of contours, and areolae enlarge Pubic hair is coarse, pigmented hair and spreads over the mons pubis Axillary hair develops Acne vulgaris develops
IV	12–15	Height increases at 7 cm/yr Breasts form secondary areolar mounds Pubic hair is adult quality and does not spread to the junction of the medial thigh and perineum
V	14–18	Height increases stop after 16 years of age Breasts show adult breast contour, areolae recess to general contour of the breast, and the nipples project Pubic hair has adult distribution (upside-down triangle), spreads to the medial thigh, and does not extend up the linea alba

VI. CLINICAL CONSIDERATIONS

A. **Atresia of the vagina** is a condition in which the vaginal lumen is blocked due to a failure of the vaginal plate to canalize and form a lumen.

B. **Uterine anomalies**

1. **Müllerian hypoplasia or agenesis anomalies (class I; Figure 14.5)** involving the paramesonephric ducts can result in vaginal, cervical, uterine, uterine tube, or combined anomalies. The diagram (Figure 14.5) depicts class I Müllerian hypoplasia and agenesis anomalies, including lower vagina agenesis, cervix agenesis, uterus and cervix hypoplasia, and uterine tube agenesis.

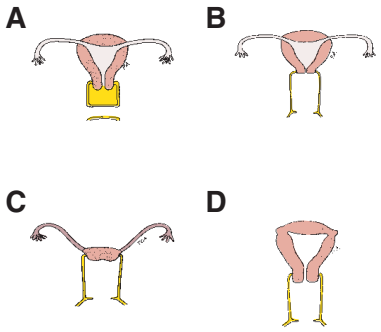

FIGURE 14.5. Class I Müllerian hypoplasia and agenesis anomalies. **A**. Lower vagina agenesis. **B**. Cervix agenesis. **C**. Uterus and cervix hypoplasia. **D**. Uterine tube agenesis.

2. **Unicornuate uterus anomalies (class II; Figure 14.6)** occur when one paramesonephric duct fails to develop or incompletely develops. The diagram (Figure 14.6) depicts class II unicornuate anomalies, including unicornuate uterus with a communicating rudimentary horn; unicornuate uterus with a noncommunicating rudimentary horn; unicornuate uterus with a rudimentary horn containing no uterine cavity; and unicornuate uterus. The hysterosalpingography (HSG) shows a single, lenticular-shaped uterine canal with no evidence of a rudimentary right horn. There is filling of the left uterine tube.

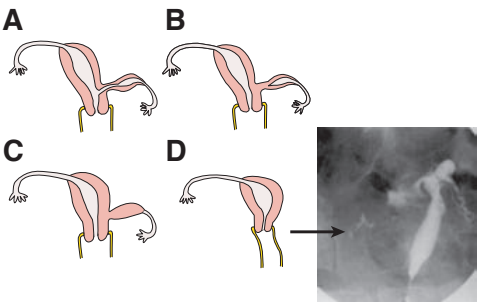

FIGURE 14.6. Class II unicornuate anomalies. **A**. Unicornuate uterus with a communicating rudimentary horn. **B**. Unicornuate uterus with a noncommunicating rudimentary horn. **C**. Unicornuate uterus with a rudimentary horn containing no uterine cavity. **D**. Unicornuate uterus.

3. **Didelphys (double uterus) anomalies (class III; Figure 14.7)** occur when there is a complete lack of fusion of the paramesonephric ducts. The diagram (Figure 14.7) depicts class III didelphys (double uterus) anomalies, including didelphys with normal vagina and didelphys with complete vaginal septum. The HSG shows a double uterus with a double vagina due to vaginal septum.

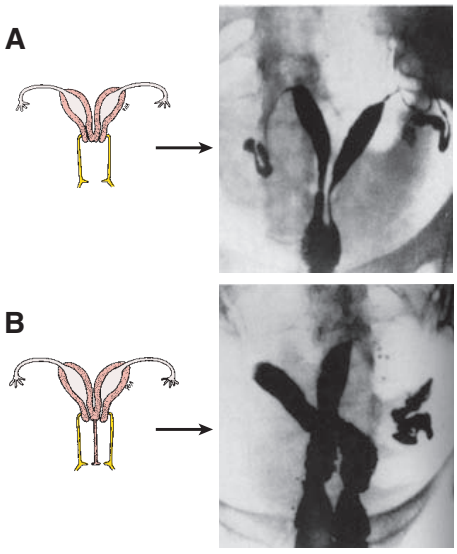

FIGURE 14.7. Class III didelphys (double uterus) anomalies. **A**. Didelphys with normal vagina. A hysterosalpingography shows a double uterus with a single normal vagina. **B**. Didelphys with complete vaginal septum. A hysterosalpingography shows a double uterus with a double vagina due to vaginal septum. This 17-year-old girl uses two tampons during menses.

4. **Bicornuate uterus anomalies (class IV; Figure 14.8)** occur when there is partial fusion of the paramesonephric ducts. The Figure 14.8 depicts class IV bicornuate anomalies, including bicornuate uterus with complete division down to the internal os and bicornuate uterus with partial division. The HSG shows the uterine cavity partitioned into two channels.

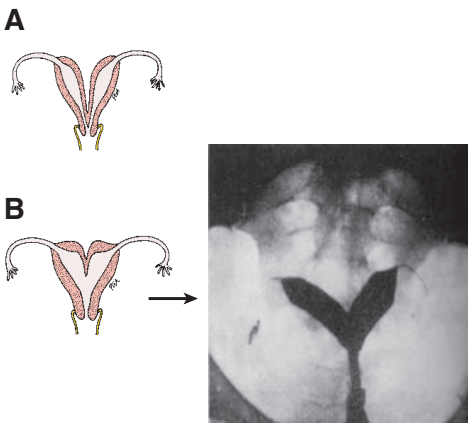

FIGURE 14.8. Class IV bicornuate anomalies. **A**. Bicornuate uterus with complete division down to the internal os. **B**. Bicornuate uterus with partial division.

5. **Septate uterus anomalies (class V; Figure 14.9)** occur when the medial walls of the caudal portion of the paramesonephric ducts partially or completely fail to resorb. The diagram (Figure 14.9) depicts class V septate uterus anomalies, including septate uterus with complete septum down to the external os and septate uterus with partial septum.

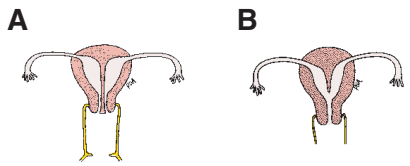

FIGURE 14.9. Class V septate uterus anomalies. **A**. Septate uterus with complete septum down to the external os. **B**. Septate uterus with partial septum.

6. **Diethylstilbestrol (DES)-related anomalies (Figure 14.10)**. DES was used until 1970 in the treatment of abortions, preeclampsia, diabetes, and preterm labor. For female offspring exposed to DES in utero, an increased incidence of **clear cell adenocarcinoma of the vagina** has been documented. In addition, many uterine anomalies that include T-shaped uterus have been observed. The diagram (Figure 14.10) depicts DES-related uterus anomalies. These anomalies typically result in a T-shaped uterus. The HSG shows a T-shaped uterus. The HSG of a normal female reproductive tract is shown for comparison.

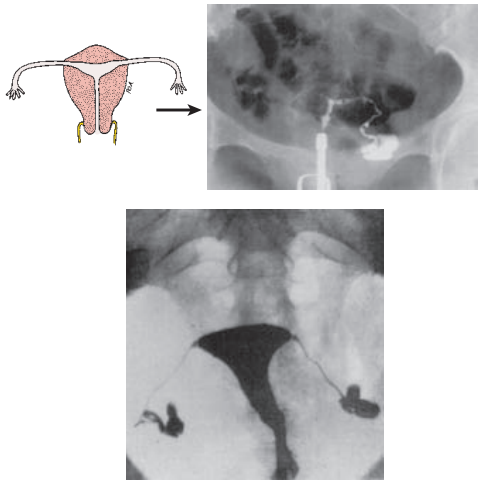

FIGURE 14.10. T-shaped uterus. HSG = hysterosalpingography.

C. **Hymen variations (Figure 14.11)** include the following:

1. **Crescentic hymen**
2. **Annular hymen**
3. **Redundant hymen**
4. **Imperforate hymen**
5. **Cribriform hymen**
6. **Microperforate hymen**
7. **Septate hymen**

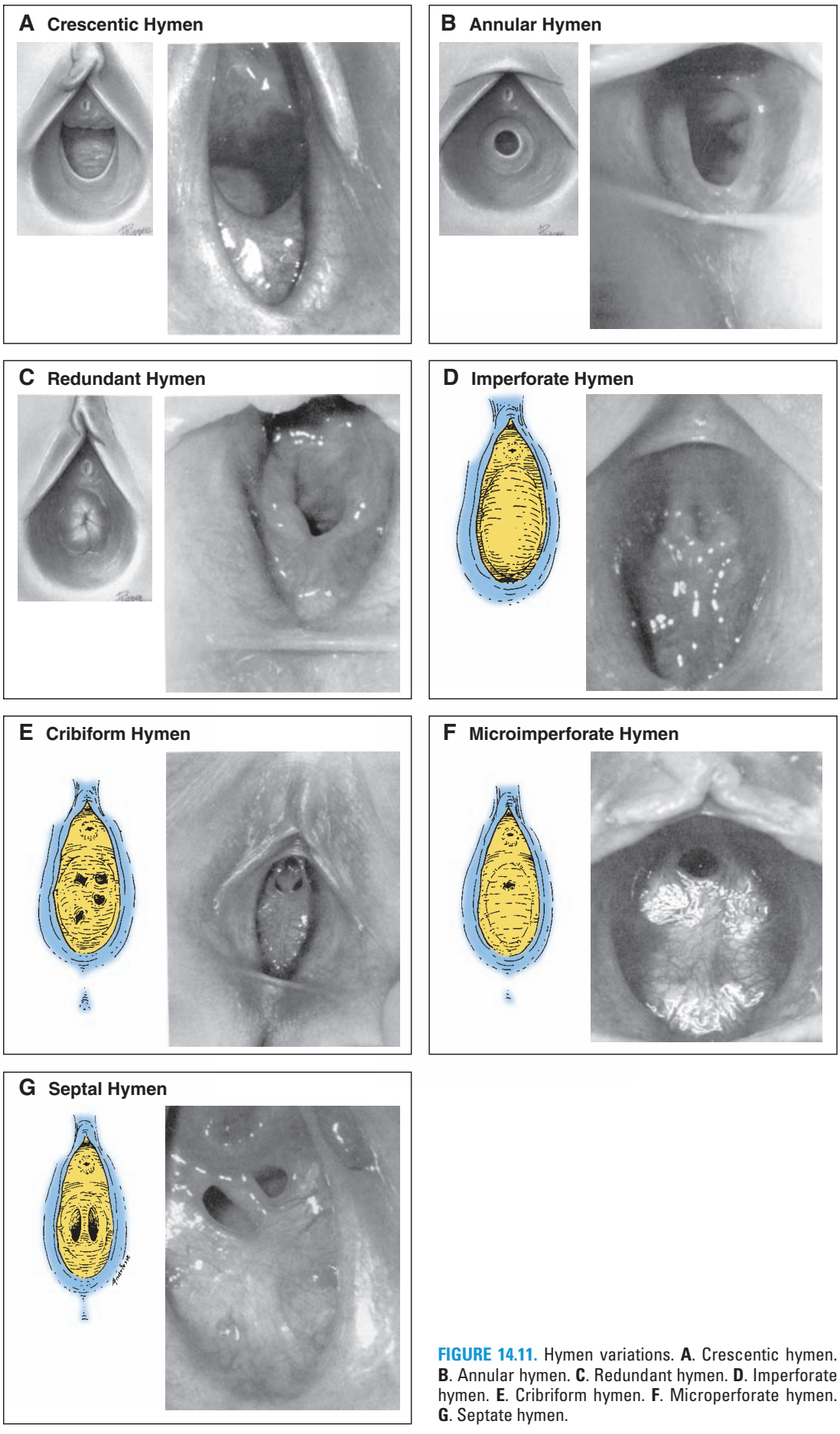

FIGURE 14.11. Hymen variations. **A**. Crescentic hymen. **B**. Annular hymen. **C**. Redundant hymen. **D**. Imperforate hymen. **E**. Cribriform hymen. **F**. Microperforate hymen. **G**. Septate hymen.

Study Questions for Chapter 14

1. The indifferent embryo begins phenotypic sexual differentiation during

(A) week 3 of development
(B) week 5 of development
(C) week 7 of development
(D) week 12 of development
(E) week 20 of development

2. The indifferent embryo completes phenotypic sexual differentiation during

(A) week 3 of development
(B) week 5 of development
(C) week 7 of development
(D) week 12 of development
(E) week 20 of development

3. After the sinovaginal bulbs have proliferated and fused, they form a solid core of endodermal cells called the

(A) vestibule of the vagina
(B) uterovaginal primordium
(C) urogenital sinus
(D) vaginal plate
(E) clitoris

4. A structure found within the adult female pelvis formed from the gubernaculum is the

(A) broad ligament
(B) suspensory ligament of the ovary
(C) round ligament of the uterus
(D) medial umbilical ligament
(E) median umbilical ligament

5. The labia minora arise embryologically from which of the following structures?

(A) Phallus
(B) Labioscrotal swellings
(C) Sinovaginal bulbs
(D) Urogenital folds
(E) Paramesonephric duct

1. The uterine tubes of the adult female are derived embryologically from which of the following?

(A) Mesonephric duct
(B) Mesonephric tubules
(C) Paramesonephric duct
(D) Paramesonephric tubules
(E) Uterovaginal primordium

Answers and Explanations

1. **C.** The embryo during weeks 1–6 remains in an indifferent or undifferentiated stage. The embryo begins phenotypic sexual differentiation during week 7.
2. **E.** By week 12, female and male characteristics can be recognized. By week 20, phenotypic sexual differentiation is complete.
3. **D.** The sinovaginal bulbs proliferate, fuse, and form the vaginal plate under the inductive influence of the paramesonephric ducts. The vaginal plate then canalizes to form the inferior two thirds of the vagina.
4. **C.** The round ligament of the uterus and the ovarian ligament both form from the gubernaculum.
5. **D.** In the female, the urogenital folds remain unfused and form the labia minora.
6. **C.** The cranial portion of the paramesonephric ducts forms the uterine tubes.

chapter 15

Male Reproductive System

I. THE INDIFFERENT EMBRYO

A. The genotype of the embryo (46, XX or 46, XY) is established at fertilization.

B. **During weeks 1–6,** the embryo remains in a sexually indifferent or undifferentiated stage. This means that genetically female embryos and genetically male embryos are phenotypically indistinguishable.

C. **During week 7,** the indifferent embryo begins phenotypic sexual differentiation.

D. **By week 12,** female or male characteristics of the external genitalia can be recognized.

E. **By week 20,** phenotypic differentiation is complete.

1. **Phenotypic sexual differentiation**
   - **a.** Phenotypic sexual differentiation is determined by the *SRY* **gene** and may result in individuals with a **female phenotype**, an **intersex phenotype**, or a **male phenotype**.
   - **b.** The *SRY* gene on chromosome Yp11.3 encodes for a **sex-determining region Y protein** (also called **testes-determining factor [TDF]**).
   - **c.** TDF is a 220–amino acid nonhistone protein that contains a highly conserved DNA-binding region called a **high mobility group box**.
   - **d.** As the indifferent gonad develops into the testes, **Leydig cells** differentiate to produce **testosterone** and **Sertoli cells** differentiate to produce **Müllerian-inhibiting factor (MIF)**.
   - **e.** **In the presence of TDF, testosterone, and MIF**, the indifferent embryo will be directed to the male phenotype.
   - **f.** **In the absence of TDF, testosterone, and MIF**, the indifferent embryo will be directed to the female phenotype.
2. **Components of the indifferent embryo**
   - **a.** The components of the indifferent embryo that are remodeled to form the adult female reproductive system include the **gonads, genital ducts**, and **primordia of external genitalia**.
   - **b.** Phenotypic sexual differentiation occurs in a sequence beginning with the gonads, then the genital ducts, and finally the primordia of external genitalia.

II. DEVELOPMENT OF THE GONADS (FIGURE 15.1)

A. **The testes**

1. The **intermediate mesoderm** forms a longitudinal elevation along the dorsal body wall, the **urogenital ridge**.

2. The coelomic epithelium and underlying mesoderm of the urogenital ridge proliferate to form the **gonadal ridge**.
3. **Primary sex cords** develop from the gonadal ridge and incorporate primordial germ cells (XY genotype), which migrate into the gonad from the wall of the yolk sac. The primordial germ cells originate from the **epiblast** in week 2 of development and then migrate into the endoderm and mesoderm layers of the yolk sac.
4. The Y chromosome carries a gene on its short arm that codes for **TDF**, which is crucial to testes differentiation.

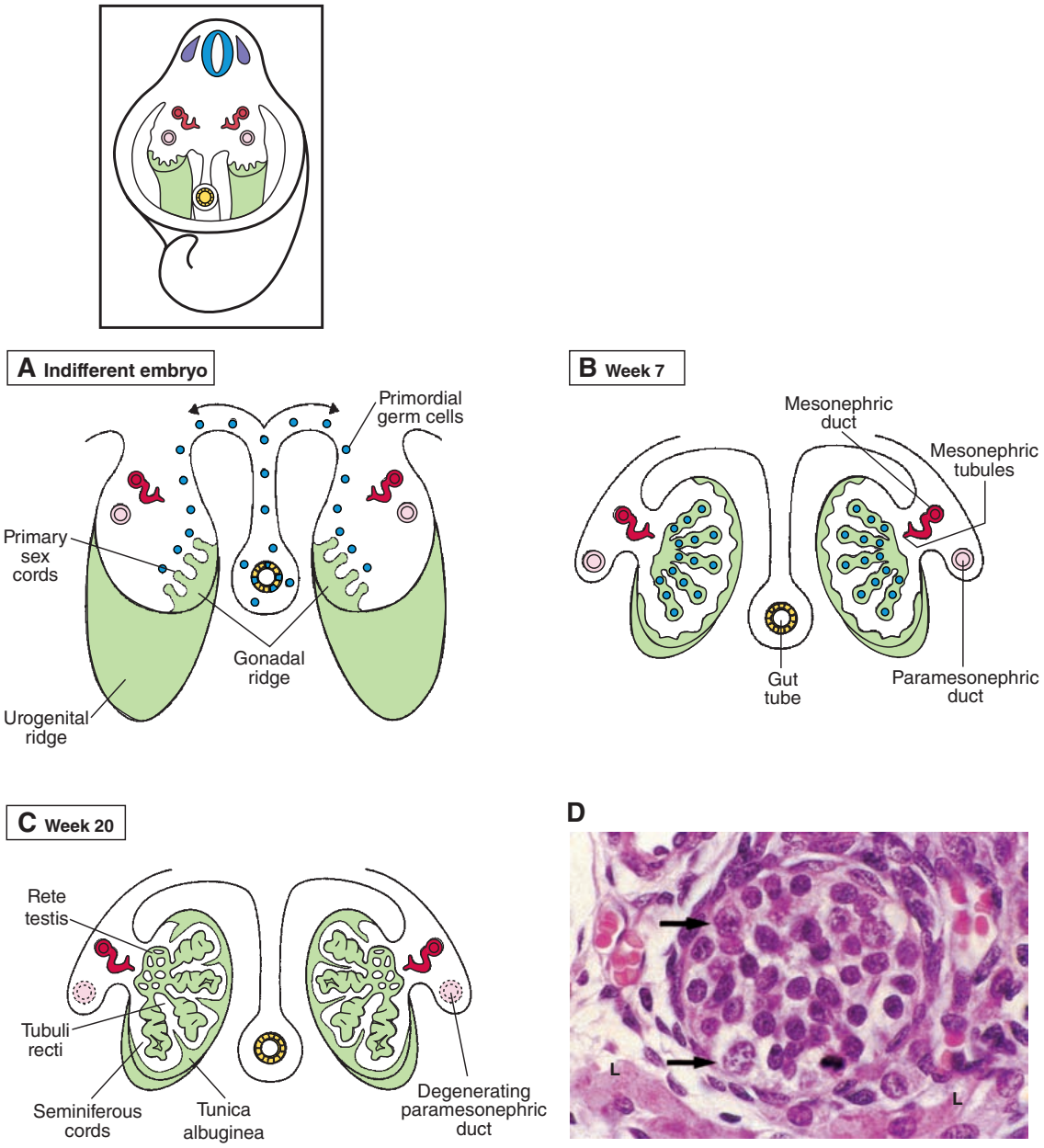

FIGURE 15.1. Development of the gonads. This diagram demonstrates the differentiation of the gonad in the male. **A**. Gonad in the indifferent embryo. This diagram shows primordial germ cells (*blue*) migrating from the yolk sac into the gonad. Urogenital ridge = green, primary sex cords = green, paramesonephric duct = light red, mesonephric duct = dark red, endodermal lining of yolk sac = yellow. **B**. Testes at week 7. This diagram shows the secondary sex cords (*green*) that have incorporated primordial germ cells (*blue*). **C**. Testes at week 20. This diagram shows the degenerating paramesonephric duct (*light red*). The mesonephric duct and tubules (*dark red*) continue to prosper. The seminiferous cords (*green*), tubuli recti (*green*), and rete testes (*green*) are shown. **D**. Light micrograph of a fetal testis, showing a seminiferous cord composed of primordial germ cells and Sertoli cells. The primordial germ cells are indicated by arrows. All the other nuclei belong to immature Sertoli cells. Leydig cells (L) are found surrounding the seminiferous cords in the interstitial space.

5. The primary sex cords extend into the medulla of the gonad and lose their connection with the surface epithelium as the thick **tunica albuginea** forms.
6. The primary sex cords form the **seminiferous cords, tubuli recti**, and **rete testes**.
7. Seminiferous cords consist of **primordial germ cells** and **sustentacular (Sertoli) cells**, which secrete **Müllerian-inhibiting factor (MIF)**.
8. The mesoderm between the seminiferous cords gives rise to the **interstitial (Leydig) cells**, which secrete **testosterone**.
9. The primordial germ cells, sustentacular (Sertoli) cells, interstitial (Leydig) cells, and connective tissue stroma of the testes are derived from **mesoderm**.
10. The seminiferous cords remain as solid cords until puberty, when they acquire a lumen and are then called **seminiferous tubules**.

B. Relative descent of the testes

1. The testes originally develop within the abdomen but later undergo a relative descent into the scrotum as a result of disproportionate growth of the upper abdominal region away from the pelvic region.
2. Other factors involved in this movement are uncertain but probably include the **gubernaculum**.
3. The gubernaculum is a band of fibrous tissue along the posterior wall that extends from the caudal pole of the testes to the scrotum.
4. Remnants of the gubernaculum in the adult male serve to anchor the testes within the scrotum.
5. The peritoneum evaginates alongside the gubernaculum to form the **processus vaginalis**.
6. Later in development, most of the processus vaginalis is obliterated except at its distal end, which remains as a peritoneal sac called the **tunica vaginalis of the testes**.

III. DEVELOPMENT OF THE GENITAL DUCTS (FIGURE 15.2)

A. Paramesonephric (Müllerian) ducts

1. The paramesonephric ducts develop as **mesodermal** invaginations of the lateral surface of the urogenital ridge.
2. The cranial portions run parallel to the mesonephric ducts.
3. The caudal portions fuse in the midline to form the **uterovaginal primordium**.
4. Under the influence of MIF, the cranial portions of the paramesonephric ducts and the uterovaginal primordium regress.

B. Mesonephric (Wolffian) ducts and tubules

1. The mesonephric ducts and tubules develop in the male as part of the urinary system because these ducts are critical in the formation of the definitive metanephric kidney.
2. The mesonephric ducts then proceed to additionally form the **epididymis, ductus deferens, seminal vesicle**, and **ejaculatory duct**.
3. A few mesonephric tubules in the region of the testes form the **efferent ductules** of the testes.

C. Vestigial remnants

1. Vestigial remnants of the paramesonephric duct (called the **appendix testis**) may be found in the adult male.
2. Vestigial remnants of the mesonephric duct (called the **appendix epididymis**) may be found in the adult male.
3. Vestigial remnants of mesonephric tubules (called the **paradidymis**) may be found in the adult male.

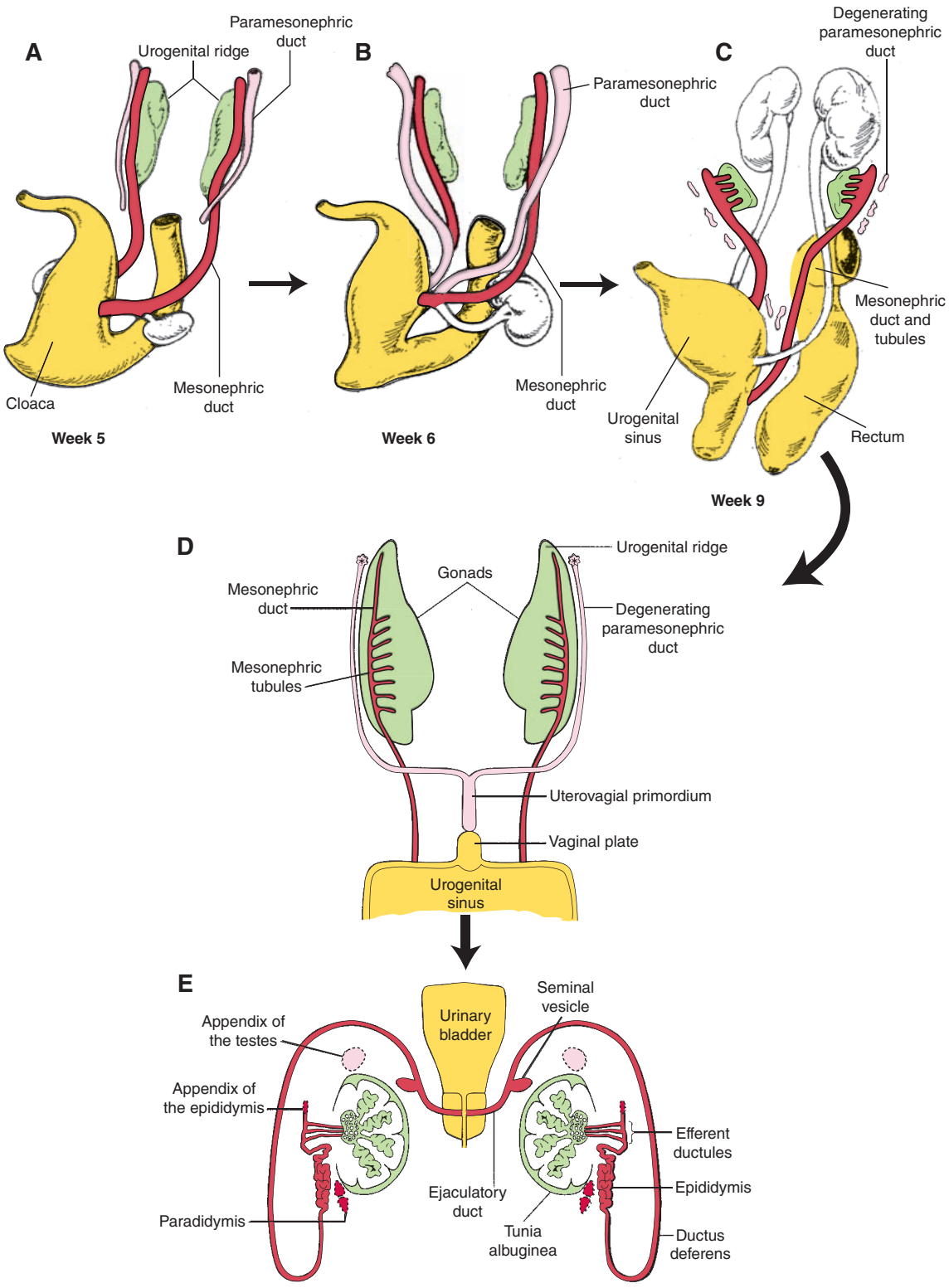

FIGURE 15.2. Development of the genital ducts. **A**–**C**. Lateral views of the embryo. **A**. At week 5. The paired paramesonephric ducts (*light red*) begin to form along the lateral surface of the urogenital ridge (*green*) and grow in close association to the mesonephric duct (*dark red*). **B**. At week 6. The paramesonephric ducts (*light red*) grow caudally and project into the dorsal wall of the cloaca (*yellow*) and induce the formation of the sinovaginal bulbs (*not shown*). The mesonephric ducts (*dark red*) continue to prosper. **C**. At week 9. The mesonephric ducts (*dark red*) and mesonephric tubules (*dark red*) establish contact with the testes and develop into definitive adult structures. During this time period, the paramesonephric ducts (*light red*) degenerate in the male. Urogenital sinus = yellow, rectum =yellow. **D**. Genital ducts in the indifferent embryo. **E**. Male components and vestigial remnants (*dotted lines*) at birth.

IV. DEVELOPMENT OF THE PRIMORDIA OF EXTERNAL GENITALIA (FIGURE 15.3)

A. A proliferation of **mesoderm** around the cloacal membrane causes the overlying **ectoderm** to rise up so that three structures are visible externally: the **phallus, urogenital folds**, and **labioscrotal swellings**.

B. The phallus forms the **penis (glans penis, corpora cavernosa penis**, and **corpus spongiosum penis)**.

C. The urogenital folds form the **ventral aspect of the penis (i.e., penile raphe)**.

D. The labioscrotal swellings form the **scrotum**.

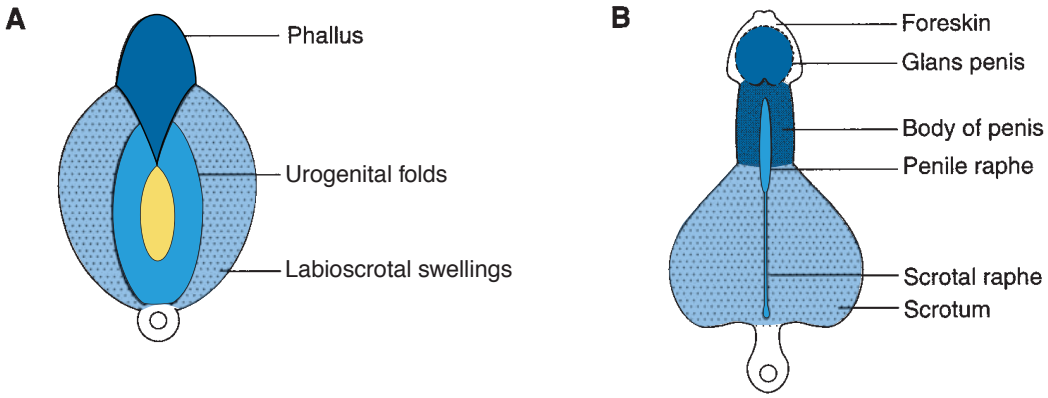

FIGURE 15.3. Development of the external genitalia. **A, B.** These diagrams indicate the differentiation of the phallus (*dark blue*), urogenital folds (*light blue*), and labioscrotal swellings (*blue shading*) in the male. **A**. At week 5. **B**. At birth.

V. TANNER STAGES OF MALE SEXUAL DEVELOPMENT (TABLE 15.1)

The Tanner scale includes stages of physical development in children, adolescents, and adults. They define physical measurements of development based on external primary and secondary sex characteristics. Due to natural variation, individuals may pass through the Tanner stages at different rates, depending on the timing of puberty.

VI. CLINICAL CONSIDERATIONS

A. Male anomalies

1. **Hypospadias (Figure 15.4)** occurs when the urethral folds fail to fuse completely, resulting in the external urethral orifice opening onto the ventral surface of the penis. It is generally associated with a poorly developed penis that curves ventrally, known as **chordee**. The upper photograph (Figure 15.4) shows hypospadias with a urethral opening on ventral surface (*arrow*). The lower photograph shows chordee. Note that the penis is poorly developed and bowed ventrally.
2. **Epispadias (Figure 15.5)** occurs when the external urethral orifice opens onto the dorsal surface of the penis. It is generally associated with **exstrophy of the bladder**. The photograph (Figure 15.5) shows epispadias with two urethral openings on the dorsal surface of the penis (*arrows*).

table 15.1 Tanner Stages for the Male

Tanner Stage	Age (years)	Characteristics
I	<10	Height increases at 5–6 cm/yr Testes are 2.5 cm in size (long axis) Penis is ~3 cm in length and shows no growth Pubic hair is villus hair only (no coarse, pigmented hair)
II	9–13	Height increases at 5–6 cm/yr Testes are 2.5–3.2 cm in size (long axis) Penis shows earliest signs of growth in length and width Pubic hair is minimally coarse, pigmented hair mainly at the base of the penis
III	12–14	Height increases at 7–8 cm/yr Testes are 3.6 cm is size (long axis) Penis shows growth in length (to ~6 cm) and width Pubic hair is coarse, pigmented hair and spreads over the pubis
IV	12–15	Height increases at 10 cm/yr (peak rate) Testes are 4–4.5 cm in size (long axis) Penis shows growth in length (to ~10 cm) and width Pubic hair is adult quality and does not spread to the junction of the medial thigh and perineum Axillary hair develops Acne vulgaris develops
V	14–18	Height increases stop after 17 years of age Testes are >4.5 cm in size (long axis) Penis shows growth in length (to ~15 cm) and width; mature penis size is reached by 16.5 years Pubic hair has adult distribution (upside-down triangle), spreads to the medial thigh, and does not extend up the linea alba

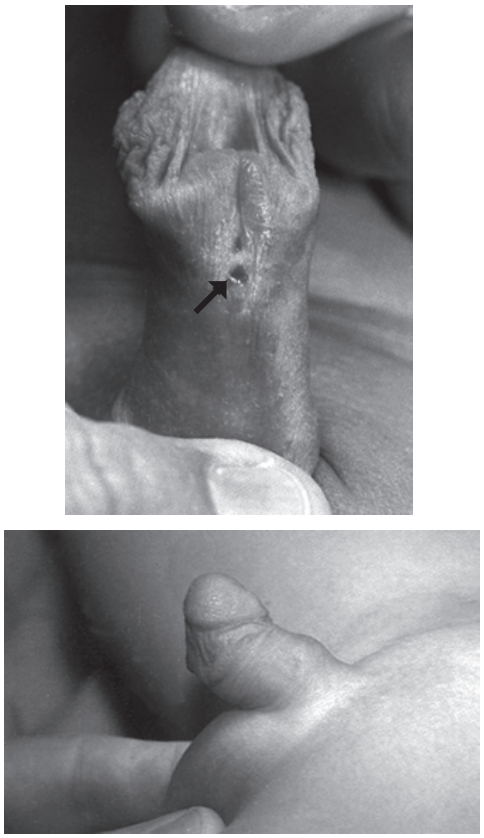

FIGURE 15.4. Hypospadias.

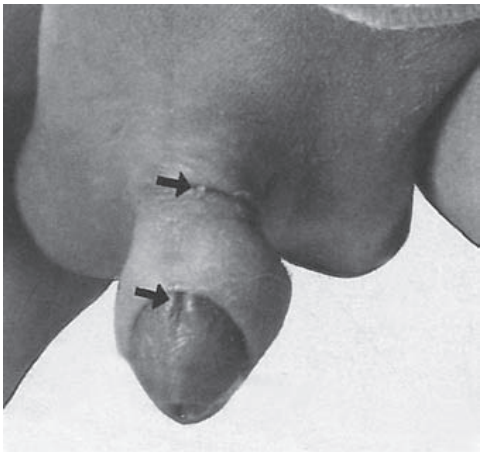

FIGURE 15.5. Epispadias.

3. **Bilateral undescended testes (cryptorchidism; Figure 15.6)** occurs when both testes fail to descend into the scrotum. Descent of the testes is evident within 3 months after birth. Cryptorchidism results in **sterility**. The undescended testes may be found in the abdominal cavity or in the inguinal canal. **Unilateral undescended testis** may also occur. The photograph (Figure 15.6) shows cryptorchidism. Note that the both testes have not descended into the scrotal sac.

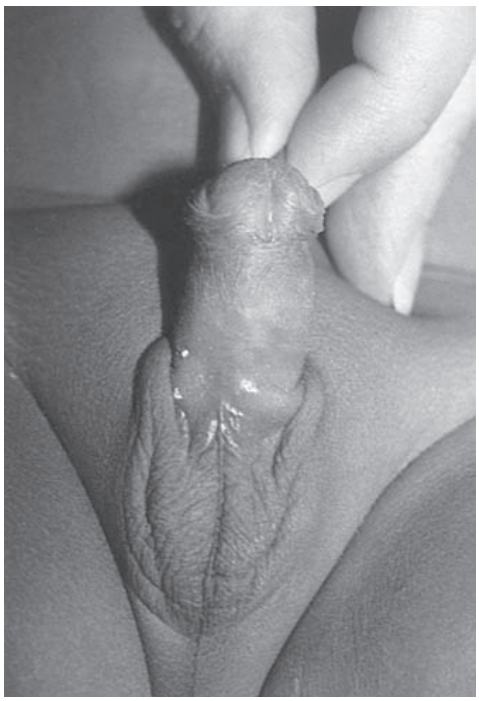

FIGURE 15.6. Cryptorchidism.

4. **Hydrocele of the testes (Figure 15.7)** occurs when a small patency of the processus vaginalis remains so that peritoneal fluid can flow into the processus vaginalis, which results in a fluid-filled cyst near the testes. The photograph (Figure 15.7) shows bilateral hydrocele.
5. **Congenital inguinal hernia** occurs when a large patency of the processus vaginalis remains so that a loop of intestine may herniate into the scrotum or labia majora.
6. It is most common in males and is generally associated with cryptorchidism.

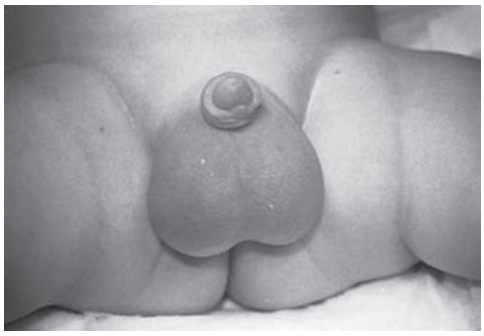

FIGURE 15.7. Bilateral hydrocele.

B. Other anomalies of the reproductive system

1. **Intersexuality**
   - **a.** Because the early embryo goes through an indifferent stage, events may occur by which a fetus does not progress toward either of the two usual phenotypes but gets caught in an intermediate stage known as intersexuality.
   - **b.** Intersexuality is classified according to the histological appearance of the **gonad** and **ambiguous genitalia**.
   - **c.** **True intersexuality** occurs when an individual has both ovarian and testicular tissue (ovotestes) histologically, ambiguous genitalia, and a 46, XX genotype.
   - **d.** True intersexuality is a rare condition whose cause is poorly understood.

2. **Female pseudo-intersexuality (FP; Figure 15.8)**
   a. FP occurs when an individual has only ovarian tissue histologically and masculinization of the female external genitalia. These individuals have a **46, XX genotype**.
   b. FP is most often observed clinically in association with a condition in which the fetus produces an **excess of androgens (e.g., congenital adrenal hyperplasia [CAH])**.
   c. CAH is caused most commonly by mutations in genes for enzymes involved in adrenocortical steroid biosynthesis (e.g., **21-hydroxylase deficiency, 11β-hydroxylase deficiency**).
   d. **21-hydroxylase deficiency** (current terminology is **CYP21A2 deficiency**) accounts for 90% of all cases of CAH.
   e. CYP21A2 deficiency is an autosomal recessive genetic disorder caused by a mutation in the ***CYP21A2* gene** located on **chromosome 6p21.3**, which encodes for the **21-hydroxylase enzyme**.

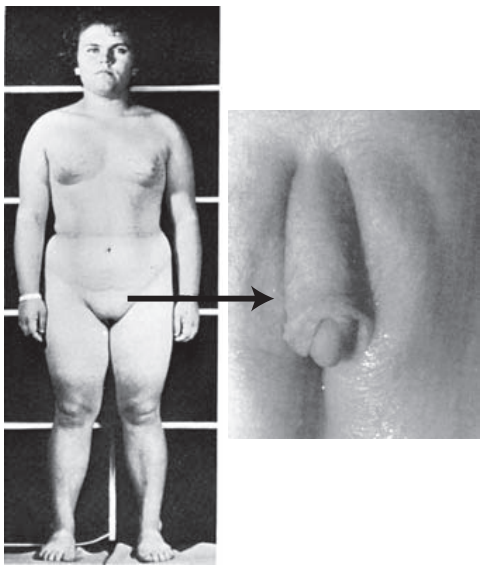

FIGURE 15.8. Female pseudo-intersexuality.

   f. In CYP21A2 deficiency, there is defective conversion of 17-hydroxyprogesterone to 11-deoxycortisol. There is virtually no synthesis of the cortisol or aldosterone, so that intermediates are funneled into androgen biosynthesis, thereby elevating androgen levels.
   g. In CYP21A2 deficiency, the characteristic biochemical finding is **elevated serum concentration of 17-hydroxyprogesterone** (i.e., >3500 ng/dL, or 105 nmol/L).
   h. The elevated levels of androgens lead to **masculinization of a female fetus** (i.e., **FP**).
   i. FP produces the following clinical findings: mild clitoral enlargement, complete labioscrotal fusion with a phalloid organ, or macrogenitosomia (in the male fetus). In clinical practice, most CYP21A2 deficiency cases are subcomplete, so that other symptoms may be the presenting condition, such as precocious puberty, virilization, and infertility.
   j. Because cortisol cannot be synthesized, negative feedback to the adenohypophysis does not occur, so adrenocorticotropic hormone (ACTH) continues to stimulate the adrenal cortex, resulting in adrenal hyperplasia.
   k. Because aldosterone cannot be synthesized, the patient presents with **hyponatremia ("salt-wasting")** with accompanying **dehydration** and **hyperkalemia**.
   l. **Treatment includes**: immediate infusion of intravenous saline and long-term steroid hormone replacement, both cortisol and mineralocorticoids (9α-fludrocortisone).
   m. The photograph (Figure 15.8) shows a patient (XX genotype) with FP due to CYP21A2 deficiency. Masculinization of female external genitalia is apparent, with fusion of the labia majora and enlarged clitoris (see *arrow* to inset).

3. **Male pseudo-intersexuality (MP; Figure 15.9)**
   a. MP occurs when an individual has only testicular tissue histologically and various stages of stunted development of the male external genitalia. These individuals have a **46, XY genotype**.
   b. MP is most often observed clinically in association with a condition in which the fetus produces a **lack of androgens (and MIF)**.
   c. This is caused most commonly by mutations in genes for androgen steroid biosynthesis (e.g., **5α-reductase 2 deficiency** or **17β-hydroxysteroid dehydrogenase**).
   d. Normally, 5α-reductase 2 catalyzes the conversion of testosterone (T) → dihydrotestosterone

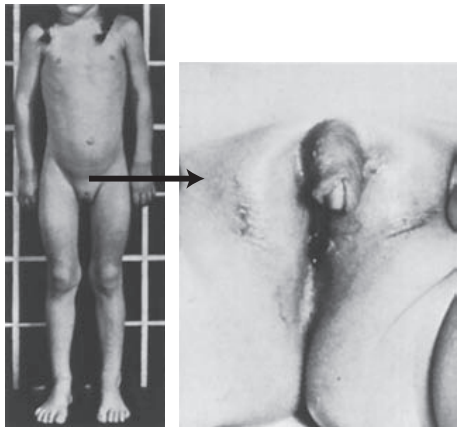

FIGURE 15.9. Male pseudo-intersexuality.

(DHT), and 17β-hydroxysteroid dehydrogenase 3 catalyzes the conversion of androstenedione → testosterone.

e. An increased **T:DHT ratio** is diagnostic (normal = 5; 5α-reductase 2 deficiency = 20–60).

f. The reduced levels of androgens lead to the **feminization of a male fetus**.

g. MP produces the following clinical findings: underdevelopment of the penis and scrotum (microphallus, hypospadias, and bifid scrotum) and prostate gland. The epididymis, ductus deferens, seminal vesicle, and ejaculatory duct are normal.

h. These clinical findings have led to inference that DHT is essential in the development of the penis and scrotum (external genitalia) and prostate gland in a genotypic XY fetus. At puberty, these individuals demonstrate a striking virilization.

i. The photograph (Figure 15.9) shows a patient (XY genotype) with MP. The stunted development of male external genitalia is apparent. The stunted external genitalia fooled the parents and physician into thinking that this XY infant was a girl. In fact, this child was raised as a girl (note pigtails). As this child neared puberty, testosterone levels increased, and clitoral enlargement ensued. This alarmed the parents, and the child was brought in for clinical evaluation.

4. Complete androgen insensitivity (CAIS; or testicular feminization syndrome; Figure 15.10)

a. CAIS is an X-linked recessive genetic disorder caused by a loss-of-function mutation in the *AR* gene on **chromosome Xq12**, which encodes for the **androgen receptor**. The androgen receptor is a member of the steroid–thyroid–retinoid superfamily of receptors.

b. The lack of androgen receptor function results in **defective virilization** in 46, XY males despite the presence of bilateral testes and normal testosterone production.

c. Even though the developing male fetus is exposed to normal levels of androgens, the lack of androgen receptors renders the phallus, urogenital folds, and labioscrotal swellings unresponsive to androgens.

d. The testes may be found in the abdomen, inguinal canals, or the labia majora. The testes are surgically removed to circumvent malignant tumor formation.

e. CAIS individuals have the following characteristics: the presenting cause is primary amenorrhea; there is little of no axillary or pubic hair; there are normal-appearing female external genitalia; the labia and clitoris are normal or slightly underdeveloped; the vagina is either absent or short and blind ending; there is absence or near absence of Müllerian structures in the urogenital tract (i.e., uterus, uterine tubes, cervix, superior third of the vagina); breast development is that of a normal female; patients are taller and heavier than normal females; psychosocial orientation is female; and maternal instincts are present.

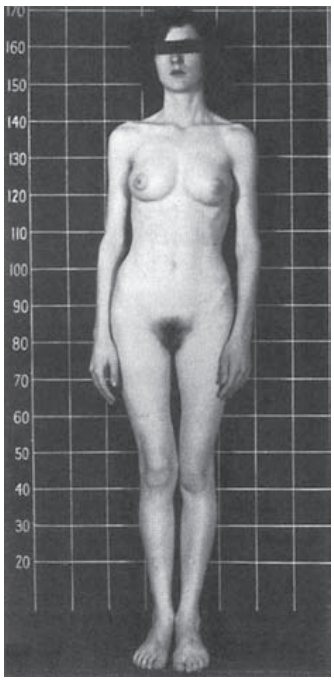

FIGURE 15.10. Complete androgen insensitivity.

f. The photograph (Figure 5-10) shows a patient (XY genotype) with CAIS. Complete feminization of male external genitalia is apparent.

5. Transsexualism. This is a condition in which a person with apparently normal bodily sexual differentiation of one gender is convinced that he or she is actually a member of the opposite gender. Although transsexualism has been traditionally considered only a psychological issue, the sexual differentiation of the brain depends on the presence or absence of androgens, and the **bed nucleus of the stria terminalis** in the brain has been implicated in sexual differentiation of the brain.

6. Transgenderism. This is a condition in which a person decides to have an in-between sex status. This type of person wants (1) to rid himself or herself of his or her natal sex without seeking reassignment to the opposite sex or (2) wants only partial adaptation to the opposite sex. There may be a part-time social transition to the opposite sex.

VII. SUMMARY (TABLE 15.2)

Table 15.2 summarizes the development of the female and male reproductive systems.

table 15.2 Summary Table of Female and Male Reproductive System Development

Adult Female	Indifferent Embryo	Adult Male
Ovary, ovarian follicles, rete ovarii	**Gonads**	Testes, seminiferous tubules, tubuli recti, rete testes, Leydig cells, Sertoli cells
Uterine tubes, uterus, cervix, superior one third of vagina *Hydatid of Morgagni*	**Paramesonephric duct**	_____ *Appendix testes*
_____ *Appendix vesiculosa, Gartner duct*	**Mesonephric duct**	Epididymis, ductus deferens, seminal vesicle, ejaculatory duct *Appendix epididymis*
_____ *Epoophoron, paroophoron*	**Mesonephric tubules**	Efferent ductules *Paradidymis*
Glans clitoris, corpora cavernosa clitoris, vestibular bulbs	**Phallus**	Glans penis, corpora cavernosa penis, corpus spongiosum
Labia minora	**Urogenital folds**	Ventral aspect of penis
Labia majora, mons pubis	**Labioscrotal swellings**	Scrotum
Ovarian ligament, round ligament of uterus	**Gubernaculum**	Gubernaculum testes
_____	**Processus vaginalis**	Tunica vaginalis

Italics indicate a vestigial structure.

Study Questions for Chapter 15

1. One day a 9-year-old girl surprisingly announces to her mother, "Guess what, mommy, I'm not a girl; I'm a boy." The mother is shocked but does act on the comment. During the next few years, the mother notices some tomboyish behavior and difficulty in social adjustment at school. When the girl is 12 years old, puberty starts with a striking virilization of the external genitalia. The mother is extremely concerned and seeks medical attention. What is the most likely cause?

(A) Male pseudo-intersexuality
(B) Female pseudo-intersexuality
(C) Congenital adrenal hyperplasia
(D) Testicular feminization
(E) Illegal use of anabolic steroids

2. The most common cause of female pseudo-intersexuality is

(A) a 46, XO genotype
(B) a 47, XXY genotype
(C) lack of androgen receptors
(D) congenital adrenal hyperplasia
(E) inadequate production of testosterone and Müllerian-inhibiting factor (MIF)

3. The most common cause of male pseudo-intersexuality is

(A) a 45, XO genotype
(B) a 47, XXY genotype
(C) inadequate production of testosterone and MIF
(D) congenital adrenal hyperplasia
(E) lack of androgen receptors

4. The most common cause of testicular feminization syndrome is

(A) a 45, XO genotype
(B) a 47, XXY genotype
(C) inadequate production of testosterone and MIF
(D) congenital adrenal hyperplasia
(E) lack of androgen receptors

5. In the male, failure of the urethral folds to fuse completely results in

(A) hypospadias
(B) epispadias
(C) cryptorchidism
(D) congenital inguinal hernia
(E) hydrocele

6. The Y chromosome carries a gene on its short arm that codes for

(A) testosterone
(B) MIF
(C) testes-determining factor (TDF)
(D) progesterone
(E) estrogen

7. Bilateral cryptorchidism usually results in

(A) impotence
(B) sterility
(C) male pseudo-intersexuality
(D) female pseudo-intersexuality
(E) testicular feminization syndrome

8. A 17-year-old girl presents with a complaint of amenorrhea. Physical examination reveals good breast development and normal amount of pubic hair. A rudimentary vagina and a mobile mass within both the right and left labia majora are found on pelvic examination. Ultrasound reveals the absence of a uterus. What is the diagnosis?

(A) Testicular feminization syndrome
(B) Gonadal dysgenesis
(C) Cryptorchidism
(D) Female pseudo-intersexuality
(E) Hypospadias

Answers and Explanations

1. **A.** Reduced levels of androgens during fetal development of an XY male fetus cause a feminization of the male external genitalia such that the baby can be phenotypically mistaken for female. Parents raise the XY male baby as a girl until puberty or other medical problems bring the child to medical attention.
2. **D.** Female pseudo-intersex individuals have a 46, XX genotype. This condition is most commonly caused by congenital adrenal hyperplasia, in which the fetus produces excessive amounts of androgens. The high androgen level will masculinize the female genitalia.
3. **C.** Male pseudo-intersex individuals have a 46, XY genotype. This condition is most commonly caused by inadequate production of testosterone and MIF by the fetal testes. The low testosterone and MIF levels will stunt the development of the male genitalia.
4. **E.** The most common cause of testicular feminization syndrome is the lack of androgen receptors in the urogenital folds and labioscrotal swellings. Because these tissues lack androgen receptors, they are blind or unresponsive to androgens. Consequently, these tissues develop into female external genitalia even though the fetus has a 46, XY genotype.
5. **A.** Failure of the urethral folds to fuse completely results in the external urethral orifice opening onto the ventral surface of the penis, a condition known as hypospadias.
6. **C.** The gene product that is coded on the short arm of the Y chromosome is called the TDF.
7. **B.** Sterility is a common result of bilateral cryptorchidism. When both testes fail to descend into the scrotum, the increased temperature to which they are exposed in the abdominal cavity will inhibit spermatogenesis.
8. **A.** This is a classic case of testicular feminization syndrome. A karyotype analysis would reveal that this normal-appearing 17-year-old girl actually has a 46, XY genotype. The mobile masses within the right and left labia majora are the testes and should be surgically removed because this tissue has a propensity toward malignant tumor formation. The most common cause of this syndrome is a lack of androgen receptors in the phallus, urogenital folds, and labioscrotal swellings.

chapter 16

Integumentary System

I. SKIN

The skin consists of two layers: the outer layer (or **epidermis**) and the deeper connective tissue layer (or **dermis**). Skin functions as a barrier against infection, serves in thermoregulation, and protects the body against dehydration.

A. Epidermis. The epidermis is derived from the **ectoderm**.

1. **Early development**
   - **a.** Initially, the epidermis consists of a single layer of ectodermal cells that give rise to an overlying **periderm** layer.
   - **b.** The epidermis soon becomes a three-layered structure consisting of the **stratum basale** (mitotically active), **intermediate layer** (progeny of stratum basale), and the **periderm**.
   - **c.** Peridermal cells are eventually desquamated and form part of the **vernix caseosa**, a greasy substance of peridermal cells and sebum from the sebaceous glands that protects the embryo's skin.
2. **Later development.** The definitive adult layers are formed through the inductive influence of the dermis. The ectodermal cells give rise to five cell layers:
   - **a.** Stratum basale (stratum germinativum)
   - **b.** Stratum spinosum
   - **c.** Stratum granulosum
   - **d.** Stratum lucidum
   - **e.** Stratum corneum. This layer is associated with the expression of 56-kDa keratin, 67-kDa keratin, and filaggrin (a binding protein).
3. **Other cells of the epidermis**
   - **a. Melanoblasts** are derived from **neural crest cells** that migrate into the stratum basal of the epidermis. They differentiate into melanocytes by mid-pregnancy, when pigment granules called **melanosomes** are observed.
   - **b. Langerhans cells** are derived from the **bone marrow (mesoderm)** and migrate into the epidermis. They are involved in antigen presentation.
   - **c. Merkel cells** are of uncertain origin. They are associated with free nerve endings and probably function as mechanoreceptors.

B. Dermis. The dermis is derived from both the **somatic mesoderm** located just beneath the ectoderm and **mesoderm of the dermatomes** of the body. In the head and neck region, the dermis is derived from **neural crest cells**.

1. **Early development**
   - **a.** The dermis is initially composed of loosely aggregated mesodermal cells frequently referred to as **mesenchymal cells** (or **mesenchyme**).
   - **b.** The mesenchymal cells secrete a watery-type extracellular matrix rich in glycogen and hyaluronic acid.
2. **Later development**
   - **a.** The mesenchymal cells differentiate into fibroblasts, which secrete increasing amounts of collagen and elastic fibers into the extracellular matrix.
   - **b.** Vascularization occurs.
   - **c.** Sensory nerves grow into the dermis.
   - **d.** The dermis forms projections into the epidermis called **dermal papillae**, which contain tactile sensory receptors (e.g., Meissner corpuscles).

C. Clinical considerations

1. **Oculocutaneous albinism (OCA) (Figure 16.1)**
   - **a. Type I OCA (tyrosinase negative; classic type; Figure 16.1)** is an autosomal recessive genetic caused by a mutation in the *TYR* **gene** on **chromosome 11q14**, which encodes for the **tyrosinase** enzyme. This results in a disorder in which melanocytes **fail to produce melanin pigment**. **Clinical features include** pink skin, gray-blue eyes, and white hair at birth and throughout life. The photograph (Figure 16.1) shows a patient with Type I OCA.
   - **b. Type II OCA (tyrosinase positive; Figure 16.2)** is an autosomal recessive genetic disorder caused by a mutation in the *OCA2* **gene** on **chromosome 15q11**, which encodes for the **P protein** that is involved in the transport of tyrosine. This results in a disorder in which melanocytes **produce some melanin pigment. Clinical features include** pink skin, gray-blue eyes, and dark hair at birth, but the pigment of the skin, eyes, and hair increases as the patient ages. The photograph (Figure 16.2) shows a female African American child with type II OCA.
   - **c. Piebaldism (Figure 16.3)** is an autosomal dominant genetic disorder caused by a mutation in the ***KIT* gene** on **chromosome 4q11**, which encodes for a **receptor tyrosine kinase**. This results in a disorder in which there is a lack of melanin in isolated patches of skin and/or hair (i.e., a localized albinism). **Clinical features include** patches of depigmented skin around the mid-forehead, neck, anterior trunk, and mid-extremities. A white forelock is a common finding. Patients are otherwise healthy and have a normal life span. Albinism predisposes to basal cell carcinoma, squamous cell carcinoma,

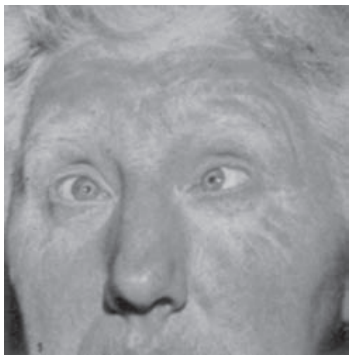

FIGURE 16.1. Type I oculocutaneous albinism (OCA).

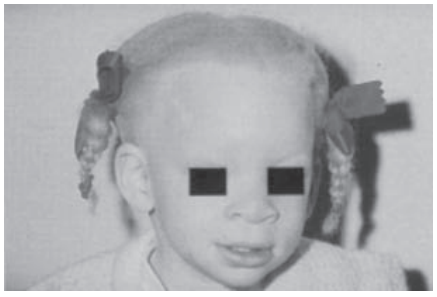

FIGURE 16.2. Type II oculocutaneous albinism (OCA) in a black female child.

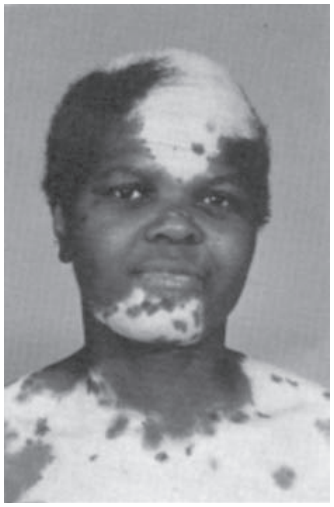

FIGURE 16.3. Piebaldism in a black female child.

and malignant melanoma. The photograph (Figure 16.3) shows a female African American child with piebaldism.

2. **Ichthyosis** refers to a group of cutaneous disorders characterized by increased or aberrant keratinization of the skin resulting in noninflammatory scaling, dryness, and cracks in the skin that may form deep fissures.
   a. **Ichthyosis vulgaris** is an autosomal dominant genetic disorder caused by a mutation in the *FLG* **gene** on **chromosome 1q21**, which encodes for the **filaggrin** protein (a major component of keratohyalin). **Clinical features include** the mildest form of ichthyosis. It presents during childhood after 3 months of age, and appearance consists of fine white scales on the extensor surfaces of the extremities.
   b. **Lamellar ichthyosis** is an autosomal recessive genetic disorder caused by a mutation in the *TGM1* **gene** on **chromosome 14q11.2**, which encodes for **transglutaminase 1**, which plays a role in the assembly of the cornified envelope of the squames. **Clinical features include** presentation as a "collodion baby" at birth; the infant is encased in a translucent, taut, parchment-like membrane. The parchment-like membrane dries out and is shed, leaving residual erythema and hyperkeratosis. Children and adults develop large, brown polygonal scales that involve the entire body.
   c. **Epidermolytic hyperkeratosis** is an autosomal dominant genetic disorder caused by a mutation in either the *KRT1* **gene** on **chromosome 12q11** for **keratin 1** protein or the *KRT10* **gene** on **chromosome 17q21** for **keratin 10** protein. Keratins are intermediate filament proteins that form the cytoskeleton in all epithelial cells, including the stratified squamous epithelium of the skin. **Clinical features include** presentation in the neonatal period with widespread blistering and erythema. Children and adults develop generalized hyperkeratosis with dark scales and spiny ridges.
   d. **Harlequin fetus (Figure 16.4)** is an autosomal recessive genetic disorder caused by a mutation in the ***ABCA12* gene** on **chromosome 2q34**, which encodes for the **adenosine triphosphate-binding cassette transporter (subfamily A, member 12)**, which functions as a lipid transporter in keratinocytes. These mutations lead to impaired lipid secretion from lamellar granules in keratinocytes. **Clinical features include** the most severe form of ichthyosis. The fetus is encased by massive, armor-like plates of scale with deep fissures; the diamond-like configuration of the scales results in the appearance of a harlequin clown. Many such infants are stillborn or die shortly after birth. The photograph (Figure 16.4) shows a harlequin fetus.

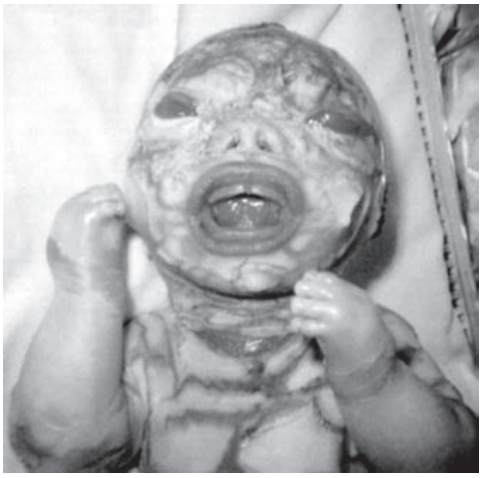

FIGURE 16.4. Harlequin fetus.

3. **Classic-type Ehlers-Danlos syndrome (EDS; Figure 16.5)** is an autosomal dominant genetic disorder caused by a mutation either in the *COL5A1* gene on chromosome 9q34.2-q34.3 for collagen a-1(V) chain protein or the *COL5A2* gene on chromosome 2q31 for collagen a-2(V) chain protein. **Clinical features include** extremely stretchable and fragile skin; hypermobile joints; aneurysms of blood vessels; rupture of the bowel; and widened atrophic scars. The photograph (Figure 16.5) shows a child with EDS. Note the extremely stretchable skin and the cigarette-paper scars over the knees (arrows).

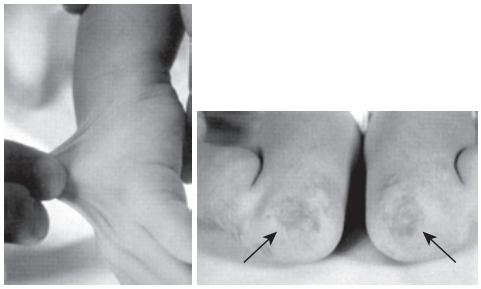

FIGURE 16.5. Ehlers-Danlos syndrome.

4. **Hemangiomas (Figure 16.6)** are vascular malformations, that is, benign tumors of endothelial cells. They produce "birthmarks" on the skin. A port-wine stain is a birthmark covering the area of distribution of the trigeminal nerve (CN V) that is frequently associated with a hemangioma of the meninges called **Sturge-Weber syndrome**. The photograph (Figure 16.6) shows an infant with an aggressive hemangioma of the face covering the distribution of the trigeminal nerve.

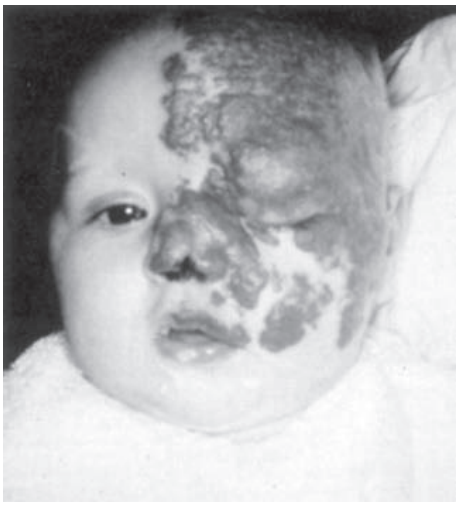

FIGURE 16.6. Hemangioma of the face.

5. **Junctional epidermolysis bullosa (JEB; Figure 16.7)** is an autosomal recessive genetic disorder caused by a mutation in the *LAMA5* **gene** on **chromosome 20q13.2**, which encodes for the **laminin α5** protein that is a component of hemidesmosomes. This results in a disorder in which the adhesion of the stratum basale to the basement membrane is weakened. **Clinical features include** onset at birth; widespread bulla (blister) formation, where the epidermis is intact but is separated from the underlying dermis; absent nails; dysplastic teeth; oral lesion. It is usually fatal by 3–4 years of age due to hypoproteinemia, anemia, and infection. The photograph (Figure 16.7) shows a young infant with widespread bullae (blisters) and erosion of the skin. The light micrograph shows a pathological cleft (*asterisk*) between the epidermis (E) and dermis (D). There is also some scarring in the dermis.
6. **Psoriasis** is a skin disease characterized by **excess cell proliferation** in the stratum basale and in the stratum spinosum. This results in thickening of the epidermis and shorter regeneration time of the epidermis.

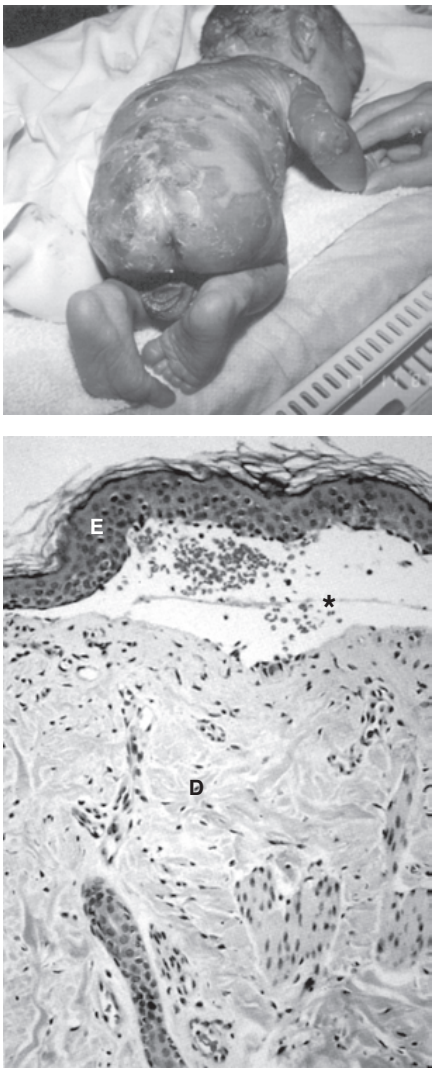

FIGURE 16.7. Epidermolysis bullosa.

II. HAIR AND NAILS

Hair and nails are derived from the **ectoderm**.

A. Hair (Figure 16.8)

1. At week 12, cells from the stratum basale grow into the underlying dermis and form the **hair follicle**.
2. The deepest part of the hair follicle soon becomes club shaped to form the **hair bulb**.
3. The hair bulbs are invaginated by **mesoderm** called the **hair papillae**, which are rapidly infiltrated by blood vessels and nerve endings.

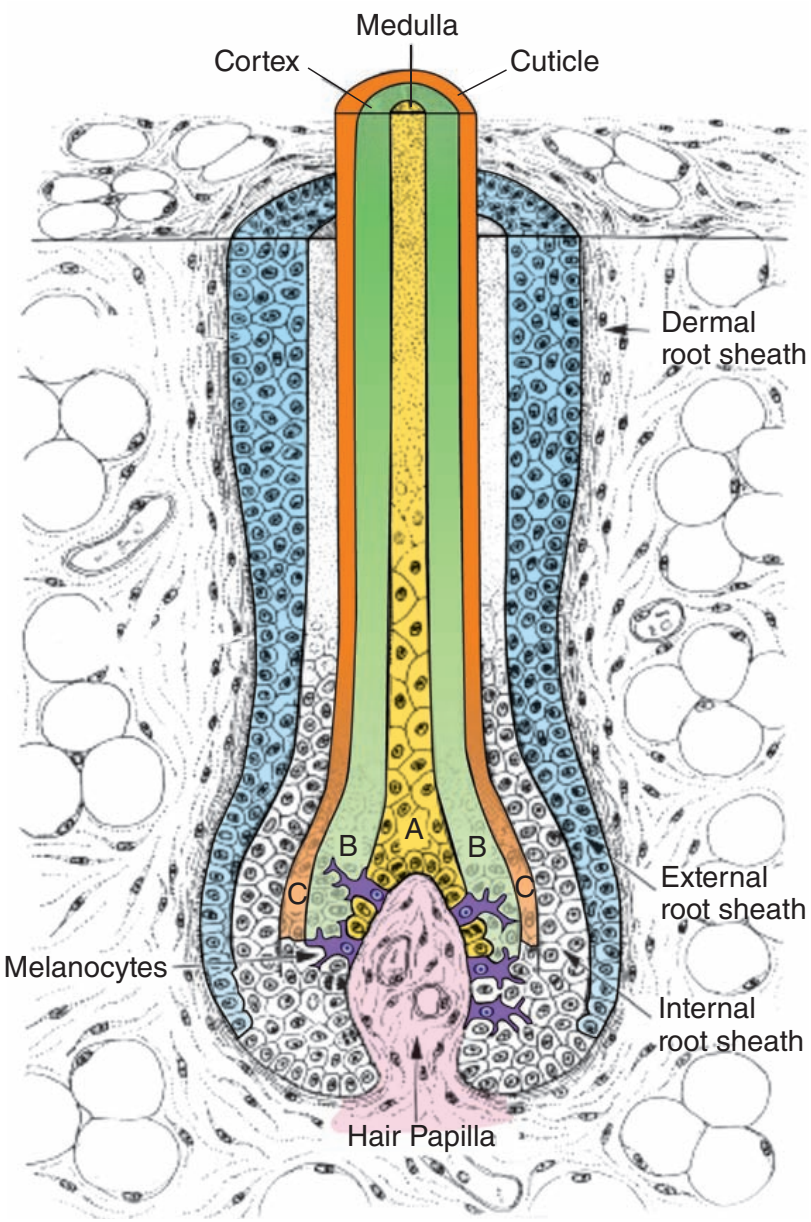

FIGURE 16.8. Diagram of a hair and its follicle. The expanded lower end of the follicle contains a hair papilla (*light red*). The formation and growth of the hair depend on the continuous proliferation and differentiation of cells around the tip of the hair papilla (*pink*). Cells in region A give rise to the hair medulla (*yellow*). Cells in region B give rise to the hair cortex (*light green*). Cells in region C give rise to the hair cuticle (*orange*). Other peripheral cells give rise to the internal root sheath (*white*) and external root sheath (*blue*). Melanocytes (*purple*) contribute to hair color.

4. The epithelial cells within the hair bulb differentiate into the **germinal matrix**, where cells proliferate, grow toward the surface, keratinize, and form the **hair shaft**. These cells also form the **internal root sheath**.
5. Other epithelial cells of the hair follicle form the **external root sheath**, which is continuous with the epidermis and has a prominent subjacent basement membrane called the **glassy membrane**.
6. Mesodermal cells of the dermis that surround the invaginating hair follicle form the **dermal root sheath** and the **arrector pili muscle**.
7. The first fine hairs, called **lanugo hairs**, are sloughed off at birth.

B. Nails develop from the epidermis. The nails first develop on the tips of the digits and then migrate to the dorsal surface, taking their innervation with them. This is why the median nerve innervates the dorsal surface of three and one-half digits (I–IV).

C. Clinical considerations

1. **Alopecia** is baldness resulting from an absence or faulty development of the hair follicles.
2. **Hypertrichosis** is an overgrowth of hair. It is frequently associated with spina bifida occulta, which is seen as a patch of hair overlying the defect.
3. **Pili torti (Figure 16.9)** is a familial disorder characterized by **twisted hairs**. It is seen in **Menkes (kinky-hair) disease**, an X-linked recessive neurological disorder involving a defect in intestinal copper transport. The photograph (Figure 16.9) shows pili torti or twisted hair condition.

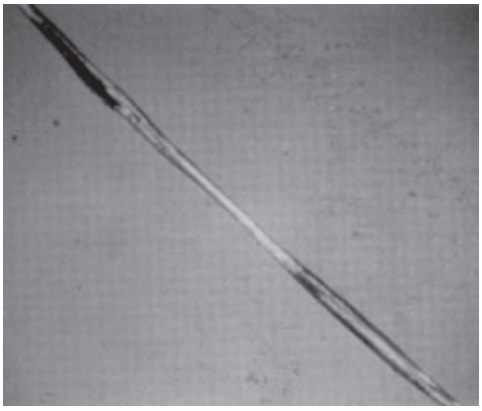

FIGURE 16.9. Pili torti.

4. **Trichorrhexis nodosa (Figure 16.10)** is **brittle hair** that breaks easily and is usually associated with metabolic disorders like **argininosuccinic aciduria**. Argininosuccinic aciduria is an autosomal recessive genetic disorder that causes a deficiency in the enzyme argininosuccinase of the urea cycle. The photograph (Figure 16.10) shows the trichorrhexis nodosa or brittle hair condition.

FIGURE 16.10. Trichorrhexis nodosa.

5. **Beaded hair (Figure 16.11)** is characterized by elliptical nodes along the hair, which breaks easily at the internodes and is usually associated with **monilethrix**. Monilethrix is an autosomal dominant genetic disorder. The photograph (Figure 6.11) shows the beaded hair condition.

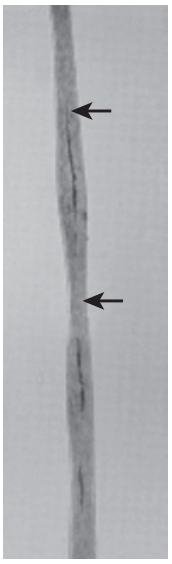

FIGURE 16.11. Beaded hair.

6. **Trichothiodystrophy (Figure 16.12)** is a very rare autosomal recessive genetic disorder characterized by short, brittle hair with alternating light and dark bands called **tiger-tail hair**. The photograph (Figure 6.12) shows the trichothiodystrophy condition.

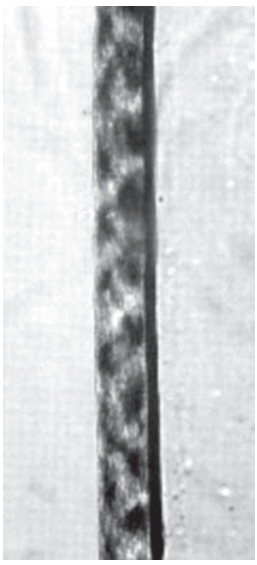

FIGURE 16.12. Tiger-tail hair.

7. **Uncombable hair syndrome (spun-glass hair; Figure 16.13)** is an autosomal dominant genetic disorder characterized by blonde, dry, shiny hair that cannot be combed into place. The hair has a triangular shape with a canal-like groove called pili trianguli et canaliculi. The photograph (Figure 16.13) shows the uncombable hair syndrome. Note the triangular-shaped hair with canal-like groove.

FIGURE 16.13. Uncombable hair syndrome.

III. MAMMARY, SWEAT, AND SEBACEOUS GLANDS

Mammary, sweat, and **sebaceous glands** are all derived from the surface ectoderm.

A. Mammary glands (Figure 16.14)

1. Mammary glands develop from the **mammary ridge**, a downgrowth of the **epidermis (ectoderm)** into the underlying **dermis (mesoderm)**.
2. Canalization of these epithelial downgrowths results in formation of **alveoli** and **lactiferous ducts**.
3. The lactiferous ducts drain into an epithelial pit, the future **nipple**.
4. The Tanner stages of breast development are guidelines in assessing whether a female adolescent is developing normally:
   a. **Stage I:** Breasts have papillae elevations only
   b. **Stage II:** Breasts have palpable buds, and areolae enlarge
   c. **Stage III:** Breasts show elevation of contours, and areolae enlarge
   d. **Stage IV:** Breasts form secondary areolar mounds
   e. **Stage V:** Breasts show adult breast contour, areolae recess to the general contour of the breast, and the nipples project

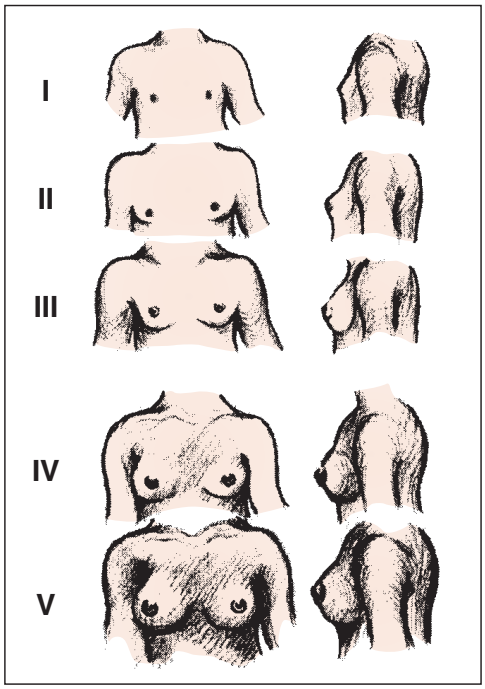

FIGURE 16.14. The Tanner stages of breast development.

B. Eccrine and apocrine sweat glands

develop from downgrowths of the epidermis into the underlying dermis.

C. Sebaceous glands

develop from the epithelial wall of the hair follicle and elaborate **sebum** into the hair follicles. The tarsal (meibomian) glands of the eyelids do not communicate with hair follicles.

D. Clinical considerations

1. **Gynecomastia (Figure 16.15)** is a condition in which there is excessive development of the male mammary glands. It is frequently associated with Klinefelter syndrome (47, XXY). The photograph (Figure 16.15) shows gynecomastia in a male with Klinefelter syndrome.

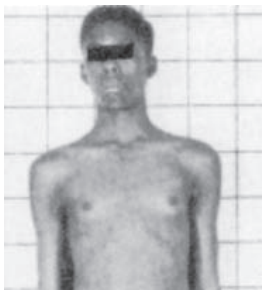

FIGURE 16.15. Gynecomastia.

2. **Breast hypertrophy (Figure 16.16)** may occur early in infancy. The photograph (Figure 16.16) shows breast hypertrophy in a 1-month-old female infant.

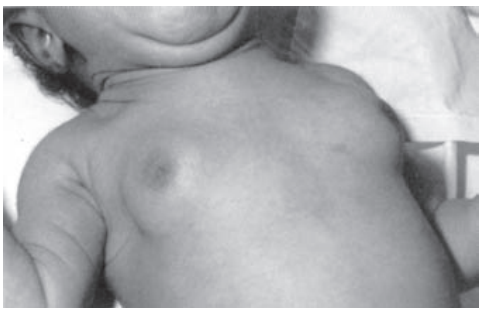

FIGURE 16.16. Breast hypertrophy.

3. **Breast hypoplasia (Figure 16.17)** generally occurs asymmetrically when one breast fails to develop completely. The photograph (Figure 16.17) shows breast hypoplasia of the right breast in a 16-year-old female.

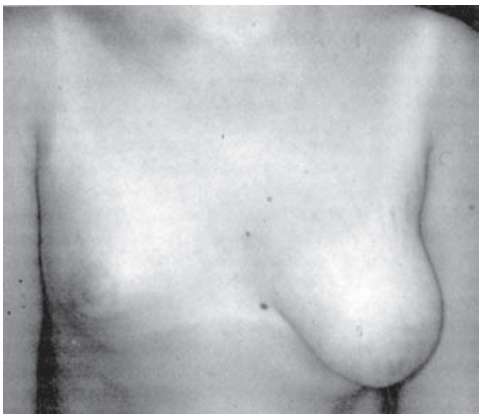

FIGURE 16.17. Breast hypoplasia.

4. **Polythelia (Figure 16.18)** is a condition in which supernumerary nipples occur along the mammary ridge. The photograph (Figure 16.18) shows two rudimentary nipples (arrows) that are located along the mammary line.
5. **Polymastia** is a condition in which supernumerary breasts occur along the mammary ridge.

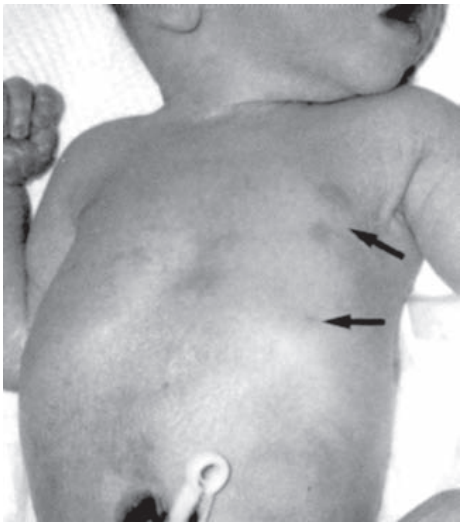

FIGURE 16.18. Polythelia.

IV. TEETH (FIGURE 16.19)

A. Development

1. The teeth develop from **ectoderm** and an underlying layer of **neural crest cells**.
2. The **dental lamina** develops from the **oral epithelium (ectoderm)** as a downgrowth into the underlying neural crest layer.
3. The dental lamina gives rise to **tooth buds**, which develop into the **enamel organs**.
4. The enamel **organs** are derived from **ectoderm** and develop first for the 20 deciduous teeth, then for the 32 permanent teeth.
5. The enamel organs give rise to **ameloblasts**, which produce **enamel**.
6. The **dental papillae** are formed by **neural crest cells** that underlie the enamel organs.
7. The dental papillae give rise to the **odontoblasts** (which produce **predentin** and **dentin)** and **dental pulp**.
8. The **dental sacs** are formed by a condensation of **neural crest cells** that surrounds the dental papillae.
9. The dental sacs give rise to **cementoblasts** (which produce **cementum**) and the **periodontal ligaments**.

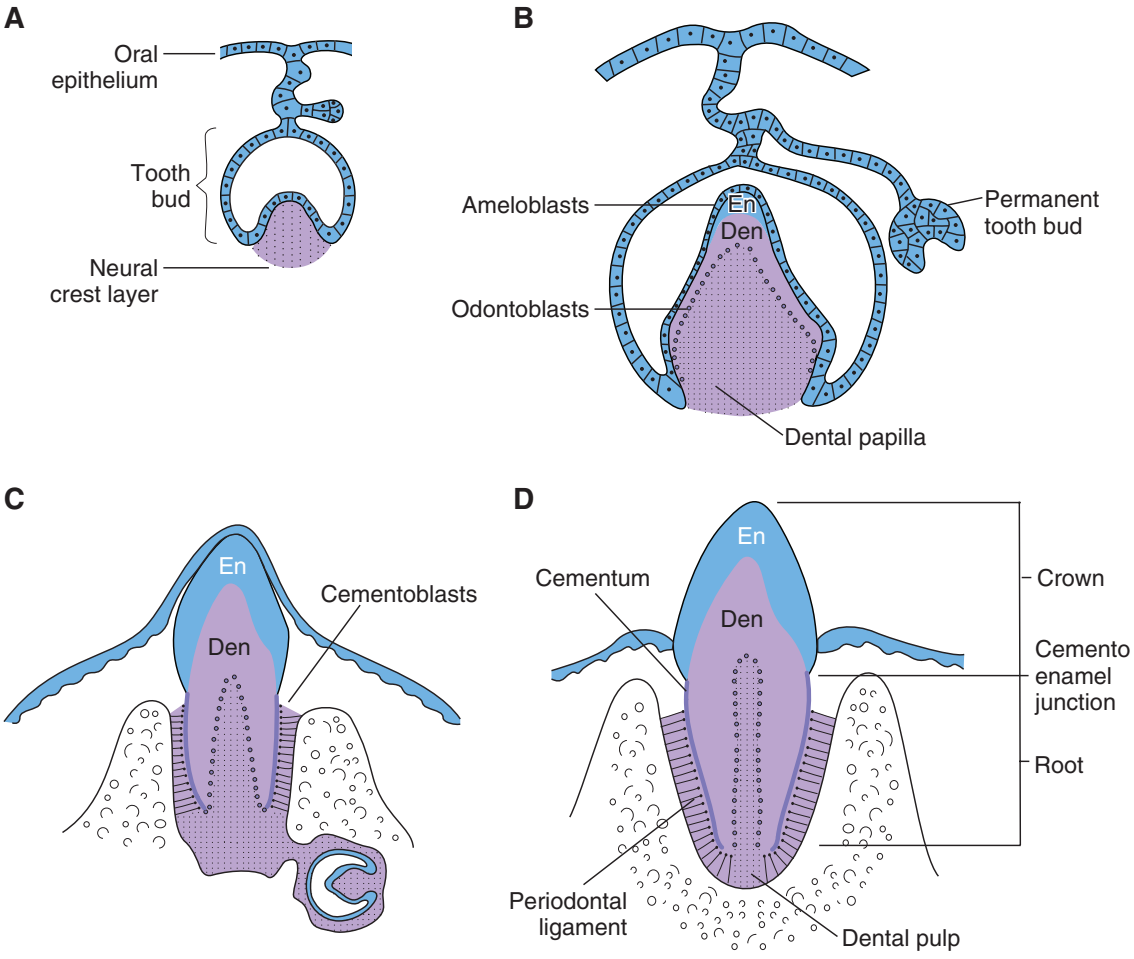

FIGURE 16.19. The successive stages in the development of a tooth. **A**. At week 8. This diagram shows the tooth bud formed by oral epithelium (ectoderm; *light blue*) and neural crest cells (*purple*). **B**. At week 28. This diagram shows the formation of enamel (En; *light blue*) by ameloblasts and dentin (Den; *purple*) by odontoblasts. **C**. At month 6 postnatal. This diagram shows the early tooth eruption. **D**. At month 18 postnatal. This diagram shows the fully erupted deciduous tooth. The ameloblasts are no longer present, which means further enamel formation is not possible.

B. Clinical considerations

1. Defective enamel formation (amelogenesis imperfecta) is an autosomal dominant trait.
2. Defective dentin formation (dentinogenesis imperfecta) is an autosomal dominant trait.
3. Vitamin A deficiency (Figure 16.20). If the vitamin A deficiency is severe, ameloblast cells will atrophy, which results in the absence of enamel. In less severe cases, there is enamel hypoplasia. The drawing (Figure 16.20) shows the clinical appearance of teeth in vitamin A deficiency.

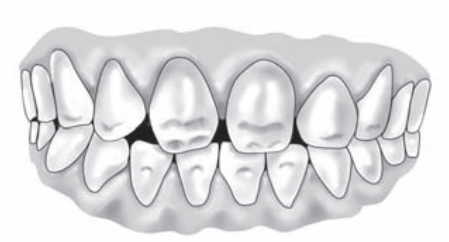

FIGURE 16.20. Clinical appearance of teeth in vitamin A deficiency.

4. Vitamin D deficiency (Figure 16.21). A severe vitamin D deficiency in children results in rickets, a condition characterized by insufficient deposition of calcium in bony tissue. In teeth, vitamin D deficiency is manifested by enamel and dentin hypoplasia. The drawing (Figure 16.21) shows the clinical appearance of teeth in vitamin D deficiency.

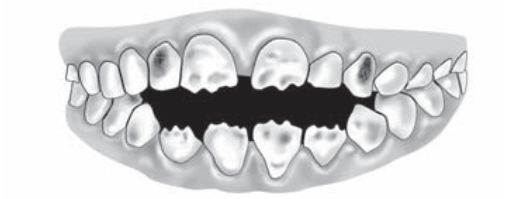

FIGURE 16.21. Clinical appearance of teeth in vitamin D deficiency.

5. Tetracycline discoloration (Figure 16.22). If tetracycline antibiotics are administered to a pregnant woman, permanent brown-gray staining of the teeth will result in the child. Tetracycline is deposited in bone and teeth during mineralization. The photograph (Figure 16.22) shows the clinical appearance of teeth in tetracycline staining.

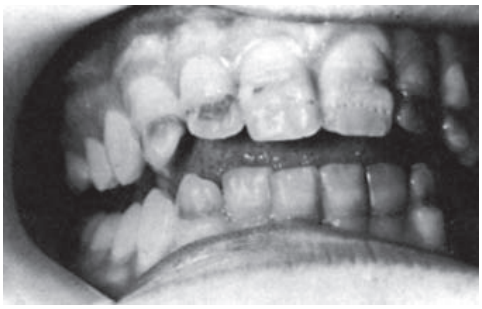

FIGURE 16.22. Clinical appearance of teeth in tetracycline staining.

Study Questions for Chapter 16

1. Melanocytes are found in which epidermal layer?

(A) Stratum basale
(B) Stratum corneum
(C) Stratum granulosum
(D) Stratum lucidum
(E) Stratum spinosum

2. A young black girl shows isolated patches of skin and hair that lack melanin pigment. In addition, other skin lesions are observed that look suspiciously like a malignant melanoma. What is the most likely diagnosis?

(A) Type I oculocutaneous albinism
(B) Type II oculocutaneous albinism
(C) Piebaldism
(D) Ichthyosis
(E) Psoriasis

3. A young infant shows extremely stretchable and fragile skin, hypermobile joints, and cigarette-paper scars over the knees. What is the most likely diagnosis?

(A) Ehlers-Danlos syndrome
(B) Junctional epidermolysis bullosa
(C) Psoriasis
(D) Ichthyosis
(E) Piebaldism

4. A young infant shows skin blisters over the entire body with generalized skin erosion. Pathology indicates a cleft between the epidermis and dermis. What is the most likely diagnosis?

(A) Psoriasis
(B) Junctional epidermolysis bullosa
(C) Ichthyosis
(D) Ehlers-Danlos syndrome
(E) Type II oculocutaneous albinism

5. The administration of which of the following agents may result in discoloration of both deciduous and permanent teeth?

(A) Cephalosporin
(B) Chloramphenicol
(C) Erythromycin
(D) Penicillin
(E) Tetracycline

Answers and Explanations

1. **A.** Melanocytes are found in the stratum basale, the deepest layer of the epidermis, at the dermoepidermal junction.
2. **C.** Piebaldism is an autosomal dominant disorder and is basically a localized albinism.
3. **A.** Ehlers-Danlos syndrome is an autosomal dominant disorder involving the gene for peptidyl lysine hydroxylase.
4. **B.** Junctional epidermolysis bullosa refers to a group of autosomal recessive disorders caused by a mutation in the gene for laminin 5.
5. **E.** Tetracyclines are bound to calcium in newly formed teeth both in utero and in young children. They may cause discoloration and enamel dysplasia.

chapter 17

Skeletal System

I. SKULL (FIGURE 17.1)

The skull can be divided into two parts: the neurocranium and viscerocranium.

A. Neurocranium

1. The neurocranium consists of the flat bones of the skull (cranial vault) and the base of the skull.
2. The neurocranium develops from **neural crest cells**, except for the basilar part of the occipital bone, which forms from **mesoderm of the occipital sclerotomes**.

B. Viscerocranium

1. The viscerocranium consists of the bones of the face involving the pharyngeal arches.
2. The viscerocranium develops from **neural crest cells**, except for the laryngeal cartilages, which form from **mesoderm within pharyngeal arches 4 and 6**.

C. Sutures

1. During fetal life and infancy, the flat bones of the skull are separated by dense connective tissue (fibrous joints) called **sutures**.
2. There are five sutures: frontal suture, sagittal suture, lambdoid suture, coronal suture, and squamous suture.
3. Sutures allow the flat bones of the skull to deform during childbirth (called **molding**) and to expand during childhood as the brain grows.
4. Molding may exert considerable tension at the **"obstetrical hinge"** (junction of the squamous and lateral parts of the occipital bone) such that the **great cerebral vein (of Galen)** may be ruptured during childbirth.

D. Fontanelles are large, fibrous areas where several sutures meet. There are six fontanelles: **anterior fontanelle, posterior fontanelle, two sphenoid fontanelles, and two mastoid fontanelles**.

1. The anterior fontanelle is the largest fontanelle and is readily palpable in the infant.
2. The anterior fontanelle pulsates because of the underlying cerebral arteries and can be used to obtain a blood sample from the underlying **superior sagittal sinus**.
3. The **anterior fontanelle** and the **mastoid fontanelles** close at about **2 years of age** when the main growth of the brain ceases.
4. The posterior fontanelle and the sphenoid fontanelles close at about 6 months of age.

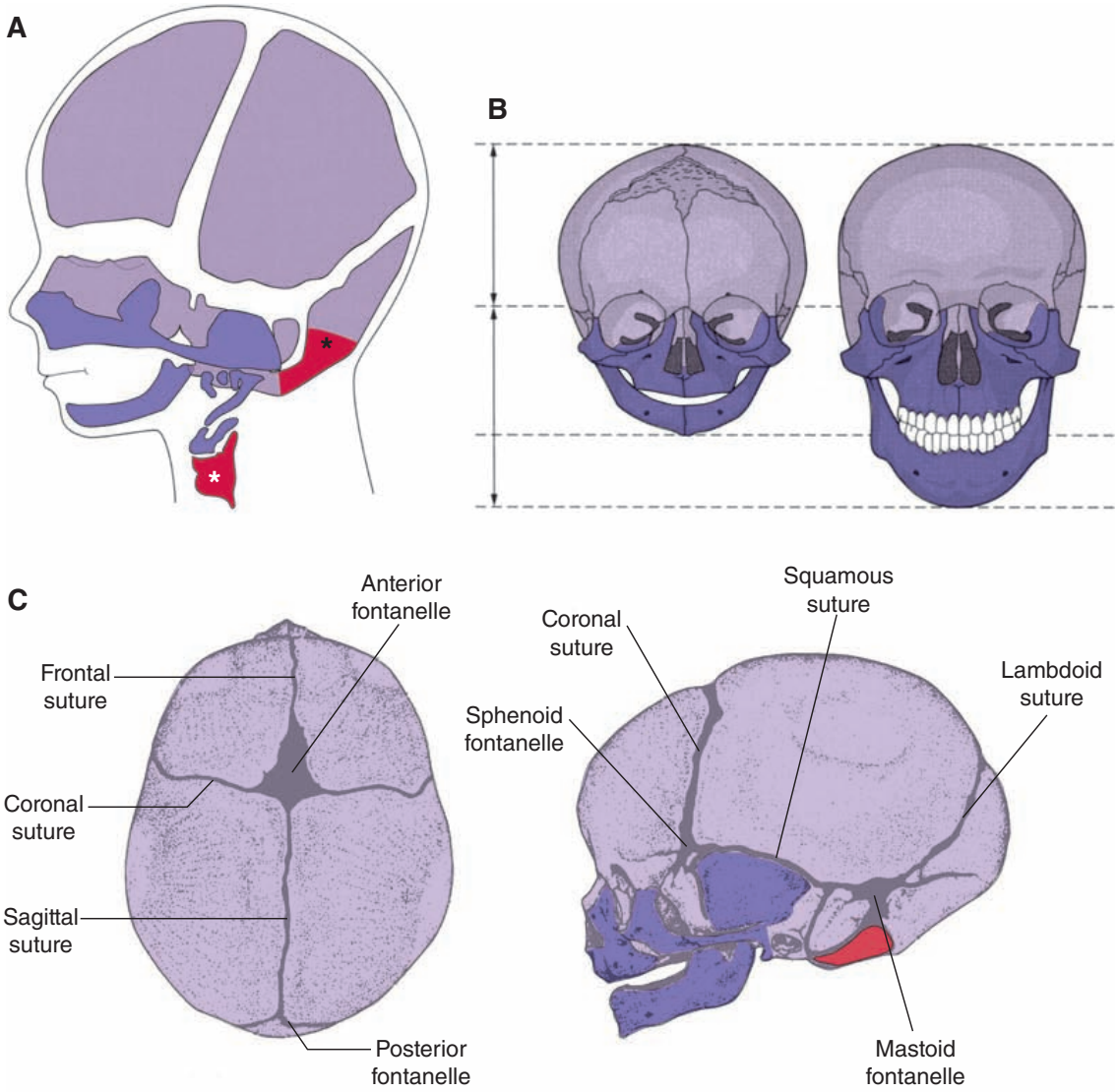

FIGURE 17.1. A. A diagram of the newborn skull indicating the neurocranium (*light purple*) and the viscerocranium (*dark purple*). The bones of the neurocranium and viscerocranium are derived almost entirely from neural crest cells. However, the basilar part of the occipital bone (*asterisk; dark red*), which forms from mesoderm of the occipital sclerotomes, and the laryngeal cartilages (*asterisk*; *dark red*), which form from mesoderm within pharyngeal arches 4 and 6. **B**. A diagram depicting the postnatal growth of the skull. After birth, the skull continues ossification toward the sutures. However, the face is relatively underdeveloped and undergoes dramatic changes during childhood and adolescence with the eruption of teeth, formation of sinuses, and elongation of the maxilla and mandible. Note that the profound postnatal changes of the skull are due to the development of the viscerocranium. **C**. Diagram of the sutures and fontanelles.

E. Clinical considerations

1. **Abnormalities in skull shape** may result from failure of cranial sutures to form or from premature closure of sutures **(craniosynostoses)**.
   a. **Microcephaly** results from failure of the brain to grow and is usually associated with mental retardation.
   b. **Oxycephaly (turricephaly or acrocephaly)** is a **tower-like skull** caused by premature closure of the **lambdoid and coronal sutures**. It should be differentiated from **Crouzon syndrome**, which is a dominant genetic condition with a presentation quite similar to that of oxycephaly but is accompanied by malformations of the face, teeth, and ears.

c. **Plagiocephaly (Figure 17.2)** is an asymmetrical skull caused by premature closure of the **lambdoid and coronal sutures** on one side of the skull. The photograph (Figure 17.2) shows an infant with plagiocephaly.

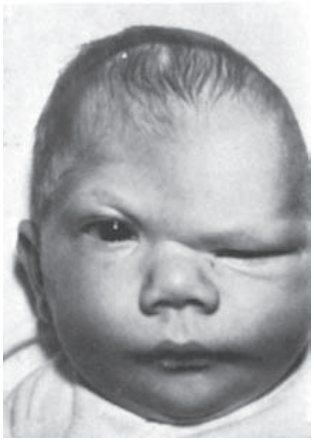

FIGURE 17.2. Plagiocephaly.

d. **Brachycephaly (Figure 17.3)** is a short, square-shaped skull caused by premature closure of the **coronal sutures**. The radiograph (Figure 17.3) shows the condition of brachycephaly.

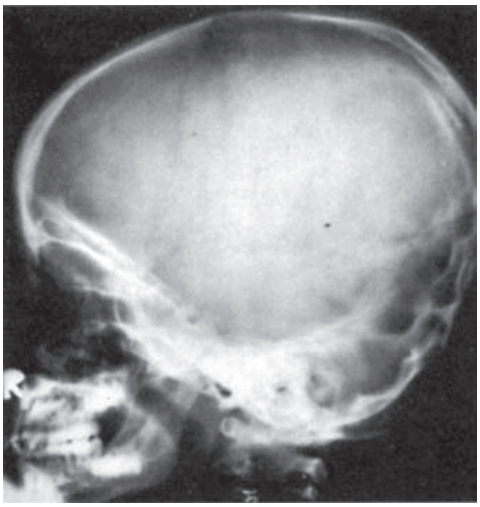

FIGURE 17.3. Brachycephaly.

e. **Scaphocephaly (Figure 17.4)** is a long skull (in the anterior/posterior plane) caused by premature closure of the **sagittal suture**. The photograph (Figure 17.4) shows an infant with scaphocephaly.

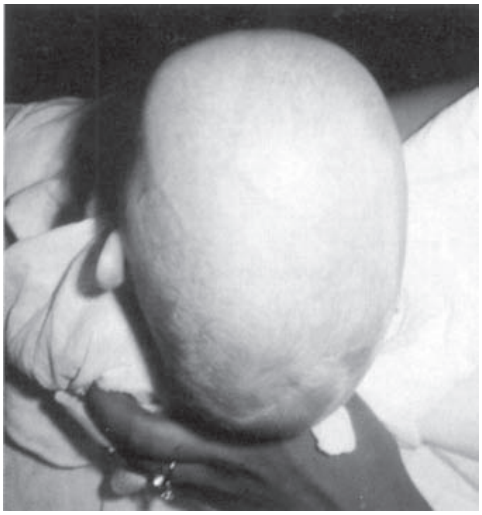

FIGURE 17.4. Scaphocephaly.

f. Kleeblattschädel (Figure 17.5) is a cloverleaf skull caused by premature closure of **all sutures**, forcing the brain growth through the anterior and sphenoid fontanelles. The photograph (Figure 17.5) shows a child with Kleeblattschädel.

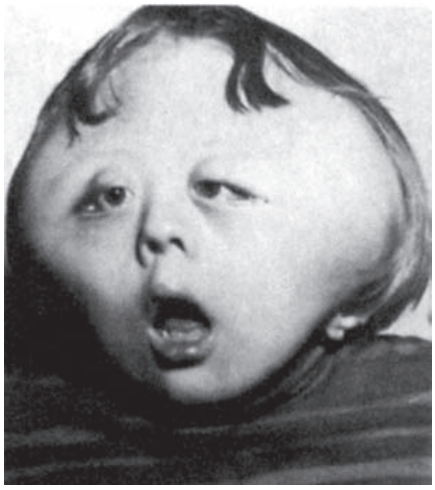

FIGURE 17.5. Kleeblattschädel.

g. Crouzon syndrome (Figure 17.6) is an autosomal dominant genetic disorder caused by a mutation in the *FGFR2* **gene** on **chromosome 10q25.3**, which encodes for **fibroblast growth factor receptor 2**. The mutation results in constitutive activation of the FGFR2 receptor (i.e., a **gain-of-function mutation**). **Clinical features include** premature craniosynostosis; midface hypoplasia with shallow orbits; ocular proptosis; mandibular prognathism; normal extremities; progressive hydrocephalus; and no mental retardation. The photograph (Figure 17.6) shows a child with Crouzon syndrome.

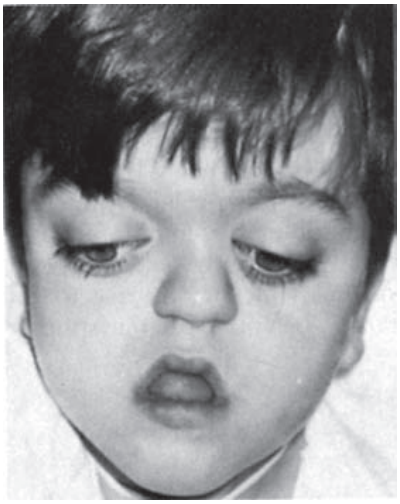

FIGURE 17.6. Crouzon syndrome.

h. Apert syndrome (Figure 17.7) is an autosomal dominant genetic disorder caused by a mutation in the *FGFR2* **gene** on **chromosome 10q25.3**, which encodes for **fibroblast growth factor receptor 2. Clinical features include** craniosynostosis leading to turribrachycephaly; syndactyl of hands and feet; various ankyloses; progressive synostoses of the hands, feet, and cervical spine; and mental retardation. The photograph (Figure 17.7) shows a child with Apert syndrome.

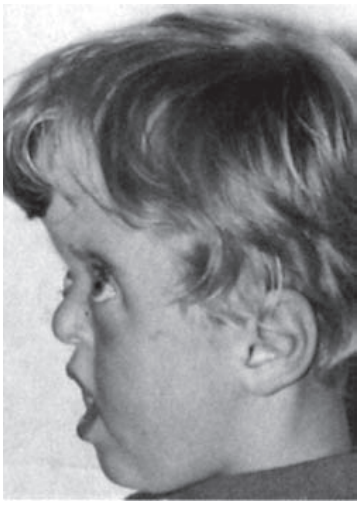

FIGURE 17.7. Apert syndrome.

i. **Pfeiffer syndrome (Figure 17.8)** is an autosomal dominant genetic disorder caused by a mutation in the ***FGFR1* gene** on **chromosome 8p12**, which encodes for **fibroblast growth factor receptor 1**, or the ***FGFR2* gene** on **chromosome 10q25.3**, which encodes for **fibroblast growth factor receptor 2. Clinical features include** craniosynostosis leading to turribrachycephaly; syndactyl of hands and feet; and broad thumbs and great toes. The photograph (Figure 17.8) shows a child with Pfeiffer syndrome.

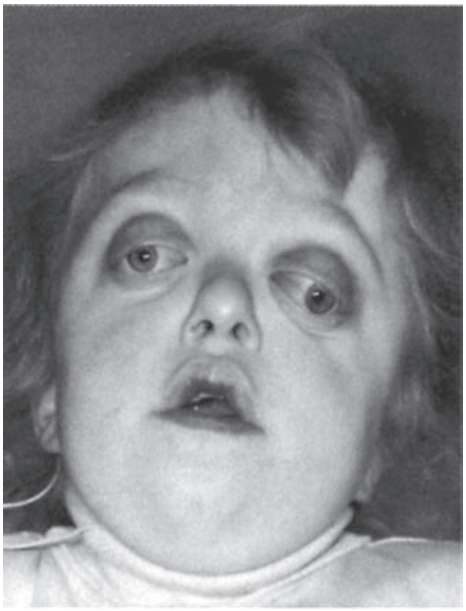

FIGURE 17.8. Pfeiffer syndrome.

2. **Temporal bone formation**
   a. **Mastoid process.** This portion of the temporal bone is absent at birth, which leaves the **facial nerve (CN VII)** relatively unprotected as it emerges from the stylomastoid foramen. In a difficult delivery, forceps may damage CN VII. The mastoid process forms by 2 years of age.
   b. **Petrosquamous fissure.** The petrous and squamous portions of the temporal bone are separated by the petrosquamous fissure, which opens directly into the mastoid antrum of the middle ear. This fissure, which may remain open until 20 years of age, provides a route for the spread of infection from the middle ear to the meninges.
3. **Spheno-occipital joint** is a site of growth up to about 20 years of age.

II. VERTEBRAL COLUMN (FIGURE 17.9)

A. Vertebrae in general

1. Mesodermal cells from the sclerotome migrate and condense around the notochord to form the **centrum**, around the neural tube to form the **vertebral arches**, and in the body wall to form the **costal processes**.
2. The centrum forms the **vertebral body**.
3. The vertebral arches form the **pedicles, laminae, spinous process, articular processes**, and the **transverse processes**.
4. The costal processes form the **ribs**.

B. The **atlas (C1) and axis (C2)** are highly modified vertebrae.

1. The atlas has no vertebral body or spinous process.
2. The axis has an **odontoid process (dens)**, which represents the vertebral body of the atlas.

C. Sacrum is a large triangular fusion of five sacral vertebrae forming the posterior/superior wall of the pelvic cavity.

D. Coccyx is a small triangular fusion of four rudimentary vertebrae.

E. Intersegmental position of vertebrae

1. As mesodermal cells from the sclerotome migrate toward the notochord and neural tube, they split into a **cranial portion** and a **caudal portion**.
2. The caudal portion of each sclerotome fuses with the cranial portion of the succeeding sclerotome, which results in the intersegmental position of the vertebra.

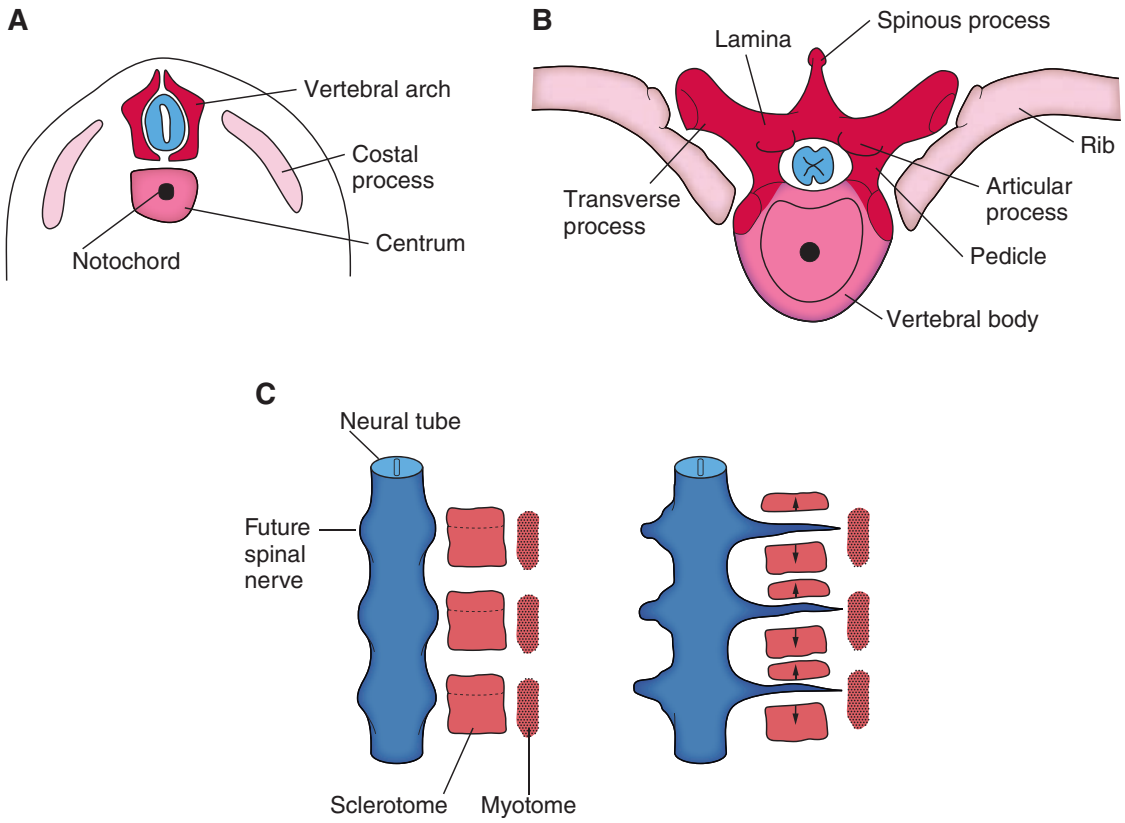

FIGURE 17.9. Development of a typical thoracic vertebra. **A**. At about 5–7 weeks. Mesodermal cells from the sclerotome demonstrate three distinct condensations: centrum (*light red*), vertebral arch (*dark red*), and costal process (*pink*). At birth, three ossification centers are present: one in the centrum and one in each vertebral arch. At 3–5 years of age, the vertebral arches fuse with each other and to the centrum. Ossification ends at about 25 years of age. **B**. Adult. Each condensation develops into distinct components of the adult vertebrae, as indicated by the shading. **C**. Diagram depicting the splitting of the sclerotome into caudal and cranial portions as the spinal nerves (*blue*) grow out to innervate the myotome. The dotted lines indicate where the sclerotome splits, thus allowing the growing spinal nerve to reach the myotome.

3. The splitting of the sclerotome is important because it allows the developing spinal nerve a route of access to the myotome, which it must innervate.
4. In the cervical region, the caudal portion of the fourth occipital sclerotome (O4) fuses with cranial portion of the first cervical (C1) sclerotome to form the base of the occipital bone, which allows C1 spinal nerve to exit between the **base of the occipital bone and C1 vertebrae**.

F. Curves

1. The **primary curves** are **thoracic** and **sacral curvatures** that form during the fetal period.
2. The **secondary curves** are **cervical** and **lumbar curvatures** that form after birth as a result of lifting the head and walking, respectively.

G. Joints of the vertebral column

1. **Synovial joints**
   a. The **atlanto-occipital joint** lies between C1 (atlas) and the occipital condyles.
   b. The **atlanto-axial joint** lies between C1 (atlas) and C2 (axis).
   c. **Facets (zygapophyseal)** are joints between the inferior and superior articular facets.
2. **Secondary cartilaginous joints (symphyses)**
   a. Symphyses are the joints between the vertebral bodies in which the **intervertebral disks** play a role. An intervertebral disk consists of the following:
      i. **Nucleus pulposus.** This is a remnant of the embryonic **notochord**. By 20 years of age, all notochordal cells have degenerated such that all notochordal vestiges in the adult are limited to just a noncellular matrix.
      ii. **Annulus fibrosus.** This is an outer rim of **fibrocartilage** derived from **mesoderm** found between the vertebral bodies.

H. Clinical considerations

1. **Congenital brevicollis (Klippel-Feil syndrome; Figure 17.10)** results from fusion and shortening of the cervical vertebrae. It is associated with shortness of neck, low hairline, and limited motion of head and neck. The radiograph (Figure 17.10) shows congenital fusion of the cervical vertebrae.

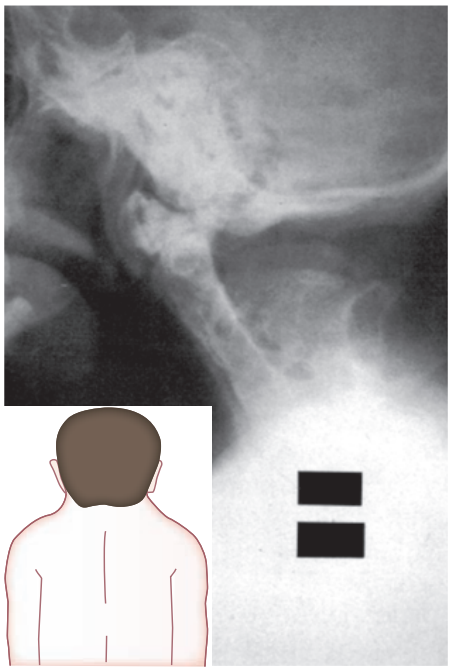

FIGURE 17.10. Congenital brevicollis.

2. **Intervertebral disk herniation (Figure 17.11)** involves the prolapse of the nucleus pulposus through the defective annulus fibrosis into the vertebral canal. The nucleus pulposus impinges on spinal roots and results in root pain, radiculopathy. The MRI (Figure 17.11) shows protrusion of the L2 disk causing extradural compression of cauda equina nerve roots (*arrows*).

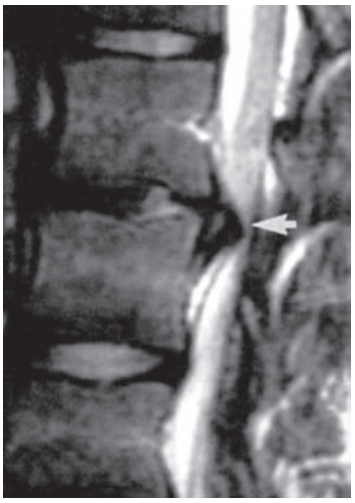

FIGURE 17.11. Intervertebral disk herniation.

3. **Spina bifida occulta (Figure 17.12)** results from failure of the vertebral arches to form or fuse. Figure 17.12 shows spina bifida occulta.

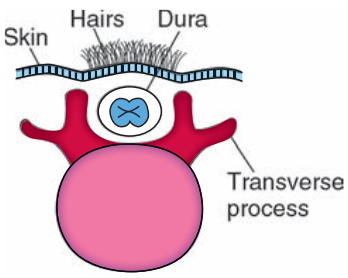

FIGURE 17.12. Spina bifida occulta.

4. **Spondylolisthesis (Figure 17.13)** occurs when the pedicles of the vertebral arches fail to fuse with the vertebral body. This allows the vertebral body to move anterior with respect to the vertebrae below it, causing **lordosis. Congenital spondylolisthesis** usually occurs at the L5–S1 vertebral level. Figure 17.13 shows spondylolisthesis. Note the congenital absence of pedicles (*arrows*).

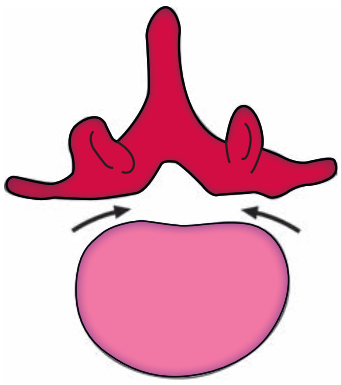

FIGURE 17.13. Spondylolisthesis.

5. **Hemivertebrae (Figure 17.14)** occur when wedges of vertebrae appear that are usually situated laterally between two other vertebrae. The radiograph (Figure 17.14) shows a hemivertebra (*arrow*).

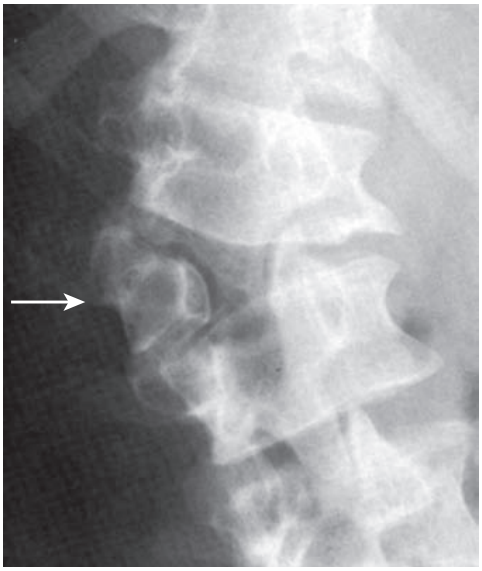

FIGURE 17.14. Hemivertebrae.

6. **Vertebral bar (Figure 17.15)** occurs when there is a localized failure of segmentation on one side of the column, usually in a posterolateral site. The MRI (Figure 17.15) shows partial fusion (*solid arrow*) of the L4–L5 vertebral bodies posteriorly. Note the single fused spinous process (*open arrow*).

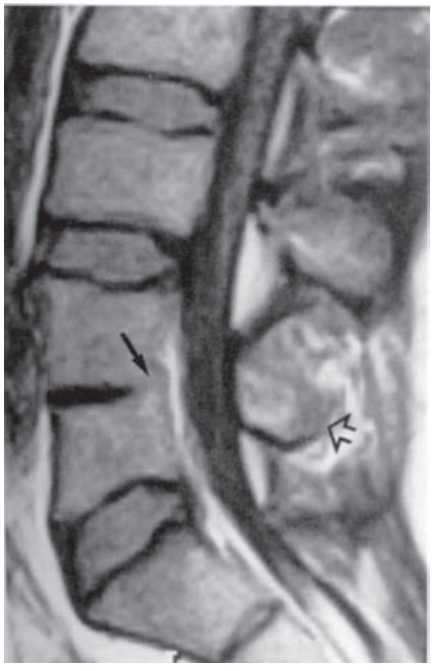

FIGURE 17.15. Vertebral bar.

7. **Block vertebra (Figure 17.16)** occurs when there is a lack of separation between two or more vertebrae, usually occurring in the lumbar region. Figure 17.16 shows a block vertebra.

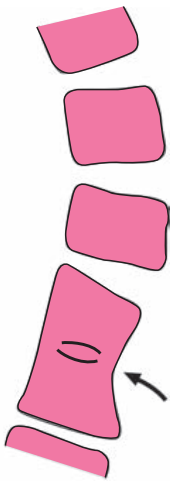

FIGURE 17.16. Block vertebra.

8. **Cleft vertebra (Figure 17.17)** occurs when a cleft develops in the vertebra, usually in a coronal or sagittal plane in the lumbar region. The drawing (Figure 17.17) shows both a coronal and a sagittal cleft vertebra. The radiograph (Figure 17.17) shows coronal clefts in vertebrae L1, L2, and L4 (*arrows*).

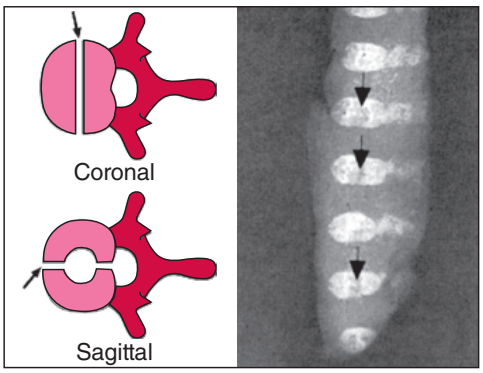

FIGURE 17.17. Coronal and sagittal cleft vertebrae.

9. **Idiopathic scoliosis (Figure 17.18)** is a lateral deviation of the vertebral column that exhibits both deviation and rotation of vertebral bodies. The photograph (Figure 17.18) shows a forward-bending patient with scoliosis, a position that will reveal even very small curvatures. The prominence (*arrow*) is produced by chest wall asymmetry.

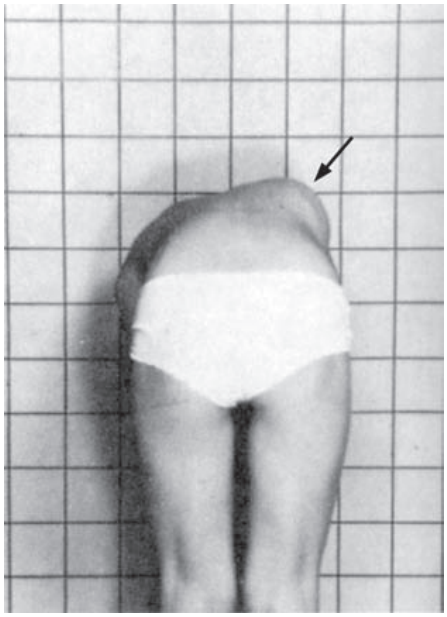

FIGURE 17.18. Scoliosis.

III. RIBS

A. Development in general. Ribs develop from costal processes, which form at all vertebral levels. However, only in the thoracic region do the costal processes grow into ribs.

B. Clinical considerations

1. **Accessory lumbar ribs** are the most common.
2. Accessory cervical ribs
   a. These ribs are attached to the C7 vertebrae and may end either freely or attached to the thoracic cage.
   b. Accessory cervical ribs may put pressure on the lower trunk of the brachial plexus and subclavian artery, causing superior **thoracic outlet syndrome**.

IV. STERNUM

A. Development in general. The sternum develops from two sternal bars that form in the ventral body wall independent of the ribs and clavicle. The sternal bars fuse with each other in a cranial–caudal direction to form the **manubrium, body**, and **xiphoid process** by week 8.

B. Clinical considerations

1. **Sternal cleft** occurs when the sternal bars do not fuse completely. It is fairly common and, if small, is generally of no clinical significance.
2. **Pectus excavatum (funnel chest)** is the most common chest anomaly, consisting of a depression of the chest wall that may extend from the manubrium to the xiphoid process. In addition to the cosmetically challenging appearance, these individuals demonstrate cardiopulmonary restriction, drooped shoulders, protuberant abdomen, and scoliosis such that early surgical intervention is generally recommended.

V. BONES OF THE LIMBS AND LIMB GIRDLES

A. Development in general

1. The bones of the limb and limb girdles develop from condensations of lateral plate mesoderm within the limb buds.
2. The limb buds are visible at week 4 of development; the upper limb appears first.
3. The limbs are well differentiated at week 8.
4. The limb tip contains the **apical ectodermal ridge**, which exerts an inductive influence on limb growth and development.

B. Clinical considerations

1. **Amelia** (an absence of one or two extremities) may result from the use of the teratogen **thalidomide**.
2. **Polydactyly** is an autosomal dominant disorder that is characterized by the presence of extra digits on the hands and feet.
3. **Syndactyly** (webbed fingers or toes), the most common limb anomaly, results from failure of the hand or foot webs to degenerate between the digits.
4. **Holt-Oram syndrome (heart–hand syndrome)** is an autosomal dominant disorder associated with chromosome 12 that causes anomalies of the upper limb and heart.

VI. OSTEOGENESIS

Osteogenesis occurs through the conversion of preexisting connective tissue (mesoderm) into bone. This process is called **ossification**. During development, two types of ossification occur:

A. Intramembranous ossification

1. Intramembranous ossification occurs in the embryo when **mesoderm** condenses into sheets of highly vascular connective tissue, which then **directly** forms a primary ossification center.
2. Bones that form via intramembranous ossification are the: **frontal bone, parietal bones, intraparietal part of occipital bone, maxilla, and zygomatic bone, squamous part of temporal bone, palatine, vomer, and mandible**.

B. Endochondral ossification

1. Endochondral ossification occurs in the embryo when **mesoderm** first forms a hyaline cartilage model, which then develops a primary ossification center at the diaphysis.
2. Bones that form via endochondral ossification are the: **ethmoid bone, sphenoid bone, petrous and mastoid parts of the temporal bone, basilar part of the occipital bone, incus, malleus, stapes, styloid process, hyoid bone, bones of the limbs, limb girdles, vertebrae, sternum, and ribs**.

VII. GENERAL SKELETAL ABNORMALITIES

A. Achondroplasia (AC; Figure 17.19) is an autosomal dominant genetic disorder caused by a mutation in the ***FGFR3* gene** on **chromosome 4p16**, which encodes for **fibroblast growth factor receptor 3**. The mutation results in constitutive activation of FGFR3 (i.e., a **gain-of-function mutation**). Approximately 80% of AC cases are not inherited but result from a de novo mutation that occurs during spermatogenesis in the unaffected advanced-aged father. Chances of AC increase with increasing paternal age. **Pathological features include** changes at the epiphyseal growth plate, where the zones of proliferation and hypertrophy are narrow and disorganized, and eventual growth of horizontal struts of bone into the growth plate, "sealing" the bone and thereby preventing bone growth. **Clinical features include** short stature, proximal shortening of arms and legs with redundant skin folds, limitation of elbow extension, trident configuration of hands, bowlegs, thoracolumbar gibbus in infancy, exaggerated lumbar lordosis, large head with frontal bossing, and midface hypoplasia. The photograph (Figure 17.19) shows a man with achondroplasia. Note the lordotic curve.

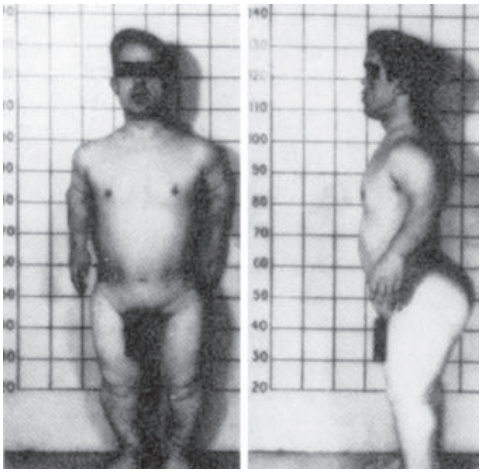

FIGURE 17.19. Achondroplasia.

B. Marfan syndrome (MS; Figure 17.20) is an autosomal dominant genetic disorder caused by a mutation in the ***FBN1* gene** on **chromosome 15q21.1**, which encodes for the **fibrillin** protein, which is an essential component of **elastic fibers. Clinical features include** unusual height, exceptionally long, thin limbs, pectus excavatum ("hollow chest"), ectopia lentis (dislocation of the lens), severe near-sightedness (myopia), and dilation or dissection of the aorta at the level of the sinuses of Valsalva, which may lead to cardiomyopathy or even a rupture of the aorta, dural ectasia, and mitral valve prolapse. The photograph (Figure 17.20) shows a boy with MS. Note the deformities of the sternum and spine.

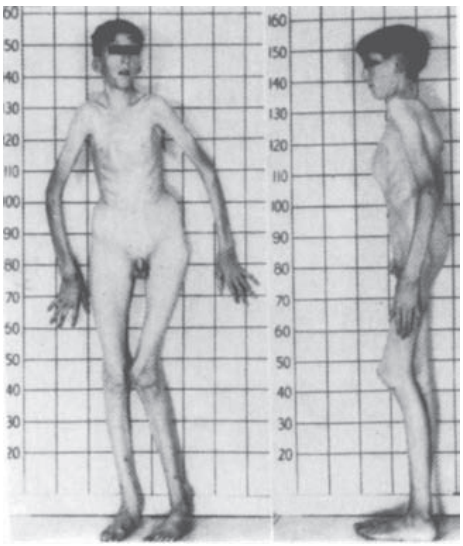

FIGURE 17.20. Marfan syndrome.

C. Osteogenesis imperfecta types I–IV (OI; Figure 17.21) are autosomal dominant genetic disorders caused by a mutation in the ***COL1A1* gene** on **chromosome 17q21.3-q22**, which encodes for the **collagen a-1(I) chain protein**, or the *COL1A2* **gene** on **chromosome 7q22.1**, which encodes for **collagen a-2(I) chain protein**. OI is a group of disorders with a continuum ranging from perinatal lethality → severe skeletal deformities → nearly asymptomatic individuals. **Clinical features include** extreme bone fragility with spontaneous fractures, short stature with bone deformities, gray or brown teeth, blue sclera of the eye, and progressive postpubertal hearing loss. Milder forms of OI may be confused with child abuse. Severe forms of OI are fatal in utero or during the early neonatal period. The radiograph (Figure 17.21) shows an infant with OI. Note the multiple bone fractures of the upper and lower limbs, resulting in an accordion-like shortening of the limbs.

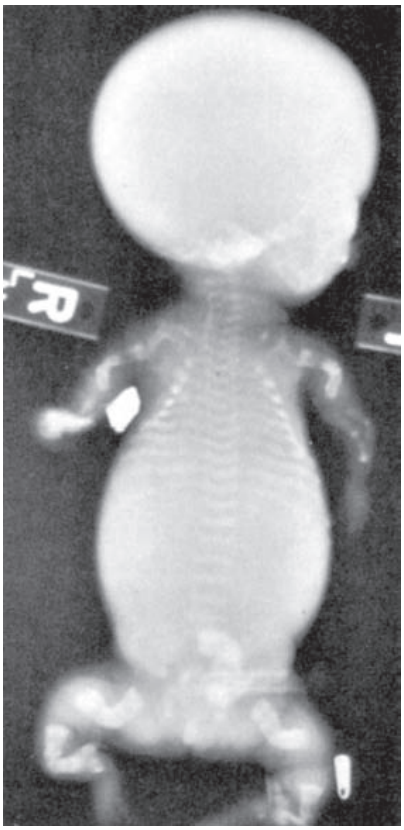

FIGURE 17.21. An infant with osteogenesis imperfecta (OI).

D. **Acromegaly (Figure 17.22)** results from hyperpituitarism. It is characterized by a large jaw, enlarged hands and feet, and sometimes by gigantism. The upper photograph (Figure 17.22) shows a 22-year-old man before he developed telltale signs of acromegaly. The lower photograph (Figure 17.22) shows the same man at 39 years old with the distinct facial appearance of acromegaly.

E. **Cretinism** occurs when there is a deficiency in fetal thyroid hormone (triiodothyronine [T3] and thyroxine [T4]) and/or thyroid agenesis. Cretinism results in growth retardation, skeletal abnormalities, mental retardation, and neurological disorders. It is rare except in areas where there is a lack of iodine in water and soil.

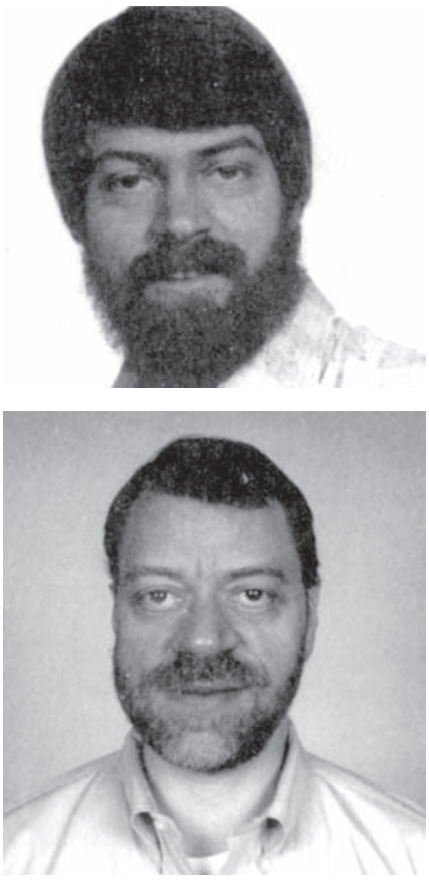

FIGURE 17.22. Acromegaly.

Study Questions for Chapter 17

1. Accessory ribs are most commonly found attached to the

(A) cervical vertebrae
(B) thoracic vertebrae
(C) lumbar vertebrae
(D) manubrium
(E) sternebrae

2. The anterior fontanelle is usually closed by

(A) birth
(B) age 6 months
(C) age 18 months
(D) age 2 years
(E) age 5 years

3. The condition where the pedicles of the vertebral arches fail to fuse with the vertebral body is called

(A) block vertebrae
(B) cleft vertebrae
(C) hemivertebrae
(D) spondylolisthesis
(E) spina bifida occulta

4. During an ultrasound examination, numerous fractures of the long bones of the fetus are observed. This condition is called

(A) achondroplasia
(B) osteogenesis imperfecta
(C) Marfan syndrome
(D) cretinism
(E) acromegaly

5. A female newborn presents with a square-shaped skull with a short occipital–frontal diameter. Premature closure of which of the following sutures is the most likely cause of this finding?

(A) Sphenofrontal
(B) Sphenoparietal
(C) Lambdoidal
(D) Sagittal
(E) Coronal

Answers and Explanations

1. **C.** Accessory ribs are most commonly attached to lumbar vertebrae. When present (incidence 0.5%–1%), a cervical rib is usually attached to the seventh cervical vertebra. Cervical ribs may compress the brachial plexus and subclavian vessels and cause superior thoracic outlet syndrome.
2. **D.** The anterior fontanelle is usually closed by 2 years of age; the posterior and sphenoid fontanelles are usually closed by the end of 6 months of age.
3. **D.** When the pedicles fail to fuse with the vertebral body, a condition called spondylolisthesis results. This allows the vertebral body to move anterior with respect to the vertebrae below it, causing lordosis.
4. **B.** Osteogenesis imperfecta is a deficiency of type I collagen and results in spontaneous fractures of fetal bones and blue sclera of the eye.
5. **E.** Brachycephaly is the premature closure of the coronal sutures, which leads to a square-shaped skull with a short occipital–frontal diameter.

chapter 18

Muscular System

I. SKELETAL MUSCLE

A. Molecular events

1. **Mesodermal (mesenchymal) cells** within somites commit to a muscle-forming cell line to form **myogenic cells**.
2. Myogenic cells undergo mitosis, which is stimulated by **FGF** (fibroblast growth factor) and **TGF-b** (transforming growth factor).
3. **Pax-3** and **myf-5** stimulate myogenic cells to express MyoD (a helix–loop–helix transcription factor).
4. MyoD binds to the **E box** (CANNTG) on DNA, which stops mitosis of the myogenic cells and switches on **muscle-specific genes** to form **postmitotic myoblasts**.
5. Myoblasts synthesize **actin** and **myosin** while they fuse with each other to form multinucleated **myotubes**.
6. Myotubes synthesize **actin, myosin, troponin, tropomyosin**, and **other muscle proteins**. These proteins aggregate into **myofibrils**, at which stage the cells are called **muscle cells (or fibers).**
7. Because muscle cells are postmitotic, further growth occurs through **satellite cells**, which operate by poorly understood mechanisms.

B. Paraxial mesoderm

1. Paraxial mesoderm is a thick plate of mesoderm on each side of the midline.
2. The paraxial mesoderm organizes into segments known as **somitomeres**, which form in a craniocaudal sequence.
3. **Somitomeres 1–7** do not form somites but contribute mesoderm to the head and neck region (pharyngeal arches).
4. **The remaining somitomeres** condense in a craniocaudal sequence to form 42–44 pairs of somites of the trunk region.
5. The somites closest to the caudal end eventually disappear, to give a final count of approximately **35 pairs of somites**.
6. Somites differentiate into the **sclerotome** (cartilage and bone component), **myotome** (muscle component), and **dermatome** (dermis of skin component).

C. Head and neck musculature

1. **Head and neck musculature** is derived from somitomeres 1–7 of the head and neck region, which participate in the formation of the pharyngeal arches.
2. **Extraocular muscles** are derived from somitomeres 1–3 and 5. Somitomeres 1–3 are called **preotic myotomes**. The extraocular muscles are innervated by cranial nerve (CN) III, CN IV, and CN VI.
3. **Tongue muscles** are derived from **occipital myotomes**. The tongue muscles are innervated by CN XII.

D. Trunk musculature (Figure 18.1)

1. **Trunk musculature** is derived from myotomes in the trunk region. Each myotome partitions into a dorsal **epimere** and a ventral **hypomere**.
   - **a. Epimere**
     - **i. The epimere** develops into the extensor muscles of the neck and vertebral column (e.g., erector spinae).
     - **ii.** The epimere is innervated by dorsal rami of spinal nerves.
   - **b. Hypomere**
     - **i. The hypomere** develops into the scalene, prevertebral, geniohyoid, infrahyoid, intercostal, abdominal muscles, lateral and ventral flexors of the vertebral column, quadratus lumborum, and pelvic diaphragm.
     - **ii.** The hypomere is innervated by **ventral rami of spinal nerves**.

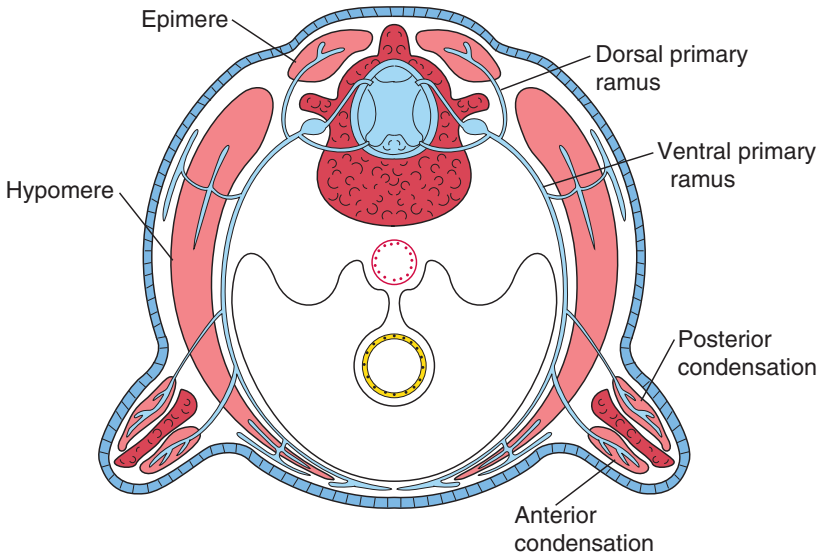

FIGURE 18.1. Trunk and limb musculature. This drawing of a transverse section through the thorax and limb bud shows the muscles of the epimere (*light red*), hypomere (*light red*), and the limb bud (*light red*). The limb bud musculature develops from mesoderm of various myotomes. The epimeric muscles are innervated by dorsal primary rami (*blue*), and the hypomeric and limb muscles are innervated by ventral primary rami (*blue*) of spinal nerves. Vertebrae and limb bones = dark red ; surface ectoderm = blue; spinal cord=blue; endoderm of gut tube=yellow

E. Limb musculature

1. Limb musculature is derived from myotomes (somites) in the upper limb bud region and lower limb bud region.
2. This mesoderm migrates into the limb bud and forms a **posterior condensation** and an **anterior condensation**.
   - **a.** Posterior condensation
     - **i.** The posterior condensation develops into the extensor and supinator musculature of the upper limb and the extensor and abductor musculature of the lower limb.
   - **b.** Anterior condensation
     - **i.** The anterior condensation develops into the flexor and pronator musculature of the upper limb and the flexor and adductor musculature of the lower limb.

II. SMOOTH MUSCLE

Smooth muscle of the gastrointestinal tract and the tunica media of blood vessels is derived from **mesoderm**.

III. CARDIAC MUSCLE

Cardiac muscle is derived from **mesoderm** that surrounds the endocardium of the primitive heart tube and becomes the myocardium.

IV. CLINICAL CONSIDERATIONS

A. Prune belly syndrome (Figure 18.2) occurs when the **abdominal musculature** is absent or very hypoplastic, most likely involving cells of the hypomere. The photograph (Figure 18.2) shows an infant with prune belly syndrome. The absence of the abdominal musculature is apparent, causing a widening of the flanks.

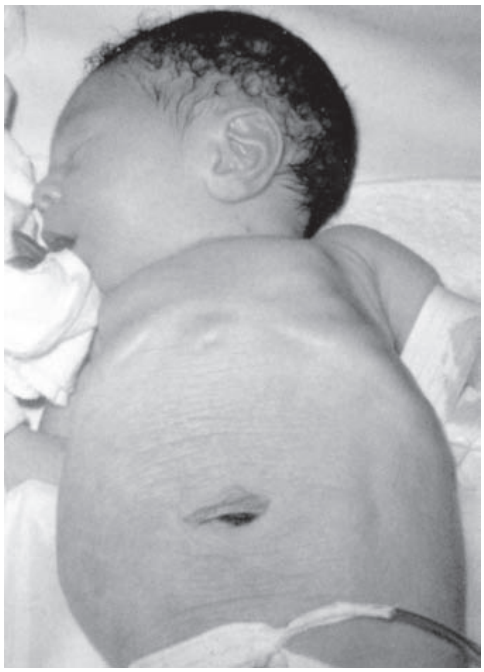

FIGURE 18.2. Prune belly syndrome.

B. Poland syndrome (Figure 18.3) is a relatively uncommon chest anomaly characterized by the **partial or complete absence of the pectoralis major muscle**. In addition, these individuals may demonstrate partial agenesis of the ribs and sternum, mammary gland aplasia, or absence of the latissimus dorsi and serratus anterior muscles. The photograph (Figure 18.3) shows an infant with Poland syndrome. The absence of the right pectoralis major muscle (*arrow*) and loss of the right anterior axillary fold are apparent.

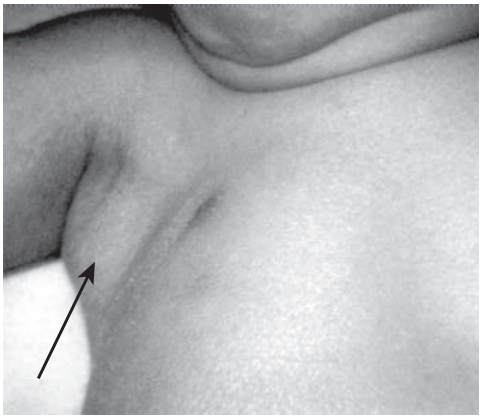

FIGURE 18.3. Poland syndrome.

C. Congenital torticollis (wryneck; Figure 18.4) occurs when the **sternocleidomastoid muscle** is abnormally shortened, causing rotation and tilting of the head. It may be caused by injury to the sternocleidomastoid muscle during childbirth, formation of a hematoma, and eventual fibrosis of the muscle. The photograph (Figure 18.4) shows an infant with congenital torticollis. Note the fibrous mass (*arrow*) in the right sternocleidomastoid muscle.

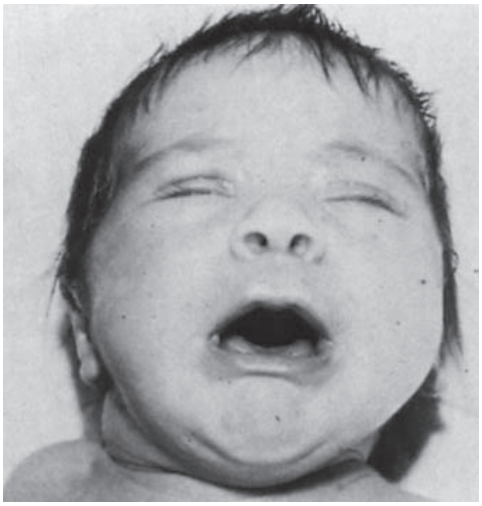

FIGURE 18.4. Congenital torticollis (wryneck).

D. Duchenne muscular dystrophy (DMD; Figure 18.5) is an X-linked recessive genetic disorder caused by a mutation in the ***DMD* gene** on chromosome Xp21.2, which encodes for dystrophin. Dystrophin anchors the cytoskeleton (actin) of skeletal muscle cells to the extracellular matrix through a transmembrane protein (α-dystroglycan and β-dystroglycan) and stabilizes the cell membrane. A mutation of the *DMD* gene destroys the ability of dystrophin to anchor actin to the extracellular matrix. **Clinical features include** progressive muscle weakness and wasting, and death occurs as a result of cardiac or respiratory failure, usually in the late teens or 20s. The immunofluorescent light micrographs (Figure 18.5) show staining for dystrophin located at the periphery of skeletal muscle cells in normal individuals and complete absence of staining in a DMD patient.

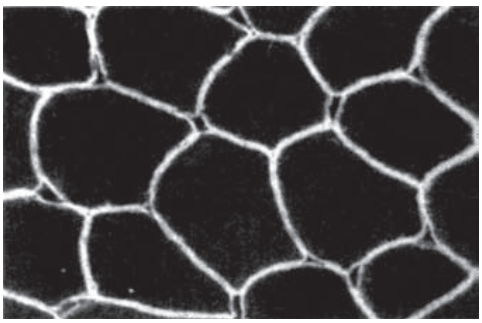

Normal

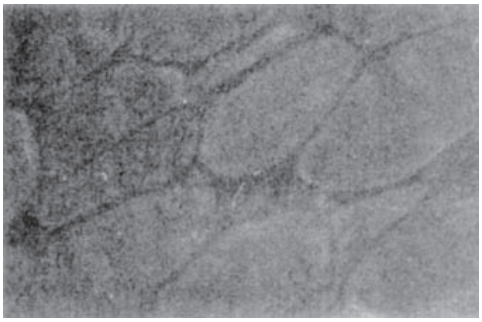

DMD

FIGURE 18.5. Duchenne muscular dystrophy (DMD).

Study Questions for Chapter 18

1. The extrinsic eye muscles develop from which of the following?

(A) Cervical somites
(B) Epimere
(C) Hypomere
(D) Occipital somites
(E) Preotic somites

2. The tongue muscles develop from which of the following?

(A) Cervical somites
(B) Epimere
(C) Hypomere
(D) Occipital somites
(E) Preotic somites

3. The biceps brachii muscle develops from which of the following?

(A) Hypomere
(B) Epimere
(C) Anterior condensation
(D) Posterior condensation
(E) Preotic somites

4. The biceps femoris muscle develops from which of the following?

(A) Hypomere
(B) Epimere
(C) Anterior condensation
(D) Posterior condensation
(E) Preotic somites

Answers and Explanations

1. **E.** The extrinsic eye muscles arise from the preotic somites (myotomes) found near the prochordal plate. Recent research indicates that the extrinsic eye muscles are derived from somitomeres 1–3, and 5.
2. **D.** The tongue muscles (intrinsic and extrinsic) arise from the occipital somites (myotomes).
3. **C.** Because the biceps brachii muscle is a flexor of the antebrachium (forearm), it develops from the anterior condensation of myotomic mesoderm.
4. **C.** Because the biceps femoris muscle is a flexor of the leg, it develops from the anterior condensation of myotomic mesoderm.

chapter 19

Upper Limb

I. OVERVIEW OF DEVELOPMENT

Lateral plate mesoderm migrates into the limb bud and condenses along the central axis to eventually form the **vasculature** and **skeletal** components of the upper limb. **Mesoderm from the somites** migrates into the limb bud and condenses to eventually form the **musculature** component of the upper limb.

A. Apical ectodermal ridge (AER)

1. The AER is a ridge of thickened **ectoderm** at the apex of the limb bud.
2. The AER produces **FGF** (fibroblast growth factor), which interacts with the underlying mesoderm to promote limb outgrowth by stimulating mitosis and preventing terminal differentiation of the underlying mesoderm.
3. The AER expresses the ***Wnt7*** **gene**, which organizes the limb bud along the dorsal–ventral axis.

B. Zone of polarizing activity (ZPA)

1. The ZPA consists of **mesodermal** cells located at the base of the limb bud.
2. The ZPA produces **sonic hedgehog**, which organizes the limb bud along the anterior–posterior axis and patterns the digits.
3. Sonic hedgehog activates the ***BMP*** **(bone morphogenetic protein) gene** and the ***Hoxd-9, Hoxd-10, Hoxd-11, Hoxd-12,*** **and** ***Hoxd-13*** **genes**.
4. **Retinoic acid** also plays a significant role in limb polarization.

C. Digit formation

1. Digit formation occurs as a result of selected **apoptosis (cell death)** within the AER such that five separate AER regions remain at the tips of the future digits.
2. The exact mechanism is poorly understood, although **BMP, Msx-1**, and **retinoic acid receptor** may play a role.

II. VASCULATURE (FIGURE 19.1)

A. The **aortic arch 4** forms the proximal part of the right subclavian artery.

B. The **seventh intersegmental artery** forms the distal part of the right subclavian artery and the entire left subclavian artery.

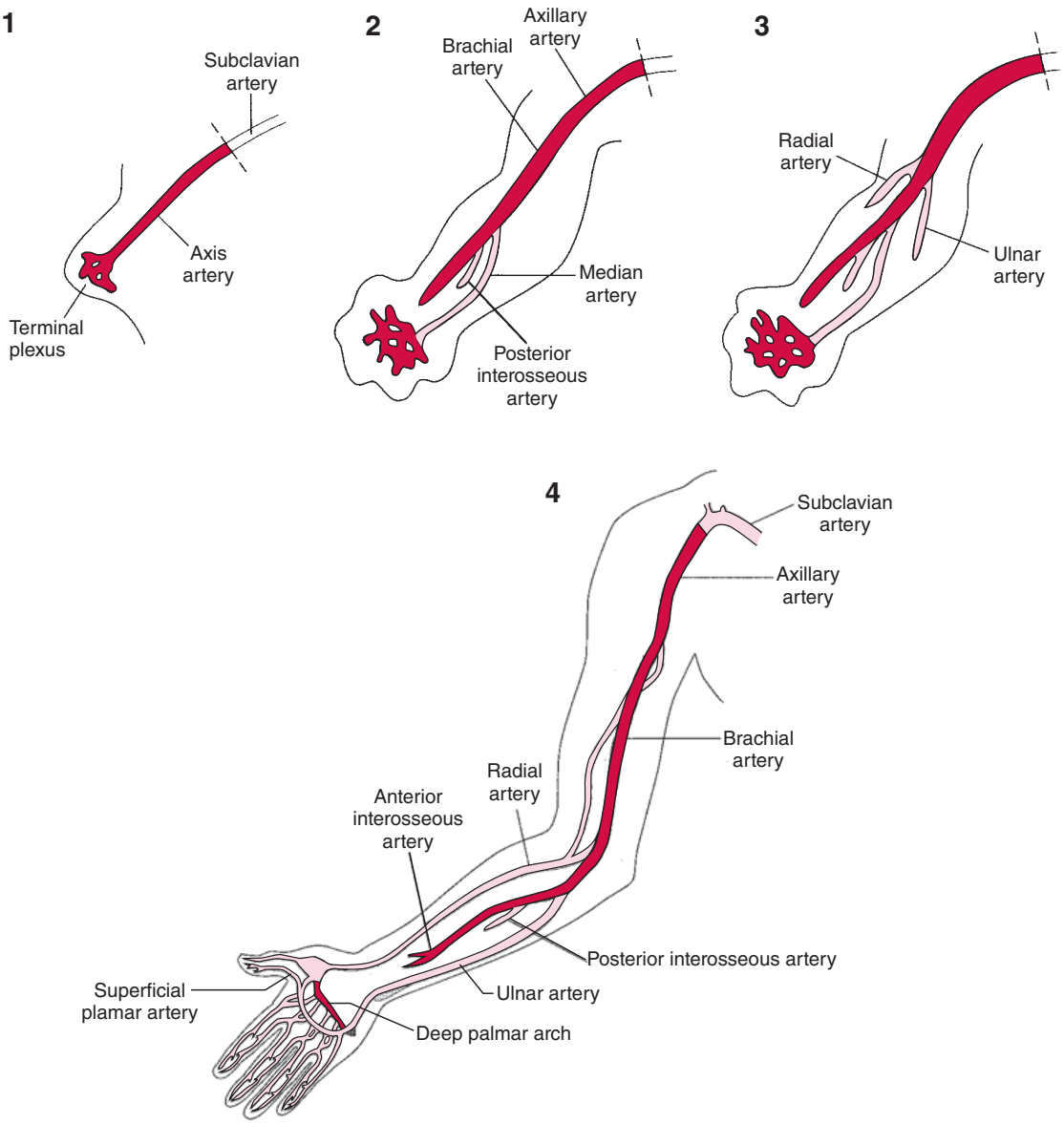

FIGURE 19.1. Development of arteries of the upper limb. **(1–3)** Early limb bud. The earliest arterial supply of the upper limb bud is the axis artery (*dark red*) and terminal plexus (*dark red*). The first branches of the axis artery are the posterior interosseous artery (*light red*) and the median artery (*light red*). The last branches of the axis artery are the radial artery (*light red*) and ulnar artery (*light red*). **(4)** Adult upper limb. The axis artery persists as the axillary artery, brachial artery, anterior interosseous artery, and deep palmar arch (*dark red*).

C. The **subclavian artery (right and left)** continues into the limb bud as the **axis artery**, which ends in a **terminal plexus** near the tip of the limb bud.

D. The **terminal plexus** participates in the formation of the **deep palmar arch** and the **superficial palmar arch**.

E. The **axis artery** initially sprouts the **posterior interosseous artery** and the **median artery**. The median artery is reduced to an unnamed vessel in the adult.

F. The axis artery later sprouts the **radial artery** and **ulnar artery**.

G. The axis artery persists in the adult as the **axillary artery, brachial artery, anterior interosseous artery, and deep palmar arch**.

III. MUSCULATURE

The upper limb bud site lies opposite somites C4–C8, T1, and T2. During week 5, mesoderm from these somites (myotomes) migrates into the limb bud and forms a **posterior condensation** and an **anterior condensation**. The mesoderm of these condensations differentiates into myoblasts. Then, the condensations split into anatomically recognizable muscles of the upper limb, although little is known about this process.

A. Posterior condensation

1. The **posterior condensation** gives rise to the following muscles: deltoid, supraspinatus, infraspinatus, teres minor, teres major, subscapularis, triceps brachii, anconeus, brachioradialis, extensor carpi radialis longus, extensor carpii radialis brevis, extensor digitorum, extensor digiti minimi, extensor carpii ulnaris, supinator, abductor pollicis longus, extensor pollicis brevis, extensor pollicis longus, and extensor indicis.
2. In general, the posterior condensation gives rise to the **extensor and supinator musculature**.

B. Anterior condensation

1. The **anterior condensation** gives rise to the following muscles: biceps brachii, brachialis, coracobrachialis, pronator teres, flexor carpii radialis, palmaris longus, flexor carpii ulnaris, flexor digitorum superficialis, flexor digitorum profundus, flexor pollicis brevis, flexor pollicis longus, pronator quadratus, abductor pollicis brevis, opponens pollicis, adductor pollicis, abductor digiti minimi, flexor digiti minimi brevis, opponens digiti minimi, lumbricales, and dorsal and palmar interossei.
2. In general, the anterior condensation gives rise to the **flexor and pronator musculature**.

IV. NERVES: THE BRACHIAL PLEXUS (FIGURE 19.2)

A. Local molecular messages produced at the base of the limb bud guide the early nerve fibers into the limb bud.

B. The muscles do not provide any specific target messages to the ingrowing nerve fibers.

C. **Ventral primary rami from C5–C8 and T1** arrive at the base of the limb bud and join in a specific pattern to form the **upper trunk, middle trunk**, and **lower trunk anterior divisions**.

D. Posterior divisions grow into the posterior condensation of mesoderm and join to form the **posterior cord**.

E. Anterior divisions grow into the anterior condensation of mesoderm and join to form the **medial cord** and **lateral cord**.

F. With further development of the limb musculature, the posterior cord branches into the **axillary nerve (C5, C6)** and **radial nerve (C5–C8, T1)**, thereby innervating all the muscles that form from the posterior condensation.

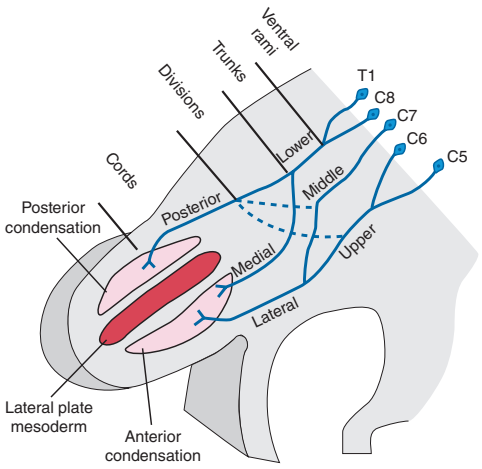

FIGURE 19.2. Muscle and nerve development of the upper limb.

G. With further development of the limb musculature, the medial cord and lateral cord branch into the musculocutaneous **nerve (C5–C7), ulnar nerve (C8, T1)**, and **median nerve (C5–C8, T1)**, thereby innervating all the muscles that form from the anterior condensation.

H. The diagram (Figure 19.2) shows the muscle and nerve development of the upper limb. Mesoderm from the somites (myotomes) migrates into the limb bud and forms a posterior and anterior condensation (*light red*). Ventral primary rami from C5–T1 (*blue*) leave the neural tube and undergo extensive rearrangement into upper, middle, and lower trunks. Each trunk divides into posterior (blue; *dotted lines*) and anterior (blue; *solid lines*) divisions. The posterior divisions selectively grow into the posterior condensation and form the posterior cord. The anterior divisions selectively grow into the anterior condensation and form the medial and lateral cords. Lateral plate mesoderm = dark red

V. ROTATION OF THE UPPER LIMB (FIGURE 19.3)

A. The upper limb buds appear at week 4 as small bulges oriented in a **coronal plane**.

B. The upper limb buds undergo a horizontal movement in week 6 so that they are now oriented in a **sagittal plane**.

C. The upper limbs **rotate laterally 908** during weeks 6–8 such that the elbow points posteriorly, the extensor compartment lies posterior, and the flexor compartment lies anterior.

D. This rotation causes the originally straight segmental pattern of innervation (dermatomes) to be somewhat modified in the adult.

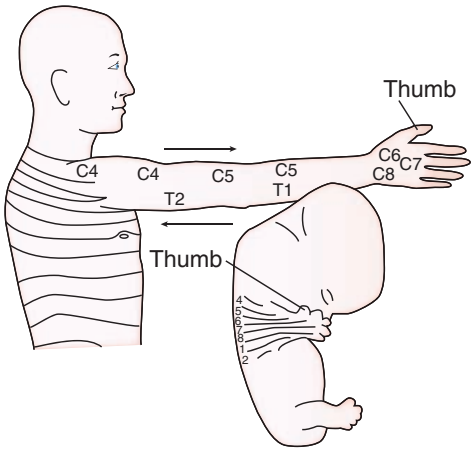

FIGURE 19.3. Dermatome pattern in the adult upper limb.

E. The drawing (Figure 19.3) shows the dermatome pattern in the adult upper limb. The 90° lateral rotation of the upper limb bud alters the originally straight segmental pattern of innervation in the embryo (i.e., twisted in a spiral"). However, an orderly dermatome pattern exists in the adult if the upper limb is positioned in the sagittal plane with the thumb pointing superiorly (as shown). The dermatomes from C4 are counted distally down the superior border of the upper limb (*arrow*) to C7 at the middle finger and then back proximally up the inferior border of the upper limb (*arrow*) to T2. Note the position of the thumb.

VI. SKELETAL

The **lateral plate mesoderm** forms the **scapula, clavicle, humerus, radius, ulnar, carpals, metacarpals**, and **phalanges**. All the bones of the upper limb undergo endochondral ossification. However, the clavicle undergoes both membranous and endochondral ossification. The **timing of bone formation** follows this time course:

A. Weeks 5, 6, and 7–9 (Figure 19.4)

1. At week 5, the lateral plate mesoderm within the limb bud condenses.
2. At week 6, the condensed mesoderm chondrifies to form a hyaline cartilage model of the upper limb bones.
3. At weeks 7–9, the primary ossification centers are seen in the clavicle, humerus, radius, and ulnar bones. The clavicle is the first bone in the entire body to ossify.
4. The drawing (Figure 19.4) shows early bone formation in the upper limb. At week 5, lateral plate mesoderm condenses (hatched). At week 6, the hyaline cartilage (light blue shading) model of future bones forms. At weeks 7–9, primary ossification centers within the diaphysis appear such that bone (dark blue shading) forms (osteogenesis).

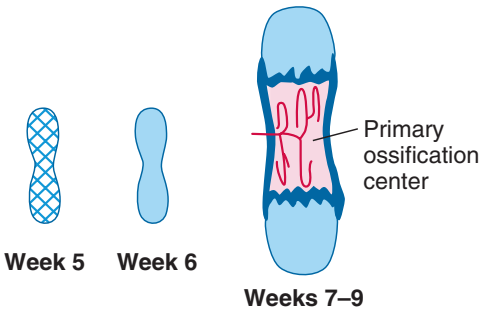

FIGURE 19.4. Early bone formation in the upper limb.

B. Week 9 to birth (Figure 19.5)

1. Primary ossification centers are seen in the scapula, metacarpals, and phalanges.
2. The diagram and radiograph (Figure 19.5) show bone formation in the upper limb at birth. The diaphysis consists of bone (*dark blue shading*), whereas the epiphysis remains hyaline cartilage (*light blue shading*). This is important to note when interpreting radiographs of newborns. The radiograph of a newborn at the shoulder region (1 = humerus, 2 = acromion, 3 = clavicle) shows the portion of the hyaline cartilage model that has been replaced by radiodense bone (*white*). Note that the epiphyseal end of the humerus (*white arrow*) is still hyaline cartilage at birth and therefore will appear radiolucent (*dark*).

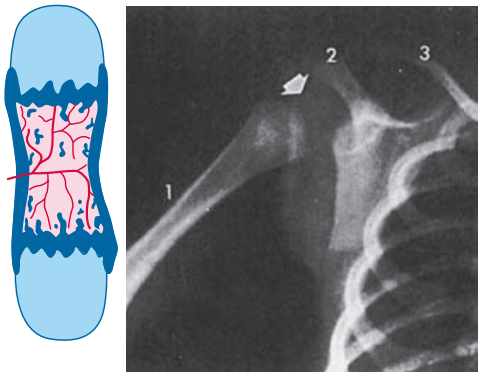

FIGURE 19.5. Bone formation in the upper limb at birth.

C. Childhood (Figure 19.6)

1. Secondary ossification centers form in the epiphyseal ends. All carpal bones begin ossification.
2. The diagram and radiograph (Figure 19.6) show bone formation in the upper limb during childhood. During childhood, secondary ossification centers form in the epiphyseal ends of the bones. During childhood and adolescence, the growth in length of long bones occurs at the epiphyseal growth plate. Note the radiograph of a 6-year-old child at the shoulder region (1 = humerus, 2 = acromion, 3 = clavicle). Because secondary ossification centers are present within the epiphyseal ends of the humerus, the head of the humerus is now radiodense (*white arrow*), and the epiphyseal growth plate (*arrowheads*) where hyaline cartilage is present remains radiolucent (dark). This is not to be confused with a bone fracture.

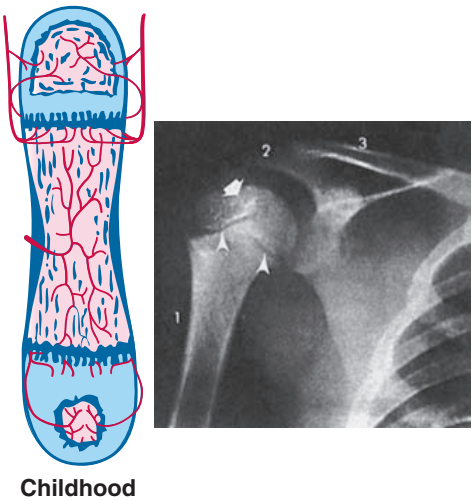

FIGURE 19.6. Bone formation in the upper limb during childhood.

Study Questions for Chapter 19

1. Which of the following arteries is one of the first branches to form from the axis artery?

(A) Radial artery
(B) Ulnar artery
(C) Axillary artery
(D) Median artery
(E) Brachial artery

2. The humerus develops from which of the following?

(A) Somite mesoderm
(B) Lateral plate mesoderm
(C) Intermediate mesoderm
(D) Extraembryonic mesoderm
(E) Sclerotome mesoderm

3. The long head of the triceps muscle develops from which of the following?

(A) Posterior condensation
(B) Anterior condensation
(C) Lateral plate mesoderm
(D) Extraembryonic mesoderm
(E) Sclerotome mesoderm

4. Which of the following muscles will the lateral cord of the brachial plexus innervate?

(A) Triceps
(B) Supinator
(C) Extensor carpi ulnaris
(D) Extensor digitorum
(E) Biceps brachii

5. During weeks 6–8, the upper limb will rotate

(A) Medially 90°
(B) Laterally 90°
(C) Medially 180°
(D) Laterally 180°
(E) No rotation occurs

Answers and Explanations

1. **D.** The median artery is one of the first branches to form from the axis artery. In the adult, the median artery does not persist and is probably reduced to a small unnamed vessel. This is why the median nerve does not have an accompanying artery in the adult like the ulnar nerve (ulnar artery) and radial nerve (radial artery).
2. **B.** All bones of the upper limb form from lateral plate mesoderm that condenses alone the central axis of the upper limb bud.
3. **A.** Somite mesoderm migrates into the limb bud and forms two condensations. The posterior condensation of the upper limb gives rise to the extensors of the upper limb, which attain a posterior location in the adult because of the lateral rotation of 90°.
4. **E.** One of the nerves that form from the lateral cord of the brachial plexus is the musculocutaneous nerve. The musculocutaneous nerve will innervate muscles derived from the anterior condensation (flexors). The biceps brachii muscle is a flexor at the elbow joint. Note that the biceps brachii muscle and the musculocutaneous nerve are related embryologically to the anterior condensation and anterior divisions (which form the lateral cord) and in the adult are located anterior. This occurs because of the lateral rotation of 90°.
5. **B.** The upper limb rotates laterally 90° so that the elbows point posteriorly.

chapter 20

Lower Limb

I. OVERVIEW OF DEVELOPMENT

Lateral plate mesoderm migrates into the limb bud and condenses along the central axis to eventually form the **vasculature** and **skeletal** components of the lower limb. **Mesoderm from the somites** migrates into the limb bud and condenses to eventually form the **musculature** component of the lower limb.

A. Apical ectodermal ridge (AER)

1. The AER is a ridge of thickened **ectoderm** at the apex of the limb bud.
2. The AER produces **FGF** (fibroblast growth factor), which interacts with the underlying mesoderm to promote outgrowth by stimulating mitosis and preventing terminal differentiation of the underlying mesoderm.
3. The AER expresses the ***Wnt7* gene**, which organizes the limb bud along the dorsal–ventral axis.

B. Zone of polarizing activity (ZPA)

1. The ZPA consists of **mesodermal** cells located at the base of the limb bud.
2. The ZPA produces **sonic hedgehog**, which organizes the limb bud along the anterior–posterior polar axis and patterns the digits.
3. Sonic hedgehog activates the ***BMP* (bone morphogenetic protein) gene** and the ***Hoxd-9, Hoxd-10, Hoxd-11, Hoxd-12,* and *Hoxd-13* genes**.
4. **Retinoic acid** also plays a significant role in limb polarization.

C. Digit formation

1. Digit formation occurs as a result of selected **apoptosis (cell death)** within the AER such that five separate AER regions remain at the tips of the future digits.
2. The exact mechanism is poorly understood, although **BMP, Msx-1**, and **retinoic acid receptor** may play a role.

II. VASCULATURE (FIGURE 20.1)

A. The **umbilical artery** gives rise to the **axis artery** of the lower limb, which ends in a **terminal plexus** near the tip of the limb bud.

B. The **terminal plexus** participates in the formation of the **deep plantar arch**.

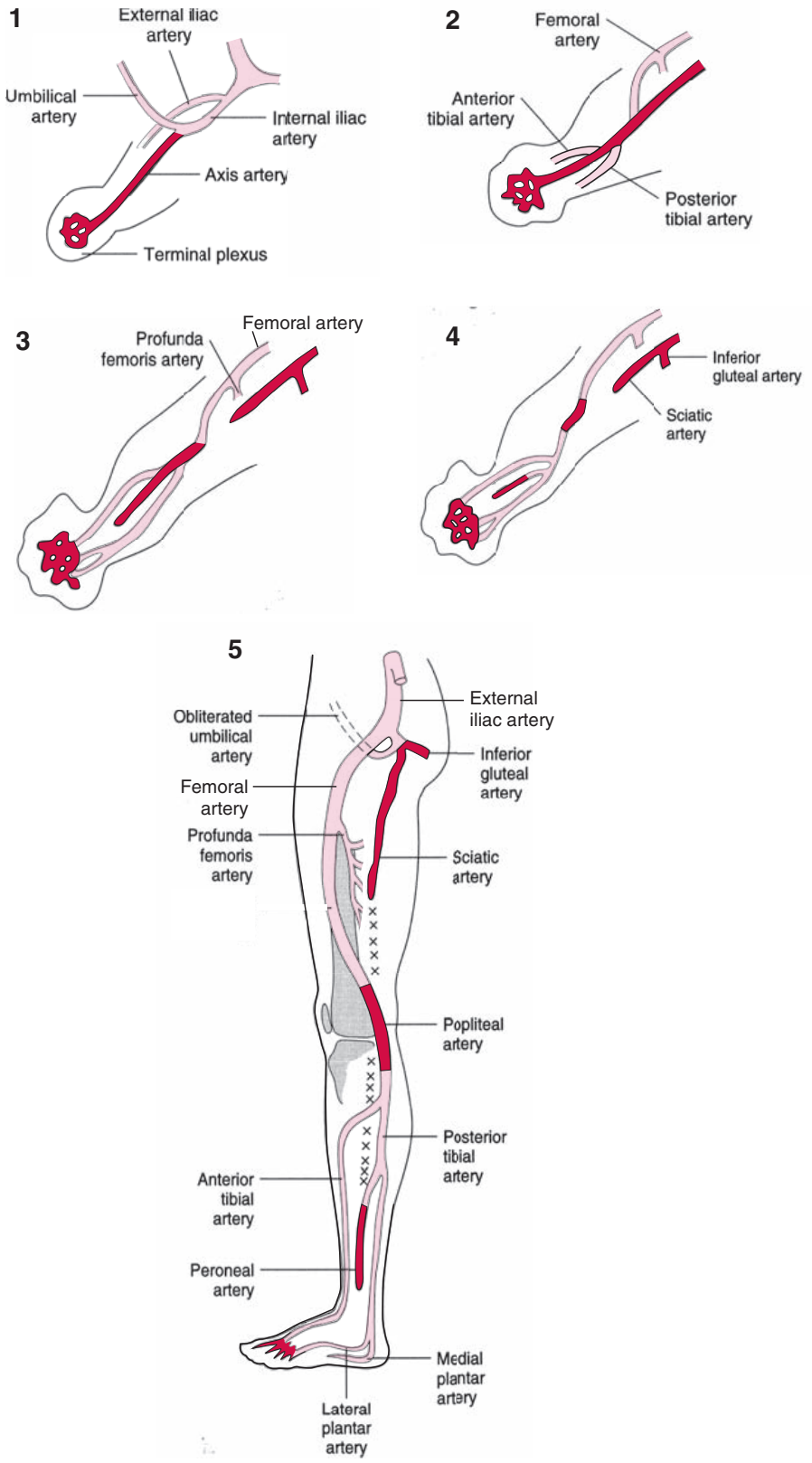

FIGURE 20.1. Development of arteries of the lower limb. **(1–4)** Early limb bud. The earliest arterial supply of the lower limb bud is the axis artery (*dark red*) and the terminal plexus (dark red), both of which arise from the umbilical artery. The axis artery gives off branches forming the anterior tibial artery (*light red*) and posterior tibial artery (*light red*). The axis artery then undergoes regression and remodeling in selected areas. The external iliac artery (light red) gives rise to the femoral artery (*light red*), which constitutes a separate second arterial channel in the lower limb.The femoral artery gives rise to the profunda femoris artery (*light red*). **(5)** Adult lower limb. In the adult, the axis artery persists as the inferior gluteal artery (*dark red*), sciatic artery (*dark red*), proximal part of the popliteal artery (*dark red*), and distal part of the peroneal artery (*dark red*). The X's indicate areas of regression.

C. The **axis artery** sprouts the **anterior tibial artery** (which continues as the **dorsalis pedis artery**) and the **posterior tibial artery** (which terminates as the **medial plantar artery** and **lateral plantar artery**).

D. Although most of the axis artery regresses, the axis artery ultimately persists in the adult as the **inferior gluteal artery, sciatic artery** (accompanying the sciatic nerve), **proximal part of the popliteal artery**, and **distal part of the peroneal artery**.

E. The **external iliac artery** gives rise to the **femoral artery** of the lower limb, which constitutes a separate second arterial channel into the lower limb that connects to the axis artery.

F. The femoral artery sprouts the **profunda femoris artery**.

III. MUSCULATURE

The lower limb bud site lies opposite somites L1–L5, S1, and S2. During week 5, mesoderm from these somites (myotomes) migrates into the limb bud and forms a **posterior condensation** and an **anterior condensation**. The mesoderm of these condensations differentiates into myoblasts. Then, the condensations split into anatomically recognizable muscles of the lower limb, although little is known about this process.

A. Posterior condensation

1. **The posterior condensation** gives rise to the following muscles: gluteus maximus, gluteus medius, gluteus minimus, piriformis, pectineus, iliacus, tensor fascia latae, sartorius, rectus femoris, vastus lateralis, vastus medialis, vastus intermedius, short head of biceps femoris, tibialis anterior, extensor hallucis longus, extensor digitorum longus, peroneus tertius, peroneus longus, peroneus brevis, extensor digitorum brevis, and extensor hallucis brevis.
2. In general, the posterior condensation gives rise to the **extensor and abductor musculature**.

B. Anterior condensation

1. The **anterior condensation** gives rise to following muscles: adductor longus, adductor brevis, adductor magnus, gracilis, obturator externus, obturator internus, superior and inferior gemelli, quadratus femoris, semitendinosus, semimembranosus, long head of biceps femoris, gastrocnemius, soleus, plantaris, popliteus, flexor hallucis longus, flexor digitorum longus, tibialis posterior, abductor hallucis, flexor digitorum brevis, abductor digiti minimi, quadratus plantae, lumbricales, flexor hallucis brevis, adductor hallucis, flexor digiti minimi brevis, and dorsal and plantar interossei.
2. In general, the anterior condensation gives rise to the **flexor and adductor musculature**.

IV. NERVES: THE LUMBOSACRAL PLEXUS (FIGURE 20.2)

A. Local cell biological messages produced at the base of the limb bud guide the early nerve fibers into the limb bud.

B. The muscles do not provide any specific target messages to the ingrowing nerve fibers.

C. **Ventral primary rami from L2–L5 and S1–S3** arrive at the base of the limb bud and divide into **posterior divisions** and **anterior divisions**.

D. Posterior divisions grow into the posterior condensation of mesoderm.

E. Anterior divisions grow into the anterior condensation of mesoderm.

F. With further development of the limb musculature, the posterior divisions branch into the **superior gluteal nerve (L4, L5, S1), inferior gluteal nerve (L5, S1, S2), femoral nerve (L2–L4)**, and **common peroneal nerve (L4, L5, S1, S2)**, thereby innervating all the muscles that form from the posterior condensation.

G. With further development of the limb musculature, the anterior divisions branch into the **tibial nerve (L4, L5, S1–S3)** and **obturator nerve (L2–L4)**, thereby innervating all the muscles that form from the anterior condensation.

H. The diagram (Figure 20.2) shows the muscle and nerve development of the lower limb. Mesoderm from somites (myotomes) migrates into the limb bud and forms a posterior and anterior condensation (light red). Ventral primary rami from L2–S3 (blue) leave the neural tube and divide into posterior (blue; *dotted lines*) and anterior (blue; *solid lines*) divisions. The posterior divisions selectively grow into the posterior condensation. The anterior divisions selectively grow into the anterior condensation. Lateral plate mesoderm = dark red

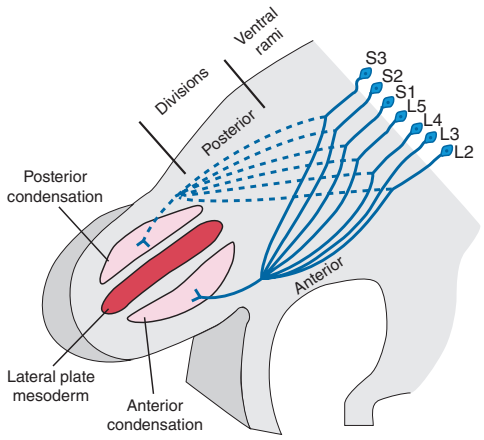

FIGURE 20.2. Muscle and nerve development of the lower limb.

V. ROTATION OF THE LOWER LIMB (FIGURE 20.3)

A. The lower limb buds appear in week 4 (about 4 days after the upper limb bud) as small bulges oriented in a **coronal plane**.

B. The lower limb buds undergo a horizontal movement in week 6 so that they are now oriented in a **sagittal plane**.

C. The lower limbs **rotate medially 90°** during weeks 6–8 such that the knee points anteriorly, the extensor compartment lies anterior, and the flexor compartment lies posterior.

D. This rotation causes the originally straight segmental pattern of innervation (dermatomes) to be somewhat modified in the adult.

E. Note that the upper limbs rotate laterally 90°, whereas the lower limbs rotate medially 90°, which sets up the following anatomical situations:

1. The flexor compartment of the upper limb is anterior, whereas the flexor compartment of the lower limb is posterior.
2. The extensor compartment of the upper limb is posterior, whereas the extensor compartment of the lower limb is anterior.
3. Flexion at the wrist joint is analogous to plantar flexion at the ankle joint.
4. Extension at the wrist joint is analogous to dorsiflexion at the ankle joint.

F. The drawing (Figure 20.3) shows the dermatome pattern in the adult lower limb. The 90° medial rotation of the lower limb bud alters the originally straight segmental pattern of innervation in the embryo (i.e., "twisted in a spiral") such that the dermatome pattern in the adult is altered. However, an orderly dermatome pattern exists in the adult if the lower limb is positioned in a parasagittal plane with the big toe pointing superiorly (as shown). The dermatomes from L1 are counted distally down the superior border of the lower limb (*arrow*) to L5 and then back proximally up the inferior border of the lower limb (*arrow*) to S2. Note the position of the big toe.

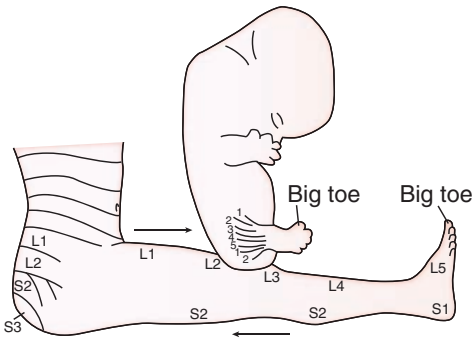

FIGURE 20.3. Dermatome pattern in the adult lower limb.

VI. SKELETAL

The **lateral plate mesoderm** forms the **ilium, ischium, pubis, femur, tibia, fibula, tarsals, metatarsals, and phalanges**. All bones of the lower limb undergo endochondral ossification. The **timing of bone formation** follows this time course:

A. Weeks 5, 6, and 7–9 (Figure 20.4)

1. At week 5, lateral plate mesoderm within the limb bud condenses.
2. At week 6, condensed mesoderm chondrifies to form a hyaline cartilage model of all the lower limb bones.
3. At weeks 7–9, primary ossification centers are seen in the femur and tibia.
4. The drawing (Figure 20.4) shows early bone formation in the lower limb. At week 5, lateral plate mesoderm condenses (hatched). At week 6, the hyaline cartilage (*light blue shading*) model of future bones forms. At weeks 7–9, primary ossification centers within the diaphysis appear such that bone (dark blue shading) forms (osteogenesis).

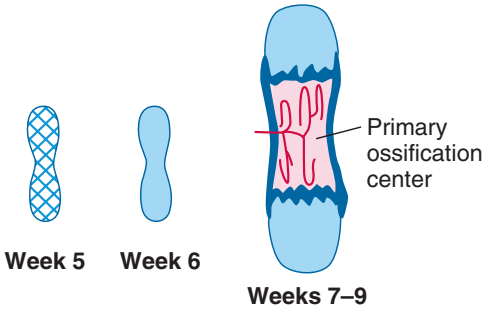

FIGURE 20.4. Early bone formation in the lower limb.

B. Week 9 to birth (Figure 20.5)

1. Primary ossification centers are seen in the ilium, ischium, pubis, fibula, calcaneus, talus, metatarsals, and phalanges.
2. The ossification of the calcaneus (weeks 16–20) is used medicolegally to establish maturity.
3. The diagram and radiograph (Figure 20.5) show bone formation in the lower limb at birth. The diaphysis consists of bone (dark blue shading), whereas the epiphysis remains hyaline cartilage (light blue shading). This is important to note when interpreting radiographs of newborns. The radiograph of a newborn at the hip region (1 = femur, 2 = ilium) shows the portions of the hyaline cartilage model that have been replaced by radiodense bone (white). Note the epiphyseal end of the femur (*white arrow*) is still hyaline cartilage at birth and therefore will appear radiolucent (dark).

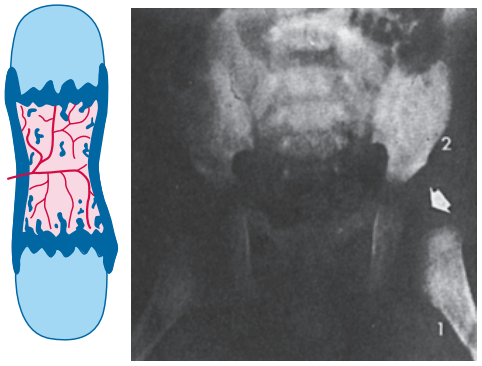

FIGURE 20.5. Bone formation in the lower limb at birth.

C. Childhood (Figure 20.6)

1. Secondary ossification centers form in the epiphyseal ends. The remaining tarsal bones begin ossification.
2. The diagram and radiograph (Figure 20.6) show bone formation in the lower limb during childhood. During childhood, secondary ossification centers form in the epiphyseal ends of the bones. During childhood and adolescence, the growth in length of long bones occurs at the epiphyseal growth plate. Note the radiograph of a 6-year-old child at the hip region (1 = femur, 2 = ilium). Because secondary ossification centers are present within the epiphyseal ends, the head of the femur is now radiodense (*white arrow*), and the epiphyseal growth plate (*arrowhead*) where hyaline cartilage is present remains radiolucent (dark). This is not to be confused with a bone fracture.

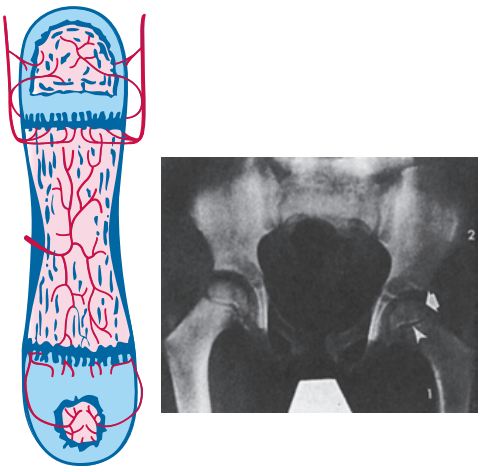

FIGURE 20.6. Bone formation in the lower limb during childhood.

Study Questions for Chapter 20

1. Which of the following arteries gives rise to the axis artery of the lower limb?

(A) External iliac artery
(B) Femoral artery
(C) Profunda femoris artery
(D) Umbilical artery
(E) Inferior gluteal artery

2. The femur develops from which of the following?

(A) Somite mesoderm
(B) Lateral plate mesoderm
(C) Intermediate mesoderm
(D) Extraembryonic mesoderm
(E) Sclerotome mesoderm

3. The rectus femoris muscle develops from which of the following?

(A) Posterior condensation
(B) Anterior condensation
(C) Lateral plate mesoderm
(D) Extraembryonic mesoderm
(E) Sclerotome mesoderm

4. Which of the following muscles will the posterior divisions of the lumbosacral plexus innervate?

(A) Semitendinosus
(B) Semimembranosus
(C) Long head of biceps femoris
(D) Rectus femoris
(E) Gastrocnemius

5. During weeks 6–8, the lower limb bud will rotate

(A) Medially 90°
(B) Laterally 90°
(C) Medially 180°
(D) Laterally 180°
(E) No rotation occurs

Answers and Explanations

1. **D.** Early in development, the umbilical artery gives rise to the axis artery.
2. **B.** All bones of the lower limb form from lateral plate mesoderm that condenses along the central axis of the lower limb bud.
3. **A.** Somite mesoderm migrates into the limb bud and forms two condensations. The posterior condensation of the lower limb gives rise to the extensors of the lower limb, which attain an anterior location in the adult because of the medial rotation of 90°.
4. **D.** One of the nerves that form from the posterior divisions of the lumbosacral plexus is the femoral nerve. Posterior divisions of the lumbosacral plexus will innervate muscles derived from the posterior condensation (extensors). Rectus femoris muscle is an extensor at the knee joint. Note that rectus femoris muscle and the femoral nerve are related embryologically to the posterior condensation and posterior divisions even though in the adult they are located anterior. This occurs because of the medial rotation of 90°.
5. **A.** The lower limb bud will rotate medially 90° so that the knee points anteriorly.

chapter 21

Body Cavities

I. FORMATION OF THE INTRAEMBRYONIC COELOM (FIGURE 21.1)

A. The formation of the intraembryonic coelom begins when spaces coalesce within the lateral mesoderm and form a horseshoe-shaped space that opens into the chorionic cavity (extraembryonic coelom) on the right and left sides.

B. The intraembryonic coelom undergoes remodeling due to the craniocaudal folding and lateral folding of the embryo.

C. The intraembryonic coelom can best be visualized as a balloon whose walls are visceral mesoderm (closest to the viscera) and somatic mesoderm (closest to the body wall).

D. The intraembryonic coelom provides the needed room for the growth of various organs.

II. PARTITIONING OF THE INTRAEMBRYONIC COELOM

The intraembryonic coelom is initially one continuous space. To form the definitive adult pericardial, pleural, and peritoneal cavities, two partitions must develop. The two partitions are the **paired pleuropericardial membranes** and the **diaphragm**.

A. Paired pleuropericardial membranes

1. The **paired pleuropericardial membranes** are sheets of **somatic mesoderm** that separate the **pericardial cavity** from the **pleural cavities**.
2. The formation of these membranes appears to be aided by lung buds invading the lateral body wall and by tension on the common cardinal veins resulting from rapid longitudinal growth.
3. These membranes develop into the definitive **fibrous pericardium** surrounding the heart.

B. Diaphragm

1. The diaphragm separates the pleural cavities from the peritoneal cavity.
2. The diaphragm is formed through the fusion of tissue from four different sources:
   a. The **septum transversum** is a thick mass of **mesoderm** located between the primitive heart tube and the developing liver. The septum transversum is the primordium of the **central tendon of the diaphragm** in the adult.

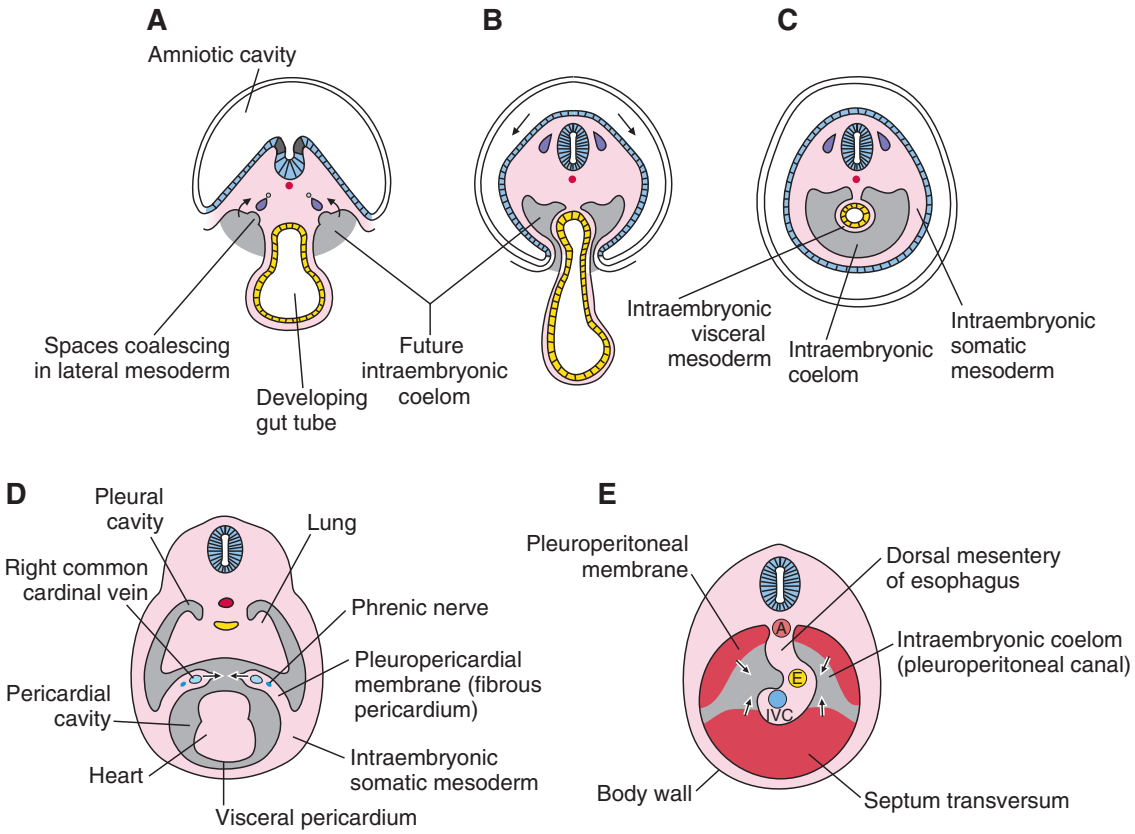

FIGURE 21.1. Formation and partitioning of the intraembryonic coelom (IC). **A–C**. The cross sections show the various stages of IC formation while the embryo undergoes lateral folding. **D**. The cross section shows two folds of intraembryonic somatic mesoderm carrying the phrenic nerves (*blue*) and common cardinal veins (*blue*). The two folds fuse in the midline (*arrows*) to form the pleuropericardial membrane (*light red*). This separates the pericardial cavity (*shaded*) from the pleural cavity (*shaded*). **E**. The cross section of an embryo at week 5 shows the four components that fuse (*arrows*) to form the diaphragm, which closes off the IC between the pleural and peritoneal cavities. The portions of the IC that connect the pleural and pericardial cavities in the embryo are called the pleuroperitoneal canals (*shaded*). A = aorta (*dark red*); E = esophagus (*yellow*); IVC = inferior vena cava (*blue*).

b. The **paired pleuroperitoneal membranes** are sheets of **somatic mesoderm** that appear to develop from the dorsal and dorsolateral body wall by an unknown mechanism.

c. The **dorsal mesentery of the esophagus** is invaded by myoblasts and forms the **crura of the diaphragm** in the adult.

d. The **body wall** contributes muscle to the peripheral portions of the definitive diaphragm.

III. POSITIONAL CHANGES OF THE DIAPHRAGM

A. During week 4 of development, the developing diaphragm becomes innervated by the **phrenic nerves**, which originate from C3, C4, and C5 and pass through the pleuropericardial membranes. This explains the definitive location of the phrenic nerves associated with the fibrous pericardium.

B. By week 8, an apparent **descent of the diaphragm to L1** occurs because of the rapid growth of the neural tube.

C. The phrenic nerves are carried along with the "descending diaphragm," which explains their unusually long length in the adult.

IV. CLINICAL CONSIDERATIONS

A. Congenital diaphragmatic hernia (Figure 21.2) is a herniation of abdominal contents into the pleural cavity caused by a **failure of the pleuroperitoneal membrane** to develop or fuse with the other components of the diaphragm. A congenital diaphragmatic hernia is most commonly found on the **left posterolateral side** and is usually life threatening because abdominal contents compress the lung buds, causing **pulmonary hypoplasia**. **Clinical features in the newborn include** an unusually flat abdomen, breathlessness, severe dyspnea, peristaltic bowel sounds over the left chest, and cyanosis. It can be detected prenatally using ultrasonography. The photograph (Figure 21.2A) shows an infant at autopsy with a congenital diaphragmatic hernia. Note the defect (*arrow*) in the diaphragm, which allows loops of intestine and a portion of the liver to enter the pleural cavity. There is attendant pulmonary hypoplasia. The radiograph (Figure 21.2B) shows a congenital diaphragmatic hernia. Note the loops of intestine within the pleural cavity as indicated by the bowel gas above and below the diaphragm and the mediastinal shift to the right.

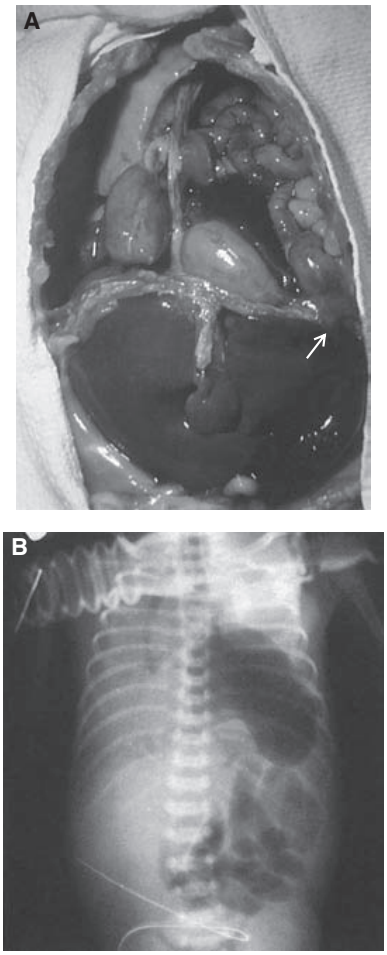

FIGURE 21.2. Congenital diaphragmatic hernia.

B. Esophageal hiatal hernia (Figure 21.3) is a herniation of the stomach through the esophageal hiatus into the pleural cavity caused by an abnormally large esophageal hiatus. An esophageal hiatal hernia renders the **esophagogastric sphincter** incompetent so that stomach contents reflux into the esophagus. **Clinical features in the newborn include** vomiting (frequently projectile) when the infant is laid on its back after feeding. The photograph (Figure 21.3) shows an esophageal hiatal hernia. Note the large saccular, discolored, ischemic portion of the stomach (*arrow*) and the deviation of the esophagus to the right.

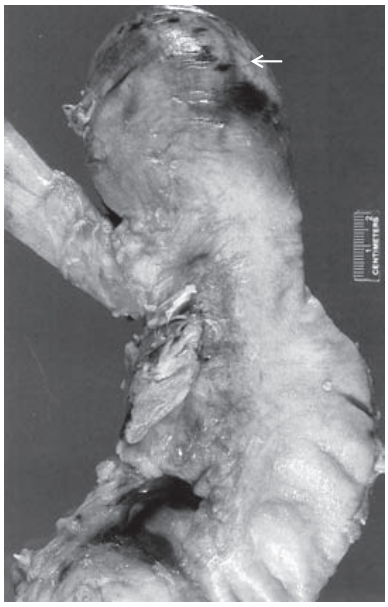

FIGURE 21.3. Esophageal hiatal hernia.

Study Questions for Chapter 21

1. A congenital diaphragmatic hernia may result from failure of the

(A) septum transversum to develop
(B) pleuroperitoneal membranes to fuse in a normal fashion
(C) pleuropericardial membrane to develop completely
(D) dorsal mesentery of the esophagus to develop
(E) body wall to form the peripheral part of the diaphragm

2. A congenital diaphragmatic hernia most commonly occurs

(A) on the right anteromedial side
(B) on the right posterolateral side
(C) on the left anteromedial side
(D) on the left posterolateral side
(E) anywhere on the left side

3. A congenital diaphragmatic hernia is usually life threatening because it is associated with

(A) pulmonary hypoplasia
(B) pulmonary hyperplasia
(C) physiological umbilical hernia
(D) liver hypoplasia
(E) liver agenesis

4. An 8-day-old boy presents with a history of complete loss of breath at times and of turning blue on a number of occasions. If the baby is placed in an upright or sitting position, his breathing improves. Physical examination reveals an unusually flat stomach when the newborn is lying down; auscultation demonstrates no breath sounds on the left side of the thorax. What is the diagnosis?

(A) Physiological umbilical herniation
(B) Esophageal hiatal hernia
(C) Tetralogy of Fallot
(D) Congenital diaphragmatic hernia
(E) Tricuspid atresia

5. During week 4, the developing diaphragm is located at

(A) C3, C4, C5
(B) T3, T4, T5
(C) T8, T9, T10
(D) L1, L2, L3
(E) L4, L5, L6

6. An apparently healthy newborn with a hardy appetite has begun feedings with formula. When she is laid down in the crib after feeding, she experiences projectile vomiting. Which of the following conditions is a probable cause of this vomiting?

(A) Physiological umbilical herniation
(B) Esophageal hiatal hernia
(C) Tetralogy of Fallot
(D) Congenital diaphragmatic hernia
(E) Tracheoesophageal fistula

Answers and Explanations

1. **B.** The formation of the diaphragm occurs through the fusion of tissue from four different sources. The pleuroperitoneal membranes normally fuse with the three other components during week 6 of development. Abnormal development or fusion of one or both of the pleuroperitoneal membranes causes a patent opening between the thorax and abdomen through which abdominal viscera may herniate.

2. **D.** Congenital diaphragmatic hernias occur most commonly on the left posterolateral side. The pleuroperitoneal membrane on the right side closes before the left for reasons that are not clear. Consequently, the patency on the left side remains unclosed for a longer time. The portion of the diaphragm formed by the pleuroperitoneal membrane in the newborn is located posterolateral.

3. **A.** The herniation of abdominal contents into the pleural cavity compresses the developing lung bud, resulting in pulmonary hypoplasia. Lung development on the ipsilateral (left) side of the herniation is most commonly affected, but lung development on the contralateral (right) side can also be compromised. The lungs may achieve normal size and function after surgical reduction of the hernia and repair of the diaphragm. However, mortality is high due to pulmonary hypoplasia.

4. **D.** Loss of breath and cyanosis result from pulmonary hypoplasia associated with congenital diaphragmatic hernia. Placing the baby in an upright position will reduce the hernia somewhat and ease the pressure on the lungs, thereby increasing the baby's comfort. The baby's stomach is flat (instead of the plump belly of a normal newborn) because the abdominal viscera have herniated into the thorax. Auscultation reveals no breath sounds on the left side because of pulmonary hypoplasia.

5. **A.** Although it may seem unusual, the adult diaphragm has its embryological beginning at the cervical level (C3, C4, C5). Nerve roots from C3, C4, and C5 enter the developing diaphragm, bringing both motor and sensory innervation. With the subsequent rapid growth of the neural tube, there is an apparent descent of the diaphragm to its adult levels (thoracic and lumbar). However, the diaphragm retains its innervation from C3, C4, and C5, which explains the unusually long phrenic nerves.

6. **B.** An esophageal hiatal hernia is a herniation of the stomach through the esophageal hiatus into the pleural cavity. This compromises the esophagogastric sphincter so that stomach contents can easily reflux into the esophagus. The combination of a full stomach after feeding and lying down in the crib will cause vomiting in this newborn.

chapter 22

Pregnancy

I. ENDOCRINOLOGY OF PREGNANCY

A. Human chorionic gonadotropin (hCG)

1. hCG is a glycoprotein hormone produced by the **syncytiotrophoblast** that stimulates the production of progesterone by the corpus luteum (i.e., maintains corpus luteum function).
2. hCG can be assayed in **maternal blood at day 8** or **maternal urine at day 10** using a radioimmunoassay, with antibodies directed against the β subunit of hCG. This is the basis of the early pregnancy test kits purchased over the counter.
3. Low hCG levels may predict a spontaneous abortion or indicate an ectopic pregnancy.
4. High hCG levels may indicate a multiple pregnancy, hydatidiform mole, or gestational trophoblastic neoplasia.
5. **Quantitative hCG dating of pregnancy.** During weeks 1–6 of a normal pregnancy, hCG levels will increase by about 70% every 48 hours.
   - **a.** 0–2 weeks: 0–250 mIU/mL
   - **b.** 2–4 weeks: 100–5000 mIU/mL
   - **c.** 1–2 months: 4000–200,000 mIU/mL
   - **d.** 2–3 months: 8000–100,000 mIU/mL
   - **e.** 2nd trimester: 4000–75,000 mIU/mL
   - **f.** 3rd trimester: 1000–5000 mIU/mL

B. Human placental lactogen (hPL)

1. hPL is a protein hormone produced by the **placenta** that induces lipolysis, thereby elevating free fatty acid levels in the mother.
2. hPL is considered the "growth hormone" of the latter half of pregnancy.
3. hPL can be assayed in **maternal blood at week 6**.
4. hPL levels vary with placental mass (i.e., may indicate a multiple pregnancy) and rapidly disappear from maternal blood after delivery.

C. Prolactin (PRL)

1. PRL is a protein hormone produced by the **maternal adenohypophysis, fetal adenohypophysis,** and **decidual tissue of the uterus** that prepares the mammary glands for lactation.
2. PRL can be assayed in **maternal blood throughout pregnancy** or in **amniotic fluid**.
3. Near term, PRL levels rise to a maximum of about 100 ng/mL (normal nonpregnant PRL levels range between 8 and 25 ng/mL).

D. Progesterone (PG)

1. PG is a steroid hormone produced by the **corpus luteum** until week 8 and then by the **placenta** until birth.
2. PG prepares the endometrium for implantation (nidation) and maintains the endometrium.
3. PG is used by the fetal adrenal cortex as a precursor for corticosteroid and mineralocorticoid synthesis.
4. PG is used by the fetal testes as a precursor for testosterone synthesis.

E. Estrone, estradiol, and estriol

1. Little is known about the specific function of these steroid hormones in the mother or fetus during pregnancy.
2. **Estrone** is a fairly weak estrogen.
3. **Estradiol** is the most potent estrogen.
4. **Estriol** is a very weak estrogen but is produced in very high amounts during pregnancy.
5. Estriol can be assayed in **maternal blood** (shows a distinct diurnal variation with peak amounts early in the morning) and **maternal urine** (24-hour urine sample shows no diurnal variation).
6. Significant amounts of estriol are produced at month 3 (i.e., early second trimester) and continue to rise until birth.
7. Maternal urinary levels of estriol have long been recognized as a **reliable index of fetal–placental function** because estriol production is dependent on a normally functioning fetal adrenal cortex, fetal liver, and placenta.
8. Estrone, estradiol, and estriol are produced by complex series of steps involving the **maternal liver, placenta, fetal adrenal gland,** and **fetal liver** as follows:
   a. Cholesterol from the maternal liver is converted to pregnenolone by the placenta.
   b. Pregnenolone is converted to pregnenolone sulfate.
   c. Pregnenolone sulfate is converted to dehydroepiandrosterone sulfate (DHEA-SO_4) by the fetal adrenal gland.
   d. DHEA-SO_4 is converted to estrone and estradiol by the placenta.
   e. DHEA-SO_4 is also converted to 16α-hydroxy DHEA-SO_4 by the fetal liver.
   f. 16α-hydroxy DHEA-SO^4 is converted to estriol by the placenta.

II. PREGNANCY DATING

A. The **estimated date of confinement (EDC)** is based on the assumption that a woman has a 28-day cycle with ovulation on day 14 or day 15.

B. In general, the duration of a normal pregnancy is **280 days (40 weeks) from the first day of the last menstrual period (LMP)**.

C. A common method for determining the EDC (Naegele rule) is to count back 3 months from the first day of the LMP and then add 1 year and 7 days. This method is reasonably accurate in women with regular menstrual cycles.

III. PREGNANCY MILESTONES

A. First trimester

1. The first trimester extends from the **LMP through week 12**. Important events that occur are:
   a. At days 8–10, a positive pregnancy test is obtained by hCG assay.
   b. At week 12, the uterine fundus is palpable at the pubic symphysis; Doppler fetal heart rate is first audible.

B. Second trimester

1. The second trimester extends from the **end of the first trimester through week 27**. Important events that occur are as follows:
   - **a.** At weeks 14–18, amniocentesis is performed when suspicion of fetal chromosomal abnormalities exist.
   - **b.** At week 16, the uterine fundus is palpable midway between the pubic symphysis and the umbilicus.
   - **c.** At weeks 16–18, first fetal movements occur **(quickening)** in a woman's second or higher pregnancy.
   - **d.** At weeks 17–20, the fetal heart rate is audible with fetoscope.
   - **e.** At week 18, female and male external genitalia can be distinguished by ultrasound (i.e., sex determination).
   - **f.** At weeks 18–20, first fetal movements occur **(quickening)** in a woman's first pregnancy.
   - **g.** At week 20, the uterine fundus is palpable at the umbilicus.
   - **h.** At weeks 25–27, lungs become capable of respiration; surfactant is produced by type II pneumocytes. There is a 70%–80% chance of survival in infants born at the end of the second trimester. If death occurs, it is generally as a result of lung immaturity and resulting respiratory distress syndrome (hyaline membrane disease).
   - **i.** At week 27, the fetus weighs about 1000 g (a little more than 2 pounds).

C. Third trimester

1. The third trimester extends from the **end of the second trimester until term or week 40**. Important events that occur are as follows:
   - **a.** Pupillary light reflex is present.
   - **b.** Descent of the fetal head to the pelvic inlet (called **lightening**) occurs.
   - **c.** Rupture of the amniochorionic membrane occurs, with labor usually beginning about 24 hours later.
   - **d.** The fetus weighs about 3300 g (about 7–7.5 pounds).

IV. PRENATAL DIAGNOSTIC PROCEDURES

Prenatal diagnosis is indicated in about **8%** of all pregnancies. Prenatal diagnostic procedures include the following:

A. Ultrasonography

1. Ultrasonography is commonly used to:
   - **a.** Date a pregnancy
   - **b.** Diagnose a multiple pregnancy
   - **c.** Assess fetal growth
   - **d.** Determine placenta location
   - **e.** Determine position and lie of the fetus
   - **f.** Detect certain congenital anomalies
   - **g.** Monitor needle or catheter insertion during amniocentesis and chorionic villus biopsy
2. In obstetric ultrasonography, 2.25- to 5.0-mHz frequencies are used for good tissue differentiation.
3. The term **anechoic** refers to tissues with few or no echoes (e.g., bladder, brain, cavities, amniotic fluid).
4. The term **echogenic** refers to tissues with a high capacity to reflect ultrasound.

B. Amniocentesis

1. Amniocentesis is a transabdominal sampling of **amniotic fluid** and **fetal cells**.
2. Amniocentesis is performed at **weeks 16–20** and is indicated in the following situations:
   - **a.** The woman is older than 35 years of age.
   - **b.** A previous child had a chromosomal anomaly.

c. One parent is a known carrier of a translocation or inversion.
d. One or both parents are known carriers of an X-linked recessive or autosomal recessive trait.
e. There is a history of neural tube defects.

3. The sample obtained is used in the following studies:
a. **α-Fetoprotein assay** is used to diagnose neural tube defects.
b. **Spectrophotometric assay of bilirubin** is used to diagnose hemolytic disease of the newborn (i.e., erythroblastosis fetalis) due to Rh incompatibility.
c. **Lecithin-sphingomyelin (L/S) ratio and phosphatidylglycerol assay** are used to determine the lung maturity of the fetus.
d. **DNA analysis:** A wide variety of DNA methodologies are available [e.g., karyotype analysis, Southern blotting, or RFLP analysis (restriction fragment length polymorphism)] to diagnose chromosomal abnormalities and single-gene defects.

C. Chorionic villus biopsy

1. Chorionic villus biopsy is a transabdominal or transcervical sampling of the chorionic villi to obtain a large amount of **fetal cells** for DNA analysis.
2. Chorionic villus biopsy is performed late in the first trimester at **weeks 10–12 (i.e., much earlier than amniocentesis)**, thereby providing an early source of fetal cells for DNA analysis.

D. Percutaneous umbilical blood sampling (PUBS)

1. PUBS is a sampling of **fetal blood** from the umbilical cord.

V. FETAL DISTRESS DURING LABOR (INTRAPARTUM)

A. Fetal distress during labor is defined in terms of **fetal hypoxia** and measured by changes in either **fetal heart rate (FHR)** or **fetal scalp capillary pH**.

B. The normal baseline FHR is **120–160 beats/min**.

C. Fetal hypoxia causes a decrease in FHR (or **fetal bradycardia**), that is, **a FHR of less than 120 beats/min**.

D. The normal fetal scalp capillary pH is **7.25–7.35**.

E. Fetal hypoxia causes a decrease in pH, that is, a **pH of less than 7.20**.

VI. THE APGAR SCORE (TABLE 22.1)

A. The **APGAR score** assesses five characteristics (**A**ppearance, **P**ulse, **G**rimace, **A**ctivity, **R**espiratory effort) in the newborn infant in order to determine which infants need resuscitation.

B. The APGAR score is calculated at 1 minute and 5 minutes after birth. To obtain an APGAR score, score 0, 1, or 2 for the five characteristics and add them together.

1. **APGAR score of 0–3** indicates a life-threatening situation.
2. **APGAR score of 4–6** indicates temperature and ventilation support is needed.
3. **APGAR score of 7–10** indicates a normal situation.

table 22.1 Assessing the APGAR Score

Characteristic	Score 0	1	2	Example[a]
Appearance, color	Blue, pale	Body pink, extremities blue	Completely pink	1
Pulse, heart rate	Absent	<100 beats/minute	>100 beats/minute	2
Grimace, reflex, irritability	No response	Grimace	Vigorous crying	0
Activity, muscle tone	Flaccid	Some flexion of extremities	Active motion, flexed extremities	0
Respiratory effort	None	Weak, irregular	Good, crying	1
APGAR score				**4**

[a]Clinical example: A newborn infant at 5 minutes after birth has a pink body but blue extremities (score 1); a heart rate of 125 beats/minute (score 2); shows no grimace or reflex (score 0); has flaccid muscle tone (score 0); and has weak, irregular breathing (score 1). The total APGAR score is 4. This infant needs ventilation and temperature support.

VII. PUERPERIUM

A. The puerperium extends from immediately after delivery of the baby until the reproductive tract returns to the nonpregnant state in approximately 4–6 weeks.

B. Important events that occur are as follows:
1. Involution of the uterus
2. Afterpains due to uterine contractions
3. Uterine discharge (lochia)
4. **In nonlactating women,** menstrual flow returns within 6–8 weeks postpartum and ovulation returns 2–4 weeks postpartum.
5. **In lactating women,** ovulation may return within 10 weeks postpartum. Birth control protection afforded by lactation is assured for only 6 weeks, after which time pregnancy is possible.

VIII. LACTATION

A. **During pregnancy**, hPL, PRL, progesterone, estrogens, cortisol, and insulin stimulate the growth of **lactiferous ducts** and proliferation of epithelial cells to form **alveoli**. The alveoli secrete **colostrum**.

B. **After delivery of the baby**, lactation is initiated by a decrease in progesterone and estrogens along with the release of PRL from the adenohypophysis. This initiates **milk production**.

C. **During suckling**, a stimulus from the breast inhibits the release of PRL-inhibiting factor from the hypothalamus, thereby causing a **surge in PRL,** which increases milk production. In addition, stimulation of the nipples during suckling causes a **surge of oxytocin,** which causes the **expulsion of accumulated milk ("milk letdown")** by stimulating myoepithelial cells.

IX. SMALL-FOR-GESTATIONAL AGE (SGA) INFANT

A. SGA, fetal growth restriction (FGR), intrauterine growth restriction (IUGR), and low birth weight are all terms used to describe a small baby or a fetus that has not reached its growth potential.

B. Although the definition is controversial, the most common definition of SGA is a body weight **below the tenth percentile for gestational age**.

C. **The clinical features of a SGA infant include** thin, loose, peeling skin; decreased skeletal muscle mass; decreased subcutaneous adipose tissue; shrunken or "wizened" facial appearance; thin umbilical cord; meconium staining; difficult cardiopulmonary transition; meconium aspiration; persistent pulmonary hypertension; greater rates of neonatal death, necrotizing enterocolitis, and respiratory distress; impaired thermoregulation; hypoglycemia; polycythemia; hyperviscosity; impaired immune function; and increased fetal, neonatal, and perinatal mortality.

D. The methods for clinically estimating gestation age include the following:
1. Measurement of the fundal height, which is the distance between the upper edge of the pubic symphysis and the top of the uterine fundus, using a tape measure.
2. Ultrasound measurement of the fetal abdominal circumference.
3. Ultrasound measurement of fetal weight.

E. SGA may be caused by **maternal factors,** which include the following:
1. Severe maternal starvation
2. Maternal hypoxemia
3. Preeclampsia
4. Maternal viral or parasitic infections
5. Maternal substance abuse
6. Toxic exposures (e.g., warfarin, anticonvulsants, antineoplastic drugs, and folic acid antagonists)
7. High altitude
8. Demographic factors (e.g., race, maternal age at first birth, and pregnancy at the extremes of reproductive life)

F. SGA may be caused by **fetal factors,** which include the following:
1. Karyotype abnormalities (e.g., trisomies, autosomal deletions, mosaicism)
2. Genetic syndromes (e.g., Bloom syndrome, dwarfism, Russell-Silver syndrome)
3. Major congenital anomalies
4. Multiple gestation (e.g., twins, triplets, quintuplets, etc.).

G. SGA may be caused by **placental factors,** which include the following:
1. Abnormal uteroplacental vasculature
2. Abruptio placenta
3. Gross placental anomalies (e.g., single umbilical artery, velamentous umbilical cord insertion, placental hemangioma).

X. COLLECTION AND STORAGE OF UMBILICAL CORD BLOOD (UCB)

A. UCB is the blood that remains in the umbilical cord and placenta following the birth of an infant.

B. The importance of the collection and storage of UCB relates to the fact that UCB contains **hematopoietic stem cells,** which can be used to reconstitute the bone marrow in patients with a wide variety of malignant and nonmalignant diseases (e.g., acute and chronic leukemia, lymphoma, aplastic anemia, sickle cell anemia, thalassemia major, etc.).

C. The in utero collection of UCB involves the following steps: after delivery of the infant, the umbilical cord is clamped and cut in the usual manner; before expulsion of the placenta, a 16 gauge needle is inserted into the umbilical vein located within the umbilical cord; UCB is allowed to drain into a collection bag containing an anticoagulant solution; collection time is usually 2–4 minutes, and ideally 40–60 mL of UCB is collected.

Study Questions for Chapter 22

1. Human chorionic gonadotropin (hCG) is produced by which of the following?

(A) Ectoderm
(B) Cytotrophoblast
(C) Decidua basalis
(D) Syncytiotrophoblast
(E) Mesoderm

2. A reliable index of fetal–placenta function is maternal urinary level of

(A) estrone
(B) human placental lactogen (hPL)
(C) prolactin (PRL)
(D) progesterone
(E) estriol

3. The first fetal movements occur in which of the following trimesters?

(A) First trimester
(B) Second trimester
(C) Third trimester

4. The Doppler fetal heart rate is first audible in which of the following trimesters?

(A) First trimester
(B) Second trimester
(C) Third trimester

5. The lungs become capable of respiration in which of the following trimesters?

(A) First trimester
(B) Second trimester
(C) Third trimester

6. Which of the following structures produces progesterone late in pregnancy?

(A) Placenta
(B) Corpus luteum
(C) Syncytiotrophoblast
(D) Fetal adenohypophysis
(E) Maternal liver

Answers and Explanations

1. **D.** The syncytiotrophoblast produces hCG.
2. **E.** Maternal urinary levels of estriol have long been recognized as a reliable index of fetal–placental function because estriol production is dependent on a normal functioning fetal adrenal cortex, fetal liver, and placenta.
3. **B.** The first fetal movements occur in the second trimester.
4. **A.** The fetal heart rate is first audible in the first trimester at around week 12.
5. **B.** The lungs become capable of respiration at weeks 25–27 in the second trimester.
6. **A.** Progesterone is a steroid hormone that is produced by the placenta up until birth. The corpus luteum also produces progesterone, but only until week 8 of pregnancy.

chapter 23

Teratology

I. INTRODUCTION

A teratogen is any infectious agent, drug, chemical, or irradiation that alters fetal morphology or fetal function if the fetus is exposed during a critical stage of development.

A. The **resistant period (week 1 of development)** is the time when the conceptus demonstrates the **"all-or-none" phenomenon** (i.e., the conceptus will either die as a result of the teratogen or survive unaffected).

B. The **maximum susceptibility period (weeks 3–8; embryonic period)** is the time when the embryo is most susceptible to teratogens because all organ morphogenesis occurs at this time.

C. The **lowered susceptibility period (weeks 9–38; fetal period)** is the time when the fetus has a lowered susceptibility to teratogens because all organs systems have already formed. A teratogen exposure at this period generally results in a *functional* derangement of an organ system.

II. INFECTIOUS AGENTS

Infectious agents may be viral or nonviral. However, bacteria appear to be nonteratogenic.

A. **Viral infections** may reach the fetus via the amniotic fluid following vaginal infection, transplacentally via the bloodstream after maternal viremia, or by direct contact during passage through an infected birth canal.

1. **Rubella virus (German measles; member of TORCH—see Section III)**
   - **a.** The rubella virus belongs to the Togaviridae family, which are enveloped, icosahedral, positive, single-stranded RNA viruses.
   - **b.** The rubella virus is transmitted to the fetus transplacentally.
   - **c.** The risk of fetal rubella infection is greatest during the first month of pregnancy and apparently declines thereafter.
   - **d.** Fetal rubella infection results in the classic triad of cardiac defects (e.g., patent ductus arteriosus, pulmonary artery stenosis, and atrioventricular [AV] septal defects), cataracts, and low birth weight.
   - **e.** With the pandemic of rubella in 1964, the complexity of this syndrome became apparent, and the term expanded rubella syndrome became standard.

f. **Clinical features of expanded rubella syndrome include** intrauterine growth retardation (most common manifestation), hepatosplenomegaly, generalized adenopathy, hemolytic anemia, hepatitis, jaundice, meningoencephalitis, eye involvement (e.g., cataracts, glaucoma, retinopathy), bluish-purple lesions on a yellow, jaundiced skin ("blueberry muffin spots"), osteitis (celery stalk appearance of long bones), and sensorineural deafness.

2. **Cytomegalovirus (CMV; member of TORCH)**
   a. CMV belongs to the Herpesvirus family, which are large, enveloped, icosahedral, double-stranded DNA viruses.
   b. CMV is a ubiquitous virus and the most common fetal infection.
   c. CMV is transmitted to the fetus transplacentally, with more severe malformations when infection occurs during the first half of pregnancy.
   d. CMV is also transmitted to perinates during passage through the birth canal or through breast milk but causes no apparent disease.
   e. The most common feature of CMV fetal infection is **sensorineural deafness**.
   f. Cytomegalic inclusion disease (characterized by multiorgan involvement) is the most serious but least common manifestation of CMV infection and results in intrauterine growth retardation, microcephaly, chorioretinitis, hepatosplenomegaly, osteitis (celery stalk appearance of long bones), discrete cerebral calcifications, mental retardation, heart block, and bluish-purple lesions on a yellow jaundiced skin ("blueberry muffin spots").
3. **Herpes simplex virus (HSV-1; HSV-2; member of TORCH)**
   a. HSV belongs to the Herpesvirus family, which are large, enveloped, icosahedral, double-stranded DNA viruses.
   b. Most neonatal infections are caused by HSV-2 (75% of the cases).
   c. HSV-2 is most commonly transmitted to the fetus by direct contact during passage through an infected birth canal (intrapartum; 85% of cases).
   d. At 10–11 days of age, some intrapartum HSV-infected infants present with the disease localized to the skin (discrete vesicular lesion, large bullae, or denuded skin; hallmark signs), eye (keratoconjunctivitis, uveitis, chorioretinitis, cataracts, retinal dysplasia), or mouth (ulcerative lesions of the mouth, tongue, or palate).
   e. At 15–17 days of age, some intrapartum HSV-infected infants present with central nervous system (CNS) involvement (with or without skin, eye, or mouth involvement) due to axonal retrograde transport of HSV to the brain. **Clinical features of CNS involvement include** lethargy, bulging fontanelles, focal or generalized seizures, opisthotonus, decerebrate posturing, and coma.
   f. The only intervention shown to prevent neonatal HSV infection is delivery by cesarean section within 4–6 hours of rupture of the amnionic membranes.
4. **Varicella zoster virus (VZV; varicella or chickenpox)**
   a. VZV belongs to the Herpesvirus family, which are large, enveloped, icosahedral, double-stranded DNA viruses.
   b. VZV is the etiology of two clinical syndromes: a primary infection (varicella or chickenpox usually occurs in children) and a secondary infection (herpes zoster or shingles usually occurs in adults along a single sensory dermatome).
   c. VZV is transmitted to the fetus transplacentally in 25% of the cases, but fetal varicella syndrome develops only when maternal VZV infection occurs in the first trimester.
   d. **Clinical features of fetal varicella syndrome include** cicatricial (scarring) skin lesions in a dermatomal pattern, limb and digit hypoplasia, limb paresis/paralysis, hydrocephalus, microcephaly/mental retardation, seizures, chorioretinitis, and cataracts.
5. **Human immunodeficiency virus (HIV)**
   a. HIV belongs to the Retroviridae family (or Lentivirus subfamily), which are diploid, enveloped, positive, single-stranded RNA viruses.
   b. Most researchers believe that HIV is the major cause of acquired immunodeficiency syndrome (AIDS). However, there exist cases of AIDS in those who are HIV-negative. Some researchers thus believe that multiple blood transfusions (e.g., hemophiliacs), consumption of megadoses of antibiotics as prophylaxis against sexually transmitted diseases, and continuous use of drugs to heighten orgasm (e.g., amyl and butyl nitrite) may destroy $CD4^{1}$ T cells and lead to AIDS.
   c. The placenta is a highly effective barrier to HIV infection of the fetus.

d. HIV may be transmitted to the fetus through blood containing HIV or HIV-infected lymphoid cells near the time of delivery or after 35 weeks of gestation.

e. HIV infection does not appear to cause any congenital malformations.

B. Nonviral infections

1. *Toxoplasma gondii* (TG; member of TORCH)

a. TG is a **protozoan parasite** whose life cycle is divided into a **sexual phase** that occurs only in cats **(the definitive host)** and an **asexual phase** that occurs in intermediate hosts.

b. Generally speaking, mice that eat cat feces contaminate fields, thereby infecting cows, sheep, and pigs.

c. TG is transmitted to humans primarily through ingestion of oocyst-containing water or food or consumption of cyst-containing raw or undercooked meat. In addition, inhalation or ingestion of oocysts from soil, dust, or cat litter box may occur.

d. TG is transmitted to the fetus **transplacentally**.

e. TG infection results in miscarriage, perinatal death, chorioretinitis, microcephaly, hydrocephalus, and encephalomyelitis with cerebral calcification.

f. About 10% of congenitally infected infants who have severe TG die, and most surviving infants are left with major neurological sequelae (e.g., mental retardation, seizures, spasticity, and visual deficits).

2. *Treponema pallidum* (TP; Figure 23.1)

a. TP is a spirochete causing syphilis.

b. TP is transmitted to the fetus trans-placentally.

c. Clinical features of TP include miscarriage; perinatal death; hepatosplenomegaly; hepatitis; joint swelling; vesiculobullous blisters whose fluid contains active spirochetes and is highly infective; nasal discharge with rhinitis; a maculopapular rash located on the extremities that is initially oval and pink but then turns copper brown and desquamates (palms and soles); eye findings that include chorioretinitis, glaucoma, cataracts, and uveitis; anemia; jaundice; focal erosions of the proximal medial tibia (Wimberger sign); osteitis (celery stalk appearance of long bones); saw-toothed appearance of the metaphysis of long bones; abnormal teeth (Hutchinson teeth); acute syphilitic leptomeningitis, which may present as neck stiffness; and chronic meningovascular syphilis (cranial nerve palsy, hydrocephalus, cerebral infarction).

d. The upper photograph (Figure 23.1) shows an infant with TP infection. Note the vesiculobullous blisters on the legs and feet along with marked skin peeling. The lower photograph (Figure 23.1) also shows an infant with TP infection. Note the nasal discharge with rhinitis.

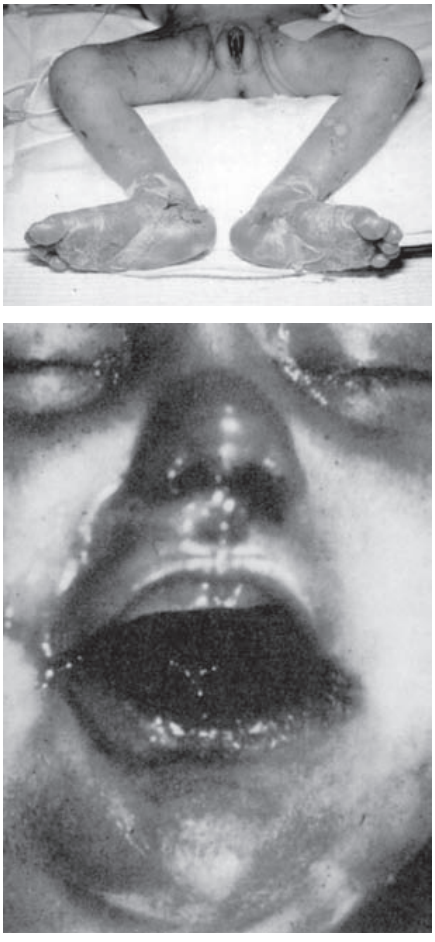

FIGURE 23.1. *Treponema pallidum* infection.

III. TORCH INFECTIONS (FIGURE 23.2)

TORCH infections are caused by ***T*oxoplasma,** **r**ubella, **c**ytomegalovirus, **h**erpes virus, and **o**ther bacterial and viral infections. They are grouped together because they cause similar clinical and pathological manifestations. See previous discussion for specifics.

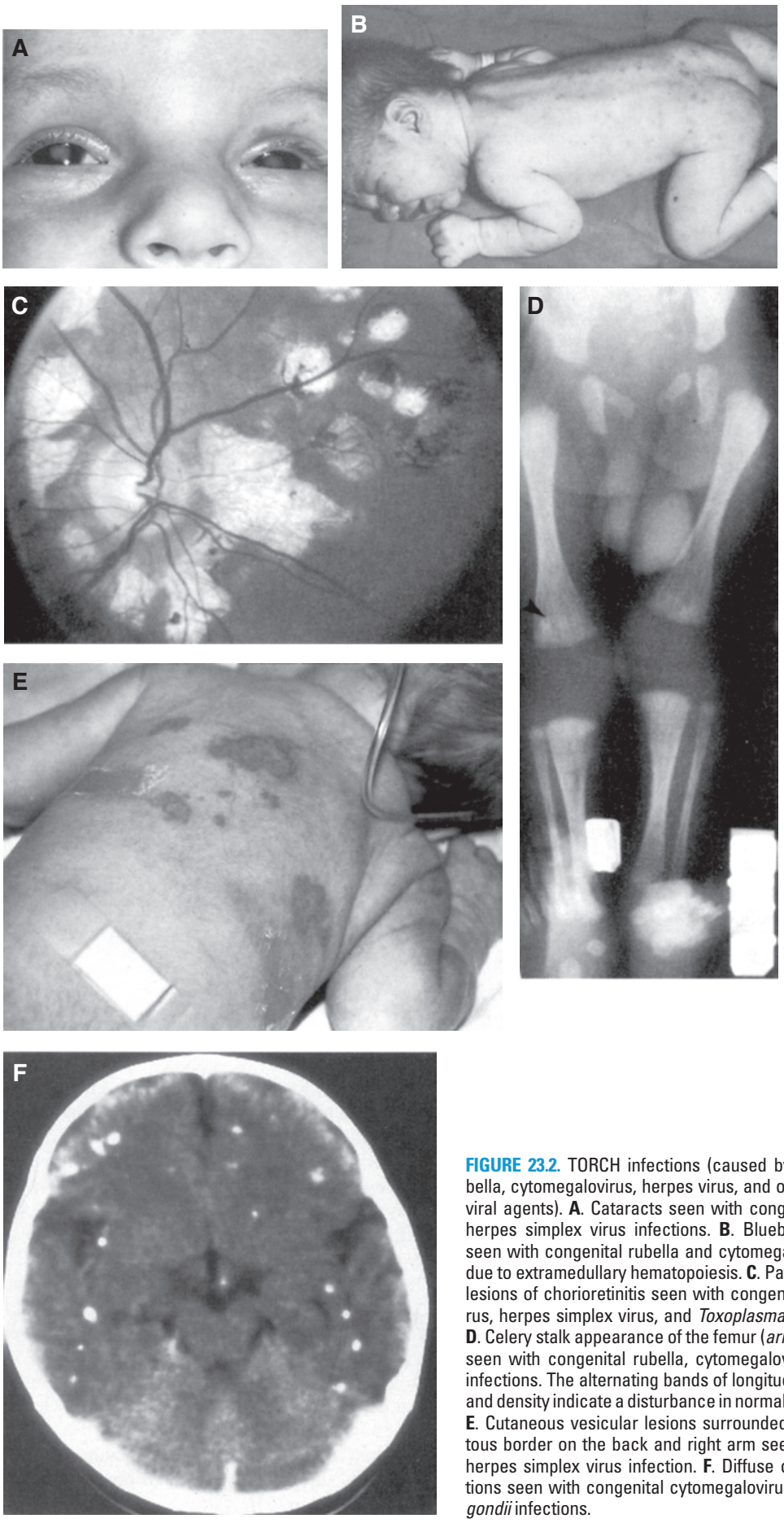

FIGURE 23.2. TORCH infections (caused by *Toxoplasma*, rubella, cytomegalovirus, herpes virus, and other bacterial and viral agents). **A**. Cataracts seen with congenital rubella and herpes simplex virus infections. **B**. Blueberry muffin spots seen with congenital rubella and cytomegalovirus infections due to extramedullary hematopoiesis. **C**. Patchy, yellow-white lesions of chorioretinitis seen with congenital cytomegalovirus, herpes simplex virus, and *Toxoplasma gondii* infections. **D**. Celery stalk appearance of the femur (*arrowhead*) and tibia seen with congenital rubella, cytomegalovirus, and syphilis infections. The alternating bands of longitudinal translucency and density indicate a disturbance in normal bone metabolism. **E**. Cutaneous vesicular lesions surrounded by an erythematous border on the back and right arm seen with congenital herpes simplex virus infection. **F**. Diffuse cerebral calcifications seen with congenital cytomegalovirus and *Toxoplasma gondii* infections.

IV. CHILDHOOD VACCINATIONS

A general practical guide to childhood vaccinations is as follows:

A. **MMR** vaccine protects against **m**easles, **m**umps, and **r**ubella and is given in two doses at 12–15 months and at 4–6 years.

B. **Polio vaccine** protects against polio and is given in four doses at 2 months, 4 months, 6–18 months, and 4–6 years.

C. **DTaP vaccine** protects against **d**iphtheria, **t**etanus, and **p**ertussis and is given in five doses at 2 months, 4 months, 6 months, 15–18 months, and 4–6 years. A tetanus booster is given at 11 years.

D. **Hib vaccine** protects against **H**aemophilus **i**nfluenza type **b** and is given in four doses at 2 months, 4 months, 6 months, and 12–15 months.

E. **HBV vaccine** protects against **h**epatitis **B** and is given in four doses at birth, 1 month, 4 months, and 6–18 months.

F. **Varicella vaccine** protects against chicken pox and is given in one dose at 12–18 months.

G. **Pneumococcal vaccine (PCV7)** protects against pneumonia, blood infections, and meningitis and is given in four doses at 2 months, 4 months, 6 months, and 12–25 months.

V. CATEGORY X DRUGS (ABSOLUTE CONTRAINDICATION IN PREGNANCY)

A. **Thalidomide** is an **antinauseant** drug that was prescribed for pregnant women (no longer used) for "morning sickness." This drug can cause limb reduction (e.g., meromelia, amelia), ear and nasal abnormalities, cardiac defects, lung defects, pyloric or duodenal stenosis, and gastrointestinal atresia. Thalidomide has undergone a resurgence in use for treatment of multiple myeloma due to its **antiangiogenic properties**.

B. **Aminopterin and methotrexate** are **folic acid antagonists** used in cancer chemotherapy. These drugs can cause small stature, abnormal cranial ossification, ocular hypertelorism, low-set ears, cleft palate, and myelomeningocele.

C. **Busulfan (Myleran), chlorambucil (Leukeran),** and **cyclophosphamide (Cytoxan)** are **alkylating agents** used in cancer chemotherapy. These drugs can cause cleft palate, eye defects, hydronephrosis, renal agenesis, absence of toes, and growth retardation.

D. **Phenytoin (Dilantin)** is an **antiepileptic** drug. In 30% of cases, this drug causes **fetal hydantoin syndrome**, which results in growth retardation, mental retardation, microcephaly, craniofacial defects, and nail and digit hypoplasia. In the majority of cases, this drug causes cleft lip, cleft palate, and congenital heart defects.

E. **Triazolam (Halcion) and estazolam (Prosom)** are **hypnotic** drugs. These drugs can cause cleft lip and cleft palate, especially if used in the first trimester of pregnancy.

F. **Warfarin (Coumadin)** is an **anticoagulant** drug that acts by inhibiting vitamin K-dependent coagulation factors. This drug can cause stippled epiphyses, mental retardation, microcephaly,

seizures, fetal hemorrhage, and optic atrophy in the fetus. Warfarin inhibits **vitamin K epoxide reductase**. Consequently, vitamin K-dependent coagulation factors (II, VII, IX, X) are not produced.

G. **Isotretinoin (Accutane)** is a **retinoic acid derivative** used in the treatment of **severe acne**. This drug can cause CNS abnormalities, external ear abnormalities, eye abnormalities, facial dysmorphia, and cleft palate (i.e., **vitamin A embryopathy**).

H. **Clomiphene (Clomid)** is a nonsteroidal **ovulatory stimulant** used in women with ovulatory dysfunction. Although no causative evidence of a deleterious effect of clomiphene on the human fetus has been established, there have been reports of birth anomalies.

I. **Diethylstilbestrol (DES)** is a **synthetic estrogen** that was used to prevent spontaneous abortion in women. This drug can cause cervical hood, T-shaped uterus, hypoplastic uterus, ovulatory disorders, infertility, premature labor, and cervical incompetence in women who were exposed to DES in utero. These women are also subject to increased risk of clear cell carcinoma of the vagina later in life.

J. **Ethisterone, norethisterone, and megestrol (Megace)** are synthetic **progesterone derivatives**. These drugs can cause masculinization of genitalia in female embryos, hypospadias in males, and cardiovascular anomalies.

K. **Norethindrone (Ovcon, Norinyl)** and **levonorgestrel (Levlen)** are **oral contraceptives** that contain a combination of estrogen (e.g., ethinyl estradiol or mestranol) and progesterone (e.g., norethindrone or levonorgestrel) derivatives. These drugs can cause an increase of fetal abnormalities, particularly the **VACTERL syndrome** consisting of vertebral, anal, cardiac, tracheoesophageal, renal, and limb malformations.

L. **Nicotine** is a **poisonous, additive alkaloid** delivered to the fetus through **cigarette smoking** by pregnant women (cigarette smoke also contains **hydrogen cyanide** and **carbon monoxide**). This drug can cause intrauterine growth retardation, premature delivery, low birth weight, and fetal hypoxia due to reduced uterine blood flow and diminished capacity of the blood to transport oxygen to fetal tissue.

M. **Alcohol** is an **organic compound** delivered to the fetus through **recreational or addictive (i.e., alcoholism) drinking** by pregnant women. This drug can cause **fetal alcohol syndrome**, which results in mental retardation, microcephaly, holoprosencephaly, limb deformities, craniofacial abnormalities (i.e., hypertelorism, smooth philtrum, short palpebral fissures, flat nasal bridge, maxillary [midface] hypoplasia, and a thin upper lip), and cardiovascular defects (i.e., ventricular septal defects). Fetal alcohol syndrome is the leading cause of preventable mental retardation. The threshold dose of alcohol has not been established, so "no alcohol is good alcohol" during pregnancy.

VI. CATEGORY D DRUGS (DEFINITE EVIDENCE OF RISK TO FETUS)

A. **Tetracycline (Achromycin) and doxycycline (Vibramycin)** are **antibiotics** in the tetracycline family. These drugs can cause permanently yellow-stained teeth and hypoplasia of enamel.

B. **Streptomycin, amikacin, and tobramycin (Nebcin)** are **antibiotics** in the aminoglycoside family. These drugs can cause **cranial nerve (CN) VIII toxicity** with permanent bilateral deafness and loss of vestibular function.

C. **Phenobarbital (Donnatal) and pentobarbital (Nembutal)** are **barbiturates** used as **sedatives**. Studies have suggested a higher incidence of fetal abnormalities with maternal barbiturate use.

D. **Valproic acid (Depakene)** is an **antiepileptic** drug. This drug can cause neural tube defects, cleft lip, and renal defects.

E. **Diazepam (Valium), chlordiazepoxide (Librium), alprazolam (Xanax), and lorazepam (Ativan)** are **anticonvulsant** or **antianxiety** drugs. These drugs can cause cleft lip and cleft palate, especially if used in the first trimester of pregnancy.

F. **Lithium** is used in the treatment of **manic-depressive disorder**. This drug can cause fetal cardiac defects (i.e., Ebstein anomaly and malformations of the great vessels).

G. **Hydrochlorothiazide (Diuril)** is a **diuretic** and **antihypertensive** drug. This drug can cause fetal jaundice and thrombocytopenia.

VII. CHEMICAL AGENTS

A. **Organic mercury.** Consumption of organic mercury during pregnancy results in fetal neurological damage, including seizures, psychomotor retardation, cerebral palsy, blindness, and deafness.

B. **Lead.** Consumption of lead during pregnancy results in abortion due to embryotoxicity, growth retardation, increased perinatal mortality, and developmental delay.

C. **Polychlorinated biphenyls (PCBs).** Consumption of PCBs during pregnancy results in result in intrauterine growth retardation, dark-brown skin pigmentation, exophthalmos, gingival hyperplasia, skull calcification, mental retardation, and neurobehavioral abnormalities.

D. **Potassium iodide (PI).** PI is found in over-the-counter cough medicines and radiograph cocktails for organ visualization. PI is involved in thyroid enlargement (goiter) and mental retardation (cretinism)

E. **Bisphenol A** is a common ingredient in plastics (e.g., reusable water bottles, computer housings, dental sealants). Bisphenol A is a well-known endocrine disruptor that mimics the effects of estrogen. Bisphenol A exposure during fetal development *in mice* results in higher rates of breast cancer later in life.

F. **Bisphenol S** is a replacement for the well-known endocrine disruptor Bisphenol A. Bisphenol S disrupts normal estrogen-induced cell signaling pathways that lead to increased cell proliferation and apoptosis (cell death) via the extrinsic pathway.

G. **Phthalates** are a common ingredient in many household products (e.g., vinyl floor covering, detergents, shampoo, deodorants, nail polish, food storage bags, and inflatable toys). It has been reported in humans that high levels of phthalates in pregnant women is associated with incomplete testicular descent in infant sons, suggesting antiandrogenic activity.

H. **Methoxychlor (an insecticide) and vinclozolin (a fungicide)** are both endocrine disruptors. It has been reported *in mice* that exposure to these endocrine disruptors during fetal development caused changes in mice that affected not only the mice exposed in utero, but also all male mice for at least four subsequent generations (i.e., a transgenerational effect).

VIII. RECREATIONAL DRUGS

A. **Lysergic acid (LSD)** has not been shown to be teratogenic.

B. **Marijuana** has not been shown to be teratogenic.

C. **Caffeine** has not been shown to be teratogenic.

D. **Cocaine** results in an increased risk of various congenital abnormalities, stillbirths, low birth weight, and placental abruption.

E. **Heroin** has not been shown to be teratogenic. It is drugs that are often taken with heroin that produce congenital anomalies. The principal adverse effect is **severe neonatal withdrawal**, causing death in 3%–5% of neonates. **Methadone** (used to replace heroin) is not teratogenic but is also associated with severe neonatal withdrawal.

IX. IONIZING RADIATION

A. **Acute high dose (>250 rads)** results in microcephaly, mental retardation, growth retardation, and leukemia. After exposure to **greater than 25 rads**, classic fetal defects will be observed so that termination of pregnancy should be offered as an option. Much information concerning acute high-dose radiation has come from studies of the atomic explosions over Hiroshima and Nagasaki.

B. **Diagnostic radiation.** Even if several radiographic studies are performed, rarely does the dose add up to exposure significant enough to produce fetal defects. **Radioactive iodine cocktails** for organ visualization should be avoided after week 10 of gestation because fetal thyroid development can be impaired.

C. **Fukishima Meltdown.** Due to the meltdown of four nuclear reactors at the Fukishima plant in Japan beginning on March 11, 2011, the I^{131} concentrations in USA precipitation increased up to 210 times above normal. The highest levels of I^{131} concentrations were documented in five US states along the Pacific Ocean coast. The incidence in congenital hypothyroidism in these five US states increased by 16% from March 17–December 31, 2011, compared to the same period in 2010.

Study Questions for Chapter 23

1. Which of the following time intervals best describes the maximum susceptibility period?

(A) Week 1
(B) Weeks 3–8
(C) Weeks 9–38

2. Which of the following time intervals best describes the resistant period?

(A) Week 1
(B) Weeks 3–8
(C) Weeks 9–38

3. The most common viral infection is

(A) cytomegalovirus
(B) rubella virus
(C) herpes virus type 2
(D) varicella zoster virus
(E) HIV

4. Which of the following is a parasite found in cats?

(A) Treponema pallidum
(B) Toxoplasma gondii
(C) Rubella virus
(D) Cytomegalovirus
(E) Varicella zoster virus

5. Warfarin falls into which category of drugs?

(A) Category X drugs
(B) Category D drugs

6. Valium falls into which category of drugs?

(A) Category X drugs
(B) Category D drugs

Answers and Explanations

1. **B.** The embryonic period (weeks 3–8) is the time when the embryo is most susceptible to teratogens because all organ morphogenesis occurs at this time.
2. **A.** Week 1 is the resistant period when the conceptus demonstrates the "all-or-none" phenomenon (i.e., the conceptus will either die as a result of the teratogen or survive unaffected).
3. **A.** Cytomegalovirus (CMV) is the most common fetal infection and is the cause of cytomegalic inclusion disease.
4. **B.** *Toxoplasma gondii* is a protozoan parasite found in cats and may be transmitted to the fetus transplacentally.
5. **A.** Warfarin is a Category X drug.
6. **B.** Valium is a Category D drug.

Comprehensive Exam

1. A 25-year-old woman comes into your office complaining of "spotting" and having "stomach pains" as she points to her lower abdominal area. She noted that she and her husband were trying to have a baby and that she had her last period about 5 weeks ago. She said that after talking with her girlfriends about her symptoms, she was a little afraid of what it could be, and so she decided to see a physician. Her chart shows that she has had a history of pelvic inflammatory disease. Relevant physical exam findings include a tender pelvic mass that was palpable, amenorrhea, light vaginal bleeding, and lower abdominal pain. Relevant laboratory findings include elevated β-human chorionic gonadotropin (hCG) levels but lower than expected for pregnancy, lower-than-normal progesterone levels, and ultrasound that showed a mass in the ampulla of the left uterine tube. Which of the following is the most likely diagnosis?

(A) Choriocarcinoma
(B) A bleeding corpus luteum
(C) A spontaneous abortion
(D) Ectopic tubal pregnancy
(E) Appendicitis

2. A 31-year-old woman comes into the office complaining of "running a fever," being nauseated, and losing weight—"about 15 pounds or so"—over the last month. She tells you that she had a miscarriage about 2 months ago and "all of a sudden these other problems come up." She added that she said that the doctors said she had "preeclampsia" during her first trimester of that pregnancy. She said that she was supposed to come back in, but she didn't because she "felt depressed about losing the baby." She remarks that she hasn't had any changes in her diet and remarked that she "thought she would have gained weight with all the food she was eating." Relevant physical exam findings include normal thyroid gland on palpation, no coughing of blood, and no diarrhea. Relevant laboratory findings include elevated hCG levels and normal thyroxine (T_4) and thyroid-stimulating hormone (TSH) levels. Which of the following is the most likely diagnosis?

(A) Achalasia
(B) Hyperthyroidism
(C) Pelvic inflammatory disease
(D) Hydatidiform mole
(E) Gestational trophoblastic neoplasia (or choriocarcinoma)

3. A 37-year-old woman who is in her third trimester comes into your clinic complaining of bleeding that lasted for about "an hour or two." She remarks she noticed that the bleeding was "very bright red" in color but felt no noticeable pain. She said that she did nothing to cause the bleeding and "was concerned for the safety of her baby." Relevant physical exam findings include no abdominal or pelvic pain on palpation. Relevant laboratory findings include transvaginal ultrasound showing an intact, normally implanted placenta; however, the placenta was located in close proximity of the internal os. Which of the following is the most likely diagnosis?

(A) Placenta previa
(B) Placental abruption
(C) Placenta accreta
(D) Velamentous placenta
(E) Membranous placenta

4. A 34-year-old woman who is in her third trimester complains of her hands and face "swelling up a few days ago." She remarks that she has also felt like "her heart was racing a mile a minute." Relevant physical exam findings include hypertension (>160/110 mm Hg) and edema of the hands and face. Relevant laboratory findings include proteinuria (>5 g/24 hours), and ultrasound was unremarkable. Which of the following is the most likely diagnosis?

(A) Molar pregnancy
(B) Severe preeclampsia
(C) Choriocarcinoma
(D) Ectopic tubal pregnancy
(E) Placental abruption

5. A distraught mother brings her 2-month-old daughter into your office saying that she noticed a "lump growing from her child's bottom." She states that she "noticed it about 2 weeks ago while changing her daughter's diaper." The lump was small and she so didn't think much of it, but over time it has "grown to the size of a baseball." Relevant physical exam findings include a large spheroid mass that appeared to be very firm on palpation. Relevant laboratory findings include biopsy of the mass showing tissue containing hair, teeth, muscle fibers, and thyroid follicular cells. Which of the following is the most likely diagnosis?

(A) Spina bifida with meningocele
(B) Sacrococcygeal teratoma
(C) Spina bifida with meningomyelocele
(D) Chordoma
(E) Caudal dysplasia (sirenomelia)

6. After the delivery of a healthy baby girl, a physician notices a tuft of hair on the lower back of the child. The physician asked the mother about her prenatal health care, and she said she didn't take folic acid until the second month of pregnancy because she didn't know she was pregnant until then. Relevant physical exam findings include a tuft of hair on the lower back with no noticeable sac formation. Relevant laboratory findings include radiograph showing a defect in the vertebral arches but no sac filled with fluid or spinal cord. Which of the following is the most likely diagnosis?

(A) Spina bifida with meningocele
(B) Spina bifida with meningomyelocele
(C) Spina bifida occulta
(D) Spina bifida with rachischisis
(E) Caudal dysplasia (sirenomelia)

7. A distraught father comes in with his 10-year-old son, saying that his son began "turning blue" when he was out playing catch with him. His son remarked that he "just felt really tired" when he was running after the ball. The father is concerned that his son will not be able to play in the big game this weekend. Relevant physical exam findings include loud holosystolic ejection murmur on auscultation, cyanosis, and clubbing of fingernails. Relevant laboratory findings include echocardiogram showing right ventricular hypertrophy. Which of the following is the most likely diagnosis?

(A) Membranous ventricular septal defect
(B) Eisenmenger complex
(C) Atrial septal defect
(D) Patent ductus arteriosus
(E) Coarctation of the aorta

8. A 39-year-old man comes to your office complaining of "heartburn after trying to eat" and not being able to swallow anything. He states, "I have tried everything from water to steaks; it doesn't matter what I eat, I always have trouble swallowing it down." Relevant physical exam findings include dysphagia and normal thyroid on palpation. Relevant laboratory findings include barium swallow radiograph showing a dilated esophagus with an area of distal stenosis (almost looks like a "bird's beak") and normal T_4 levels. Which of the following is the most likely diagnosis?

(A) Esophageal atresia
(B) Thyroid tumor
(C) Esophageal stenosis
(D) Reflux esophagitis
(E) Achalasia

9. A mother brings her 1-month-old son into the clinic, complaining of her son "vomiting all over the place when he tries to eat something." She said her son's vomiting looks like it was "shot out of a cannon." Relevant physical findings include a small, nontender, palpable mass on the right costal margin. Relevant laboratory findings include barium swallow radiograph showing a narrow pyloric channel and abdominal ultrasound showing a hypertrophic pylorus. Which of the following is the most likely diagnosis?

(A) Esophageal hiatal hernia
(B) Hypertrophic pyloric stenosis
(C) Malrotation of the midgut with volvulus
(D) Esophageal stenosis
(E) Biliary atresia

10. A man brings his 3-year-old son into the office, complaining that his son is having "bad stomach pains" and talks about him "running a fever" and "being thirsty all the time." He remarks that his son has not had a bowel movement lately. Relevant physical exam findings include painless rectal bleeding, dark-red stools, and abdominal distention. Relevant laboratory findings include radiograph showing a remnant of the vitelline duct that was estimated to be about 2 feet from the ileocecal valve and a biopsy showing ectopic gastric and pancreatic mucosal tissue. Which of the following is the most likely diagnosis?

(A) Volvulus
(B) Intussusception

(C) Foreign-body obstruction
(D) Meckel diverticulum
(E) Biliary atresia

11. A nurse comes into your office informing you that the child you delivered yesterday failed to pass meconium. The nurse remarks that the child also cries on palpation of the abdominal area. Relevant physical exam finding include abdominal distention, megacolon on palpation, and gushing of fecal material on a rectal digital exam. Relevant laboratory findings include barium enema showing a dilated proximal segment and a narrow distal segment of the sigmoid colon. Which of the following is the most likely diagnosis?

(A) Rectal atresia
(B) Rectovesical fistula
(C) Hirschsprung disease
(D) Anorectal agenesis
(E) Intussusception

12. A 33-year-old man comes in complaining of "fever and chills" and that he "has to constantly go to the bathroom." He also indicates that he has pain just below the abdominal area on the right side. He states he has not had sexual intercourse in more than 6 months. He suspects that it may be urinary tract infection because he "has had a lot of them over the years." Relevant physical exam findings include flank pain and costovertebral angle tenderness. Relevant laboratory findings include normal calcium levels and computed tomography (CT) scan showing an unusual kidney appearance. Which of the following is the most likely diagnosis?

(A) Urachal fistula
(B) Horseshoe kidney
(C) Pyelonephritis
(D) Kidney stones
(E) Polycystic kidney disease

13. A 16-month-old boy has had recurrent bouts of cyanosis since birth. His parents tell you that "he cannot keep up with the other children of his age." The parents indicate that their boy frequently turns blue, breathes heavily on exertion, and sometimes experiences these difficulties for no reason. On many occasions, they observed their son in a squatting position. Relevant physical exam findings include systolic ejection murmur, cyanosis, clubbing of the fingernails, and a parasternal heave. Relevant laboratory findings include radiographs showing an enlarged right ventricle and "boot-shaped" heart, electrocardiogram showing right ventricular hypertrophy, and echocardiogram showing pulmonary stenosis, right ventricular hypertrophy, overriding aorta, and a ventricular septal defect. Which of the following is the most likely diagnosis?

(A) Tetralogy of Fallot
(B) Tricuspid atresia
(C) Total anomalous pulmonary venous return
(D) Transposition of the great arteries
(E) Persistent truncus arteriosus

14. A 40-year-old mother brings in her 4-week-old baby boy and tells you that "my baby's face looks funny and he keeps sticking his tongue out." The mother recalls that during the pregnancy she had low α-fetoprotein (AFP) levels. Relevant physical exam findings include a flat occiput; white spots in the iris (Brushfield spots); a large, protruding tongue; small, low-set ears; short feet and hands; a flexion crease across the palms (simian crease); curvature of the fifth digit; systolic ejection murmur; and hypotonia. Relevant laboratory findings include echocardiogram showing an endocardial cushion defect (atrioventricular septal defect) and karyotype analysis showing an extra chromosome 21. Which of the following is the most likely diagnosis?

(A) Cri-du-chat syndrome
(B) Edwards syndrome
(C) Fragile X syndrome
(D) Down syndrome
(E) Patau syndrome

15. A 25-year-old woman who is CEO of a new biotech company has been under considerable stress this last year trying to negotiate a contract with a major drug company. She has also been under a very rigorous exercise program because "she just can't stand any fat on her body" and ran in the Boston marathon 4 months ago. Due to her busy schedule, her eating habits have radically changed, and sometimes "the sight of food just disgusts me." She is not on any drug or medication. She tells you that recently she met "the guy" and has been sexually active with him for "about 2 months now." She comes to you because her menstrual cycle is 2 weeks late and sometimes she feels nauseated, especially in the morning. Relevant physical exam findings were unremarkable. Relevant laboratory findings include a positive β-human chorionic gonadotropin (hCG) test. Which of the following is the most likely diagnosis?

(A) Secondary amenorrhea due to stress
(B) Secondary amenorrhea due to anorexia nervosa
(C) Pregnancy
(D) Turner syndrome
(E) Secondary amenorrhea due to antipsychotic drug therapy

16. A father brings his 1-month-old daughter into the clinic, complaining that his daughter frequently "throws up after she eats" and "it just shoots across the room." Relevant physical exam findings include projectile vomiting when the infant is laid on its back after a feeding. Relevant laboratory findings include radiograph showing a portion of the stomach located in the pleural cavity. Which of the following is the most likely diagnosis?

(A) Hypertrophic pyloric stenosis
(B) Gastroesophageal reflux disease
(C) Esophageal hiatal hernia
(D) Congenital diaphragmatic hernia
(E) Tracheoesophageal fistula

17. A father brings his 4-year-old daughter into the clinic. He says he noticed "a lump on her lower right side" and that "it has gotten bigger over time." Relevant physical exam findings include a large, palpable mass on the right flank and no evidence of a urinary tract infection (UTI). Relevant laboratory findings include normal catecholamine levels and normal androgen levels, and genetic testing reveals a deletion of a tumor suppression gene on chromosome 11. Which of the following is the most likely diagnosis?

(A) Neuroblastoma
(B) Pheochromocytoma
(C) Congenital adrenal hyperplasia
(D) Wilms tumor
(E) Childhood polycystic kidney disease

18. A 45-year-old man comes in complaining of chest and abdominal pain. He also says that his "blood pressure rises every so often" even when he is relaxing at home and that "it's been happening more and more." He says he exercises often and tries to stay in shape because he has a family history of obesity. Relevant physical exam findings include profuse sweating, hypertension, abdominal discomfort, and lungs clear on auscultation. Relevant laboratory findings include radiograph negative for a pulmonary embolism, hyperglycemia, increased urinary vanillylmandelic acid (VMA) and metanephrine levels, and inability to suppress catecholamines with clonidine. Which of the following is the most likely diagnosis?

(A) Angina
(B) Pneumothorax
(C) Myocardial infarction
(D) Neuroblastoma
(E) Pheochromocytoma

19. A woman comes in with her 16-year-old daughter and states that her daughter "has not had a menstrual period yet." The daughter says that she is not sexually active and that she is not on any form of birth control. Relevant physical exam findings include ambiguous genitalia, amenorrhea, and early appearance of axillary and pubic hair. Relevant laboratory findings include elevated urinary 17-ketosteroids, elevated serum dehydroepiandrosterone (DHEA) sulfate, and normal or decreased 17-hydroxycorticosteroids, genetic testing reveals 46,XX genotype, and CT head scan reveals no sign of tumor. Which of the following is the most likely diagnosis?

(A) Female pseudo-intersexuality
(B) Turner syndrome
(C) Complete androgen insensitivity
(D) Pituitary tumor
(E) Male pseudo-intersexuality

20. A concerned couple brings their 3-week-old son into your office, stating that they think something is wrong with his genital area. They noticed that his testicles appeared to be swollen when they were changing his diaper a week ago. They said that his scrotum felt like a "water-filled balloon." Neither parent could recall any traumatic episode with their son, saying that they have been very protective of him. Relevant physical exam findings include an enlarged, nontender scrotum, testicles not immediately palpable, and no herniated bulge, and flashlight test through the enlarged area showed illumination. Relevant laboratory findings include absence of blood on fluid collection. Which of the following is the most likely diagnosis?

(A) Hypospadias
(B) Hematocele
(C) Congenial inguinal hernia
(D) Cryptorchidism
(E) Hydrocele of the testes

21. A mother brings her 5-year-old son into your office for a follow-up visit. The child previously

had a bout with pneumonia, and the mother remarked that the child has been coughing up "yellow and green stuff." The mother mentioned that he has had a number of coughs and colds that were just like this in the past. Relevant physical exam findings include foul-smelling, greenish sputum with speckles of blood, orthopnea, and fever, and his chart is remarkable for cystic fibrosis. Relevant laboratory findings include spirometry showing a reduced forced expiratory volume in 1 second/forced vital capacity (FEV_1/FVC) ratio, radiograph showing multiple cysts that have a "honeycomb" appearance, and CT scanning shows a dilation of bronchi. Which of the following is the most likely diagnosis?

(A) Asthma
(B) Bronchitis
(C) Bronchiectasis
(D) Pneumonia
(E) Influenza

22. While delivering a newborn baby girl, you notice that she has abnormal facies, but otherwise the delivery is uncomplicated. About 48 hours after birth, the baby girl develops seizures and muscle spasms. She is lethargic, mildly tachypneic, and jittery. Relevant physical findings include peculiar facies, low-set ears, widely spaced eyes, small mandible, no detectable thymus on palpation, muscle rigidity, harsh holosystolic murmur along the lower left sternal border, and a slight cyanotic tinge to the skin. Relevant laboratory findings include hypocalcemia, a low T lymphocyte count, radiograph showing absent thymic shadow, and cardiac ultrasound showing a congenital heart defect in the conotruncal region, and genetic testing reveals a deletion on chromosome 22q. Which of the following is the most likely diagnosis?

(A) Patau syndrome
(B) DiGeorge syndrome
(C) Miller-Decker syndrome
(D) Prader-Willi syndrome
(E) Treacher Collins syndrome

23. A mother brings in her 2-year-old son to the clinic, stating that she "thinks her son can't hear her when she calls to him." She also indicates that he seems "slower mentally than the other kids" and he isn't "saying any works like Mommy." Her son has been in and out of the hospital a lot due to congenital heart defects and recently had his cataracts removed. She remarks that while she was pregnant toward the beginning she was little sick and "broke out in a rash," but she thinks that "was due to a new lotion she was using." Relevant physical exam findings include microcephaly, deafness, hepatosplenomegaly, blueberry muffin spots, and a hint of jaundice. Which of the following is the most likely diagnosis?

(A) HIV infection
(B) Herpes simplex virus infection
(C) Rubella virus infection
(D) Patau syndrome
(E) Down syndrome

24. A young mother brings in her 3-year-old son because of "a white spot in his right eye" that she first noticed in a photograph taken 2 weeks ago. She also tells you that "he seems to be always squinting with his right eye." She remembers hearing about distant family member with the same sort of spot who eventually went blind. Relevant physical exam findings include leukocoria (whitish spots in the pupillary area behind the lens), strabismus (squinting; deviation of the eye that the patient cannot overcome), poor vision in the right eye, and curious family history. Relevant laboratory findings include CT scan showing a solid intraocular tumor with intratumoral calcifications, and genetic testing reveals a deletion on chromosome 13q. Which of the following is the most likely diagnosis?

(A) Congenital cataract
(B) Congenital glaucoma
(C) Retinitis pigmentosa
(D) Papilledema
(E) Retinoblastoma

25. A father brings his 8-year-old son to the clinic and tells you that "he is bleeding a lot" and that "the kid comes in from playing with a lot of bruises." When talking to the son, he tells you that he is "one of the coolest kids in school" because "he can pull his skin out all over the place." Then, he proceeds to demonstrate this fact by pulling his ears out several inches away from his body. His father tells you that last year his son was rushed to the hospital and had emergency surgery because "he had a hole in his intestines." Relevant physical findings include highly elastic, velvety skin; fragile skin that bruises easily; and loose, unstable, hypermobile joints. Relevant laboratory findings include genetic testing revealing a mutation in the gene for peptidyl lysine hydroxylase. Which of the following is the most likely diagnosis?

(A) Ehlers-Danlos syndrome
(B) Marfan syndrome
(C) Junctional epidermolysis bullosa

(D) Osteogenesis imperfecta
(E) Achondroplasia

26. A frantic father rushes his 1-year-old daughter to your clinic, saying that he "thinks his daughter's leg is broken." He says that this is the third time that his daughter has broken a bone in the last 2 months, and he thinks his wife may be abusing the child while he is at work. Relevant physical exam findings include short, deformed limbs, blue sclera of the eye, and kyphoscoliosis, and medical history indicates that there may have been bone fractures at birth. Relevant laboratory findings include radiographs showing multiple, healed fractures of the limbs, and genetic testing reveals a mutation in the gene for type 1 collagen on chromosome 7q22. Which of the following is the most likely diagnosis?

(A) Marfan syndrome
(B) Child abuse
(C) Osteogenesis imperfecta
(D) Ehlers-Danlos syndrome
(E) Achondroplasia

27. A 22-year-old man comes into the office complaining of blurred vision. He states that he "has not had problems seeing before." He remarks that "his dad and sister had the same problem around his age." Relevant physical exam findings include long, spidery fingers (arachnodactyly), hypermobile joints, arm span much greater than body height, and dislocation of the lens (ectopia lentis). Relevant laboratory findings include CT scan showing a dilated aorta, and genetic testing reveals a mutation for the fibrillin-1 gene on chromosome 15q21.1. Which of the following is the most likely diagnosis?

(A) Marfan syndrome
(B) Klippel-Feil syndrome
(C) Osteogenesis imperfecta
(D) Ehlers-Danlos syndrome
(E) Achondroplasia

28. A father brings his 12-year-old son and tells you that "his son is feeling weakness in his legs and is beginning to fall a lot." The father says "he can't run as good as he used to." He also says it's gotten so bad that when "he is sitting down he has to put his hands on his thighs just to stand up." Relevant physical exam findings include rapidly progressive muscle weakness with frequent falls; muscle wasting in the legs and pelvis and progressing to shoulders and neck; and pseudohypertrophy of calf muscles. Relevant laboratory findings include no sign of myoglobulinuria, highly elevated creatine phosphokinase (CPK), and electromyography (EMG) showing weakness due to muscle tissue destruction and not nerve damage, and genetic testing reveals a mutation on chromosome Xp21. Which of the following is the most likely diagnosis?

(A) Achondroplasia
(B) Myasthenia gravis
(C) McArdle disease
(D) Polymyositis
(E) Duchenne muscular dystrophy

29. A mother brings in her 5-year-old son at the request of his summer camp counselor, who claims "the boy is hyperactive and doesn't seem to be as smart as the other kids." The mother agrees but has not done anything about until now. The mother indicates that her son was "pretty small at birth" and had a ventricular septal defect that was repaired soon after birth. The mother further tells you that "except for being small and the heart problem, everything else in the pregnancy was just fine; but you know I did have a drink every now and then." Relevant physical exam findings include hypertelorism, smooth philtrum, short palpebral fissures, flat nasal bridge, maxillary (midface) hypoplasia, and a thin upper lip. Relevant laboratory findings include magnetic imaging (MRI) showing holoprosencephaly. Which of the following is the most likely diagnosis?

(A) Alcohol consumption during pregnancy
(B) Thalidomide consumption duringpregnancy
(C) Phenytoin consumption during pregnancy
(D) Prader-Willi syndrome
(E) Wolf-Hirschhorn syndrome

30. A 25-year-old woman who is 32 weeks pregnant comes into the emergency room while in labor. The infant is stillborn. The mother is obviously upset and says "I want to know what happened." Although the mother had no prenatal care, she says "I am shocked that something went wrong because I had no problems with my first pregnancy; that baby is fine." The mother is sincere when she states that she did not smoke or drink alcohol during the pregnancy. The mother says, "Everything was going along just fine with this pregnancy until just few hours ago." The mother requests an autopsy on the infant. Relevant physical findings of the autopsy

include the finding that the body is swollen and jaundiced; yellow deposits in several areas of the brain, especially the basal ganglia; and ascites. Relevant laboratory findings of the autopsy include severe anemia, high serum bilirubin levels, and infant's blood type O positive. Further lab tests were done on the blood of the mother and father. The mother's blood was O negative. The father's blood was O positive. Which of the following is the most likely diagnosis?

(A) Oligohydramnios
(B) Polyhydramnios
(C) Severe preeclampsia
(D) Erythroblastosis fetalis
(E) Placental abruption

31. A mother brings in her 6-week-old infant son because "I just want him to get checked out." She further tells you that "you know he was born prematurely, and thank God he didn't have any serious breathing problems; but I'm still worried." Relevant physical exam findings include the finding that the infant is small but active and appears to be mildly short of breath, and a harsh, machine-like, continuous murmur in the upper left parasternal area. Which of the following is the most likely diagnosis?

(A) Coarctation of the aorta
(B) Membranous ventricular septal defect
(C) Patent ductus arteriosus
(D) Double aortic arch
(E) Tetralogy of Fallot

32. A mother brings in her newborn baby girl and says, "My baby coughs and gags every time I try to feed her; one time she even turned blue and it scared me." The mother also indicates that her baby always has a "mouthful of saliva." Relevant physical exam findings include a distended stomach, excessive saliva accumulation, a hint of pneumonitis, and inability to pass a catheter into the infant's stomach. Relevant laboratory findings include radiograph showing a large amount of air in the stomach. Which of the following is the most likely diagnosis?

(A) Esophageal hiatal hernia
(B) Hypertrophic pyloric stenosis
(C) Tracheoesophageal fistula
(D) Respiratory distress syndrome
(E) Congenital diaphragmatic hernia

33. A frantic mother brings her newborn infant into the emergency room. You immediately notice that the infant is pale, irritable, diaphoretic, and dyspneic. A quick physical exam reveals hepatomegaly, absent femoral pulses, and pulses poor in all four extremities. The infant shows signs of heart failure and shock. An ECG shows pure right ventricular hypertrophy. A chest radiograph reveals generalized cardiomegaly with increased pulmonary vascular markings due to pulmonary venous congestion. The mother tells you that her baby was released from the hospital given a clean bill of health. Which of the following is the most likely diagnosis?

(A) Postductal coarctation of the aorta
(B) Membranous ventricular septal defect
(C) Patent ductus arteriosus
(D) Tetralogy of Fallot
(E) Congenital diaphragmatic hernia

34. A 40-year-old man comes to your office complaining that he has a gradual swelling in the front of his neck that has been growing over the last 6 months. He says, "Doc, at first I did not pay any attention to it, but now it is so big that other people are starting to notice it." He does not complain of any pain, difficulty in swallowing, or problems with breathing. There is no history of trauma, fever, or change in his voice. A physical exam reveals a nontender, nonerythematous fluctuant mass in the midline lower neck with a slight extension to the right side of the neck. The mass moves up and down when the patient swallows and displaces anteriorly with protrusion of the tongue. No cervical lymphadenopathy is noticed. The lung fields are clear, and the heart rate and rhythm are normal. You order a CT scan, which shows a cystic mass extending to the thyroid gland and under the strap muscles. Routine lab blood tests and thyroid function tests are all normal. Which of the following is the most likely diagnosis?

(A) Esophageal hiatal hernia
(B) Hypertrophic pyloric stenosis
(C) Tracheoesophageal fistula
(D) Thyroglossal duct cyst
(E) Congenital diaphragmatic hernia

35. A mother is holding her newborn baby in the hospital bed just a few hours after giving birth. The mother becomes alarmed when her baby begins to have a difficult time breathing and rings for help. You arrive at the bedside and observe that the baby is in severe respiratory distress. A quick physical exam reveals that the baby has a barrel-shaped chest, a

scaphoid-shaped abdomen, and absence of breath sounds on the left side, and the heartbeat is displaced to the right side. A chest radiograph reveals air/fluid containing bowel in the left-side hemithorax, no visible aerated lung on the left side, contralateral displacement of the heart and other mediastinal structures, compression of the contralateral lung, and reduced size of the abdomen. Which of the following is the most likely diagnosis?

(A) Esophageal hiatal hernia
(B) Hypertrophic pyloric stenosis
(C) Tracheoesophageal fistula
(D) Respiratory distress syndrome
(E) Congenital diaphragmatic hernia

Answers and Explanations

1. **D.** Ectopic tubal pregnancy (ETP) occurs when the blastocyst implants within the uterine tube due to delayed transport. The ampulla of the uterine tube is the most common site of an ectopic pregnancy. The rectouterine pouch (pouch of Douglas) is a common site for an ectopic abdominal pregnancy. ETP is most commonly seen in women with endometriosis or pelvic inflammatory disease. ETP leads to uterine tube rupture and hemorrhage if surgical intervention (i.e., salpingectomy) is not performed. ETP presents with abnormal uterine bleeding and unilateral pelvic pain, which must be differentially diagnosed from appendicitis, an aborting intrauterine pregnancy, or a bleeding corpus luteum of a normal intrauterine pregnancy. See Chapter 2, IV.A.

2. **E.** Gestational trophoblastic neoplasia (GTN; or choriocarcinoma). GTN is a malignant tumor of the trophoblast that may occur following a normal or ectopic pregnancy, abortion, or a hydatidiform mole. With a high degree of suspicion, elevated hCG levels are diagnostic. Nonmetastatic GTN (i.e., confined to the uterus) is the most common form of the neoplasia, and treatment is highly successful. However, the prognosis of metastatic GTN is poor if it spreads to the liver or brain. See Chapter 3, IV.D.

3. **A.** Placenta previa. Placenta previa occurs when the placenta attaches in the lower part of the uterus, covering the internal os. The placenta normally implants in the posterior superior wall of the uterus. Uterine (maternal) blood vessels rupture during the later part of pregnancy as the uterus begins to gradually dilate. The mother may bleed to death, and the fetus will also be placed in jeopardy because of the compromised blood supply. Because the placenta blocks the cervical opening, delivery is usually accomplished by cesarean section. This condition is clinically associated with repeated episodes of bright, red vaginal bleeding. Placental abruption would have shown a separation of the placenta and showed dark-red bleeding accompanied by abdominal pain. Placenta accreta would have shown the placenta implanted much deeper in the myometrium. See Chapter 6, IX.G.

4. **B.** Severe preeclampsia. Preeclampsia is a complication of pregnancy characterized by hypertension, edema, and/or proteinuria. Severe preeclampsia refers to the sudden development of maternal hypertension (blood pressure >160/110 mm Hg), edema (hands and/or face), and proteinuria (>5 g/24 hours), usually after week 32 of gestation (third trimester). Eclampsia includes the additional symptom of convulsions. The pathophysiology of preeclampsia involves a generalized arteriolar constriction that affects the brain (seizures and stroke), kidneys (oliguria and renal failure), liver (edema), and small blood vessels (thrombocytopenia and disseminated intravascular coagulation). Treatment of severe preeclampsia involves magnesium sulfate (for seizure prophylaxis) and hydralazine (blood pressure control); once the patient is stabilized, delivery of the fetus should ensue immediately. Risk factors include nulliparity, diabetes, hypertension, renal disease, twin gestation, or hydatidiform mole (produces first trimester preeclampsia). Her symptoms of hypertension, proteinuria, and edema are all telltale signs of preeclampsia. In addition, her advancing age has left to susceptible to this condition. A molar pregnancy is normally seen in the first trimester. Renal disease is unlikely because there were no findings other than proteinuria. See Chapter 6, IX.S.

5. **B.** Sacrococcygeal teratoma. Sacrococcygeal teratoma (ST) is a tumor that arises from remnants of the primitive streak, which normally degenerates and disappears. ST is derived from

pluripotent cells of the primitive streak and often contains various types of tissue (e.g., bone, nerve, hair). ST occurs more commonly in female infants and usually becomes malignant during infancy (must be removed by age 6 months). Caudal dysplasia (sirenomelia) refers to a constellation of syndromes ranging from minor lesions of lower vertebrae to complete fusion of the lower limbs. Caudal dysplasia is caused by abnormal gastrulation, whereby the migration of mesoderm is disturbed. Spina bifida occurs when the bony vertebral arches fail to form properly, thereby creating a vertebral defect, usually in the lumbosacral region. See Chapter 4, V.E.

6. **C.** Spina bifida occulta. Spina bifida occurs when the bony vertebral arches fail to form properly, thereby creating a vertebral defect, usually in the lumbosacral region. Spina bifida occulta is evidenced by a tuft of hair in the lumbosacral region. Spina bifida occulta is the least severe variation and occurs in 10% of the population. Spina bifida with meningocele occurs when the meninges protrude through a vertebral defect and form a sac filled with cerebrospinal fluid (CSF). The spinal cord remains in its normal position. Spina bifida with meningomyelocele occurs when the meninges and spinal cord protrude through a vertebral defect and form a sac filled with CSF. Spina bifida with rachischisis occurs when the posterior neuropore of the neural tube fails to close during week 4 of development. This condition is the most severe type of spina bifida, causing paralysis from the level of the defect caudally. See Chapter 7, XVIII.A.

7. **A.** Membranous ventricular septal defect (VSD). Membranous VSD is caused by faulty fusion of the right bulbar ridge, left bulbar ridge, and atrioventricular (AV) cushions. It results in a condition in which an opening between the right and left ventricles allows free flow of blood. A large VSD is initially associated with a left → right shunting of blood, increased pulmonary blood flow, and pulmonary hypertension. One of the secondary effects of a large VSD and its associated pulmonary hypertension is proliferation of the tunica intima and tunica media of pulmonary muscular arteries and arterioles, resulting in a narrowing of their lumen. Ultimately, pulmonary resistance may become higher than systemic resistance and cause right → left shunting of blood and cyanosis. At this stage, the characteristic of the patient has been termed the "Eisenmenger complex." This is the most common type of VSD. An atrial septal defect (ASD) would have a fixed, split S2, systolic ejection murmur. A patent ductus arteriosus (PDA), which is normally detected in infants, would have a continuous, machine-like murmur. Coarctation of the aorta would show a holosystolic murmur; however, there was no finding of a lack of a femoral pulse or rib notching. See Chapter 5, VII.B.3.

8. **E.** Achalasia. Achalasia occurs due to the loss of ganglion cells in the myenteric (Auerbach) plexus and is characterized by the failure to relax the lower esophageal sphincter, which will cause progressive dysphagia and difficulty in swallowing. The "bird's beak" appearance on the radiograph is a telltale sign of achalasia. Another telltale sign is that patients have a dysphagia involving both solids and liquids. The physical and lab findings exclude both thyroid disease and masses. Although reflux esophagitis would present with heartburn, it is limited to dysphagia of solids only, not solids and liquid. See Chapter 10, II.A.3.

9. **B.** Hypertrophic pyloric stenosis. Hypertrophic pyloric stenosis occurs when the muscularis externa in the pyloric region hypertrophies, causing a narrow pyloric lumen that obstructs food passage. It is associated clinically with projectile, nonbilious vomiting after feeding and a small, palpable mass at the right costal margin. An increased incidence of hypertrophic pyloric stenosis has been found in infants treated with the antibiotic erythromycin. See Chapter 10, II.B.3.

10. **D.** Meckel diverticulum. Meckel diverticulum (ileal diverticulum) occurs when a remnant of the vitelline duct persists, thereby forming an outpouching located on the antimesenteric border of the ileum. The outpouching may connect to the umbilicus via a fibrous cord or fistula. A Meckel diverticulum is usually located about 30 cm proximal to the ileocecal valve in infants and varies in length from 2 to 15 cm. Heterotopic gastric or pancreatic mucosa may be present, which leads to ulceration, perforation, or gastrointestinal bleeding, especially if a large number of parietal cells are present. It is associated clinically with symptoms resembling appendicitis and bright-red or dark-red stools (i.e., bloody). See Chapter 10, III.B.3c.

11. **C.** Hirschsprung disease (colonic aganglionosis). Hirschsprung disease is caused by the arrest of the caudal migration of neural crest cells. The hallmark is the absence of ganglionic cells in the

myenteric and submucosal plexuses, most commonly in the sigmoid colon and rectum, resulting in a narrow segment of colon (i.e., the colon fails to relax). Although the ganglionic cells are absent, there is a proliferation of hypertrophied nerve fiber bundles. The most characteristic functional finding is the failure of internal anal sphincter to relax following rectal distention (i.e., abnormal rectoanal reflex). Mutations of the RET protooncogene (chromosome 10q.11.2) have been associated with Hirschsprung disease. It is associated clinically with a distended abdomen, inability to pass meconium, gushing of fecal material on a rectal digital exam, and a loss of peristalsis in the colon segment distal to the normal innervated colon. See Chapter 10, IV.B.3a.

12. B. Horseshoe kidney. The symptoms that the man had (fevers, chills, flank pain, and costovertebral angle tenderness) are classic signs of pyelonephritis as a result of a urinary tract infection (UTI). In this case, the UTI is a result of a urinary tract obstruction caused by a horseshoe kidney. The most common type of renal fusion is the horseshoe kidney. A horseshoe kidney occurs when the inferior poles of the kidneys fuse across the midline. Normal ascent of the kidneys is arrested because the fused portion gets trapped behind the inferior mesenteric artery. Kidney rotation is also arrested so that the hilum faces ventrally. See Chapter 13, VIII.E.

13. A. Tetralogy of Fallot. Tetralogy of Fallot (TF) is caused by an abnormal neural crest cell migration such that there is *skewed* development of the aorticopulmonary (AP) septum. TF results in a condition in which the pulmonary trunk obtains a small diameter while the aorta obtains a large diameter. TF is characterized by four classic malformations: pulmonary stenosis, right ventricular hypertrophy, overriding aorta, and a ventricular septal defect (VSD). Note the mnemonic PROVE. TF is associated clinically with marked cyanosis, in which the clinical consequences depend primarily on the severity of the pulmonary stenosis. See Chapter 5, III.B.4.

14. D. Down syndrome (Trisomy 21) is characterized by moderate mental retardation (leading cause of inherited mental retardation), microcephaly, microphthalmia, colobomata, cataracts and glaucoma, flat nasal bridge, epicanthic folds, protruding tongue, simian crease in hand, increased nuchal skin folds, appearance of an "X" across the face when the baby cries as the upward-slanted palpebral fissures run in a line with the nasolabial folds, and congenital heart defects. Alzheimer neurofibrillary tangles and plaques are found in Down syndrome patients after 30 years of age. Acute megakaryocytic leukemia (AMKL) is frequently present. Trisomy 21 is the most common type of trisomy, and its frequency increases with advanced maternal age. Trisomy 21 is associated with low α-fetoprotein levels in amniotic fluid or maternal serum. A specific region on chromosome 21 seems to be markedly associated with numerous features of Trisomy 21. This region is called DSCR (Down syndrome critical region). The genes for the following have been mapped to the DSCR (although their role is far from clear): carbonyl reductase, SIM2 (a transcription factor), p60 subunit of chromatin assembly factor, holocarboxylase synthetase, ERG (a protooncogene), GIRK2 (a K^+ ion channel), and PEP19 (a Ca^{2+}-dependent signal transducer). Trisomy 21 may also be caused by a chromosomal translocation between chromosomes 14 and 21 [i.e., t(14;21)]. See Chapter 1, VI.A.

15. C. Pregnancy. Amenorrhea can be primary or secondary. Primary amenorrhea is the complete absence of menstruation in a woman from puberty. The most common cause of primary amenorrhea is Turner syndrome. Secondary amenorrhea is the absence of menstruation for at least 3 months in a woman who previously had normal menstruation. Many factors can cause secondary amenorrhea, including stress, anorexia nervosa, elevated prolactin levels (e.g., prolactinoma or antipsychotic drug therapy), and pregnancy. Of these factors, only pregnancy is associated with a positive hCG test. See Chapter 22, I, and Chapter 4, V.B.

16. C. Esophageal hiatal hernia. Esophageal hiatal hernia is a herniation of the stomach through the esophageal hiatus into the pleural cavity caused by an abnormally large esophageal hiatus. An esophageal hiatal hernia renders the esophagogastric sphincter incompetent so that stomach contents reflux into the esophagus. Clinical signs in the newborn include vomiting (frequently projectile) when the infant is laid on its back after feeding. See Chapter 21, IV.B.

17. D. Wilms tumor (WT). WT is the most common renal malignancy of childhood. WT presents as a large, solitary, well-circumscribed mass that on cut section is soft, homogeneous, and tan-gray in color. WT is interesting histologically, in that this tumor tends to recapitulate different

stages of embryological formation of the kidney, so that three classic histological areas are described: a stromal area; a blastemal area of tightly packed embryonic cells; and a tubular area. Neuroblastoma is ruled out because there was no mention of an increase in urine vanillylmandelic acid (VMA) and metanephrine levels. See Chapter 13, VIII.I.

18. E. Pheochromocytoma (PH). PH is a relatively rare neoplasm that contains both epinephrine and norepinephrine. PH occurs mainly in adults 40 to 60 years old and is generally found in the region of the adrenal gland, but it may be found in extrasuprarenal sites. PH is associated with persistent or paroxysmal hypertension, anxiety, tremor, profuse sweating, pallor, chest pain, and abdominal pain. Laboratory findings include increased urine VMA and metanephrine levels, inability to suppress catecholamines with clonidine, and hyperglycemia. PH is treated by surgery or phenoxybenzamine (an α-adrenergic antagonist). See Chapter 13, IX.C.2.

19. A. Female pseudo-intersexuality (FP) occurs when an individual has only ovarian tissue histologically and masculinization of the female external genitalia. These individuals have a 46,XX genotype. FP is most often observed clinically in association with a condition in which the fetus produces an excess of androgens (e.g., congenital adrenal hyperplasia [CAH]). CAH is caused most commonly by mutations in genes for enzymes involved in adrenocortical steroid biosynthesis (e.g., 21-hydroxylase deficiency, 11 β-hydroxylase deficiency). In 21-hydroxylase deficiency (90% of all cases), there is virtually no synthesis of cortisol or aldosterone, so intermediates are funneled into androgen biosynthesis, thereby elevating androgen levels. The elevated levels of androgens lead to masculinization of a female fetus. FP produces the following clinical findings: mild clitoral enlargement, complete labioscrotal fusion with a phalloid organ, or macrogenitosomia (in the male fetus). Because cortisol cannot be synthesized, negative feedback to the adenohypophysis does not occur, so adrenocorticotropic hormone (ACTH) continues to stimulate the adrenal cortex, resulting in adrenal hyperplasia. Because aldosterone cannot be synthesized, the patient presents with hyponatremia ("salt-wasting") with accompanying dehydration and hyperkalemia. Treatment includes immediate infusion of intravenous saline and long-term steroid hormone replacement, both cortisol and mineralocorticoids (9α-fludrocortisone). Although Turner syndrome is also a cause of primary amenorrhea, individuals with Turner syndrome have a 45,XO genotype. A pituitary tumor can be excluded due to negative CT scan findings. See Chapter 15, VI.B.2.

20. E. Hydrocele of the testes. Hydrocele of the testes occurs when a small patency of the processus vaginalis remains, so that peritoneal fluid can flow into the processus vaginalis, which results in a fluid-filled cyst near the testes. Peritoneal fluid drains from the abdomen through the tunica vaginalis. The fluid accumulates in the scrotum, becomes trapped, and causes the scrotum to enlarge. A hydrocele is usually harmless and in most cases resolves within a few months after birth. A hydrocele is normally treated only when there is discomfort or when the testicular blood supply is threatened. A hematocele could have also been considered, but a hematocele is typically due to trauma, and blood would have been seen on fluid collection. Inginual hernias usually accompany hydroceles, but there was no bulge detected on physical examination. See Chapter 15, VI.A.4.

21. C. Bronchiectasis. Bronchiectasis is the abnormal, permanent dilation of bronchi due to chronic necrotizing infection (e.g., *Staphylococcus*, *Streptococcus, Haemophilus influenzae*), bronchial obstruction (e.g., foreign body, mucous plugs, or tumors), or congenital conditions (e.g., Kartagener syndrome, cystic fibrosis, immunodeficiency disorders). The lower lobes of the lung are predominately affected, and the affected bronchi have a saccular appearance. Clinical signs include cough, fever, and expectoration of large amounts of foul-smelling purulent sputum. Bronchiectasis may also be classified to a group of disorders known as chronic obstructive pulmonary disease (COPD), which are characterized by increased resistance to airflow during both inspiration and expiration due to airway obstruction. Other members of COPD include emphysema, chronic bronchitis, and asthma. See Chapter 11, II.C.3d.

22. A. DiGeorge syndrome (DS) is caused by a microdeletion in the long arm of chromosome 22 (22q11), which is also called the DiGeorge chromosomal region (DGCR). DS occurs when pharyngeal pouches 3 and 4 fail to differentiate into the thymus and parathyroid glands. DS is usually accompanied by facial anomalies resembling first arch syndrome (micrognathia, low-set ears) due to

abnormal neural crest cell migration, cardiovascular anomalies due to abnormal neural crest cell migration during formation of the aorticopulmonary septum, immunodeficiency due to absence of thymus gland, and hypocalcemia due to absence of parathyroid glands. DS has a phenotypic and genotypic similarity to velocardiofacial syndrome (VCFS), that is, both DS and VCFS are manifestations of a microdeletion at 22q11. The genes for the following have been mapped to 22q11 or the DGCR (although their role is far from clear): catechol-*O*-methyltransferase (COMT; an enzyme used in catecholamine metabolism), GpIbb (receptor for von Willebrand factor), DGCR3 (a leucine zipper transcription factor), and citrate transport protein (CTP). See Chapter 12, VIII.I.

23. C. Rubella virus infection. Rubella virus (German measles; member of TORCH) belongs to the Togaviridae family, which are enveloped, icosahedral, positive, single-stranded RNA viruses. The rubella virus is transmitted to the fetus transplacentally. The risk of fetal rubella infection is greatest during the first month of pregnancy and apparently declines thereafter. Fetal rubella infection results in the classic triad of cardiac defects (e.g., patent ductus arteriosus, pulmonary artery stenosis, atrioventricular [AV] septal defects), cataracts, and low birth weight. With the pandemic of rubella in 1964, the complexity of this syndrome became apparent, and the term expanded rubella syndrome became standard. The clinical manifestations include intrauterine growth retardation (most common manifestation), hepatosplenomegaly, generalized adenopathy, hemolytic anemia, hepatitis, jaundice, meningoencephalitis, eye involvement (e.g., cataracts, glaucoma, retinopathy), bluish-purple lesions on a yellow, jaundiced skin ("blueberry muffin spots"), osteitis (celery stalk appearance of long bones), and sensorineural deafness. Exposure of pregnant women requires immediate assessment of their immune status. If the exposed pregnant woman is known to be immune (i.e., antibodies present), the woman can be assured of no risk. Postexposure prophylaxis of pregnant women with immune globulin (IG) is not recommended and should be considered only if abortion is not an option. Control measures for rubella prevention should be placed on immunization of children. Other members of TORCH include *Toxoplasma gondii* (a protozoan parasite), cytomegalovirus (CMV), herpes simplex virus, varicella zoster virus, *Treponema pallidum* (a spirochete), and hepatitis B virus. TORCH infections are caused by *Toxoplasma* (T), rubella (R), cytomegalovirus (C), herpes virus (H), and other (O) bacterial and viral infections that are grouped together because they cause similar clinical and pathological manifestations. See Chapter 23, II.A.1.

24. E. Retinoblastoma. Retinoblastoma (RB) is a tumor of the retina that occurs in childhood and develops from precursor cells in the immature retina. The RB gene is located on chromosome 13q and encodes for RB protein, which binds to a gene regulatory protein and causes suppression of the cell cycle, that is, the RB gene is a tumor-suppressor gene (also called an anti-oncogene). A mutation in the RB gene will encode an abnormal RB protein such that there is no suppression of the cell cycle. This leads to the formation of RB. Hereditary RB causes multiple tumors in both eyes. Nonhereditary RB causes one tumor in one eye. See Chapter 9, III.M.

25. A. Ehlers-Danlos syndrome. Ehlers-Danlos syndrome is an autosomal dominant genetic disorder involving the gene for peptidyl lysine hydroxylase, which is an enzyme necessary for the hydroxylation of lysine residues of collagen. It affects mainly type I and type III collagen. It is characterized by extremely stretchable and fragile skin, hypermobile joints, aneurysms of blood vessels, and rupture of the bowel. See Chapter 16, I.C.4.

26. C. Osteogenesis imperfecta. Osteogenesis Imperfecta (OI) is an autosomal dominant (types I and IV) or recessive (types II and III) genetic disorder caused by a mutation in the gene for type I collagen subunits on chromosome 7q22 or 17q22. OI is characterized by extreme bone fragility, with spontaneous fractures occurring when the fetus is still in the womb and blue sclera of the eye. Severe forms of OI are fatal in utero or during the early neonatal period. Milder forms of OI may be confused with child abuse. See Chapter 17, VII.C.

27. A. Marfan syndrome. Marfan syndrome (MS) is an autosomal dominant genetic disorder caused by a mutation in the gene for the protein fibrillin-1 on chromosome 15q21.1, which is an essential component of elastic fibers. These individuals are unusually tall and have exceptionally long, thin limbs, ectopia lentis (dislocation of the lens), severe near-sightedness, and heart valve incompetence. See Chapter 17, VII.B.

28. E. Duchenne muscular dystrophy. Duchenne muscular dystrophy (DMD). DMD is an X-linked recessive disorder caused by a mutation in the gene for dystrophin on the short arm of chromosome X (Xp21). X-linked recessive inheritance means that males who inherit only one defective copy of the DMD gene from the mother have the disease. Dystrophin anchors the cytoskeleton (actin) of skeletal muscle cells to the extracellular matrix through a transmembrane protein (α-dystroglycan and β-dystroglycan) and stabilizes the cell membrane. A mutation of the DMD gene destroys the ability of dystrophin to anchor actin to the extracellular matrix. The characteristic dysfunction in DMD is progressive muscle weakness and wasting. Death occurs as a result of cardiac or respiratory failure, usually in the late teens or 20s. The description of how the boy arose from a seated position is called the Gower maneuver, which is classically seen in DMD. Becker muscular dystrophy normally begins around the third decade of life, whereas DMD can begin much earlier. McArdle disease is excluded because there was no sign of myoglobinuria, which would be a result of muscle glycogen phosphorylase deficiency. See Chapter 18, IV.D.

29. A. Alcohol consumption during pregnancy. Alcohol is an organic compound delivered to the fetus through recreational or addictive (i.e., alcoholism) drinking by pregnant women. This drug can cause fetal alcohol syndrome, which results in mental retardation, microcephaly, holoprosencephaly, limb deformities, craniofacial abnormalities (i.e., hypertelorism, smooth philtrum, short palpebral fissures, flat nasal bridge, maxillary (midface) hypoplasia, and a thin upper lip), and cardiovascular defects (i.e., ventricular septal defects). Fetal alcohol syndrome is the leading cause of preventable mental retardation. The threshold dose of alcohol has not been established, so "no alcohol is good alcohol" during pregnancy. See Chapter 23, V.M.

30. D. Erythroblastosis fetalis. The Rh factor is clinically important in pregnancy. If the mother is Rh–, she will produce Rh antibodies if the fetus is Rh+. This situation will not affect the first pregnancy but will affect the second pregnancy with an Rh+ fetus. In the second pregnancy with an Rh+ fetus, a hemolytic condition of red blood cells (RBCs) occurs known as Rh-hemolytic disease of newborn (erythroblastosis fetalis). This causes destruction of fetal RBCs, which leads to the release of large amounts of bilirubin (a breakdown product of hemoglobin). This causes fetal brain damage due to a condition called kernicterus, which is a pathological deposition of bilirubin in the basal ganglia. Severe hemolytic disease in which the fetus is severely anemic and demonstrates total body edema (i.e., hydrops fetalis) may lead to death. In these cases, an intrauterine transfusion is indicated. Rh_0(D) immune globulin (RhoGAM, MICRhoGAM) is a human immunoglobulin (IgG) preparation that contains antibodies against Rh factor and prevents a maternal antibody response to Rh+ cells that may enter the maternal bloodstream of an Rh–mother. This drug is administered to Rh– mothers within 72 hours after the birth of an Rh+ baby to prevent erythroblastosis fetalis during subsequent pregnancies. See Chapter 6, IX.O.

31. C. Patent ductus arteriosus. Patent ductus arteriosus occurs when the ductus arteriosus—a connection between the left pulmonary artery and aorta—fails to close. Normally, the ductus arteriosus functionally closes within a few hours after birth via smooth muscle contraction to ultimately form the ligamentum arteriosum. A patent ductus arteriosus causes a left → right shunting of oxygen-rich blood from the aorta back into the pulmonary circulation. This can be treated with prostaglandin synthesis inhibitors (such as indomethacin), which promote closure. It is very common in premature infants and maternal rubella infection. Clinical signs include a harsh, machine-like, continuous murmur in the upper left parasternal area. See Chapter 5, IX.B.4.

32. C. Tracheoesophageal fistula. Tracheoesophageal fistula is an abnormal communication between the trachea and esophagus that results from improper division of foregut by the tracheoesophageal septum. It is generally associated with esophageal atresia and polyhydramnios. Clinical features include excessive accumulation of saliva or mucus in the nose and mouth; episodes of gagging and cyanosis after swallowing milk; abdominal distention after crying; and reflux of gastric contents into lungs, causing pneumonitis. Diagnostic features include inability to pass a catheter into the stomach and radiographs demonstrating air in the infant's stomach. See Chapter 11, II.B.2.

33. A. Postductal coarctation of the aorta. Postductal coarctation of the aorta occurs when the aorta is abnormally constricted distal to the origin of the left subclavian artery and inferior to the ductus arteriosus. Congenital coarctation reveals tunica intima hyperplasia and tunica media thickening that forms a posterolateral ridge that encircles the aortic lumen. Symptoms may occur in the neonatal period when the patent ductus arteriosus and the patent foramen ovale close, so that the entire cardiac output to the lower extremity must cross the narrowed aortic segment. See Chapter 5, IX.B.5.

34. D. A thyroglossal duct cyst occurs when parts of the thyroglossal duct persist and thereby form a cyst. These cysts can be present anywhere along the line of descent in fetal development of the thyroid gland, from the foramen cecum at the base of the tongue to the level of the thyroid gland. There are four types of thyroglossal duct cysts: thyrohyoid cysts (61% of cases), suprahyoid cysts (24%), suprasternal cysts (13%), and intralingual cysts (2%). See Chapter 12, VIII.E.

35. E. A congenital diaphragmatic hernia is a herniation of abdominal contents into the pleural cavity caused by a failure of the pleuroperitoneal membrane to develop or fuse with other components of the diaphragm. Affected neonates usually present in the first few hours of life with respiratory distress that may be mild or so severe as to be incompatible with life. See Chapter 21, IV.A.

Credits

CHAPTER 2

Figure 2.1. From Dudek R, Fix J. *High-Yield Embryology*. Baltimore, MD: Lippincott Williams & Wilkins; 1996:5.

CHAPTER 3

Figure 3.1. E. From Sauerbrei EE, Nguyen KT, Nolan RL. *A Practical Guide to Ultrasound in Obstetrics and Gynecology*. 2nd ed. Philadelphia, PA: Lippincott Williams & Wilkins; 1998:115.

Figure 3.2. From Sternberg SS. *Diagnostic Surgical Pathology*. Vol 2. 3rd ed. Philadelphia, PA: Lippincott Williams & Wilkins; 1999:2070.

Figure 3.3. A, B. From Sternberg SS. *Diagnostic Surgical Pathology*. Vol 2. 3rd ed. Philadelphia, PA: Lippincott Williams & Wilkins; 1999:2077, 2078.

CHAPTER 4

Figure 4.1. From Dudek RW. *High-Yield Embryology*. Baltimore, MD: Williams & Wilkins; 1996:9.

Figure 4.2. A, B. From Johnson KE. *NMS Human Developmental Anatomy*. Baltimore, MD: Williams & Wilkins; 1988:79. **C.** From Sadler TW. *Langman's Medical Embryology*. 7th ed. Baltimore, MD: Williams & Wilkins; 1995:77.

Figure 4.4. From Sadler TW. *Langman's Medical Embryology*. 7th ed. Baltimore, MD: Williams & Wilkins; 1995:62.

Figure 4.5. From Sadler TW. *Langman's Medical Embryology*. 7th ed. Baltimore, MD: Williams & Wilkins; 1995:61.

CHAPTER 5

Figure 5.2. (Table) From Dudek RW. *High-Yield Embryology*. 2nd ed. Philadelphia, PA: Lippincott Williams & Wilkins; 2001:27. **B, C.** From Johnson KE. *NMS Human Developmental Anatomy*. Baltimore, MD: Williams & Wilkins; 1988:147. **D.** From Kirks DR. *Practical Pediatric Imaging*. 3rd ed. Philadelphia, PA: Lippincott Williams & Wilkins; 1997:591.

Figure 5.4. From Avery GB, Fletcher MA, MacDonald MG. *Neonatology Pathophysiology and Management of the Newborn*. 5th ed. Philadelphia, PA: Lippincott Williams & Wilkins; 1999:602.

Figure 5.5. From Donnelly LF, Higgin CB. MR imaging of conotruncal abnormalities. *Am J Roentgenol.* 1996;166:925. Reprinted with permission from the *American Journal of Roentgenology*.

Figure 5.6. From Fletcher MA, MacDonald MG. *Neonatology Pathophysiology and Management of the Newborn*. 5th ed. Philadelphia, PA: Lippincott Williams & Wilkins; 1999:605.

Figure 5.7. From Bisset GS III. Magnetic resonance imaging of the pediatric cardiovascular system. In: Cohen MD, Edwards MK, eds. *Pediatrics Magnetic Resonance Imaging.* Philadelphia, PA: BC Decker; 1990:541–548.

Figure 5.8. Modified from Johnson KE. *NMS Human Developmental Anatomy*. Baltimore, MD: Williams & Wilkins; 1988:149.

Figure 5.9. B. From McMillan JA, DeAngelis CD, Feigin RD, et al., eds. *Oski's Pediatrics*. 3rd ed. Philadelphia, PA: Lippincott Williams & Wilkins; 1999:1349.

Figure 5.13. B. From Kirks DR. *Practical Pediatric Imaging*. 3rd ed. Philadelphia, PA: Lippincott Williams & Wilkins; 1997:553.

Figure 5.15. B. From Kirks DR. *Practical Pediatric Imaging*. 3rd ed. Philadelphia, PA: Lippincott Williams & Wilkins, 1997:553.

Figure 5.17. B. From McMillan JA, DeAngelis CD, Feigin RD, et al., eds. *Oski's Pediatrics*. 3rd ed. Philadelphia, PA: Lippincott Williams & Wilkins; 1999:1356.

Figure 5.18. A, B. From Johnson KE. *NMS Human Developmental Anatomy*. Baltimore, MD: Williams & Wilkins; 1988:154. **D1.** From McMillan JA, DeAngelis CD, Feigin RD, et al., eds. *Oski's Pediatrics*. 3rd ed. Philadelphia, PA: Lippincott Williams & Wilkins; 1999:1369.

Figure 5.19. A–C. Modified from Johnson KE. *NMS Human Developmental Anatomy*. Baltimore, MD: Williams & Wilkins; 1988:159.

CHAPTER 6

Figure 6.1. B–D. (left part only) From Johnson KE. *NMS Human Developmental Anatomy*. Baltimore, MD: Williams & Wilkins; 1988:96.

Figure 6.2. D, E. From Sadler TW. *Langman's Medical Embryology*. 7th ed. Baltimore, MD: Williams & Wilkins; 1995:108. **A. (sonogram only)** From Sauerbrei EE. *A Practical Guide to Ultrasound in Obstetrics and Gynecology*. 2nd ed. Philadelphia, PA: Lippincott Williams & Wilkins; 1998:116.

Figure 6.3. C. From Gartner LP, Hiatt JL. *Color Atlas of Histology*. 4th ed. Philadelphia, PA: Lippincott Williams & Wilkins; 2006:365. **D.** From Thornberg KL, Faber JJ. *Placental Physiology*. New York: Raven Press, 1983:19. **E.** From Dudek R. *High-Yield Embryology*. 2nd ed. Philadelphia, PA: Lippincott Williams & Wilkins; 2000:21.

Figure 6.4. From Sternberg SS. *Histology for Pathologists*. 2nd ed. Philadelphia, PA: Lippincott Williams & Wilkins; 1997:967.

Figure 6.5. From Dudek RW. *High-Yield Embryology*. 2nd ed. Philadelphia, PA: Lippincott Williams & Wilkins; 2000:24.

Figure 6.6. A–C. From Dudek RW. *High-Yield Embryology*. 2nd ed. Philadelphia, PA: Lippincott Williams & Wilkins; 2000:8. **A1.** From Dudek RW. *High-Yield Embryology*. 2nd ed. Philadelphia, PA: Lippincott Williams & Wilkins, 2000:20. **A2.** Courtesy of Dr. R. W. Dudek. **B1.** From Dudek RW. *High-Yield Embryology*. 2nd ed. Philadelphia, PA: Lippincott Williams & Wilkins; 2000:20. **B2.** Courtesy of Dr. R. W. Dudek. **C1.** From Sadler TW. *Langman's Medical Embryology*. 6th ed. Baltimore, MD: Williams & Wilkins; 1990:156.

Figure 6.7. From Sternberg SS. *Diagnostic Surgical Pathology*. Vol 2. 3rd ed. Philadelphia, PA: Lippincott Williams & Wilkins; 1999:2091.

Figure 6.8. From Sternberg SS. *Diagnostic Surgical Pathology*. Vol 2. 3rd ed. Philadelphia, PA: Lippincott Williams & Wilkins; 1999:2089.

Figure 6.9. From Fletcher, MA. *Physical Diagnosis in Neonatology*. Philadelphia, PA: Lippincott-Raven; 1997:85.

Figure 6.10. From Benirschke K, Kaufmann P. *The Pathology of the Human Placenta*. 3rd ed. New York, NY: Springer-Verlag; 1995. With permission of Springer Science+Business Media.

CHAPTER 7

Figure 7.1. A, C, E. Modified from Truex RC, Carpenter MB. *Human Neuroanatomy*. Baltimore, MD: Williams & Wilkins; 1969:91. **B, D, F.** From Carpenter MB, Sutin J. *Human Neuroanatomy*. 8th Ed. Baltimore, MD: Lippincott Williams & Wilkins; 1983:63.

Figure 7.2. From Spitz JL. *Genodermatoses: A Full Color Clinical Guide to Genetic Skin Disorders*. Baltimore, MD: Lippincott Williams & Wilkins; 1996:76. Courtesy of Lawrence Gordon, MD.

Figure 7.3. From Gold DH, Weingeist TA, eds. *Color Atlas of the Eye in Systemic Diagnosis*. Philadelphia, PA: Lippincott Williams & Wilkins; 2001:499.

Figure 7.4. Modified from Johnson KE. *NMS Human Developmental Anatomy*. Baltimore, MD: Lippincott Williams & Wilkins; 1988:177.

Figures 7.5, 7.6, 7.10. From Cormack DH. *Essential Histology*. 2nd ed. Philadelphia, PA: Lippincott Williams & Wilkins; 2001:221.

Figure 7.17. From Fix J. *BRS Neuroanatomy*. 4th ed. Philadelphia, PA: Lippincott Williams & Wilkins; 2008:70.

Figure 7.18. From Johnson KE. *NMS Human Developmental Anatomy*. Baltimore, MD: Williams & Wilkins; 1988:181.

Figure 7.19. Redrawn from Larsen WJ. *Human Embryology*. 2nd ed. New York, NY: Churchill Livingston; 1997:439.

Figure 7.20. Modified from Haines DE. *Fundamental Neuroscience*. New York, NY: Churchill Livingston; 1997:69.

Figure 7.21. From Haines DE. *Fundamental Neuroscience*. New York, NY: Churchill Livingston; 1997:69. Copyright Elsevier.

Figure 7.22. Courtesy of Dr. T. Naidich, Miami, FL.

Figure 7.23. From Papp Z. *Atlas of Fetal Diagnosis*. Amsterdam, Netherlands: Elsevier; 1992:128.

Figure 7.24. From Haines DE. *Fundamental Neuroscience*. New York, NY: Churchill Livingston; 1997:68. Copyright Elsevier.

Figure 7.25. From Carlson BM. *Human Embryology and Developmental Biology*. 2nd ed. St. Louis, MO: Mosby; 1999:244.

Figure 7.26. From Haines DE. *Fundamental Neuroscience*. New York, NY: Churchill Livingston; 1997:69.

Figure 7.27. From Dudek RW. *High-Yield Embryology*. 2nd ed. Philadelphia, PA: Lippincott Williams & Wilkins; 2001:76.

Figure 7.28. From Swischuk LE. *Imaging of the Newborn, Infant, and Young Child*. 5th ed. Philadelphia, PA: Lippincott Williams & Wilkins; 2004:1016.

Figure 7.29. From Swischuk LE. *Imaging of the Newborn, Infant, and Young Child*. 5th ed.

Philadelphia, PA: Lippincott Williams & Wilkins; 2004:1017.

Figure 7.30. From Siegel MJ. *Pediatric Sonography*. 3rd ed. Philadelphia, PA: Lippincott Williams & Wilkins; 2001:111.

Figure 7.31. From Siegel MJ. *Pediatric Sonography*. 3rd Ed. Philadelphia: Lippincott Williams & Wilkins; 2001:92.

Figure 7.32. From Siegel MJ. *Pediatric Sonography*. 3rd ed. Philadelphia, PA: Lippincott Williams & Wilkins; 2001:103.

Figure 7.33. From Swischuk LE. *Imaging of the Newborn, Infant, and Young Child*. 5th ed. Philadelphia, PA: Lippincott Williams & Wilkins, 2004:1018.

Figure 7.34. From Siegel MJ. *Pediatric Sonography*. 3rd ed. Philadelphia, PA: Lippincott Williams & Wilkins; 2001:102.

Figure 7.35. From Siegel MJ. *Pediatric Sonography*. 3rd ed. Philadelphia, PA: Lippincott Williams & Wilkins; 2001:97.

Figure 7.36. Courtesy of Dr. James E. Rytting.

CHAPTER 8

Figure 8.1. C. Redrawn from Moore KL, Persaud TVN. *The Developing Human*. 6th ed. Philadelphia, PA: WB Saunders; 1998:505. **E.** From Rohen JW, Yokochi C, Lütjen-Drecoll E. *Color Atlas of Anatomy*. 4th ed. Philadelphia, PA: Lippincott Williams & Wilkins; 1998:124.

Figure 8.2. From Fletcher MA. *Physical Diagnosis in Neonatology*. Philadelphia, PA: Lippincott Williams & Wilkins; 1998:285.

Figure 8.3. From Fletcher MA. *Physical Diagnosis in Neonatology*. Philadelphia, PA: Lippincott Williams & Wilkins; 1998:288.

Figure 8.4. From Fletcher MA. *Physical Diagnosis in Neonatology*. Philadelphia, PA: Lippincott Williams & Wilkins; 1998:289.

Figure 8.5. From Fletcher MA. *Physical Diagnosis in Neonatology*. Philadelphia, PA: Lippincott Williams & Wilkins; 1998:294.

Figure 8.6. From Fletcher MA. *Physical Diagnosis in Neonatology*. Philadelphia, PA: Lippincott Williams & Wilkins; 1998:295.

Figure 8.7. From Fletcher MA. *Physical Diagnosis in Neonatology*. Philadelphia, PA: Lippincott Williams & Wilkins; 1998:292.

Figure 8.8. From Sternberg SS. *Diagnostic Surgical Pathology*. Vol 1. 3rd ed. Philadelphia, PA: Lippincott Williams & Wilkins; 1999:963.

Figure 8.9. From Fletcher MA. *Physical Diagnosis in Neonatology*. Philadelphia, PA: Lippincott Williams & Wilkins; 1998:296.

CHAPTER 9

Figure 9.3. From Tasman W, Jaeger EA. *Wills Eye Hospital Atlas of Clinical Ophthalmology*. Philadelphia, PA: Lippincott-Raven; 1996.

Figure 9.4. From Gilbert-Barness E. *Potter's Atlas of Fetal and Infant Pathology*. St. Louis, MO: Mosby; 1998:366, 370. Copyright Elsevier.

Figure 9.5. From Tasman W, Jaeger EA. *The Wills Eye Hospital Atlas of Clinical Ophthalmology*. 2nd ed. Philadelphia, PA: Lippincott Williams & Wilkins; 2001.

Figure 9.6. From Gilbert-Barness E. *Potter's Atlas of Fetal and Infant Pathology*. St. Louis, MO: Mosby; 1998:366, 370. Copyright Elsevier.

Figure 9.7. From Avery GB. *Neonatology: Pathophysiology and Management of the Newborn*. 5th ed. Philadelphia, PA: Lippincott Williams & Wilkins; 1999:1286.

Figure 9.8. From Kirks DR. *Practical Pediatric Imaging*. 3rd ed. Philadelphia, PA: Lippincott Williams & Wilkins; 1997:205.

Figure 9.9. From Kirks DR. *Practical Pediatric Imaging*. 3rd ed. Philadelphia, PA: Lippincott Williams & Wilkins; 1997:211.

CHAPTER 10

Figure 10.1. From Dudek R. *High-Yield Embryology*. 2nd ed. Philadelphia, PA: Lippincott Williams & Wilkins; 2000:35.

Figure 10.2. From Fenoglio-Preiser CM, Noffsinger AE, Stemmermann GN, et al., eds. *Gastrointestinal Pathology: An Atlas and Text*. 2nd ed. Philadelphia, PA: Lippincott Williams & Wilkins; 1999:33.

Figure 10.3. From Fenoglio-Preiser CM, Noffsinger AE, Stemmermann GN, et al., eds. *Gastrointestinal Pathology: An Atlas and Text*. 2nd ed. Philadelphia, PA: Lippincott Williams & Wilkins; 1999:37.

Figure 10.4. From Fenoglio-Preiser CM, Noffsinger AE, Stemmermann GN, et al., eds. *Gastrointestinal Pathology: An Atlas and Text*. 2nd ed. Philadelphia, PA: Lippincott Williams & Wilkins; 1999:36.

Figure 10.5. From Yamada T, Alpers DH, Laine L, et al., eds. *Textbook of Gastroenterology*. Vol 1. Philadelphia, PA: Lippincott Williams & Wilkins; 1999:1189.

Figure 10.6. From Fenoglio-Preiser CM, Noffsinger AE, Stemmermann GN, et al., eds. *Gastrointestinal Pathology: An Atlas and Text*. 2nd ed. Baltimore, MD: Lippincott Williams & Wilkins; 1999:624.

Figure 10.7. From Johnson KE. *NMS Human Developmental Anatomy*. Baltimore, MD: Williams & Wilkins; 1988:211.

Figure 10.8. From Yamada T, Alpers DH, Laine L, et al., eds. *Textbook of Gastroenterology*. Vol 1. Philadelphia, PA: Lippincott Williams & Wilkins; 1999:1337.

Figure 10.9. From Johnson KE. *NMS Human Developmental Anatomy*. Baltimore, MD: Williams & Wilkins; 1988:215.

Figure 10.10. From Lindner H. Embryology and anatomy of the biliary tree. In: Way LW. *Surgery of the Gallbladder and Bile Ducts*. Philadelphia, PA: WB Saunders; 1987.

Figure 10.11. From Yamada T, Alpers DH, Laine L, et al., eds. *Textbook of Gastroenterology*. Vol 1. Philadelphia, PA: Lippincott Williams & Wilkins; 1999:2250.

Figure 10.12. From Lindner H. Embryology and anatomy of the biliary tree. In: Way LW. *Surgery of the Gallbladder and Bile Ducts*. Philadelphia, PA: WB Saunders; 1987.

Figure 10.13. Redrawn and modified from Cubilla AL, Fitzgerald PJ. Tumors of the exocrine pancreas. In: Hartman WH, Sobin LH, eds. *Atlas of Tumor Pathology*. 2nd ed. Washington, DC: Armed Forces Institute of Pathology; 1984.

Figure 10.14. A. Redrawn and modified from Cubilla AL, Fitzgerald PJ. Tumors of the exocrine pancreas. In: Hartman WH, Sobin LH, eds. *Atlas of Tumor Pathology*. 2nd ed. Washington, DC: Armed Forces Institute of Pathology; 1984. **B.** From Yamada T, Alpers DH, Laine L, et al., eds. *Textbook of Gastroenterology*. Vol 1. Philadelphia, PA: Lippincott Williams & Wilkins; 1999:2118. Courtesy of Peter B. Cotton, MD, Durham, NC.

Figure 10.15. From Misiewicz JJ, Bartram CI. *Atlas of Clinical Gastroenterology*. London: England, Gower Medical Publishing; 1987.

Figure 10.16. From Johnson KE. *NMS Human Developmental Anatomy*. Baltimore, MD: Williams & Wilkins; 1988:218.

Figure 10.17. From Sadler TW. *Langman's Medical Embryology*. 8th ed. Baltimore, MD: Lippincott Williams & Wilkins; 2000:294.

Figure 10.18. From Sadler TW. *Langman's Medical Embryology*. 8th ed. Baltimore, MD: Lippincott Williams & Wilkins; 2000:294. Courtesy of Dr. S. Lacey, Department of Surgery, University of North Carolina, Chapel Hill, North Carolina.

Figure 10.19. From Fenoglio-Preiser CM, Noffsinger AE, Stemmermann GN, et al., eds. *Gastrointestinal Pathology: An Atlas and Text*. 2nd ed. Baltimore, MD: Lippincott Williams & Wilkins; 1999:321.

Figure 10.20. From Fenoglio-Preiser CM, Noffsinger AE, Stemmermann GN, et al., eds. *Gastrointestinal Pathology: An Atlas and Text*. 2nd ed. Baltimore, MD: Lippincott Williams & Wilkins; 1999:310.

Figure 10.21. From Yamada T, Alpers DH, Laine L, et al., eds. *Textbook of Gastroenterology*. Vol 1. Philadelphia, PA: Lippincott Williams & Wilkins; 1999:259.

Figure 10.22. From Fenoglio-Preiser CM, Noffsinger AE, Stemmermann GN, et al., eds. *Gastrointestinal Pathology: An Atlas and Text*. 2nd ed. Philadelphia, PA: Lippincott Williams & Wilkins; 1999:315. **(Inset)** From Smith GH, Glasson M. Intestinal atresia: factors affecting survival. *Aust N Z J Surg.* 1989;59:151.

Figure 10.23. From Yamada T, Alpers DH, Laine L, et al., eds. *Textbook of Gastroenterology*. Vol 1. Philadelphia, PA: Lippincott Williams & Wilkins; 1999:259. **(Inset)** From Smith GH, Glasson M. Intestinal atresia: factors affecting survival. *Aust N Z J Surg.* 1989;59:151.

Figure 10.24. From Sadler TW. *Langman's Embryology*. 10th ed. Philadelphia, PA: Lippincott Williams & Wilkins; 2006:224.

Figure 10.25. From Fenoglio-Preiser CM, Noffsinger AE, Stemmermann GN, et al., eds. *Gastrointestinal Pathology: An Atlas and Text*. 2nd ed. Baltimore, MD: Lippincott Williams & Wilkins; 1999:318. **(Inset)** From Fenoglio-Preiser CM, Noffsinger AE, Stemmermann GN, et al., eds. *Gastrointestinal Pathology: An Atlas and Text*. 2nd ed. Baltimore, MD: Lippincott Williams & Wilkins; 1999:318.

Figure 10.26. (line drawings) From Sadler TW. *Langman's Medical Embryology*. 8th ed. Philadelphia, PA: Lippincott Williams & Wilkins; 2000:299. **(Photo)** From Sternberg SS. *Histology for Pathologists*. 2nd ed. Philadelphia, PA: Lippincott-Raven; 1997:554.

Figure 10.27. From Swischuk LE. *Imaging of the Newborn, Infant, and Young Child*. 5th ed. Philadelphia, PA: Lippincott Williams & Wilkins; 2004:448.

Figure 10.28. From Larsen WJ. *Human Embryology*. 2nd ed. New York, NY: Churchill Livingstone; 1997:268. Copyright Elsevier.

Figure 10.29. From Larsen WJ. *Human Embryology*. 2nd ed. New York, NY: Churchill Livingstone; 1997:268.

Figure 10.30. From Larsen WJ. *Human Embryology*. 2nd ed. New York, NY: Churchill Livingstone; 1997:268.

CHAPTER 11

Figure 11.1. (bottom) From Dudek R. *High-Yield Embryology*. 2nd ed. Philadelphia, PA: Lippincott Williams & Wilkins; 2000:56.

Figure 11.2. A. From Yamada T, Alpers DH, Laine L, et al., eds. *Textbook of Gastroenterology*. Vol 1. Philadelphia, PA: Lippincott Williams & Wilkins; 1999:1186. **B.** From Kirks DR. *Practical Pediatric Imaging*. 3rd ed. Philadelphia, PA: Lippincott Williams & Wilkins; 1998:845.

Figure 11.3. From Yamada T, Alpers DH, Laine L, et al., eds. *Textbook of Gastroenterology*. Vol 1. Philadelphia, PA: Lippincott Williams & Wilkins; 1999:1186.

Figure 11.4. A. From Yamada T, Alpers DH, Laine L, et al., eds. *Textbook of Gastroenterology*. Vol 1. Philadelphia, PA: Lippincott Williams & Wilkins; 1999:1186. **B.** From Avery GB. Neonatology Pathophysiology and Management of the Newborn. 5th ed. Philadelphia, PA: Lippincott Williams & Wilkins; 1999:1018.

Figure 11.5. From Yamada T, Alpers DH, Laine L, et al., eds. *Textbook of Gastroenterology*. Vol 1. Philadelphia, PA: Lippincott Williams & Wilkins; 1999:1186.

Figure 11.6. From Yamada T, Alpers DH, Laine L, et al., eds. *Textbook of Gastroenterology*. Vol 1. Philadelphia, PA: Lippincott Williams & Wilkins; 1999:1186.

Figure 11.7. From Rohen JW, Yokochi C, Lütjen-Drecoll E. *Color Atlas of Anatomy*. 4th ed. Philadelphia, PA: Lippincott Williams & Wilkins; 1998:235.

Figure 11.8. From Kirks DR. *Practical Pediatric Imaging*. 3rd Ed. Philadelphia, PA: Lippincott Williams & Wilkins; 1998:671.

Figure 11.9. From Kirks DR. *Practical Pediatric Imaging*. 3rd Ed. Philadelphia, PA: Lippincott Williams & Wilkins; 1998:674.

Figure 11.10. (Left) Modified from Rohen JW, Yokochi C, Lütjen-Drecoll E. *Color Atlas of Anatomy*. 4th ed. Philadelphia, PA: Lippincott Williams & Wilkins; 1998:235. **(Right)** Redrawn from Sweeney LJ. *Basic Concepts in Embryology*. New York, NY: McGraw-Hill; 1998:321.

Figure 11.11. (Left) Modified from Rohen JW, Yokochi C, Lütjen-Drecoll E. *Color Atlas of Anatomy*. 4th ed. Philadelphia, PA: Lippincott Williams & Wilkins; 1998:235. **(Right)** Redrawn from Sweeney LJ. *Basic Concepts in Embryology*. New York, NY: McGraw-Hill; 1998:321.

Figure 11.12. (Left) Modified from Rohen JW, Yokochi C, Lütjen-Drecoll E. *Color Atlas of Anatomy*. 4th ed. Philadelphia, PA: Lippincott Williams & Wilkins; 1998:235. **(Right)** Redrawn from Sweeney LJ. *Basic Concepts in Embryology*. New York, NY: McGraw-Hill; 1998:321.

Figure 11.13. (Left) Modified from Rohen JW, Yokochi C, Lütjen-Drecoll E. *Color Atlas of Anatomy*. 4th ed. Philadelphia, PA: Lippincott Williams & Wilkins; 1998:235. **(Right)** From Gartner LP, Hiatt JL. *Color Atlas of Histology*. 4th ed. Philadelphia, PA: Lippincott Williams & Wilkins; 2006:253.

Figure 11.14. A. From Dudek RW. *High-Yield Embryology*. 2nd ed. Philadelphia, PA: Lippincott Williams & Wilkins; 2000:59. **B.** From Kirks DR. *Practical Pediatric Imaging*. 3rd ed. Philadelphia, PA: Lippincott Williams & Wilkins; 1998:695.

CHAPTER 12

Figure 12.4. From Sadler TW. *Langman's Medical Embryology*. 9th ed. Philadelphia, PA: Lippincott Williams & Wilkins; 2004:391–393.

Figure 12.5. From McMillan JA, DeAngelis CD, Feigin RD, et al., eds. *Oski's Pediatrics*. 3rd ed. Philadelphia, PA: Lippincott Williams & Wilkins; 1999:394.

Figure 12.6. From Moore KL. *The Developing Human*. 6th ed. Philadelphia, PA: WB Saunders; 1998:228. Copyright Elsevier.

Figure 12.7. Courtesy of Dr. A. Shaw, Department of Surgery, University of Virginia, Charlottesville, VA.

Figure 12.8. From Laeung AKC. Ectopic thyroid gland simulating a thyroglossal duct cyst. *Can J Surg* 1995;38:87.

Figure 12.9. A. From Fletcher A. *Physical Diagnosis in Neonatology*. Philadelphia, PA: Lippincott Williams & Wilkins; 1997:225. **B.** From Kirks DW. *Practical Pediatric Imaging*. 3rd ed. Philadelphia, PA: Lippincott Williams & Wilkins; 1997:246.

Figure 12.10. From Bickley LS, Szilagyi P. *Bates' Guide to Physical Examination and History Taking*. 8th ed. Philadelphia, PA: Lippincott Williams & Wilkins; 2003.

Figure 12.11. Courtesy of Dr. M. Edgerton, Department of Plastic Surgery, University of Virginia, Charlottesville, VA.

CHAPTER 13

Figure 13.4. A. From Johnson KE. *NMS Human Developmental Anatomy*. Baltimore, MD: Williams & Wilkin;, 1988:269. **C.** Redrawn from Stevenson RE. *Human Malformation and Related Anomalies*. New York, NY: Oxford University Press; 1993.

Figure 13.5. A. From Stevenson RE. *Human Malformation and Related Anomalies*. New York, NY: Oxford University Press; 1993. **B.** From Kirks DW. *Practical Pediatric Imaging*. 3rd ed. Philadelphia, PA: Lippincott Williams & Wilkins; 1997:1091.

Figure 13.6. From Kirks DW. *Practical Pediatric Imaging*. 3rd ed. Philadelphia, PA: Lippincott Williams & Wilkins; 1997:1038.

Figure 13.7. A. From Kelalis PP, King LR. *Clinical Pediatric Urology*. Vol 2. Philadelphia, PA: WB Saunders, 1976:210. **B.** From Kirks DW. *Practical Pediatric Imaging*. 3rd ed. Philadelphia, PA: Lippincott Williams & Wilkins; 1997:1050.

Figure 13.8. A. From Papp Z. *Atlas of Fetal Diagnosis*. New York, NY: Elsevier; 1992:178. **B.** Courtesy of Dr. R. W. Dudek.

Figure 13.9. A. From Sternberg SS. *Diagnostic Surgical Pathology*. Vol 2, 3rd ed. Philadelphia, PA: Lippincott Williams & Wilkins; 1999:1827. **B.** Courtesy of Dr. R. W. Dudek.

Figure 13.10. From Belman AB. The clinical significance of vesicoureteral reflux. *Pediatr Clin North Am.* 1976;23:707.

Figure 13.11. From Malek RS, Kelalis PP. Simple and ectopic ureterocele in infancy and childhood. *Surg Gynecol Obstet.* 1972;134:611.

Figure 13.13. A. From Sternberg SS. *Diagnostic Surgical Pathology*. Vol 1, 3rd ed. Philadelphia, PA: Lippincott Williams & Wilkins; 1999:609. **B.** Courtesy of Dr. R. W. Dudek.

Figure 13.14. A. From DeLellis RA. Diseases of the adrenal glands. In: Murphy WM. *Urological Pathology*. Philadelphia, PA: WB Saunders; 1997: 539–584. **B.** From Sternberg SS. *Diagnostic Surgical Pathology*. Vol 1. 3rd ed. Philadelphia, PA: Lippincott Williams & Wilkins; 1999:616.

Figure 13.15. From Wilkins L. *The Diagnosis and Treatment of Endocrine Disorders in Childhood and Adolescence*. 3rd ed. Springfield, IL: Courtesy of Charles C Thomas Publisher, Ltd. 1965:439.

CHAPTER 14

Figure 14.1. Courtesy of Dr. R.W. Dudek.

Figure 14.2. A–C. Modified from Shakzkes DR, Haller JO. Imaging of Uterovaginal Anomalies in the Pediatric Population. *Urol Radiol.* 1991;13:58; and Markham SM, Waterhouse TB. Structural anomalies of the reproductive tract. *Curr Opin Obstet Gynecol.* 1992;4:867.

Figure 14.3. From Janovski NA. *Ovarian Tumors*. Vol 4. Major Problems in Obstetrics and Gynecology. Philadelphia, PA: WB Saunders; 1973:191.

Figure 14.4. C. From Fletcher MA. *Physical Diagnosis in Neonatology*. Philadelphia, PA: Lippincott Williams & Wilkins; 1998:179. **D.** From Sternberg SS. *Histology for Pathologists*. 2nd ed. Philadelphia, PA: Lippincott Williams & Wilkins; 1997:852.

Figures 14.5, 14.6 (A–D), 14.7 (A, B), 14.8 (A, B), 14.9, 14.10 (A). From Emans SJ, Laufer MR, Goldstein DP. *Pediatric and Adolescent Gynecology*. 4th ed. Philadelphia, PA: Lippincott-Raven; 1998:322–331. Originally adapted from American Fertility Society. The American Fertility Society classifications of adnexal adhesion, distal tubal occlusion, tubal occlusion secondary to tubal ligation, tubal pregnancies, Müllerian anomalies, and intrauterine adhesions. *Fertil Steril*. 1988;49(6):944. Reprinted by permission from the American Society for Reproductive Medicine.

Figure 14.6. (Photo) From Fleischer AC, Javitt MC, Jeffrey RB, et al. *Clinical Gynecologic Imaging*. Philadelphia, PA: Lippincott-Raven; 1997:304.

Figure 14.7. (Photos), 14.8 (Photo), 14.10 (Lower photo). Courtesy of Dr. A. Gerbie. From Spitzer IB, Rebar RW. Counseling for women with medical problems: ovary and reproductive organs. In: Hollingsworth D, Resnik R, eds. *Medical Counseling before Pregnancy*. New York, NY: Churchill Livingston;, 1988:216.

Figure 14.10. (Upper photo) From Gidwani G, Falcone T. *Congenital Malformations of the Female Genital Tract: Diagnosis and Management.* Philadelphia, PA: Lippincott Williams & Wilkins, 1999:81.

Figure 14.11. A, B. From Pokorny SF. Configuration of the Prepubertal Hymen. *Am J Obstet Gynecol.* 1987;157:950. **B1, C, C1.** From Emans SJ, Laufer MR, Goldstein DP. *Pediatric and Adolescent Gynecology*. 4th ed. Philadelphia, PA: Lippincott Williams & Wilkins; 1998:9. **D, E.** From Goldstein DP, Laufer MR, Davis AF. *Gynecologic Surgery in Children and Adolescents: A Text Atlas.* New York, NY: Springer-Verlag. **F, F1, G, G1.** From Emans SJ, Laufer MR, Goldstein DP. *Pediatric and Adolescent Gynecology*. 4th ed. Philadelphia, PA: Lippincott Williams & Wilkins; 1998:11.

CHAPTER 15

Figure 15.1. D. From Trainer TD. Testis and excretory duct system. In: Mills SE, ed. *Histology for Pathologists*. 3rd ed. Philadelphia, PA: Lippincott Williams & Wilkins; 2007:951.

Figure 15.2. A–C. Modified from Shakzkes DR, Haller JO. Imaging of uterovaginal anomalies in the pediatric population. *Urol Radiol.* 1991;13:58; and Markham SM, Waterhouse TB. Structural anomalies of the reproductive tract. *Curr Opin Obstet Gynecol.* 1992;4:867.

Figure 15.4. A. From Gilbert-Barness E. *Potter's Atlas of Fetal and Infant Pathology*. St. Louis, MO: Mosby; 1998:294. Copyright Elsevier. **B.** Courtesy of Dr. T. Ernesto Figuero.

Figure 15.5, 15.6. From Gilbert-Barness E. *Potter's Atlas of Fetal and Infant Pathology*. St. Louis, MO: Mosby; 1998:294.

Figure 15.7. Courtesy of Dr. T. Ernesto Figuero.

Figure 15.8. Courtesy of Dr. J. Kitchin, Department of Obstetrics and Gynecology, University of Virginia, Charlottesville, VA.

Figure 15.9. From Warkany J. *Congenital Malformations: Notes and Comments*. Chicago, IL: Year Book Medical Publishers; 1971:337. Copyright Elsevier.

Figure 15.10. From Jones HW, Scott WW. *Hermaphroditism, Genital Anomalies and Related Endocrine Disorders.* Baltimore, MD: Williams & Wilkins; 1958.

CHAPTER 16

Figure 16.1. Reprinted from Pehamberger H, Honigsmann H, Wolff K. Dysplastic nevus syndrome with multiple primary amelanotic melanomas in oculocutaneous albinism. *J Am Acad Dermatol.* 1984;11:731, with permission from Elsevier.

Figure 16.2. Courtesy of the Department of Dermatology, Columbia University, New York, NY.

Figure 16.3. Courtesy of Ingrid Winship, MBChB, MD, Cape Town, South Africa.

Figure 16.4. From Fletcher MA. *Physical Diagnosis in Neonatology*. Philadelphia, PA: Lippincott Williams & Wilkins; 1997:130.

Figure 16.5. A, B. From Bernice R, Karachi ND, Toronto, Canada, from Mallory SB. What syndrome is this? Ehlers-Danlos syndrome. *Pediatr Dermatol.* 1991;8:348.

Figure 16.6. Reprinted from Reese V, Frieden IJ, Paller AS, et al. Association of facial hemangiomas with Dandy-Walker and other posterior fossa malformations. *J Pediatr.* 1993; 122:379, with permission from Elsevier.

Figure 16.7. A. Courtesy of Gilles G. Lestringang, MD, Abu Dhabi, United Arab Emirates. **B.** From Sternberg SS. *Diagnostic Surgical Pathology*. Vol 1, 3rd ed. Philadelphia, PA: Lippincott Williams & Wilkins; 1999:24.

Figure 16.8. From Junqueira LC, Carneiro J. *Basic Histology*. 9th ed. Stamford, CT: Appleton & Lange; 1998:335.

Figure 16.9. Courtesy of Dr. Antoine Petit, Argenteuil, France.

Figure 16.10. Courtesy of Peter H. Itin, MD, Basel, Switzerland.

Figure 16.11. Courtesy of Marc E. Grossman, New York, NY.

Figure 16.12. From Spitz JL. *Genodermatoses*. Baltimore, MD: Williams & Wilkins; 1996:241.

Figure 16.13. Courtesy of Paulus T. V. M. de Jong, MD, Rotterdam, Netherlands.

Figure 16.14. Adapted from Grumback MM, Styne DM. Puberty: ontogeny, neuroendocrinology, physiology, and disorders. In: Wilson JD, Foster DW, eds. *Williams Textbook of Endocrinology*. 8th ed. Philadelphia, PA: WB Saunders; 1992; and Marshall WA, Tanner JM. Variations in pattern of pubertal changes in girls. *Arch Dis Child.* 1969;44:291.

Figure 16.15. Reprinted from McKusick VA, Abbey H, Bannerman RM, et al. Medical genetics. *J Chronic Dis.* 1959;12:1, with permission from Elsevier.

Figure 16.16. From Fletcher MA. *Physical Diagnosis in Neonatology*. Philadelphia, PA: Lippincott Williams & Wilkins; 1997:330.

Figure 16.17. Courtesy of George E. Giffor, MD, Children's Hospital, Boston, MA.

Figure 16.18. From Fletcher MA. *Physical Diagnosis in Neonatology*. Philadelphia, PA: Lippincott Williams & Wilkins; 1997:330.

Figure 16.20. Redrawn from Avery JK. *Oral Development and Histology*. 2nd ed. New York, NY: Thieme Medical Publishers; 2002:131, 133.

Figure 16.21. Redrawn from Avery JK. *Oral Development and Histology*. 2nd ed. New York, NY: Thieme Medical Publishers; 2002:131, 133.

Figure 16.22. Redrawn from McMillan JA, DeAngelis CD, Feigin RD, et al., eds. *Oski's Pediatrics*. 3rd ed. Philadelphia, PA: Lippincott Williams & Wilkins; 1999:645.

CHAPTER 17

Figure 17.1. B. Redrawn from *Gray's Anatomy: The Anatomical Basis of Medicine and Surgery*. 38th ed. Edinburgh: Churchill Livingstone; 1995:372. **C.** Modified from Sadler TW. *Langman's Medical Embryology*. 8th ed. Philadelphia, PA: Lippincott Williams & Wilkins; 2000:164.

Figure 17.2. From Sadler TW. *Langman's Medical Embryology*. 8th ed. Philadelphia, PA: Lippincott Williams & Wilkins; 2000:169.

Figure 17.3. From McMillan JA, DeAngelis CD, Feigin RD, et al., eds. *Oski's Pediatrics*. 3rd ed. Philadelphia, PA: Lippincott Williams & Wilkins; 1999:396.

Figure 17.4. From Fletcher MA. *Physical Diagnosis in Neonatology*. Philadelphia, PA: Lippincott Williams & Wilkins; 1997:188.

Figure 17.5. From McMillan JA, DeAngelis CD, Feigin RD, et al., eds. *Oski's Pediatrics*. 3rd ed. Philadelphia, PA: Lippincott Williams & Wilkins; 1999:398.

Figure 17.6. Courtesy of M. M. Cohen, Jr., Halifax, Nova Scotia, Canada.

Figure 17.7. Courtesy of M. M. Cohen, Jr., Halifax, Nova Scotia, Canada.

Figure 17.8. From McMillan JA, DeAngelis CD, Feigin RD, et al., eds. *Oski's Pediatrics*. 3rd ed. Philadelphia, PA: Lippincott Williams & Wilkins; 1999.

Figure 17.9. B. Redrawn from Larsen WJ. *Human Embryology*. 2nd ed. New York, NY: Churchill Livingston; 1997:77.

Figure 17.10. From Esses SI. *Textbook of Spinal Disorders*. Philadelphia, PA: Lippincott Williams & Wilkins; 1995:44.

Figure 17.11. From Kirks DR. *Practical Pediatric Imaging*. 3rd ed. Philadelphia, PA: Lippincott Williams & Wilkins; 1997:314.

Figure 17.14. From Esses SI. *Textbook of Spinal Disorders*. Philadelphia, PA: Lippincott Williams & Wilkins; 1995:259.

Figure 17.15. From Jinkins JR. *Neurodiagnostic Imaging*. Philadelphia, PA: Lippincott Williams & Wilkins; 1997:69.

Figure 17.17. Courtesy of Derek C. Harwood-Nash, MD, Toronto, Ontario, Canada.

Figure 17.18. From McMillan JA, DeAngelis CD, Feigin RD, et al., eds. *Oski's Pediatrics*. 3rd ed. Philadelphia, PA: Lippincott Williams & Wilkins; 1999:2118.

Figure 17.19. From McKusick VA. *Heritable Disorders of Connective Tissue*. 4th ed. St. Louis, MO: CV Mosby; 1972:758. Copyright Elsevier.

Figure 17.20. From McKusick VA. *Heritable Disorders of Connective Tissue*. 4th ed. St. Louis, MO: CV Mosby; 1972:67. Copyright Elsevier.

Figure 17.21. From McMillan JA, DeAngelis CD, Feigin RD, et al., eds. *Oski's Pediatrics*. 3rd ed. Philadelphia, PA: Lippincott Williams & Wilkins; 1999:2149.

Figure 17.22. From Kaufman CE. *Essentials of Pathophysiology*. Philadelphia, PA: Lippincott Williams & Wilkins; 1996:261. Used with permission of the patient.

CHAPTER 18

Figures 18.2, 18.3. From Fletcher MA. *Physical Diagnosis in Neonatology*. Philadelphia, PA: Lippincott Williams & Wilkins; 1997:309, 355.

Figure 18.4. From Avery GB. *Neonatology: Pathophysiology and Management of the Newborn*. 5th ed. Philadelphia, PA: Lippincott Williams & Wilkins; 1999:1271.

Figure 18.5. Reprinted from Nicholson LV, Davison K, Johnson MA, et al. Dystrophin in skeletal muscle II. Immunoreactivity in patients with Xp21 muscular dystrophy. *J Neurol Sci*. 1989;94:137, with permission from Elsevier.

CHAPTER 19

Figures 19.5B, 19.6B. From Keats TE, Smith TH. *Atlas of Normal Developmental Roentgen Anatomy*. 2nd ed. Chicago, IL: Year Book Medical Publishers; 1977:33, 292, 295. Copyright Elsevier.

CHAPTER 20

Figures 20.5B, 20.6B. From Keats TE, Smith TH. *Atlas of Normal Developmental Roentgen Anatomy*. 2nd ed. Chicago, IL: Year Book Medical Publishers; 1977:31, 237, 289. Copyright Elsevier.

CHAPTER 21

Figure 21.2A. From Gilbert-Barness E. *Potter's Atlas of Fetal and Infant Pathology*. St. Louis, MO: Mosby; 1998:172. Copyright Elsevier.

Figure 21.2B. From Aladjen S, Vidyasagar D. *Atlas of Perinatology*. Philadelphia, PA: WB Saunders; 1982:295, 375.

Figure 21.3. From Fenoglio-Preiser CM. *Gastrointestinal Pathology: An Atlas and Text*. 2nd ed. Philadelphia, PA: Lippincott, Williams & Wilkins; 1998:43.

CHAPTER 23

Figure 23.1. A. From Fletcher MA. *Physical Diagnosis in Neonatology*. Philadelphia, PA: Lippincott Williams & Wilkins; 1997:133. **B.** Courtesy of Dr. George H. McCracken, Jr., Dallas, TX.

Figure 23.2. A. From Avery GB. *Neonatology: Pathophysiology and Management of the Newborn*. 5th ed. Philadelphia, PA: Lippincott Williams & Wilkins; 1999:1293. **B.** From McMillan JA, DeAngelis CD, Feigin RD, et al., eds. *Oski's Pediatrics*. 3rd ed. Philadelphia, PA: Lippincott Williams & Wilkins; 1999:687. **C.** Courtesy of Dr. George H. McCracken, Jr., Dallas, TX. **D.** Courtesy of Dr. Guido Currarinao, Dallas, TX. **E.** From Avery GB. *Neonatology: Pathophysiology and Management of the Newborn*. 5th ed. Philadelphia, PA: Lippincott Williams & Wilkins; 1999:1154. **F.** From Avery GB. *Neonatology: Pathophysiology and Management of the Newborn*. 5th ed. Philadelphia, PA: Lippincott Williams & Wilkins; 1999:1136.

Index

Note: Page numbers followed by f denote figures; those followed by t denote tables.